The mechanism of action of Clioquinol for the treatment of Alzheimer's disease

presented by

Yifat Biran

Submitted in total fulfillment of the requirements of the degree of Doctor of Philosophy

March 2018

The Florey Institute of Neuroscience and Mental Health
Faculty of Medicine, Dentistry and Health Sciences
The University of Melbourne
Victoria, Australia

Abstract

Alzheimer's disease (AD) is an irreversible, progressive neurodegenerative disorder, which is characterised by an increasing impairment in memory and cognitive skills that significantly hinders a person's daily functioning. As it stands today, AD is a fatal condition that affects millions of people around the world and is expected to reach mammoth proportions by mid-century. Despite decades of research, key findings in disease aetiology and pathogenesis, discovery of new biomarkers and development of novel brain imaging compounds, AD remains incurable and an effective disease-modifying treatment is still proving to be elusive.

In parallel, numerous compounds are currently undergoing pre-clinical and clinical evaluations. These candidate pharmacotherapeutics are aimed at various aspects of the disease, such as the microtubule-associated tau protein, the amyloid beta (Aβ) peptide and metal ion dyshomeostasis – all of which are involved in the origin and/or progression of AD, as reviewed in **Chapter 1**.

This thesis aims to expand our knowledge on the mechanism of action (MOA) of one such investigational drug, clioquinol (CQ), which serves as an 8-hydroxyqionoline (8-HQ) prototype therapeutic for AD.

To this end, the interaction between CQ, metal ions and Aβ was studied *in vitro*. Together, results in **Chapter 3** and **Chapter 5** demonstrate that CQ binds directly to Aβ and metals (presumably by forming a ternary complex), and delivers them into neuronal cells and primary neurons, respectively. Once internalized, the ions are either retained or removed, the protein is degraded and the drug continues to recycle. This may account for the reduction in plasma and/or cerebrospinal fluid (CSF) Aβ, and improvement in cognitive functions observed in AD animal models and patients following intake of CQ.

During the experimental process of this dissertation (methodology detailed in **Chapter 2**), different neuronal cell lines were observed to be prone to cytotoxicity induced by metal-CQ complexes. Findings in **Chapter 4** add to a growing literature on the anti-cancer effects of metal chelates of CQ and other compounds that, so far, have only been tested in non-neuronal cell lines and tumours.

As concluded in **Chapter 6**, it is hoped that this new level of understanding of CQ's operating mode can assist in the rational development of 8-HQ derivatives and their metal complexes as medical imaging, diagnostic and/or therapeutic agents for AD and brain cancer.

Declaration

This is to certify that

i. the thesis comprises only my original work towards the PhD except where indicated in the Preface,

ii. due acknowledgement has been made in the text to all other material used,

iii. the thesis is less than 100,000 words in length, exclusive of tables, maps, bibliographies and appendices.

Yifat Biran
The Florey Institute of Neuroscience and Mental Health
Faculty of Medicine, Dentistry and Health Sciences
The University of Melbourne
Victoria, Australia

Preface

It is acknowledged that:

- synthesis of ^{125}I-CQ was carried out by Dr. Ivan Greguric and Ms. Naomi Wyatt (Australian Nuclear Science and Technology Organisation (ANSTO)).
- metal and iodine analysis was performed by Ms. Irene Volitakis (The Florey Institute of Neuroscience and Mental Health).
- Aβ was occasionally prepared by or with the aid of Dr. Adam Gunn and Dr. Bruce Wong (The Florey Institute of Neuroscience and Mental Health).
- Aβ analysis was conducted by or with the help of Dr. Qiao-Xin Li and Ms. Katrina Laughton (The University of Melbourne).

Acknowledgments

First, I would like to thank my supervisors, Prof. Ashley Bush and A/Prof. Kevin ("Macduff") Barnham, for their guidance in experimental design and result analysis, as well as their assistance in compiling this thesis.

Of the "old" Mental Health Research Institute (MHRI) crew, I am grateful to Prof. Colin Masters, A/Prof. Robert Cherny, Prof. David Finkelstein, A/Prof. Paul Adlard and A/Prof. Victor Villemagne for their advice along the way. I would also like to thank the entire administrative team and the animal facility staff for their help during my PhD.

I wish to thank the Preventative Health Flagship at the Commonwealth Scientific and Industrial Research Organisation (CSIRO) for the productive collaboration and generous scholarship. I would especially like to acknowledge Prof. Peter Hudson, Dr. Jose Varghese, Dr. Victor Streltsov and Dr. Julie Nigro.

Thank you to Dr. Ivan Greguric and Ms. Naomi Wyatt at the Australian Nuclear Science and Technology Organisation (ANSTO) for your hard work and persistence in the synthesis of radiolabeled CQ, despite all the obstacles. Although the experimental results using ^{125}I-CQ were not included in this thesis, I appreciate the time and effort you have dedicated to this project.

I would like to thank few members of the Oxidation Biology laboratory for all the coffees, drinks and comic relief during my PhD: Dr. Chris Lim, Dr. Simon James, Dr. Adam Gunn, Dr. Elysia Robb, Dr. Andrew Tsatsanis and Ms. Mikhalina Cortes. I wish to single out Ms. Irene Volitakis, to whom I owe my deepest appreciation for working tirelessly to analyse my samples in the quickest and most accurate way possible.

I would like to express my immense gratitude to my colleagues at Bio21 Institute, Dr. Lin Hung and Ms. Keyla Perez, for your friendship, inspiration and for making this journey all the more bearable.

I wish to convey my appreciation to my former colleagues and classmates for taking interest in my studies and encouraging me to complete them: Dr. Steven Petratos, Dr. Michael Azari, Dr. Jennifer Cottee, Ms. Karen Frontanilla and Ms. Soniya Suvase.

I am grateful to my friends, near and far, for their patience and understanding through all my trials and tribulations over the last few years: the Richwol family, Schwartz family, Rosenblum and Rozen families, Krycer family, Miri Senecky, Simone and David Spark, Boyd Strauss, Gisella Wilcox and Galina Hitchen, Yehuda and Orly Kaplan, Tammy Freadman, Hilit Adler, Jasmine Bar-Gad, Len Addabo and Sanjay Sharma.

My biggest thanks and appreciation by far go out to my parents, Jacob and Mira, sister Chen and extended family! Despite being so far away for so many years, you have been by my side every step of the way and shared all of my highs and lows. You listened to me, reassured me, given me (endless) advice and pushed me to do my best. I could not have done this without you.

Finally, to my men - Kobi and Oz, who have given me a much needed boost of confidence and energy, love and support that made it possible for me to cross the line and finish this race.

I wish to dedicate this thesis to my beloved grandparents Kehat, Devora, Isaac and Rachel blessed be their memory, and to my colleague and friend Dr. Alan Rembach, who cared so deeply about my thesis but regrettably passed away suddenly before it was complete.

Publications

- **Biran Y**, Masters CL, Barnham KJ, Bush AI, Adlard PA (2009). Pharmacotherapeutic targets in Alzheimer's disease. *Journal of Cellular and Molecular Medicine*, 13(1):61-86.
- James SA, Opazo C, **Biran Y**, Lim CM, Ciccotosto GD, Altissimo M, Paterson D, Vogt S, Lai B, McLean C, Masters CL, Cappai R, Cherny RA and Bush AI. Protease-Resistant Ubiquitin Aggregates as an Index of Intraneuronal Cu^{2+} Release in Neurodegenerative Disease. *Submitted, but not yet published*

Table of Contents

List of Figures

List of Tables

Abbreviations

α2M	Alpha 2-macroglobulin
2DE	Two-dimensional gel electrophoresis
3-MA	3-methyladenine
6-OHDA	6-hydroxydopamine
8-BQ	8-(1*H*-benzoimidazol-2-yl)-quinoline
8-HQ	8-hydroxyquinoline
AAS	Atomic absorption spectrometry
ACE	Angiotensin-converting enzyme
AChE	Acetylcholinesterase
AChEI	Acetylcholinesterase inhibitor
AChR	Acetylcholine receptor
AD	Alzheimer's disease
ADAS-Cog	Alzheimer's Disease Assessment Scale-Cognitive section
ADDL	Amyloid-beta (Aβ) derived diffusible ligands
ADEAR	Alzheimer's Disease Education and Referral
ADGC	Alzheimer's Disease Genetics Consortium
ADGI	Alzheimer's Disease Genetics Initiative
ADME	Absorption, distribution, metabolism and excretion
ADNI	Alzheimer's Disease Neuroimaging Initiative
ADR	Adverse drug reaction
ADRDA	Alzheimer's Disease and Related Disorders Association
ADSP	Alzheimer's Disease Sequencing Project
AEC	Animal Ethics Committee
AIBL	Australian Imaging, Biomarker and Lifestyle Flagship Study of Ageing
AICD	Amyloid precursor protein (APP) intracellular domain
AIT	Amyloid Imaging Taskforce
ALS	Amyotrophic lateral sclerosis
ANOVA	Analysis of variance
ANSTO	Australian Nuclear Science and Technology Organisation
AP	Amyloid plaque
API	Alzheimer's Prevention Initiative
APLP	Amyloid precursor-like protein

ApoE	Apolipoprotein E
ApoJ	Apolipoprotein J
APP	Amyloid precursor protein
ATCC	American Type Culture Collection
ATP	Adenosine triphosphatase
ATSM	Diacetyl*bis*(N^4-methylthiosemicarbazone)
AV	Autophagic vacuole
Aβ	Amyloid beta
BACE	Beta-site APP cleaving enzyme
BBB	Blood brain barrier
BC	Bathocuproine
BCA	Bicinchoninic acid
BDNF	Brain-derived neurotrophic factor
BIMC	Blessed Information, Memory and Concentration
BSA	Bovine serum albumin
BTSC	*Bis*thiosemicarbazone
BuChE	Butyrylcholinesterase
BuChEI	Butyrylcholinesterase inhibitor
C. elegans	*Caenorhabditis elegans*
CAA	Cerebral amyloid angiopathy
CCK	Cell Counting Kit
CD	Circular dichroism
cDNA	Complimentary deoxyribonucleic acid (DNA)
CHO	Chinese hamster ovary
CNS	Central nervous system
CoQ	Coenzyme Q
Cp	Ceruloplasmin
CQ	Clioquinol
CSF	Cerebrospinal fluid
CSIRO	Commonwealth Scientific and Industrial Research Organisation
CTF	C-terminal fragment
CTR	Copper transporter
Cu	Copper
CuBD	Copper binding domain

CuDDL	Copper-derived diffusible ligand
D.I.V	Day *in vitro*
DBH	Dopamine-beta-hydroxylase
DFO	Desferrioxamine
DHA	Docosahexaenoic acid
DIAN	Dominantly Inherited Alzheimer Network
DLB	Diffuse Lewy body
DMD	Disease-modifying drug
DMEM	Dulbecco's Modified Eagle's Medium
DMSO	Dimethyl sulfoxide
DMT	Divalent metal transporter
DNA	Deoxyribonucleic acid
DPBS	Dulbecco's phosphate-buffered saline (PBS)
DSM	Diagnostic and Statistical Manual of Mental Disorders
ECE	Endothelin-converting enzyme
EDTA	Ethylenediaminetetraacetic acid
EGCG	Epigallocatechin gallate
ELISA	Enzyme-Linked Immunosorbent Assay
EMA	European Medicines Agency
EMEM	Eagles' minimal essential medium
EPR	Electron paramagnetic resonance
ER	Endoplasmic reticulum
ESI-MS	Electrospray-ionization mass spectrometry
EXAFS	Extended X-ray absorption fine structure
FAD	Familial Alzheimer's disease
FCS	Foetal calf serum
FDA	Food and Drug Administration
Fe	Iron
FTD	Frontotemporal dementia
GC-MS	Gas chromatography mass spectroscopy
GDNF	Glial-derived neurotrophic factor
GLC	Gas-liquid chromatography
GLP	Good laboratory practice
GMP	Good manufacturing practice

GPCR	G-protein coupled receptor
GSH	Glutathione
GSK	Glycogen synthase kinase
GTSM	Glyoxal*bis*(N^4-methylthiosemicarbazone)
GWAS	Genome-wide association studies
HBSS	Hank's Balanced Salt Solution
HD	Huntington disease
HFI	Howard Florey Institute
HHC	Hereditary hemochromatosis
HO	Heme oxygenase
HPLC	High-performance liquid chromatography
ICPMS	Inductively-coupled plasma mass spectrometry
IDE	Insulin degrading enzyme
Ig	Immunoglobulin
IGAP	International Genomics of Alzheimer's Project
IMAC	Immobilised metal-ion affinity chromatography
IND	Investigational new drug
IPG	Immobilized pH gradient
IRE	Iron-responsive element
IRE-BP	Iron-responsive element-binding protein
IRP	Iron regulatory protein
IV	Intravenous
IVIg	Intravenous immunoglobulin
JNK	c-Jun N-terminal kinase
KO	Knock out
LA-ICPMS	Laser-ablation inductively-coupled plasma mass spectrometry (ICPMS)
LDH	Lactate dehydrogenase
LDLR	Low-density lipoprotein receptor
LF	Lactoferrin
LOAD	Late-onset Alzheimer's disease
LRP	Low-density lipoprotein receptor (LDL) related protein
Ltd.	Limited
LTP	Long-term potentiation
LXR	Liver X receptor

MAO	Monoamine oxidase
MAPK	Mitogen-activated protein kinase
MCI	Mild cognitive impairment
MDH	Malondialdehyde
MEA	Multi-electrode array
MHRI	Mental Health Research Institute
MMP	Matrix metalloproteinase
MMSE	Mini-Mental State Examination
MOA	Mechanism of action
MPAC	Metal-protein attenuating compound
mRNA	Messanger ribonucleic acid (RNA)
MS	Multiple sclerosis
MT	Metallothionein
MTF	Metal regulatory factor
MWM	Morris Water Maze
MβCD	Methyl-beta-cyclodextrin
NADH	Nicotinamide adenine dinucleotide
NBIA	Neurodegenerative disorders with brain iron accumulation
NBT	Neuropsychological test battery
NCD	Neurocognitive disorder
NCE	New chemical entity
NCRAD	National Cell Repository for Alzheimer's Disease
NDA	New drug application
NEP	Neprilysin
NF	Neurofilament
NFT	Neurofibrillary tangles
NF-κB	Nuclear factor-kappa B
NHMRC	National Health and Medical Research Council
NIA	National Institute on Aging
NIAGADS	National Institute on Aging (NIA) Genetics of Alzheimer's Disease Data Storage Site
NINCDS	National Institute of Neurological and Communicative Disorders and Stroke
NMDA	N-methyl-D-aspartate
NMDAR	N-methyl-D-aspartate receptor
NMR	Nuclear magnetic resonance

NPC	Neiman-Pick’s disease
NSAID	Non-steroidal anti-inflammatory drug
NTA	Nitrilotriacetic acid
OGTR	Office of Gene Technology Regulator
PAGE	Polyacrylamide gel electrophoresis
PBS	Phosphate-buffered saline
PBS-T	Phosphate-buffered saline-Tween 20
PC2	Physical Containment Level 2
PD	Parkinson’s disease
PDTC	Pyrolidium dithiocarbamate
PET	Positron emission tomography
P-gp	P-glycoprotein
PHF	Paired helical filament
PI3K	Phosphatidylinositol 3-kinase
PK	Pharmacokinetics
PKC	Protein kinase C
PP2	Protein phosphatase 2
PPARγ	Peroxisome proliferator-activated receptor-gamma
PrP	Prion protein
PS	Presenilin
PSP	Progressive Supranuclear Palsy
QC	Glutaminyl cyclase
R&D	Research and development
RAGE	Receptor for advanced glycation end products
RNA	Ribonucleic acid
RNS	Reactive nitrogen species
ROS	Reactive oxygen species
RPMI	Roswell Park Memorial Institute
S.E.M	Standard error of the means
SAE	Severe adverse event
sAPP	Soluble amyloid precursor protein (APP)
SBTI	Soybean trypsin inhibitor
SDS	Sodium dodecyl sulphate
siRNA	Small interfering ribonucleic acid (RNA)

SMON	Sub-acute myelo-optico-neuropathy
SNMMI	Society of Nuclear Medicine and Molecular Imaging
SNP	Single nucleotide polymorphism
SOD	Superoxide dismutase
SSV	Standard suspension vehicle
TAI	Tau aggregation inhibitor
TB	Tuberculosis
Tf	Transferrin
TfR	Transferrin receptor
Tg	Transgenic
TGA	Transient global amnesia
TGN	Trans-Golgi network
TH	Tyrosine hydroxylase
ThT	Thioflavin T
TMAH	Tetramethylammonium hydroxide
TREM	Triggering receptor expressed on myeloid
UK	United Kingdom
UPS	Ubiquitin–proteasome system
USA	United States of America
UTR	Untranslated region
UV	Ultra violet
WT	Wild type
XFM	X-ray fluorescent microscopy
Zn	Zinc
ZnT	Zinc transporter

Chapter 1

Introduction

Chapter 1

LEAR:
"Pray, do not mock me:
I am a very foolish fond old
man,
Four score and upward, not
an hour more nor less;
And, to deal plainly,
I fear I am not in my perfect
mind.
Methinks I should know you,
and know this man;
Yes I am doubtful: for I am
mainly ignorant
What place this is; and all the
skill I have
Remembers not these
garments; nor I know not
Where I did lodge last night.
Do not laugh at me;
For, as I am a man, I think
this lady
To be my child Cordelia."

CORDELIA:
"And so I am, I am."

"King Lear" Act 4, Scene 7:60-70 by William Shakespeare

1.1 Overview of Alzheimer's disease (AD)

For millennia, senile dementia had been viewed in the arts (see former page) and in science as an intrinsic feature of ageing (1, 2). It was not until the turn of the 20th century, the German psychiatrist and neuropathologist Dr Alois Alzheimer correlated the clinical signs of demented patients Auguste Deter and Johann Feigl with abnormal bodies and fibrils in their brain tissue post-mortem (3, 4). Today, AD is the most prevalent form of dementia accounting for 60-80 % of all dementia cases. AD is also ranked the third leading cause of death in Australia (5) and sixth in the United States of America (USA) (6).

Over 0.5 % of the world's population (nearly 50 million people) is now living with AD and other dementias (7). Among them, at least quarter of a million Australians (8) and approximately 5.5 million Americans (6). According to the latest incident reports, there are 9.9 million new AD patients per annum globally (7), including 454,000 in the USA and 78,000 in Australia (9). With the rapidly growing elderly population in general and the "baby-boomer" generation in particular, it is projected that by 2050, unless an effective remedy can be employed, the prevalence and incidence figures of AD will at least double; if not triple (6, 7, 10).

Perhaps even more alarming are predictions that the costs of caring for people with AD and other dementias are likely to rise at an even faster rate than their prevalence. The total (direct and indirect) worldwide cost of dementia will surpass US$1 trillion in 2018, and is estimated to double by 2030 (7). Considering these costs are already taking an enormous toll on the global economy, and are only set to soar over the next few decades, it is believed that AD will pose as the most significant health epidemic and greatest socioeconomic challenge of the 21st century.

AD associations around the world are promoting legislation, policies and strategies, and working to raise awareness and educate about dementia, outreach programs and community support, to train additional professionals and carers, and to invest in dementia-dedicated care facilities. In this regard, Australia has set the standard when in 2004 it was the first country to make dementia a national priority. In parallel to advocacy, there is also increasing demand to invest more funds in AD research as there is a consensus that advancing our knowledge and understanding of the disease risk factors, causes and underlying mechanisms will form the basis for developing preventative and/or therapeutic approaches for AD in the quest to eradicate the disease.

1.1.1 Aetiology of AD

Despite age being the greatest risk factor for AD, such that prevalence doubles with every five-year increment over the age of 65, Alzheimer's is a disease and is not part of natural ageing. Age of disease onset is used to distinguish between the two sub-types of AD. Persons over 65 years of age are considered as sporadic or late-onset AD, while those aged 65 years or under are classified as early-onset AD. In the USA and Australia, respectively, there are currently 5.3 million and 200,000 people living with late-onset AD, as well as 200,000 and 24,000 individuals living with early-onset AD (6, 11).

Early-onset AD accounts for only 5-10 % of all AD cases and includes the rare form of familial AD (FAD). FAD is caused due to the autosomal dominant inheritance of mutations in the genes encoding for amyloid precursor protein (APP) presenilin1 (PS1) and presenilin2 (PS2) (*APP* on chromosome 21, *PSEN1* on chromosome 14 and *PSEN2* on chromosome 1, respectively) (12). To date, a single deletion mutation (13) and 35 missense mutations in the *APP* gene are known to predispose to FAD (14-16). FAD is also attributed to the number of *APP* gene copies in a person's genome. People with Down's syndrome, who have a chromosome 21 trisomy and carry an additional copy of the *APP* gene, exhibit progressive cognitive and behavioural deficits and in their final stages of life have fully expressed AD (17). 193 FAD mutations in *PSEN1* and 20 in *PSEN2* have also been identified (14-16). FAD-linked mutations in *PSEN1* are likely to cause the most aggressive form of AD and/or earliest onset of the disease, with reports of patients as young as 30 years of age (18). Carriers of FAD-related *PSEN2* gene mutations demonstrate a more variable age of onset and AD phenotype (19).

While exact figures are unavailable, it is estimated that FAD accounts for less than 1% of all AD cases worldwide, with descendants of FAD-mutation carriers having a 50% chance of developing FAD themselves. The largest known cluster of families carrying FAD-associated gene mutations resides in Antioquia, Colombia. To study this cluster and others, the National Institute on Aging (NIA) has instigated the Dominantly Inherited Alzheimer Network (DIAN) and the Alzheimer's Prevention Initiative (API), which will hopefully provide researchers with vital clues as to the genetic origin of familial and non-familial early-onset AD, and perhaps even late-onset AD (LOAD). Understanding the potential risk factors and the preventative measures that can be applied in order to delay, stop or even prevent LOAD is of great importance as studies show that impeding the onset of sporadic AD by 5 years will halve not only the number of AD cases, but also the associated health care costs (20-23).

Gender, race and ethnicity, socioeconomic status, education and intellectual stimulation, social interaction, physical activity, diet, hormone and vitamin levels, underlying health conditions (cardiovascular disease, type II diabetes mellitus, cancer, obesity, inflammation, depression and head injury), anaesthesia, smoking, as well as intake of alcohol, drugs and toxins are some of the lifestyle and environmental factors suggested to be associated with susceptibility to and/or prevention of LOAD, yet none of which have been proven (24).

As for genetic contributors to sporadic AD, the apolipoprotein E (ApoE) gene (*APOE*) is the strongest confirmed risk factor for LOAD. *APOE* is a polymorphic gene mapped to chromosome 19 that encodes the 299 amino-acid long ApoE protein (25, 26), which is vital for the transport, distribution and metabolism of lipids in the periphery and central nervous system (CNS) (27, 28). ApoE plays a role in dendrite and spine growth (29) and is also associated with numerous acute and chronic neurological disorders and/or diseases, including AD (30).

Pivotal studies have found the predisposition to sporadic AD, age of disease onset, degree of amyloid burden and rate of cognitive decline with disease progression are dependent on the variant and number of copies of the ApoE epsilon (ε) alleles. Two copies of the ApoE-ε3 allele confer a normal risk for AD, while the presence of one or both copies of the ApoE-ε2 allele is indicative of either a neutral or reduced risk for developing AD (31, 32). Conversely, homozygous and heterozygous ApoE-ε4 allele carriers have a 10-30 fold increase risk of developing AD, disease onset is 10-20 years earlier and they display higher amyloid burden compared to non-carriers (33-35).

The mechanism by which ApoE polymorphism serves as a risk factor for LOAD is still unresolved. In the early 1990s, isoform-specific differences in the binding of ApoE to amyloid beta (Aβ) (36, 37) and tau (38) were stipulated. More recent studies revealed that, despite minimal interaction (39), ApoE affects the structure and clearance of Aβ in the brain and cerebrospinal fluid (CSF) (40); possibly by isoform-specific variations in the half-life of ApoE (41) or competition by ApoE for receptor-mediated Aβ uptake and subsequent degradation in astrocytes (39).

These days, ApoE genotyping is used not only to assist with diagnosis, but also in the enrolment of AD patients into clinical trials and interpretation of trials' results. It is, however, important to recognize that although up to two thirds of AD patients carry at least one copy of the ApoE-ε4 allele; a third of AD patients do not carry this allele at all and some carriers of one or both copies of the ApoE-ε4 allele never develop AD.

Recent large-scale, independent genome-wide association studies (GWAS) and integrated genetic network analysis, have identified novel susceptibility loci and genes, single nucleotide polymorphisms (SNPs) and/or sequence variants with an effect on AD risk, onset and progress (42-53). Rare SNPs were discovered in the *APP* and triggering receptor expressed on myeloid cells 2 (*TREM2*) genes. The former might reduce the likelihood of LOAD by interfering with proteolysis of APP at the β-secretase cleavage site (see **section 1.3**) (54); while the latter may increase the risk for sporadic AD, possibly due to impaired microglia function (55, 56).

Discovery, mapping and characterization of these and other candidate genes have been made possible in recent years, at least in part, due to readily accessible resources, such as the vast number of biological specimens at the National Cell Repository for Alzheimer's Disease (NCRAD) and the large volume of data at the NIA Genetics of Alzheimer's Disease Data Storage Site (NIAGADS). Additional breakthroughs and advances are expected to emerge in the near future from collaborations formed between international AD genetics research teams, such as the Alzheimer's Disease Genetics Initiative (ADGI), Alzheimer's Disease Genetics Consortium (ADGC), Alzheimer's Disease Sequencing Project (ADSP) and the International Genomics of Alzheimer's Project (IGAP), which have set to promote understanding of the disease inheritance, explore epigenetic mechanisms (i.e., interplay between genetic and environmental factors) involved in AD, and ultimately discover new drug targets.

1.1.2 Clinical Symptoms of AD

Regardless of its form, early- or late-onset, AD patients present with similar symptoms as the disease progresses. Whilst the preliminary signs of AD are usually associated with difficulties in remembering names and recent events, new findings allude to certain movement difficulties, changes in gait and balance, sleep disturbances, and/or loss of the sense of smell as symptoms that may precede memory problems.

At the early to mild stages of the disease, AD patients exhibit a gradual loss of cognitive functions, orientation and speech that are often accompanied by agitation, aggression, apathy and depression. Mild to moderate AD patients experience further cognitive decline, as well as anxiety, confusion, impaired judgment, sensory and motor dysfunction, personality and behavioural changes. Hallucinations, delusions and paranoia are also common. During these advanced stages of the disease, patients need assistance with all daily activities and require full-time formal and informal care.

While AD patients continue to deteriorate, becoming more physically and mentally debilitated until they cease to recognize their family and friends; they themselves become unrecognizable. Gradually losing their ability to talk, think and reason this, inevitably fatal disease, strips patients away from their independence, individual identity and humanity. As difficult as it is for AD patients, it is also important to recognize that caring for a family member who slowly changes and weathers away takes a heavy physical, psychological, social and financial toll on caregivers. At the severe stage of the disease, AD patients become paralysed, vegetative and bed-ridden, which makes them more prone to infections that eventually lead to death (57). In the USA and Australia, 1.4 million and 164,000 patients are classified as mild AD, 1.6 million and 90,000 are considered as moderate AD, and as many as 2 million and 45,000 are diagnosed as having severe AD, respectively (11, 58).

The average life expectancy of AD patients from initial diagnosis, through the different clinical stages, until death is 3-10 years depending on the patient's age at the time of diagnosis (59). However, it is now known that the pathological changes in the brain begin several decades prior to signs and symptoms manifesting (60-70). Therefore, there is an urgent need for developing a range of tools to allow for early detection and reliable diagnosis of the disease. This will enable patients, their families and professionals to put in place a care and support management plan, provide them access to drug and non-drug interventions, allow them the opportunity to enrol into clinical trials, as well as lead to substantial lower medical and healthcare costs (71).

1.1.3 Diagnosis of AD

The aforementioned clinical symptoms, which form the basis for an AD diagnosis, are also common to other types of dementia and/or neurological disorders. Even today, expert clinicians can only diagnose a person with "possible AD" (dementia that could be due to another condition) or "probable AD" (no other cause of dementia can be found), and they can do so with only 80-90% accuracy. The only existing method allowing "definite AD" diagnosis is by means of brain autopsy, wherein gross atrophy is observed, followed by a microscopic histopathological examination that reveals gliosis, neuronal and synaptic loss, as well as the hallmark pathological lesions of the disease – amyloid plaques (APs) and neurofibrillary tangles (NFTs). Since this can only be achieved post mortem, there is a great need for safe and reliable diagnostic tools that could be applied to living people as earlier in the disease pathogenesis as possible.

At present, clinical diagnosis of AD is done by way of exclusion of any underlying conditions, such as fatigue, stress, depression, vitamin deficiency, thyroid hormone imbalance and/or other types of dementia. AD diagnosis relies on a comprehensive health and wellbeing evaluation including the patient's medical history, physical and neurological exams and an array of mental status tests, such as the Mini-Mental State Examination (MMSE) (72) and the Alzheimer's Disease Assessment Scale-Cognitive section (ADAS-Cog) (73). The combined results of the various assessments listed above are required to demonstrate impairment in memory, language, attention, orientation, perceptual skills, problem solving and executive function, as well as constructive, motor and social abilities of sufficient severity to compromise daily independent function in order to satisfy a diagnosis of AD (74, 75).

However, this criteria were originally set by the National Institute of Neurological and Communicative Disorders and Stroke-Alzheimer's Disease and Related Disorders Association (NINCDS-ADRDA) workgroup (74), and later reiterated by the American Psychiatric Association in the Diagnostic and Statistical Manual of Mental Disorders Fourth Edition Text Revision (DSM-IV-TR) (75), more than 25 years ago. The existing standards for diagnosis of AD are not only outdated, but also restrict its use for research, clinical and drug development purposes. Therefore, the scientific community has set to revise and update the AD diagnostic criteria so that it will redefine the distinct clinical stages of the disease, integrate the latest research discoveries, and incorporate new cognitive tests to assist in risk prediction, early detection and/or evaluation of disease progression (76, 77). To this end, the International Working Group for New Research Criteria for Diagnosis of AD has been commissioned to formally classify the unique features of prodormal AD (78), mild cognitive impairment (MCI) (79) and Alzheimer's dementia (80); termed mild or major neurocognitive disorder (NCD) in DSM-5 (81).

Development and validation is underway of new and improved cognitive tests that are still simple, brief and inexpensive; yet, more sensitive in detecting the earliest stages of the disease and more accurate in discerning between those, normal ageing or diseases other than AD. The new guidelines for AD diagnosis (82) are also set to encompass clinically-relevant, specific and quantitative blood- and/or CSF-based (83), as well as neuroimaging (84), parameters. These biomarkers could serve as prognostic, diagnostic and/or theragnostic tools to predict the likelihood to develop and/or convert from one disease stage to another, to detect and/or monitor AD, to select patients for prevention and/or intervention trials, and/or to measure the efficacy of drugs.

Testing is ongoing towards formulating a unique panel of CSF or, better yet, blood-borne proteins, lipids, minerals and other analytes; the levels of which could accurately predict disease onset and/or correlate with the severity of the disease. There are also continuing efforts to validate AD-specific and sensitive structural and functional radiography probes, as well as to standardize protocols for training, performance, interpretation and reporting of neuroimaging scans by healthcare professionals.

The fluorine-18 radiolabeled (^{18}F) florbetapir/amyvid (Avid Radiopharmaceuticals, Philadelphia, PA, USA and Eli Lilly, Indianapolis, IN, USA) (85), flutemetamol/ vizamyl (GE Healthcare, Little Chalfont, Buckinghamshire, United Kingdom (UK)) (86) and florbetaben/neuraceq (Piramal Imaging, Berlin, Germany) have recently gained regulatory approval as the first amyloid positron emission tomography (PET) tracers. In conjunction, the Alzheimer's Association and the Society of Nuclear Medicine and Molecular Imaging (SNMMI) joint Amyloid Imaging Taskforce (AIT) published recommendations for the appropriate clinical use of brain amyloid PET scans to support or corroborate (but not substitute or constitute) the diagnosis of MCI and AD (87, 88).

In future, early AD diagnosis may also permit targeted therapeutic intervention that could carry great personal, emotional, medical, social and financial benefits to patients, caregivers, clinicians and the community at large. In the meantime, the AD field is at a bridging stage where research in being translated from the bench to the clinic.

Alzheimer’s Disease Neuroimaging Initiative (ADNI) and Australian Imaging, Biomarker and Lifestyle Flagship Study of Ageing (AIBL) are prospective longitudinal studies currently being conducted simultaneously in four continents in an effort to improve AD diagnosis and monitoring of disease progression. In these multi-modality cohorts, diet and lifestyle questioners, neuropsychological assessments and neuroimaging scans are being employed, as well as blood and CSF specimens collected for genomics, proteomics, lipidomics and elementomics studies from hundreds of men and women over the age of 60, who are healthy or have either MCI or AD (89, 90).

The main objectives of these studies are to predict which individuals and/or population are more prone to develop AD, to design a simple, minimally-invasive, cost-effective and accessible screening test for early diagnosis of AD, and to establish preventative strategies. In the process, these initiatives are creating global harmonized procedures for gathering and evaluating biological samples and neuroimaging scans. Sharing, comparing and combined analysis of the extensive data will not only increase the power of these studies, but will also broaden their implications.

Preliminary results from both the ADNI and AIBL studies are becoming available and although no definitive conclusions can be drawn as yet, the data is already providing researchers with useful information about tracking the course of the disease. If these initiatives indeed achieve their goals, their results are also expected to aid in the development of effective pharmacological treatments that will prevent, delay, slow down, halt or even reverse the course of the disease.

1.1.4 Pharmacotherapeutics for AD-related Symptoms

AD is the third largest market in the world in terms of cost of treatment, following cardiovascular diseases and cancer (91). The global AD drug market in 2009 was evaluated at US$8 billion; comprising of US$6 billion of approved symptomatic drugs (see **Table 1.1**), a US$439 million segment of medications for AD-related disorders, US$1.2 billion worth of diagnostics and a US$361 million neuroimaging sector (92). In 2012, the world-wide market for AD therapeutic and diagnostic agents reached US$10.2 billion (with the imaging section having the highest growth rate); however, analysts forecast revenues will decline to US$9.5 billion in 2017, due to patent expiry of currently-approved AD pharmaceuticals in the leading markets, and despite anticipated growth in diagnostics and biomarkers sales (93).

To date, the only European Medicines Agency (EMA) and US Food and Drug Administration (FDA)-approved classes of therapeutics for the treatment of AD-related symptoms are acetylcholinesterase inhibitors (AChEIs) and an N-methyl-D-aspartate receptor (NMDAR) antagonist (listed in **Table 1.1** below).

The AChEIs exert their affect by preventing the enzymatic degradation of acetylcholine, resulting in increased concentrations of the neurotransmitter in the synaptic cleft and enhanced cholinergic transmission, which are implicated in the processes of memory, thinking and reasoning (94).

AChEIs currently on the market are donepezil (Aricept®; Eisai, Woodcliff Lake, NJ, USA and Pfizer, New-York, NY, USA), galantamine (Reminyl ER®/Razadyne ER®; Ortho-McNeil-Janssen Pharmaceuticals, Titusville, NJ, USA) and rivastigmine (Exelon® oral formulation and transdermal patch; Novartis, Basel, Switzerland). While galantamine is used for mild to moderate AD, rivastigmine and donepezil are approved for mild through to severe AD. However, since less acetylcholine is being synthesized as the disease progresses, the AChEIs provide certain benefits for a limited time, but eventually become ineffective.

Drug Name	Chemical Structure	Mechanism of Action	Drug Indication	Manufacturer's Recommended Use	Common Adverse Drug Reactions
Galantamine (Razadyne®)	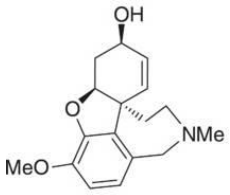	AChEI	Mild to moderate AD	• Tablet*: Initial dose of 8 mg/day (4 mg twice a day); may increase dose to 16 mg/day (8 mg twice a day) and 24 mg/day (12 mg twice a day) at minimum 4-week intervals if well tolerated • Oral solution*: same dosage as above • Extended-release capsule*: same dosage as above, taken once a day	Nausea, vomiting, diarrhoea, weight loss, loss of appetite
Rivastigmine (Exelon®)	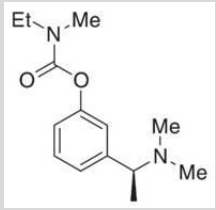	AChEI	Mild to severe AD	• Capsule*: Initial dose of 3 mg/day (1.5 mg twice a day); may increase dose to 6 mg/day (3 mg twice a day), 9 mg (4.5 mg twice a day), and 12 mg/day (6 mg twice a day) at minimum 2-week intervals if well tolerated • Patch: Initial dose of 4.6 mg once a day; may increase to 9.5 and 13.3 mg once a day after at least 4 weeks if well tolerated • Oral solution: same dosage as capsule	Nausea, vomiting, diarrhoea, weight loss, loss of appetite, muscle weakness
Donepezil (Aricept®)	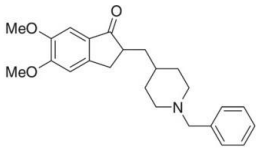	AChEI	Mild to severe AD	• Tablet*: Initial dose of 5 mg once a day; may increase dose to 10 mg/day after 4-6 weeks if well tolerated, then to 23 mg/day (available as brand-name tablet only) after at least 3 months • Orally disintegrating tablet*: same dosage as above	Nausea, vomiting, diarrhoea
Memantine (Namenda®)	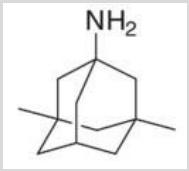	NMDAR antagonist	Moderate to severe AD	• Oral solution: Initial dose of 5 mg once a day; may increase dose to 10 mg/day (5 mg twice a day), 15 mg/day (5 mg and 10 mg as separate doses), and 20 mg/day (10 mg twice a day) at minimum 1-week intervals if well tolerated • Extended-release tablet: Initial dose of 7 mg once a day; may increase dose to 14 mg/day, 21mg/day, and 28 mg/day at minimum 1-week intervals if well tolerated	Dizziness, headache, constipation, confusion

Table 1.1 Current Medications for the Symptomatic Treatment of AD

Modified from the Alzheimer's Disease Education and Referral (ADEAR) Centre's Alzheimer's Disease Medications Fact Sheet (95) and updated
** Also available as a generic drug. Abbreviations: AChEI, acetylcholinesterase inhibitor; NMDAR, N-methyl-D-aspartate receptor*

The non-competitive NMDA-receptor antagonist, memantine (Namenda®; Forest Laboratories, New-York, NJ, USA), protects neurons against glutamate excitotoxicity-mediated cell death (96-98), as well as inhibits tau hyperphosphorylation and aggregation (99). Memantine is prescribed for moderate to severe AD; yet, much like the AChEIs, it only delays symptoms for a brief period and does not address the root cause of the disease. A new approach, using combination therapy of donepezil and memantine, has been reported to have beneficial effects on cognitive performance, activities of daily living and behaviour (100).

In conjunction with the abovementioned medications, various types of psychological interventions as well as antipsychotic, anxiolytic and other drugs are commonly used to help AD patients manage their mood, emotion and behavioural disturbances, performance of daily activities and quality of life. Nevertheless, irrespective of the form of therapy utilised, the current drugs only temporarily alleviate AD-related symptoms and do not inhibit and/or reverse the underlying disease mechanisms (101). Therefore, potent and more selective AChEIs, butyrylcholinesterase inhibitors (BuChEIs), acetylcholine receptor (AChR) agonists, and second-generation NMDAR antagonists are being assessed in pre-clinical and early clinical trials. So far, none of the aforementioned classes of agents has been demonstrated to either arrest or prevent the progression of AD. Trajectories show that even if there were to be a drug, which could slow down AD progression, this will actually result in an increase number of AD patients (58). This stresses the urgent need for disease-modifying drugs (DMD) for AD: small, easily administrated, well-tolerated, bioavailable compounds that cross the blood-brain-barrier (BBB) and have little or no adverse drug reactions (ADRs).

In a bid to diversify the pipeline, numerous compounds are now in various stages of clinical investigation for the treatment of AD (102, 103), including: statins (104-107); non-steroidal anti-inflammatory drugs (NSAIDs) (108, 109); intranasal insulin (110, 111); peroxisome proliferator-activated receptor-gamma (PPARγ) agonists (112, 113); serotonin and histamine receptor modulators; hormonal, stem-cell and nerve growth factor gene therapy (114-117); neurosteroid, neurotrophic and nootropic molecules; and even metabolic drinks and medical foods. There are also copious new chemical entities (NCEs) at the pre-clinical stages of research and development, natural compounds (based on plant, herb and food fractions and/or extracts) and non-pharmacological therapies (psychosocial interventions, trans-cranial electromagnetic treatment or deep brain stimulation) – all of which exceed the scope of this thesis' background.

Most of the pharmacological agents being tested have been designed based upon a notion that has been dominating the AD field for the past two decades - the “amyloid cascade hypothesis” (118-120). This theory, postulated by Hardy and Higgins (118), claims that the metabolism of the Aβ peptide (both generation and clearance) is the main initiator of AD that, together with downstream tau hyperphosphorylation and aggregation, leads to neuronal and synaptic dysfunction and loss, microglial activation and neuronal death (119-121).

Thus, the leading experimental pharmacological approaches target one or both principal cerebral proteins implicated in the causation and/or progression of AD: tau and Aβ. As these pharmacotherapeutic strategies have been extensively covered in a peer-reviewed publication by the author of this thesis (122), which appears in **Appendix A**, they will only be briefly outlined in the introduction to this dissertation. Instead, this chapter will focus on the relevant literature with regards to a growing field of research into the role of metal ions in the pathogenesis of AD and, as a result, the development of pharmaceutics for the treatment of AD that target metals, and which are at different levels of clinical investigations – Phase I, II or III (see **Fig. 1.1**).

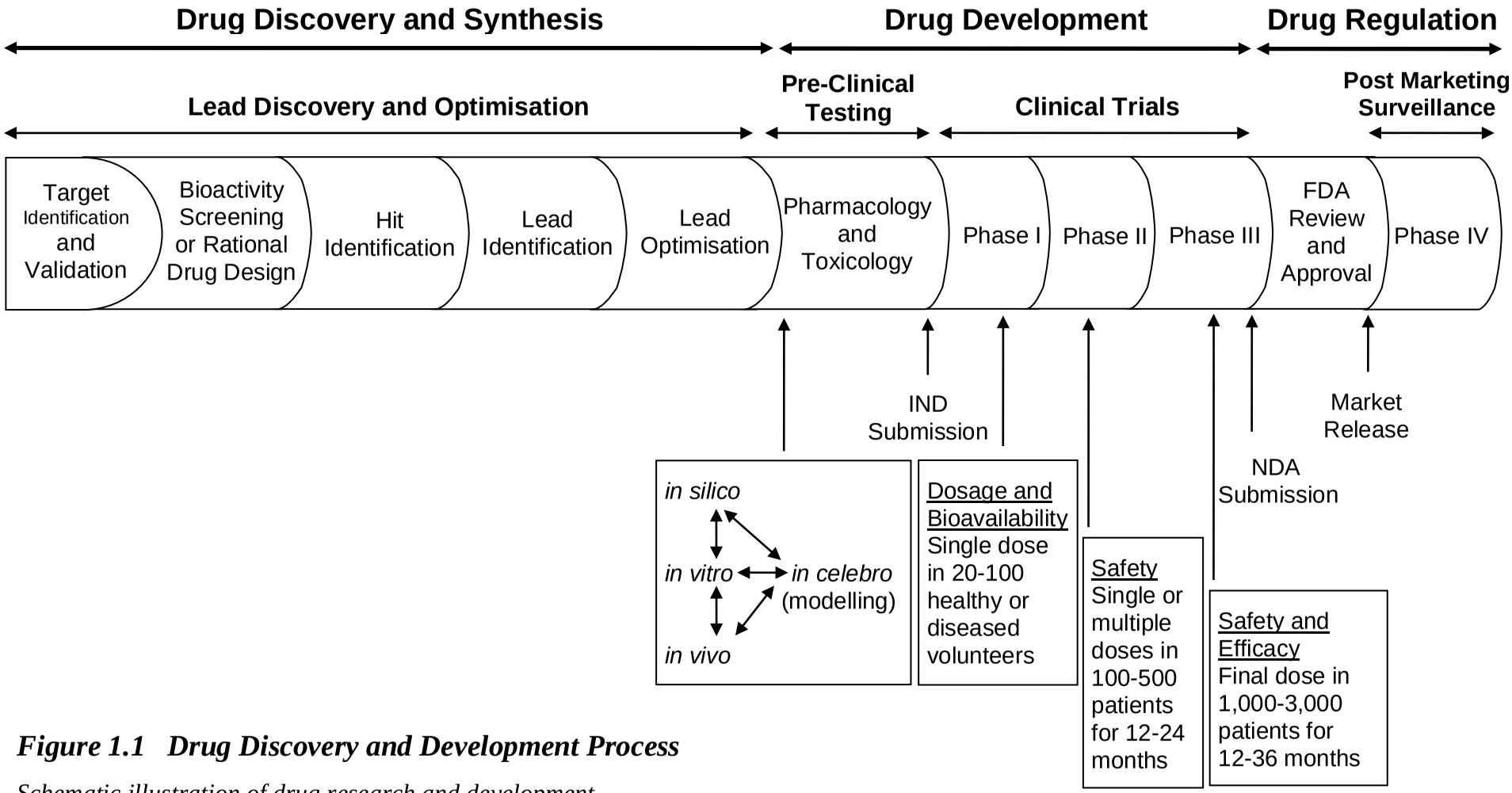

Figure 1.1 Drug Discovery and Development Process

Schematic illustration of drug research and development
Abbreviations: FDA, Food and Drug Administration; IND, investigational new drug; NDA, new drug application

1.2 Tau Neurobiology of AD

The *MAPT* gene on chromosome 17 can be alternatively spliced to produce six different isoforms of the microtubule-associated tau protein (123-125). Native tau is a soluble cytoplasmic protein with a predominantly random coil structure that interacts with tubulin to stabilize microtubules, which preserve the cell's cytoskeletal structure and enable neurogenesis, neuronal migration, axonal transport and neurotransmission (125-127). During the pathogenesis of AD and other tauopathies, tau dissociates from microtubules, misfolds and aggregates into soluble oligomers, immature filaments/pre-tangles and insoluble, intra-neuronal NFTs (128). In AD, NFTs begin to form in the locus coeruleus, then propagate across synapses and along neuronal circuits into the transentorhinal cortex, hippocampus, isocortex, striatum and substantia nigra (129-131).

NFTs are comprised of paired helical filaments (PHFs) that consist of hyperphosphorylated tau with a cross β-sheet conformation (132-134). It has long been hypothesized that NFTs lead to destabilization of microtubules, loss of neuronal cytoskeletal architecture and/or plasticity (135), impaired neuronal transport, dystrophy and ultimately neuronal cell death (136, 137). The latest findings, however, point to tau oligomers being present in human brains at early stages of AD (138), and to neurodegenerative events occurring prior to the appearance of NFTs in brains of transgenic (Tg) mice (139) or without the formation of NFTs all together in *Drosophila melanogaster* flies that express human tau mutants (140). Furthermore, suppression of tau in a transgenic mouse model resulted in restoration of cognitive functions, despite the ongoing accumulation of NFTs (141), thus supporting the notion that tau oligomers and/or pre-filaments are in fact the toxic species (142).

Based on these findings, small molecules that interfere with the formation of tau aggregates, selectively inhibit tau-kinases and/or activate tau-phosphatases, as well as tau-based immunization are being pursued as therapeutic targets (depicted in **Fig. 1.2**) and are now in pre-clinical and clinical stages of testing (refer to **Table 1.2**). Information on the candidate AD pharmacotherapeutics targeting tau that fall under each of the above categories has been reviewed by Biran *et. al.,* (122); herein **Appendix A**.

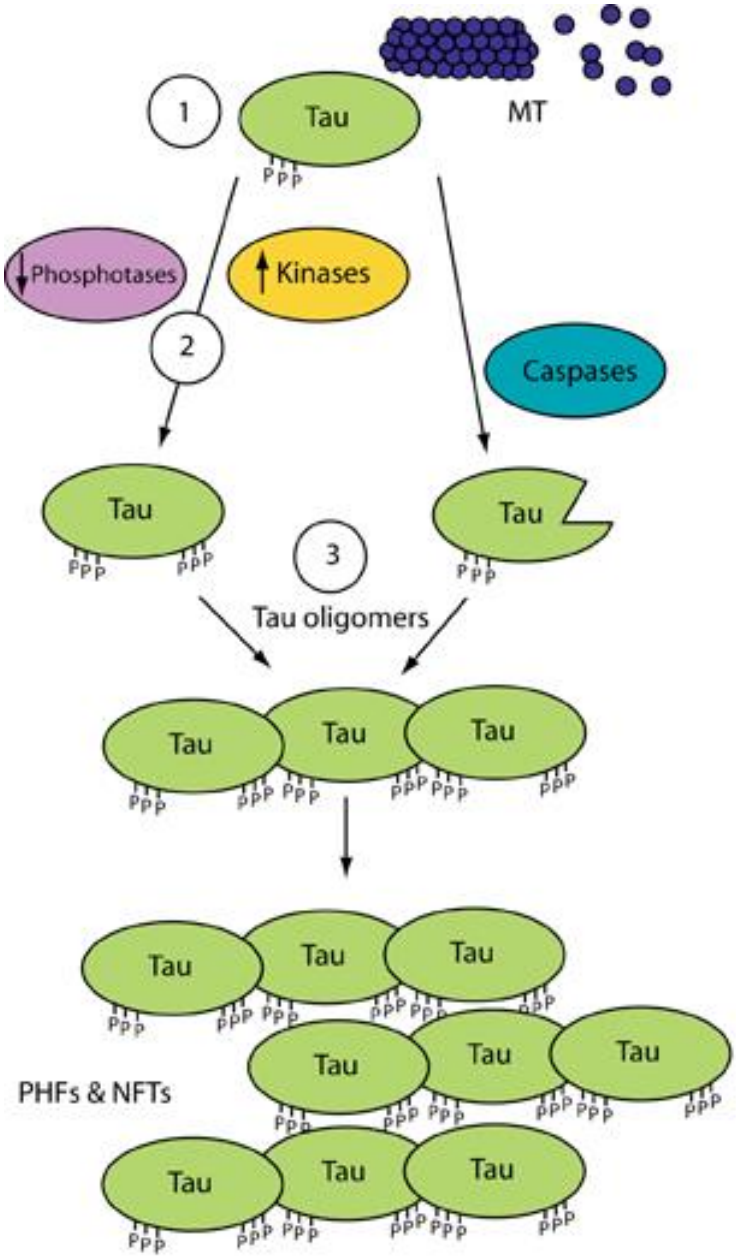

Figure 1.2 Pharmacotherapeutic strategies targeting tau for the treatment of AD

Schematic representation of the anti-tau targets for candidate pharmacotherapies:

1. *Tau-targeted immunotherapy*
2. *Modulators of tau kinases or phosphatases*
3. *Tau aggregation inhibitors (TAIs)*

Abbreviations: MT, microtubule; NFTs, neurofibrillary tangles; P, phosphate group; PHFs, paired helical filaments

Class	Drug Name	Developing Pharma	MOA	Developmental Phase
Modulators of Tau Kinases or Phosphatases	Nypta/ NP-12/ tideglusib	Noscira and Zeltia	Glycogen synthase kinase (GSK)-3 inhibitor	Phase IIb discontinued
Tau Aggregation Inhibitors (TAIs)	TPI 287	Cortice Biosciences	Microtubule stabilizer	Phase I
	BMS-241027	Bristol-Myers Squibb	Microtubule stabilizer	Phase I discontinued
	Davunetide/ AL-108/ NAP	Allon Therapeutics	Microtubule stabilizer	Phase II discontinued
	Rember/ MT/ Trx0014	TauRx Therapeutics	Unclear	Phase II discontinued
	LMTM/ LMT-X/ Trx0237	TauRx Therapeutics	Unclear	Phase III
Tau Active Immunotherapy	ACI-35	AC Immune	$Tau_{393-408}$ [pS396/pS404] liposomes	Phase I
	AADvac-1	Axon Neuroscience	Axon peptide 108 coupled to keyhole limpet hemocyanin (KLH)	Phase II
Tau Passive Immunotherapy	RG7345/ RO6926496	Roche	humanized monoclonal antibody against tau pS422	Phase I discontinued
	RG6100/ RO7105705	AC Immune and Genentech	Anti-tau antibody	Phase I
	C_2N-8E12/ ABBV-8E12	C2N Diagnostics and AbbVie	recombinant humanized anti-tau antibody	Phase II

Table 1.2 Tau-Targeting AD Pharmacotherapeutics in Clinical Trials

1.3 Amyloid Neurobiology of AD

The amyloid precursor protein (APP) is an ancient, evolutionary conserved (143) type I trans-membrane glycoprotein (144-146) that belongs to a family of proteins, including amyloid protein precursor-like protein (APLP) 1 and 2 (147, 148). Both the amino (N) and carboxyl (C) terminals of APP can be divided into several regions, each with its own characteristics and functions (149). The overall function of APP is unclear, however it is believed to be important during the development of the CNS and in response to stress or injury (150). It has been suggested that APP can act as a cell-surface receptor and may be involved in the modulation of processes, such as insulin secretion, cell adhesion, synapse formation, neurite outgrowth, as well as plasticity and memory (151-156).

APP is synthesised in the endoplasmic reticulum (ER), N- and O-glycosylated in the Golgi, and translocated from the trans-Golgi network (TGN) to the cell surface *via* the secretory pathway (157). During and/or post trafficking, APP undergoes degradation by the ubiquitin–proteasome system (UPS) (158) and/or various forms of autophagy (159, 160). Neuronal macroautophagy induction and impaired clearance of several autophagy intermediates is evident in the AD brain, leading to over-production and accumulation of intracellular Aβ in autophagic vacuoles (AVs) (161, 162). APP also undergoes proteolytic processing through either the non-amyloidogenic or the amyloidogenic pathways (163) (illustrated in **Fig. 1.3**).

During the non-amyloidogenic pathway, the membrane-bound enzyme α-secretase cleaves APP within its Aβ domain, resulting in the extracellular secretion of soluble APP alpha (sAPPα) and the production of a short membrane-bound C-terminal fragment (CTF), α-CTF or C83 (164). Subsequent γ-secretase cleavage of C83 results in the secretion of a 3 kDa peptide termed p3 out of the cell (165), and release of the APP intracellular domain (AICD) into the cytoplasm (166).

The amyloidogenic pathway is initiated when β-secretase, identified as β-site APP cleaving enzyme (BACE1, Asp-2 or memapsin-2) (167-170), cleaves APP at the N-terminal part of the Aβ domain. This cleavage leads to the extracellular release of sAPPβ, while the β-CTF or C99 fragment remains membrane bound. Sequential γ-secretase cleavage of C99, at the C-terminal of Aβ, allows the shedding of the AICD and the secretion of Aβ species of variable length, into the lumen or extracellular space (171).

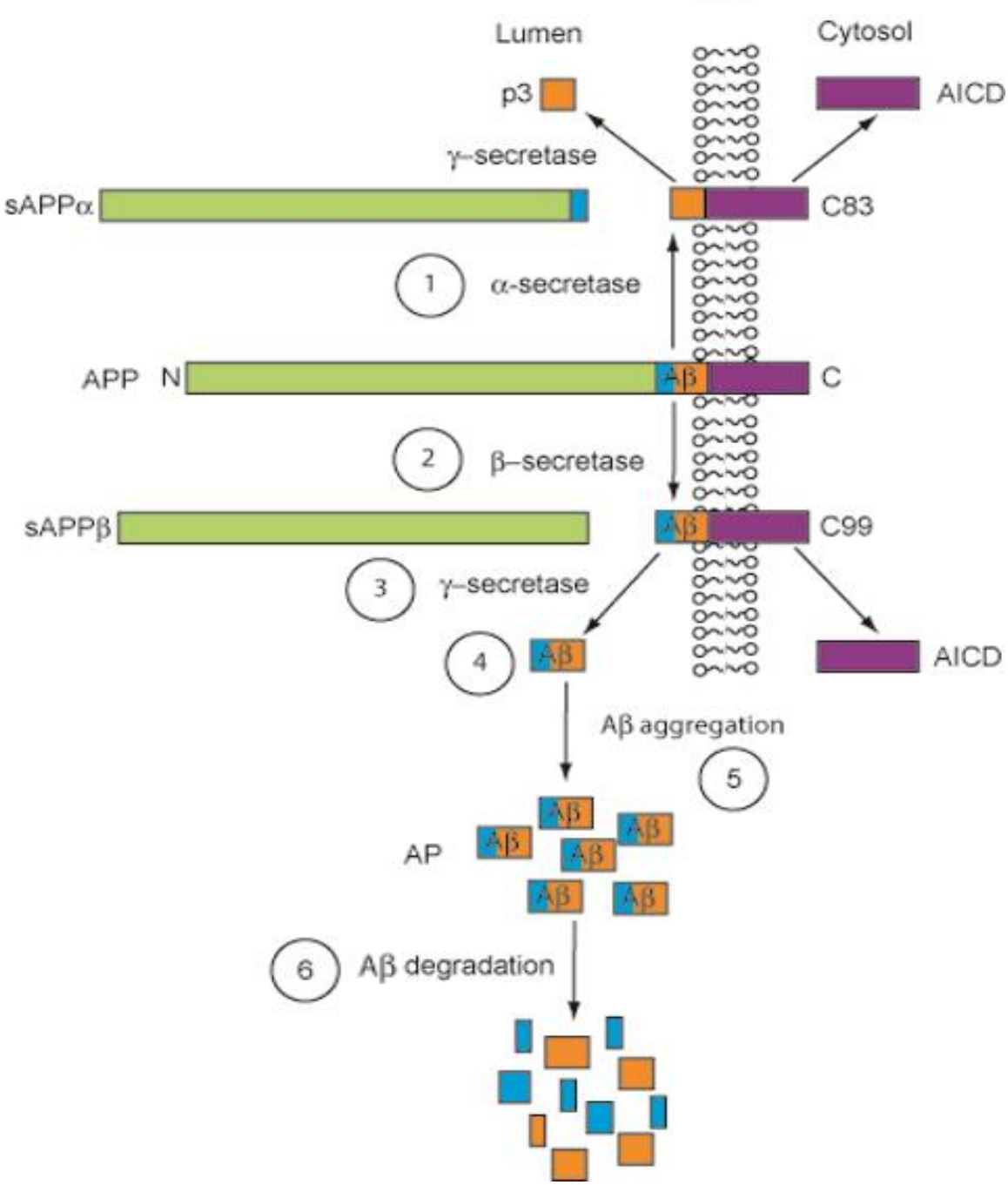

Figure 1.3 Pharmacotherapeutic strategies targeting Aβ for the treatment of AD

Diagrammatic illustration of the anti-amyloidogenic targets for candidate pharmacotherapies:

1. *α-Secretase activators*
2. *β-Secretase modulators/inhibitors*
3. *γ-Secretase modulators/inhibitors*
4. *Aβ-targeted immunotherapy*
5. *Aβ aggregation inhibitors*
6. *Aβ degradation enhancers*

Abbreviations: Aβ, amyloid beta; AICD, APP intracellular domain; APP, amyloid precursor protein; sAPPα, soluble APP alpha; sAPPβ, soluble APP beta

Following their discovery and characterisation, the APP secretases became prime targets in the quest for an AD treatment and/or cure. The rational for modulating the APP secretases is twofold: stimulating α-secretase cleavage in order to direct APP processing towards the non-amyloidogenic pathway or suppressing β- and/or γ-secretase cleavage in order to reduce the amount of Aβ produced. The clinical development of key experimental pharmacotherapeutics for each of these categories is summarized in **Table 1.3** and expanded upon by Biran *et. al.,* (122); attached as **Appendix A**.

Others argue that, rather than focus on Aβ production, a wiser strategy is to target Aβ (itself, its aggregation or its degradation) after it has been synthesized.

Aβ is constitutively synthesized at the membrane surface by proteolytic cleavage and is then secreted (172). Aβ typically ranges between 38 to 43 amino acid residues in length, yet $A\beta_{45}$, $A\beta_{48}$, $A\beta_{49}$ and $A\beta_{50}$ species have also been reported (173). $A\beta_{40}$ and $A\beta_{42}$ are the most prominent types in AD (174), however a new publication claims $A\beta_{43}$ is equally important in AD (175).

Following its secretion, extracellular Aβ can later be internalized back into the cell by poorly understood molecular mechanisms. New evidence suggests that in the absence of ApoE, Aβ is internalized in axons of primary neurons *via* a clathrin-independent endocytic pathway involving lipid rafts (176). Another study established that microglia is responsible for the uptake of Aβ, which is modulated by the lipidation state of ApoE (177). The rapid turnover of Aβ in the brain (178, 179) suggests efficient clearance and/or degradation mechanism(s) of the peptide are in place.

Detection of Aβ in plasma and CSF (180), implies that Aβ can be transported from the CNS across the BBB into the periphery. In this regard, a few receptors (associated with cholesterol and/or lipid metabolism) have been suggested to mediate Aβ efflux from the brain, including P-glycoprotein (P-gp)1 (181), receptor for advanced glycation end products (RAGE) (182), low-density lipoprotein receptor (LDLR) (183) and LDLR-related protein (LRP) (184). Aβ has been shown to bind directly to LRP1 and LRP2/ megalin or indirectly, by binding to their ligands: α2-macroglobulin (α2M), clusterin/ apolipoprotein J and E (ApoJ and ApoE, respectively) (185-187). Aβ-LRP1/2 complexes can be internalised and delivered to the endosomal/lysosomal compartments, where they undergo either autophagy or transcytosis into the CSF or plasma (188, 189). Aβ is finally eliminated through the kidney and liver *via* LRP (190, 191) or liver X receptor (LXR) (192-194).

Alternatively, Aβ can be degraded and cleared by several classes of enzymes (195), including angiotensin-converting enzyme (ACE), the metalloproteases insulin degrading enzyme (IDE) (196-199), neprilysin (NEP) (200-203) and its homologue endothelin-converting enzyme 1 (ECE1) (204, 205), the zinc-dependant matrix metalloproteinases 2 and 9 (MMP2 and MMP9, respectively) (206-208), as well as the recently discovered BACE2 (209). Examples of Aβ-degradation enhancers under investigation for the treatment of AD can be found in **Table 1.3** as well as **Appendix A**.

The fact that Aβ is normally produced in the body throughout life, is present in various organs and bodily fluids, and that the body has evolved sophisticated mechanisms for its metabolism suggest that Aβ may have a physiological role (210). Aβ has been proposed to act as an antimicrobial peptide (211) or as an acute-phase apolipoprotein with metal-binding and antioxidant activities (212-217). Recent work demonstrated Aβ's abilities to mediate synaptic vesicle release (218) and modulate connectivity of olfactory neurons (219). In parallel, an age-related decrease in CSF Aβ was found to be inversely correlated with a rise in cerebral Aβ load in mouse models of AD (220). Assuming Aβ may have a functional role, it had been hypothesized that with ageing, and more so with AD, Aβ either losses its physiological function or gains a pathological one (213, 215).

Researchers have turned to the study of Aβ structure in search of clues as to its neurotoxic and/or synaptotoxic effects (221, 222). It was found that soluble Aβ monomers assume a random coil or α-helix conformation; yet, in AD they undergo a structural change into a pleated β-sheet (223). This induces the peptide to form low molecular weight oligomers, higher molecular weight intermediates (protofibrils and amyloid-β derived diffusible ligands (ADDLs)), mature fibrils and APs in the neuropil and the vasculature (224-227).

It has long been thought that in early stages of AD low-density amyloid deposits appear in the neocortex (frontal, occipital, parietal and temporal lobes, as well as the cingulate cortex). As the disease progresses, amyloid pathology extends towards the medial temporal lobe (hippocampus and amygdala) and the nucleus basalis of Meynert located within the substantia innominata (129). In advance stages of AD, dense APs are widespread throughout the entire neocortex and major part of the hippocampus (129). Brain areas outside the cerebral cortex are affected by AD-related amyloid pathology to a lesser extent (129).

Recent findings challenge Braak and Braak's staging of amyloid deposition. Using cutting-edge neuroimaging techniques, scientists can now visualise amyloid deposits in older people, who are cognitively normal and do not exhibit any clinical signs of AD (63, 228-231). This amyloid burden reaches a plateau early in the disease course, when patients are still classified as prodormal or MCI (232-234). Early detection of amyloid could, in future, allow for early pharmaceutical intervention (refer to **section 1.1.3**).

Kinetic studies have shown that amyloidogenesis and fibrillogenesis can be affected not only by the type of Aβ and its conformation (i.e., secondary structure, flexibility, ampiphilic nature and morphology); but also by factors, such as time, concentration, temperature, pH and metal ions (235). For many years, it was widely believed that the toxic effects of Aβ were a result of the mature Aβ fibrils. However, current data suggest that low molecular weight, soluble, oligomeric forms of Aβ are more neurotoxic and correlate more closely with the disease severity rather than Aβ fibrils or APs (236-247).

In the quest for the definitive synaptotoxic Aβ entity, several research teams found *in vitro* evidence to suggest that the surface of Aβ fibrils actually acts as a secondary nucleation site that catalyzes the conversion of Aβ monomers into toxic oligomers (248-250). This was supported by an *in vivo* study that showed APs surrounded by halos of oligomeric Aβ triggered the collapse of dendritic spines and excitatory synapse loss upon contact (251). It is, therefore, plausible that neurotoxicity is not due to either Aβ oligomers or APs, but rather a consequence of their equilibrium (252-254).

As progress is gained in understanding of Aβ structure and dynamics, and with the advent of more sophisticated analytical techniques, the development of Aβ aggregation inhibitors is also set to improve (refer to **Table 1.3** and to **Appendix A**).

A different approach has been to try to characterize the mechanisms involved in Aβ neurotoxicity as a basis for developing pharmacological agents that modulate these processes. Aβ-associated neurotoxicity may be attributed to assorted factors (255), including Aβ interactions with: membrane surface receptors, intracellular organelles, lipids, protein or lipoproteins (256-260). Activation of inflammatory factors and microglia (261), as well as induction of apoptosis by Aβ-mediated activation of cysteine aspartyl proteases termed caspases (262-264), have also been postulated to be involved. Alternatively, modification of Aβ by enzymes, such as aminopeptidases, isomerases, transglutaminase or glutaminyl cyclase (QC), could account for the peptide's toxicity.

Another proposed mode of Aβ toxicity is the promotion of ion-channel formation and calcium ion (Ca^{2+}) influx (265, 266). This theory gained support from pre-clinical and preliminary clinical trials with different neuronal L-type Ca^{2+} channel blockers (see **Table 1.3**).

A dominant strategy in the field of AD pharmacotherapeutics, which some consider to be a primary test of the "amyloid cascade hypothesis" (see **section 1.1.4**), is based on Aβ vaccination. Tg mouse models of AD immunized actively with Aβ (267-274) or passively with anti-Aβ antibodies (274-290) showed reduced Aβ and tau pathology, neutralized soluble Aβ oligomers, attenuated synaptic degeneration and improved synaptic plasticity; all of which were accompanied by improved learning.

These data prompted many pharmaceutical companies to test both active immunotherapies (using synthetic Aβ peptide) and passive immunotherapies (in the form of intravenous immunoglobulin (IVIg) infusions, as well as humanized monoclonal anti-Aβ antibodies) in humans (examples listed in **Table 1.3**).

The safety and efficacy outcomes of prominent clinical trials of Aβ-based immunotherapies have been thoroughly assessed by Biran *et. al.*, ((122); **Appendix A**) and, therefore, need not be repeated herein. It is only important to note that, whilst few Aβ-targeted immunotherapeutics are still undergoing clinical studies, most have been terminated due to serious adverse events (SAEs) or discontinued as their primary endpoints were not achieved (i.e., the treatment arm showed no difference compared with placebo).

Currently, it appears the much-anticipated breakthrough in the development of AD pharmacotherapeutics has not been fulfilled by Aβ-targeted immunization.

Class	Drug Name	Developing Pharma	MOA	Developmental Phase
Inhibitors and/or Modulators of the Secretases	Begacestat/ GSI-953	Pfizer	γ-secretase inhibitor	Phase I
	Etazolate/ EHT 0202	ExonHit	α-secretase stimulator	Phase II
	Avagacestat/ BMS-708163	Bristol-Myers Squibb	γ-secretase inhibitor	Phase II discontinued
	Verubecestat/ MK-8931	Merck	β-secretase inhibitor	Phase II/III discontinued
	Semagacestat/ LY450139	Eli Lilly	γ-secretase inhibitor	Phase III discontinued
	Flurizan/ tarenflurbil/ MPC-7869	Myriad Genetics	γ-secretase modulator	Phase III discontinued
Aβ Degradation Enhancers	Azeliragon/ PF-04494700/ TTP488	vTv Therapeutics	RAGE inhibitor	Phase III
Aβ Aggregation Inhibitors	MEM 1003	Memory Pharmaceuticals	L-type calcium channel blocker	Phase II discontinued
	Scyllo-inositol/ ELND005/ AZD-103	Elan	Aβ aggregation blocker	Phase II
	Alzhemed/ tramiprosate/ NC-531	Bellus Health	homo-taurine	Phase III discontinued
	Nilvadipine	Roskamp Institute	L-type calcium channel blocker	Phase III
Aβ Active Immunotherapy	V950	Merck	N-terminal Aβ conjugate	Phase I
	MimoVax/ Affitope AD03	Affiris and GSK	$Aβ_{3(pE)–x}$	Phase I
	Betabloc/ AN-1792	Elan and Wyeth	synthetic $Aβ_{1-42}$	Phase II discontinued
	Vanutide cridificar/ ACC-001	Janssen and Pfizer	$Aβ_{1-6}$ conjugate	Phase II discontinued
	Mimotope/ Affitope AD02	Affiris and GSK	$Aβ_{1-6}$ mimetic	Phase II
	CAD-106	Novartis	$Aβ_{1-6}$ coupled to Qβ-virus like particles	Phase II/III
Aβ Passive Immunotherapy	Ponezumab/ PF-04360365	Pfizer	humanized IgG2Δa monoclonal antibody against Aβ's C-terminal	Phase II discontinued
	Crenezumab/ MABT5102A/ RG7412	Roche	humanized IgG4 monoclonal anti-$Aβ_{12-23}$ antibody	Phase III
	Octagam	Octapharma	IVIg	Phase II/III
	Gammagard	Baxter	IVIg	Phase III discontinued
	Bapineuzumab/ ELN115727/ AAB-001	Janssen and Pfizer	humanized IgG1 monoclonal antibody against Aβ's N-terminal	Phase III discontinued
	Solanezumab/ LY2062430	Eli Lilly	humanized IgG1 monoclonal antibody to Aβ‘s mid-region	Phase III discontinued

Table 1.3 Aβ-Targeting AD Pharmacotherapeutics in Clinical Trials

1.4 Metal Neurobiology of AD

1.4.1 Metals and Neurodegenerative Diseases

It is evident that both Aβ and tau are implicated in the onset and/or progression of AD; however, pharmacological strategies directed at these targets have not yet proven to be disease modifying in human studies. In particular, investigational drugs that target Aβ have failed to show any correlation between a reduction in amyloid burden and improvement in cognitive functions in large-scale clinical trials. While such data do not necessarily invalidate the "amyloid hypothesis", there remains considerable debate as to whether it has yet to be properly tested in the clinic.

Numerous factors have been proposed to account for the poor performance of several frontline drugs, including: patient confounds (ApoE genotype, rate of cognitive decline in placebo groups), trial design (single, add-on or combination of drugs tested, treatment as oppose to prevention protocol), drug pharmacodynamic profile (poor BBB penetration and/or bioavailability) and outcome measures (reduction in total amyloid *versus* oligomers as the appropriate indication for a drug's disease modifying effect).

Whilst the debate over the validity of the "amyloid cascade hypothesis" will no doubt continue, it remains likely that there are other critical co-factors partaking in AD pathogenesis. Metal ions are one such possibility, as they have been implicated in the pathogenesis of numerous neurodegenerative diseases (291-293), including AD (293-298) (refer to **Table 1.4**). While the link between toxicological metals, such as lead (Pb), aluminium (Al) and mercury (Hg), and AD remains controversial; the relation between transition biometals copper (Cu), zinc (Zn) and iron (Fe) and AD pathogenesis (as well as other neurodegenerative diseases) is becoming more widely accepted.

Perhaps even more interesting, neurodegeneration and dementia are common pathological and clinical signs in many metal metabolism disorders (299, 300), such as Menkes disease (mutation in the copper-transporting P-type adenosine triphosphatase (ATP)7a leading to systemic Cu deficiency), Wilson's diseases (mutation in the copper-transporting P-type adenosine triphosphatase (ATP)7b resulting in Cu toxicosis), aceruloplasminaemia (absence of the copper-carrier ceruloplasmin and Fe overload), neuroferritinopathy (impaired assembly of the iron-storage ferritin protein and brain Fe accumulation), neurodegenerative disorders with brain iron accumulation (NBIA; genetic mutations causing increased Fe and childhood neurodegeneration) and possibly also in hereditary hemochromatosis (HHC; an Fe accumulation disorder).

Neurodegenerative disease	Proteinaceous deposits	Abnormal protein	Associated metal(s)
Alzheimer's disease (AD)	Extracellular amyloid plaques Intracellular neurofibrillary tangles	Amyloid-β (Aβ) Tau	Cu, Zn, Fe
Amyotrophic lateral sclerosis (ALS)	Intraneuronal hyaline inclusions	Superoxide dismutase-1 (SOD1)	Cu, Zn, Fe
Diffuse Lewy body dementia (DLB)	Lewy bodies	α-synuclein	Cu, Fe (?)
Frontotemporal dementia (FTD)	Intracellular neurofibrillary tangles	Tau	Zn (?)
Huntington disease (HD)	Intranuclear neuronal inclusions	Huntingtin	Cu, Fe
Neiman-Pick's disease (NPC)	Pick bodies	Tau	Fe, Cu
Parkinson's disease (PD)	Lewy bodies	α-synuclein	Cu, Fe
Prion diseases	Extracellular prion plaques	Protease-resistant prion protein (PrP)	Cu, Fe
Progressive Supranuclear Palsy (PSP)	Intracellular neurofibrillary tangles	Tau	Fe, Cu
Spinocerebellar ataxia	Intranuclear neuronal inclusions	Ataxin	Fe, Cu, Zn

Table 1.4 Neurodegenerative diseases - defining pathological proteins and associated metals

Adapted from a review by Skovronsky, Lee and Trojanowski (301)

1.4.2 Metals and Metalloproteins in AD – Biological Samples

Valuable information from human specimens implicates changes in the level, oxidation state and location of metals, metalloproteins and/or metal-binding proteins as being fundamental in the pathogenesis of AD.

1.4.2.1 Blood Metals and Metalloproteins in Ageing and AD

As humans and rats age, their serum and plasma Cu levels increase (302-308), while those of Fe and Zn decrease (307-313). Interestingly, community-based prospective (314) and cross-sectional (315) studies in 3718 Americans and 800 Australians 60 years of age or older, respectively, found neither Cu, Zn or Fe dietary intake were related to cognitive function. In contrast, the prospective Zincage project (853 Europeans aged 60 or older) found an age-independent correlation between plasma Zn and cognitive status (316) and the cross-sectional Rancho Bernardo study (~1500 non-demented elderly) found an association between plasma Zn and the Blessed Information, Memory and Concentration (BIMC) test scores in women, but not men (317).

While Zn deficiency is common in the elderly, studies have shown serum Zn levels to be markedly decreased even further in AD patients *versus* age-matched controls (318-321). AD patients have lower plasma Fe levels (321, 322), yet equivalent serum Fe and transferrin levels (323), to healthy subjects of similar age. AD patients were also recently found to have an increased risk for anaemia (unrelated to deficient dietary Fe intake), while anaemic patients are more likely to develop AD (324, 325).

Although several research teams found serum (320, 326) and plasma (321, 327, 328) Cu levels did not vary between AD patients and age-matched controls; the latest meta-analysis was inconclusive with regards to plasma Cu, and found serum Cu to be significantly elevated in AD patients, compared to healthy individuals (329, 330).
Extensive work by Squitti and colleagues has shown that AD patients, compared to healthy controls, exhibit significantly elevated serum levels of freely circulating Cu (i.e. non-ceruloplasmin bound Cu), which correlate with their lower MMSE scores and may even be predictive of their cognitive decline over time (331-333). Others, however, have reported low plasma Cu levels correlates with higher ADAS-Cog scores in AD patients (334). More recent studies have confirmed a higher percentage of ”loosely bound” Cu and peroxides, in parallel to reduced oxidase activity of ceruloplasmin (Cp), in serum of AD patients compared to healthy controls (323, 335-339).

1.4.2.2 CSF Metals and Metalloproteins in Ageing and AD

Data on changes in CSF levels of metal and metalloprotein during normal ageing is scarce; yet, AD patients have been shown to have similar Fe levels and considerably lower Zn levels in CSF than their age-matched healthy controls (320). As for Cu in CSF, one study found AD patients to have significantly higher levels compared to controls (321); while others found them to be no different (320, 327, 329). Interestingly, CSF levels of Cu, Zn and Fe have been shown to be inversely correlated with $A\beta_{42}$ levels (340).

While levels of ferritin (341) and Cp (342) were shown to be relatively elevated, the ferroxidase activity of Cp and that of Cu/Zn superoxide dismutase (SOD) have been found to be reduced (343), in CSF from AD patients. Importantly, CSF ferritin levels inversely associated with cognitive performance and disease progression (344).

1.4.2.3 Brain Metals and Metalloproteins in Ageing and AD

Information on the level and activity of cerebral metalloproteins during distinct stages in life is limited. AD brains, however, have been shown to have an imbalance in metalloproteins, especially Fe-related ones, in comparison with brains of age-matched healthy individuals. Levels of the Cp enzyme (345), neuroglobin (an Fe heme binding, reactive oxygen and nitrogen species (ROS and RNS, respectively) scavenger) (346), lactoferrin (LF; involved in Fe binding, transport and storage) (347) and the iron-storage protein ferritin are all elevated within brains of AD patients, whilst levels of transferrin (Tf; an Fe-transport protein) and its receptor (TfR) are reduced (348, 349).

The AD brain is also deficient in metal regulatory factor 1 (MTF1) (350), metallothionein III (MT-III; a metalloprotein that is responsible for the regulation of neuronal Zn (351)) (350, 352-354) and Zn transporter 3 (ZnT3; a brain-specific transporter responsible for sequestering Zn into pre-synaptic vesicles (355, 356)) (357). In addition, the activity of complex IV or cytochrome c oxidase, a metalloenzyme in the mitochondrial respiratory chain, has been found to be diminished in AD brains (358).

Metal ions are normally concentrated in specific brain regions, for example Cu levels are high in the neuropil (359), the hippocampus is rich in Zn and Fe is concerted in the substantia nigra and putamen (360, 361). With healthy ageing, regional levels of Cu and Fe in the human brain are increased (361-366), however Zn levels remain the same or are decreased (367). Similar trends were seen in WT mice (368-371), though an age-dependent increase in synaptic Zn was recently reported in non-Tg mice (372).

In brains of AD patients, Zn (359, 373-377) and Cu (345, 359, 376, 377) seem to be elevated in some areas and lower in others. Importantly, the AD brain contains a pool of redox-active, labile Cu (378). While a single meta-analysis implied that bulk cerebral Fe levels are unchanged in AD (379), most reports claim they are increased (374-376, 380, 381) and that hippocampal Fe levels in AD patients correlate with their cognitive function (382). In a Tg-mouse model of AD, elevated brain Fe content was detected at the earliest stage of AP formation and continue to increase with time (383).

Interestingly, these biometals are naturally more concentrated in areas where AD lesions are the most profound, as compared to other areas of the brain. Indeed, Cu and Fe are deposited in cerebral amyloid angiopathy (CAA; the vascular lesion associated with AD) (384), intracellular NFTs have been found to co-localize with zinc ions (Zn^{2+}) (385) and with the iron regulatory protein 2 (IRP2) (386), while ferritin (387-390) and some zinc transporters (ZnTs) (372, 391, 392) have been found to co-localize with APs. Extracellular APs have also been shown to be enriched with Cu (400 μM), Zn (1 mM) and Fe (1 mM) (359, 372, 385, 393-397). Considering neurotransmission results in peak concentrations of ~300 μM Zn^{2+} (398, 399) and up to 100 μM Cu^{2+} (400-402), the synaptic cleft would be the ideal location for Aβ metalation and oligomerization (403).

Taken together, this evidence suggests that there may be an interaction between biometals and the main proteins implicated in AD (i.e. APP, Aβ and tau), and that these factors may influence one another at various levels.

1.4.3 Metals and Metalloproteins in AD – *in vitro*

A variety of cell-free, cell-based and animal studies support the binding and effects of metals on tau, APP and Aβ's localization, metabolism, aggregation and toxicity.

1.4.3.1 Metals and Tau

Ferric (Fe^{3+}) and cupric (Cu^{2+}) ions can bind to various "repeat" motifs on tau, thus altering its conformation, phosphorylation and aggregation states. In the case of iron, this effect can be reversed by reducing Fe^{3+} to Fe^{2+} (ferrous ions) (404) or by chelating Fe altogether (405). Treatment of human tau with low concentrations of Zn^{2+} induced non-fibrillar aggregates, which became fibrillar *via* intermolecular bridging of cysteine residues at positions 291 and 322 upon treatment with TPEN (N,N,N′,N′-tetrakis(2-pyridinylmethyl)-1,2-ethanediamine; a chelator with high affinity to Zn^{2+}) (406).

The addition of Zn^{2+} to mouse and human neuroblastoma cells (N2a and SH-SY5Y, respectively) (407-410), as well as rat brains, hippocampal brain slices and neurons (410, 411) induces tau hyperphosphorylation; whereas the opposite result is seen with the addition of pyrolidium dithiocarbamate (PDTC) (412), clioquinol (CQ) and Ca^{2+}-ethylenediaminetetraacetic acid (EDTA) (410, 411). This hyperphosphorylation of tau is a result of the Zn-induced activation of many tau kinases (407-410) and inactivation of protein phosphatase 2A (PP2A) (410, 411). In addition to tau, Zn^{2+} (and Cu^{2+}) has also been shown to bind to neurofilaments (NFs; another protein component of NFTs) (413) and stimulate their phosphorylation (408).

1.4.3.2 Metals and APP

On a gene level, researchers discovered that the translation of APP messenger ribonucleic acid (mRNA) is governed by the binding of an iron-regulatory element (IRE) to its 5'-untranslated region (5'UTR) such that in an Fe-enriched environment APP translation is up-regulated, whereas it is down-regulated in response to either an Fe (414-417) or a Cu deficient milieu (418). Cu deficiency has been proposed to either enhance APP translation or inhibit its degradation (419), while Cu overload has been shown to up-regulate *APP* expression (420, 421). Interestingly, deletion of the *APP* gene causes an increase in cellular Cu (422).

Posiphen® (QR Pharma, Berwyn, PA, USA) is a small, orally-bioavailable, BBB-permeable positive enantiomer of phenserine (423) that normalized CSF levels of APP, total and phosphorylated tau in 30 MCI patients, comparable to that of healthy controls, in a 10-day Phase I/II trial. It was revealed that Posiphen® achieved these outcomes by enhancing the binding of iron-regulatory protein 1 (IRP1)/iron-responsive element-binding protein (IRE-BP) to the 5'UTR IRE mRNA, thereby repressing the translation of APP (and other proteins) (424). It would be of interest to examine any effects on metal metabolism in the planned Phase II/III trial of Posiphen®.

On a protein level, APP contains putative zinc and copper-binding domains (CuBD) both in its ectodomain (E1 and E2 sections) and in its Aβ sequence (425-428) (see **Fig. 1.4**). Little is known about the Zn-binding site within the E1 domain of APP other that it spans residues 181 to 188 (425). However, it has been established that the E1 CuBD on APP consists of a tyrosine (Tyr^{168}), a methionine (Met^{170}) and two histidine ($His^{147, 151}$) residues that facilitate the coordination of Cu^{2+} and its reduction to Cu^{+} (427).

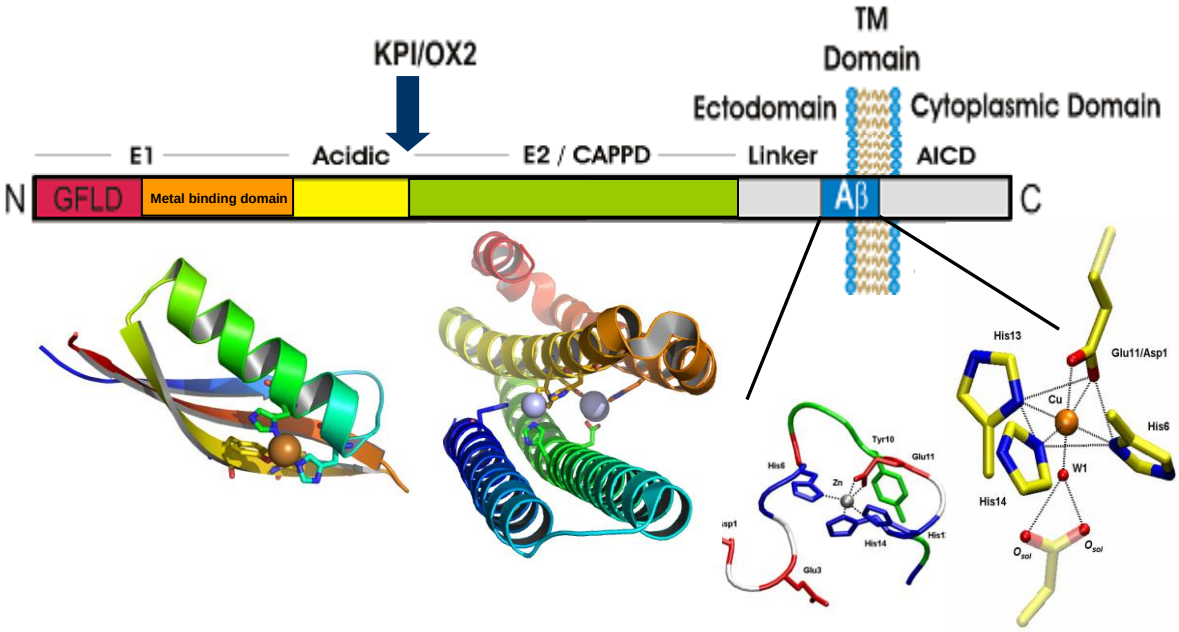

Figure 1.4 Structure of APP_{695} isoform and its metal binding domains

The amyloid precursor protein (APP) is comprised of three parts: the N-terminus ectodomain, the trans-membrane (TM) domain and the C-terminus cytoplasmic domain.

The ectodomain of APP consists of the E1 and acidic domains, sequentially followed by the E2 or central APP domain (CAPPD) and an unstructured linker region.

The E1 domain is sub-divided into a heparin or growth factor-like domain (GFLD) and a metal-binding domain.

The arrow points to the site of the Kunitz-type protease inhibitor (KPI) and OX2 homology domains in the $APP_{751/770}$ isoforms.

The Aβ sequence spans across the ectodomain and part of the TM domain.

The copper and zinc-binding ligands within the E1 (427) and E2 metal-binding domains (428) and within the Aβ sequence (429, 430) are shown.

A competitive high-affinity metal-binding site was newly discovered within the E2 domain of APP, in which Cu^{2+} is coordinated by four histidines ($His^{313, 382, 432, 436}$) in a square planar arrangement and Zn^{2+} is coordinated by three histidines ($His^{382, 432, 436}$) and a water molecule in a tetrahedral geometry (428). In addition, a non-specific, low-affinity Zn^{2+}-binding site, consisting of a glutamate (Glu^{387}), an aspartate (Asp^{429}), a histidine (His^{458}) and a water molecule, was identified in the E2 sequence of APP (428).

It was suggested that the binding of metals to APP selectively regulates the protein's flexibility and conformation, depending on the ions' coordination sphere that, in turn, may alter the function, trafficking and processing of APP (428). Zn binding leads to local stabilization of APP (428), yet permits the amyloidogenic cleavage of APP and increase Aβ deposition (431); whereas, Cu binding restricts the overall flexibility of APP (428), perhaps by causing its homodimerization (432).

The effect of metals on APP and Aβ has been difficult to reconcile, as it seems to differ depending on the cell type. Decreased intracellular Cu levels in WT and APP_{695}-expressing SY5Y and M17 human neuroblastoma cells and in human fibroblasts led to increased Aβ production (419). Elevated Cu levels did not change Aβ levels secreted from SY5Y cells transfected with APP_{695} (419); however, it resulted in trafficking of APP to the cell surface and reduced Aβ synthesis in SY5Y cells transfected with APP_{695} that contains the Swedish mutation (433, 434).

Increased Cu in Chinese hamster ovary (CHO) cells and human fibroblasts shifted APP processing towards the non-amyloidogenic pathway, resulting in increased secretion of full-length and soluble α-cleaved APP ectodomain (sAPPα), and decreased Aβ synthesis (419, 435, 436). This may result from an increase in glycogen synthase kinase (GSK)3β phosphorylation, which activates phosphatidylinositol 3 kinase (PI3K) leading to secretion of matrix metalloproteinases (MMPs) that can degrade Aβ (436).

Other than direct binding, Cu and Zn might also affect APP (and Aβ) indirectly by altering the expression, synthesis and activity of its secretases (421, 437-440). In turn, PSs have been demonstrated to foster a cellular Cu and Zn uptake activity (441, 442).

Whilst the reciprocal relations between APP, Cu and/or Zn have been extensively investigated, research is lacking into that of APP and Fe. One study demonstrated that Fe treatment promotes the amyloidogenic processing of APP (417). Our research team has recently shown that ablation of APP resulted in Fe accumulation and *vice versa*, both *in vitro* and *in vivo* (443). Fe retention was also observed in tau-null cells and mice, and was attributed to decreased APP trafficking to the cell surface (444).

These studies shed light on the potential effect of APP and Fe on one another; although it remains to be determined whether Fe interacts directly with APP through a defined binding site, or whether APP affects Fe *via* certain intermediates, such as ferroportin.

1.4.3.3 Metals and Aβ

As previously described, Aβ also possess metal binding domain(s), however the complicated process of Aβ aggregation makes it is difficult to characterise the binding of metals to Aβ. While there have been numerous reports on the stoichiometry and affinity of Aβ-metal binding, results have varied depending on: the Aβ source (mouse, rat or human), Aβ sequence or length ($Aβ_{x\text{-}16/28/40/42}$), Aβ species (monomers, dimers, trimers, oligomers), as well as the reaction conditions (sample preparation, buffer type and concentration, pH, incubation time and/or technique used) (445). For example, low concentrations of Zn^{2+} can promote a morphological change and rapid aggregation of Aβ at physiological pH (446-452); however, Cu^{2+} (and Fe^{3+}) have been shown to induce Aβ precipitation at mildly acidic pH (453, 454) and, under acidic conditions (pH 6.6), Cu^{2+} has totally displaced Zn^{2+} from Aβ (455).

Most researchers are in agreement that Aβ binds Cu^{2+} and Zn^{2+} in a 1:1 ratio (456-460); however, there have been reports of Zn^{2+} binding to Aβ in a 2:1 (461) or 3:1 ratio (462), and of Cu^{2+} binding to Aβ in a 2:1 ratio, when in excess (463, 464). One study concluded that Fe^{2+} binds to $Aβ_{40}$ in a 1:1 stoichiometry, while binding to $Aβ_{42}$ occurs in a 2:1 ratio (465). There is mounting evidence that the Aβ:metal ion ratio modulates not only Aβ conformation (random coil, α-helix or β-sheet) and aggregation kinetics (466-468), but also the morphology of the Aβ aggregates (amorphous, non-fibrillar or fibrillar) (464, 469-471) and, possibly, its function and/or activity.

Indeed, Zn^{+2} was reported to induce $Aβ_{16}$ binding to deoxyribonucleic acid (DNA) (472). Interestingly, it has been suggested that Fe^{2+} binding to $Aβ_{28}$ at low concentrations serves as an antioxidant protective mechanism, while aggregated Fe^{2+}-$Aβ_{28}$ complexes actively partake in the production of harmful oxygen radicals (473). Others found $Aβ_{16}$ binds strongly to Fe^{3+} and, with lesser affinity, to Fe^{2+} forming a 1:1 complex in the presence of stabilizing nitrilotriacetic acid (NTA) (474).

Similar to their action on Cu^{2+}, $Aβ_{16}$ (474), $Aβ_{40}$ and $Aβ_{42}$ (475) were shown to be redox active in that it can bind Fe^{3+} and reduce it to Fe^{2+} thereby facilitating the generation of ROS.

This oxidative stress may be related to the observed neurotoxicity of Fe^{2+} and Fe^{3+} in the presence of $A\beta_{25-35}$ (476) and $A\beta_{1-42}$ (477). Importantly, several metal chelators (discussed later in **section 1.5.4**) have been shown to solubilise synthetic Aβ aggregates and brain amyloid extracts, as well as inhibit Aβ's redox activity and toxicity (478-481).

There is an ongoing debate as to the binding affinity and kinetics of Aβ to Cu^{2+} and Zn^{2+}, with dissociation constants (K_D) ranging from nM to μM for Cu^{2+}-Aβ (455, 456, 482) and for Zn^{2+}-Aβ (447, 457, 458, 465, 482-484). To resolve these issues, it is imperative that the metal-binding site(s) of Aβ and APP are defined and that the relationship between the structural features of the protein and its function in health and disease can be elucidated.

Contemporary studies (429, 482) utilising circular dichroism (CD), electron paramagnetic resonance (EPR), nuclear magnetic resonance (NMR), Raman spectroscopy, electrospray-ionization mass spectrometry (ESI-MS), X-ray diffraction and extended X-ray absorption fine structure (EXAFS) spectroscopies have determined the coordination of Cu, Zn and Fe by His^6, His^{13}, His^{14} (223, 430, 447, 454-456, 469, 474, 485-494) and a fourth ligand. The fourth donor could be Asp^1 (456, 492, 493), Ala^2 (495) or Tyr^{10} (486, 487) for Cu^{2+}, Tyr^{10} (487, 488) or Glu^{11} (484, 496) for Zn^{2+}, and Asp^1 or Glu^3 for Fe^{2+} (474, 494). Recent work by our group and by others in an attempt to reconcile the different reports as to Aβ's CuBD concluded that it is most likely to be pleomorphic and to exist in two distinct coordination modes (497-500).

1.4.4 Metals and Metalloproteins in AD - *in vivo*

Yeast does not express APP or its homologues and, therefore, present a useful model for investigating the effects of these protein family members on metals. Indeed, sAPP and sAPLP2-expressing yeast have been shown to have significantly reduced Cu levels and bioavailability with no effect on Zn levels (501).

Curiously, mouse and rat's endogenous Aβ contains three amino acid substitutions (R5G, Y10F, H13R), which prevent the formation of intermolecular histidine bridges (223, 466, 487) and, therefore, do not allow metal-induced Aβ aggregation *in vitro* (448, 453) and cerebral Aβ deposits *in vivo* (502, 503). Thus, transgenic rodents provide vital clues as to the effects of APP and Aβ on metal-ions, and *vice versa*.

1.4.4.1 Metals and Metalloproteins in Tg mouse models of AD

Tg2576 mice that over-express the Swedish double mutant human APP_{695} (K670N and M671L) exhibit AD-related behavioural and cognitive changes (memory and spatial learning impairments) (504) and AD-related pathology (substantially elevated cerebral levels of full-length APP, CTFs, Aβ and APs) (505) as they age. APs in these mice are surrounded by dystrophic neurites and reactive astrocytes, which are abundant in Zn and ZnT3; despite an age-dependent decrease in ZnT3 expression and synaptic Zn^{+2} (372). Tg2576 mice also have significantly reduced cerebral Cu (but not Fe) levels (369, 422, 506). C100 mice over-express Aβ and the C-terminal of APP (507), and have markedly lower levels of both Cu and Fe in the brain (369).

While cerebral Cu levels in a triple Tg mouse model of AD (harboring the mutant APP_{Swe}, $PS1_{M146V}$ and tau_{P301L} transgenes (264)) were reportedly no different to WT mice (327); others found total brain Cu and Fe to be elevated in the former (508). APP (and APLP2) knock out (KO) mice (509) also have raised brain Cu and Fe levels (443, 510). Aged tau-KO mice exhibit increased Fe in some brain areas, but not others (444).

It had been postulated that co-existence of endogenous murine Aβ and transgene-derived human Aβ (511, 512) may contribute to the disparity in the type and level of metals in APs observed in various Tg-mouse models, and compared to those of humans (513). Alternatively, in some strains, like Tg2576, the transgene is governed by the hamster prion protein gene promoter, which is known to be modulated by Cu (420, 514), as well as to modulate Cu and other metal ions (515, 516).

Regardless, these studies all suggest that APP and/or Aβ are involved in metal homeostasis; however, the opposite has also been shown to be true.

1.4.4.2 Effect of Cu on AD-related Pathology and Cognition

Using a genetic approach, TgCRND8 mice (expressing the Swedish and Indiana-mutant human APP as well as $PS1_{P264L}$, and have ~15% lower brain Cu levels, compared to non-Tg controls (517)) were crossed with tx^{J} "toxic milk" mice (that have a mutated ATPase7b transporter and a consequent elevation in Cu levels (518)). This led to markedly reduced plaque load and Aβ levels in the resulting progeny (506).

Attempts to increase cerebral Cu levels by means of a Cu-enriched diet have yielded conflicting results. APP23 mice (carrying the Swedish mutation of human APP_{751} and an inherent brain Cu deficiency (519)) given Cu-supplemented drinking water for three months had normalized brain Cu levels and reduced Aβ levels (520).

Conversely, increasing dietary Cu intake in triple Tg mice led to an increase in APP, C99, Aβ as well as tau (521). Both studies used the same concentration of sucrose and Cu in the treated drinking water; yet, they used different strains of Tg mice, at different ages, and the number of mice in both the treated and the control groups were vastly different between the two studies, which could account for the discordance in data.

Others observed no change in plaque burden or learning and memory between WT mice (522, 523), PSAPP mice (Tg2576 crossed with a $PS1_{M164L}$ line (524)) (525) or APP_{Swe}/PS1ΔE9 mice (expressing chimeric APP_{695} with the Swedish double mutation and an exon-9-deleted variant of human PS1 (526)) (527) allowed distilled drinking water to those provided with Cu-containing drinking water. No behavioral differences were observed in aged WT mice provided with either normal or Cu-restricted diet (528).

In line with these findings, studies have demonstrated that nutritional Cu intake and supplementation in healthy adults (314) and those with AD (529, 530), respectively, did not influence cognition. Cognitive scores of patients with mild AD were unaffected by oral intake of Cu^{2+}-orotate-dihydrate (8 mg/day for a year as add-on to donepezil); yet, the decline in CSF $A\beta_{42}$ was stabilized in a prospective, randomized, double-blind, placebo-controlled Phase II clinical trial (529, 530).

Evidence suggests that Cu exacerbates the effect of dietary fats on the translation and expression of AD-related proteins, as well as on cognition (reviewed by Hung *et. al.* (531)). Consumption of a high-cholesterol diet, together with Cu-supplemented drinking water, potentiated the up-regulation of APP, increased Aβ deposition, as well as learning and memory impairments observed in cholesterol-fed WT mice (522, 523).

Sparks and colleagues demonstrated that trace Cu levels in the drinking water of cholesterol-fed rabbits and beagle dogs elicited cognitive deficits and elevated brain Aβ (194, 525, 532) concurrently with reduced cerebral tau levels (533). These results were paralleled in a study showing dietary Cu intake, in conjunction with a high-fat diet, correlated with an accelerated rate of cognitive decline in older individuals (314). Also, a year-long observational study showed that hyper-lipidemic mild to moderate AD patients with high levels of serum Cu were more prone to cognitive impairment (333).

In contrast, our laboratory has reported that a combined high Cu and cholesterol diet resulted in decreased APP expression and Aβ levels, and did not affect the spatial learning and working memory of APP/PS1 mice performance (527). Variations in animal models (genotype and phenotype), treatments (dose and period) and analytical techniques utilized may have attributed to the discrepancy in the above findings.

1.4.4.3 Effect of Zn on AD-related Pathology and Cognition

Like Cu, the effect of Zn modulation on APP and Aβ was also tested in various mammalian cells, yeast strains and animal models, as well as in humans. Using genetic manipulation, ZnT3 KO mice that lack a synaptic Zn pool and exhibit age-dependant cognitive deficits (357) were crossed with Tg2576 mice (Tg2576/ZnT3$^{-/-}$), which caused a significant reduction in plaque formation (534, 535). Reducing Zn levels by dietary means, however, elicited the opposite effect. A Zn-depleted diet led to increased volume of APs in brains of APP/PS1 mice (536).

On the other hand, Zn-supplemented drinking water, with and without cholesterol chow, had no effect on the amyloid burden in rabbits (525) or C100 mice (537). A Zn-enriched diet was recently shown to decease cerebral Cu, Zn and Fe (508), reduce both Aβ and tau pathologies, as well as prevent long-term memory deficits in a 3xTg AD mouse model (538); yet, it led to impaired learning and memory in WT littermates and even more so in multiple Tg mouse models of AD (431, 539). Provision of dietary Zn enhanced APP expression, and increased levels of Aβ and other BACE1 cleavage products in APP/PS1 mice (431). It also reduced hippocampal APs in TgCRND8 and Tg2576 mice (539). Interestingly, parallel dietary supplementation of both Cu and Zn annulled the spatial memory impairment in Tg2576 (540).

The confounding results are likely to stem from the use of different animal models (rabbits *versus* WT and Tg mice) and varied concentration of Zn provided (deficiency, trace amount or high). Nonetheless, findings suggest the effects of Zn on pathological and cognitive aspects in AD may be linked to other factors, such as lipids and/or Cu.

Zn therapy in healthy adults and AD patients has, thus far, yielded inconclusive results (541). In the prospective, randomized, double-blind, placebo-controlled Zenith study, Zn-gluconate supplementation (15 or 30 mg/day for 6 months) was associated with improvement in attention and spatial working memory of 387 healthy adults (542).

In separate trials, oral administration of zinc-sulphate and zinc-aspartate to AD patients had to be discontinued due to gastrointestinal disturbances (543). To avoid the intolerability of its oral formulation, zinc-aspartate was intravenously administered every other day for 3-12 months to 10 AD patients (543). Improvement in cognition was seen in 8 of them, which was abolished during periods of discontinuing treatment, yet this was a small and uncontrolled cohort (543). Gastrointestinal irritation was also reported in a cohort of five MCI and AD patients following a single oral dose of zinc acetate (Galzin®; FDA-approved drug for treatment of Wilson's disease) (544).

Synthetic Biologics (formally Adeona Pharmaceuticals; Ann Arbor, MI, USA) recently completed a 6-month prospective, randomized, double-blind Phase I trial of a gastro-retentive, sustained-release oral preparation of zinc-cysteine (reaZin™) in 64 patients with MCI or mild to moderate AD. Zinc-cysteine treatment (150 mg/day) was reported to be bioavailable (significantly elevated Zn and reduced Cu in serum, compared to placebo) and well tolerated (substantially less gastrointestinal symptoms, compared to Galzin®) (544). Post-hoc analysis of trial participants 70 years of age or older revealed that treatment with zinc-cysteine stabilized the cognitive deterioration of AD patients, compared to placebo (544). The company is now developing reaZin™ as a medicinal food, as well as an IND for the treatment of AD (AEN-100).

1.4.4.4 Effect of Fe on AD-related Pathology and Cognition

A recent study demonstrated that treatment of APP/PS1 mice with Fe-supplemented drinking water resulted in elevated PS1 levels, and induced expression, phosphorylation and amyloidogenic processing of APP, as well as suppressed non-amyloidogenic APP proteolytic pathway (417). No memory, behavioural or cognitive tests were performed.

1.4.5 The Metal Hypothesis of AD

Collectively, the above findings constitute a compelling argument for APP and/or Aβ playing a major physiological role in regulating metal-ion levels and *vice versa*. These lines of evidence led Bush, Tanzi and colleagues to propose "the metal theory of AD" (545, 546), which stipulates that an age-related endogenous metal imbalance in the brain allows binding of redox-active metal ions (Cu^{2+} and Fe^{3+}) to Aβ. This can lead to neurotoxicity as Cu^{2+} stabilizes the neurotoxic oligomeric Aβ assemblies (547, 548), induces the covalent di-tyrosine crosslink of Aβ (459, 462, 482, 549-556) and promotes the generation of SDS-resistant copper-derived diffusible ligands (CuDDLs) (455, 462, 550). Metallated-Aβ also has an increased affinity for the phospholipid heads of the membrane bi-layer, which acts as a reductant in the production of ROS *via* Fenton and Haber-Weiss chemistry (557-560). The resulting radicals, hydrogen peroxide (H_2O_2) and superoxide (OH^-), induce oxidative stress damage of lipids, proteins and DNA, ultimately leading to synaptic and neuronal loss (291, 294, 475, 480, 554, 559-563). Based on this hypothesis, therapeutics that aim to restore metal homeostasis, inhibit Aβ-metal interactions and/or inhibit metallated Aβ-catalysed oxidation are being developed.

1.5 AD Pharmacotherapies Targeting Metal Ions

The equilibrium (concentrations, distribution, stability and bio-availability) of metal ions is critical for many physiological functions. This is particularly true for the CNS, where metals are essential for development and maintenance of enzymatic activities, mitochondrial function (564, 565), myelination (566), neurotransmission (567), learning and memory (568, 569). In light of their importance, cells have evolved complex machinery for controlling metal-ion homeostasis. However, when these mechanisms fail, the altered homeostasis of metal ions can result in a disease state, including several neurodegenerative disorders (570, 571). Understanding the complex structural and functional interactions of metal ions with the various intracellular and extracellular components of the CNS, under normal conditions and during neurodegeneration, is critical for the development of effective therapies (572). Accordingly, modulation of metal ions has been proposed as a disease-modifying therapeutic strategy for AD (573-576) and other neurodegenerative diseases (576, 577).

1.5.1 Antioxidants

Antioxidant molecules are capable of neutralizing free metals, thereby interfering with the 'down-stream' generation of ROS and other reactive radicals. Hence, antioxidants may be used mainly as a preventative approach (578). Numerous molecules with antioxidant properties, such as oestrogen, melatonin, vitamin C and E (L-ascorbate and α-topopherol, respectively), coenzyme Q (CoQ), docosahexaenoic acid (DHA), ginkgo bilboa extract, the green tea extract EGCG (epigallocatechin gallate), curcumin and flavonoids, have been shown to have neuroprotective effects against Aβ-induced toxicity in cell-based experiments (579, 580) and animal models (581-585), but have had conflicting results in a clinical setting (586-588).

Owing to the complex nature of AD, it is highly likely that antioxidants alone will be inadequate to cause disease-modifying effects. Therefore, an emerging strategy in the AD therapeutics field is the rational design of multi-modal/targeted drugs combining antioxidant with other beneficial properties (refer to **section 1.5.4**). By incorporating the 1,4-benzoquinone radical scavenger moiety of CoQ into the polyamine backbone of AChEI caproctamine (589), scientists created memoquin (see **Fig. 1.5**), which is currently undergoing pre-clinical evaluations (590). It would be of interest to know whether memoquin can cross the BBB and study its therapeutic effect in clinical trials.

1.5.2 Metal Chelators

By definition, metal chelators (meaning "claw" in Greek) bind a metal ion, *via* two or more atoms, to form a cyclic ring; unlike chelation therapy, wherein chelating agents are used to systemically deplete metals, usually as treatment for heavy metal poisoning.

Desferrioxamine (DFO; **Fig 1.5**), an Fe chelator with high binding-affinities for Zn, Cu and Al (591), was the first such agent to enter clinical investigations for the treatment of AD. Results of a 2-year long, blinded Phase II trial of a 48 AD patient cohort demonstrated that 125mg intramuscular injections twice daily for 5 days a week significantly slowed down the decline of some cognitive functions and lowered their cerebral Zn and Fe levels, in comparison with the two control arms (an oral placebo or no treatment) (592, 593). However, DFO is a large hydrophilic molecule that is not orally bio-available, and therefore requires painful intramuscular injections, after which it degrades quickly and does not penetrate the BBB easily (594). Hence, it is unknown whether the beneficial effect seen with the DFO treatment was due to the drug's interaction and/or chelation of metals, or due to a different mechanism all together (593). In an attempt to overcome these limitations, an intranasal formulation of DFO, SAN-121 (DiaMedica, Winnipeg, Canada), is now being assessed (417, 595).

Another hexadentate chelator, DP-109 (DPharm, Rehovot, Israel), is a large synthetic analogue of the Ca^{2+} chelator BAPTA that becomes activated following cleavage of its two long-chain esters (596) and insertion into lipid membranes (597). Administration of DP-109 (5 mg/kg daily) by oral gavage to female Tg2576 mice over a 3-month period reduced the formation and deposition of CAA and APs, as well as re-solubilised Aβ (598). Recently, DP-109 and DP-460 (another Ca, Cu and Zn lipophilic chelator) were reported to have neuroprotective effects in a transgenic *Drosophila* fly model of AD (599), a 6-hydroxydopamine (6-OHDA)-lesioned mouse model of PD (596) and a G93A transgenic mouse model of ALS (600). Like DFO, DP-109 is not expected to cross the BBB; therefore, the mechanism by which it exerts its effects in the above models is still unclear.

Injection of the bicyclam analogue, JKL169, to rats resulted in a slight reduction to serum Cu, yet significant decrease of Cu in the CSF and significant increase of Cu in the brain cortex (601). Further *in vivo* assessments of JKL169 and other metal chelators to determine their bioavailability, BBB penetration capability and specificity is pending in order to rule out any harmful systemic effects due to indiscriminate scavenging of essential metals, metal-binding and/or metalloproteins.

The latest advancement in this field is the conjugation of chelating agents onto various nanoparticles. The nanoparticles deliver the metal chelators across the BBB and into the brain, where the metals are chelated, bind to the nanoparticles, exit the brain and naturally degrade (602). This intends to be a safer and efficient way of specifically removing metal ions from the brain of patients with AD and other neurodegenerative diseases. Indeed, preliminary studies demonstrated that nanoparticle-chelator conjugates are able to remove Fe from AD brain sections (603), solubilise Cu- and Zn-Aβ aggregates (604, 605), as well as protect and rescue human cortical neurons from Aβ-mediated toxicity (606). However, any neurotoxic and/or other ADRs that could stem from the nanoparticles themselves, the linkers used, or the nanochelators as a whole need to be examined thoroughly prior to their testing in humans.

Rather than using nanoparticles to transport metal chelators, a new approach utilizes nanoparticles to deliver metals themselves in order to increase metal ion bioavailability in a more efficient, controlled, and perhaps even safer manner.

1.5.3 Metal Complexes

Metallo-nanoparticles and metallo-complexes of pyrrolidine dithiocarbamate (M^{2+}-PDTC) or *bis*(thiosemicarbazone) (M^{2+}-BTSC) (see **Fig. 1.5**) are emerging as promising AD diagnostics and therapeutics that facilitate the targeted delivery of metal ions to specific cells and/or cellular compartments (607-609). Gerd Multhaup's group designed these two distinct Cu-carrier nanoparticles that are able to cross plasma membranes and release the Cu molecules they encapsulate, thereby increasing Cu bioavailability and decreasing $A\beta_{40}$ and $A\beta_{42}$ secretion from APP-transfected SY5Y cells (609).

PDTC is traditionally considered an inhibitor of the transcription-factor regulator nuclear factor-κB (NF-κB) with anti-inflammatory, anti-oxidant and anti-apoptotic properties (610-612) – all of which have been attributed to the synergistic interaction between PDTC and endogenous Cu and/or Zn (613-619). Therefore, PDTC could potentially remove metals from biologically deleterious sites and deliver them to areas of deficiency, thus maintaining overall metal steady state. Indeed, oral PDTC treatment of APP/PS1 double transgenic mice resulted in increased cerebral Cu levels, compared to non-treated APP/PS1 mice, as well as down-regulation of the GSK-3β signalling cascade, which led to a decrease in tau phosphorylation and an improvement in spatial memory, but had no effect on amyloid burden, glial activation or oxidative stress (412).

A later study, in which PDTC was administered to APP/PS1 mice by intraperitoneal injections, attenuated astrogliosis and increased cerebral Aβ were observed (620). The latest data to emerge indicates that PDTC complexed to either Cu^{2+} or Zn^{2+} can act as a proteasome inhibitor to induce apoptosis in several human cancer cells (621-623). It is expected that metallo-PDTC complexes would be carefully evaluated in additional cellular and/or animal models of AD prior to being assessed in humans.

The metallo-complexes of diacetyl*bis*(N^4-methylthiosemicarbazone) (M^{2+}-ATSM) and glyoxal*bis*(N^4-methylthiosemicarbazone) (M^{2+}-GTSM) are small, stable, neutral and easily synthesized molecules (624, 625) with anti-bacterial, anti-fungal and anti-neoplastic activities by selectively delivering exogenous metal ions into metal-deficient cells (626, 627). Cu^{2+}-ATSM is membrane permeable, selective for hypoxic cells and is redox inactive, therefore the ligand retains its Cu molecule (624, 628). These properties are being exploited for its development as a radiotherapeutic agent (629-631) and as a radiopharmaceutical for PET imaging (632, 633). Cu^{2+}-GTSM can also cross the BBB, however, once inside the cell it is readily reduced by various cellular reductants and releases its Cu^{1+} molecule, which is made available for the cell (624, 634, 635).

Treatment of human APP_{695}-overexpressing CHO cells with Cu^{2+}/Zn^{2+}-BTSC ligands resulted in increased intracellular metal levels that, in turn, activated Akt/PI3K, c-Jun N-terminal kinase (JNK) and GSK3 (607). Phosphorylation of these kinases led to the up-regulation of MMPs, which reduced extracellular levels of Aβ (607). Low doses of Cu^{2+}-GTSM were shown to prevent the Aβ-inhibition of long-term potentiation (LTP) in mouse hippocampal brain slices (608). Treatment of SY5Y cells and APP/PS1 mice with Cu^{2+}-GTSM caused an increase in cellular Cu bioavailability, which inhibited GSK3β and, in turn, decreased the phosphorylation of tau (608). While oral treatment of APP/PS1 mice with Cu^{2+}-GTSM did not result in improved cognitive performance in Morris water maze (MWM (636)), it did restore their spatial working memory and learning, as tested by a three-arm radial maze (Y-maze; (637)), which directly correlated with decreased Aβ trimers (608). Reduction in Aβ oligomeric species was previously shown to correlate with diminished binding to lipid membranes and neurotoxicity (638).

Other radiopharmaceutical-based compounds being evaluated for treatment of AD are 1,10-phenanthroline derivatives complexed to platinum (Pt^{2+}). These ligand-$PtCl_2$ planar aromatic complexes are stable, redox inactive and have been designed to bind and alkylate the imidazole side chains on histidine residues 6, 13 and 14 on Aβ, thereby competing with metals for Aβ's putative metal binding site (639).

In addition to displacing Cu^{2+} and/or Zn^{2+} from their binding site on Aβ, Pt^{2+}-phenanthroline compounds can also change the peptide's conformation, hinder its aggregation, inhibit neurotoxicity and reverse synaptotoxicity (639, 640). Yet, these complexes were found to be unsuited for *in vivo* testing.

Nonetheless, a novel class of 8-(1*H*-benzoimidazol-2-yl)-quinoline (8-BQ)-Pt^{2+} complexes has been synthesized, and is currently undergoing *in vitro* and *in vivo* pre-clinical assessments (641). Further evaluation of the lead compound of this Pt^{2+}-8-BQ series is needed prior to its advanced development as an AD pharmacotherapeutic.

1.5.4 Multi-functional Chelators

Rather than interrupting the detrimental Aβ-metal interaction by targeting *either* the metals themselves or the Aβ sequence that binds metals, sophisticated ligands have been rationally designed to target *both* metals and the metal binding site on Aβ. Two such molecules are XH1 (General Hospital Corporation, Charlestown, MA, USA) and L2-b (Université de la Méditerranée, Marseille, France). Both are bi-functional compounds with metal-complexing and Aβ-binding properties (642).

XH1 treatment led to decreased Zn-induced $Aβ_{40}$ aggregates in a human neuroblastoma cell line, while a 4-week treatment of APP/PS1 mice with XH1 resulted in a reduction of brain amyloid load (642). L2-b is a small, BBB permeable molecule, effective at inhibiting metal-triggered Aβ fibril formation, ROS production and neurotoxicity, as well as disaggregating pre-formed metal-Aβ aggregates and disassembling Aβ deposits from human AD brain homogenates (643). There are also several thioflavin T (ThT) and stilbene derivatives that are currently being optimized and developed as bi-functional AD diagnostics and/or therapeutics (644, 645).

Recently, Italian (646), Spanish (647) and German (648) scientists have taken this approach a step further by designing tacrine-based tri-functional agents for the treatment of AD, which are capable of blocking the enzymatic activity of AChE, able to inhibit AChE-induced Aβ aggregation and possess metal chelating and/or antioxidant activities.

Other examples of multi-functional molecules currently in development for the treatment of AD, as well as other neurodegenerative diseases, are ladostigil/TV-3326 (Avraham Pharmaceuticals, Tel Aviv-Jaffa, Israel) and M30/VAR10300 (Varinel, West Chester, PA, USA) (see **Fig. 1.5**).

Ladostigil combines the pharmacophore component of rasagiline/azilect (Teva Pharmaceutical Industries, Petah Tikva, Israel) with the carbamate moiety of rivastigmine/exelon (649). As a result, ladostigil possesses neuroprotective properties (reversible cholinesterase inhibition and irreversible monoamine oxidase B (MAO-B) inhibition), as well as neurorescue abilities *via* the enhanced expression of brain-derived neurotrophic factor (BDNF) and glial-derived neurotrophic factor (GDNF), and through induction of neurogenesis (649, 650). For the synthesis of M30/VAR10300, the propargylamine moiety of rasagiline/exelon was embedded onto the backbone of the 8-hydroxyquinoline (8-HQ)-derivative VK28/VAR10100 (Varinel, West Chester, PA, USA) (651, 652). Amongst its many pharmacological activities, M30/VAR10300 has been shown to be a Fe chelator, antioxidant and brain selective MAO-A/B inhibitor (653, 654).

Both ladostigil and M30/VAR10300 also regulate the proteolytic processing of APP *in vitro* and *in vivo*. Treatment of neuronal cell lines and mouse hippocampal slices with M30/VAR10300 and ladostigil resulted in lower APP and elevated sAPPα levels (655-659). M30/VAR10300 was also shown to increase α-CTF and to decrease β-CTF and Aβ, correspondingly (659). The effects of ladostigil and M30/VAR10300 on APP metabolism have been attributed to suppression of APP translation, stimulation of the non-amyloidogenic processing pathway of APP and *via* the activation of protein kinase C (PKC), mitogen-activated protein kinase (MAPK) and tyrosine kinase signalling pathways (655-658).

While M30/VAR10300 is still being investigated pre-clinically, Avraham Pharmaceuticals (Tel Aviv-Jaffa, Israel) is conducting a randomized, double-blind, placebo-controlled European Phase II study with ladostigil (10 mg, once a day for 36 months) in 200 patients diagnosed with MCI subsequent to a completed 26-week long Phase II trial with ladostigil in 200 patients with mild to moderate AD, which failed to meet its primary efficacy endpoints (660).

Antioxidants

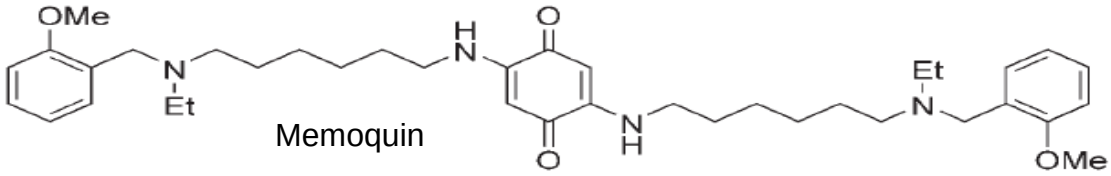

Memoquin

Metal chelators

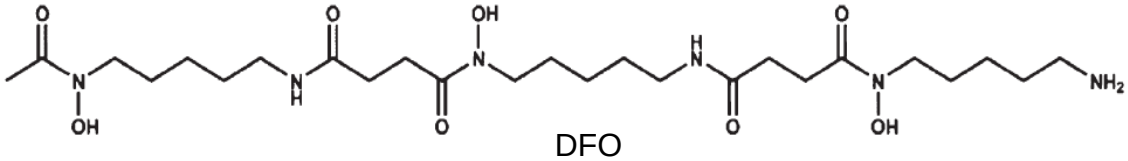

DFO

Metal Complexes

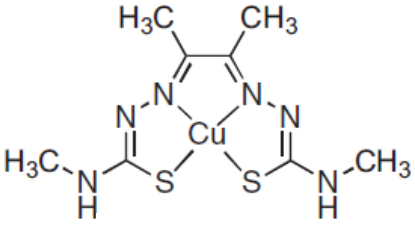

Cu^{2+}-ATSM

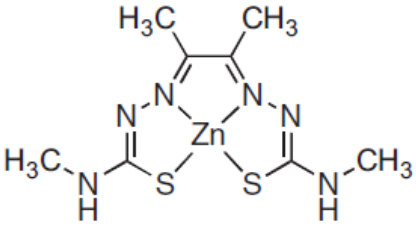

Zn^{2+}-ATSM

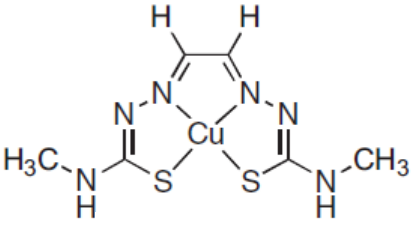

Cu^{2+}-GTSM

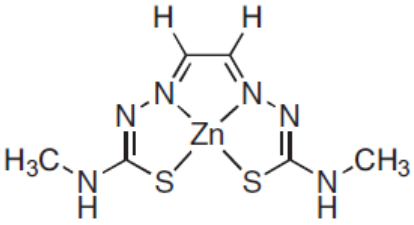

Zn^{2+}-GTSM

Multi-Functional Chelators

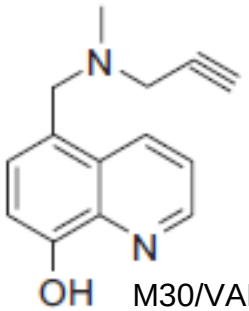

M30/VAR10300

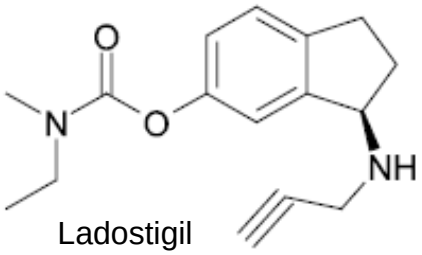

Ladostigil

Figure 1.5 Pharmacotherapeutic strategies and representative compounds targeting metal ions for the treatment of AD

Classes of metal-targeting pharmacotherapies and chemical structures of candidate compounds in each category.

Abbreviations: ATSM, diacetylbis(N^4-methylthiosemicarbazone); DFO, desferrioxamine; GTSM, glyoxalbis(N^4-methylthiosemicarbazone)

1.5.5 Metal-Protein Attenuating Compounds

Metal-protein attenuating compounds (MPACs) have moderate, reversible affinity towards metals, which enables them to compete with endogenous ligands for metal ions, target the harmful 'up stream' metal-protein reactions and restore normal metal levels in specific cellular compartments (661). The first-generation series of MPACs were based on clioquinol (CQ; 5-chloro-7-iodo-8-hydroxyquinoline). CQ is a small and highly lipophilic molecule (see **Table 1.5**), which absorbs quickly, can convert to glucuronated and sulfate metabolites, crosses the BBB and is excreted in urine and feces (662-668).

For decades, CQ (Ciba-Geigy; Basel, Switzerland) was used topically (as an ointment or cream) in cattle and humans for treatment of congenital or acquired Zn-deficiencies, and for the treatment of bacterial or fungal dermatological infections (669-671). CQ was also administered orally as an anti-parasitic/protozoal/microbial for vaginal trichomonacide, and as prophylactic or therapeutic for amebiasis, shigellosis, dysentery or diarrhea (672-674); however, its oral preparation was withdrawn from the market during the 1960s-1970s, due to suspected links to transient global amnesia (TGA) and sub-acute myelo-optico-neuropathy (SMON) (675-682).

SMON is characterized by abdominal symptoms followed by sensory and motor disorders in the lower limbs, peripheral neuropathy and visual impairment due to de-myelation of the spinal cord, optic and peripheral nerves (683). SMON affected people worldwide; though, it reached near-epidemic proportions in Japan, where even a few related blindness and death cases were reported (684). At the time, association between CQ and SMON was circumstantial and no mechanistic relation was established (685).

Later, it was suggested that CQ may transport metals into the CNS, which leads to neurotoxicity. Early observations indicated that CQ-Fe, but not CQ or Fe alone, stimulated degeneration of cultured retinal neuroblasts (686) by increasing cellular Fe levels and promoting lipid peroxidation (687). Enhanced lipid peroxidation with CQ-Fe, but not CQ alone, was also demonstrated in a sciatic nerve isolated from rabbit (688). Some researchers suggested CQ-Zn chelate as being the toxic entity (689), while others proposed that CQ induced Cu deficiency myelopathy, which resembled SMON (690).

However, it is now believed that intake of CQ, at doses far exceeding the recommended ones and for prolonged periods, together with a post-world war II deficient diet, led to a vitamin B12 deficiency that presented as SMON in Japan (691, 692). This is supported by claims that there were no diagnosed SMON cases in Bombay in the years 1977-1984, despite CQ being widely used in India during that time (693).

Drug Name	Clioquinol (CQ)
IUPAC Nomenclature	5-chloro-7-iodo-8-hydroxyquinoline
Chemical Structure	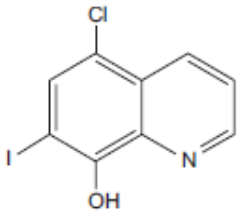
Chemical Formula	C_9H_5ClINO
Molecular Weight	305.5 g/mol
Physiological Charge	0
Hydrogen-Bond Acceptors	2
Hydrogen-Bond Donors	1
Water Solubility	$2.64e^{-01}$ g/L
Partition Coefficient	logP = 3.66
Distribution Coefficient	logD = 3.75
Polar Surface Area (PSA)	33.12
Refractivity	60.13
Polarizability	22.63
State	solid (powder)
Colour	yellowish
Melting Point	178.5 ^oC

Table 1.5 Physiological and Chemical Properties of CQ

CQ binds Cu and Zn (2:1 ratio (694-698)) and was shown to exert diverse effects on these metals (and other biological components) depending on its route of administration and the *in vitro* and/or *in vivo* system in which it was tested in. The well-known interaction of CQ with Cu and Zn prompted our laboratory to investigate the effects of CQ on AD-related pathology.

CQ was originally shown to potently disassemble synthetic Aβ-Cu/Zn aggregates and solubilise amyloid deposits from postmortem AD brain (699). Subsequently, it was confirmed that CQ dissolves synthetic Aβ-Zn aggregates (700, 701), inhibits Cu-induced di-tyrosine cross-linking of Aβ and diminishes Aβ-Cu-mediated hydrogen peroxide production in a dose-dependent manner (644, 700). Others have demonstrated that CQ can influence synthetic metal-dependant and independent Aβ aggregation (702-705) and/or disassembly (705, 706), rescue Aβ toxicity in neuronal cultures (707), reduce Aβ oligomer formation (403) and prevent tau hyperphosphorylation (411) in stimulated hippocampal slices, as well as prevent Aβ-induced LTP inhibition (700).

A pilot study revealed significant reduction in APs in brains of 12-month old Tg2576 mice orally gavaged with 20 mg CQ/kg/day for 12 weeks (699). In another pre-clinical trial, the oral administration of 30 mg/kg/day of CQ to 21-month old Tg2576 mice over 9 weeks resulted in the normalization of cerebral Cu and Zn levels, reduction in hydrogen peroxide synthesis, significant decrease in insoluble Aβ and increase in soluble Aβ, and overall decrease in plaque burden, as compared to control littermates (699). In both animal studies, not only was there no toxicity reported on a neurological index, but the CQ-treated mice were physically superior to the sham-treated mice (699).

These results are consistent with two independent studies that showed significant reduction in the number and area size of cerebral APs in 7 month-old male APP/PS1 mice treated with 30 mg CQ/kg/day for 2 months (708) and in 5 months-old male and female APP/PS1 mice treated with 6 mg CQ/kg/day for 6 months (709). The former report found these to be a result of decreased Zn within APs (but not overall brain Zn) and the attenuation of amyloidogenic processing of APP, with no adverse impact on the animals' behavior (708); whilst the later provided evidence of increased plasma Aβ levels and myelin-related pathological abnormalities (709).

Extension pre-clinical studies found that CQ does not only affect the brain biochemistry, but also affects behavior and cognition. While CQ treatment did not affect the cognitive performance of WT mice, it improved that of female APP/PS1 mice, compared to standard suspension vehicle (SSV)-treated Tg animals (700).

These data led to clinical assessment of CQ in Phase I (20 or 80 mg/day (*n*=10 mild to moderate AD patients, each) for 21 days) and IIa (250 or 375 mg/day (*n*=3 and 12 moderate to severe AD patients, respectively) *versus* placebo (*n*=16) for 36 weeks) trials (710, 711). CQ intake significantly elevated Zn and lowered $A\beta_{42}$ in plasma, and slowed cognitive decline with no signs of SAEs (710, 711). Advanced clinical studies, however, were stalled by Good Manufacturing Practice (GMP) difficulties encountered in preventing a di-iodo-8-hydroxyquinoline contamination during the required larger scale chemical synthesis for such studies. At the same time, Prana Biotechnology (Parkville, Melbourne, VIC, Australia) identified PBT2 (2-(dimethylamino) methyl-5, 7-dichloro-8-hydroxyquinoline) as an 8-HQ derivative that lacks iodine, contains an exocyclic amine, and has higher solubility and increased BBB permeability than CQ (712). This compound was then extensively screened in a variety of pre-clinical assays.

In vitro, PBT2 has been shown to be more effective than CQ in the dissolution of synthetic Aβ-Zn aggregates, inhibition of Cu-induced di-tyrosine cross-linked Aβ oligomers and accompanied hydrogen peroxide (H_2O_2) production (700). PBT2 was also able to remove Zn from APs in brain slices of APP/PS1 mice and to prevent Aβ-driven inhibition of LTP in hippocampal slices (700).

Similar to CQ, PBT2 also exhibits a wide range of effects in cultured cells. Exposure of differentiated PC12 cells to PBT2 markedly increased neurite outgrowth, which was exaggerated by the co-administration with either Cu or Zn, but abolished upon addition of metal chelator $(NH_2)_2$sar (diamsar) (713). Diamsar also prevented the PBT2-induced elevation in NMDAR 1A sub-unit levels and phosphorylation of GSK3 in SY5Y human neuroblastoma cells (714), suggesting that PBT2's ability to promote neuritogenesis and to inhibit the activity of GSK-3 are mediated by metals.

Further investigation has revealed that the drug has a dual mode of action as an AD therapeutic. PBT2 mobilizes the Zn trapped by extracellular amyloid and chaperones its uptake into cells, where it increases MMP activity that, consequently, facilitates the protease degradation of Aβ. Intracellularly, Zn also inhibits the phosphatase activity of calcineurin/PP2B, which enables the increased phosphorylation of GSK3 and, in turn, the reduced phosphorylation of tau (714).

Reduced hyperphosphorylation of tau (by modulating the activity of its kinases and phosphatases) and enhanced Aβ degradation are both desired strategies in developing pharmacotherapeutics for AD (as described in detail in **Appendix A**).

In vivo, PBT2 treatment protected *Caenorhabditis elegans* (*C. elegans*) nematodes against Aβ-induced paralysis (715) and did not affect WT mice; yet, it had differential effects on spatial learning and memory, as well as several neuropathological biomarkers (soluble and insoluble Aβ species, total and/or phosphorylated soluble and insoluble tau, and the pre-synaptic marker synaptophysin) in Tg2576 *versus* APP/PS1 mice (700). Out of the array of biological indices tested, the rapid and significant decrease in interstitial fluid Aβ observed in both Tg mouse strains following PBT2 treatment was the only one to correlate with the remarkable cognitive improvement (to levels either equivalent to or greater than WT controls) (700).

In another series of studies in young and old female WT and Tg2576 mice, PBT2 treatment was also shown to elicit a range of synaptotrophic responses, including restored dendritic spine density and normalized levels of protein markers for synaptic function and plasticity (713). Administration of PBT2 (30 mg/kg by daily oral gavage for six weeks) in aged Tg mice that model human tauopathy (141) was recently found to inactivate GSK3β, significantly reduce NFT burden, increase the number of cortical and hippocampal neurons and improve cognitive performance, independent of Aβ (716).

PBT2 progressed into human clinical trials, and following a successful Phase I study, it entered into a randomized, double blind, placebo-controlled, multi-centred, 12-week long Phase IIa trial in 78 mild AD patients. This study demonstrated safety and tolerability, reduced CSF levels of $A\beta_{42}$ and improved neuropsychological test battery (NBT) executive function in patients taking a daily dose of 250 mg PBT2, as compared to placebo (717, 718). PBT2 (single daily dose of 250 mg) was later evaluated in an open-label, extension study to a double blind, placebo-controlled, 12-month Phase IIb IMAGINE trial, in which it did not show a significant effect on cerebral amyloid load, brain activity, cognition or function in 40 prodromal or mild AD patients (719).

Subsequent to proof-of-concept studies with both CQ (720, 721) and PBT2 (722), Prana Biotechnology (Parkville, Melbourne, VIC, Australia) also conducted a randomized, double-blind, placebo-controlled Phase II trial (Reach2HD) into the safety and efficacy of PBT2 (100 or 250 mg once daily for 6 months) in 109 patients with early- to mid-stage Huntington disease (HD). The treatment was safe and well tolerated, but did not result in changes in biomarkers, motor abilities, functional or behavioural capacities; yet, its high dose, did result in statistically significant improvement in a particular measure of cognitive performance (723).

Taken together, these data support the notion that the modulation of metals may be sufficient to significantly alter the onset and/or progression of AD, and may represent a more potent disease intervention than systemically targeting the production or degradation of the Aβ protein.

While CQ continues to be examined as an imaging agent for AD (724, 725), as well as a proof-of-principle therapeutic for a wide spectrum of diseases (including PD, HD, multiple sclerosis (MS), prion diseases, diabetes, cancer and even tuberculosis (TB) (444, 621, 689, 720, 726-736)), a finer dissection of the mechanism of action of drugs, such as CQ and PBT2, will enable researchers to better design additional therapeutics for AD and other diseases.

1.6 Thesis Outline and Aims

This body of work focuses on deepening the understanding of the therapeutic MOA of CQ in relation to AD with the aim of implementing this knowledge in the research and development (R&D) of similar compounds for the treatment of AD, as well as other neurodegenerative diseases.

Chapter 1 provides a critical appraisal of the relevant approaches and pharmaceutics currently in clinical development for the treatment of AD, with an emphasis on metal-targeted candidate drugs. This chapter highlights the therapeutic benefits of 8-HQ derivatives, CQ and PBT2, but also identifies a gap in the understanding of their MOA.

Chapter 2 lists the reagents, general experimental methods and statistical analysis tools used in the procedures detailed in Chapters 3-5.

Chapter 3 examines the interaction between CQ, metals (Cu and Zn) and $A\beta_{42}$, using mouse neuroblastoma cells.

Chapter 4 explores the toxicity of CQ and/or metal ions in an array of cell lines.

Chapter 5 focuses on the relationship between CQ, metals (Cu, Zn and Fe) and $A\beta_{42}$ in mouse primary cortical neuronal cultures.

Chapter 6 summarizes the key findings in this dissertation and discusses their significance in context of work by the wider scientific community. It includes concluding remarks and comments on future directions of this work.

Appendix A compliments Chapter 1, as it affords greater insight into the molecular targets in the development of pharmacotherapeutics for AD.

Chapter 2

Materials and Methods

Chapter 2

2.1 Procedures

All tissue culture procedures were conducted, in accordance with good laboratory practice (GLP) and under sterile conditions, in a Physical Containment Level 2 (PC2)-accredited Tissue Culture Facility (issued by the Office of Gene Technology Regulator (OGTR)).

All procurement, transport, storage and use of radioisotopes were carried out in keeping with a radiation management licence, issued by the Department of Health (Victoria, Australia).

All other procedures were also GLP-compliant and performed in OGTR-accredited PC2 Laboratories.

2.2 Materials

All chemical reagents were of analytical grade and were purchased from Sigma-Aldrich (Castle Hill, Sydney, NSW, Australia), unless stated otherwise.

All tissue culture reagents were of tissue culture grade and purchased from Invitrogen (Mulgrave, Melbourne, VIC, Australia), unless indicated otherwise.

All 1.5 and 2 mL polypropylene tubes were purchased from Eppendorf (North Ryde, Sydney, NSW, Australia) and all 15 and 50 mL polypropylene tubes were purchased from Interpath Services (Heidelberg West, Melbourne, VIC, Australia).

All other plastic-ware were purchased from Thermo Fisher Scientific (Scoresby, Melbourne, VIC, Australia), unless otherwise specified.

Milli-Q® ultrapure water (resistivity $\geq$ 18.2 MΩ.cm at 25 °C), purified by a Milli-Q Academic System (Merck Millipore; Kilsyth, VIC, Australia), was used in all experimental procedures.

All buffers and stock solutions were filtered though a 0.22 μm membrane (Merck Millipore; Kilsyth, VIC, Australia) in order to remove particulate matter.

2.3 Cell culture

The work described in this thesis utilized a variety of neuronal and non-neuronal cell lines (**Chapters 3** and **4**), as well as primary neuronal cells (**Chapter 5**), as *in vitro* model systems for investigating different aspects relating to the MOA of CQ.

Clonal cell lines and mouse primary cortical neuronal cells were maintained and treated at 37 ^{o}C in separate 5 % carbon dioxide (CO_2)-humidified incubators (Binder; Tuttlingen, Germany) to prevent cross-contamination.

See individual chapters for description of types of cell lines, procedures for preparation of primary neuronal cells, and culture conditions.

2.4 Cellular ^{125}I-CQ uptake studies

Radiolabelled CQ (^{125}I-CQ) was prepared by and purchased from the Australian Nuclear Science and Technology Organisation (ANSTO; Lucas Heights, Sydney, NSW, Australia) (737). Since each CQ molecule contains a sole ^{125}I moiety, direct correlation was made between ^{125}I radiation measurement and cellular CQ levels.

Using Online Radiation Calculator (http://graphpad.com/quickcalcs/radcalcform.cfm by GraphPad Software; La Jolla, CA, USA), the isotope decay from the day ^{125}I-CQ was synthesised until the experimental day was calculated based on the known half-life ($t_{1/2}$) of the ^{125}I isotope being 60 days. The fraction (%) of ^{125}I-CQ remaining from its original concentration (mCi/mL) and its original specific activity (Ci/mmole) were used to calculate the concentration of ^{125}I-CQ stock solution (μM). The ^{125}I-CQ stock solution was diluted in treatment media to the desired final concentration.

On experimental days, growing media was aspirated and confluent cells in well-plates were briefly rinsed with phosphate-buffered saline (PBS). To study the uptake of CQ, cells were treated in triplicates with various concentrations of ^{125}I-CQ, in the absence and presence of metal ions at different doses. Following different incubation times, either on ice at 4 ^{o}C or in a 5 % carbon dioxide (CO_2)-humidified incubator at 37 °C, treatment media was removed and collected. To stop its uptake and remove any unbound ^{125}I-CQ, cells were washed twice with ice-cold PBS, and both washes were collected. For cell lysis, cells were incubated for 5 minutes at room temperature with PBS containing 0.15 % (w/v) sodium dodecyl sulphate (SDS). Cell lysates were harvested by scraping and collected.

2 mL microtubes (Biocorp; Huntingdale, Melbourne, VIC, Australia) containing: ^{129}I calibration standard, blanks, controls, original ^{125}I-CQ stock, experimental stock solutions, as well as collected treatment media, both PBS washes and cell lysates, were all placed within individual sample holders in racks and onto a conveyer. Samples were then robotically lifted into a lead (Pb)-shielded detector and ^{125}I-emitted gamma radiation was measured (counts per minute; cpm), using WIZARD$^{3®}$ 1480 Automatic Gamma Counter and Data Analyser Software (PerkinElmer; Glen Waverley, Melbourne, VIC, Australia).

While this technique proved sensitive and efficient, for reasons beyond the operator's control (explained in **sections 3.4** and **5.3.4**) data was not included in this thesis.

2.5 Preparation of CQ

Since the use of ^{125}I-CQ (see **section 2.4** above) had to be abandoned, "cold" CQ was used. Due to its physical and chemical properties (listed in **Table 1.5**), CQ (5-chloro-7-iodo-8-hydroxy-quinoline; C_9H_5ClINO) does not dissolve well in water; however, it dissolves well in organic solvents. Therefore, CQ stock solutions were freshly prepared by dissolving the drug in dimethyl sulfoxide (DMSO; $(CH_3)_2SO$/Me_2SO).

CQ stock solutions were diluted in DMSO and kept in the dark (due to photosensitivity) at room temperature until same-day use (due to stability properties). Since DMSO itself can be harmful to cells, CQ was added to the treatment media, at < 0.5 % (v/v), immediately prior to cell exposure to desired final concentrations.

2.6 Preparation of metals

Stock solutions of metals were prepared by dissolving metal ions in water (H_2O). Following their initial preparation, the actual (as oppose to theoretical) concentrations of metals in stock solutions were determined by inductively-coupled plasma mass spectrometry (ICPMS; see **section 2.8** below).

Metal stock solutions were stored at 4 ^{o}C and were periodically monitored by ICPMS.

Metal ion stock solutions were diluted in water and added, at the desired final concentrations, to treatment media immediately prior to cell exposure.

2.7 Preparation of Aβ

Human $A\beta_{1-42}$ (here on referred to as $A\beta_{42}$; molecular weight 4514 g/mol) was synthesised, purified, characterized by and purchased from The Keck Biotechnology Resource Laboratory (Yale University; New Haven, CT, USA).

2.8 Metal analysis

Initially, cellular Cu levels were analysed by atomic absorption spectrometry (AAS), using an AA240 Spectrometer (Varian; Mulgrave, Melbourne, VIC, Australia) with a graphite tube electrothermal atomizer (378).

However, due to the limitation of measuring one metal ion per sample and other technical difficulties, this method was replaced by ICPMS. ICPMS is a highly sensitive and accurate technique for multi-elemental quantification to a resolution of parts per billion (ppb).

To determine the cellular levels of Cu, Zn, Fe, I and other elements, different sample preparation procedures, instrument models, calibration measures, operating modes and data analysis software were used (see **sections 3.2.8**, **5.2.7** and **5.2.8**).

2.9 Aβ analysis

Originally, cellular Aβ levels were detected, using 4-12 % NuPAGE® Novex® Bis-Tris polyacrylamide gel electrophoresis (Invitrogen; Mulgrave, Melbourne, VIC, Australia) and analysed by Western blot (700), however results were found to vary.

Instead, DELFIA® Double Antibody Capture Enzyme-Linked Immunosorbent Assay (ELISA) was utilized (436, 738, 739). This method was found to be more sensitive and consistent than PAGE.

To quantify the cellular Aβ concentrations, different sample preparation procedures, antibodies and operating modes were used (see **sections 3.2.10** and **5.2.9**).

2.10 Toxicity assays

All toxicity assays were carried out according to individual manufacturer's protocols.

Neuronal and non-neuronal cell lines, as well as mouse primary cortical neuronal cells, were treated with CQ, metal ions and/or Aβ (see **sections 4.2.4** and **5.2.5**, respectively).

Each assay included a blank (i.e., media alone without cells) to account for background absorbance in the media, and a low control (i.e., untreated cells) to establish the basal intra- or extra-cellular activity.

All incubations were performed at 37 ^{o}C in a 5 % carbon dioxide (CO_2)-humidified incubator.

All absorbance measures (0.1 seconds) were performed, using BioTek's PowerWave Microplate Spectrophotometer and Gen5™ Data Analysis Software (Millennium Science; Mulgrave, Melbourne, VIC, Australia). Primary absorbance measurements were corrected for reference absorbance readings, and the average blank absorbance values were subtracted from those of all treatments and controls.

2.10.1 CCK-8 assay

The highly stable and water-soluble, yellow-coloured 2-(2-methoxy-4-nitrophenyl)-3-(4-nitrophenyl)-5-(2,4-disulfophenyl)-2H-tetrazolium salt (WST-8) is reduced by cellular dehydrogenase activity, through electron mediator 1-methoxy phenazine methosulphate (PMS), and generates a soluble, orange-colour formazan dye (740). This measurable colour change (as a surrogate for the number of live cells) was assessed, using the Cell Counting Kit (CCK)-8 (Dojindo Laboratories; Kumamoto, Japan).

In principal, post treatment, media was aspirated and replaced with media containing 10 % (v/v) CCK-8. Following further 1-2 hour incubation, aliquots of media containing CCK-8, were transferred to corresponding wells in 96-well micro-titre plates and their absorbance was measured at 450 nm wavelength.

Percentage cell viability was ascertained by normalizing the average absorbance values of treated cells to the average absorbance values of untreated cells, which were used as positive control and set at 100 %.

2.10.2 MTT assay

An assay aimed at measuring the metabolic activity of mitochondrial dehydrogenase and oxidoreductase enzymes, which reduce the yellow 3-(4,5-dimethylthiazol-2-yl)-2,5-diphenyltetrazolium bromide (MTT) to its insoluble, purple-coloured formazan crystals. The formazan precipitates are solubilised and the absorbance of the coloured solution is measured spectrophotometrically, which correlates to the number of viable cells (741, 742). Since the cells are lysed in this process, the MTT assay does not allow further analysis of the cells to be conducted.

Post treatment, media was aspirated to remove traces of coloured compounds (that may increase background absorbance and decrease the assay's sensitivity) and metal ions (which can chelate to the formazan) and replaced with media, containing 10 % (v/v) reconstituted MTT (3 mg/mL in PBS). Following additional two-hour incubation, MTT-containing media was aspirated, the formazan precipitates were dissolved in DMSO, aliquots of the coloured solution were transferred to corresponding wells in 96-well microplates and their absorbance was measured at 570 nm and 690 nm (background) wavelengths.

Percentage cell viability (*via* mitochondrial function) was calculated by comparing the average absorbance readings of treated cells to untreated cells (i.e., 100 % live cells).

2.10.3 MTS assay

Similar to the MTT assay, the MTS is a colourimetric test that reflects enzymatic activity in living, proliferating cells. In the presence of PMS, the water-soluble 3-(4,5-dimethylthiazol-2-yl)-5-(3-carboxymethoxyphenyl)-2-(4-sulfophenyl)-2H-tetrazolium salt (MTS) produces a formazan end product (743).

The lack for an intermediate solubilisation step in the MTS, as opposed to the MTT, assay renders it more convenient (i.e., simpler and faster); however, it also increases the susceptibility to colourimetric and other interference from residual material, which may affect its accuracy and reliability.

Post three-hour treatment, media was aspirated and replaced with media, containing 10 % (v/v) CellTiter 96® AQueous One Solution Reagent (Promega; Alexandria, Sydney, NSW, Australia). Following further two-hour incubation, aliquots of supernatant were transferred to corresponding wells in 96-well micro-titre plates and absorbance was measured at 492 nm and 690 nm (reference) wavelengths.

MTS reduction was quantified as a marker of cellular survival by standardising the average absorbance measures of treated with those of untreated cells (considered as 100 % viable).

2.10.4 LDH assay

Lactate dehydrogenase (LDH) is a ubiquitous and stable cytoplasmic enzyme that catalytically converts pyruvate, the final product of glycolysis, into lactate; coupled by the oxidation of nicotinamide adenine dinucleotide (NADH) into its NAD^+ form.

The LDH assay detects compromised membrane integrity and cell lysis by measuring the activity of LDH released from the cytosol of damaged or dying cells into the culture milieu (744). The increase in LDH enzymatic activity in the cell culture supernatant is relative to the amount of water-soluble, red formazan formed by catalyst cleavage of the yellow 2-(4-iodophenyl)-3-(4-nitrophenyl)-5-phenyl-2H-tetrazolium chloride (INT) and, thus, to the level of cell toxicity. In this manner, the LDH assay allows repeated sample of the media over time.

The extracellular LDH activity was assessed, using the Cytotoxicity Detection Kit (Roche; Hawthorn, Melbourne, VIC, Australia). In brief, following treatment, 48-well plates were centrifuged at 200 × *g* for 5 minutes at 4 ^oC to remove cells and cell debris from the serum-free media. Subsequently, aliquots of supernatant were transferred into corresponding wells in 96-well plates. Supernatant in each well was then diluted 1:2 in freshly prepared reaction mixture (1:45 ratio), consisting of reconstituted catalyst (diaphorase/NAD^+ mix) and dye solution (INT and sodium lactate). Microplates were shaken briefly and incubated for 30-45 minutes in the dark at room temperature. The absorbance of the coloured solution was measured at 490 nm and 630 nm (background) wavelengths.

In addition to the blank and low control (described in **section 2.10**), the LDH assay also included a high control (i.e., cells lysed with 2 % (v/v) Triton X-100 detergent) in order to establish the maximal LDH efflux into the media.

Percentage of cellular toxicity (proportional to LDH activity release) was expressed, using the following equation:

$$\text{Cytotoxicity (\%)} = \frac{\text{(sample – low control) x 100}}{\text{(high control – low control)}}$$

2.11 Bibliography software

Thomson Reuters EndNote X.8® Software was used to cite references appropriately in this dissertation.

2.12 Statistical analysis

All analyses described in this thesis comprised of 3-4 samples per treatment ($n \geq 3$) and a sample size of two or more independent experiments ($N \geq 2$).

Since each data set consisted of, at least, three unmatched groups (i.e. treatments), one-way analysis of variance (ANOVA) with a *post-hoc* test was performed. ANOVA with Dunnett's post-test was used to compare the means of all groups to the mean of the vehicle control. ANOVA with Tukey's post-test was used to compare the means of all groups to each other.

Where indicated, differences between means of two specific groups were identified by an unpaired Student's *t*-test, assuming unequal variance.

Means were determined to be significantly different when the probability value was equal to or less that 0.05 ($p \leq 0.05$).

GraphPad Prism® version 5.01 Software (San Diego, CA, USA) was used for to plot the data into tables and graphs, as well as for statistical data analysis. In all figures, data points represent average means and bars represent standard error of the means (S.E.M).

Chapter 3

Characterisation of CQ, metals and Aβ interactions in a mouse neuroblastoma cell line

Chapter 3

3.1 Introduction

As AD is becoming a global epidemic and the handful of FDA-approved medications for AD provides all but symptomatic relief to patients, the need for disease-modifying drugs (DMDs) is greater than ever. Based on the widely-accepted "amyloid hypothesis", scientists all over the world have been devoting a great deal of effort and funds to the discovery, research, pre-clinical and clinical development of experimental drugs that target different aspects of the tau and/or Aβ proteins (see **sections** and **Tables 1.2 - 1.3**, as well as **Appendix A**). Yet, all of these pharmacotherapeutics, including those that have reached advanced large-scaled human studies, have so far failed regardless of which class of drugs they belong to. Regrettably, one by one pharmaceutical companies have had to terminate the R&D of their lead candidates; some due to safety concerns and most due to lack of efficacy in humans.

These discouraging outcomes suggest one or more of the following possibilities: the investigational drugs tested so far did not target the pathological or toxic species of tau and/or Aβ, the current design of AD clinical trials does not allow the appropriate testing of "the amyloid hypothesis", or that "the amyloid hypothesis" does not (fully) explain the root cause of AD. If the latter one is true, there is a need for an alternative and/or complementary theory as to the underlying cause of AD and the identification of novel drug targets, which may still affect Aβ and/or tau indirectly.

One of many theories on AD pathogenesis, "the metal hypothesis" (545, 546), is based on a large and continually growing body of evidence of metal dyshomeostasis in AD (as detailed in **section 1.4**), as well as other neurodegenerative diseases (291-298). Our laboratory has been developing MPACs and other classes of DMDs aimed at preventing the binding of metals to pathologically-linked proteins and restoring metal homeostasis for the treatment AD and several other diseases (refer to **section 1.5.5**).

CQ is small, lipophilic, orally bioavailable, BBB-permeable and able to bind divalent metal ions with moderate affinity (see **section 1.5.5**, including **Table 1.5**). Owing to these properties, CQ was chosen as an archetype MPAC (PBT1; Prana Biotechnology, Parkville, Melbourne, Victoria, Australia) and tested, by us and by others, as a potential therapeutic for various diseases, including AD.

As proof-of-principle, our group has shown that CQ inhibits metal-induced Aβ aggregation and toxicity *in vitro* (479, 700). Subsequent studies found that CQ also prevents and rescues Aβ-mediated toxicity in cultured astrocytes (707) and neuronal cells (549), respectively. It was later demonstrated that administration of CQ led to decreased amyloid burden in brains of Tg2576 (699) and APP/PS1 mice (708, 709), as well as improved cognitive performance (700).

In human studies, CQ treatment of two FAD patients was reported to stop further cognitive deterioration and improve brain glucose metabolism (745). CQ given to small cohorts of LOAD patients in early-stage clinical trials also led to a slowing of cognitive decline, which was accompanied by increased plasma Zn and decreased plasma $A\beta_{42}$ levels, but had no effect on plasma Cu or CSF $A\beta_{42}$ levels (710, 711). Further clinical development of CQ was discontinued due to manufacturing impurities; however, its MOA remains of great interest as it affects the ongoing R&D of more advanced 8-HQs, such as PBT2 (700, 713, 714, 717, 718).

CQ is referred to as a conventional metal chelator; yet, pre-clinical and clinical data indicate that CQ affects not only several metal ions, but also an array of biological molecules (746-751). While the mechanism(s) by which CQ exerts these effects remain poorly understood, it is unlikely that CQ acts as a mere chelator. The complex MOA of CQ is evident as different effects of the drug on metals and/or Aβ have been reported in a variety of AD models. Equally important, and still unexplored, is the effect(s) of metal ions and/or Aβ on CQ.

Answering this question is difficult as CQ has poor solubility in neutral aqueous solutions, it adsorbs strongly onto various surfaces, and its structure does not allow it to be biotin-labelled or fluorescently tagged. Moreover, since marked differences were observed between 8-HQ, CQ (5-chloro-7-iodo-8-HQ) and PBT2 (2-(dimethylamino) methyl-5, 7-dichloro-8-HQ) and other 8-HQ derivatives (700, 714, 751-753), any change to the structure of CQ may affect its activity.

In the past, the levels of CQ and its metabolites in biological samples, as well its pharmacokinetics (PK) (i.e., absorption, distribution, metabolism and excretion; ADME) in animals and humans, were determined by using gas-liquid chromatography (GLC) (754), gas chromatography mass spectroscopy (GC-MS) (662, 666, 755, 756), high-performance liquid chromatography (HPLC) (667, 668, 711, 757, 758), or carbon 14 and/or iodine 123, 125 or 131-radiolabelled CQ (^{14}C-CQ and $^{123/125/131}$I-CQ) (663, 664, 759-763).

In recent years, our research team established that the binding affinity of ^{125}I-CQ (737) to synthetic and brain-derived Aβ-Zn aggregates occurs in a saturated manner, and determined the PK of CQ in Tg2576 mice compared to WT mice (763). In addition, Dr. Opazo C. and Dr. Bellingham S. in our laboratory set to utilize ^{125}I-CQ in order to investigate the interplay between CQ, metals and Aβ in an Neuro-2a (N2a) mouse neuroblastoma cell line (described in **section 3.2.1**).

In pilot experiments, N2a cells were incubated for an hour with 100 pM ^{125}I-CQ in the absence or presence of several metals (10 μM) in Locke's buffer (pH 7.4; as per **section 2.4**). Under these conditions, it was found that levels of ^{125}I-CQ in N2a cell lysates were significantly higher in the presence of $CuCl_2$ and $ZnCl_2$, but not in the presence of $AgNO_3$ or $FeSO_4$, compared to ^{125}I-CQ alone (depicted in **Fig. 3.1.1**).

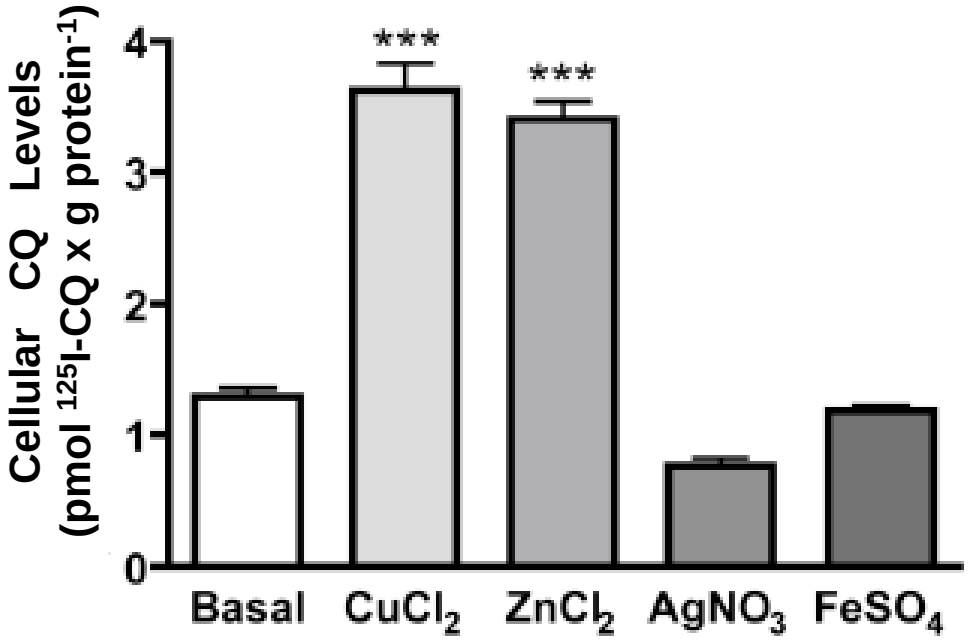

Figure 3.1.1 Effect of metals on the levels of CQ in N2a cells

Exposure to ^{125}I-CQ in the presence of $CuCl_2$ and $ZnCl_2$ selectively induced an increase in the levels of ^{125}I-CQ in N2a cell lysates, compared to ^{125}I-CQ alone.
*ANOVA; ***p < 0.001, compared to basal. Bars represent mean ± S.E.M, n = 5*
(Modified from Bellingham S. et. al., unpublished data).

The experiments described in this chapter were designed to further investigate the interplay between CQ and metals (Cu and Zn), as well as Aβ, using a similar experimental set-up in a continuing effort to elucidate the MOA of CQ.

3.2 Experimental Methods

3.2.1 Cell line and culture conditions

The Neuro-2a (N2a) clone was established in 1967 by Klebe and Ruddle from a spontaneous tumour in a strain A albino mouse (764). N2a cells are morphologically rounded with extended neurite-like processes and are known to contain substantial amount of microtubules and filaments.

Mouse N2a neuroblastoma cells were obtained from the American Type Culture Collection (ATCC; Manassas, VA, USA). Cells were cultured in Dulbecco's Modified Eagle's Medium (DMEM) containing GlutaMAX™ (stabilized L-alanyl-L-glutamine di-peptide; 4 mM), HEPES (4-(2-hydroxyethyl)-1-piperazineethanesulfonic acid; 25 mM) and high D-glucose (25 mM), which was supplemented with 10 % (v/v) heat-inactivated foetal calf serum (FCS) (Bovogen Biologicals; Essendon, Melbourne, VIC, Australia) and penicillin (100 units/mL)/streptomycin sulphate (100 μg/mL) antibiotic agents.
Upon reaching confluence, cells were sub-cultivated (i.e., dispersed by 0.25 % (w/v) trypsin/0.2 % (w/v) EDTA solution and re-seeded) 2-3 times per week at a 1:10-1:15 (v/v) ratio.

3.2.2 Preparation of Locke's buffer

To avoid any metal chelation by components of culture media (**section 3.2.1** above), serum-free and neutral (pH 7.4) Locke's buffer was used as the experimental media.
Locke's buffer consisted of: 154 mM sodium chloride (NaCl), 5.6 mM potassium chloride (KCl), 2.3 mM calcium chloride ($CaCl_2$), 1 mM magnesium chloride ($MgCl_2$), 3.6 mM sodium bicarbonate ($NaHCO_3$), 5 mM glucose and 5 mM HEPES.
Locke's buffer was stored at 4 ^oC and, prior to experimental use, was heated to 37 ^oC in a water bath.

3.2.3 Preparation of CQ

1 mM CQ stock solutions were freshly prepared by dissolving the drug in DMSO. Serial dilution in DMSO was performed in order to reach a concentration of 100 nM.
According to preliminary data (see **Fig. 3.1.1**), CQ was added to Locke's buffer immediately prior to exposure of N2a cells at a final concentration of 100 pM.

3.2.4 Preparation of metals

1 mM copper glycine stock solution was prepared by dissolving cupric chloride ($CuCl_2$) and glycine (1:6 molar ratio) in water (765).

2 mM stock solution of Zn was prepared by dissolving zinc chloride ($ZnCl_2$) in water.

Metal ions were added to Locke's buffer immediately prior to exposure of N2a cells at a final concentration of 10 μM.

3.2.5 Preparation of soluble Aβ

Following an established method (639), lyophilised $A\beta_{42}$ powder was equilibrated from -80 ^{o}C to room temperature for 30 minutes to minimize condensation. The peptide was weighed on a microbalance, dissolved in 1,1,1,3,3,3-hexafluoro-2-propanol (HFIP), aliqouted (~0.3 mg/mL) into 1.5 mL tubes and air-dried at room temperature for two hours to remove any pre-formed aggregated material. Excess HFIP was evaporated by vacuum centrifugation for 30 minutes. Aliquots were then stored at -20 ^{o}C.

On experimental days, $A\beta_{42}$ films were thawed on ice, re-suspended in 20 mM sodium hydroxide (NaOH; 1:2 w/v) and briefly mixed, using a vortex instrument. The NaOH-$A\beta_{42}$ mixture was diluted 1:4 (v/v) in Dulbecco's PBS (DPBS; PBS with 0.9 mM calcium chloride ($CaCl_2$) and 0.5 mM magnesium chloride ($MgCl_2$); pH 7.4). The $A\beta_{42}$ solution was briefly mixed, using a vortex instrument, followed by sonication in an ice-containing Ultrasonic Cleaner (Unisonics; Brookvale, Sydney, NSW, Australia) for 10 minutes and centrifugation at 16,000 × *g* for 15 minutes at 4 ^{o}C to remove any aggregates. The supernatant was transferred to a 1.5 mL tube and placed on ice.

To determine the soluble $A\beta_{42}$ stock concentration, an aliquot of the supernatant was diluted 1:50 (v/v) in PBS (pH 7.4; at room temperature), mixed and transferred into a 1 cm quartz cuvette. Triplicate absorbance measurements (optical density units; OD) were performed at 214 nm wavelength, using Lambda 25 UV/Vis Spectrophotometer and WinLab Software (PerkinElmer; Glen Waverley, Melbourne, VIC, Australia). Average $A\beta_{42}$ content (ng/μL) was corrected for background signal (i.e., PBS blank) and the molar concentration of $A\beta_{42}$ was calculated, using Lambert-Beer's law:

$A_{214\ nm}$ × dilution factor (= 50) / molar extinction coefficient (= 75887 litre/mole/cm)

Based on the $A\beta_{42}$ concentration, the volumes required for treating N2a cells with soluble $A\beta_{42}$ at a final concentration of 10 μM or for preparing stock solutions of aggregated $A\beta_{42}$ (see **section 3.2.6** below), with and without metals, were calculated.

3.2.6 Preparation of aggregated Aβ and Aβ-metal complexes

In order to prepare stock solutions of self-aggregated $A\beta_{42}$ and aggregated metal-$A\beta_{42}$ complexes (~100-180 μM), $A\beta_{42}$ was prepared as described above in **section 3.2.5** and respectively incubated alone or together with either $CuCl_2$ or $ZnCl_2$ (1:1 molar ratio in PBS; pH 7.4) overnight at 37 ^oC on a rotating wheel. The following day, 2 mL tubes were centrifuged at 16,000 × *g* for 15 minutes at 4 ^oC, supernatants were discarded of and pellets, containing $A\beta_{42}$ and metal-$A\beta_{42}$ aggregates, were re-suspended in original volume of PBS.

Aggregated $A\beta_{42}$ and metal-$A\beta_{42}$ complexes were kept on ice until added to Locke's buffer immediately prior to exposure of N2a cells at a final concentration of 10 μM.

3.2.7 Pharmacokinetic assays

For all experimental procedures described in this chapter, N2a cells were seeded in 75 cm^2 flasks at a density of 1 $\times 10^6$ cells/cm^2 (determined by a haemocytometer and trypan blue staining) and grown for 3-4 days until reaching ~85-90 % confluence.

On experimental days, culture media was aspirated and cells were rinsed with PBS, prior to incubation in triplicates with a variety of treatments or with vehicle control (equal volumes of water and DMSO as treatments) at 37 ^oC in a 5 % carbon dioxide (CO_2)-humidified incubator.

For uptake experiments (see **sections 3.3.1-3.3.4**), N2a cells were incubated for an hour with Locke's buffer, containing either vehicle control, 100 pM CQ or 10 μM: soluble $A\beta_{42}$ (Sol. $A\beta_{42}$), $CuCl_2$, $ZnCl_2$, soluble $A\beta_{42}$ together with either $CuCl_2$ or $ZnCl_2$ (1:1 molar ratio), pre-aggregated $A\beta_{42}$ (Agg. $A\beta_{42}$), and either pre-aggregated Cu-$A\beta_{42}$ or Zn-$A\beta_{42}$ (1:1 molar ratio) – in the absence and presence of 100 pM CQ.

For endocytosis/exocytosis inhibition experiments (refer to **sections 3.3.5-3.3.8**), N2a cells were pre-incubated for two hours with Locke's buffer, containing either vehicle control or 20 μM nocodazole, and subsequently co-incubated for a further hour with Locke's buffer, containing either 100 pM CQ alone or together with 10 μM: soluble $A\beta_{42}$ (Sol. $A\beta_{42}$), $CuCl_2$, $ZnCl_2$, soluble $A\beta_{42}$ together with either $CuCl_2$ or $ZnCl_2$ (1:1 molar ratio), pre-aggregated $A\beta_{42}$ (Agg. $A\beta_{42}$), and either pre-aggregated Cu-$A\beta_{42}$ or Zn-$A\beta_{42}$ (1:1 molar ratio) – in the continuing absence and presence of 20 μM nocodazole.

For lysosomal/autophagy inhibition experiments (see **sections 3.3.9-3.3.15**), N2a cells were pre-incubated for two hours with Locke's buffer, containing either vehicle control or 3-methyladenine (3-MA; 5mM) and ammonium chloride (NH_4Cl; 20 mM). Then, cells were co-incubated for a further hour with Locke's buffer, containing 100 pM CQ alone or 10 μM of: soluble $A\beta_{42}$ (Sol. $A\beta_{42}$), $CuCl_2$, $ZnCl_2$, soluble $A\beta_{42}$ together with either $CuCl_2$ or $ZnCl_2$ (1:1 molar ratio), pre-aggregated $A\beta_{42}$ (Agg. $A\beta_{42}$), and either pre-aggregated Cu-$A\beta_{42}$ or Zn-$A\beta_{42}$ (1:1 molar ratio) – in the absence and presence of 100 pM CQ, and the continuing absence or presence of 5 mM 3-MA and 20 mM ammonium chloride (NH_4Cl).

Following incubation in these three types of pharmacokinetic assays, treatment media was aspirated and cells were rinsed with ice-cold Locke's buffer. Cells were then incubated with 0.25 % (w/v) trypsin/0.2 % (w/v) EDTA solution for 2 minutes at 37 °C in a 5 % carbon dioxide (CO_2)-humidified incubator to remove membrane-bound material and disperse cells. Cell detachment was verified, using an inverted microscope. To stop the reaction, ice-cold Locke's buffer was added to the flasks and cells were harvested into 15 mL tubes, using a rubber-bladed cell scraper (Sigma-Aldrich; Castle Hill, Sydney, NSW, Australia). To remove cell debris and/or un-bound material, the cell suspension was centrifuged at 1,200 × *g* for 5 minutes at 4 ^{o}C and supernatant was discarded. The cell pellets were immediately frozen and stored at -80 °C.

Cell pellets were later thawed on ice and re-suspended in ice-cold PBS with added EDTA-free protease inhibitor cocktail (Roche; Hawthorn, Melbourne, VIC, Australia). Cell suspensions were transferred into 1.5 mL tubes on ice and manually homogenised, using a 25 gauge needle. Aliquots of the cell lysates were re-frozen and stored at -80 °C, until analyses were performed.

To assess the cellular uptake of Aβ and metals (as oppose to material that may still be bound to the outer cell membrane even after several washes post treatment), N2a lysates were fractionated in a step-wise centrifugation process. In order to separate the nuclear fraction (whole cells and nuclei), the remainder cell lysates were centrifuged at 1,000 × *g* for 10 minutes at 4 ^{o}C and the supernatants transferred into 2 mL ultra-centrifuge tubes. The post-nuclear supernatant fractions were then centrifuged at 100,000 × *g* for an hour at 4 ^{o}C, using an Optima MAX-E Ultracentrifuge (Beckman Coulter; Lane Cove, Sydney, NSW, Australia). Pellets (containing microsomal fractions) and supernatants (containing soluble cytosolic fractions) were immediately frozen and stored at -80 ^{o}C, until analyses were performed.

3.2.8 Protein analysis using BSA assay

The widely-used bicinchoninic acid (BCA) protein assay (766) is based on the reduction of Cu^{2+} by peptide bonds in an alkaline environment (known as the biuret reaction), and the coordination of Cu^{1+} by BCA (1:2 molar ratio). This results in a colourimetric reaction (colour changes from pale blue to deep purple), which can be spectrophotometrically detected and exhibits high linearity with protein concentrations near 562 nm absorbance wavelength.

Cellular protein levels were determined, using the Pierce™ BCA™ Protein Assay Kit (Thermo Fisher Scientific; Scoresby, Melbourne, VIC, Australia), according to the manufacturer's instructions. In brief, an Albumin Standard ampoule (2 mg/mL bovine serum albumin (BSA)) was serially diluted in order to create a standard curve of known concentrations (0.05-2 mg/mL). Samples (100,000 × *g* supernatant; i.e., cytosolic N2a fractions) were thawed on ice, diluted 1:1 (v/v) in water and centrifuged at 13,000 revolutions per minute (rpm) for 15 seconds at room temperature.

BCA standards and samples were pipetted onto a 96-well microplate. Working BCA reagent A (BCA in 0.1 M sodium hydroxide (NaOH)) and reagent B (consisting of 4 % (w/v) copper sulphate ($CuSO_4$) in water) were combined at a 50:1 (v/v) ratio and mixed for 5-10 seconds, using a vortex instrument. Using a multi-pipette, the BCA reagent mixture was added to the BCA standards and samples at a 20:1 (v/v) ratio. Microplate was covered in foil and incubated at 60 ºC for 25 minutes. Microplate was subsequently removed from the incubator and equilibrated to room temperature for 5 minutes, prior to being placed in BioTek's PowerWave Microplate Spectrophotometer (Millennium Science; Mulgrave, Melbourne, VIC, Australia) and shaken for 3 seconds.

For each sample, triplicate absorbance measurements (optical density units; OD) were performed at 540 nm wavelength. Using Gen5™ Data Analysis Software (Millennium Science; Mulgrave, Melbourne, VIC, Australia), the protein content (mg/mL) in each sample was corrected for background signal/blank (i.e., BCA working solutions mix only) and for dilution factor (i.e., 2), extrapolated from the linear curve fit, and average of triplicate readings was calculated.

3.2.9 Metal analysis using ICPMS

To determine the Cu and Zn levels in control and treated N2a cells, aliquots of the 100,000 × *g* supernatant fractions were diluted in 1 % (v/v) nitric acid (HNO_3; Merck; Kilsyth, VIC, Australia) at a 1:10 (v/v) ratio (the minimum dilution needed to overcome matrix interference with the instrument).

ICPMS measurements of ^{57}Fe, ^{65}Cu, ^{66}Zn and other isotopes were performed, using an Ultramass 700 Spectrometer (Varian; Mulgrave, Melbourne, VIC, Australia) under operating conditions suitable for routine multi-element analysis: peak-hopping scan mode, 1 point per peak, 50 scans per replicate, 0.163 seconds per scan, 3 replicates per sample. Plasma gas (Argon) and auxiliary flow rates of 15 and 1.5 litre per minute, respectively. R_F power was 1.2 kW. Samples were introduced, using a concentric glass nebulizer, at a flow rate of 0.92 litres per minute.

The instrument was calibrated, using a certified multi-element ICPMS standard solution (ICPMS-CAL2-1, AccuStandard; New Haven, CT, USA), containing 0, 10, 50 and 100 parts per billion (ppb) of the elements of interest in 1 % (v/v) nitric acid. A certified internal standard solution (ICPMS-IS-MIX1-1, AccuStandard; New Haven, CT, USA), containing 100 ppb of Yttrium (^{89}Y), was added as an internal matrix and instrument performance control.

Sample measurements were usually above the ICPMS detection limits; however, in samples that contained metal levels (mainly pertaining to Cu) close to or below the detection limits of the instrument, the values were corrected to zero.

WinMass™ Software for ICPMS (Varian; Mulgrave, Melbourne, VIC, Australia) was used for data analysis and for conversion of metal concentrations from ppb to μM, using the following formula:

(μmol/L) = [(raw ppb value) x (dilution factor; 10)] / (molecular weight of the element)

Cellular metal levels (μmol/L) were then normalised to corresponding protein levels (g/L; as determined by BCA assay described in **section 3.2.8**), and are expressed as the fold change relative to metal concentrations in vehicle-treated N2a cells (set at 100 %).

3.2.10 Aβ analysis using double antibody capture ELISA

To determine the $A\beta_{42}$ levels in N2a cells, C384-well OptiPlate microplates (Greiner; Frickenhausen, Germany) were coated with G2-11 capture antibody (monoclonal IgG1 antibody with high binding affinity and specificity towards the C-terminal of $A\beta_{42}$ (767); 0.02 μg/μL in a carbonate buffer (15 mM sodium carbonate (Na_2CO_3) and 35 mM sodium bicarbonate ($NaHCO_3$); pH 9.6)), at a final concentration of 0.5 μg/well. Microplates were incubated overnight at 4 ^oC.

The following day, plates were washed with PBS, containing 0.05 % (v/v) Tween-20 (PBS-T; pH 7.4), in order to remove any un-bound antibody. To prevent non-specific binding, plates were incubated with blocking buffer (pH 7.4), consisting of 3.5 % (w/v) superblock (Thermo Fisher Scientific; Scoresby, Melbourne, VIC, Australia) in PBS-T, for one hour at room temperature. Plates were again washed with PBS-T, followed by the addition of biotin-labelled W0-2 detection antibody (monoclonal IgG2a antibody that binds to $A\beta_{5\text{-}8}$ (767); 2 ng/μL in blocking buffer), at a final concentration of 20 ng/well.

$A\beta_{42}$ standards and samples (aliquots of 100,000 × *g* supernatants), diluted 1:4 (v/v) in guanidine hydrochloride (final concentration of 0.5 M), were added in triplicates and the plates were incubated overnight at 4° C. Microplates were then washed with PBS-T to remove any un-bound peptide. Next, streptavidin-labelled Europium (PerkinElmer; Glen Waverley, Melbourne, VIC, Australia), diluted 1:1000 (v/v) in blocking buffer, was added and the plates were incubated for an hour at room temperature. Microplates were subsequently washed with PBS-T, prior to the addition of an enhancement solution (PerkinElmer; Glen Waverley, Melbourne, VIC, Australia), in order to detect the bound antibody.

Spectroscopic measurements (optical density units; OD) were performed at 340 nm excitation and 613 nm emission wavelengths, using a WALLAC Victor^2 1420 Multilabel Plate Reader (PerkinElmer; Glen Waverley, Melbourne, VIC, Australia). $A\beta_{42}$ levels were above the detection limit of the assay and their quantification was calibrated against peptide standards, after subtraction of background fluorescence in the absence of sample (i.e., blank). Cellular $A\beta_{42}$ levels (pmol/mL) were normalised to the cellular protein levels (mg/mL; as determined by BCA assay described in **section 3.2.8**) and are expressed relative to $A\beta_{42}$ concentrations in vehicle-treated mouse N2a cells (set at 0% since the antibodies used in this procedure specifically identify human Aβ).

3.3 Experimental Results

3.3.1 Effect of CQ and/or Aβ on the cellular uptake of Cu

The Cu-promoted uptake of CQ into N2a cells (illustrated in **Fig. 3.1.1**) prompted an examination into the reciprocal effect of CQ on the cellular uptake of Cu. Thus, the uptake of $CuCl_2$ into N2a cells was studied on its own, with soluble $A\beta_{42}$ or as pre-aggregated Cu-$A\beta_{42}$ complexes, in the absence and presence of CQ (refer to **section 3.2.7**). Concomitant incubation of $CuCl_2$ with soluble $A\beta_{42}$ was performed to try and imitate toxic Cu-derived diffusible ligands (CuDDLs) (554, 768, 769), while pre-aggregated Cu-$A\beta_{42}$ complexes were used to emulate Cu-enriched amyloid plaques (APs) (359, 395-397).

Following one-hour incubation in Locke's buffer, Cu levels in N2a cells treated with CQ alone or with soluble $A\beta_{42}$, in the absence and presence of CQ, were not different to each other or to Cu levels in vehicle-treated N2a cells (**Fig. 3.3.1**). Therefore, it can be deduced that Aβ and/or CQ do not modulate endogenous neuronal Cu levels.

As expected, significant Cu uptake was observed in N2a cells treated with $CuCl_2$, both in the absence and presence of CQ, compared to vehicle-treated N2a cells (~5 fold increase; **Fig. 3.3.1**). Yet, this significant Cu uptake was similar in N2a cells treated with $CuCl_2$ in the absence, as compared to in the presence, of CQ (**Fig. 3.3.1**).
The rapid Cu uptake suggests that Cu enters neuronal cells by an active transport mechanism that is unrelated to CQ.

Interestingly, significant Cu uptake occurred in N2a cells co-treated with $CuCl_2$ and soluble $A\beta_{42}$; not only compared to vehicle-treated N2a cells, but also compared to N2a cells treated with $CuCl_2$ alone (~6.5 and 1.5 fold increase, respectively; **Fig. 3.3.1**). Significant Cu uptake, compared to vehicle-treated N2a cells, was also detected in N2a cells co-treated with $CuCl_2$ and soluble $A\beta_{42}$ in the presence of CQ; however, Cu uptake was considerably diminished in N2a cells treated with $CuCl_2$ and soluble $A\beta_{42}$ in the presence, compared to the absence, of CQ (~1.5 fold decrease; **Fig. 3.3.1**). In fact, Cu uptake into N2a cells treated with $CuCl_2$ and CQ, in the presence of soluble $A\beta_{42}$, was comparable to Cu uptake in N2a cells treated with $CuCl_2$, with and without CQ, in the absence of soluble $A\beta_{42}$ (**Fig. 3.3.1**).
Together, these data confirmed that soluble Aβ interacts with Cu and impacts on Cu uptake into neuronal cells, while CQ may sequester Cu in the presence of soluble Aβ.

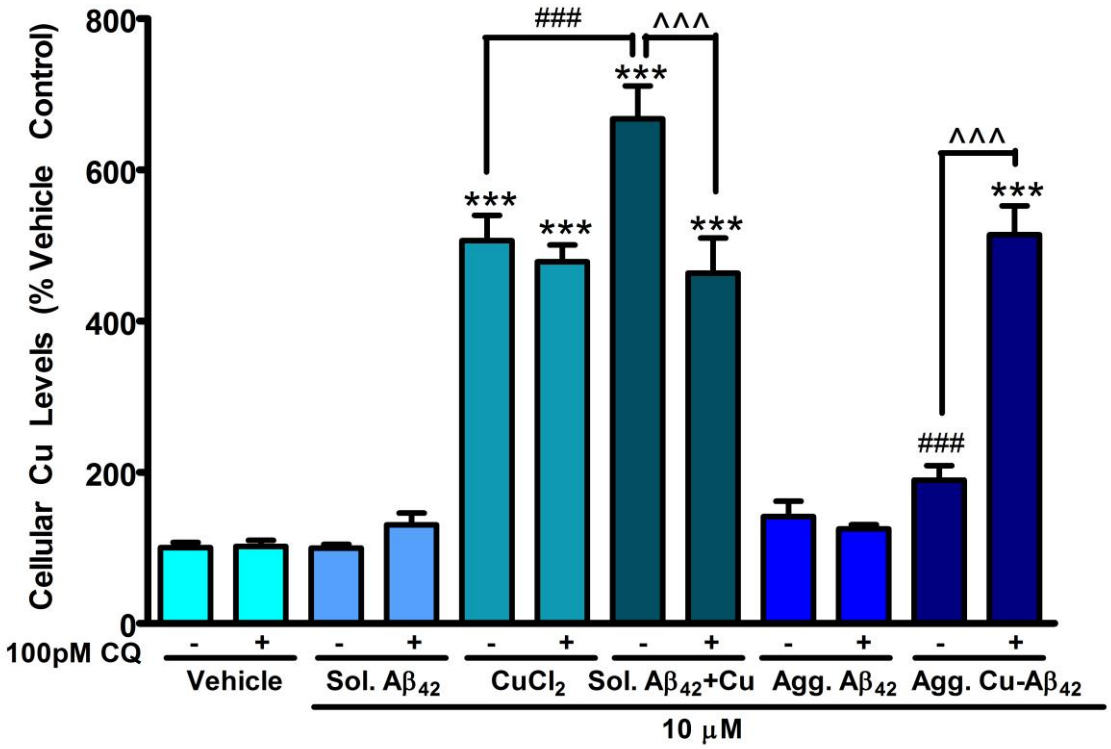

Figure 3.3.1 Effect of CQ and/or Aβ on the uptake of Cu into N2a cells

Exposure of N2a cells to $CuCl_2$, with and without CQ, resulted in significant Cu uptake, which was further potentiated by soluble $A\beta_{42}$ (Sol. $A\beta_{42}$). However, addition of CQ suppressed the soluble $A\beta_{42}$-induced Cu uptake to levels comparable to those of N2a cells exposed to $CuCl_2$, with or without CQ.

The opposite effect was observed when Cu was complexes to aggregated $A\beta_{42}$ (Agg. $A\beta_{42}$). Exposure of N2a cells to pre-aggregated Cu-$A\beta_{42}$ did not result in significant Cu uptake; but, addition of CQ resulted in significant Cu uptake.

ANOVA with Tukey post-hoc test;

****$p < 0.001$ compared to vehicle; ###$p < 0.001$ compared to $CuCl_2$; ^^^$p < 0.001$*

Bars represent mean ± S.E.M, $n \geq 3$

Following one hour incubation in Locke's buffer, Cu levels in N2a cells treated with pre-aggregated $A\beta_{42}$, in the absence and presence of CQ, were no different to each other or to Cu levels in vehicle-treated N2a cells (**Fig. 3.3.1**).

Cu levels in N2a cells treated with pre-aggregated Cu-$A\beta_{42}$ complexes in the absence of CQ were also similar to vehicle-treated N2a cells and were significantly lower than Cu levels in N2a cells treated with $CuCl_2$ alone (~2.5 fold decrease; **Fig. 3.3.1**). Conversely, significant Cu uptake was observed in N2a cells co-treated with pre-aggregated Cu-$A\beta_{42}$ complexes and CQ; not only compared to vehicle-treated N2a cells, but also compared to N2a cells treated with pre-aggregated Cu-$A\beta_{42}$ complexes in the absence of CQ (~5 and 2.5 fold increase, respectively; **Fig. 3.3.1**).

Overall, data indicated that once Cu was complexed to aggregated Aβ it could not be delivered into neuronal cells, which might contribute to the abnormal distribution of Cu seen in the AD brain (345, 359, 376-378). Importantly, treatment with CQ was able to free Cu from its complex with Aβ and facilitate its uptake into neuronal cells.

3.3.2 Effect of CQ and/or Aβ on the cellular uptake of Zn

Similar to Cu, the Zn-induced uptake of CQ into N2a cells (see **Fig. 3.1.1**) has also instigated an investigation into the effect of CQ on the cellular uptake of Zn. Therefore, the uptake of $ZnCl_2$ into N2a cells was examined alone, together with soluble $A\beta_{42}$ or as pre-aggregated Zn-$A\beta_{42}$ complexes, in the absence and presence of CQ (**section 3.2.7**). Co-incubation of $ZnCl_2$ with soluble or pre-aggregated $A\beta_{42}$ was performed in order to determine whether the solubility state of the Aβ impacted on the cellular uptake of Zn.

Under the conditions tested, Zn levels in vehicle-treated N2a cells were no different to Zn levels in N2a cells treated with $ZnCl_2$, soluble $A\beta_{42}$ with and without $ZnCl_2$, and pre-aggregated $A\beta_{42}$ with and without $ZnCl_2$ - either in the absence or presence of CQ (**Fig. 3.3.2**).

This was surprising as these experiments were done under physiological, neutral conditions (Locke's buffer; pH 7.4) that have been shown to favour Zn binding to Aβ (447, 448, 450). On the other hand, it is known that the binding affinity and stability of CQ are greater for Cu^{2+} than it is for Zn^{2+} (695, 770); which could explain why, under the same conditions, $A\beta_{42}$ and CQ affected Cu, but not Zn, uptake into N2a cells.

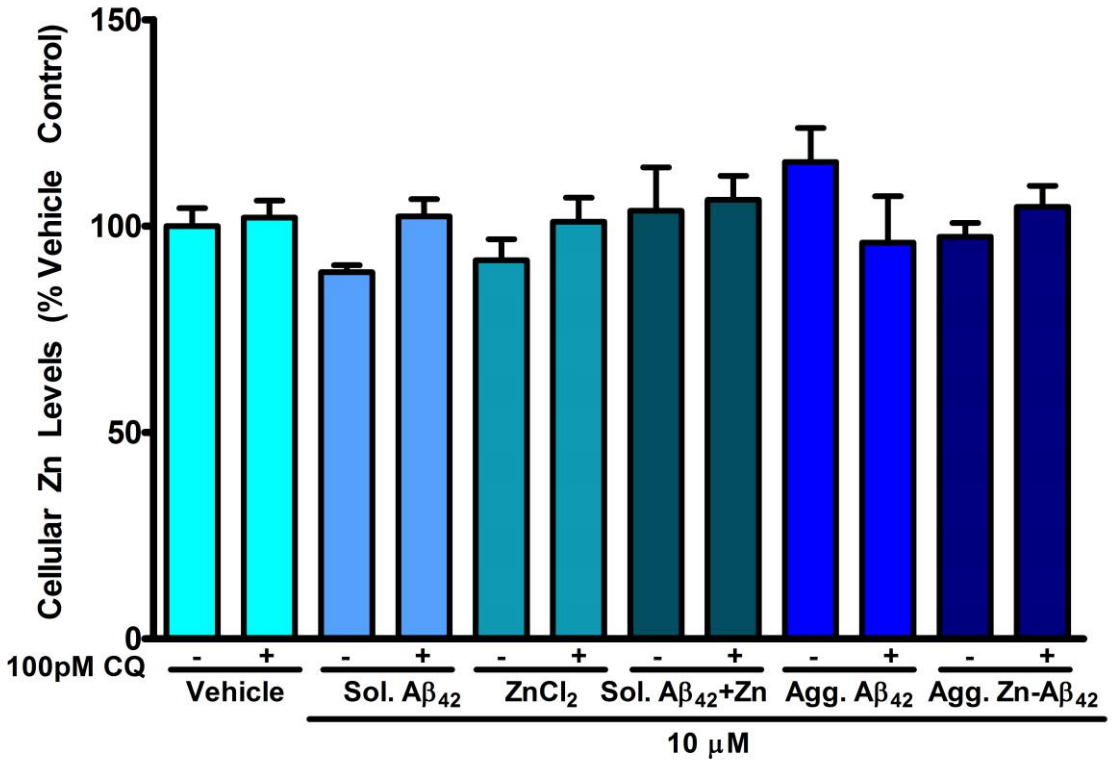

Figure 3.3.2 Effect of CQ and/or Aβ on the uptake of Zn into N2a cells

Exposure of N2a cells to $ZnCl_2$ and/or $A\beta_{42}$ (soluble or aggregated), did not result in cellular uptake of Zn. Addition of CQ to these conditions did not affect the uptake of Zn into N2a cells.

ANOVA with Tukey post-hoc test; Bars represent mean ± S.E.M, $n \geq 3$

3.3.3 Effect of CQ and/or Cu on the cellular uptake of Aβ

Since it was determined that Cu uptake into N2a cells was influenced by Aβ and CQ (**Fig. 3.3.1**); the uptake of $A\beta_{42}$ into N2a cells was explored, under the same conditions (as per **section 3.2.7**).

Following one hour incubation in Locke's buffer, $A\beta_{42}$ levels in N2a cells treated with CQ and/or $CuCl_2$, were not different to each other or to $A\beta_{42}$ levels in vehicle-treated N2a cells (**Fig. 3.3.3**). This is not surprising since these conditions only included endogenous murine Aβ (i.e., no exogenously added human $A\beta_{42}$), which cannot be detected by the ELISA used (see **section 3.2.10**).

Interestingly, $A\beta_{42}$ levels in N2a cells treated with either soluble or pre-aggregated $A\beta_{42}$, both in the absence and presence of CQ, were also similar to $A\beta_{42}$ levels in vehicle-treated N2a cells (**Fig. 3.3.3**).

These findings suggest that Aβ does not readily enter neuronal cells, regardless of its solubility state, and may require other factors to facilitate its influx.

$A\beta_{42}$ levels in N2a cells co-treated with soluble $A\beta_{42}$ and $CuCl_2$ were no different to $A\beta_{42}$ levels in N2a cells treated with either vehicle or with soluble $A\beta_{42}$ (**Fig. 3.3.3**). Conversely, significant $A\beta_{42}$ uptake was detected in N2a cells treated with soluble $A\beta_{42}$ and $CuCl_2$ in the presence of CQ, compared to vehicle-treated N2a cells, as well as to N2a cells treated with soluble $A\beta_{42}$ and either CQ or $CuCl_2$ (**Fig. 3.3.3**).

Similar results were observed with pre-aggregated Cu-$A\beta_{42}$ complexes. $A\beta_{42}$ levels in vehicle-treated N2a cells were comparable to $A\beta_{42}$ levels in N2a cells treated with pre-aggregated Cu-$A\beta_{42}$ complexes in the absence of CQ (**Fig. 3.3.3**). Yet, significant $A\beta_{42}$ uptake occurred in N2a cells treated with pre-aggregated Cu-$A\beta_{42}$ complexes in the presence of CQ; not only compared to vehicle-treated N2a cells, but also compared to N2a cells treated with either pre-aggregated $A\beta_{42}$ and CQ in the absence of $CuCl_2$ or with pre-aggregated Cu-$A\beta_{42}$ complexes in the absence of CQ (**Fig. 3.3.3**).

Collectively, the results demonstrated that Cu and CQ, each on its own, do not affect the cellular uptake of Aβ. Instead, Cu and CQ act synergistically to enhance the uptake of both soluble and aggregated Aβ into neuronal cells.

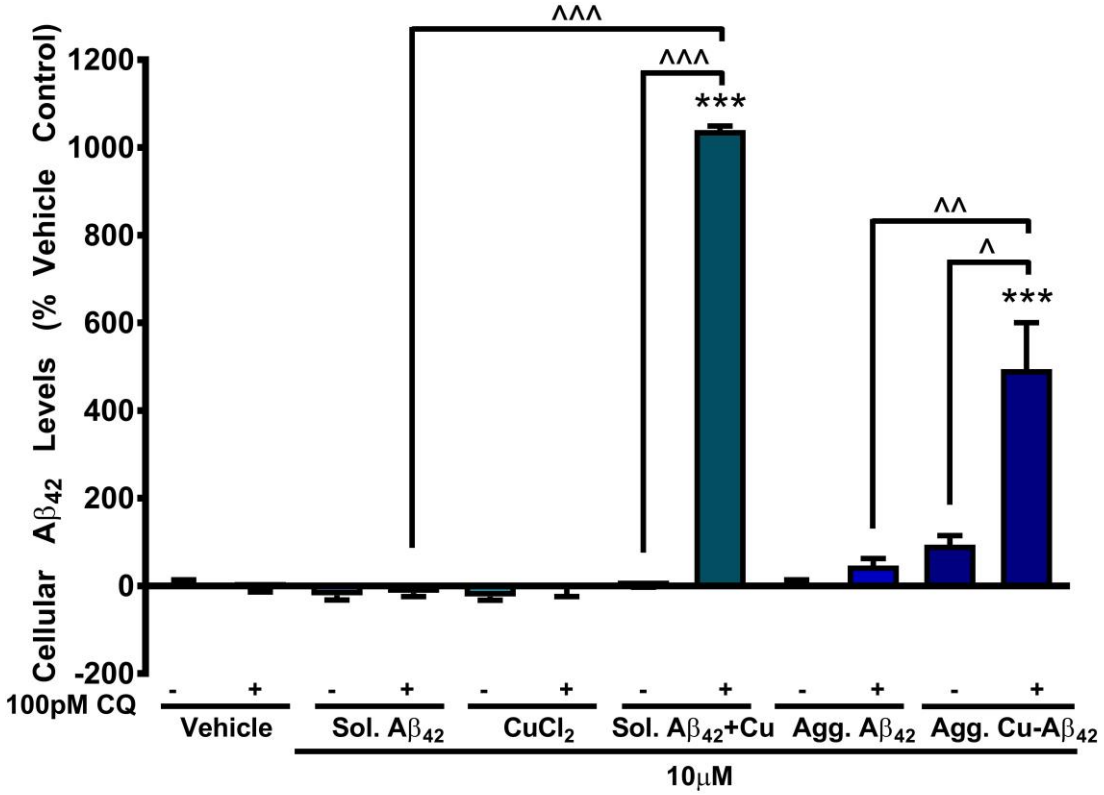

Figure 3.3.3 Effect of CQ and/or Cu on the uptake of Aβ into N2a cells

Exposure of N2a cells to soluble $A\beta_{42}$ (Sol. $A\beta_{42}$) or aggregated $A\beta_{42}$ (Agg. $A\beta_{42}$), with and without either CQ or CuCl2, did not result in cellular uptake of Aβ.

In contrast, addition of both $CuCl_2$ and CQ together to N2a cells exposed to aggregated (Agg. $A\beta_{42}$), and especially, soluble $A\beta_{42}$ (Sol. $A\beta_{42}$) resulted in significant Aβ uptake.

ANOVA with Tukey post-hoc test;

****$p < 0.001$ compared to vehicle; ^$p < 0.05$, ^^$p < 0.01$, ^^^$p < 0.001$*

Bars represent mean ± S.E.M, $n \geq 3$

3.3.4 Effect of CQ and/or Zn on the cellular uptake of Aβ

Despite CQ and/or Aβ having no effect on Zn uptake into N2a cells (see **Fig. 3.3.2**), Zn is known to affect the aggregation and/or fibrillization of Aβ (446-452) and it was, therefore, of interest to determine whether CQ and/or Zn influenced the cellular uptake of Aβ (experimental procedure described in **section 3.2.7**).

Consistent with data depicted in **Fig. 3.3.3**, $A\beta_{42}$ levels in N2a cells treated with CQ alone and in N2a cells treated with either soluble or pre-aggregated $A\beta_{42}$, both in the absence and presence of CQ, were similar to each other and to $A\beta_{42}$ levels in vehicle-treated N2a cells (**Fig. 3.3.4**). $A\beta_{42}$ levels in N2a cells treated with $ZnCl_2$, with and without CQ, were also no different to each other or to $A\beta_{42}$ levels in vehicle-treated N2a cells (**Fig. 3.3.4**). Notably, the non-significant negative values for these treatments do not reflect that cells are depleted of Aβ; rather, they are an artefact of data analysis.

Similar to treatment with soluble $A\beta_{42}$ and $CuCl_2$ (**Fig. 3.3.3**), $A\beta_{42}$ levels in N2a cells treated with soluble $A\beta_{42}$ and $ZnCl_2$ were comparable to $A\beta_{42}$ levels in N2a cells treated with either vehicle or with soluble $A\beta_{42}$ alone (**Fig. 3.3.4**). However, while treatment with soluble $A\beta_{42}$, $CuCl_2$ and CQ led to significant $A\beta_{42}$ uptake into N2a cells (**Fig. 3.3.3**); $A\beta_{42}$ levels in N2a cells treated with soluble $A\beta_{42}$, $ZnCl_2$ and CQ were not different to $A\beta_{42}$ levels in vehicle-treated N2a cells or in N2a cells treated with either soluble $A\beta_{42}$ and CQ in the absence of $ZnCl_2$ or with soluble $A\beta_{42}$ and $ZnCl_2$ in the absence of CQ (**Fig. 3.3.4**).

These unexpected results may relate to the different conformation Aβ oligomers assume in the presence of Zn, as oppose to Cu, which could impact on CQ's ability to facilitate their neuronal uptake.

While treatment with pre-aggregated Cu-$A\beta_{42}$ did not lead to $A\beta_{42}$ uptake into N2a cells (**Fig. 3.3.3**); treatment with pre-aggregated Zn-$A\beta_{42}$ did result in significant $A\beta_{42}$ uptake, both compared to vehicle-treated N2a cells and to N2a cells treated with pre-aggregated $A\beta_{42}$ (**Fig. 3.3.4**). Significant $A\beta_{42}$ uptake was also detected in N2a cells treated with pre-aggregated Zn-$A\beta_{42}$ complexes and CQ, as compared to N2a cells treated with either vehicle or with aggregated $A\beta_{42}$ and CQ, but not compared to N2a cells treated with pre-aggregated Zn-$A\beta_{42}$ complexes in the absence of CQ (**Fig. 3.3.4**).

These interesting observations imply that Aβ uptake from Zn-enriched APs into nearby neurons may be achieved by a non-CQ dependant mechanism.

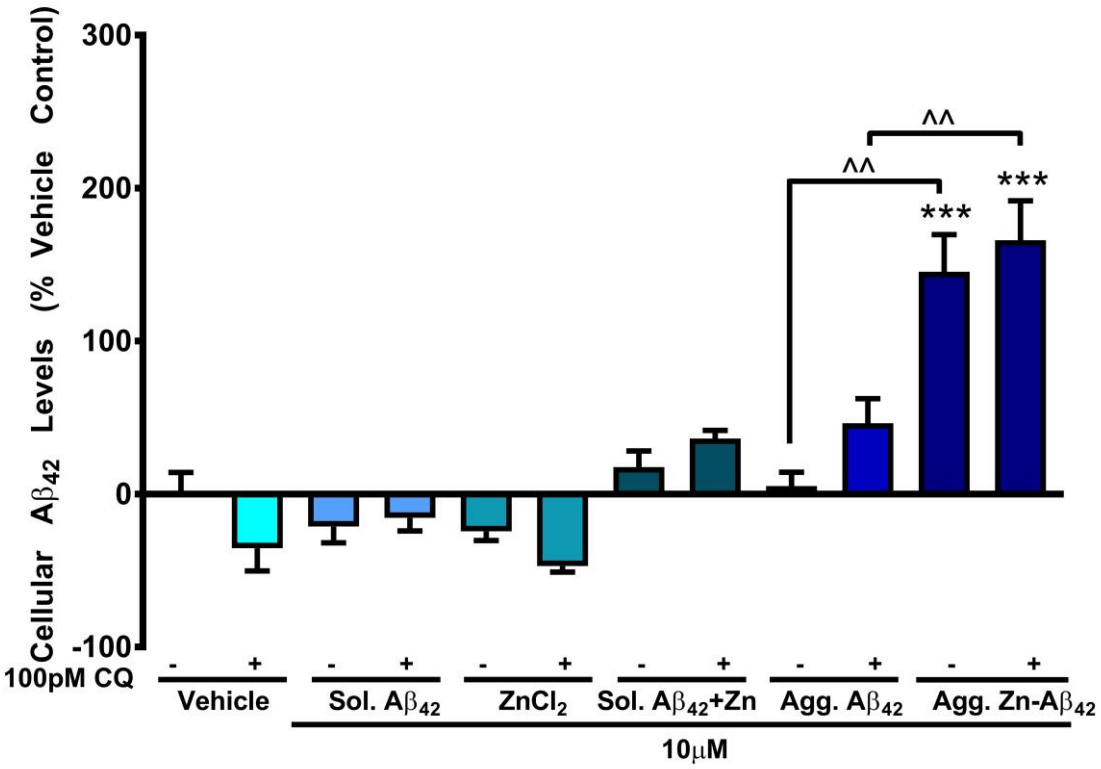

Figure 3.3.4 Effect of CQ and/or Zn on the uptake of Aβ into N2a cells

Exposure of N2a cells to soluble Aβ42 (Sol. Aβ42), with and without CQ and/or $ZnCl_2$, did not result in cellular uptake of Aβ.

Exposure of N2a cells to pre-aggregated Zn-Aβ42, with and without CQ, resulted in significant cellular uptake of Aβ.

*ANOVA with Tukey post-hoc test; ***p < 0.001 compared to vehicle; ^^p < 0.01*

Bars represent mean ± S.E.M, n ≥ 3

3.3.5 Effect of nocodazole on the cellular uptake of Cu in the presence of CQ and Aβ

Having observed that CQ and Aβ markedly modulate the cellular uptake of Cu (**Fig. 3.3.1**), the mechanism by which this uptake takes place was further characterized. Most molecules and/or drugs, both biological and synthetic, are able to exert their effect(s) on cells and/or cellular components either by passive uptake (i.e., energy-free facilitated diffusion across the cell membrane according to a concentration gradient) or by means of active transport (i.e., binding to a voltage- or ligand-gated ion channel, G-protein coupled receptor (GPCR) or enzyme-linked receptor on the surface of the cell and internalisation that require energy).

To test whether the cellular internalisation of Cu and Aβ occurs *via* a passive or active transport mechanism, the experiments described in **sections 3.3.1-3.3.4** that included CQ were repeated in the absence and presence of nocodazole (method outlined in **section 3.2.7**). Nocodazole is an anti-neoplastic agent that acts as a general endocytosis inhibitor by binding to tubulin and interfering with microtubule assembly (771-773).

Results showed that, under control conditions, Cu levels in N2a cells treated with CQ, alone or together with either soluble or pre-aggregated $A\beta_{42}$, were comparable to each other and to Cu levels in vehicle-treated N2a cells (**Fig. 3.3.5**), as in **Fig. 3.3.1**. Likewise, in the presence of nocodazole, Cu levels in N2a cells treated with CQ, alone or together with either soluble or pre-aggregated $A\beta_{42}$, were no different to each other or to Cu levels in nocodazole-treated N2a cells (**Fig. 3.3.5**). In addition, Cu levels were similar in vehicle and nocodazole-treated N2a cells, as well as in N2a cells treated with CQ alone or together with either soluble or pre-aggregated $A\beta_{42}$ in the presence, compared to the absence, of nocodazole (**Fig. 3.3.5**).

These findings support the notion that CQ and Aβ, each on its own or combined, do not affect neuronal Cu, irrespective of endocytosis.

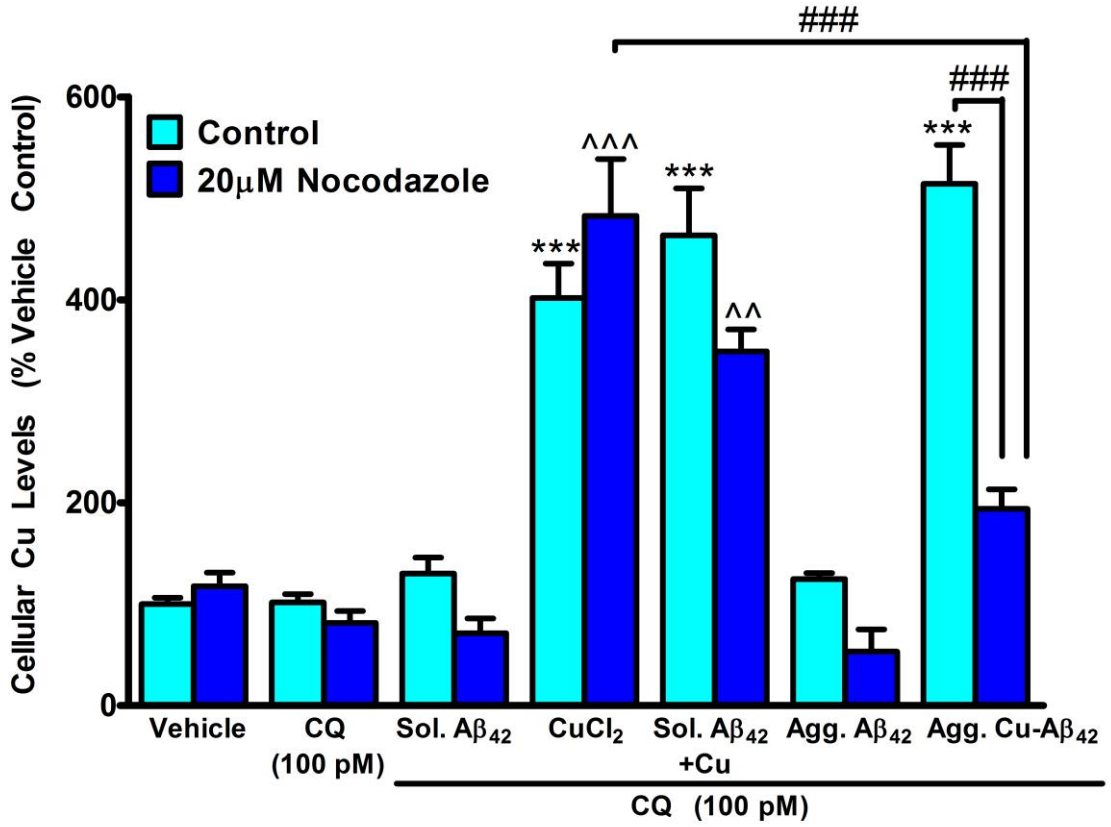

Figure 3.3.5 Effect of nocodazole on the uptake of Cu into N2a cells in the presence of CQ and Aβ

Exposure of N2a cells to CQ and $CuCl_2$, with and without soluble $A\beta_{42}$, resulted in significant Cu uptake, which was unaffected by nocodazole.

On the other hand, exposure of N2a cells to CQ and pre-aggregated Cu-$A\beta_{42}$ resulted in significant Cu uptake, which was inhibited by nocodazole.

*Unpaired two-tailed t-test; ***$p < 0.001$ compared to vehicle;*

^^$p < 0.01$, ^^^$p < 0.001$ compared to nocodazole; ###$p < 0.001$

Bars represent mean ± S.E.M, $n \geq 3$

In line with data depicted in **Fig. 3.3.1**, under control conditions, significant Cu uptake was detected in N2a cells co-treated with $CuCl_2$ and CQ, both in the absence and presence of soluble $A\beta_{42}$, compared to vehicle-treated N2a cells (~4-5 fold increase); but was not different to each other (**Fig. 3.3.5**). Similarly, in the presence of nocodazole, significant Cu uptake was observed in N2a cells treated with $CuCl_2$ and CQ, both in the absence and presence of soluble $A\beta_{42}$, compared to nocodazole-treated N2a cells (~4-5 fold increase); yet, was not different to each other (**Fig. 3.3.5**). Of note, Cu uptake was similar in N2a cells co-treated with $CuCl_2$ and CQ alone or together with soluble $A\beta_{42}$ in the presence, as compared to the absence, of nocodazole (**Fig. 3.3.5**).

Nocodazole's inability to alter Cu levels, including in the presence of soluble $A\beta_{42}$, signifies that neuronal Cu uptake occurs *via* a mechanism other than endocytosis.

Under control conditions, significant Cu uptake occurred in N2a cells co-treated with pre-aggregated Cu-$A\beta_{42}$ complexes and CQ, compared to vehicle-treated N2a cells (~5-6 fold increase; **Fig. 3.3.5**), similar to results illustrated in **Fig. 3.3.1**. However, Cu levels in N2a cells treated with pre-aggregated Cu-$A\beta_{42}$ complexes and CQ in the presence of nocodazole were significantly diminished; not only compared to N2a cells co-treated with $CuCl_2$ and CQ in the absence of $A\beta_{42}$ and presence of nocodazole, but also compared to N2a cells treated with pre-aggregated Cu-$A\beta_{42}$ complexes and CQ in the absence of nocodazole (~3 fold decrease; **Fig. 3.3.5**). In fact, Cu levels in N2a cells treated with pre-aggregated Cu-$A\beta_{42}$ complexes and CQ in the presence of nocodazole were equivalent to Cu levels in nocodazole-treated N2a cells (**Fig. 3.3.5**).

Nocodazole's capacity to inhibit the synergistically-induced Cu uptake by CQ and aggregated Aβ indicates that the mechanism by which CQ elicits ion influx from Cu-enriched APs into neurons involves endocytosis.

3.3.6 Effect of nocodazole on the cellular uptake of Zn in the presence of CQ and Aβ

Next, endocytosis/exocytosis inhibition experiments were performed in N2a cells co-incubated with CQ alone or together with either $ZnCl_2$, soluble or pre-aggregated $A\beta_{42}$ - in the continuing presence and absence of nocodazole (procedure outlined in **section 3.2.7**).

Consistent with earlier observations (**Fig. 3.3.2**), Zn levels in vehicle-treated N2a cells were not statistically different to Zn levels in N2a cells treated with CQ alone or together with either $ZnCl_2$, soluble $A\beta_{42}$, soluble $A\beta_{42}$ and $ZnCl_2$, pre-aggregated $A\beta_{42}$ or pre-aggregated Zn-$A\beta_{42}$ complexes (**Fig. 3.3.6**).

These findings were paralleled in the presence of nocodazole. Zn levels in N2a cells treated with CQ alone or together with either $ZnCl_2$, soluble $A\beta_{42}$, soluble $A\beta_{42}$ and $ZnCl_2$, pre-aggregated $A\beta_{42}$ or pre-aggregated Zn-$A\beta_{42}$ complexes – all in the presence of nocodazole were similar to Zn levels in nocodazole-treated N2a cells (**Fig. 3.3.6**).

Zn levels in vehicle-treated N2a cells and in N2a cells treated with CQ alone and together with $ZnCl_2$, soluble $A\beta_{42}$ and $ZnCl_2$, or pre-aggregated Zn-$A\beta_{42}$ complexes were also comparable in the absence, as opposed to the presence, of nocodazole (**Fig. 3.3.6**).

Surprisingly, there was a significant difference between Zn levels in N2a cells co-treated with CQ and either soluble $A\beta_{42}$ or pre-aggregated $A\beta_{42}$ in the absence of nocodazole, and their respective treatments in the presence of nocodazole. In both cases, Zn levels were almost halved in the presence, compared to the absence, of nocodazole (**Fig. 3.3.6**).

These data imply that CQ, together with Aβ (regardless of its solubility state), can modulate neuronal Zn; however, this could only be appreciated under conditions in which endocytosis was inhibited.

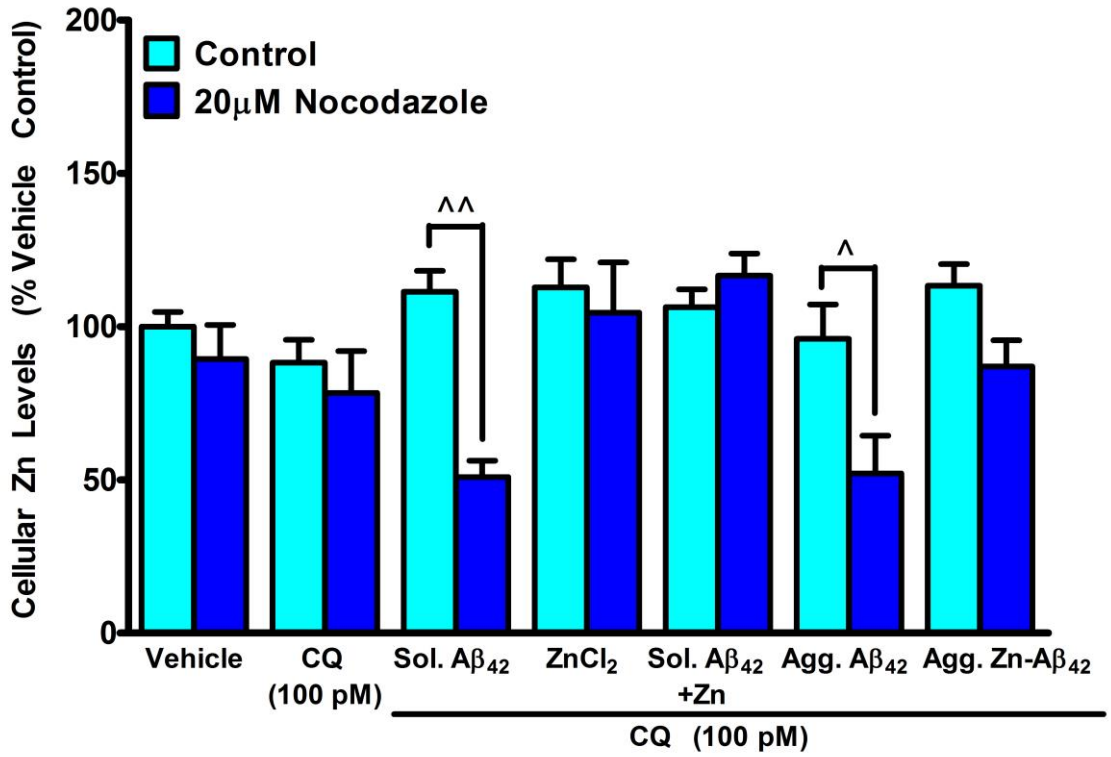

Figure 3.3.6 Effect of nocodazole on the uptake of Zn into N2a cells in the presence of CQ and Aβ

Exposure of N2a cells to CQ and $ZnCl_2$, with and without $A\beta_{42}$ (soluble or aggregated), did not affect cellular Zn levels, either in the absence or presence of nocodazole.

On the other hand, Zn levels were significantly lower in N2a cells exposed to CQ and either soluble or aggregated $A\beta_{42}$ (Sol. or Agg. $A\beta_{42}$, respectively) in the presence, as compared to the absence, of nocodazole.

Unpaired two-tailed t-test; ^$p < 0.05$; ^^$p < 0.01$

Bars represent mean ± S.E.M, $n \geq 3$

3.3.7 Effect of nocodazole on the cellular uptake of Aβ in the presence of CQ and Cu

Since it had been established that Cu and CQ synergistically potentiate the cellular uptake of both soluble and aggregated Aβ (**Fig. 3.3.3**) and that nocodazole mitigates the CQ and aggregated, but not soluble, Aβ-induced cellular Cu uptake (**Fig. 3.3.5**), it was hypothesized that nocodazole may also affect the joint Cu and CQ-induced Aβ uptake. This was put to the test, using an endocytosis/exocytosis pharmacokinetic assay (refer to **section 3.2.7**).

In line with previous findings (**Fig. 3.3.3**), $A\beta_{42}$ levels in N2a cells treated with CQ alone or together with $CuCl_2$ were comparable to each other and to $A\beta_{42}$ levels in vehicle-treated N2a cells (**Fig. 3.3.7**). In the presence of nocodazole, $A\beta_{42}$ levels in N2a cells treated with CQ alone or together with $CuCl_2$ were similar to each other, to nocodazole-treated N2a cells, as well as to their respective treatments in the absence of nocodazole (**Fig. 3.3.7**).

While $A\beta_{42}$ levels were no different in N2a cells treated with CQ and soluble $A\beta_{42}$, compared to vehicle-treated N2a cells (**Fig. 3.3.3** and **Fig. 3.3.7**); $A\beta_{42}$ levels in N2a cells treated with CQ and soluble $A\beta_{42}$ in the presence of nocodazole were higher than $A\beta_{42}$ levels in N2a cells treated with CQ and soluble $A\beta_{42}$ in the absence of nocodazole and in nocodazole-treated N2a cells (**Fig. 3.3.7**).

This result was unexpected, as it was predicted that following pre-treatment with nocodazole, intracellular $A\beta_{42}$ levels would be either similar to, or lower than, those in control conditions depending on whether Aβ uptake occurred *via* an endocytosis-independent or dependant pathway, respectively. However, nocodazole does not only block endocytosis; it can also inhibit exocytosis (774). Accordingly, elevated $A\beta_{42}$ levels in the presence, compared to the absence, of nocodazole point to accumulation of intracellular soluble $A\beta_{42}$ that would, otherwise, be excreted *via* a secretory pathway.

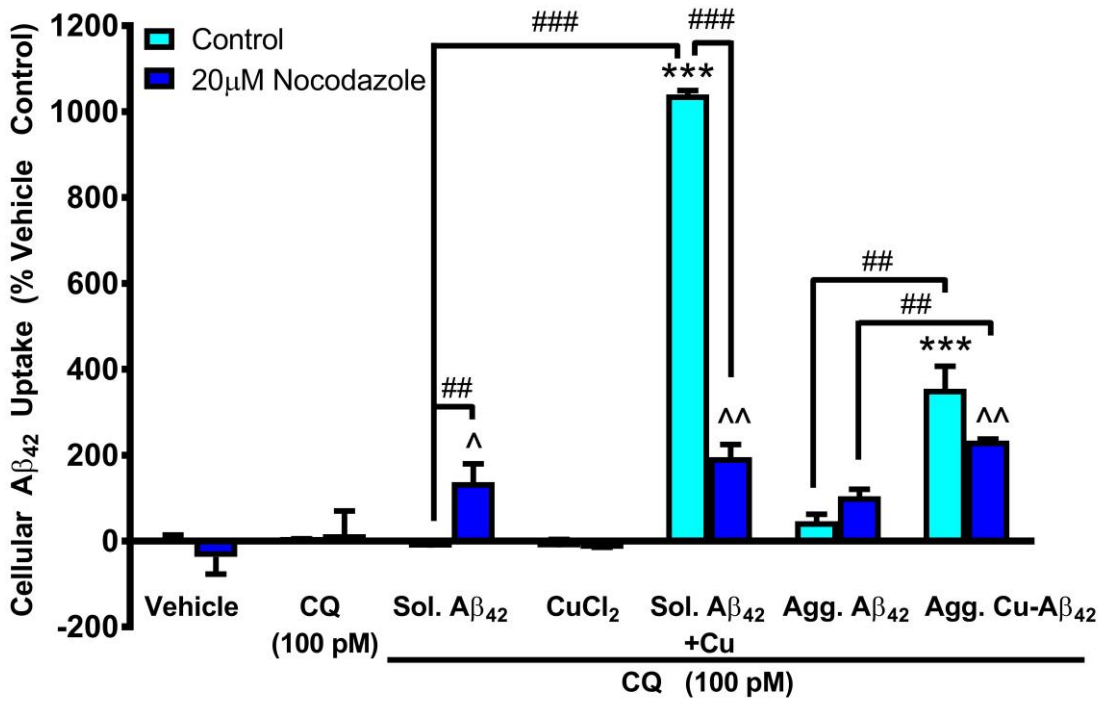

Figure 3.3.7 Effect of nocodazole on the uptake of Aβ into N2a cells in the presence of CQ and Cu

In the presence of nocodazole, exposure of N2a cells to soluble $A\beta_{42}$ and CQ resulted in accumulation of Aβ; whereas addition of $CuCl_2$ resulted in inhibition of the Cu-induced Aβ uptake, in the absence of nocodazole.

In the presence of nocodazole, Aβ uptake continued to be enhanced in N2a cells exposed to pre-aggregated Cu-$A\beta_{42}$, compared to self-aggregated $A\beta_{42}$, and CQ.

*Unpaired two-tailed t-test; ***$p < 0.001$ compared to vehicle;*

^$p < 0.05$, ^^$p < 0.01$ compared to nocodazole; ##$p < 0.01$; ###$p < 0.001$

Bars represent mean ± S.E.M, $n \geq 3$

Under control conditions, $A\beta_{42}$ uptake was significantly elevated in N2a cells treated with soluble $A\beta_{42}$, $CuCl_2$ and CQ, compared to N2a cells treated with either vehicle or with soluble $A\beta_{42}$ and CQ (**Fig. 3.3.3** and **Fig. 3.3.7**). Although, in the presence of nocodazole, $A\beta_{42}$ uptake into N2a cells treated with soluble $A\beta_{42}$, $CuCl_2$ and CQ was higher, compared to nocodazole-treated N2a cells (**Fig. 3.3.7**); $A\beta_{42}$ uptake was significantly lower in N2a cells treated with soluble $A\beta_{42}$, $CuCl_2$ and CQ in the presence, compared to the absence, of nocodazole (**Fig. 3.3.7**). In fact, $A\beta_{42}$ levels in N2a cells treated with soluble $A\beta_{42}$, $CuCl_2$ and CQ in the presence of nocodazole were equivalent to $A\beta_{42}$ levels in N2a cells treated with soluble $A\beta_{42}$ and CQ in the presence of nocodazole (**Fig. 3.3.7**).

These results indicate that CuDDLs may be internalized into neuronal cells, to a great extent, by endocytosis.

In accordance with **Fig. 3.3.3**, though $A\beta_{42}$ levels in N2a cells treated with CQ and pre-aggregated $A\beta_{42}$ were not statistically different to $A\beta_{42}$ levels vehicle-treated N2a cells; $A\beta_{42}$ levels in N2a cells treated with CQ and pre-aggregated Cu-$A\beta_{42}$ complexes were significantly enhanced, compared to N2a cells treated with either vehicle or with pre-aggregated $A\beta_{42}$ and CQ (**Fig. 3.3.7**).

These outcomes were paralleled in the presence of nocodazole. $A\beta_{42}$ levels in N2a cells treated with CQ and pre-aggregated $A\beta_{42}$ in the presence of nocodazole were no different to $A\beta_{42}$ levels in nocodazole-treated N2a cells or in N2a cells treated with CQ and pre-aggregated $A\beta_{42}$ in the absence of nocodazole (**Fig. 3.3.7**). In addition, $A\beta_{42}$ levels in N2a cells treated with CQ and pre-aggregated Cu-$A\beta_{42}$ in the presence of nocodazole were statistically elevated, compared to in N2a cells treated with either nocodazole alone or together with pre-aggregated $A\beta_{42}$ and CQ (**Fig. 3.3.7**). However, $A\beta_{42}$ levels were similar in N2a cells treated with CQ and pre-aggregated Cu-$A\beta_{42}$ complexes in the presence, *versus* the absence, of nocodazole (**Fig. 3.3.7**).

These data imply that, under conditions wherein endocytosis is inhibited, Cu retains its ability to facilitate the influx of Aβ from Cu-enriched APs into nearby neurons.

3.3.8 Effect of nocodazole on the cellular uptake of Aβ in the presence of CQ and Zn

As Zn complexed to $A\beta_{42}$ stimulated the uptake of Aβ into N2a cells (**Fig. 3.3.4**), and since nocodazole suppressed the endogenous Zn levels in N2a cells treated with CQ and either soluble or aggregated $A\beta_{42}$ (**Fig. 3.3.6**); it remained to be tested whether nocodazole affected Aβ uptake in the presence of CQ with and without Zn (as outlined in **section 3.2.7**).

Expectedly, results demonstrated that $A\beta_{42}$ levels in N2a cells treated with CQ alone and together with $ZnCl_2$, were comparable to each other and to $A\beta_{42}$ levels in vehicle-treated N2a cells (**Fig. 3.3.8**), as in **Fig. 3.3.4**. In the presence of nocodazole, $A\beta_{42}$ levels in N2a cells treated with CQ on its own or together with $ZnCl_2$ were similar to each other, to nocodazole-treated N2a cells, as well as to their respective treatments in the absence of nocodazole (**Fig. 3.3.8**).

In keeping with earlier findings (**Fig. 3.3.3**, **Fig. 3.3.4** and **Fig. 3.3.7**), $A\beta_{42}$ levels in N2a cells treated with soluble $A\beta_{42}$ and CQ were no different to $A\beta_{42}$ levels in vehicle-treated N2a cells (**Fig. 3.3.8**). In the presence of nocodazole, however, $A\beta_{42}$ levels in N2a cells treated with soluble $A\beta_{42}$ and CQ were significantly increased; not only compared to nocodazole-treated N2a cells, but also compared to $A\beta_{42}$ levels in N2a cells treated with soluble $A\beta_{42}$ and CQ in the absence of nocodazole (**Fig. 3.3.8**), similar to **Fig. 3.3.7**.

Again, these observations could be explained by nocodazole's ability to block exocytosis (774), as well as endocytosis, and implicate the secretory pathway as being involved in the removal of soluble Aβ, most likely, as a turn-over mechanism and a way of achieving balanced levels of the protein within neurons.

$A\beta_{42}$ uptake was markedly different in N2a cells treated with soluble $A\beta_{42}$, CQ and $CuCl_2$ *versus* $ZnCl_2$ (**Fig. 3.3.7** and **Fig. 3.3.8**, respectively). $A\beta_{42}$ levels in N2a cells treated with soluble $A\beta_{42}$, $ZnCl_2$ and CQ were equivalent to $A\beta_{42}$ levels in vehicle-treated N2a cells (**Fig. 3.3.8**), as seen in **Fig. 3.3.4**. In contrast, $A\beta_{42}$ levels in N2a cells treated with soluble $A\beta_{42}$, $ZnCl_2$ and CQ in the presence of nocodazole were slightly higher than $A\beta_{42}$ levels in nocodazole-treated N2a cells, yet were comparable to $A\beta_{42}$ levels in N2a cells treated with soluble $A\beta_{42}$ and CQ in the presence of nocodazole or treated with soluble $A\beta_{42}$, $ZnCl_2$ and CQ in the absence of nocodazole (**Fig. 3.3.8**).

Findings with soluble $A\beta_{42}$ were not paralleled upon treatment with aggregated $A\beta_{42}$. $A\beta_{42}$ levels in N2a cells treated with pre-aggregated $A\beta_{42}$ and CQ were not statistically different to $A\beta_{42}$ levels vehicle-treated N2a cells (similar to data depicted in **Fig. 3.3.3**, **Fig. 3.3.4** and **Fig. 3.3.7**); while $A\beta_{42}$ levels in N2a cells treated with pre-aggregated Zn-$A\beta_{42}$ complexes and CQ were significantly elevated, compared to N2a cells treated with either vehicle or with pre-aggregated $A\beta_{42}$ and CQ (**Fig. 3.3.8**), as in **Fig. 3.3.4**.

Though $A\beta_{42}$ levels in N2a cells treated with CQ and pre-aggregated Zn-$A\beta_{42}$ complexes in the presence of nocodazole were slightly higher than $A\beta_{42}$ levels in nocodazole-treated N2a cells (**Fig. 3.3.8**); they were similar to $A\beta_{42}$ levels in N2a cells treated with either pre-aggregated $A\beta_{42}$ and CQ in the presence of nocodazole or with pre-aggregated Zn-$A\beta_{42}$ complexes and CQ in the absence of nocodazole (**Fig. 3.3.8**). Taken together, it seems that, under conditions where endocytosis is inhibited, Zn losses its capability to enhance the uptake of aggregated Aβ into neuronal cells.

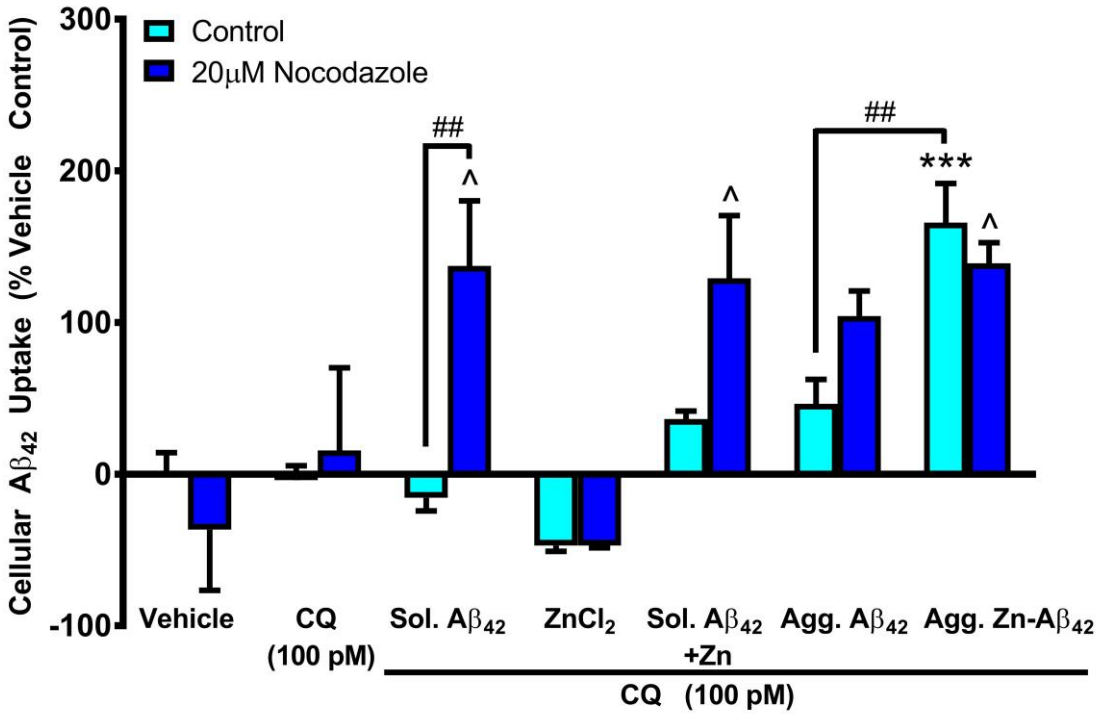

Figure 3.3.8 Effect of nocodazole on the uptake of Aβ into N2a cells in the presence of CQ and Zn

In the presence of nocodazole and CQ, accumulation of Aβ was observed in N2a cells exposed to soluble $A\beta_{42}$ without, but not with, Zn.

In the presence of nocodazole and CQ, addition of Zn no longer enhanced the uptake of aggregated Aβ into N2a cells.

*Unpaired two-tailed t-test; ***$p < 0.001$ compared to vehicle;*

^$p < 0.05$ compared to nocodazole; ##$p < 0.01$

Bars represent mean ± S.E.M, $n \geq 3$

3.3.9 Effect of lysosomal and autophagy inhibitors on cellular Cu levels in the absence and presence of Aβ

It was determined that particular settings enable the influx of Cu and/or Aβ; yet, once inside neuronal-like cells, their fate remained unclear (i.e., do the metal and/or protein accumulate in the cytoplasm or in particular cellular organelle(s)). Due to the chemical and/or optical properties of Cu, there are no validated fluorescent tracers that can be used to visualize intracellular Cu and it is therefore difficult to ascertain to which cellular compartment(s) Cu is directed towards.

Anomalies in the endosomal-lysosomal-autophagy pathway have been reported with relation to AD (775, 776). Ammonium chloride (NH_4Cl) is a weak base, which increases the pH of acidic lysosomes thus inhibiting their enzymes (777); while, 3-methyladenine (3-MA) blocks autophagic vacuole formation by inhibiting type III PI3K (778, 779). These inhibitors were used to evaluate if disrupting the lysosomal-autophagy pathway affects Cu levels in N2a cells in the presence and absence of Aβ (**section 3.3.9**) and/or CQ (**section 3.3.10**).

Results showed that Cu levels in N2a cells treated with lysosomal-autophagy inhibitors were similar to Cu levels in vehicle-treated N2a cells (**Fig. 3.3.9**). Cu levels in N2a cells treated with soluble $A\beta_{42}$ were also comparable to Cu levels in vehicle-treated N2a cells (**Fig. 3.3.9**), akin to data illustrated in **Fig. 3.3.1**. In the presence of lysosomal-autophagy inhibitors, Cu levels in N2a cells treated with soluble $A\beta_{42}$ were not different to Cu levels in N2a cells treated with lysosomal-autophagy inhibitors or in N2a cells treated with soluble $A\beta_{42}$ in the absence of lysosomal-autophagy inhibitors (**Fig. 3.3.9**). These observations strengthen the impression that soluble Aβ does not affect neuronal Cu, even under conditions wherein the lysosomal-autophagy pathway is inhibited.

As seen in **Fig. 3.3.1**, Cu uptake was significantly elevated in N2a cells treated with $CuCl_2$, compared to vehicle-treated N2a cells (~4.5 fold increase; **Fig. 3.3.9**). In the presence of lysosomal-autophagy inhibitors, Cu uptake in N2a cells treated with $CuCl_2$ was significantly enhanced, compared to N2a cells treated with lysosomal-autophagy inhibitors alone (~5.5 fold increase); but, was no different to N2a cells treated with $CuCl_2$ in the absence of lysosomal-autophagy inhibitors (**Fig. 3.3.9**).
These results confer that Cu ions, which readily enter neuronal cells, are not directed towards the endosomal-lysosomal-autophagy pathway.

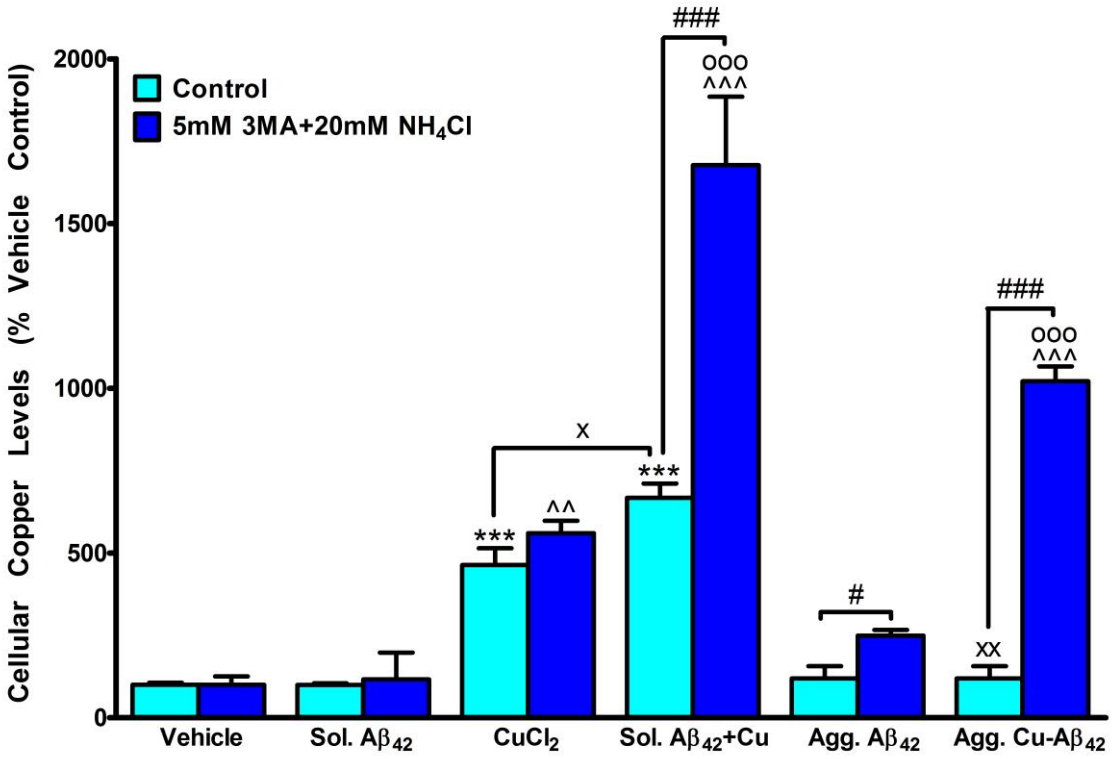

Figure 3.3.9 Effect of lysosomal and autophagy inhibitors on the uptake of Cu into N2a cells in the absence and presence of Aβ

While inhibition of the lysosomal-autophagy pathway did not affect the significant uptake of Cu into N2a cells exposed to $CuCl_2$, it further enhanced the intracellular Cu levels in N2a cells exposed to $CuCl_2$ and soluble $A\beta_{42}$ (Sol. $A\beta_{42}$).

Inhibition of the lysosomal-autophagy pathway resulted in increased Cu levels in N2a cells exposed to aggregated $A\beta_{42}$ (Agg. $A\beta_{42}$) with and without $CuCl_2$.

*Unpaired two-tailed t-test; ***$p < 0.001$ compared to vehicle;*

^^$p < 0.01$, ^^^$p < 0.001$ compared to lysosomal-autophagy inhibitors;

$^{x}p < 0.05$, $^{xx}p < 0.01$ compared to $CuCl_2$;

$^{ooo}p < 0.001$ compared to $CuCl_2$ + lysosomal-autophagy inhibitors;

$^{\#}p < 0.05$, $^{\#\#}p < 0.01$; $^{\#\#\#}p < 0.001$

Bars represent mean ± S.E.M, $n \geq 3$

Under control conditions, similar to **Fig. 3.3.1**, significant Cu uptake was detected in N2a cells co-treated with soluble $A\beta_{42}$ and $CuCl_2$, compared to N2a cells treated with either vehicle or with $CuCl_2$ (~6.5 and 1.5 fold increase, respectively; **Fig. 3.3.9**). These results were paralleled in the presence of lysosomal-autophagy inhibitors. Significant Cu uptake was observed in N2a cells co-treated with soluble $A\beta_{42}$ and $CuCl_2$ in the presence of lysosomal-autophagy inhibitors, compared to N2a cells treated with lysosomal-autophagy inhibitors alone or together with $CuCl_2$ (~10 and 3 fold increase, respectively; **Fig. 3.3.9**). Importantly, Cu levels were markedly elevated in N2a cells co-treated with soluble $A\beta_{42}$ and $CuCl_2$ in the presence, compared to the absence, of lysosomal-autophagy inhibitors (~2.5 fold increase; **Fig. 3.3.9**).

Accumulation of Cu in N2a cells co-treated with soluble $A\beta_{42}$ and $CuCl_2$, under conditions in which the lysosomal-autophagy system was blocked, implies that Aβ can mediate the uptake of Cu into neuronal cells, where it is distributed to and/or secreted by the lysosomal-autophagy pathway.

As expected, Cu levels in N2a cells treated with pre-aggregated $A\beta_{42}$ were not different to vehicle-treated N2a cells (**Fig. 3.3.1** and **Fig. 3.3.9**). Surprisingly, Cu levels were higher in N2a cells treated with pre-aggregated $A\beta_{42}$ in the presence, as compared to the absence, of lysosomal-autophagy inhibitors (~2 fold increase; **Fig. 3.3.9**).

These data suggest that aggregated Aβ may impact on neuronal Cu homeostasis, but this can only be appreciated where the lysosomal-autophagy system is inhibited.

Cu levels in N2a cells treated with pre-aggregated Cu-$A\beta_{42}$ complexes were similar to Cu levels in vehicle-treated N2a cells and were significantly lower than Cu levels in N2a cells treated with $CuCl_2$ alone (~4 fold decrease; **Fig. 3.3.1** and **Fig. 3.3.9**). However, in the presence of lysosomal-autophagy inhibitors, Cu levels in N2a cells treated with pre-aggregated Cu-$A\beta_{42}$ complexes were markedly greater than N2a cells treated with lysosomal-autophagy inhibitors alone or together with $CuCl_2$ (~10 and 2 fold increase, respectively; **Fig. 3.3.9**). Moreover, Cu levels in N2a cells treated with pre-aggregated Cu-$A\beta_{42}$ complexes were significantly elevated in the presence, *versus* the absence, of lysosomal-autophagy inhibitors (~8.5 fold increase; **Fig.3.3.9**).

These findings suggest that APs could sequester Cu and prevent it from being taken into neighbouring neurons. Yet, when the lysosomal-autophagy pathway is disrupted, as has been reported in the case of AD and other neurodegenerative diseases (159, 160, 776, 780), Cu may accumulate in neuronal cells.

3.3.10 Effect of lysosomal and autophagy inhibitors on cellular Cu levels in the presence of CQ and Aβ

Overall, the results in **section 3.3.9** pointed to the lysosomal-autophagy machinery as being involved in the metabolism of excess Cu ions and in maintenance of Cu equilibrium under conditions where it would be overloaded by the impact of Aβ. With this in mind, the same experimental conditions were used; but, with the addition of CQ (described in **section 3.2.7**).

Once more, Cu levels in N2a cells treated with lysosomal-autophagy inhibitors were similar to Cu levels in vehicle-treated N2a cells (**Fig. 3.3.9** and **Fig. 3.3.10**). Cu levels in N2a cells treated with CQ alone or together with soluble $A\beta_{42}$ were also comparable to Cu levels in vehicle-treated N2a cells (**Fig. 3.3.10**), as in **Fig. 3.3.1** and **Fig. 3.3.5**. In the presence of lysosomal-autophagy inhibitors, Cu levels in N2a cells treated with CQ alone or together with soluble $A\beta_{42}$ were not statistically different to each other and to Cu levels in N2a cells treated with lysosomal-autophagy inhibitors alone or with their respective treatments in the absence of lysosomal-autophagy inhibitors (**Fig. 3.3.10**).
These observations reinforce the supposition that CQ, on its own or combined with Aβ, does not affect endogenous neuronal Cu, regardless of the lysosomal-autophagy pathway.

Consistent with data depicted in **Fig. 3.3.1** and **Fig. 3.3.5**, Cu uptake in N2a cells co-treated with $CuCl_2$ and CQ, in the absence and presence of lysosomal-autophagy inhibitors, was significantly elevated compared to N2a cells treated with vehicle or with lysosomal-autophagy inhibitors, respectively (~4 fold increase; **Fig. 3.3.10**); though, the significant Cu uptake into N2a cells treated with $CuCl_2$ and CQ was no different in the presence, compared to the absence, of lysosomal-autophagy inhibitors (**Fig. 3.3.10**).
These data suggest that CQ alone does not affect the uptake of Cu ions into neuronal cells, or their processing by the endosomal-lysosomal-autophagy pathway.

While Cu levels in N2a cells treated with soluble $A\beta_{42}$, $CuCl_2$ and CQ were higher than Cu levels in vehicle-treated N2a cells (~4.5 fold increase); they were equivalent to Cu levels in N2a cells treated with $CuCl_2$ and CQ (**Fig. 3.3.10**; as well as **Fig. 3.3.1** and **Fig. 3.3.5**). Similar to results in the absence of CQ (**Fig. 3.3.9**), significant Cu retention was observed in N2a cells treated with soluble $A\beta_{42}$, $CuCl_2$ and CQ in the presence of lysosomal-autophagy inhibitors, compared to N2a cells treated with lysosomal-autophagy inhibitors alone or together with $CuCl_2$ and CQ (~12.5 and 2.5 fold increase,

respectively; **Fig. 3.3.10**). Moreover, Cu levels were markedly elevated in N2a cells treated with soluble $A\beta_{42}$, $CuCl_2$ and CQ in the presence, compared to the absence, of lysosomal-autophagy inhibitors (~2.5 fold increase; **Fig. 3.3.10**).

The enhanced accumulation of Cu in N2a cells treated with soluble $A\beta_{42}$ and $CuCl_2$, with and without CQ (**Fig. 3.3.10** and **Fig. 3.3.9**, respectively), where the endosomal-lysosomal-autophagy system is inhibited, indicates that the excess Cu taken up by neuronal cells from CuDDLs is targeted to the lysosomal-autophagy pathway for clearance in a CQ-independent manner.

Expectedly, Cu levels in N2a cells co-treated with pre-aggregated $A\beta_{42}$ and CQ were not different to vehicle-treated N2a cells (**Fig. 3.3.1**, **Fig. 3.3.5** and **Fig. 3.3.10**). Whilst Cu levels in N2a cells co-treated with pre-aggregated $A\beta_{42}$ and CQ in the presence of lysosomal-autophagy inhibitors were no different to Cu levels in N2a cells treated with lysosomal-autophagy inhibitors alone (**Fig. 3.3.10**); they were slightly higher than Cu levels in N2a cells co-treated with pre-aggregated $A\beta_{42}$ and CQ in the absence of lysosomal-autophagy inhibitors (1-2 fold increase; **Fig. 3.3.10**).
As similar results were observed in the absence of CQ (**Fig. 3.3.9**), it seems CQ does not impact the role aggregated Aβ may play in influencing neuronal Cu levels.

Under control conditions, Cu uptake in N2a cells treated with pre-aggregated Cu-$A\beta_{42}$ complexes and CQ was markedly elevated, compared to vehicle-treated N2a cells (~5 fold increase); yet, was no different to N2a cells treated with $CuCl_2$ and CQ (**Fig. 3.3.1**, **Fig. 3.3.5** and **Fig. 3.3.10**). In the presence of lysosomal-autophagy inhibitors, Cu retention in N2a cells co-treated with pre-aggregated Cu-$A\beta_{42}$ complexes and CQ was significantly enhanced; not only compared to N2a treated with lysosomal-autophagy inhibitors (~10 fold increase), but also compared to N2a cells treated with $CuCl_2$ and CQ in the presence of lysosomal-autophagy inhibitors and N2a cells treated with pre-aggregated Cu-$A\beta_{42}$ complexes and CQ in the absence of lysosomal-autophagy inhibitors (~2 and fold increase; **Fig. 3.3.10**).

Since inhibition of the lysosomal-autophagy system led to a similar magnitude of Cu accumulation in N2a cells treated with pre-aggregated Cu-$A\beta_{42}$ complexes, both in the absence and presence of CQ (**Fig. 3.3.9** and **Fig. 3.3.10**, respectively), it can be inferred that CQ may potentially enable the uptake of Cu from APs into neurons by a separate pathway to that which is facilitated by Aβ.

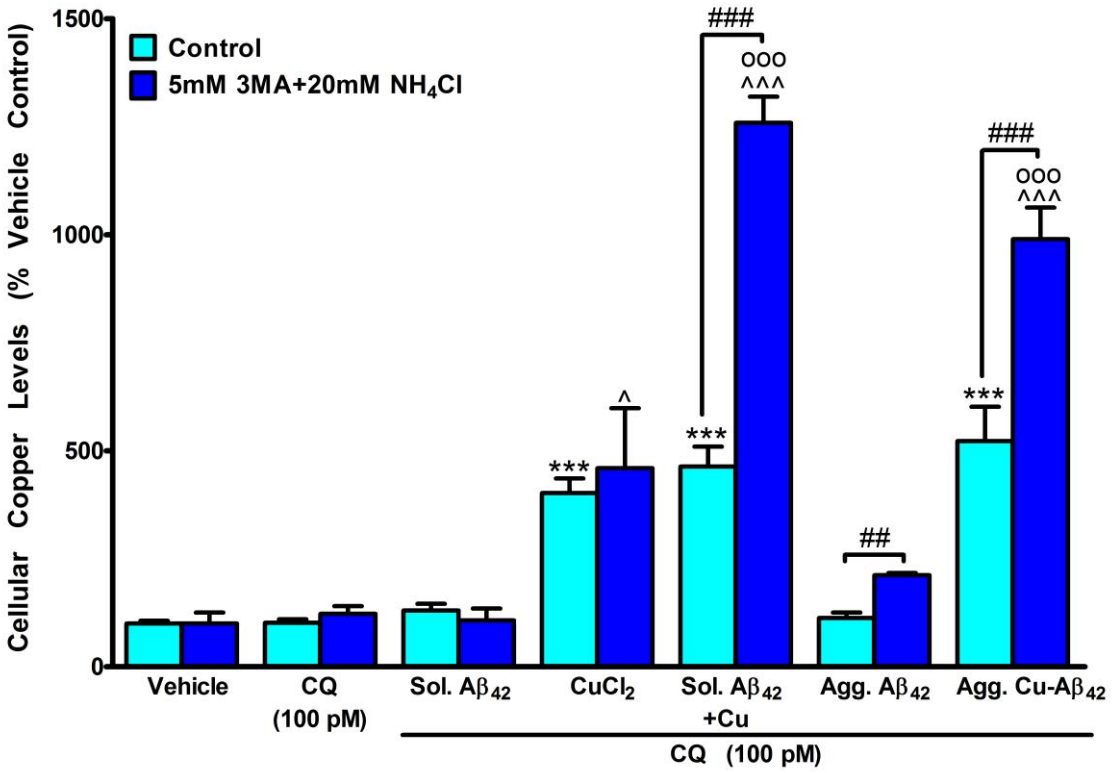

Figure 3.3.10 Effect of lysosomal and autophagy inhibitors on the uptake of Cu into N2a cells in the presence of CQ and Aβ

Inhibition of the lysosomal-autophagy pathway further enhanced Cu levels in N2a cells exposed to $CuCl_2$ and CQ with soluble $A\beta_{42}$ (Sol. $A\beta_{42}$) or aggregated $A\beta_{42}$ (Agg. $A\beta_{42}$). Additionally, inhibition of the lysosomal-autophagy pathway resulted in increased Cu levels in N2a cells exposed to CQ and aggregated $A\beta_{42}$ (Agg. $A\beta_{42}$).

*Unpaired two-tailed t-test; ***$p < 0.001$ compared to vehicle;*

^$p < 0.05$, ^^^$p < 0.001$ compared to lysosomal-autophagy inhibitors;

$^{ooo}p < 0.001$ compared to CQ and $CuCl_2$ + lysosomal-autophagy inhibitors;

$^{\#\#}p < 0.01$; $^{\#\#\#}p < 0.001$

Bars represent mean ± S.E.M, $n \geq 3$

3.3.11 Effect of lysosomal and autophagy inhibitors on cellular Zn levels in the absence and presence of Aβ and/or CQ

Ammonium chloride (NH_4Cl) and 3-MA were then used to assess whether inhibiting the lysosomal and autophagy pathways, respectively, has a similar effect on Zn, as for Cu, in the presence and absence of Aβ and/or CQ (detailed in **section 3.2.7**).

Zn levels in N2a cells treated with CQ and/or either $ZnCl_2$, soluble $A\beta_{42}$ with and without $ZnCl_2$, or pre-aggregated $A\beta_{42}$ with and without $ZnCl_2$, in the absence and presence of lysosomal-autophagy inhibitors were not statistically different to each other or to Zn levels in N2a cells treated with either vehicle or lysosomal-autophagy inhibitors alone, respectively (**Fig. 3.3.11**).

These data suggest that neuronal cells do not direct Zn towards the lysosomal-autophagy pathway. This is reasonable considering that, under the conditions examined, Zn ions do not enter neuronal cells (**Fig. 3.3.2** and **Fig. 3.3.6**); therefore, no excess Zn need be removed.

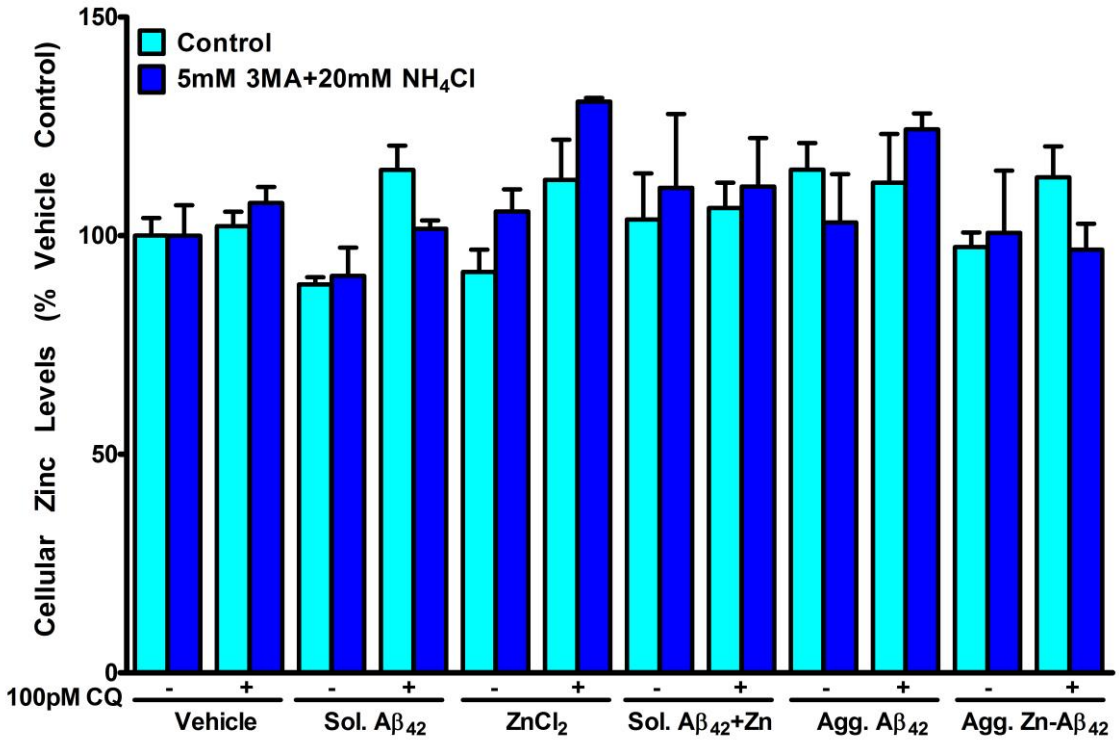

Figure 3.3.11 Effect of lysosomal and autophagy inhibitors on the uptake of Zn into N2a cells in the absence and presence of Aβ and/or CQ

Exposure of N2a cells to CQ and/or either $ZnCl_2$ and/or $A\beta_{42}$ (soluble or aggregated) did not result in cellular uptake of Zn.

Inhibition of the lysosomal-autophagy pathway did not affect the uptake of Zn into N2a cells either.

ANOVA with Tukey post-hoc test; Bars represent mean ± S.E.M, $n \geq 3$

3.3.12 Effect of lysosomal and autophagy inhibitors on cellular Aβ levels in the absence and presence of Cu

Despite Aβ being taken into neuronal-like cells only by Cu and CQ acting synergistically (**Fig. 3.3.3**); the effect of inhibiting the lysosomal-autophagy system on Cu uptake in the presence of Aβ, but in the absence of CQ (**Fig. 3.3.9**), warranted an examination into the effect on the retention of Aβ in the presence of Cu, but in the absence of CQ (as outlined in **section 3.2.7**).

Results showed that $A\beta_{42}$ levels in N2a cells treated with lysosomal-autophagy inhibitors were similar to $A\beta_{42}$ levels in vehicle-treated N2a cells (**Fig. 3.3.12**).

$A\beta_{42}$ levels in N2a cells treated with $CuCl_2$ were also equivalent to $A\beta_{42}$ levels in vehicle-treated N2a cells (**Fig. 3.3.3** and **Fig. 3.3.12**). In the presence of lysosomal-autophagy inhibitors, $A\beta_{42}$ levels in N2a cells treated with $CuCl_2$ were not different to $A\beta_{42}$ levels in N2a cells treated with lysosomal-autophagy inhibitors alone or in N2a cells treated with $CuCl_2$ in the absence of lysosomal-autophagy inhibitors (**Fig. 3.3.12**).

$A\beta_{42}$ levels in N2a cells treated with soluble $A\beta_{42}$, in the absence and presence of lysosomal-autophagy inhibitors, were comparable to each other and to $A\beta_{42}$ levels in vehicle-treated N2a cells (**Fig. 3.3.3**, **Fig. 3.3.4** and **Fig. 3.3.12**) and in N2a cells treated with lysosomal-autophagy inhibitors (**Fig. 3.3.12**), respectively.

While $A\beta_{42}$ levels in N2a cells co-treated with soluble $A\beta_{42}$ and $CuCl_2$ were not statistically different to $A\beta_{42}$ levels in vehicle-treated N2a cells (**Fig. 3.3.3** and **3.3.12**); in the presence of lysosomal-autophagy inhibitors, $A\beta_{42}$ levels in N2a cells treated with soluble $A\beta_{42}$ and $CuCl_2$ were higher not only compared to $A\beta_{42}$ levels in N2a cells treated with lysosomal-autophagy inhibitors, but also compared to $A\beta_{42}$ levels in N2a cells co-treated with soluble $A\beta_{42}$ and $CuCl_2$ in the absence of lysosomal-autophagy inhibitors (**Fig. 3.3.12**).

Combined, these data suggest that when the lysosomal-autophagy pathway is inhibited, as is evident in AD (159, 160, 776, 780), CuDDLs may accumulate within neuronal cells.

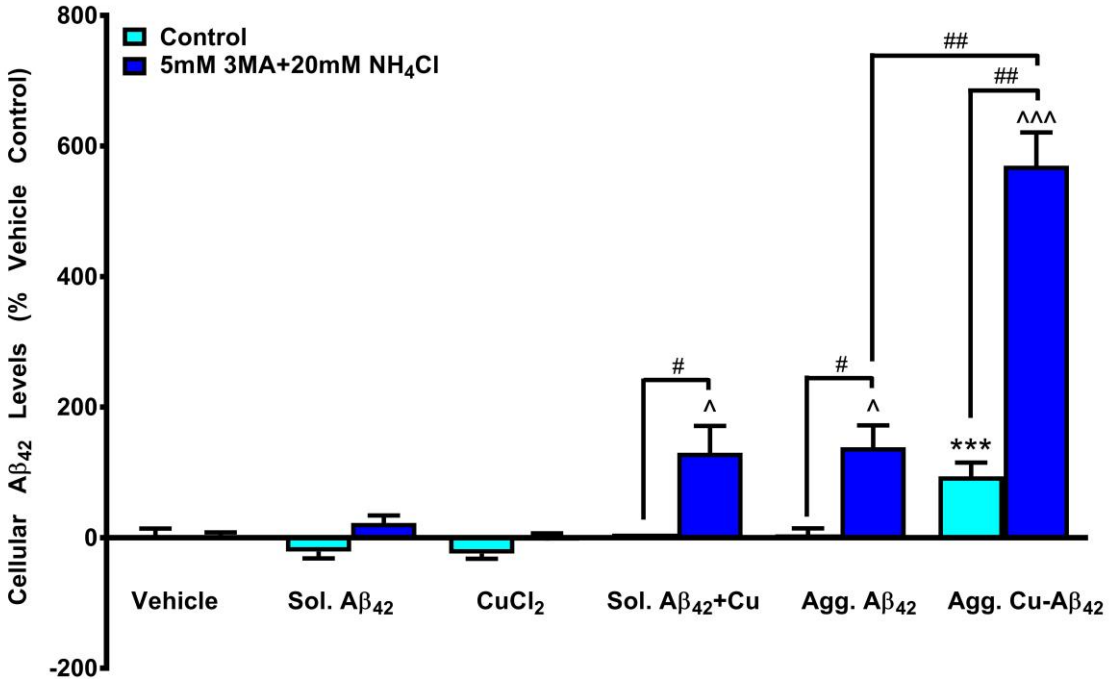

Figure 3.3.12 Effect of lysosomal and autophagy inhibitors on the uptake of Aβ into N2a cells in the absence and presence of Cu

Upon inhibition of the lysosomal-autophagy pathway, exposure of N2a cells to $CuCl_2$ and either soluble or aggregated $A\beta_{42}$ (Sol. $A\beta_{42}$ or Agg. $A\beta_{42}$, respectively) resulted in accumulation of intracellular $A\beta_{42}$.

*Unpaired two-tailed t-test; ***p < 0.001 compared to vehicle;*

^p < 0.05, ^^^p < 0.001 compared to lysosomal-autophagy inhibitors;

#p < 0.05, ##p < 0.01

Bars represent mean ± S.E.M, $n \geq 3$

Under control conditions, $A\beta_{42}$ levels in N2a cells treated with pre-aggregated $A\beta_{42}$ were no different to vehicle-treated N2a cells (**Fig. 3.3.3**, **Fig. 3.3.4** and **Fig. 3.3.12**); yet, in the presence of lysosomal-autophagy inhibitors, $A\beta_{42}$ levels in N2a cells treated with pre-aggregated $A\beta_{42}$ were increased, compared to $A\beta_{42}$ levels in N2a cells treated with lysosomal-autophagy inhibitors alone, as well as N2a cells treated with pre-aggregated $A\beta_{42}$ in the absence of lysosomal-autophagy inhibitors (**Fig. 3.3.12**).

Whilst $A\beta_{42}$ levels in N2a cells treated with pre-aggregated Cu-$A\beta_{42}$ complexes were increased relative to $A\beta_{42}$ levels in vehicle-treated N2a cells; they were equivalent to $A\beta_{42}$ levels in N2a cells treated with pre-aggregated $A\beta_{42}$ (**Fig. 3.3.12**). On the other hand, $A\beta_{42}$ levels in N2a cells treated with pre-aggregated Cu-$A\beta_{42}$ complexes in the presence of lysosomal-autophagy inhibitors were significantly higher, not only relative to $A\beta_{42}$ levels in N2a cells treated with lysosomal-autophagy inhibitors alone, but also compared to N2a cells treated with pre-aggregated $A\beta_{42}$ in the presence of lysosomal-autophagy inhibitors (**Fig. 3.3.12**). Importantly, $A\beta_{42}$ levels were significantly elevated in N2a cells treated with pre-aggregated Cu-$A\beta_{42}$ complexes in the presence, compared to the absence, of lysosomal-autophagy inhibitors (**Fig. 3.3.12**).

Collectively, these findings indicate that Cu has the potential to promote the uptake of Aβ from APs into neurons, where it is destined to the lysosomal-autophagy pathway, most probably, for degradation.

3.3.13 Effect of lysosomal and autophagy inhibitors on cellular Aβ levels in the presence of CQ and Cu

Since it was established that Cu uptake into neuronal-like cells was synergistically promoted by Aβ and CQ, and that these ions were delivered to the endosomal-lysosomal-autophagy pathway (**Fig. 3.3.9** and **Fig. 3.3.10**); it was important to ascertain if Aβ, synergistically taken into neuronal-like cells by Cu and CQ (**Fig. 3.3.3**), is also targeted towards the same organelles.

Again, $A\beta_{42}$ levels in N2a cells treated with lysosomal-autophagy inhibitors were equivalent to $A\beta_{42}$ levels in vehicle-treated N2a cells (**Fig. 3.3.12** and **Fig. 3.3.13**).

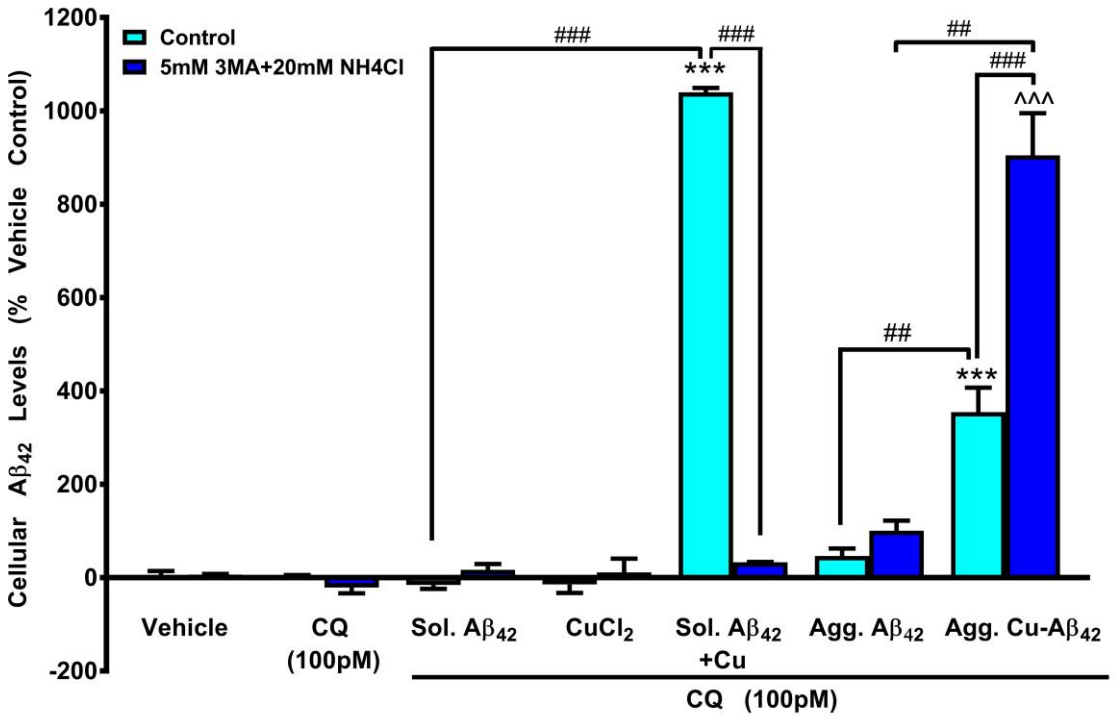

Figure 3.3.13 Effect of lysosomal and autophagy inhibitors on the uptake of Aβ into N2a cells in the presence of CQ and Cu

Blocking the lysosomal-autophagy pathway resulted in opposite effects on $CuCl_2$ and CQ's synergistically-induced cellular $A\beta_{42}$ uptake: a complete inhibition of $CuCl_2$ and CQ's synergistically-induced uptake of soluble $A\beta_{42}$ (Sol. $A\beta_{42}$) into N2a cells, as oppose to further enhancement of $CuCl_2$ and CQ's synergistically-induced uptake of aggregated $A\beta_{42}$ (Agg. $A\beta_{42}$) into N2a cells.

*Unpaired two-tailed t-test; ***p < 0.001 compared to vehicle;*

^^^p < 0.001 compared to lysosomal-autophagy inhibitors;

##p < 0.01, ###p < 0.001

Bars represent mean ± S.E.M, n ≥ 3

$A\beta_{42}$ levels in N2a cells treated with CQ alone or together with either soluble $A\beta_{42}$ or $CuCl_2$ were similar to each other, as well as to $A\beta_{42}$ levels in vehicle-treated N2a cells (**Fig. 3.3.13**; similar to **Fig. 3.3.3** and **Fig. 3.3.7**). In the presence of lysosomal-autophagy inhibitors, $A\beta_{42}$ levels in N2a cells treated with CQ alone or together with either soluble $A\beta_{42}$ or $CuCl_2$ were not statistically different to each other nor to $A\beta_{42}$ levels in N2a cells treated with lysosomal-autophagy inhibitors (**Fig. 3.3.13**). Furthermore, $A\beta_{42}$ levels in N2a cells treated with CQ alone or together with either soluble $A\beta_{42}$ or $CuCl_2$ were no different in the presence, compared to their respective treatments in the absence, of lysosomal-autophagy inhibitors (**Fig. 3.3.13**).

In keeping with data illustrated in **Fig. 3.3.3** and **Fig. 3.3.7**, $A\beta_{42}$ levels in N2a cells treated with soluble $A\beta_{42}$, $CuCl_2$ and CQ were significantly higher than $A\beta_{42}$ levels both in vehicle-treated N2a cells and in N2a cells treated with soluble $A\beta_{42}$ and CQ in the absence of $CuCl_2$ (**Fig. 3.3.13**). In the presence of lysosomal-autophagy inhibitors, $A\beta_{42}$ levels in N2a cells treated with soluble $A\beta_{42}$, $CuCl_2$ and CQ were significantly lower, compared to $A\beta_{42}$ levels in N2a cells treated with soluble $A\beta_{42}$, $CuCl_2$ and CQ in the absence of lysosomal-autophagy inhibitors (**Fig. 3.3.13**). Actually, $A\beta_{42}$ levels in N2a cells treated with soluble $A\beta_{42}$, $CuCl_2$ and CQ in the presence of lysosomal-autophagy inhibitors were equivalent to $A\beta_{42}$ levels in N2a cells treated with lysosomal-autophagy inhibitors either alone or together with soluble $A\beta_{42}$ and CQ (**Fig. 3.3.13**).

The complete inhibition of the synergistically-induced uptake of Aβ by Cu and CQ upon impeding lysosomal and autophagy activities indicated that CQ acted to deliver CuDDLs into neuronal cells to be eliminated by the process of macroautophagy.

Consistent with earlier findings (**Fig. 3.3.3**-**3.3.4** and **Fig. 3.3.7**-**3.3.8**), $A\beta_{42}$ levels in N2a cells treated with pre-aggregated $A\beta_{42}$ and CQ were comparable to $A\beta_{42}$ levels in vehicle-treated N2a cells (**Fig. 3.3.13**). While in the absence of CQ, $A\beta_{42}$ levels were slightly increased in N2a cells treated with pre-aggregated $A\beta_{42}$ in the presence, compared to the absence, of lysosomal-autophagy inhibitors (**Fig. 3.3.12**); $A\beta_{42}$ levels in N2a cells treated with pre-aggregated $A\beta_{42}$ and CQ in the presence of lysosomal-autophagy inhibitors were no different to $A\beta_{42}$ levels in N2a cells treated with either lysosomal-autophagy inhibitors alone or in N2a cells treated with pre-aggregated $A\beta_{42}$ in the absence of lysosomal-autophagy inhibitors (**Fig. 3.3.13**).

$A\beta_{42}$ levels in N2a cells co-treated with pre-aggregated Cu-$A\beta_{42}$ complexes and CQ were significantly elevated, compared to $A\beta_{42}$ levels in vehicle-treated N2a cells, as well as N2a cells treated with pre-aggregated $A\beta_{42}$ and CQ (**Fig. 3.3.13**; as in **Fig. 3.3.3** and **Fig. 3.3.7**). Likewise, $A\beta_{42}$ levels in N2a cells treated with pre-aggregated Cu-$A\beta_{42}$ complexes and CQ in the presence of lysosomal-autophagy inhibitors were significantly higher than $A\beta_{42}$ levels in N2a cells treated with lysosomal-autophagy inhibitors alone or together with pre-aggregated $A\beta_{42}$ and CQ (**Fig. 3.3.13**). Importantly, $A\beta_{42}$ levels were significantly enhanced in N2a cells treated with pre-aggregated Cu-$A\beta_{42}$ complexes and CQ in the presence, compared to the absence, of lysosomal-autophagy inhibitors (**Fig. 3.3.13**).

Taken together, these data imply that Cu and CQ jointly affect Aβ in distinct modes of action. While Cu and CQ evoked the neuronal uptake of both soluble and aggregated Aβ; once inside the cells, CuDDLs were removed by the lysosomal-autophagy system, whereas Aβ originating from AP-like aggregates did not undergo autophagy.

3.3.14 Effect of lysosomal and autophagy inhibitors on cellular Aβ levels in the absence and presence of Zn

Subsequently, the cellular uptake of Aβ, with and without Zn, was determined in the presence and absence of lysosomal-autophagy inhibitors (as per **section 3.2.7**).

$A\beta_{42}$ levels in N2a cells treated with lysosomal-autophagy inhibitors were similar to $A\beta_{42}$ levels in vehicle-treated N2a cells (**Fig. 3.3.12-3.3.14**). Similar to **Fig. 3.3.4**, $A\beta_{42}$ levels in N2a cells treated with soluble $A\beta_{42}$ and/or $ZnCl_2$ were also equivalent to $A\beta_{42}$ levels in vehicle-treated N2a cells and to one another (**Fig. 3.3.14**). As expected, $A\beta_{42}$ levels in N2a cells treated with soluble $A\beta_{42}$ and/or $ZnCl_2$ in the presence of lysosomal-autophagy inhibitors were not different to each other, to $A\beta_{42}$ levels in N2a cells treated with lysosomal-autophagy inhibitors alone or with their respective treatments in the absence of lysosomal-autophagy inhibitors (**Fig. 3.3.14**).

Once more, all negative cellular $A\beta_{42}$ values are an artefact of data analysis that is related to fact that the W0-2 antibody utilised in the ELISA can detect only human, and not murine, Aβ (refer to **section 3.2.10**); thus, these are simply background readings.

Consistent with prior findings (**Fig. 3.3.3**, **Fig. 3.3.4** and **Fig. 3.3.12**), under control conditions, $A\beta_{42}$ levels in N2a cells treated with pre-aggregated $A\beta_{42}$ were no different to $A\beta_{42}$ levels in vehicle-treated N2a cells (**Fig. 3.3.14**). On the other hand, $A\beta_{42}$ levels in N2a cells treated with pre-aggregated $A\beta_{42}$ in the presence of lysosomal-autophagy inhibitors were higher than $A\beta_{42}$ levels in N2a cells treated with either lysosomal-autophagy inhibitors alone or with pre-aggregated $A\beta_{42}$ in the absence of lysosomal-autophagy inhibitors (**Fig. 3.3.14**).

These results were paralleled in the presence of $ZnCl_2$. $A\beta_{42}$ levels in N2a cells treated with pre-aggregated Zn-$A\beta_{42}$ complexes were significantly elevated, relative to $A\beta_{42}$ levels in vehicle-treated N2a cells, as well as N2a cells treated with pre-aggregated $A\beta_{42}$ (**Fig. 3.3.4** and **Fig. 3.3.14**). $A\beta_{42}$ levels in N2a cells treated with pre-aggregated Zn-$A\beta_{42}$ complexes in the presence of lysosomal-autophagy inhibitors were significantly higher than $A\beta_{42}$ levels in N2a cells treated with lysosomal-autophagy inhibitors either alone or together with pre-aggregated $A\beta_{42}$ (**Fig. 3.3.14**). Notably, $A\beta_{42}$ levels were also significantly elevated in N2a cells treated with pre-aggregated Zn-$A\beta_{42}$ complexes in the presence, compared to the absence, of lysosomal-autophagy inhibitors (**Fig. 3.3.14**).

These results suggest that Zn may be able to stimulate the import of aggregated, but not soluble, Aβ into surrounding neurons, where the protein is degraded in a lysosomal-autophagy compartment.

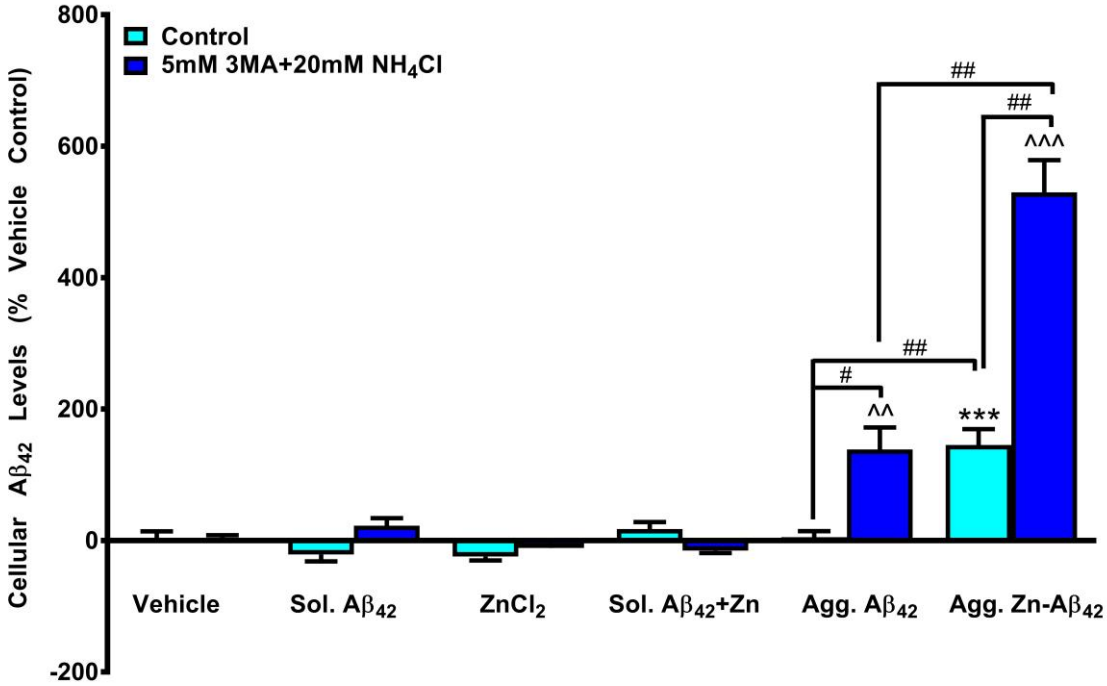

Figure 3.3.14 Effect of lysosomal and autophagy inhibitors on the uptake of Aβ into N2a cells in the absence and presence of Zn

Compared to control conditions, inhibition of the lysosomal-autophagy pathway did not impact $A\beta_{42}$ levels in N2a cells exposed to soluble $A\beta_{42}$ (Sol. $A\beta_{42}$) with and without $ZnCl_2$; yet, it resulted in increased $A\beta_{42}$ levels in N2a cells exposed to aggregated $A\beta_{42}$ (Agg. $A\beta_{42}$) with and without $ZnCl_2$.

*Unpaired two-tailed t-test; ***$p < 0.001$ compared to vehicle;*

^^$p < 0.01$, ^^^$p < 0.001$ compared to lysosomal-autophagy inhibitors;

$^{\#}p < 0.05$; $^{\#\#}p < 0.01$

Bars represent mean ± S.E.M, $n \geq 3$

3.3.15 Effect of lysosomal and autophagy inhibitors on cellular Aβ levels in the presence of CQ and Zn

Finally, the cellular uptake of Aβ was examined in the presence of CQ with and without Zn and/or lysosomal-autophagy inhibitors (according to **section 3.2.7**).

Data demonstrated that $A\beta_{42}$ levels in N2a cells treated with lysosomal-autophagy inhibitors were comparable to $A\beta_{42}$ levels in vehicle-treated N2a cells (**Fig. 3.3.15**; as in **Fig. 3.3.12-3.3.14**). Similar to **Fig. 3.3.4** and **Fig. 3.3.8**, $A\beta_{42}$ levels in N2a cells treated with CQ alone or together with soluble $A\beta_{42}$ and/or $ZnCl_2$ were no different to each other or to $A\beta_{42}$ levels in vehicle-treated N2a cells (**Fig. 3.3.15**). Likewise, in the presence of lysosomal-autophagy inhibitors, $A\beta_{42}$ levels in N2a cells treated with CQ alone or together with soluble $A\beta_{42}$ and/or $ZnCl_2$ were not different to one another or to $A\beta_{42}$ levels in N2a cells treated with lysosomal-autophagy inhibitors alone (**Fig. 3.3.15**).

$A\beta_{42}$ levels in N2a cells treated with pre-aggregated $A\beta_{42}$ and CQ were equivalent to $A\beta_{42}$ levels in vehicle-treated N2a cells (**Fig. 3.3.15**; similar to **Fig. 3.3.3-3.3.4**, **Fig. 3.3.7-3.3.8** and **Fig. 3.3.13**). Unlike in the absence CQ, where $A\beta_{42}$ levels in N2a cells treated with pre-aggregated $A\beta_{42}$ were higher in the presence, compared to the absence, of lysosomal-autophagy inhibitors (**Fig. 3.3.12** and **Fig. 3.3.14**); $A\beta_{42}$ levels were similar in N2a cells treated with pre-aggregated $A\beta_{42}$ and CQ both in the absence and presence of lysosomal-autophagy inhibitors (**Fig. 3.3.13** and **Fig. 3.3.15**).

Similar to results in the absence of CQ (**Fig. 3.3.14**), $A\beta_{42}$ levels in N2a cells treated with pre-aggregated Zn-$A\beta_{42}$ complexes and CQ were significantly higher than $A\beta_{42}$ levels in N2a treated with either vehicle or with pre-aggregated $A\beta_{42}$ and CQ (**Fig. 3.3.15**; as in **Fig. 3.3.4** and **Fig. 3.3.8**). In parallel, $A\beta_{42}$ levels in N2a cells treated with pre-aggregated Zn-$A\beta_{42}$ complexes and CQ in the presence of lysosomal-autophagy inhibitors were significantly elevated, compared to $A\beta_{42}$ levels in N2a cells treated with lysosomal-autophagy inhibitors alone or together with pre-aggregated $A\beta_{42}$ and CQ (**Fig. 3.3.15**). Importantly, $A\beta_{42}$ levels were significantly enhanced in N2a cells treated with pre-aggregated Zn-$A\beta_{42}$ complexes and CQ in the presence, compared to the absence, of lysosomal-autophagy inhibitors (**Fig. 3.3.15**).

These data imply that CQ does not affect Zn's ability to enhance neuronal uptake of aggregated Aβ, where it is degraded by the lysosomal-autophagy pathway.

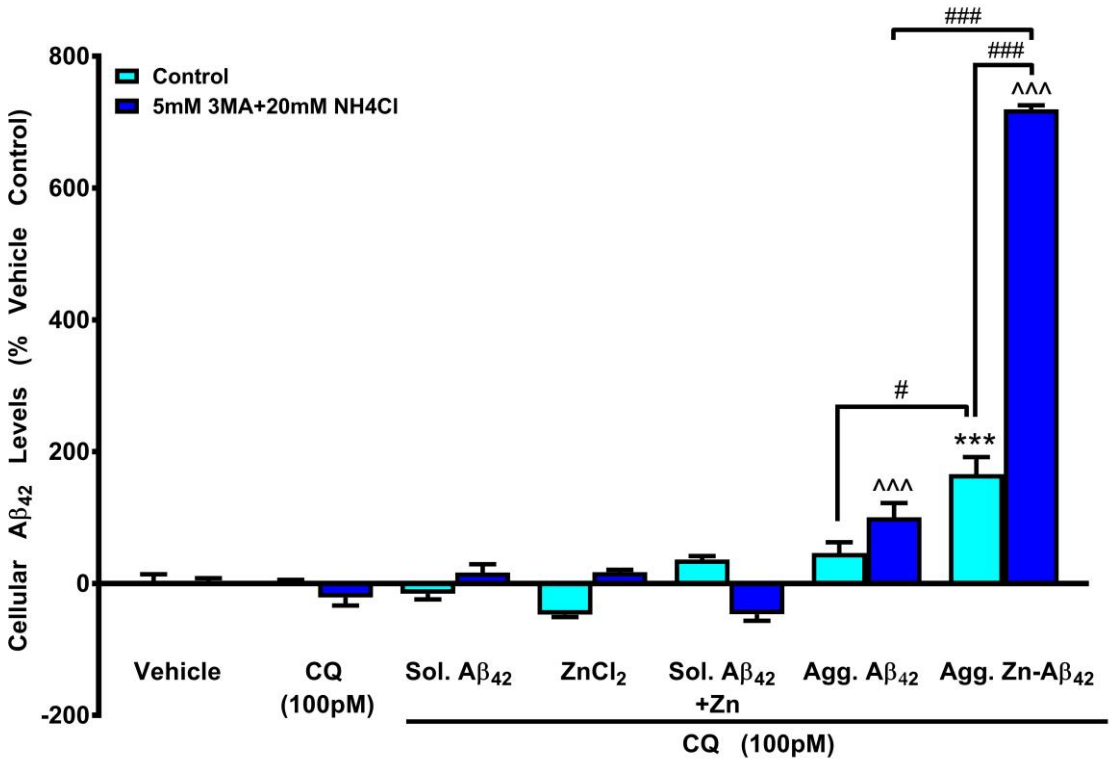

Figure 3.3.15 Effect of lysosomal and autophagy inhibitors on the uptake of Aβ into N2a cells in the presence of CQ and Zn

Blocking the lysosomal-autophagy pathway resulted in further enhancement of the $ZnCl_2$-induced uptake of aggregated $A\beta_{42}$ into N2a cells.

*Unpaired two-tailed t-test; ***$p < 0.001$ compared to vehicle;*

^^^$p < 0.001$ compared to lysosomal-autophagy inhibitors; $^{\#\#}p < 0.01$; $^{\#\#\#}p < 0.001$

Bars represent mean ± S.E.M, $n \geq 3$

3.4 Discussion

In recent years, there is an increasing interest in pharmacotherapeutics that target metal ions for the treatment of a range of diseases, including neurodegenerative diseases. These experimental drugs fall into different categories depending on their presumed mechanism of action (as detailed in **section 1.5**); yet, their exact therapeutic mechanism is usually ill defined and is based on the molecule's structure.

One such pharmaceutical agent is CQ (refer to **Table 1.5**), which has been in use for many years in both animals and humans due to its known ability to bind cations (694-696). CQ has demonstrated promising results both *in vitro* and *in vivo* (see **section 3.1**); however, each study used a dissimilar investigational setting and examined different end points. Consequently, CQ has been shown to exert various effects on animal and/or human biomarkers, behaviour, memory and learning depending on the system and the disease it has been tested in (elaborated on in **section 1.5.5**).

As more findings were published, it became increasingly apparent that CQ does not function as a simple metal chelator; but rather, in a more complex manner. This led to the hypothesis that CQ may, in fact, be a metal-protein attenuating compound (MPAC), which can disrupt the interaction of metals with Aβ, by binding either to the ion or to the peptide's metal-binding site(s), and the neurotoxic cascade that ensues (781).

Past investigations, however, looked only at the effects of CQ on metals and/or Aβ (436, 699, 700, 752); they did not look at any effects metals and Aβ may have on CQ itself. Opazo and colleges attempted to address this issue, using radioiodinated CQ (763). The experimental procedures in this chapter were designed with the intention of capitalizing on ^{125}I-CQ in order to investigate the relationship between CQ, metals and Aβ in a cell culture model relevant to AD.

The N2a murine neuroblastoma cell line (described in **section 3.2.1**) was chosen as it is neuronal-like, easy to culture and suitable for high throughput studies. Metal ions were used at a concentration of 10 μM throughout these experiments because they are believed to be at similar levels in the synaptic cleft during neurotransmission (355, 401, 782). Since it was previously determined that neurotoxicity is highest when Cu^{2+} and Aβ are at a 1:1 molar ratio (554), human $A\beta_{42}$ was also used at 10 μM. Pilot experiments by Opazo and Bellingham established that, even when ^{125}I-CQ was used at 100 pM, selective metals (Cu and Zn; 10 μM) significantly increased its cellular levels in N2a cells following an hour incubation in Locke's buffer (**Fig. 3.1.1**).

Whilst the use of ^{125}I-CQ yielded promising results, it was also met with many obstacles, such as a breakdown of the laboratory's gamma counter, worldwide supply shortage of ^{125}I isotope for an extended period, issues with ANSTO's nuclear reactor and courier company's license, to name a few. While trying to solve these problems, experiments continued, using 100 pM "cold" CQ instead of ^{125}I-CQ, and looked at its interplay with Cu and Zn ions, as well as with Aβ_{42}.

To distinguish cellular uptake from cellular retention, post-treatments the cells were extensively washed in order to strip any material that may be attached to the outer plasma membrane. The cells were subsequently fractionated by centrifugation, and all data presented in this chapter are of analyses performed on the cytoplasmic fraction.

This chapter's main conclusions are that, in a neuronal-like environment, not only are Cu and Zn ions different to one another in terms of their uptake and metabolism; but they also distinctly alter the entry and degradation of Aβ, depending on the protein's state (i.e., soluble *versus* aggregated). Moreover, while CQ does not affect the internalization and removal of Cu, Zn or Aβ individually; it acts synergistically, yet differentially, with these metal ions and either soluble or aggregated Aβ, to modulate the neuronal uptake and/or processing of both the metals and peptide, in parallel.

Under the experimental settings used in this chapter, it was shown that Cu, but not Zn or Aβ (soluble or self-aggregated), readily entered N2a cells (**Fig. 3.3.1** - **Fig. 3.3.4**) and was removed by an alternate pathway to macroautophagy (**Fig. 3.3.9 – Fig. 3.3.10**). The rapid, non-endocytic uptake of Cu into neuronal cells, irrespective of CQ (**Fig. 3.3.5**), points to active Cu transport, potentially by copper transporter 1 (CTR1) (783) or divalent metal transporter 1 (DMT1) (784). These receptors are known as the main mammalian trans-membrane Cu transporters in both the periphery and CNS. Lately, DMT1 has even been linked to the expression and processing of APP (785). To verify if one or both of these Cu transporters are involved in Cu uptake into N2a cells, their expression or activity could be suppressed by means of small interfering RNA (siRNA) or pharmacological inhibitors, respectively, and Cu uptake compared to WT N2a cells.

As for Zn and Aβ, it is hypothesized that the cells type (murine neuroblastoma cells), media type (serum-free Locke's buffer), exposure time (one hour) and/or dose (10 μM metals and Aβ; 100 pM CQ) were not sufficient to cause a change in their intracellular levels.

While there are no known publications in which Cu or Zn were added to N2a cells; there have been several studies in which immortalized neuronal-like and non-neuronal cell lines were incubated with these metals (in the absence and presence of CQ) at different doses, culture media and/or periods. Of these, only a few reported the cellular metal levels. Metal measurements were usually performed in cell pellets or lysates, using ICPMS, and resulted in heterogeneous outcomes.

Exposure of APP_{695}-overexpressing SY5Y cells for 16 hours to 200 μM $CuCl_2$ in basal Eagle's media, containing 20 % (v/v) FCS, led to significantly elevated Cu levels (41). While metal levels in APP_{695}-transfected CHO cells, exposed for six hours to $CuCl_2$ or $ZnCl_2$ (10 or 25 μM) in serum-free RPMI media, remained unaffected; cellular Cu and Zn levels were significantly increased in response to CQ and either $CuCl_2$ or $ZnCl_2$ (1:1; 10 or 25 μM) (166, 786). On the other hand, five hour exposure of M17 cells to CQ and $CuCl_2$, but not $ZnCl_2$ (1:1; 10 μM), in Opti-MEM® media supplemented with 10 % (v/v) foetal bovine serum (FBS), resulted in elevated cellular metal levels (434). Recently, one hour exposure of SY5Y cells to 10 μM $ZnSO_4$ in serum-free Hank's Balanced Salt Solution (HBSS) was sufficient to cause an increase to Zn levels (255).

Cu and Zn affect Aβ differently with relation to binding, conformation, aggregation and toxicity, and *vice versa* (evidence outlined in **sections 1.4.3.3–1.4.5**). Results of procedures that make up this chapter demonstrated that, in the presence of soluble metal-Aβ oligomers, neuronal-like cells do not take up the protein (**Fig. 3.3.3**-**3.3.4**, **Fig. 3.3.12** and **Fig. 3.3.14**) or Zn (**Fig. 3.3.2** and **Fig. 3.3.11**); but do take up Cu and deliver it to lysosomal-autophagy compartments for removal (**Fig. 3.3.1** and **Fig. 3.3.9**).

These findings probably reflect the different binding affinities of Cu and Zn ions towards Aβ and dissimilar resulting conformations. These outcomes may also indicate that Aβ is either able to interact with the empiric neuronal Cu importer or is capable of facilitating the uptake of Cu by an additional mechanism. Either way, based on the fact that Cu entered neuronal-like cells without Aβ, it is assumed that the metal would have a higher binding affinity to its transporter than it does towards Aβ. Once the neuronal Cu transporter is identified, it could be either knocked out or targeted by pharmacological agonists and/or antagonists, and CuDDLs-induced cellular Cu uptake compared to normal N2a cells. The significance of these findings is that the neurotoxicity attributed to CuDDLs (554, 768, 769) might be due to a considerable increase in neuronal Cu levels and may not be directly related to Aβ itself.

The observations also shed light on the unique MOA of CQ on Aβ oligomers, which are considered as the instigators of AD toxicity (236-246). While CQ did not affect Cu, Zn or soluble Aβ on their own (**Fig. 3.3.1**-**3.3.4**); together, CQ and Cu led to enhanced uptake of soluble Aβ (**Fig. 3.3.3**), and CQ and soluble Aβ led to suppressed uptake of Cu (**Fig. 3.3.1**). Interestingly, CQ simultaneously decreased the cellular uptake of Cu and increased that of soluble Aβ (**Fig. 3.3.1** and **Fig. 3.3.3**, respectively). The influx of Cu ions did not involve endocytosis (**Fig. 3.3.5**), while soluble Aβ entered neuronal cells *via* a secretory pathway (**Fig. 3.3.7**); however, both Cu and Aβ ended up being cleared by autophagy (**Fig. 3.3.10** and **3.3.13**, respectively).

The parallel, yet opposing, action of CQ implies that the drug may form a complex with CuDDLs that could separate at the cell surface, as its components are internalized by distinct pathways. The present data also stress that the therapeutic abilities of CQ may involve rescue from CuDDLs-related toxicity by reducing neuronal Cu down to sub-neurotoxic levels and by stimulating the removal and degradation of extracellular soluble Aβ; however, such an effect needs to be verified by toxicity assay(s).

Not surprisingly, the exact opposite effects were observed with aggregated Aβ. Experimental results showed that aggregated Aβ did not impact neuronal cell uptake of either Cu or Zn (**Fig. 3.3.1** and **Fig. 3.3.2**, respectively). On the other hand, metals that were complexes to Aβ, differentially affected the neuronal cell uptake of the protein. While Cu did not modulate aggregated Aβ entry into neuronal-like cells (**Fig. 3.3.3**); Zn induced the internalization (**Fig. 3.3.4**) and transport to the lysosomal-autophagy degradation system (**Fig. 3.3.14**) of aggregated Aβ.

These data suggest that the metal-enriched APs observed in brains of AD patients (359, 372, 385, 393-397) could be intimately involved in the dynamic homeostasis of cerebral Aβ. Whether this action is a harmful or a beneficial one remains to be determined.

Again, CQ exerted simultaneous dual action on metals and aggregated Aβ. The drug led to neuronal uptake of Cu-Aβ aggregates (**Fig. 3.3.1** and **Fig. 3.3.3**). While Cu was endocytosed, aggregated Aβ entered cells by an alternative mechanism (**Fig. 3.3.5** and **Fig. 3.3.7**, respectively); however, both components were eventually metabolized by the lysosomal-autophagy machinery (**Fig. 3.3.10** and **Fig. 3.3.13**). Conversely, CQ did not alter the lack of Zn entry, or the enhanced neuronal uptake of Aβ, from Zn-Aβ aggregates (**Fig. 3.3.2** and **Fig. 3.3.4**, respectively). These findings may be reconciled by the varying affinities of Cu and Zn to Aβ *versus* CQ.

Taken together, these data imply that, in addition to its CuDDLs inhibition effect, the therapeutic MOA of CQ in AD patients might also rely on its capability to disaggregate Cu-enriched APs and deliver them into the surrounding neurons, where they are cleared by the endogenous cellular systems.

In summary, whilst still unable to shed light on the pharmacokinetics of CQ, this chapter provides evidence that allows an initial and broader appreciation of CQ's differential effect on metals and Aβ in a cell-based model of AD. Further *in vitro* and *in vivo* experimentations are required to substantiate these findings and to determine the pharmacodynamics and MOA of CQ in the AD brain.

Chapter 4

Investigating the toxicity of CQ and metals in cultured cell lines

Chapter 4

4.1 Introduction

The results described in **Chapter 3** show that N2a cells take up, process and/or eliminate Cu differently from Zn, both in the absence and presence of CQ and/or Aβ (**Fig. 3.3.1-3.3.2**, **Fig. 3.3.5-3.3.6** and **Fig. 3.3.9-3.3.11**). N2a cells also metabolise soluble Aβ differently from aggregated Aβ, in the absence and presence of CQ, Cu and/or Zn (**Fig. 3.3.3-3.3.4**, **Fig. 3.3.7-3.3.8** and **Fig. 3.3.12-3.3.15**). Based on these findings and on work by White *et. al.* (436, 752), initial experiments were carried out with the intention of exploring the signalling cascades that may be initiated in N2a cells following exposure to and/or uptake of CQ, metals and Aβ.

Meanwhile, a growing literature has emerged with regards to the anti-cancer properties of CQ. A series of publications demonstrated *in vitro* that CQ decreased the viability of cell lines derived from human B-cell lymphoma, fibrosarcoma, bladder, breast, cervical, ovarian and pancreatic tumours (787-791). Naturally, the half maximal inhibitory concentration (IC_{50}) of CQ varied (within μM range), depending on the cell type and the exposure time of the cells to the drug (729, 787-792). *In vivo*, using X-ray fluorescent microscopy (XFM), it was shown that CQ treatment (10 mg/kg/day for 15 days) in mice implanted with human prostate tumour xenografts led to a significant decrease in Cu and Zn levels within tumour tissue; while sparing normal tissue (793).

Contrary to these authors' supposition, CQ-metal complexes did not rescue the cytotoxicity observed with CQ alone; instead, they further enhanced it (Cu > Zn > Fe) by virtue of increasing intracellular metal levels (621, 622, 748, 787, 790, 791, 794-796). Detailed investigation revealed that, together, CQ and Zn resulted in elevated labile Zn (particularly in lysosomes) and heme oxygenase 1 (HO1) levels, suppressed cell survival signalling pathways, and induced apoptotic and necrotic death in human blood, ovarian, breast and prostate cancer cell lines (622, 729, 787, 794, 797-799). Combination of CQ with Cu led to increased Cu, decreased metabolic activity, proteasome inhibition, arrested proliferation and apoptotic cell death in human breast, cervical, prostate, leukaemia and myeloma cancer cells (621, 735, 748, 791, 796, 799-802). Importantly, at the concentrations tested, CQ and its metal chelates exhibited selective toxicity towards xenografts and primary or secondary cells from solid malignancies, while sparing normal tissue or cells (621, 787, 791, 793, 800).

Notably, none of the cells used in the abovementioned studies were propagated from neuronal tumours. As our laboratory's research activities focus on neurodegenerative diseases, in particular AD and PD, we routinely utilize a range of neuronal cell lines as a means for *in vitro* testing. Therefore, the objective of this chapter was to ascertain the validity of using murine and human neuroblastoma and neuroglioma cells as pre-clinical models for evaluating CQ and/or metal ions (Cu, Zn and Fe) for various brain disorders.

As noted in **section 2.5**, CQ can be dissolved in organic solvents. In practice, CQ can be dissolved in DMSO up to 5 mM; it precipitates out of solution at higher concentrations. Preliminary results indicated that cells can only tolerate up to 0.5 % DMSO (v/v of experimental media). Hence, the highest concentration of CQ used in the studies described in this chapter was 25 μM. Since CQ is known to bind metals at a 2:1 stoichiometry (694-697), the highest concentration of Cu, Zn and Fe used in the experimental procedures described in this chapter was 12.5 μM.

Previous studies have shown that radioiodiniated CQ (^{123}I-CQ) injected into healthy volunteers, AD patients, Tg and non-Tg mice, as well as CQ administered to mice by oral gavage, was absorbed and almost completely cleared within 2-3 hours (700, 763). Accordingly, a three-hour incubation period was applied to all experiments described in this chapter.

To mimic the environment in the brain and in order to avoid chelation of CQ and/or exogenous metal ions by components in the serum, all incubations were conducted in serum-free media (after verifying that three-hour serum deprivation did not alter cell viability). Following this treatment regime (i.e., dose and exposure time of CQ and/or metals in serum-free media), various toxicity and/or cell viability assays were employed to measure the effect of CQ and metal-CQ complexes on an array of neuronal cells and on control CHO cells.

4.2 Experimental Methods

4.2.1 Cell lines and culture conditions

In addition to the N2a mouse neuroblastoma cell line (764), the characterisation and cultivation of which have been described in **section 3.2.1**, two human neuroblastoma cell lines were also obtained from the ATCC (Manassas, VA, USA) and used in this chapter: SH-SY5Y and BE(2)-M17 (henceforth, SY5Y and M17, respectively).

SY5Y cells were sub-cloned (803) from the parental SK-N-SH line, which was isolated from the bone marrow of a four year-old female with metastatic neuroblastoma (804). Neuroblast-like SY5Y cells grow in clusters with small, round cell bodies and fine, extended neurites, and possess moderate dopamine-β-hydroxylase (DBH) activity (805). Similarly, M17 cells were cloned from the original SK-N-BE(2) line that was derived from a bone marrow biopsy of a two year-old male with disseminated neuroblastoma (806). M17 cells appear as rounded cells with sporadic neuritic processes, and exhibit high tyrosine hydroxylase (TH) activity (807).

Other than the aforementioned neuroblastoma cell lines, H4 human neuroglioma cells were also obtained (kind gift of Dr Avril Pereira). The epithelial-like H4 clone was established from a 37 year-old male with neuroglioma (808). N2a, SY5Y and H4 cells were grown in DMEM, containing 25 mM D-glucose, 25 mM HEPES and 4 mM GlutaMAX™. M17 cells were grown in Opti-MEM® media (optimized Eagle's Minimal Essential Medium), containing 2 mM L-glutamine and buffered with HEPES.

The Chinese Hamster Ovary (CHO) cell line, isolated by Puck *et. al.* in 1957 from a biopsy of an ovary of an adult Chinese hamster (809), is not tumorigenic, but has been transformed in order to render it continuous. CHO-APP cells have been generated by transfecting CHO cells with pIRESpuro2 vector expressing human APP_{695} complimentary DNA (cDNA) (436). For the purpose of these studies, CHO cells transfected with empty vector or with APP_{695} (kind gift of Prof Andrew Hill), served as control to the tumorigenic neuronal cells and were maintained in Roswell Park Memorial Institute (RPMI) 1640 media, containing 0.003 mM of the antioxidant glutathione (GSH), 2 mM GlutaMAX™, 11 mM D-glucose and 25 mM HEPES.

All media were supplemented with 10 % (v/v) heat-inactivated FCS (Bovogen Biologicals; Essendon, Melbourne, VIC, Australia) and penicillin/streptomycin sulphate antibiotics (100 units/mL and 100 μg/mL, respectively).

Media of transfected CHO cells were also supplemented with 7.5 μg/mL puromycin (Sigma-Aldrich; Castle Hill, Sydney, NSW, Australia), as a selective agent.
Once confluent, cells were propagated (manner outlined in **section 3.2.1**) 2-3 times per week at a 1:5-1:15 ratio (depending on the growth rate of the cell line).

4.2.2 Preparation of CQ

5 mM CQ stock solutions were freshly prepared by dissolving the compound in DMSO. On experimental days, serial dilution in DMSO was performed in order to reach the following concentrations: 4, 3.2, 2, 1.6, 1, 0.4 and 0.2 mM. CQ was added to treatment media immediately prior to exposure of different cell lines at final concentrations ranging from 1 to 25 μM.

4.2.3 Preparation of metals

Metal stock solutions were prepared by dissolving cupric chloride ($CuCl_2$), zinc chloride ($ZnCl_2$) and ferric chloride ($FeCl_3$) in water. Following their initial preparation, stock solutions were analysed by ICPMS and their concentrations were determined to be 9.5 mM, 10.8 mM Zn and 6.9 mM Fe.
On experimental days, serial dilution in water was conducted in order to reach the following metal concentrations: 2.5, 2, 1.6, 1, 0.8, 0.5, 0.2 and 0.1 mM. Cu, Zn and Fe were added to treatment media immediately prior to exposure of various cell lines at final concentrations ranging from 0.5 to 12.5 μM.

4.2.4 Cellular toxicity studies of CQ and/or metals

Cells were seeded at a density of 0.5-1 $\times 10^5$ cells/cm^2 in the inner wells of 48-well plates (to ensure even evaporation) and maintained in serum-containing media (up to 2 days), until reaching ~90 % confluence. On experimental days, culture media was aspirated, and cells were rinsed with PBS, prior to three-hour treatment in serum-free media with CQ (up to 25 μM), metals ($CuCl_2$, $ZnCl_2$, $FeCl_3$; up to 12.5 μM), CQ-metal complexes (2:1 molar ratio; up to 25 μM CQ and up to 12.5 μM metals) or vehicle control (equal volumes of water and DMSO as treatments) in triplicates. CCK-8 was employed as the primary cell survival assay (as per **section 2.10.1**) and its results were verified by other cell viability and/or cytotoxicity assays (see **sections 2.10.2-2.10.4**).

4.3 Experimental Results

4.3.1 Toxicity of CQ and/or metals in N2a cells

As the N2a mouse neuroblastoma cell line was used in all experimental procedures described in **Chapter 3**, it was the first to be investigated for the effect of CQ, metals and CQ-metal complexes on its survival (see **section 4.2.4**).

The viability of N2a cells treated with 8, 10 or 25 μM CQ was lower than vehicle-treated N2a cells (~81, 80 and 75 %, respectively; **Fig. 4.3.1 A**). However, treatment with 16 or 20 μM CQ did not alter the viability of N2a cells, compared to vehicle-treated N2a cells (**Fig. 4.3.1 A**).

In comparison to vehicle-treated N2a cells, the number of live N2a cells treated with 0.5, 1, 5 or 12.5 μM $CuCl_2$ was variably decreased (**Fig. 4.3.1 B**); yet, no difference was observed in the survival of N2a cells co-treated with any of the tested doses of CQ and $CuCl_2$ (up to and including 25 μM CQ and 12.5 μM $CuCl_2$; **Fig. 4.3.1 C**).

There was no change in the viability of N2a cells treated with $ZnCl_2$ (equal to or less than 12.5 μM) in the absence or presence of CQ (equal to or less than 20 μM CQ and 10 μM $ZnCl_2$; **Fig. 4.3.1 D** and **E**, respectively). The survival rate of N2a cells was only affected by co-treatment with 25 μM CQ and 12.5 μM $ZnCl_2$ (~60 % of vehicle-treated N2a cells; **Fig. 4.3.1 E**). Although it may appear as if co-treatment with 8 μM CQ and 4 μM $ZnCl_2$ enhanced the number of live N2a cells, this difference was found to be not statistically significant.

Similar to $ZnCl_2$, treatment with $FeCl_3$ did not affect the number of viable N2a cells (**Fig. 4.3.1 F**). Concomitant treatment with either low or high doses of CQ and $FeCl_3$ (up to 5 μM CQ and 2.5 μM $FeCl_3$ or 16-25 μM CQ and 8-12.5 μM $FeCl_3$, respectively) also did not impact the viability of N2a cells (**Fig. 4.3.1 G**). Interestingly, treatment with moderate concentrations of CQ and $FeCl_3$ in parallel (8-10 μM CQ and 4-5 μM $FeCl_3$, respectively) significantly diminished the survival of N2a cells (~82 %, relative to vehicle-treated N2a cells; **Fig. 4.3.1 G**)

These findings indicate that, under the conditions used, CQ and its metal chelates are toxic to the N2a neuroblastoma cell line; however, only at doses higher than 5 μM. In addition, while N2a cells are sensitive to Cu, they are not sensitive to Fe or Zn.

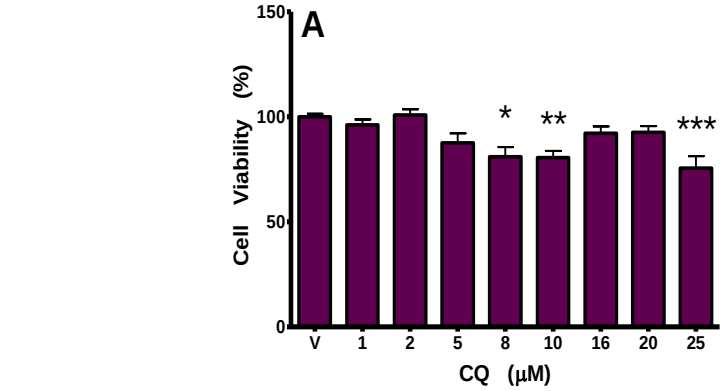
A
Cell Viability (%)
150
100
50
0
*
**
***
V 1 2 5 8 10 16 20 25
CQ (μM)

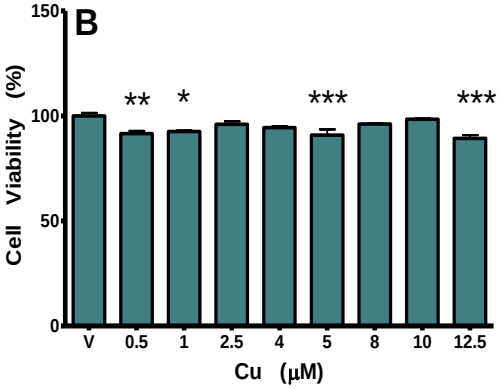
B
Cell Viability (%)
150
100
50
0
** * *** ***
V 0.5 1 2.5 4 5 8 10 12.5
Cu (μM)

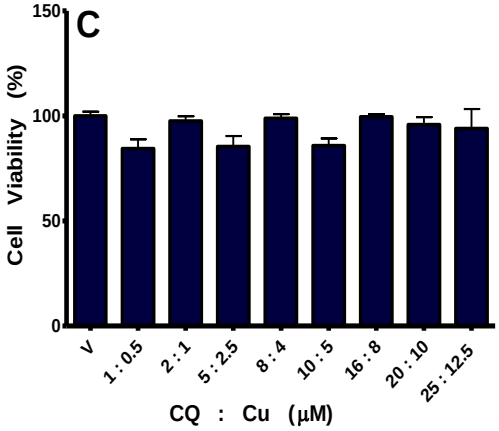
C
Cell Viability (%)
150
100
50
0
V 1 : 0.5 2 : 1 5 : 2.5 8 : 4 10 : 5 16 : 8 20 : 10 25 : 12.5
CQ : Cu (μM)

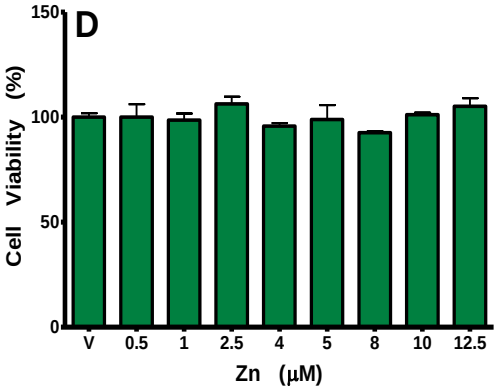
D
Cell Viability (%)
150
100
50
0
V 0.5 1 2.5 4 5 8 10 12.5
Zn (μM)

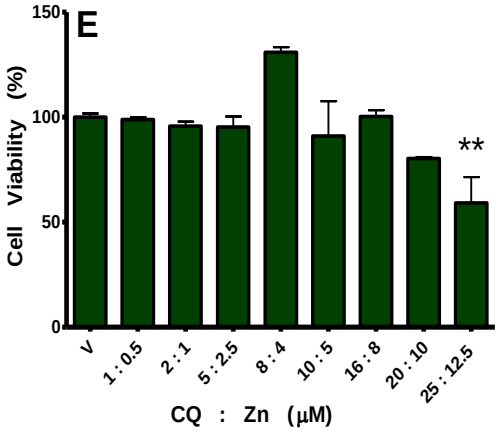
E
Cell Viability (%)
150
100
50
0
**
V 1 : 0.5 2 : 1 5 : 2.5 8 : 4 10 : 5 16 : 8 20 : 10 25 : 12.5
CQ : Zn (μM)

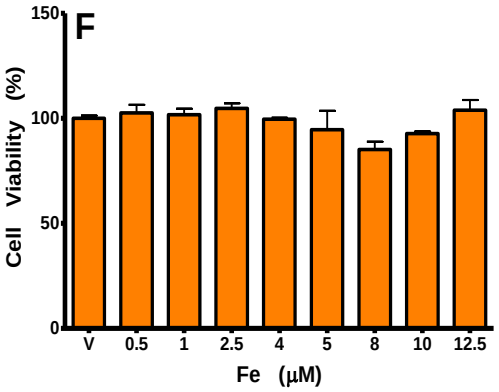
F
Cell Viability (%)
150
100
50
0
V 0.5 1 2.5 4 5 8 10 12.5
Fe (μM)

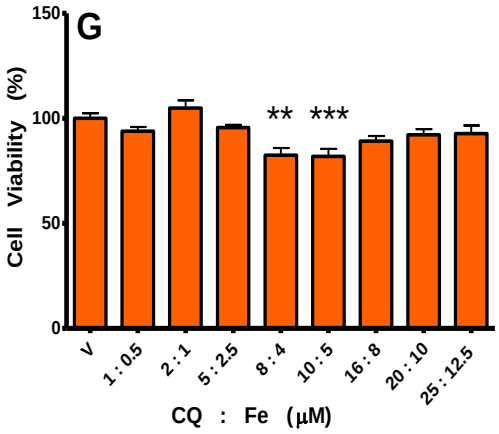
G
Cell Viability (%)
150
100
50
0
** ***
V 1 : 0.5 2 : 1 5 : 2.5 8 : 4 10 : 5 16 : 8 20 : 10 25 : 12.5
CQ : Fe (μM)

Figure 4.3.1 Dose-response effect of CQ and/or metal ions on the viability of N2a cells

*Exposure to CQ (8-10 and 25 μM; **A**) and Cu (0.5, 1, 5 and 12.5 μM; **B**) was generally dose-dependently toxic to N2a cells. Neither Zn nor Fe (≤ 12.5 μM; **D** and **F**, respectively) were cytotoxic to N2a cells.*

*Metal complexes of the drug were variably toxic to N2a cells, depending on the metal and/or the dose of the metal-CQ complex. Cytotoxicity was not observed in N2a cells exposed to CQ-Cu complexes (≤ 25 μM CQ and 12.5 μM Zn; **C**); but, was observed at the highest dose of CQ-Zn complexes (25 μM CQ and 12.5 μM Zn; **E**) and at moderate doses of CQ-Fe complexes (8-10 μM CQ and 4-5 μM Fe, respectively; **G**).*

*ANOVA with Dunnett's multiple comparison test; *p < 0.05, **p < 0.01, ***p < 0.001 compared to vehicle-control*

Bars represent mean ± S.E.M, n = 2

4.3.2 Toxicity of CQ and/or metals in BE(2)-M17 cells

Next, the response to various concentrations of CQ and metal ions, either alone or together, was examined in M17 cells (procedure outlined in **section 4.2.4**). Our research group has previously utilised the M17 human neuroblastoma cell line (described in **section 4.2.1**) to evaluate metal uptake with ascending doses of either CQ or PBT2 (700). The study showed that co-treatment with PBT2 led to a dose-dependent increase in cellular Cu, Zn and Fe levels; however, with CQ, this effect was only observed for Cu (700).

Under the experimental conditions used in this chapter, there was a dose-dependent loss in viability of M17 cells following treatment with 20 and 25 μM CQ, (~70 % and 67 % of vehicle-treated M17 cells, respectively; **Fig. 4.3.2 A**).

Compared to vehicle-treated M17 cells, the survival of M17 cells treated with either 1 or 8 μM $CuCl_2$ was slightly decreased (~91 %; **Fig. 4.3.2 B**). On the other hand, the viability of M17 cells co-incubated with CQ and $CuCl_2$ (as low as 2 μM CQ and 1 μM $CuCl_2$ and as high as 25 μM CQ and 12.5 μM $CuCl_2$) was significantly diminished (varied between 80 and 57 %, as compared to vehicle-treated M17 cells; **Fig. 4.3.2 C**).

Other than treatment with 1 μM $ZnCl_2$, which slightly reduced the number of live M17 cells; the survival of M17 cells treated with $ZnCl_2$ was unaffected, compared to vehicle-treated M17 cells (**Fig. 4.3.2 D**). In contrast, the survival rate of M17 cells co-treated with doses equal to or higher than 8 μM CQ and 4 μM $ZnCl_2$ was diminished in a dose-dependent manner (down to 62 % of vehicle-treated cells; **Fig. 4.3.2 E**).

The viability of M17 cells treated with $FeCl_3$, in the absence or presence of CQ, was mostly unchanged (**Fig. 4.3.2 F** and **G**, respectively); with the exception of treatment with 1 μM $FeCl_3$, which decreased M17 cell survival (~92 %; **Fig. 4.3.2 F**) and co-treatment with 25 μM CQ and 12.5 μM $FeCl_3$, which increased cell viability (~110 %; **Fig. 4.3.2 G**), relative to vehicle-treated M17 cells.

Collectively, these observations imply that, under the test conditions, metals alone are variably toxic to M17 cells (Cu > Fe > Zn). CQ, alone or with either Cu or Zn, is dose-dependently toxic to M17 cells (CQ-Cu > CQ-Zn > CQ). Surprisingly, as opposed to Fe on its own, Fe in combination with CQ may be protective to M17 human neuronal-like cells. In general, M17 cells were more sensitive to CQ-metal toxicity than N2a cells.

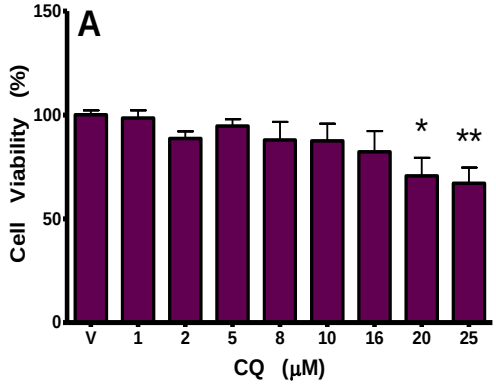
A
Cell Viability (%)
150
100
50
0
*
**
V 1 2 5 8 10 16 20 25
CQ (μM)

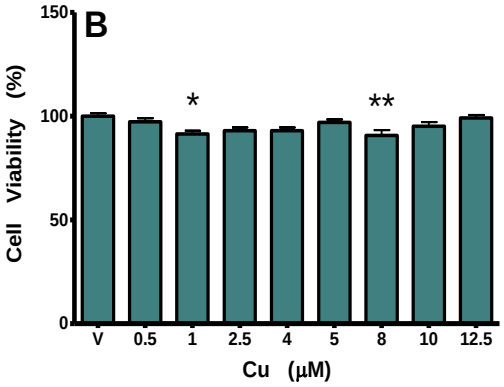
B
Cell Viability (%)
150
100
50
0
*
**
V 0.5 1 2.5 4 5 8 10 12.5
Cu (μM)

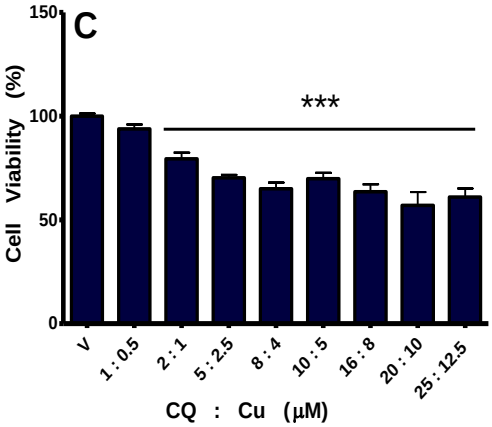
C
Cell Viability (%)
150
100
50
0
***
V 1 : 0.5 2 : 1 5 : 2.5 8 : 4 10 : 5 16 : 8 20 : 10 25 : 12.5
CQ : Cu (μM)

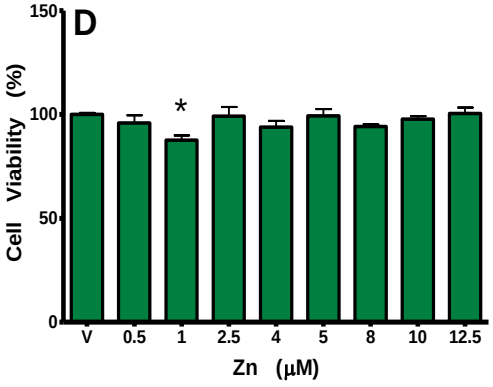
D
Cell Viability (%)
150
100
50
0
*
V 0.5 1 2.5 4 5 8 10 12.5
Zn (μM)

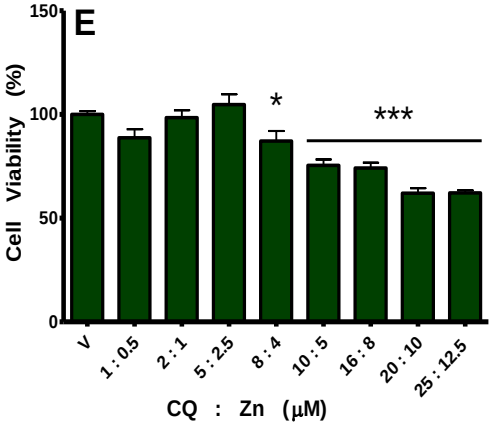
E
Cell Viability (%)
150
100
50
0
*
***
V 1 : 0.5 2 : 1 5 : 2.5 8 : 4 10 : 5 16 : 8 20 : 10 25 : 12.5
CQ : Zn (μM)

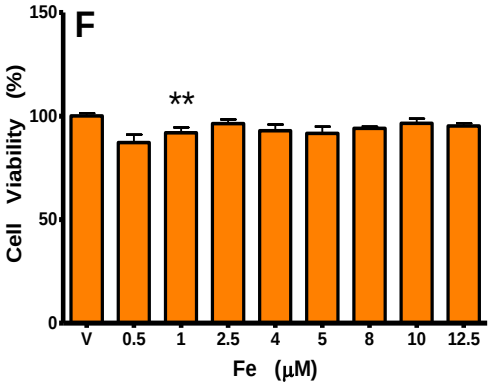
F
Cell Viability (%)
150
100
50
0
**
V 0.5 1 2.5 4 5 8 10 12.5
Fe (μM)

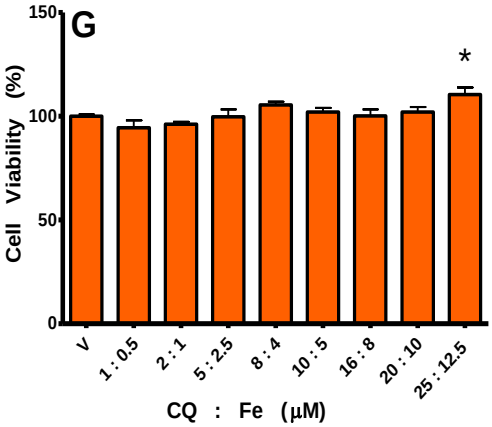
G
Cell Viability (%)
150
100
50
0
*
V 1 : 0.5 2 : 1 5 : 2.5 8 : 4 10 : 5 16 : 8 20 : 10 25 : 12.5
CQ : Fe (μM)

Figure 4.3.2 Dose-response effect of CQ and/or metals on the viability of M17 cells

*Exposure to Cu, Zn or Fe (≤ 12.5 μM; **B, D** and **F**, respectively) lowered the survival rate of M17 cells to varying degrees.*

*The viability of M17 cells was significantly diminished following exposure to high doses of CQ (≥ 20 μM; **A**), moderate to high doses of CQ-Zn complexes (≥ 8 μM CQ and 4 μM Zn; **E**) and low to high doses of CQ-Cu complexes (≥ 2 μM CQ and 1 μM Cu; **C**). Exposure to CQ-Fe complexes, not only did not decrease the survival of M17 cells, but in the highest tested dose (25 μM CQ and 12.5 μM Fe) it elevated their viability (**G**).*

*ANOVA with Dunnett's multiple comparison test; *p < 0.05, **p < 0.01, ***p < 0.001 compared to vehicle-control*

Bars represent mean ± S.E.M, n = 2

4.3.3 Toxicity of CQ and/or metals in SH-SY5Y cells

Neuroblastomas are clinically heterogeneous tumours that vary in location, histopathologic appearance and biologic characteristics. Therefore, an additional human neuroblastoma cell line, SY5Y (described in **section 4.2.1**), was employed to explore the impact of the CQ, metal ions and CQ-metal chelates on cell viability (**section 4.2.4**).

Interestingly, treatment with CQ at low to moderate concentrations (2-8 μM) modestly elevated the number of viable SY5Y cells (~123-132 %, in comparison to vehicle-treated SY5Y cells; **Fig. 4.3.3 A**). Treatment with CQ at concentrations equal to or higher than 10 μM did not alter SY5Y cell survival (**Fig. 4.3.3 A**).

Of all the $CuCl_2$ doses tested, only 1 μM $CuCl_2$ affected the viability of SY5Y cells (increased to ~134 %, compared to vehicle control; **Fig. 4.3.3 B**). To rule this out as an artefact, repeated experimentation is needed. Surprisingly, while co-treatment with 8 or 16 μM CQ and 4 or 8 μM $CuCl_2$, respectively, resulted in higher SY5Y cell survival; the opposite effect was observed following concomitant treatment with 25 μM CQ and 12.5 μM $CuCl_2$ (decreased to ~70 % of vehicle-treated SY5Y cells; **Fig. 4.3.3 C**).

Following three-hour incubation with all tested doses of $ZnCl_2$, other than 1 μM, the survival rate of SY5Y cells was variably increased (~127-137 %, as compared to vehicle-treated SY5Y cells; **Fig. 4.3.3 D**). Similarly, the viability of SY5Y cells incubated with low doses of $ZnCl_2$ in the presence of CQ (1 or 2 μM CQ and 0.5 or 1 μM $ZnCl_2$, respectively) was enhanced, relative to vehicle control (~125 and 134 %, respectively; **Fig. 4.3.3 E**). However, at doses equal to or higher than 5 μM CQ and 2.5 μM $ZnCl_2$, the number of live SY5Y cells was significantly diminished (~30 % of vehicle-treated SY5Y cells; **Fig. 4.3.3 E**), similar to M17 cells (**Fig. 4.3.2 E**).

The survival rate of SY5Y cells remained unchanged following treatment with $FeCl_3$, either in the absence or presence of CQ (**Fig. 4.3.3 F** and **G**, respectively); except for treatment with either 2.5 μM $FeCl_3$ alone (**Fig. 4.3.3 F**) or parallel treatment with 0.5 μM $FeCl_3$ and 1 μM CQ (**Fig. 4.3.3 G**) that led to a slight rise in viability of SY5Y cells, compared to vehicle-treated SY5Y cells.

Like N2a cells, CQ at doses lower than 5 μM, in the absence and presence of metals, is not toxic to SY5Y cells. In fact, results show that low doses of CQ or metals may stimulate growth and/or proliferation of SY5Y neuronal-like cells. In contrast, combination of CQ and metal ions (Zn > Cu > Fe) at moderate to high concentrations could induce SY5Y neuroblastoma cell death.

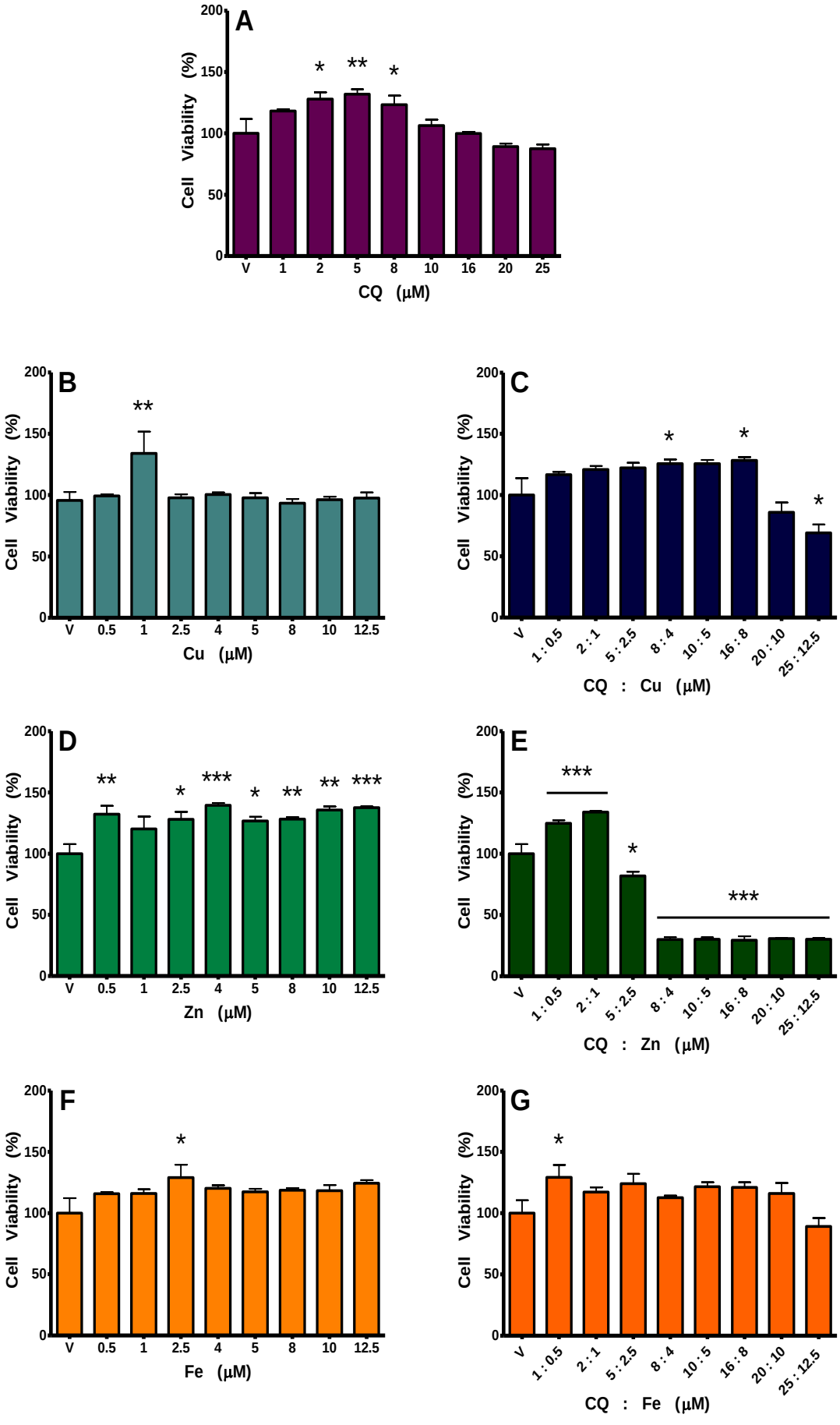
A
Cell Viability (%)
200
150
100
50
0
V 1 2 5 8 10 16 20 25
CQ (μM)
B
Cell Viability (%)
V 0.5 1 2.5 4 5 8 10 12.5
Cu (μM)
C
Cell Viability (%)
V 1 : 0.5 2 : 1 5 : 2.5 8 : 4 10 : 5 16 : 8 20 : 10 25 : 12.5
CQ : Cu (μM)
D
Cell Viability (%)
V 0.5 1 2.5 4 5 8 10 12.5
Zn (μM)
E
Cell Viability (%)
V 1 : 0.5 2 : 1 5 : 2.5 8 : 4 10 : 5 16 : 8 20 : 10 25 : 12.5
CQ : Zn (μM)
F
Cell Viability (%)
V 0.5 1 2.5 4 5 8 10 12.5
Fe (μM)
G
Cell Viability (%)
V 1 : 0.5 2 : 1 5 : 2.5 8 : 4 10 : 5 16 : 8 20 : 10 25 : 12.5
CQ : Fe (μM)

Figure 4.3.3 Dose-response effect of CQ and/or metals on the viability of SY5Y cells

*The survival of SY5Y cells was enhanced following exposure to CQ (2-8 μM; **A**), Cu (1 μM; **B**), CQ-Cu complexes (8-16 μM CQ and 4-8 μM Cu, respectively; **C**), Zn (≥ 12.5 μM; **D**), CQ-Zn complexes (≥ 2 μM CQ and 1 μM Zn; **E**), Fe (2.5 μM; **F**) and CQ-Fe complexes (1 μM CQ and 0.5 Fe; **G**).*

*Loss in viability of SY5Y cells was only seen upon exposure to the highest dose of CQ-Cu complexes (25 μM CQ and 12.5 μM Cu; **C**) and moderate to high doses of CQ-Zn complexes (≤ 5 μM CQ and 2.5 μM Zn; **E**).*

*ANOVA with Dunnett's multiple comparison test; *p < 0.05, **p < 0.01, ***p < 0.001 compared to vehicle-control*

Bars represent mean ± S.E.M, n = 2

4.3.4 Toxicity of CQ and/or metals in H4 cells

In contrast to neuroblastomas, gliomas are rapidly progressive brain malignancies. After studying both murine and human neuroblastoma cell lines (**sections 4.2.1-4.2.3**), the effect of CQ and/or metals was assessed in H4 neuroglioma cells (see **section 4.2.1**).

Results showed that treatment with moderate to high doses of CQ (10-20 μM) significantly decreased the number of live H4 cells (~83 %, compared to vehicle-treated H4 cells; **Fig. 4.3.4 A**). Unexpectedly, at its highest tested concentration (25 μM), CQ did not impact the survival rate of H4 cells (**Fig. 4.3.4 A**).

None of the $CuCl_2$ concentrations tested (equal to or less than 12.5 μM), either in the absence or presence of CQ (equal to or less than 25 μM), altered the number of viable H4 cells (**Fig. 4.3.4 B** and **C**, respectively).

On the other hand, treatment with $ZnCl_2$, with and without CQ, resulted in variably decreased viability of H4 neuroglioma cells (**Fig. 4.3.4 E** and **D**, respectively). H4 cell survival was reduced following incubation with 0.5, 5 or 8 μM $ZnCl_2$ alone (**Fig. 4.3.4 D**), and was lowered further upon co-treatment with 1, 10 or 16 μM CQ, respectively (**Fig. 4.3.4 E**). Of note, treatment with 1 or 2.5 μM $ZnCl_2$, with and without 2 or 5 μM CQ, did not compromise the survival rate of H4 cells (**Fig. 4.3.4 D** and **E**). Importantly, while the viability of H4 cells was unaffected by treatment with 4, 10 or 12.5 μM $ZnCl_2$ alone (**Fig. 4.3.4 D**); in the presence of CQ (8, 20 or 25 μM, respectively), H4 cell viability was significantly decreased (88, 60 and 40 % of vehicle-treated H4 cells, respectively; **Fig. 4.3.4 E**).

In comparison to vehicle-treated H4 cells, treatment with $FeCl_3$ (equal to or less than 12.5 μM), either alone or together with CQ (equal to or less than 25 μM), did not alter the number of viable H4 cells (**Fig. 4.3.4 F** and **G**, respectively); the only exception being 0.5 μM $FeCl_3$ that slightly lowered the survival of H4 cells (~91 %; **Fig. 4.3.4 F**).

Taken together, these findings suggest that neither Cu, Fe or their complexes with CQ are toxic to the H4 neuroglioma cell line. Conversely, H4 cells are sensitive to CQ alone at doses equal to or exceeding 10 μM, as well as to free and CQ-coordinated Zn.

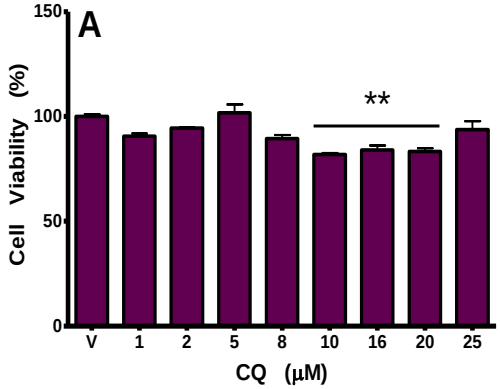
A
Cell Viability (%)
150
100
50
0
**
V 1 2 5 8 10 16 20 25
CQ (μM)

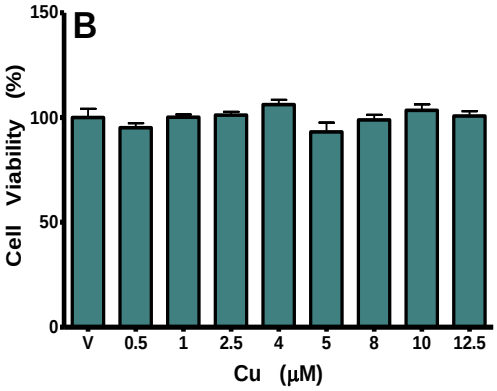
B
Cell Viability (%)
150
100
50
0
V 0.5 1 2.5 4 5 8 10 12.5
Cu (μM)

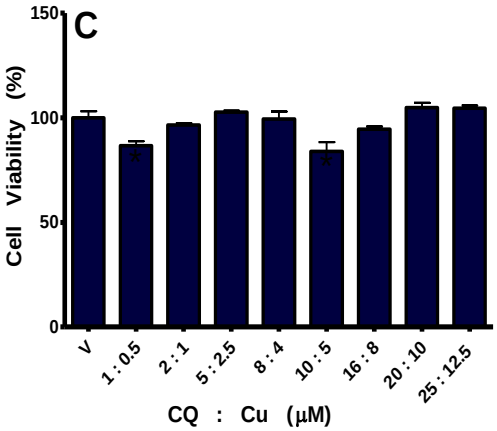
C
Cell Viability (%)
150
100
50
0
*
*
V 1 : 0.5 2 : 1 5 : 2.5 8 : 4 10 : 5 16 : 8 20 : 10 25 : 12.5
CQ : Cu (μM)

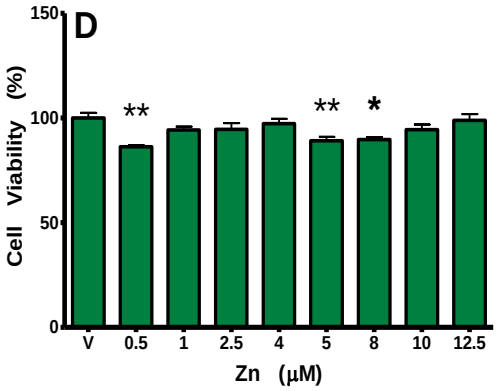
D
Cell Viability (%)
150
100
50
0
**
**
*
V 0.5 1 2.5 4 5 8 10 12.5
Zn (μM)

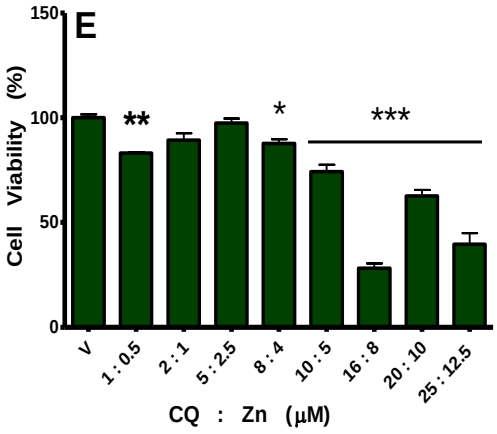
E
Cell Viability (%)
150
100
50
0
**
*
***
V 1 : 0.5 2 : 1 5 : 2.5 8 : 4 10 : 5 16 : 8 20 : 10 25 : 12.5
CQ : Zn (μM)

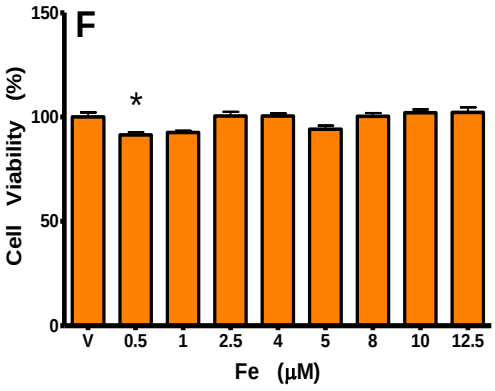
F
Cell Viability (%)
150
100
50
0
*
V 0.5 1 2.5 4 5 8 10 12.5
Fe (μM)

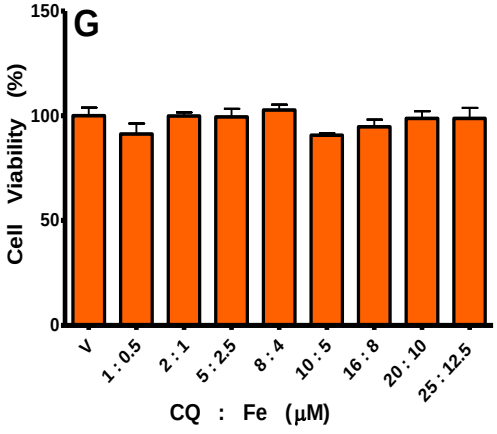
G
Cell Viability (%)
150
100
50
0
V 1 : 0.5 2 : 1 5 : 2.5 8 : 4 10 : 5 16 : 8 20 : 10 25 : 12.5
CQ : Fe (μM)

Figure 4.3.4 Dose-response effect of CQ and/or metal ions on the viability of H4 cells

*Exposure to 10-20 μM CQ significantly decreased the viability of H4 cells (**A**).*

*The viability of H4 cells was unaffected by exposure to Cu (≤ 12.5 μM; **B**), alone or together with CQ (≤ 25 μM; **C**).*

*Exposure of H4 cells to 0.5, 5 and 8 μM Zn reduced their survival (**D**), which was further diminished in the presence of 1, 10 and 16 μM CQ, respectively (**E**). The viability of H4 cells co-exposed to the highest doses of CQ-Zn complexes (20-25 μM CQ and 10-12.5 μM Zn, respectively) was also significantly compromised (**E**).*

*The survival of H4 cells exposed to 0.5 μM Fe was slightly lowered (**F**); but was, otherwise, unaffected by exposure to Fe (1-25 μM; **F**) or CQ-Fe complexes (≤ 25 μM CQ and 12.5 μM Fe).*

*ANOVA with Dunnett's multiple comparison test; *p < 0.05, **p < 0.01, ***p < 0.001 compared to vehicle-control*

Bars represent mean ± S.E.M, n = 2

4.3.5 Toxicity of CQ and/or metals in CHO cells

The cytotoxicity of CQ and/or metals was established in an array of neuronal (**sections 4.3.1-4.3.4**) and non-neuronal (621, 622, 729, 787, 789-795, 797, 800-802) cancerous cell lines. The effect of CQ and other metal-chelators (in the presence and absence of metal ions) on the viability, metal uptake, signalling cascade induction and Aβ degradation was also ascertained in continuous CHO epithelial cells transfected with APP (436, 607, 752, 810, 811). For the purpose of the studies performed as part of this chapter, both empty-vehicle and APP-transfected CHO cells were used (**sections 4.3.5** and **4.3.6**, respectively).

Data demonstrated that treatment with CQ (equal to or less than 25 μM), $CuCl_2$ (equal to or less than 12.5 μM) or combination of the two (all doses but 20 μM CQ and 10 μM $CuCl_2$) did not affect CHO cell survival, in comparison to vehicle-treated CHO cells (**Fig. 4.3.5 A**, **B** and **C**, respectively).

Unlike $CuCl_2$, incubation with $ZnCl_2$ (at all doses up to and including 12.5 μM) significantly and dose-dependently diminished the survival of CHO cells (down to 70 % of vehicle-treated CHO cells; **Fig. 4.3.5 D**). Surprisingly, only co-treatment with 25 μM CQ and 12.5 μM $ZnCl_2$ resulted in a significant decrease in CHO cell viability (~76 %, relative to vehicle-treated CHO cells; **Fig. 4.3.5 E**); while all other tested doses (up to and including 20 μM CQ and 10 μM $ZnCl_2$) had no effect on the survival of CHO cells.

Following treatment with $FeCl_3$, the survival rate of CHO cells was not compromised (**Fig. 4.3.5 F**); whereas, parallel treatment with CQ and $FeCl_3$ at doses equal to or higher than 5 μM CQ and 2.5 μM $FeCl_3$ resulted in a significant loss in the number of viable CHO cells (down to ~86 %, compared to vehicle-treated cells; **Fig. 4.3.5 G**).

Overall, these observations point to CQ, Cu and Fe on their own not being toxic to CHO cells; however, CHO cells being highly sensitive to Zn. In addition, while combination of CQ with either Cu or Zn is toxic to CHO cells only at high doses; all CQ-Fe complexes are toxic to CHO cells (CQ-Fe > CQ-Zn > CQ-Cu).

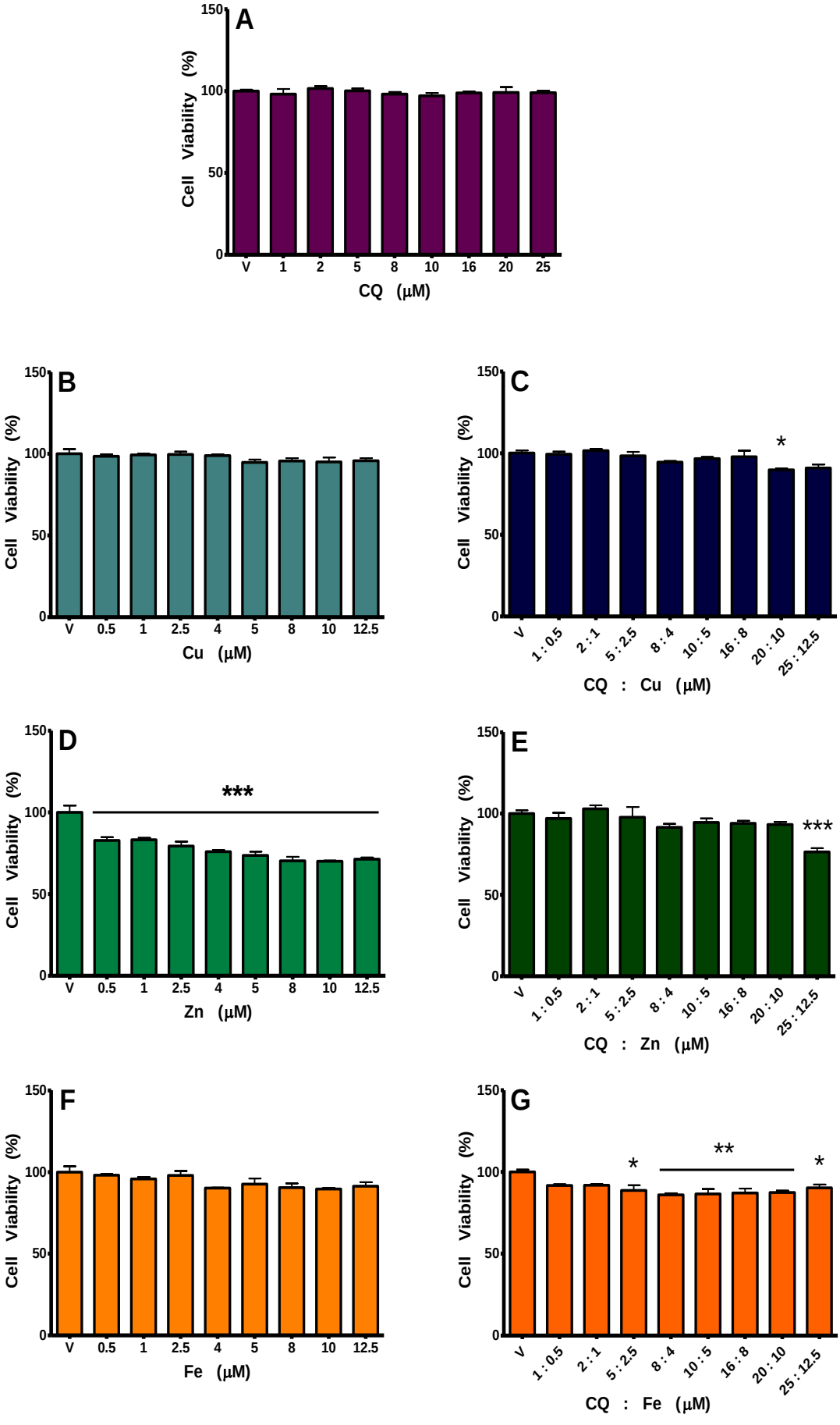
A
Cell Viability (%)
150
100
50
0
V 1 2 5 8 10 16 20 25
CQ (μM)
B
Cell Viability (%)
V 0.5 1 2.5 4 5 8 10 12.5
Cu (μM)
C
*
V 1 : 0.5 2 : 1 5 : 2.5 8 : 4 10 : 5 16 : 8 20 : 10 25 : 12.5
CQ : Cu (μM)
D
***
V 0.5 1 2.5 4 5 8 10 12.5
Zn (μM)
E
***
V 1 : 0.5 2 : 1 5 : 2.5 8 : 4 10 : 5 16 : 8 20 : 10 25 : 12.5
CQ : Zn (μM)
F
V 0.5 1 2.5 4 5 8 10 12.5
Fe (μM)
G
* ** *
V 1 : 0.5 2 : 1 5 : 2.5 8 : 4 10 : 5 16 : 8 20 : 10 25 : 12.5
CQ : Fe (μM)

Figure 4.3.5 Dose-response effect of CQ and/or metals on the viability of CHO cells

*The survival of CHO cells was unaffected by exposure to CQ (≥ 25 μM; **A**), Cu (≥ 12.5 μM; **B**) or both (except for 20 μM CQ and 10 μM Cu; **C**).*

*Exposure to Zn significantly diminished the viability of CHO cells (≥ 12.5 μM; **D**); however, in the presence of CQ, only exposure to the highest dose decreased the survival of CHO cells (25 μM CQ and 12.5 μM Zn; **E**).*

*Viability of CHO cells was unaltered by Fe alone (≥ 12.5 μM; **F**); but, it was significantly reduced following exposure to moderate to high concentrations of Fe in the presence of CQ (≤ 5 μM CQ and 2.5 μM Fe; **G**).*

*ANOVA with Dunnett's multiple comparison test; *p < 0.05, **p < 0.01, ***p < 0.001 compared to vehicle-control*

Bars represent mean ± S.E.M, n = 2

4.3.6 Toxicity of CQ and/or metals in CHO-APP cells

Finally, the response of stably-transfected CHO-APP_{695} cells (refer to **section 4.2.1**) to a range of CQ and/or metals ions treatments was tested (as detailed in **section 4.2.4**).

Similar to CHO cells, viability of CHO-APP cells treated with CQ (equal to or less than 25 μM), $CuCl_2$ (equal to or less than 12.5 μM) or both (equal to or less than 25 μM CQ and 12.5 μM $CuCl_2$) remained unaffected (**Fig. 4.3.6 A**, **B** and **C**, respectively).

Also comparable to CHO cells, incubation with most tested doses of $ZnCl_2$ alone (equal to or higher than 2.5 μM), and co-incubation with the highest dose of $ZnCl_2$ and CQ (12.5 and 25 μM, respectively), significantly compromised the survival of CHO-APP cells, relative to vehicle-treated CHO-APP cells (**Fig. 4.3.6 D** and **E**, respectively). At low doses of $ZnCl_2$ (0.5-1 μM) and at low to high doses of CQ and $ZnCl_2$ (up to and including 20 μM CQ and 10 μM $ZnCl_2$), there was no difference in viability, compared to vehicle-treated CHO-APP cells (**Fig. 4.3.6 D** and **E**, respectively).

As with $CuCl_2$, none of the tested doses of $FeCl_3$ (equal to or less than 12.5 μM) impacted the number of viable CHO-APP cells (**Fig. 4.3.6 F**). Parallel treatment with either low doses of CQ and $FeCl_3$ (1-2 μM and 0.5-1 μM, respectively) or high doses (20-25 μM CQ and 10-12.5 μM $FeCl_3$) also did not alter the survival of CHO-APP cells, in comparison to vehicle-treated CHO-APP cells (**Fig. 4.3.6 G**). In contrast, co-treatment with moderate to high concentrations of the drug and metal (5-16 μM CQ and 2.5-8 μM $FeCl_3$, respectively) moderately diminished the number of live CHO-APP cells (~89-93 % of vehicle-treated CHO-APP cells; **Fig. 4.3.6 G**).

These outcomes suggest that whilst CQ, Cu and Fe are not cytotoxic, Zn is highly toxic to CHO-APP cells, even at relatively low amounts. As for CQ complexes with metals, CHO-APP cells are only sensitive to high levels of CQ-Zn, but are quite sensitive to moderate CQ-Fe (CQ-Fe > CQ-Zn > CQ-Cu).

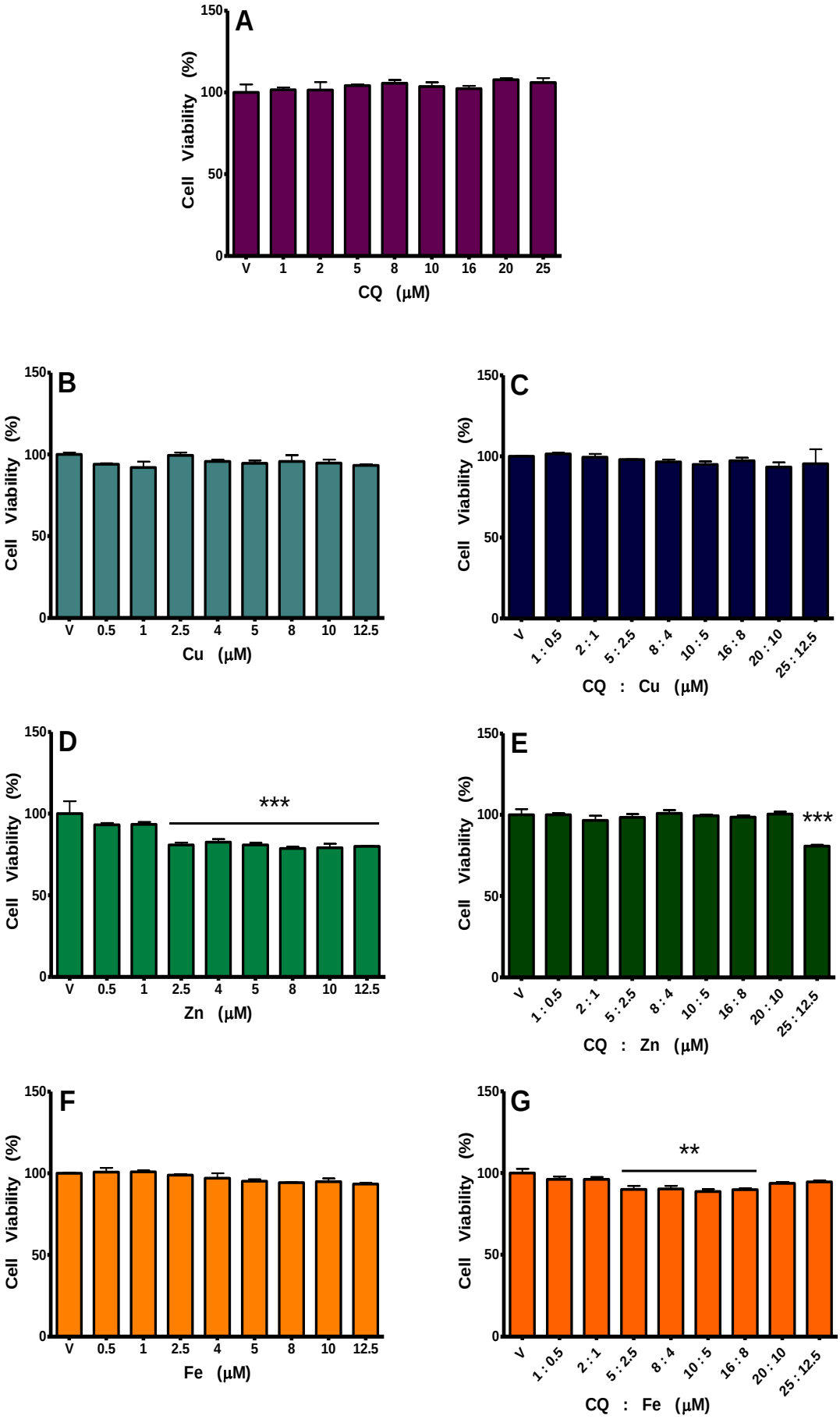
A
Cell Viability (%)
150
100
50
0
V 1 2 5 8 10 16 20 25
CQ (μM)
B
Cell Viability (%)
V 0.5 1 2.5 4 5 8 10 12.5
Cu (μM)
C
Cell Viability (%)
V 1 : 0.5 2 : 1 5 : 2.5 8 : 4 10 : 5 16 : 8 20 : 10 25 : 12.5
CQ : Cu (μM)
D
Cell Viability (%)
***
V 0.5 1 2.5 4 5 8 10 12.5
Zn (μM)
E
Cell Viability (%)
***
V 1 : 0.5 2 : 1 5 : 2.5 8 : 4 10 : 5 16 : 8 20 : 10 25 : 12.5
CQ : Zn (μM)
F
Cell Viability (%)
V 0.5 1 2.5 4 5 8 10 12.5
Fe (μM)
G
Cell Viability (%)
**
V 1 : 0.5 2 : 1 5 : 2.5 8 : 4 10 : 5 16 : 8 20 : 10 25 : 12.5
CQ : Fe (μM)

Figure 4.3.6 Dose-response effect of CQ and/or metals on the viability of CHO-APP cells

*Exposure to CQ (≤ 25 μM; **A**), Cu (≤ 12.5 μM; **B**) or both (≤ 25 μM CQ and 12.5 μM Cu; **C**) did not alter the survival of CHO-APP cells.*

*While exposure to Zn significantly decreased the viability of CHO-APP cells (≥ 2.5 μM; **D**); in the presence of CQ, only exposure to the highest concentration reduced the survival rate of CHO-APP cells (25 μM CQ and 12.5 μM Zn; **E**).*

*On the other hand, none of the Fe doses affected the number of viable CHO-APP cells (≤ 12.5 μM; **F**); whereas, exposure to Fe in the presence of CQ significantly diminished the number of live CHO-APP cells (5-16 μM CQ and 2.5-8 μM Fe, respectively; **G**).*

*ANOVA with Dunnett's multiple comparison test; **p < 0.01, ***p < 0.001 compared to vehicle-control*

Bars represent mean ± S.E.M, n = 2

4.4 Discussion

Acute and chronic toxicology testing represents a major part of the safety evaluation of compounds in environmental, food, cosmetic, medical and pharmaceutical industries. In the pre-clinical drug development process, rodent and non-rodent *in vivo* models are employed for examining ocular and/or dermal irritation, immunotoxicity, carcinogenicity, genotoxicity, developmental and reproductive toxicology.

Guided by the three R's (replacement, reduction and refinement) principle (812), toxicology studies also utilise myriad *in silico* and/or *in vitro* techniques. The latter consist of simple, inexpensive, sensitive and high-throughput analyses that quantify the degree of cell growth/arrest (cytostasis, division or proliferation) and survival/death (senescence, cytolysis or cytotoxicity) caused by experimental drugs in a wide variety of models (isolated organs, tissue slices, primary cultures, cell lines and sub-cellular preparations).

Traditional toxicity methods are based on manual or automated counting of cells that, depending on cell membrane permeability, either absorb or exclude staining dyes, such as propidium iodide or trypan blue. This could be time consuming and may under-estimate cell death. Other conventional cytotoxicity protocols are based on nucleotide uptake activity that require pre-labelling with radioactive isotopes or fluorescence dyes, and involve extensive washing of the cells. Advanced toxicity assays, including the ones used in this chapter, rely on a more rapid, accurate and reproducible measure of colour change due to impaired membrane integrity or enzymatic activity in a large number of cells, as an indication of cell lysis or viability, respectively.

In this chapter, cytotoxicity assays were utilized to validate the use of murine and human cells, derived from neuroblastoma and neuroglioma tumours, as pre-clinical models for assessing the therapeutic MOA of CQ and/or metals (Cu, Zn and Fe) for various neurodegenerative diseases (as described in **section 1.5.5**).

For these studies, cell survival was primarily determined, using the CCK-8 assay (refer to **section 2.10.1**). The CCK-8 assay was preferred to the MTT and MTS assays (see **sections 2.10.2** and **2.10.3**, respectively), as it did not warrant reconstituting or thawing of the reagent, did not entail a solubilisation step; nor did it affect the cells (thereby, allowing additional experiments to be carried out using the same cells). In addition to being easier and quicker to perform, the CCK-8 assay was also found to be more reproducible and sensitive than the abovementioned assays (i.e., able to distinguish between reversible mitochondrial impairment and cell death).

In vitro experiments comprising this chapter revealed that CQ, metals and CQ-metal complexes yielded differential effects (no change, decrease or increase) on the viability of several neuronal cell lines; some of which were dose-dependent. Due to time constraints, the corresponding cellular metal levels, gene or protein expression profiles, and the type of cell death were not determined; however, it is possible to draw from past publications in order to speculate, with high probability, on the reasons for the differential sensitivity of the various cell lines to the aforementioned treatments.

Results showed that CQ was toxic to N2a and H4 cells, at similar concentrations (ranging between 8 and 25 μM) (**A** panel in **Fig. 4.3.1** and **Fig. 4.3.4**, respectively).
Following the discovery that IRE binding to the APP 5'UTR directs the protein's mRNA translation, Bandyopadhyay *et. al.* tested the dose-response effect of several known Fe-binding compounds on the viability of H4 and SY5Y cells at 48 hours (416). Using an MTS assay, the authors showed that 50 μM CQ reduced the viability of H4 cells by half and 100 μM CQ rendered almost 100 % of H4 cells non-viable (416). The treatment media was not described in the article, but it is assumed to contain serum.

In all experiments constituting this chapter, cells were incubated for three hours in serum-free media with CQ in doses no greater than 25 μM, and cell survival was primarily assessed, using the CCK assay (rational explained in **section 4.1**). Therefore, a direct comparison between these results is not possible; though, it is plausible that the high concentrations of CQ and its prolonged exposure time to H4 cells were, at least in part, the reasons for the reported cytotoxicity.

Despite having found CQ, at relatively high concentrations, to be toxic to M17 cells; at low to moderate levels, CQ enhanced the viability of SY5Y cells (**A** panel in **Fig. 4.3.2** and **Fig. 4.3.3**, respectively). Interestingly, an increased number of viable SY5Y cells was also observed subsequent to 48 hour exposure to low levels of CQ (416). Conversely, 24 hour exposure to CQ did not affect SY5Y cell proliferation at low doses; but did suppress the proliferation of SY5Y cells, at doses higher than 25 μM (750).

As for the effect of CQ on M17 cell survival, one study found that 8-hour incubation of M17 cells with 25 μM CQ was not toxic in serum-free Opti-MEM® media, but was highly toxic in Locke's buffer (810). Disparity in these outcomes, most likely, stems from variability in the type of treatment media. Recently it was reported, also by the White group, that 26 hour exposure of M17 cells to 20 μM CQ in serum-free Opti-MEM® media led to decreased viability and increased cell death (813). Inconsistencies between these data may be attributed to different incubation period of the cells with CQ.

At the experimental settings used, the survival rate of H4 human neuroglioma cells was unaffected by Cu, either in the absence or presence of CQ (**Fig. 4.3.4 B** and **C**, respectively). Interestingly, 1 μM Cu was found to enhance the viability of one human neuroblastoma cell type (SY5Y; **Fig. 4.3.3 B**), but to diminish that of another (M17; **Fig. 4.3.2 B**) and of a mouse neuroblastoma cell line (N2a; **Fig. 4.3.1 B**).

Similarly, CQ-Cu complexes decreased the survival of M17 cells (low to high doses; **Fig. 4.3.2 C**) and increased that of SY5Y cells (moderate doses; **Fig. 4.3.3 C**). However, the viability of SY5Y cells was reduced subsequent to treatment with the highest tested concentration of CQ-Cu chelates (**Fig. 4.3.3 C**). In a paper published by Adlard and colleagues, it was shown that M17 cellular Cu levels were significantly raised in response to five hour incubation with 10 μM CQ-Cu, in comparison to 10 μM Cu (700). It is, therefore, surprising that such significant toxicity was observed in M17 cells in response to CQ-Cu (with the exception of the lowest tested dose; **Fig. 4.3.2 C**).

It would be reasonable to speculate that factors, which may be involved in these differences, could include the drug-metal molar ratios (1:1 as oppose to 2:1) and the absence *versus* presence of serum in the treatment media. Two molecules of CQ are required to coordinate Cu (694-696); therefore, when CQ and Cu are used at an equal molar ratio, only half of the Cu molecules will be coordinated by CQ (697); leaving 50 % of Cu ions free. This could have major consequences on metal uptake and cell viability. As for using cell culture medium including or excluding serum, serum is supplemented to media in order maintain cell cultures for long periods, as it contains all the necessary nutrients. These include metal ions, as well as proteins, lipids and lipoproteins, which could chelate CQ and/or Cu; thus, influencing the assay's outcomes.

Taken together, these findings support a role for CQ in modulating cellular Cu metabolism, which could be different in mouse *versus* human neuroblastoma cells, as well as in between human neuroglioma and neuroblastoma cell lines. In addition, the data imply that the therapeutic window of CQ-Cu complexes (be it for cancer, neurodegenerative or other diseases) may be narrow and that caution is warranted.

Of the neuronal-like cell lines examined, N2a and M17 neuroblastoma cells were not affected by Zn in terms of viability (**D** panel in **Fig. 4.3.1** and **4.3.2**, respectively). As opposed to Zn alone, CQ-Zn complexes did induce toxicity in N2a cells (at the highest concentration; **Fig. 4.3.1 E**) and M17 cells (at moderate to high doses; **Fig. 4.3.2 E**). Of note, Zn levels were no different in M17 cells exposed for five hours to 10 μM Zn, alone or with 10 μM CQ, compared to control (700).

Zn evoked toxicity in H4 cells, which was further exacerbated in the presence of CQ (**Fig. 4.3.4 D** and **E**, respectively). While moderate to high doses of CQ-Zn complexes were toxic to SY5Y cells, low concentrations of CQ-Zn elevated SY5Y cell survival (**Fig. 4.3.3 E**); as did most levels of Zn (**Fig. 4.3.3 D**).

Combined, these results suggest that binding of Zn by CQ may enhance the toxic effect and/or oppose the growth or proliferative effect of Zn alone on neuronal cells, in a dose-dependent manner. This information is important for the use of neuronal-like cell lines as *in vitro* models for testing the actions of therapeutic and/or imaging agents which target Zn, in pre-clinical and/or clinical development.

With regards to Fe, the metal ion did not alter the survival of N2a or H4 cells (**F** panel in **Fig. 4.3.1** and **Fig. 4.3.4**, respectively); yet, while the viability of H4 cells was also unchanged by CQ-Fe, that of N2a cells was compromised by moderate doses of CQ-Fe chelates (**G** panel in **Fig. 4.3.4** and **Fig. 4.3.1**, respectively).

In relation to human neuroblastoma cell lines, treatment with 1 μM Fe resulted in impaired M17 cell survival (**Fig. 4.3.2 F**). Conversely, exposure to 2.5 μM Fe caused an elevation in SY5Y cell viability (**Fig. 4.3.3 F**). The lowest and highest tested doses of CQ-Fe complexes were found to slightly increase the viability of SY5Y and M17 cells, respectively (**G** panel in **Fig. 4.3.3** and **Fig. 4.3.2**, respectively).
These data may point to differential impact of Fe *versus* CQ-Fe in neuroblastoma cells, originating from both mice and humans, as opposed to neuroglioma cells.

To control for data obtained from neuronal cell lines (**sections 4.3.1-4.3.4**), the effects of CQ, metal ions and CQ-metal complexes on cellular survival rate were also assessed in non-neuronal, non-cancerous cells (**sections 4.3.5-4.3.6**). For availability and convenience purposes, CHO and CHO-APP cells were utilized (see **section 4.2.1**).

CQ was not cytotoxic to either CHO or CHO-APP cells (**A** panel in **Fig. 4.3.5** and **Fig. 4.3.6**, respectively). CQ was previously shown to elevate Cu and Zn, but not Fe, levels in CHO-APP cells (436). It is unknown whether changes in metal levels, in response to CQ, occur in CHO cells as well; thus, the role of APP in modulating CHO cellular metals and viability and its affect by CQ remain unclear. Still, the lack of CQ-mediated toxicity in WT and APP-transfected CHO cells is a positive result for the development of CQ analogues for the treatment of AD and other neurodegenerative diseases (refer to **section 1.5**).

The survival rate of both CHO and CHO-APP cells was unaffected by Cu or CQ-Cu complexes (**B** and **C** panels in **Fig. 4.3.5** and **4.3.6**, respectively). Experimental evidence exist to show that treatment with Cu did not modulate metal levels in CHO-APP cells; but, two hour incubation with CQ-Cu was sufficient to elevate Cu levels in these cells (436, 607, 752). Therefore, it can be inferred that normal cells (with or without APP over-expression) may be able maintain their survival despite the CQ-mediated rise in cellular Cu. This is not to say that at intracellular Cu levels exceeding the ones tested here, cellular survival rate will not be diminished.

In CHO and CHO-APP cells, while significant toxicity was observed in most tested Zn doses; it was evident only at the highest tested concentration of CQ-Zn complexes (**D** and **E** panels in **Fig. 4.3.5** and **Fig. 4.3.6**, respectively). These results were unexpected as Zn alone was not shown to regulate metal levels in CHO-APP cells, even after six hour exposure; but, together with CQ, led to a significant increase in cellular Zn in CHO-APP cells (436, 752). This indicates that, at low to moderate doses, CQ may prevent and/or protect against Zn-mediated cellular toxicity.

Though Fe was not toxic to either CHO or CHO-APP cells (**F** panel in **Fig. 4.3.5** and **Fig. 4.3.6**, respectively); significant cytotoxicity was observed in response to most doses of CQ-Fe chelates in both CHO and CHO-APP cells (**G** panel in **Fig. 4.3.5** and **Fig. 4.3.6**, respectively). This is somewhat surprising since treatment of CHO-APP cells with Fe, in the absence or presence of CQ, resulted in a similarly significant elevation to cellular Fe levels (436, 752). Hence, it was hypothesised that Fe and Fe-CQ complexes would both be either toxic or non-toxic to CHO-APP cells. This means that perhaps the toxicity seen with CQ-Fe complexes, as oppose to Fe alone, is caused by a mechanism unrelated to Fe uptake. The fact that there is no differential variance in toxicity between CHO and CHO-APP cells challenged with Fe or CQ-Fe complexes, could suggest that APP may not be involved in these processes; despite the fact that APP translation and expression are regulated by Fe (416), and that APP KO cells and mice exhibit Fe retention (443).

Overall, at the concentrations tested, neuronal-like cell lines were variably susceptible to toxicity by metals (mainly Cu); whereas, Zn was the only metal to impair the viability of normal cells. On the other hand, CQ did not affect the survival of CHO or CHO-APP cells, yet exerted preferential cytotoxicity on most neuronal cell lines (at different doses, depending on the cell line); apart from SY5Y cells, in which certain doses of CQ had the opposite consequence (i.e., proliferative effect).

In general, cell lines derived from neuronal tumours were more prone to CQ-metal complexes-induced toxicity than normal CHO cells; although, the latter were sensitive to CQ-Fe chelates. Based on the literature available on CHO-APP (but not CHO) and neuronal cancer cell lines, it is possible to speculate that the enhanced cytotoxic effect of metal-free and metal-coordinated CQ may be credited to CQ's ability to increase intracellular metal levels. Regardless, these observations stress that toxicity of test compounds is dependant, not only on their concentration and exposure time of the cells, but also on the cell type and characteristics (genotype and phenotype).

The demonstrated cytotoxicity of CQ and, more so, of CQ-metal chelates in cell lines, originating from neuronal tumours (**sections 4.3.1 – 4.3.4**) and from malignancies in internal organs and the blood system (refer to **section 4.1**), is vital for the continued pre-clinical (787, 797, 814) and clinical (815) investigation into the anti-neoplastic properties of CQ and its metal complexes.

On a broader scope, these data contribute to the understanding of metal ions' involvement in cancer, and are of significance for the development of metal-ligands, either as PET imaging tracers for the diagnosis and monitoring of tumours or as potential targeted therapeutics for various cancers (816). Drawing from the experimental results of this chapter and of recent publications, Prana biotechnology (Parkville, Melbourne, VIC, Australia) has initiated a collaborative research programme into the potential of MPACs and other metal-targeting compounds as chemotherapeutic agents, especially for brain cancer, with PBT519 as its lead candidate drug currently in pre-clinical testing (660).

In conclusion, the findings in this chapter have immediate and important implications for the use of immortalized, neuronal-like cell lines (with inherently altered metabolism and cell signal transduction) for pre-clinical screening of metal-targeting agents, such as CQ, PBT2 (Prana biotechnology; Parkville, Melbourne, VIC, Australia) and others (discussed in **section 1.5**), as therapeutics for neurological disorders and/or neurodegenerative diseases. It is, therefore, recommended that the experimental cell-based disease model and the therapeutic window would be optimized individually for each compound and specifically for each therapeutic indication.

Chapter 5

Characterisation of CQ, metals and Aβ interactions in mouse primary cortical neuronal cells

Chapter 5

5.1 Introduction

Over the years, whole books, journal issues (and parts thereof) have been dedicated to the pharmacology and/or toxicology study of CQ (679, 770, 817-819) in numerous models: murine and human cell lines (WT, KO and/or transfected) (416, 436, 607, 621, 622, 644, 689, 700, 721, 728, 729, 748-750, 752, 787-792, 794-802, 810, 811, 813, 820-823), primary retinal (686, 687) and cortical neuronal cultures (444, 549, 707, 721, 813, 824, 825), yeast strains (501, 747, 751), *C. elegans* nematodes (746), *Drosophila melanogaster* flies (826), mice (Tg and non-Tg) (444, 671, 691, 692, 699, 700, 709, 720, 725, 726, 733, 736, 746, 759, 761, 763, 787, 793, 800, 827-832), rats (601, 666, 730, 731, 830, 833-842), gerbils (843), hamsters (667, 668, 727, 732, 844), cats and dogs (755, 845-856), monkeys (857) and humans (710, 711, 745, 754). Interestingly, in each of these experimental settings, CQ exhibited differential effects on metal ions, and the combination of CQ with metals altered a myriad of genes, multiple proteins and/or diverse signalling pathways.

Although *in vivo* models are considered the ultimate determinants of systemic drug effects, they are also complex and may mask the therapeutic MOA of a particular drug. On the other hand, *in vitro* methods are generally simpler; yet, allow for rapid, reliable and inexpensive testing of a drug's actions at the cellular and molecular levels.

In an effort to elucidate the MOA of CQ as an AD therapeutic, several cell-free and cell-based *in vitro* studies were conducted. The cell-free investigations combined CQ, metals and synthetic Aβ preparations with outcome measures including: oxidative stress markers, metal levels and bioavailability, and/or Aβ levels, species and aggregation state (699-701). Most of the cell-based examinations of CQ, metal ions and Aβ were performed, using continuous CHO-APP cells (436, 752, 811) and/or cell lines derived from malignant tumours, such as HeLa cervical cancer cells or N2a, M17 and SY5Y neuroblastoma cells (436, 811). These types of studies mainly looked at cellular toxicity, metal levels and/or the degree of Aβ degradation.

Unfortunately, as demonstrated in **Chapter 4** of this thesis and elsewhere (607, 621, 622, 644, 728, 729, 787-789, 792, 794, 795, 797, 799-802, 810, 821, 822), treatment of clonal cell lines with CQ in combination with metals leads to metal uptake, enhanced toxicity, and activation of various cell death pathways. Owing to their cytostatic and/or cytotoxic effects, metallo-complexes are now being assessed as cancer therapeutics (797, 814, 858). Whilst the discovery of CQ's selective anti-neoplastic activity is highly valuable and warrants additional R&D, this thesis focuses on CQ as a candidate pharmacotherapeutic for AD.

Despite the fact that CQ itself is no longer being developed as an AD therapeutic agent; CQ serves as a commercially-available proto-type for other 8-HQ analogues and/or derivatives, including PBT2 (Prana Biotechnology; Parkville, Melbourne, VIC, Australia), which are currently undergoing pre-clinical and clinical trials for the treatment of AD and a range of other conditions (see **section 1.5.5**). It is expected that CQ and PBT2 share a similar MOA in the treatment of neurodegenerative diseases – the aetiology of which involves metal dyshomeostasis (see **section 1.4.1** and **Table 1.4**). Yet, it has not been established whether the therapeutic benefits seen in CQ and PBT2-treated AD animal models (699, 700, 703, 704, 709, 713, 715, 725, 746, 763, 829, 832) and patients (710, 711, 717, 718, 745, 754) are a result of the drug's capacity to interact with metals and chaperon and/or deliver them into cells (as seems to be the case in cancer), or whether they are due to another mechanism all together.

Based on findings in **Chapter 4**, cell lines had to be excluded as a viable tool for further *in vitro* testing CQ-metal chelates. Consequently, the overall goal of this chapter is to explore the MOA of CQ, in relation to metals and Aβ, within an alternative cell-based system that is *suitable* and *relevant* to AD.

Cortical cultures (method outlined in **section 5.2.1**) enable the evaluation of neuronal processes in isolation (i.e., independent of other CNS cell-types and/or hormonal, vascular and inflammatory influences). It is, however, noteworthy that neuronal cell culture is a "closed" system, which does not allow treatments to be completely eliminated (unlike *in vivo* models, wherein substances are metabolised and then excreted from the body). With the limitations of this experimental technique in mind, it is still believed that the drug, ion and peptide concentrations used in this chapter's procedures reflect their levels in the brains of animals and humans with AD.

To date, only few studies have been performed with CQ in rat and mouse primary cultures of astrocytes and/or neurons (retinal, cortical or hippocampal) (444, 549, 686, 687, 704, 707, 813, 824, 825). Of these, CQ was shown to be pro-oxidant and toxic in some cases (686, 687, 824) and non-toxic in others (444, 549, 707, 813), depending on the experimental conditions. Importantly, in these studies primary cultures were treated with CQ alone (444, 813) and/or in the presence of *either* metals (686, 687, 813, 824, 825) or Aβ (549, 704, 707); however, none were treated with *all* three factors (i.e., drug, ion and peptide).

To address these shortcomings, murine primary cortical neuronal cultures were used in this chapter as a platform to characterise the interaction between CQ, metals and Aβ and to clarify how it may contribute to the therapeutic MOA of CQ in AD.

5.2 Experimental Methods

5.2.1 Preparation of primary cortical neuronal cultures

All procedures involving animals were approved by the Howard Florey Institute's (HFI; Parkville, Melbourne, Victoria, Australia) Animal Experimentation Ethics Committee (AEC; approval number 10-057) and performed in accordance with the National Health and Medical Research Council of Australia's (NHMRC) Code of Practice and for the Care and Use of Animals for Scientific Purposes.

Plugged female C57BL/6 WT mice were purchased from Monash University Animal Services (Clayton, Melbourne, Victoria, Australia), transported by a licensed animal carrier and housed in the animal facility at the Mental Health Research Institute (MHRI; Parkville, Melbourne, Victoria, Australia) under standard animal care conditions (pathogen-free environment, kept at 23 ± 1 ^{o}C temperature and 55 ± 5 % humidity, and with access to tap water and food *ad libitum*). All dead animals and animal tissue waste were autoclaved and disposed of by a licensed medical waste contractor.

On day 14 of gestation, C57BL/6 dams were killed by cervical dislocation and their abdomen was rinsed with 70 % (v/v) ethanol. Using sterile scissors and tweezers, a midline excision was made through the dams' abdominal wall, individual embryos were removed from the embryonic sack and placed in a 60 mm Petri dish, containing cold Krebs buffer (124 mM sodium chloride (NaCl), 5.4 mM potassium chloride (KCl), 1 mM sodium phosphate monobasic monohydrate ($NaH_2PO_4.H_2O$), 14.4 mM D-glucose, 28.2 mM phenol red and 25 mM HEPES; pH 7.4) with added 45 mM BSA and 2 mM magnesium sulphate anhydrous ($MgSO_4$; Merck Millipore, Kilsyth, VIC, Australia).

Under a dissection microscope and using sterile tweezers, brains of embryonic day 14 (E14) C57BL/6 mice were removed from the skull and transferred to another 60 mm Petri dish containing cold Krebs buffer (as above). At this embryonic developmental stage, tissue is relatively easy to dissociate, synaptogenesis has yet to occur and there is no fragmentation of dendrites and/or axons. Cortices were then separated from the midbrain and their enveloping meninges were carefully peeled away to ensure better isolation and recovery of neurons. Cortical tissue was transferred into a 35 mm Petri dish, diced with a sterile razor blade, and dissociated in Krebs buffer with added 5.36 mM trypsin (Sigma-Aldrich; Castle Hill, Sydney, NSW, Australia) for 15-20 minutes at 37 ^{o}C in an orbital shaker (Ratek Instruments; Boronia, Melbourne, VIC, Australia).

Krebs buffer, supplemented with 2.6 mM DNase and 12 mM soybean trypsin inhibitor (SBTI; both by Sigma-Aldrich; Castle Hill, Sydney, NSW, Australia), was then added to the dissociated cells, mixed gently and centrifuged at 1,200 rpm for 3 minutes at 4 ^{o}C.

Supernatant was discarded, and cell pellet was re-suspended in DNase/SBTI-containing Krebs buffer (as above), triturated into a single cell suspension with a filter-plugged fine pipette tip, mixed gently and centrifuged again at 1,200 rpm for 3 minutes at 4 ^{o}C. Supernatant was aspirated off and the cortical cell pellet was re-suspended in plating medium (DMEM supplemented with 5 and 10 % (v/v) heat-inactivated horse and foetal calf serum, respectively, and 100 μg/mL of gentamycin sulphate antibiotics).

Aliquot of neuronal cell suspension was stained with trypan blue and counted on a haemocytometer. Viable mouse primary cortical neurons were seeded at a density of 2 $\times 10^5$ cells/cm^2 in poly-L-lysine (5 μg/mL)-coated well-plates (for neurotoxicity assays; see **section 5.2.5**) or flasks (for neuronal uptake studies; refer to **section 5.2.6**). Cultures were maintained at 37 ^{o}C in a 5 % carbon dioxide (CO_2)-humidified incubator for 150 minutes prior to the plating medium being aspirated off and replaced with NeuroBasal® medium, containing added antioxidants with B27 supplements, 0.5 mM GlutaMAX™ and 100 μg/mL gentamycin. This serum-free, B27-supplemented NeuroBasal® medium enables the cultivation of neurons at either low or high densities, for relatively long periods, and without the need for a glial feeder layer (859).

Mouse cortical neuronal cultures were maintained at 37 ^{o}C in a 5 % carbon dioxide (CO_2)-humidified incubator for 6 *in vitro* (6 D.I.V). This commonly-used technique was shown to yield cultures highly enriched with neurons that developed elongated axons, dendrites and synaptic networks; yet, contain minimal astrocytes and microglial cells (549, 559, 860-864).

5.2.2 Preparation of CQ

CQ stock and working solutions were prepared as per **section 4.2.3**.

5.2.3 Preparation of metals

Metal ion stock and working solutions were prepared as per **section 4.2.4**.

5.2.4 Preparation of Aβ

Soluble $A\beta_{42}$ stock solutions were prepared according to an improved protocol, which was developed in our laboratory (765) and was shown to result in increased peptide solubility and data reproducibility (559, 862, 865, 866).

On experimental days, lyophilised $A\beta_{42}$ (see **section 2.7**) was weighed into a 1.5 mL tube on a microbalance, under minimal static conditions (with the aid of an anti-static gun). The peptide was re-suspended in 20 mM sodium hydroxide (NaOH; 1:2 w/v), incubated for 3 minutes at room temperature and briefly mixed, using a vortex instrument. This $A\beta_{42}$ solution was diluted in water (H_2O; 1:3.5 v/v) and briefly mixed, using a vortex instrument. The solution was then neutralised by adding of 10× PBS (137 mM sodium chloride (NaCl), 2.7 mM potassium chloride (KCl), 10 mM sodium phosphate dibasic (Na_2HPO_4) and 2 mM potassium phosphate monobasic (KH_2PO_4); pH 7.4. 1:7 v/v).

The $A\beta_{42}$ preparation was sequentially sonicated for 5 minutes in an ice-containing Ultrasonic Cleaner (Unisonics; Brookvale, Sydney, NSW, Australia), and centrifuged at 16,000 × *g* for 10 minutes at 4 ^{o}C to remove any aggregated material. Subsequently, the supernatant (containing soluble peptide) was transferred to a pre-chilled 1.5 mL tube and placed on ice.

To determine the $A\beta_{42}$ stock concentration, an aliquot of the supernatant was diluted 1:50 (v/v) in PBS (pH 7.4; at room temperature), mixed and transferred into a 96-well black quartz plate. Triplicate absorbance measurements at 214 nm wavelength were performed, using BioTek's PowerWave Microplate Spectrophotometer and Gen5™ Data Analysis Software (Millennium Science; Mulgrave, Melbourne, VIC, Australia) set to a spectrum scanning mode (350 to 200 nm wavelengths). Average $A\beta_{42}$ content (ng/μL) was corrected for background signal (i.e., PBS blank) and the molar concentration of $A\beta_{42}$ was calculated, using Lambert-Beer's law:

$A_{214\,nm}$ × dilution factor (= 50) / molar extinction coefficient (= 94526 litre/mole/cm)

Based on concentration of the $A\beta_{42}$ stock solution, the volumes required to treat mouse primary cortical neuronal cells with soluble $A\beta_{42}$ at a final concentration of 5, 8 and 12.5 μM, in the absence and presence of metals and/or CQ (see **sections 5.2.5-5.2.6** below), were calculated.

5.2.5 Neuronal toxicity assays of CQ, metal ions and/or Aβ

On experimental days (i.e., 6 D.I.V), NeuroBasal® growth medium (refer to **section 5.2.1**) was aspirated off 48-well plates, mouse primary cortical neuronal cells were rinsed with PBS and incubated in triplicates with treatments or vehicle control (equal volumes of water and DMSO as treatments) in fresh NeuroBasal® medium for three hours at 37 ºC in a 5 % carbon dioxide (CO_2)-humidified incubator.

In **section 5.3.1**, neuronal cultures were treated with vehicle, CQ (up to and including 25 μM), metals ($CuCl_2$, $ZnCl_2$, $FeCl_3$; up to and including 12.5 μM) or CQ-metal complexes (up to and including 25 μM CQ and 12.5 μM metal ions).

In **section 5.3.9**, neuronal cultures were treated with vehicle control or with soluble $A\beta_{42}$ (5, 8 and 12.5 μM), in the absence and presence of metals (5 μM $CuCl_2$, 8 μM $ZnCl_2$ and 12.5 μM $FeCl_3$) and/or CQ (10, 16 and 25 μM), respectively.

Following three-hour incubation, treatment media was aspirated, and neuronal cell viability was determined primarily, using the CCK-8 assay (see **section 2.10.1**).

5.2.6 Neuronal uptake of CQ, metal ions and/or Aβ studies

On experimental days (i.e., 6 D.I.V), NeuroBasal® growth medium (described in **section 5.2.1**) was aspirated off, mouse primary cortical neuronal cells were rinsed with PBS and incubated in triplicates with treatments or vehicle control (equal volumes of water and DMSO as treatments) in fresh NeuroBasal® medium at 37 ºC in a 5 % carbon dioxide (CO_2)-humidified incubator.

In **sections 5.3.2-5.3.7**, neuronal cultures in 75 cm^2 flasks were treated for three hours with vehicle control, CQ (up to and including 25 μM), metal ions ($CuCl_2$, $ZnCl_2$, $FeCl_3$; up to and including 12.5 μM) and/or CQ-metal complexes (up to and including 25 μM CQ and 12.5 μM metals; 2:1 molar ratio).

In another set of uptake studies (**sections 5.3.10-5.2.12**), neuronal cultures in 75 cm^2 flasks were treated for three hours with vehicle control or with soluble $A\beta_{42}$ (5, 8 and 12.5 μM), in the absence and presence of metals (5 μM $CuCl_2$, 8 μM $ZnCl_2$ and 12.5 μM $FeCl_3$, respectively) and/or CQ (10, 16 and 25 μM, respectively).

In **section 5.3.8**, neuronal cultures in 25 cm^2 flasks were treated with vehicle control or with soluble $A\beta_{42}$ (5, 8 and 12.5 μM), in the absence and presence of metals (5 μM $CuCl_2$, 8 μM $ZnCl_2$ and 12.5 μM $FeCl_3$, respectively) and/or CQ (10, 16 and 25 μM, respectively) for 10, 20, 30, 40, 50, 60, 80, 100, 120, 140, 160 and 180 minutes.

Following incubation, aliquots of treatment media were collected into 1.5 mL tubes and the remaining media was aspirated. Neuronal cultures were rinsed with ice-cold, 0.1 M sodium carbonate (Na_2CO_3; pH 10) to discard any membrane-bound material. PBS was then added to the flasks and cells were harvested into 15 mL tubes, using a rubber-bladed cell scraper (Sigma-Aldrich; Castle Hill, Sydney, NSW, Australia).

In order to remove cell debris and/or unbound material, the cell suspension was centrifuged at 13,000 rpm for 10 minutes at 4 ^oC and supernatant was discarded. Cortical cell pellets and media aliquots were immediately frozen and stored at -80 °C, until analyses were performed.

5.2.7 Metal analysis using ICPMS

The metal content of mouse primary cortical neuronal cells and their media was measured, using ICPMS. The calibration and operating conditions of the instrument were identical to those listed in **section 3.2.9**; only the sample preparation and analysis were slightly modified.

To determine the Cu, Zn and Fe levels in control and treated mouse primary cortical neurons, cell pellets were dissolved in concentrated nitric acid (HNO_3; Merck; Kilsyth, VIC, Australia) overnight at room temperature. To determine the levels of Cu, Zn and Fe in the culture and treatment media of mouse primary cortical neurons, aliquots were diluted in 1 % (v/v) nitric acid (HNO_3; Merck; Kilsyth, VIC, Australia) at a 1:10 (v/v) ratio (the minimum dilution required to overcome matrix interference with the instrument).

To complete the digestion process, all samples were heated at 90 ^oC for 15 minutes, using a heating block. Due to evaporation, there was a slight loss of sample volume. Samples were allowed to equilibrate to room temperature for 5 minutes prior to a short centrifugation in order to minimize condensation. A set volume of 1 % (v/v) nitric acid (HNO_3; Merck; Kilsyth, VIC, Australia) was added to each sample and the final sample volume was then measured.

WinMass™ Software for ICPMS (Varian; Mulgrave, Melbourne, VIC, Australia) was used for data analysis and for conversion of metal concentrations in the media and in the cell pellets from ppb to μM, using the following formulas, respectively:

(μmol/L) = [(raw ppb value) x (dilution factor; 10)] / (molecular weight of the element)

(μmol/L) = [(raw ppb value) x (final sample volume)] / (molecular weight of the element)

Metal ion levels in mouse primary cortical neuronal cells and in media are expressed either as their absolute amount (μmol) or as the fold change, in comparison to their respective concentrations (μmol/L) in vehicle-controls (set at 100 %).

5.2.8 CQ analysis using ICPMS

ICPMS can also serve as an analytical tool for quantifying the concentrations of iodine (I) in biological samples; however, measurements need to be performed under alkaline conditions due to its instability (becomes volatile) in acidic matrices (867-870). Since each CQ molecule contains a single iodine moiety (at position 7), ICPMS was used to analyse the levels of iodine as a measure of CQ in the samples (1:1 ratio).

To determine the cellular CQ and metal levels in control and treated mouse primary cortical neurons, cell pellets were dissolved in 25 % (w/v) tetramethylammonium hydroxide (TMAH; $N(CH_3)_4^+$ OH^-) overnight at room temperature. To determine the levels of CQ and metals in the culture and treatment media of mouse primary cortical neurons, aliquots were diluted at a 1:10 (v/v) ratio in a basic matrix, containing 1 % (w/v) TMAH, 0.01 % (v/v) Triton X-100 and 0.01 % (w/v) EDTA, to overcome any matrix interference with the instrument.

To complete the digestion process, all samples were heated at 90 ^oC for 15 minutes, using a heating block. Due to evaporation, there was a slight loss of sample volume. Following equilibration to room temperature for 5 minutes, samples were centrifuged briefly in order to minimize condensation. A set volume of the above alkaline matrix was added to each sample and the final sample volume was then measured.

Measurements of ^{127}I (as well as ^{56}Fe, ^{63}Cu, ^{66}Zn and others) were conducted, using an Agilent 7700 ICPMS (Agilent Technologies; Mulgrave, Melbourne, VIC, Australia) with a Helium reaction gas cell, under operating conditions suitable for routine multi-element analysis: peak-hopping scan mode, 1 point per peak, 100 scans per replicate, 3 replicates per sample. Plasma gas (Argon) and auxiliary flow rates of 15 and 0.9 litre per minute, respectively. R_F power was 1.2 kW. Samples were introduced, using a micromist nebulizer, at a flow rate of 1.15 litres per minute.

The instrument was calibrated, using an iodine internal standard (Thermo Fisher Scientific; Scoresby, Melbourne, VIC, Australia) (871) and a mixture of certified multi-element ICPMS standard solution (ICPMS-CAL2, ICPMS-CAL-3 and ICPMS-CAL-4, AccuStandard; New Haven, CT, USA), containing 0, 2.5, 5, 10, 25, 50 and 100 ppb of the elements of interest in the alkaline matrix. A certified internal standard solution

(ICPMS-IS-MIX1-1, AccuStandard; New Haven, CT, USA), containing 200 ppb of Yttrium (^{89}Y), was added as an internal matrix and instrument performance control.

MassHunter Software for ICPMS (Agilent Technologies; Mulgrave, Melbourne, VIC, Australia) was used for data analysis and for conversion of iodine concentrations in the media and in the cell pellets from ppb to μM, using the following formulas, respectively:

(μmol/L) = [(raw ppb value) x (dilution factor; 10)] / (molecular weight of the element; 127)

(μmol/L) = [(raw ppb value) x (final sample volume)] / (molecular weight of the element; 127)

CQ levels in mouse primary cortical neuronal cells and in media are expressed either as their absolute amount (μmol) or as the fold change, in comparison to their respective concentrations (μmol/L) in vehicle-controls (set at 100 %).

5.2.9 Aβ analysis using double antibody capture ELISA

$A\beta_{42}$ levels in mouse primary cortical neuronal cells and their media were analysed, using DELFIA® Double Antibody Capture ELISA (436, 738, 739), in a slightly modified manner to that described in **section 3.2.10**.

C384-well OptiPlate microplates (Greiner; Frickenhausen, Germany) were coated with W0-2 detection antibody (monoclonal IgG2a antibody that binds to $A\beta_{5-8}$ (767); 0.02 μg/μL in a carbonate buffer (15 mM sodium carbonate (Na_2CO_3) and 35 mM sodium bicarbonate ($NaHCO_3$); pH 9.6)), at a final concentration of 0.5 μg/well.

Plates were incubated overnight at 4 ºC. The following day, microplates were washed with PBS, containing 0.05 % (v/v) Tween-20 (PBS-T; pH 7.4), in order to remove any un-bound antibody. To prevent non-specific binding, plates were incubated with blocking buffer (0.5 % (w/v) casein in PBS; pH 7.4) for two hours at 37 ºC. Plates were again washed with PBS-T prior to the addition of biotin-labelled 1E8 detection antibody (monoclonal IgG1 antibody that recognises $A\beta_{18-22}$ (872); 2 ng/μL) in a PBS solution (pH 7.4), containing 0.025 % (v/v) Tween-20 and 0.25 % (w/v) casein, at a final concentration of 20 ng/well.

$A\beta_{42}$ standards and NeuroBasal® treatment media aliquots were diluted 1:2000 (v/v) in guanidine hydrochloride (final concentration of 0.1 M). Cortical cell pellets were dissolved in a lysis buffer (6 M urea and 2 % (v/v) CHAPS), followed by a 1:150 (v/v) dilution in guanidine hydrochloride (final concentration of 0.1 M). $A\beta_{42}$ standards and samples were added in triplicates, and the plates were incubated overnight at 4° C.

Next, the microplates were washed with PBS-T to remove any un-bound peptide. Streptavidin-labelled Europium (PerkinElmer; Glen Waverley, Melbourne, VIC, Australia), diluted 1:1000 (v/v) in blocking buffer, was then added and the plates were incubated for an hour at room temperature. Plates were subsequently washed with PBS-T, prior to the addition of an enhancement solution (PerkinElmer; Glen Waverley, Melbourne, VIC, Australia), at a final volume of 80 μL/well, in order to detect the bound antibody.

Plates were placed in a WALLAC Victor^2 1420 Multilabel Plate Reader (PerkinElmer; Glen Waverley, Melbourne, VIC, Australia), shaken for 5 minutes and spectroscopic measurements (optical density units; OD) were performed at 340 nm excitation and 650 nm emission wavelengths. $A\beta_{42}$ levels were above the detection limit of the assay and their quantification was calibrated against peptide standards, after subtraction of background fluorescence in the absence of sample (i.e., blank).

$A\beta_{42}$ levels in mouse primary cortical neuronal cells are expressed as their absolute amount (μmol).

5.3 Experimental Results

5.3.1 Determining the therapeutic window of CQ and/or metals in mouse primary cortical neuronal cells

In order to validate the use of cortical neuronal cells (as oppose to neuronal-like cell lines used in **chapter 4**) and to examine the toxic *versus* therapeutic range of CQ and its metal complexes, the effect of CQ, in the absence and presence of metals, on the survival of mouse primary cortical neuronal cells was investigated (as described in **section 5.2.5**), using the CCK-8 assay (refer to **section 2.10.1**).

Following three-hour incubation, there was no difference in viability between non-treated and vehicle-treated mouse primary cortical neuronal cells (data not shown); hence, any change in cell survival would be a result of the treatment, and not its vehicle.

Results also showed that the number of viable mouse primary cortical neuronal cells treated with CQ (equal to or less than 25 μM) was no different to that of vehicle-treated cultured neurons (**Fig. 5.3.1 A**). These findings are consistent with a report, in which the viability of cortical neurons was found not to be affected by 10 μM CQ even after 26-hour treatment (813). On the other hand, Benvenisti-Zarom and colleagues published conflicting data wherein CQ, as low as 1 μM, was neurotoxic to primary cultures (824). The multitude of possible explanations for the contradictory results include: disparate mouse strains (C57BL/6 as opposed to B6/129), primary cell types (cortical neurons with or without astrocytes), treatment medium (serum-free NeuroBasal® medium as opposed to Eagles' minimal essential medium (EMEM)), exposure period (3 *versus* 24 hours) and/or method for assessing toxicity (CCK-8 *versus* LDH and malondialdehyde (MDH) assays).

Data demonstrated that there was no difference in the survival rate of mouse primary cortical neuronal cells treated with $CuCl_2$ (equal to or less than 12.5 μM), as compared to vehicle-treated cultured neurons (**Fig. 5.3.1 B**). Viability of mouse primary cortical neuronal cells treated with $CuCl_2$ and CQ (equal to or less than 5 and 10 μM, respectively) was also similar to that of vehicle-treated neuronal cultures (**Fig. 5.3.1 C**). However, co-treatment with $CuCl_2$ and CQ (equal to or more than 8 and 16 μM, respectively) led to diminished mouse primary cortical neuronal cell survival, relative to vehicle-treated cultured neurons (**Fig. 5.3.1 C**). The effect was so great, in fact, that upon treatment with 25 μM CQ and 12.5 μM $CuCl_2$ there were almost no remaining viable cultured neurons (~6 %; **Fig. 5.3.1 C**), in line with a previous report (824).

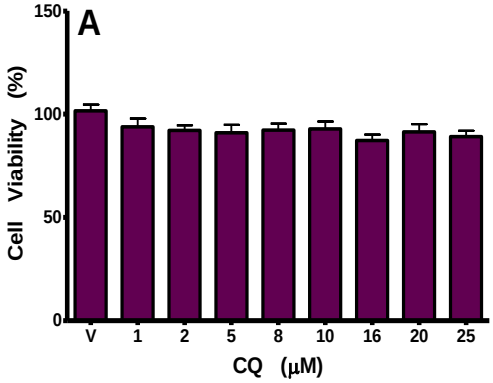
A
Cell Viability (%)
150
100
50
0
V 1 2 5 8 10 16 20 25
CQ (μM)

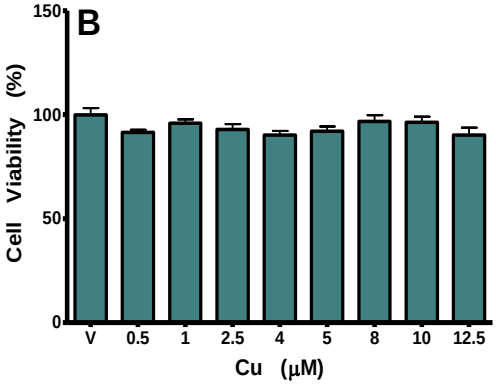
B
Cell Viability (%)
150
100
50
0
V 0.5 1 2.5 4 5 8 10 12.5
Cu (μM)

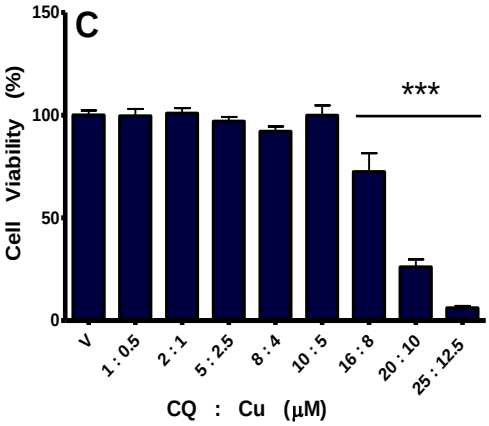
C
Cell Viability (%)
150
100
50
0
***
V 1 : 0.5 2 : 1 5 : 2.5 8 : 4 10 : 5 16 : 8 20 : 10 25 : 12.5
CQ : Cu (μM)

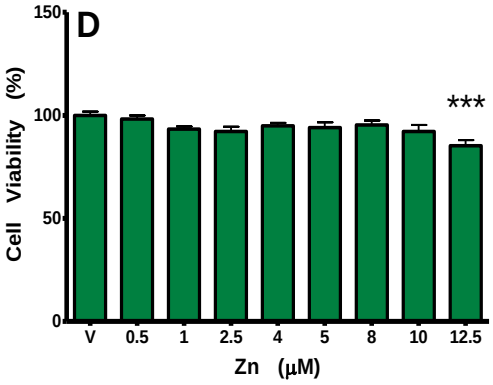
D
Cell Viability (%)
150
100
50
0
***
V 0.5 1 2.5 4 5 8 10 12.5
Zn (μM)

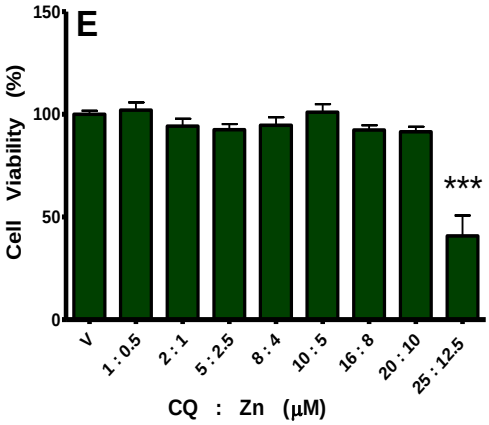
E
Cell Viability (%)
150
100
50
0
***
V 1 : 0.5 2 : 1 5 : 2.5 8 : 4 10 : 5 16 : 8 20 : 10 25 : 12.5
CQ : Zn (μM)

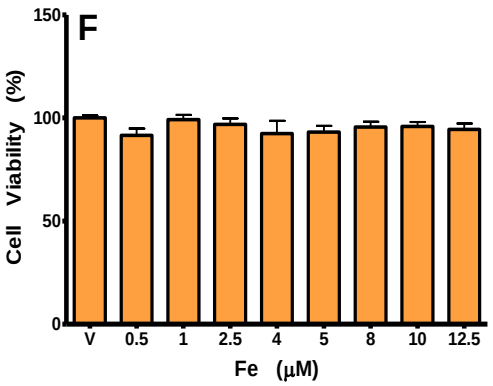
F
Cell Viability (%)
150
100
50
0
V 0.5 1 2.5 4 5 8 10 12.5
Fe (μM)

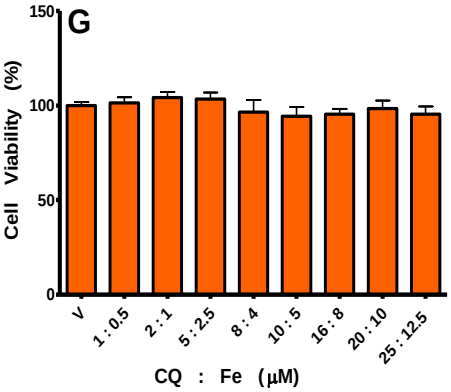
G
Cell Viability (%)
150
100
50
0
V 1 : 0.5 2 : 1 5 : 2.5 8 : 4 10 : 5 16 : 8 20 : 10 25 : 12.5
CQ : Fe (μM)

Figure 5.3.1 Dose-response effect of CQ, metals and CQ-metal complexes on neuronal cell viability

*Exposure to CQ (≤ 25 μM; **A**), Cu (≤ 12.5 μM; **B**), Zn (≤ 10 μM; **D**) or Fe (≤ 12.5 μM; **F**) was not toxic to neuronal cultures.*

*While exposure to high concentrations of CQ-Cu (≥ 16 μM CQ and 8 μM Cu; **C**) or CQ-Zn (25 μM CQ and 12.5 μM Zn; **E**) was significantly cytotoxic to neuronal cells; exposure to CQ-Fe complexes (≤ 25 μM CQ and 12.5 μM Fe; **G**) was not toxic to cultured neurons.*

*ANOVA with Dunnett's multiple comparison test; ***p < 0.001 compared to vehicle-control*

Bars represent mean ± S.E.M, n ≥ 3

Compared to vehicle-treated cultured neurons, the number of live mouse primary cortical neuronal cells treated with $ZnCl_2$ (equal to or less than 10 μM), either in the absence or presence of CQ (equal to or less than 20 μM), was unaltered (**Fig. 5.3.1 D** and **E**, respectively). However, treatment of mouse primary cortical neuronal cells with the highest dose of $ZnCl_2$ (12.5 μM), alone or together with CQ (25 μM), resulted in significant viability loss (~85 and 40 %, respectively, in comparison to vehicle-treated cultured neurons; **Fig. 5.3.1 D** and **E**, respectively).

No change was observed in the survival rate of mouse primary cortical neuronal cells treated with $FeCl_3$ (equal to or less than 12.5 μM; **Fig. 5.3.1 F**). These results were expected, as past reports have demonstrated that the viability of mouse primary cortical neuronal cells was compromised as a result of treatment with Fe at doses far exceeding those used in this study (443, 444, 863, 873).

Unlike parallel treatment with CQ and either $CuCl_2$ or $ZnCl_2$ (**Fig. 5.3.1 C** and **E**, respectively), contaminant treatment with CQ and $FeCl_3$ (equal to or less than 25 and 12.5 μM, respectively), did not affect the number of live mouse primary cortical neuronal cells, relative to vehicle-treated cultured neurons (**Fig. 5.3.1 G**).

These data oppose a study in which 24-hour exposure to 30 μM CQ-Fe complexes, but not CQ or Fe alone, resulted in significantly increased LDH release from co-cultured mouse cortical neurons and astrocytes (824). Earlier studies also showed 2-24 hour treatment with 50 μM or 4-day treatment with 2.5 mM CQ-Fe led to degeneration and/or significantly elevated lipid peroxidation in embryonic chick retinal neuroblasts (686, 687) and isolated adult rabbit sciatic nerve (688), respectively. The lengthen incubation of the various primary cell cultures with high concentrations of CQ-Fe complexes presumably account for the conflicting results.

In summary, under the experimental conditions used, CQ itself was not neurotoxic. However, high doses of CQ, complexed to either Cu or Zn (but not Fe), exerted a clear toxic effect on cortical neuronal cultures.

5.3.2 Effect of CQ on endogenous metal levels in mouse primary cortical neuronal cells

In the previous section, CQ was found not to affect neuronal cell viability, under the setting used (illustrated in **Fig. 5.3.1 A**). Conversely, previous reports have determined that CQ was neurotoxic and may be linked to SMON (see **section 1.5.5**); likely due to the drug's ability to modulate (directly or indirectly) the levels of Fe (686-688), Zn (689) or Cu (690) in the CNS. Therefore, it was important to evaluate the effect of CQ on metal levels in mouse primary cortical neuronal cells (as per **section 5.2.6**).

Following three-hour incubation, the endogenous levels of Cu, Zn and Fe were not statistically different in mouse primary cortical neuronal cells treated with ascending doses of CQ (equal to or less than 25 μM), compared to vehicle-treated cultured neurons (**Fig. 5.3.2**). Unfortunately, at the time these experiments were carried out, we were still unable to simultaneously measure the neuronal levels of CQ and ascertain their correlation with the dose of the drug applied externally.

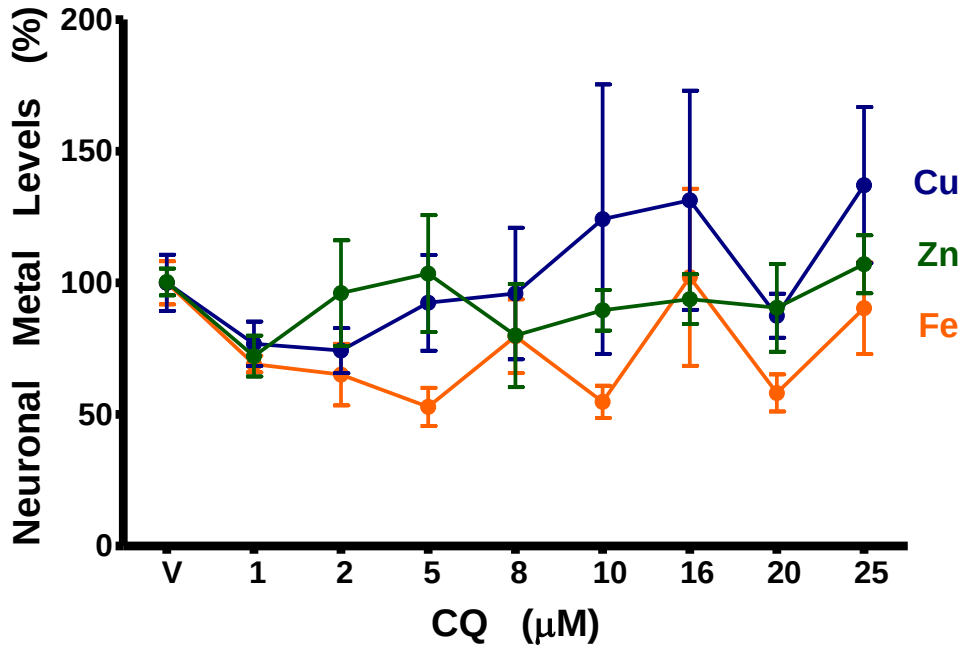

Figure 5.3.2 Dose-response effect of CQ on neuronal metal levels

The endogenous Cu, Zn and Fe levels in neuronal cells treated with ascending doses of CQ (≤ 25 μM) were similar to their respective metal levels in vehicle-treated neuronal cultures.

ANOVA with Dunnett's multiple comparison test compared to vehicle-control

Bars represent mean ± S.E.M, n ≥ 3

5.3.3 Effect of metals and CQ-metal complexes on metal levels in mouse primary cortical neuronal cells

Whilst CQ on its own was not neurotoxic (**Fig. 5.3.1 A**), nor did it affect neuronal metal levels (**Fig. 5.3.2**); data had suggested that high doses of Cu and Zn (but not Fe), with and without CQ, may have a neurotoxic effect (**Fig. 5.3.1 B-G**). To test whether the observed neurotoxicity is a consequence of altered neuronal metal levels, the effect of metals (Cu, Zn and Fe), in the absence and presence of CQ, on metal uptake into mouse primary cortical neuronal cells was investigated (detailed in **section 5.2.6**).

Results showed that treatment with $CuCl_2$, at doses equal to or higher than 4 μM, led to a dose-dependent rise in Cu levels within mouse primary cortical neuronal cells (~2-3 fold increase, relative to vehicle-treated cultured neurons; **Fig. 5.3.3 A**). Significant dose-dependent rise in Cu levels within mouse primary cortical neuronal cells was also observed following concomitant treatment with CQ and $CuCl_2$ at concentrations equal to or higher than 10 and 5 μM, respectively (~16-110 fold increase, in comparison to vehicle-treated cultured neurons; **Fig. 5.3.3 B**).

Similarly, treatment with $ZnCl_2$ alone, at doses equal to or higher than 4 μM (excluding 8 and 12.5 μM $ZnCl_2$), resulted in significantly higher Zn levels in mouse primary cortical neuronal cells (~2 fold increase, as compared to vehicle-treated cultured neurons; **Fig. 5.3.3 C**). Data also demonstrated a significant and dose-dependent elevation in Zn levels within mouse primary cortical neuronal cells following co-treatment with CQ and $ZnCl_2$ at concentrations equal to or higher than 20-25 and 10-12.5 μM, respectively (~3.5 and 7 fold increase, respectively, relative to vehicle-treated cultured neurons; **Fig. 5.3.3 D**).

While Fe levels were significantly elevated only in mouse primary cortical neuronal cells treated with the highest tested dose of $FeCl_3$ (12.5 μM; ~4 fold increase, compared to vehicle-treated cultured neurons; **Fig. 5.3.3 E**); significant and dose-dependent increase in Fe levels was observed in mouse primary cortical neuronal cells treated in parallel with CQ and $FeCl_3$ at concentrations equal to or higher than 10 and 5 μM, respectively (~3 fold increase, relative to vehicle-treated cultured neurons; **Fig. 5.3.3 F**).

Overall, these findings confirm a dose-dependent neuronal uptake of metal ions (Cu > Zn > Fe), either alone or in combination with CQ, which inversely correlated with neuronal viability (see **Fig. 5.3.1 B-G**).

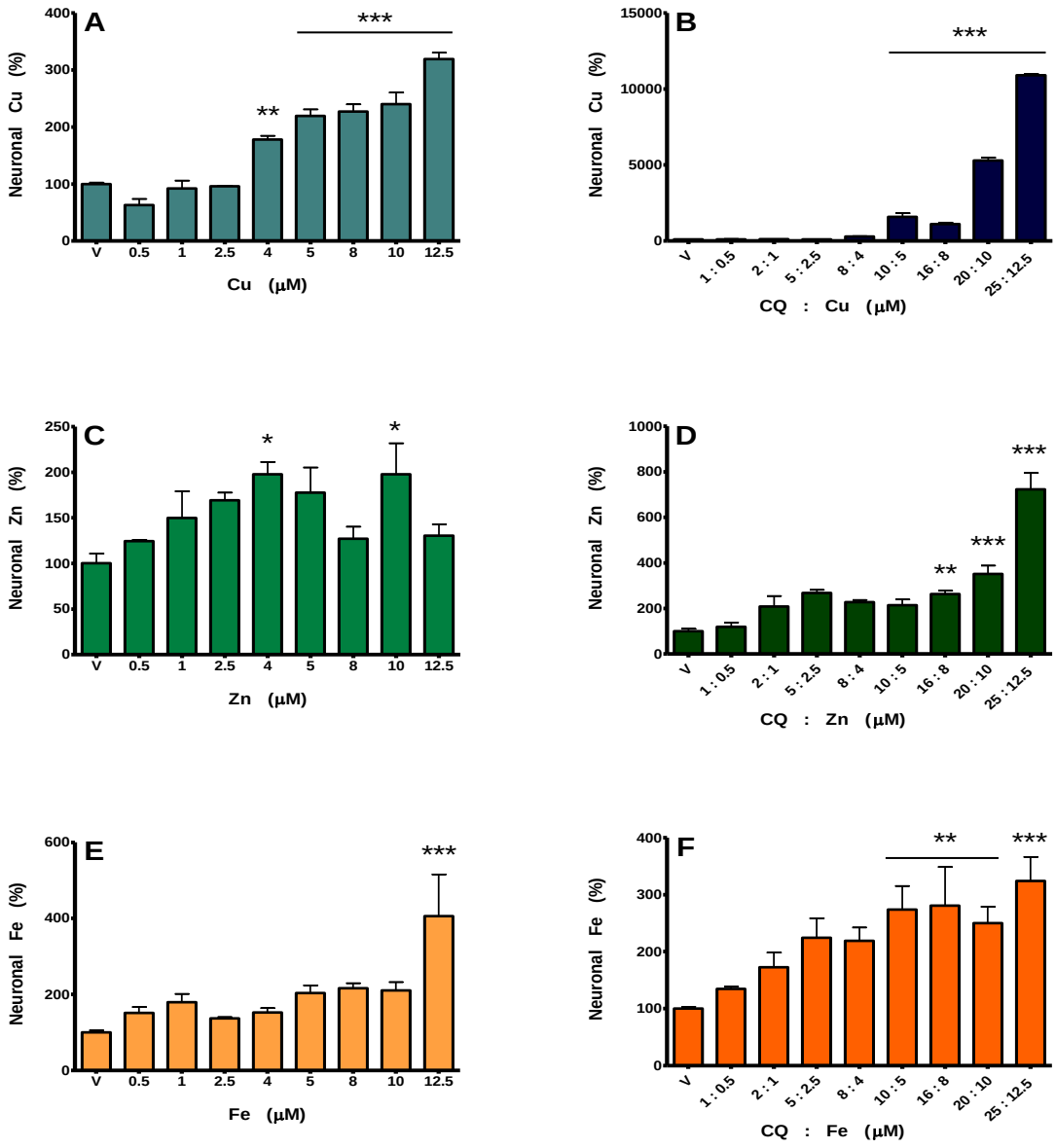

Figure 5.3.3 Dose-response effect of metals and CQ-metal complexes on neuronal metal levels

*Exposure to Cu (≥ 4 μM; **A**) and CQ-Cu complexes (≥ 10 μM CQ and 5 μM Cu; **B**) significantly elevated Cu levels in neuronal cells in a dose-dependant manner.*

*Exposure to Zn (4 and 10 μM; **C**) and CQ-Zn complexes (≥ 20 μM CQ and 10 μM Zn; **D**) raised neuronal Zn levels significantly.*

*Exposure to Fe (12.5 μM; **E**) and CQ-Fe complexes (≥ 10 μM CQ and 5 μM Fe; **F**) significantly and doe-dependantly increased Fe levels in cultured neurons.*

*ANOVA with Dunnett's multiple comparison test; *$p < 0.05$, **$p < 0.01$, ***$p < 0.001$ compared to vehicle-control*

Bars represent mean ± S.E.M, $n \geq 3$

5.3.4 Effect of CQ on exogenous metal neuronal uptake

Guided by the enhanced neurotoxicity of metallo-CQ complexes, compared to metals on their own (**Fig. 5.3.1 C**, **E** and **G** *versus* **B**, **D** and **F**, respectively), it was hypothesized that metallo-CQ complexes may also augment neuronal metal uptake, compared to metals alone.

Indeed, there was significant Cu uptake into mouse primary cortical neuronal cells concurrently treated with concentrations equal to or higher than 10 μM CQ and 5 μM $CuCl_2$, in comparison to mouse primary cortical neuronal cells treated with doses equal to or higher than 5 μM $CuCl_2$ on its own (~5-45 fold increase; **Fig. 5.3.4 A**).

There was also significant Zn uptake into mouse primary cortical neuronal cells, with *versus* without CQ, but at doses higher than Cu. Significant and dose-dependent Zn uptake occurred in mouse primary cortical neuronal cells co-treated with doses equal to or higher than 16 μM CQ and 8 μM $ZnCl_2$, compared to mouse primary cortical neuronal cells treated with $ZnCl_2$, at concentrations equal to or higher than 8 μM, in the absence of CQ (~2-5 fold increase; **Fig. 5.3.4 B**).

Using ICPMS, ^{65}Zn isotope and a Zn fluorophore, significant neuronal Zn uptake in the presence, as compared to the absence, of CQ had also been reported in rat primary cortical neuronal cultures, despite different exposure time, doses and ratio of Zn and CQ (825).

While significant Fe uptake was observed in mouse primary cortical neuronal cells treated with either 12.5 μM $FeCl_3$ alone or with concentrations equal to or higher than 10 μM CQ and 5 μM $FeCl_3$, as compared to vehicle-treated mouse primary cortical neuronal cells **Fig. 5.3.3 E** and **F**, respectively); there was no statistical difference in Fe uptake between mouse primary cortical neuronal cells treated with $FeCl_3$ in the absence, as opposed to the presence, of CQ at any of the tested concentrations (**Fig. 5.3.4 C**).

Taken together, these data provide additional and compelling evidence as to the capacity of metallo-CQ complexes to deliver Cu and Zn, but not Fe, into neurons.

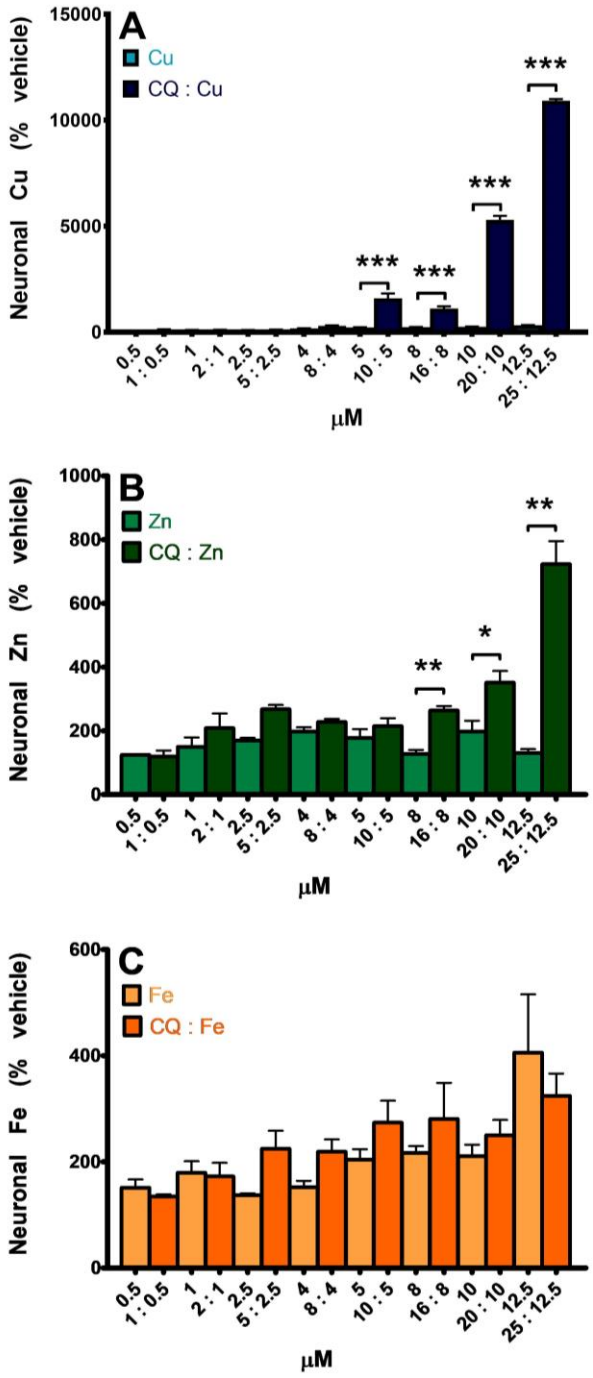

Figure 5.3.4 Dose-response effect of CQ on neuronal metal uptake

*Exposure to Cu (≥ 5 µM), in the presence compared to the absence of CQ (≥ 10 µM), significantly enhanced Cu levels in neuronal cultures (**A**).*

*Exposure to Zn (≥ 8 µM) with as opposed to without CQ (≥ 16 µM), significantly enhanced Zn levels in neuronal cells (**B**).*

*Exposure to Fe (≤ 12.5 µM) and CQ (≤ 25 µM) had no effect on Fe levels in cultured neurons, in comparison to neuronal cultures exposed to Fe (≤ 12.5 µM) alone (**C**).*

*Unpaired two-tailed t-test; *p < 0.05, **p < 0.01, ***p < 0.001*

Bars represent mean ± S.E.M, n ≥ 3

5.3.5 Effect of Cu and CQ on each other's neuronal uptake

While several research groups (including our own) have revealed the additive effect of CQ-metal complexes on cellular toxicity and metal uptake (see **chapter 4**); there have been no previous studies on the impact metals may have on the cellular uptake of CQ. To fill in this gap, the effect of CQ uptake into mouse primary cortical neuronal cells was examined, in the absence and presence of metals.

Initially, ^{125}I-CQ (737) was to be used to monitor CQ uptake (as per **section 2.4**), however numerous attempts failed due to difficulties in synthesizing pure ^{125}I-CQ (devoid of any by-products). When these issues were resolved, purified ^{125}I-CQ could only be synthesized in small volumes (~150 μL), at a low concentration (usually less than 1 nM) and was not stable for long (the ^{125}I tracer started to dissociate from CQ within days). As ^{125}I-CQ could not be used in a consistent and reliable manner, another technique was required to track CQ. Conjugation to biotin or tagging with a fluorophore could potentially alter the coordination of metals to CQ and/or other properties of the drug (listed in **Table 1.5**) and were, therefore, deemed unsuitable methods for this type of investigation.

It finally became possible to study the effect of metals on neuronal CQ uptake, and *vice versa*, simultaneously with the purchase of an advanced ICPMS model and a new sample preparation procedure that allowed the detection of naturally occurring iodine (^{127}I) (see **section 5.2.8**). As there was negligible endogenous iodine in neuronal cells (i.e., below the detection limit of the ICMPS; refer to panel **B** in **Fig. 5.3.5 – Fig. 5.3.7**) and since each CQ molecule contains a single iodine moiety (1:1 ratio), any iodine detected post treatment is directly proportional to CQ and can serve as a surrogate measure for CQ levels and/or uptake.

Rather than repeating the full dose-response curves as in **section 5.3.3**, only the minimum concentrations in which there was significant neuronal metal uptake in the presence of CQ (**Fig. 5.3.4**) *and* at which neuronal cells were still viable (**Fig. 5.3.1**) were selected. As CQ-metal chelates affected neuronal survival and metal uptake to a different extent, the doses chosen in order to determine the CQ uptake into neuronal cultures, in the presence and absence of metals, were different for each metal ion (i.e., 10 μM CQ, with and without 5 μM $CuCl_2$; 16 μM CQ, with and without 8 μM $ZnCl_2$; 25 μM CQ with and without 12.5 μM $FeCl_3$).

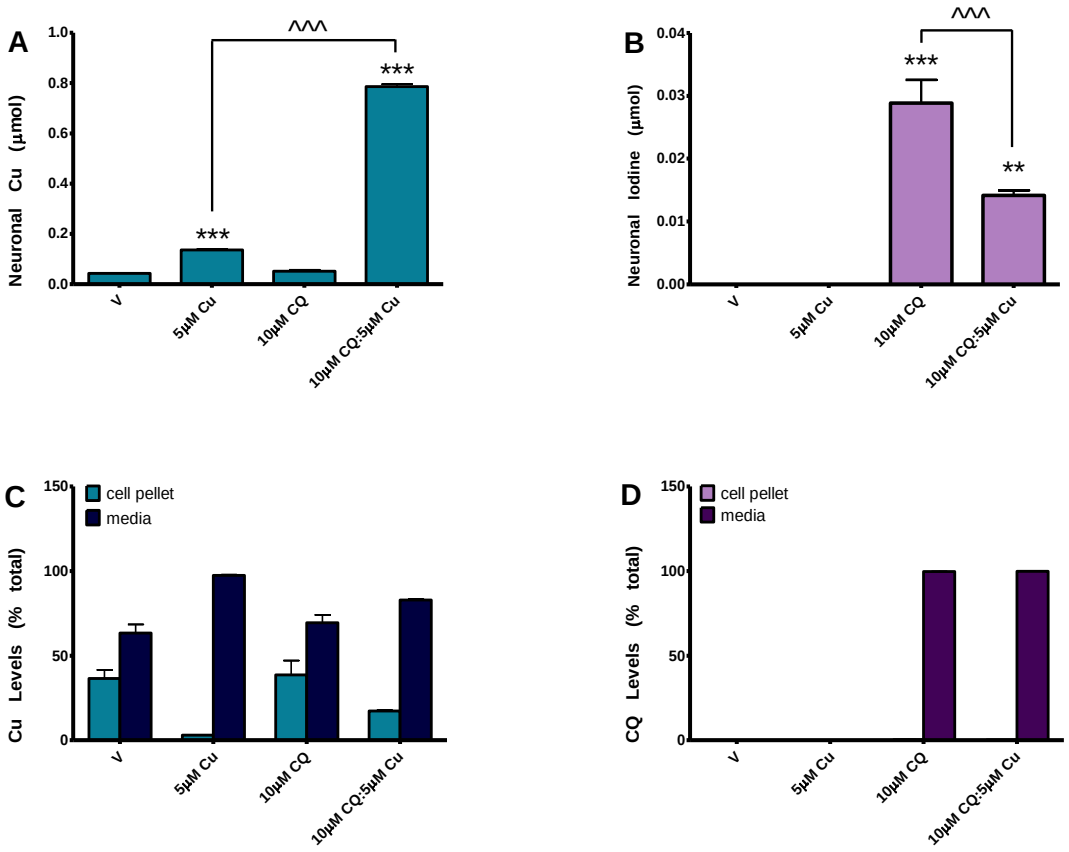

Figure 5.3.5 Neuronal uptake of Cu, CQ and CQ-Cu

*CQ enhanced the neuronal uptake of Cu (**A**) by re-distributing the metal from the media into the cells (**C**). Conversely, Cu suppressed the retention of CQ in neuronal cells (**B**), seemingly without changing the levels of the drug in the media (**D**).*

ANOVA with Tukey post-hoc test;

***p < 0.01, ***p < 0.001 compared to vehicle-control; ^^^p < 0.001*

Bars represent mean ± S.E.M, n = 3

Results depicted in **Fig. 5.3.5 A** showed that mouse primary cortical neuronal cells contained low basal levels of Cu (~0.04 μmol), which were not altered by 10 μM CQ (as in **Fig. 5.3.2**). Data illustrated in **Fig. 5.3.5 A** also confirmed that treatment with 5 μM $CuCl_2$ induced significant Cu uptake into mouse primary cortical neuronal cells (~3 fold, compared to vehicle-treated cultured neurons; similar to **Fig. 5.3.3 A**), which was further exacerbated in the presence of 10 μM CQ (~18 and 6 fold, compared to cultured neurons treated with either vehicle or 5 μM $CuCl_2$ alone, respectively; similar to **Fig. 5.3.3 B** and **Fig. 5.3.4 A**, respectively). Thus, CQ enhanced neuronal Cu uptake.

As expected, no iodine was detected in mouse primary cortical neuronal cells treated with either vehicle or 5 μM $CuCl_2$, since no CQ was added (**Fig. 5.3.5 B**). Conversely, significant levels of iodine were measured in mouse primary cortical neuronal cells treated with 10 μM CQ, in the absence and presence of 5 μM $CuCl_2$ (~0.03 and 0.015 μmol, respectively; **Fig. 5.3.5 B**), indicating significant neuronal CQ uptake.

Surprisingly, while significant CQ uptake into mouse primary cortical neuronal cells occurred following co-treatment with 10 μM CQ and 5 μM $CuCl_2$, as compared to vehicle-treated cultured neurons; it was half that of mouse primary cortical neuronal cells treated with 10 μM CQ alone (**Fig. 5.3.5 B**), suggesting that coordinating Cu attenuated neuronal CQ uptake. In addition, comparing the uptake of the metal and the drug, there was significantly greater Cu than CQ uptake into mouse primary cortical neuronal cells treated with 5 μM $CuCl_2$ and 10 μM CQ in parallel (~55 fold difference; **Fig 5.3.5 A** and **B**, respectively).

To reconcile the opposing effects CQ-Cu complexes had on neuronal uptake of Cu *versus* CQ (i.e., CQ enhanced neuronal Cu uptake, but Cu diminished neuronal CQ uptake), the levels of Cu and CQ in the media and neuronal cell cultures were determined following three-hour incubation with each of the treatments (refer to **sections 5.2.6 – 5.2.8**).

Interestingly, data showed that while concomitant treatment with 10 μM CQ and 5 μM $CuCl_2$ led to re-distribution of Cu from the treatment media to the cellular fraction, compared to treatment with 5 μM $CuCl_2$ alone (**Fig. 5.3.5 C**); it did not affect the distribution of CQ, relative to treatment with 10 μM CQ alone (i.e., over 99% of CQ remained in the treatment media fraction of neuronal cultures treated with CQ, both in the absence and presence of Cu; **Fig. 5.3.5 D**). Therefore, relatively small amount of CQ influenced the distribution of a much greater amount of Cu.

5.3.6 Effect of Zn and CQ on each other's neuronal uptake

Unlike Cu, mouse primary cortical neuronal cells contain substantial basal levels of Zn (~0.75 μmol), which remained constant following treatment with 8 μM $ZnCl_2$ alone (**Fig. 5.3.6 A**; similar to **Fig. 5.3.3 C**). Data depicted in **Fig. 5.3.6 A** also confirmed that treatment with 16 μM CQ did not impact neuronal Zn levels (as in **Fig. 5.3.2**); however, treatment with 16 μM CQ and 8 μM $ZnCl_2$ together evoked significant Zn uptake into mouse primary cortical neuronal cells, both compared to vehicle-treated cultured neurons and cultured neurons treated with 8 μM $ZnCl_2$ alone (~3 fold increase; like in **Fig. 5.3.3 D** and **Fig. 5.3.4 B**, respectively). Hence, CQ promoted neuronal Zn uptake.

As shown in **Fig. 5.3.5 B**, no iodine was detected in mouse primary cortical neuronal cells with no added CQ (i.e. cultured neurons treated with vehicle or 8 μM $ZnCl_2$; **Fig. 5.3.6 B**). Conversely, significant levels of iodine were identified in mouse primary cortical neuronal cells treated with 16 μM CQ, with and without 8 μM $ZnCl_2$ (~0.16 and 0.088 μmol, respectively; **Fig. 5.3.6 B**), indicative of significant CQ uptake into cultured neurons.

Contrary to Cu (see **Fig. 5.3.5 B**), CQ uptake into mouse primary cortical neuronal cells treated with 16 μM CQ in the presence, as opposed to the absence, of 8 μM $ZnCl_2$ was almost double (**Fig. 5.3.6 B**). This suggests that Zn further augmented the neuronal uptake of CQ. Interestingly, mouse primary cortical neuronal cells concurrently treated with 8 μM $ZnCl_2$ and 16 μM CQ displayed significantly greater metal uptake, relative to CQ uptake (~15 fold; **Fig. 5.3.6 A** and **B**, respectively).

Similar to neuronal cells treated with CQ-Cu complexes (**Fig. 5.3.5 C** and **D**), results demonstrated that while the co-treatment with 16 μM CQ led to a re-distribution of Zn from the treatment media to the cellular fraction, in comparison to treatment with 8 μM $ZnCl_2$ alone (**Fig. 5.3.6 C**); co-tratment with 8 μM $ZnCl_2$ did not affect the distribution of CQ, compared to treatment with 16 μM CQ alone (i.e., over 99% of CQ remained in the treatment media fraction of neuronal cultures, regardless of Zn; **Fig. 5.3.6 D**).

The fact that CQ-Zn complexes led to reciprocal, yet greater uptake of Zn over CQ into neurons; accompanied by reduced proportion of Zn, but not CQ, in the media fraction, could all infer that CQ may be recycling to deliver Zn into neurons.

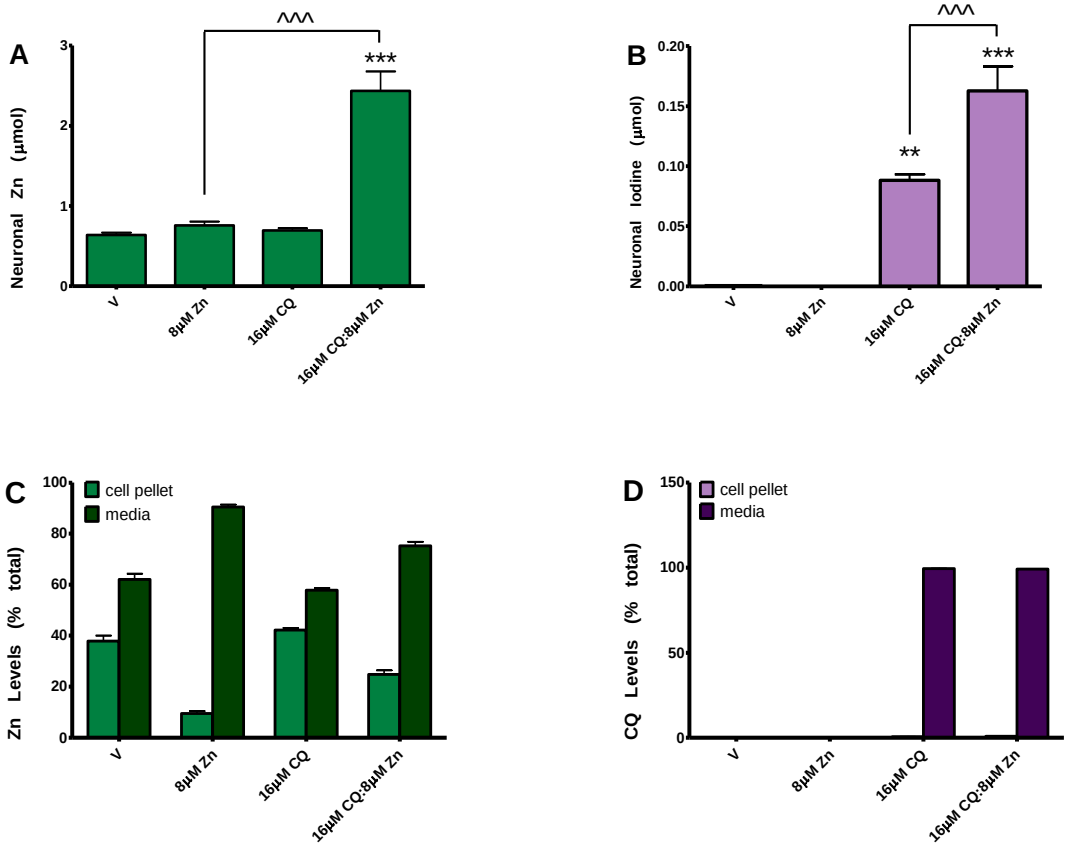

Figure 5.3.6 Neuronal uptake of Zn, CQ and CQ-Zn

*CQ facilitated the uptake of Zn (**A**), while Zn impeded the uptake of CQ (**B**) into neuronal cultures. However, while CQ re-distributed Zn from the media to the cellular phase (**C**), Zn perceivably did not alter the distribution of CQ, which remained almost exclusively in the media (**D**).*

ANOVA with Tukey post-hoc test;

***p < 0.01, ***p < 0.001 compared to vehicle-control; ^^^p < 0.001*

Bars represent mean ± S.E.M, n = 3

5.3.7 Effect of Fe and CQ on each other's neuronal uptake

Cortical neuronal cells contained relatively high levels of endogenous Fe (~2 μmol) that were not affected following treatment with either 12.5 μM $FeCl_3$ or 25 μM CQ, compared to vehicle-treated cultured neurons (**Fig. 5.3.7 A**). Yet, treatment with 25 μM CQ and 12.5 μM $FeCl_3$ in parallel stimulated significant Fe uptake into mouse primary cortical neuronal cells, relative to neuronal cultures treated with either vehicle or with 12.5 μM $FeCl_3$ alone (~3 and 2 fold increase, respectively; **Fig. 5.3.7 A**). Therefore, CQ enabled the neuronal uptake of Fe. These results are consistent with a report by Yagi *et. al*., which demonstrated significant Fe uptake into embryonic chick retinal neuroblasts co-treated for 1-10 hours with 15 μM ^{59}Fe and ^{14}C-CQ (3:10 molar ratio), compared to ^{59}Fe alone (687).

As expected, no iodine was identified in vehicle-treated mouse primary cortical neuronal cells (similar to panel **B** in **Fig. 5.3.5-5.3.6)**; nor was there any iodine found in mouse primary cortical neuronal cells treated with 12.5 μM $FeCl_3$ (**Fig. 5.3.7 B**). On the other hand, elevated levels of iodine were measured in mouse primary cortical neuronal cells following treatment with 25 μM CQ, alone and together with 12.5 μM $FeCl_3$ (~0.55 and 1 μmol, respectively; **Fig. 5.3.7 B**), pointing to significant CQ uptake into cultured neurons.

Opposite to Cu, but similar to Zn (refer to panel **B** in **Fig. 5.3.5** and **Fig. 5.3.6**, respectively), CQ uptake into mouse primary cortical neuronal cells concomitantly treated with 25 μM CQ and 8 μM $ZnCl_2$ was about twice as high as the CQ uptake into mouse primary cortical neuronal cells treated with 25 μM CQ alone (**Fig. 5.3.7 B**). This suggests that Fe further amplified the neuronal uptake of CQ. Importantly, mouse primary cortical neuronal cells treated simultaneously with 12.5 μM $FeCl_3$ and 25 μM CQ showed greater metal uptake, in comparison to CQ uptake (~3 fold; **Fig. 5.3.7 A** and **B**, respectively).

As for the effect of CQ and Fe on each other's distribution, results showed that treatment with 25 μM CQ and 12.5 μM $FeCl_3$ in parallel led to a re-distribution of Fe from the media to the cellular fraction, in comparison to treatment with 12.5 μM $FeCl_3$ alone (**Fig. 5.3.7 C**); yet, it did not influence the distribution of CQ, compared to treatment with 25 μM CQ alone (**Fig. 5.3.7 D**).

Altogether, this evidence supports a synergistic relationship between CQ and Fe, in terms of neuronal uptake, similar to that exhibited by CQ and Zn.

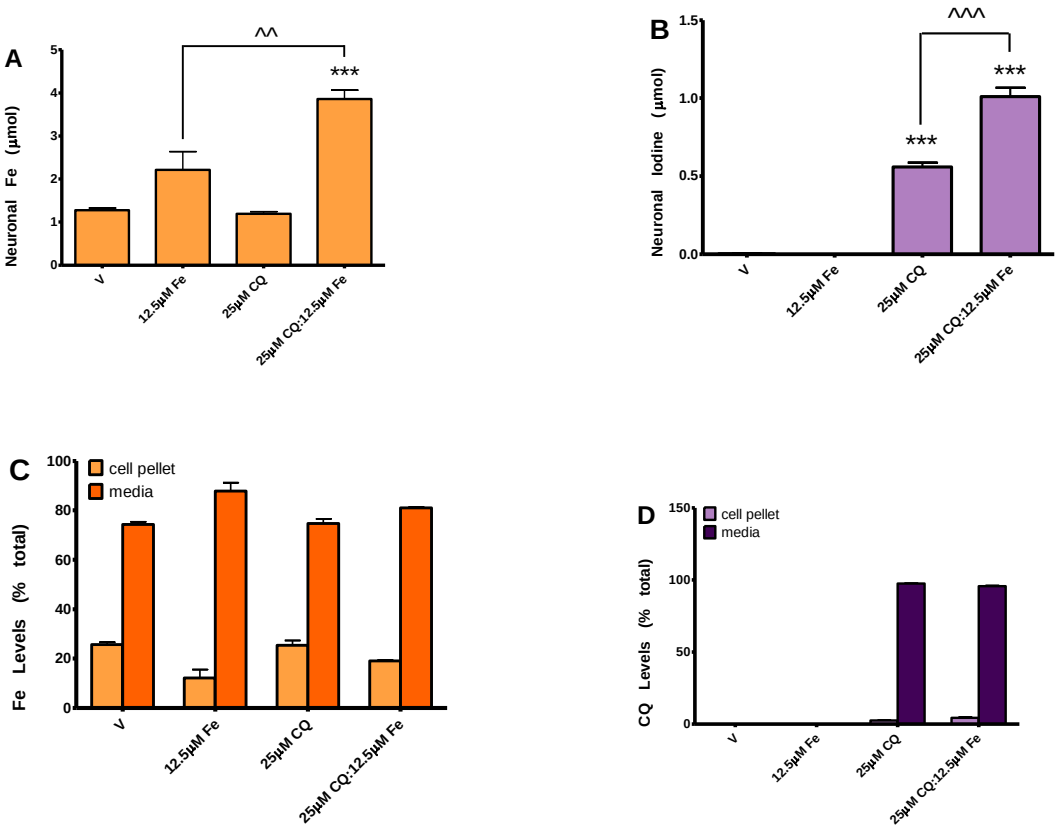

Figure 5.3.7 Neuronal uptake of Fe, CQ and CQ-Fe

*CQ induces the uptake of Fe (**A**) from the media into neurons (**C**). In turn, Fe enhances the uptake of CQ into neurons (**B**) without major changes to its distribution (**D**).*

ANOVA with Tukey post-hoc test;

****p < 0.001 compared to vehicle-control; ^^p < 0.01, ^^^p < 0.001*

Bars represent mean ± S.E.M, n = 3

5.3.8 Rate of neuronal CQ and metals uptake

In **sections 5.3.5 – 5.3.7**, it has been established that metals and CQ mutually affect each other's neuronal uptake. While CQ delivered metals from the extracellular environment into neuronal cells, in a mole ratio far exceeding CQ-metal stoichiometry; metal-stimulated neuronal uptake of CQ occurred to a lesser extent and with no apparent change to the drug's localization (refer to **Fig. 5.3.5 – 5.3.7**).

Drawing on these results, it was speculated that CQ might transport metals into neurons (where they can be utilized for cellular functions or destined for removal), and then recycle in order to bind and ferry additional metal ions across into neurons. To test this hypothesis, neuronal cultures were incubated with CQ-metal complexes and the rate of metals and CQ uptake into mouse primary cortical neuronal cells was studied simultaneously at time intervals up to three hours (as detailed in **section 5.2.6**).

Data confirmed that, at time zero, neuronal cultures contained low basal Cu levels (0.04 μmol), higher levels of endogenous Zn and Fe (0.36 and 0.25 μmol, respectively), and no detectable iodine (**Fig. 5.3.8 A-C**), similar to **Fig. 5.3.5 - 5.3.7 A-B**.

During treatment with 10 μM CQ and 5 μM $CuCl_2$, CQ entered cultured neurons within the first 10 minutes, whereas significant Cu uptake was observed from 60 minutes on (**Fig. 5.3.8 A**). Strikingly, while the rate of neuronal Cu uptake was linear, CQ maintained a constant, low level throughout the incubation period (**Fig. 5.3.8 A**).

Mouse primary cortical neuronal cells treated with 16 μM CQ and 8 μM $ZnCl_2$ displayed quick intake of the drug and metal (both within 10 minutes; **Fig. 5.3.8 B**). Following their initial rise, CQ kept a steady low level, while Zn levels increased gradually (**Fig. 5.3.8 B**).

Significant CQ and Fe uptake into mouse primary cortical neuronal cells occurred 10 and 40 minutes, respectively, from the start of the treatment with 25 μM CQ and 12.5 μM $FeCl_3$ (**Fig. 5.3.8 C**). From those time points onwards, the levels of both drug and ion were progressively elevated (**Fig. 5.3.8 C**).

In summary, when CQ-metal complexes are found in the vicinity of neurons, CQ is rapidly taken up by the cells and either remains at a constant level (in the case of Cu and Zn; **Fig. 5.3.8 A** and **B**, respectively) or slowly accumulates in neuronal cells (in the case of Fe; **Fig. 5.3.8 C**). At the same time, Cu ions are rapidly internalised and continue to accumulate within neurons (**Fig. 5.3.8 A**); whereas, Zn and Fe seem to reach steady-state levels within neuronal cells (**Fig. 5.3.8 B** and **C**, respectively).

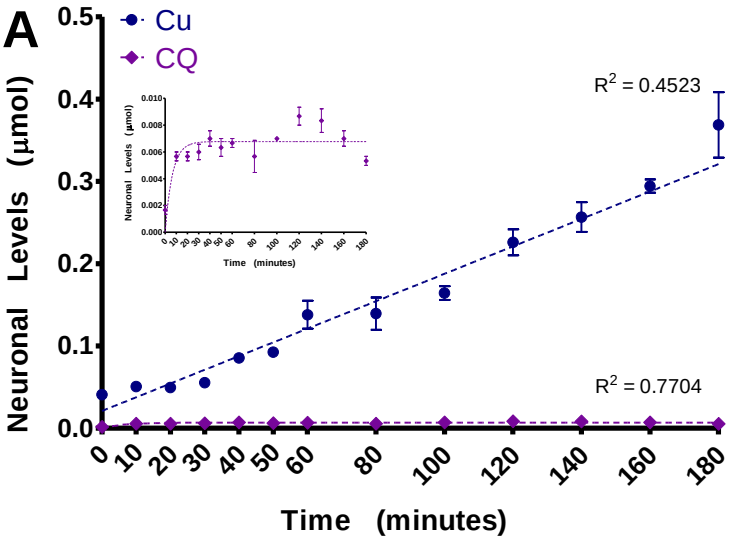
A
Cu
CQ
R2 = 0.4523
R2 = 0.7704
Neuronal Levels (µmol)
Time (minutes)

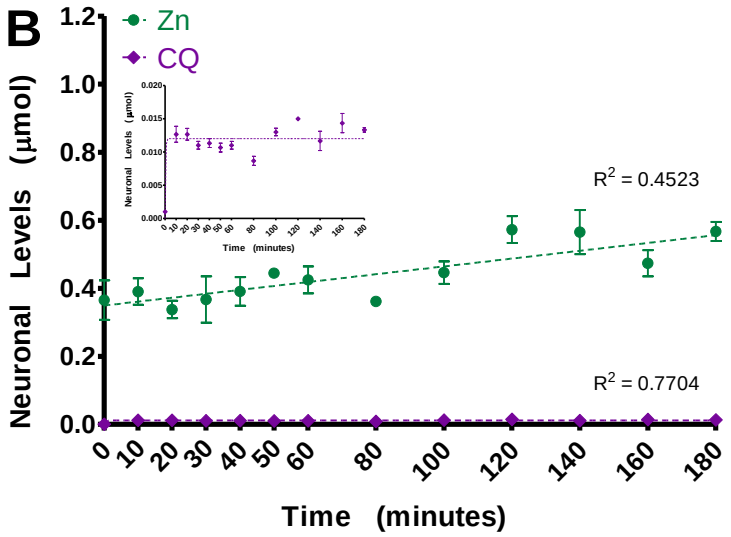
B
Zn
CQ
R2 = 0.4523
R2 = 0.7704
Neuronal Levels (µmol)
Time (minutes)

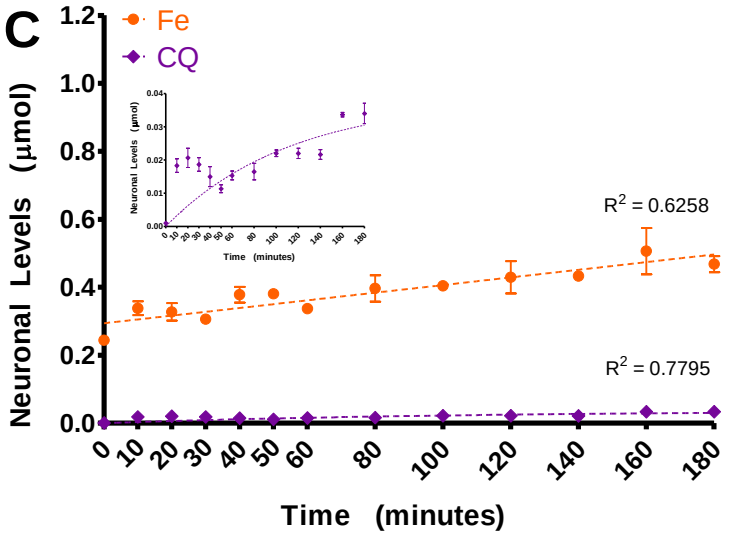
C
Fe
CQ
R2 = 0.6258
R2 = 0.7795
Neuronal Levels (µmol)
Time (minutes)

Figure 5.3.8 Time-course of neuronal CQ-metal uptake

*While neuronal uptake of Fe (**C**) and Zn (**B**) occurred slowly and gradually over time, neuronal uptake of Cu (**A**) was relatively quick and metal levels increased in a linear fashion.*

*Neuronal CQ uptake occurred within 10 minutes of its introduction and was followed by a steady state of drug levels (**A-B insert**); except for CQ-Fe complexes, where CQ levels continue to rise (**C insert**).*

Data were plotted, using non-linear regression fit and analysed by ANOVA with Dunnett's multiple comparison test compared to baseline (i.e., time zero).

Bars represent mean ± S.E.M, n = 3

5.3.9 Neurotoxicity of CQ, metals and/or Aβ

After establishing the mutual effect of CQ and metal ions on each other's level and rate of neuronal uptake, as well as distribution (**sections 5.3.2 - 5.3.8**), the effect of Aβ on the aforementioned was explored.

To ensure that any changes observed are not due to neurons being under stress conditions, the impact of Aβ on neuronal survival, in the absence and presence of metal ions and/or CQ, was first ascertained (see **section 5.2.5**).

The results confirmed earlier findings (refer to **Fig. 5.3.1**) that treatment with $CuCl_2$ (5 μM), $ZnCl_2$ (8 μM), $FeCl_3$ (12.5 μM) and/or CQ (10, 16 or 25 μM, respectively) had no effect on the viability of mouse primary cortical neuronal cells, compared to vehicle-treated cultured neurons (**Fig. 5.3.9 A-C**).

Data also showed that treatment with $A\beta_{42}$ (5, 8 or 12.5 μM), in the presence and absence of $CuCl_2$ (5 μM), $ZnCl_2$ (8 μM), $FeCl_3$ (12.5 μM) and/or CQ (10, 16 or 25 μM, respectively), did not alter the number of live mouse primary cortical neuronal cells, relative to vehicle-treated neuronal cultures (**Fig. 5.3.9 A-C**).

These findings were to be expected, especially due to the short treatment duration. The survival rate of mouse primary cortical neuronal cells was shown to be compromised by 10 and 20 μM Aβ following a longer treatment period of 96 hours (862). Also, while the viability of mouse cortical neuronal cultures was not affected by 5 μM Aβ (768, 862), it was significantly impaired by 5 μM Aβ-Cu (1:1 ratio) following a 96-hour incubation (768).

Importantly, for the purpose of all following studies, the chosen concentrations of Aβ, metal ions and/or CQ were proven to be sub-neurotoxic, under the tested conditions.

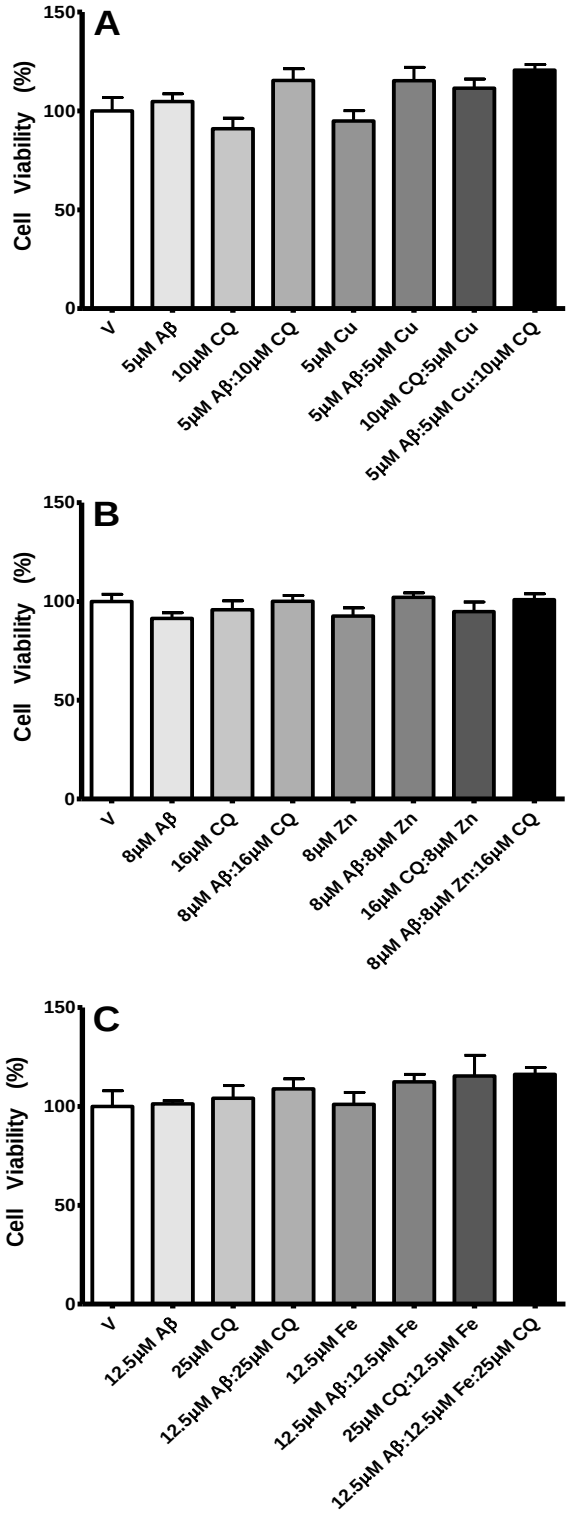

Figure 5.3.9 Effect of Aβ, metals and/or CQ on neuronal cell viability

*Exposure to Aβ (5, 8 and 12.5 μM), metals (5, 8 and 12.5 μM Cu, Zn and Fe) and/or CQ (10, 16 and 25 μM) had no effect on neuronal cell survival, relative to vehicle-treated neuronal cultures (**A-C**, respectively).*

ANOVA with Dunnett's multiple comparison test;

Bars represent mean ± S.E.M, n = 3

5.3.10 Effect of Aβ and/or CQ on neuronal metal uptake

After validating that, under the specified experimental conditions, neuronal cultures were viable (refer to **Fig. 5.3.9**), the effects of Aβ, biometals (Cu, Zn and Fe) and CQ on each other's neuronal uptake were tested next (as per **section 5.2.6**).

Initially, the influence of Aβ on metal and CQ-induced metal uptake into mouse primary cortical neurons was studied. Results confirmed that treatment with 10, 16 or 25 μM CQ did not alter the neuronal levels of Cu, Zn or Fe, respectively, as compared to vehicle-treated neuronal cultures (**Fig. 5.3.10 A-C**; similar to **Fig. 5.3.2**).

As anticipated, treatment with 5, 8 or 12.5 μM $A\beta_{42}$, in the absence and presence of CQ (1:2 molar ratio), also did not change the neuronal levels of Cu, Zn or Fe, respectively, in comparison to vehicle-treated cultured neurons (**Fig. 5.3.10 A-C**).

Data showed that treatment with 5 μM $CuCl_2$ or 8 μM $ZnCl_2$ did not impact the respective neuronal metal levels; but, treatment with 12.5 μM $FeCl_3$ led to significant Fe uptake, relative to vehicle-treated neuronal cultures (**Fig. 5.3.10 A-C**). With regards to Zn and Fe, these results verify previous evidence presented in **Fig. 5.3.3 C** and **E**, as well as **panel A** in **Fig. 5.3.6** and **Fig. 5.3.7**, respectively.

Data also confirmed findings highlighted in **Fig. 5.3.3** panels **B**, **D** and **F**, as well as **panel A** in **Fig. 5.3.5 - 5.3.7**, demonstrating that metallo-CQ complexes promoted Cu, Zn and Fe uptake into mouse primary cortical neuronal cells, compared to cultured neurons treated with either vehicle or metal alone (**Fig. 5.3.10 A-C**).

Interestingly, co-treatment with 5, 8 or 12.5 μM $A\beta_{42}$ and $CuCl_2$, $ZnCl_2$ or $FeCl_3$ (1:1 molar ratio, respectively) did not affect the respective neuronal metal levels, compared to mouse primary cortical neuronal cells treated with either vehicle, Aβ alone or metal alone (**Fig. 5.3.10 A-C**).

Conversely, treatment with $A\beta_{42}$ (5, 8 or 12.5 μM), in the presence of both metals (1:1 molar ratio) and CQ (1:2 molar ratio), suppressed the CQ-induced neuronal uptake of Cu and Fe (to levels still significantly higher than vehicle-treated neuronal cultures; **Fig. 5.3.10 A** and **C**, respectively); yet exacerbated the CQ-induced neuronal uptake of Zn (**Fig. 5.3.10 B**).

These results may infer that Aβ in itself does not influence neuronal metal levels; nor do metal-Aβ oligomers. However, the combination of Aβ, metals and CQ could differentially modulate neuronal metal intake (i.e., increase Zn, but decrease Cu and Fe uptake into neurons).

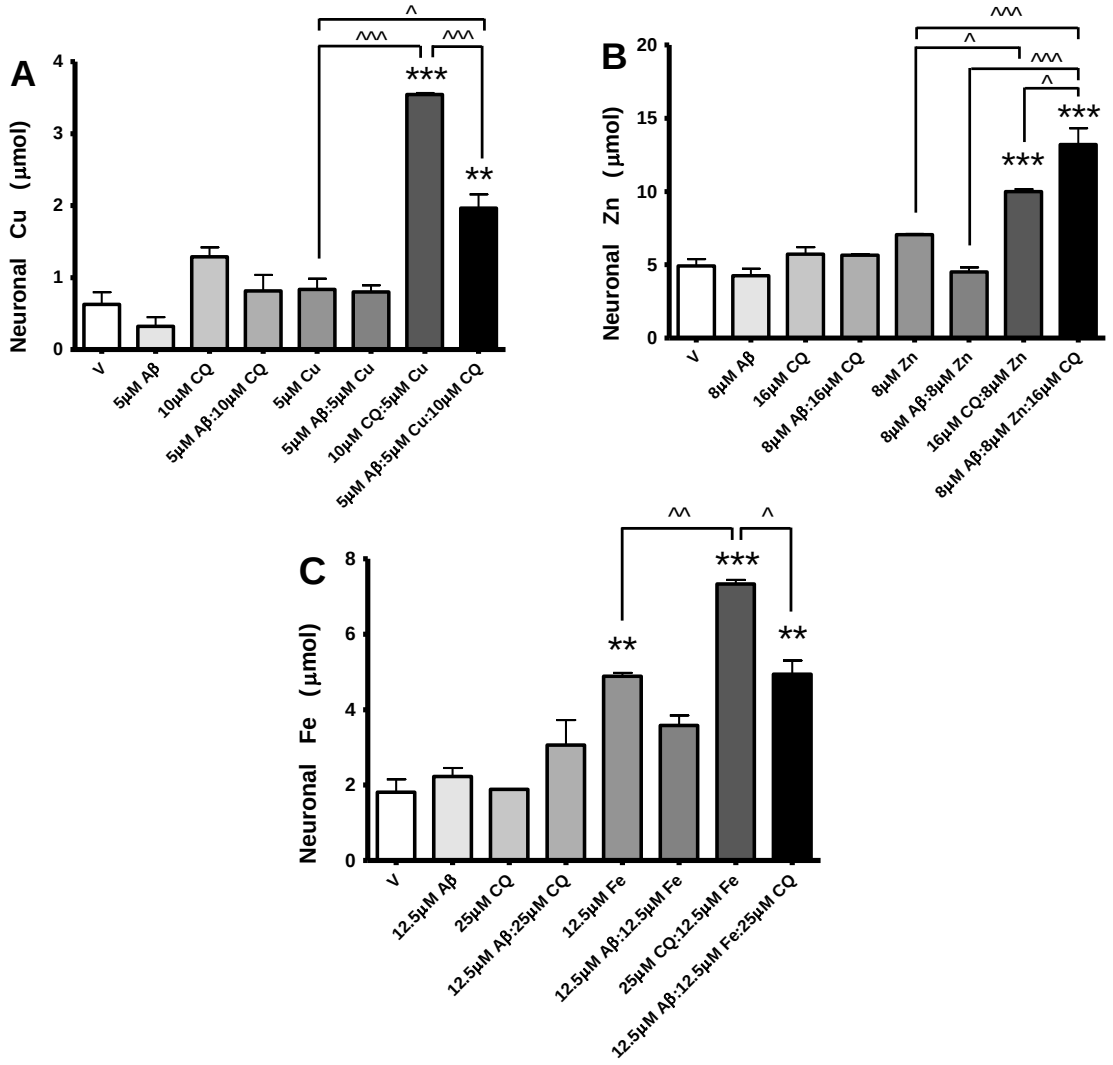

Figure 5.3.10 Effect of Aβ and/or CQ on neuronal metal uptake

*Aβ, in the absence and presence of metals or CQ, did not affect neuronal metal uptake (**A**-**C**). Aβ augmented the CQ-induced neuronal Zn uptake (**B**) but suppressed the CQ-induced neuronal uptake of Cu (**A**) and Fe (**C**).*

*ANOVA with Tukey post-hoc test;**p < 0.01, ***p < 0.001 compared to vehicle-control ^p < 0.05; ^^p < 0.01; ^^^p < 0.001*

Bars represent mean ± S.E.M, n ≥ 2

5.3.11 Effect of Aβ and/or metals on neuronal CQ uptake

In parallel to determining the effect of Aβ, with and without CQ, on neuronal metals uptake (see **section 5.3.10**); the effect of Aβ, with and without metal ions, on neuronal uptake of CQ was also investigated (procedure described in **section 5.2.6**).

As expected, iodine (^{127}I) was detected (refer to **section 5.2.8**) only in neuronal cultures that were treated with CQ, in the absence and presence of metals and/or $A\beta_{42}$ (**Fig. 5.3.11 A-C**; similar to **panel B** in **Fig. 5.3.5 – 5.3.7**); thereby, serving as a surrogate measure for neuronal CQ levels.

Results showed that treatment of mouse primary cortical neuronal cells with 10, 16 or 25 μM CQ and $A\beta_{42}$ (2:1 molar ratio) had no effect on neuronal CQ uptake, compared to cultured neurons treated with CQ alone (**Fig. 5.3.11 A-C**).

Data demonstrated that co-treatment with 5 μM $CuCl_2$ and 10 μM CQ mitigated CQ uptake, relative to mouse primary cortical neuronal cells treated with CQ alone (**Fig. 5.3.11 A**; as in **Fig. 5.3.5 B**). Results also confirmed that treatment with CQ (16 or 25 μM) and $ZnCl_2$ or $FeCl_3$ (2:1 molar ratio, respectively) stimulated CQ uptake, in comparison to neuronal cultures treated with CQ on its own (**Fig. 5.3.11 B-C**; similar to **panel B** in **Fig. 5.3.6** and **5.3.7**, respectively).

Importantly, the combined treatment of mouse primary cortical neuronal cells with $A\beta_{42}$, metals and CQ had a differential effect on neuronal CQ uptake. Parallel treatment with 5 μM $A\beta_{42}$, 5 μM $CuCl_2$ and 10 μM CQ significantly increased CQ uptake, relative to cultured neurons treated with 10 μM CQ, in the absence and presence of either 5 μM $A\beta_{42}$ or 5 μM $CuCl_2$ (**Fig. 5.3.11 A**). This implies that there is a synergistic relation between the Aβ peptide, Cu ions and the drug.

Treatment of neuronal cultures with 8 μM $A\beta_{42}$, 8 μM $ZnCl_2$ and 16 μM CQ also induced neuronal CQ uptake, as compared to treatment with 16 μM CQ, in the absence and presence of 8 μM $A\beta_{42}$; but, unlike Cu, it did not lead to further enhanced neuronal CQ uptake, compared to mouse primary cortical neuronal cells treated with 8 μM $ZnCl_2$ and 16 μM CQ (**Fig. 5.3.11 B**). These findings suggest the Zn, regardless of Aβ, is sufficient for neuronal uptake of CQ.

Surprisingly, treatment with 12.5 μM $A\beta_{42}$, 12.5 μM $FeCl_3$ and 25 μM CQ suppressed the uptake of CQ into mouse primary cortical neuronal cells, compared to treatment with 12.5 μM $FeCl_3$ and 25 μM CQ, in the absence or presence of 12.5 μM $A\beta_{42}$ (**Fig. 5.3.11 C**).

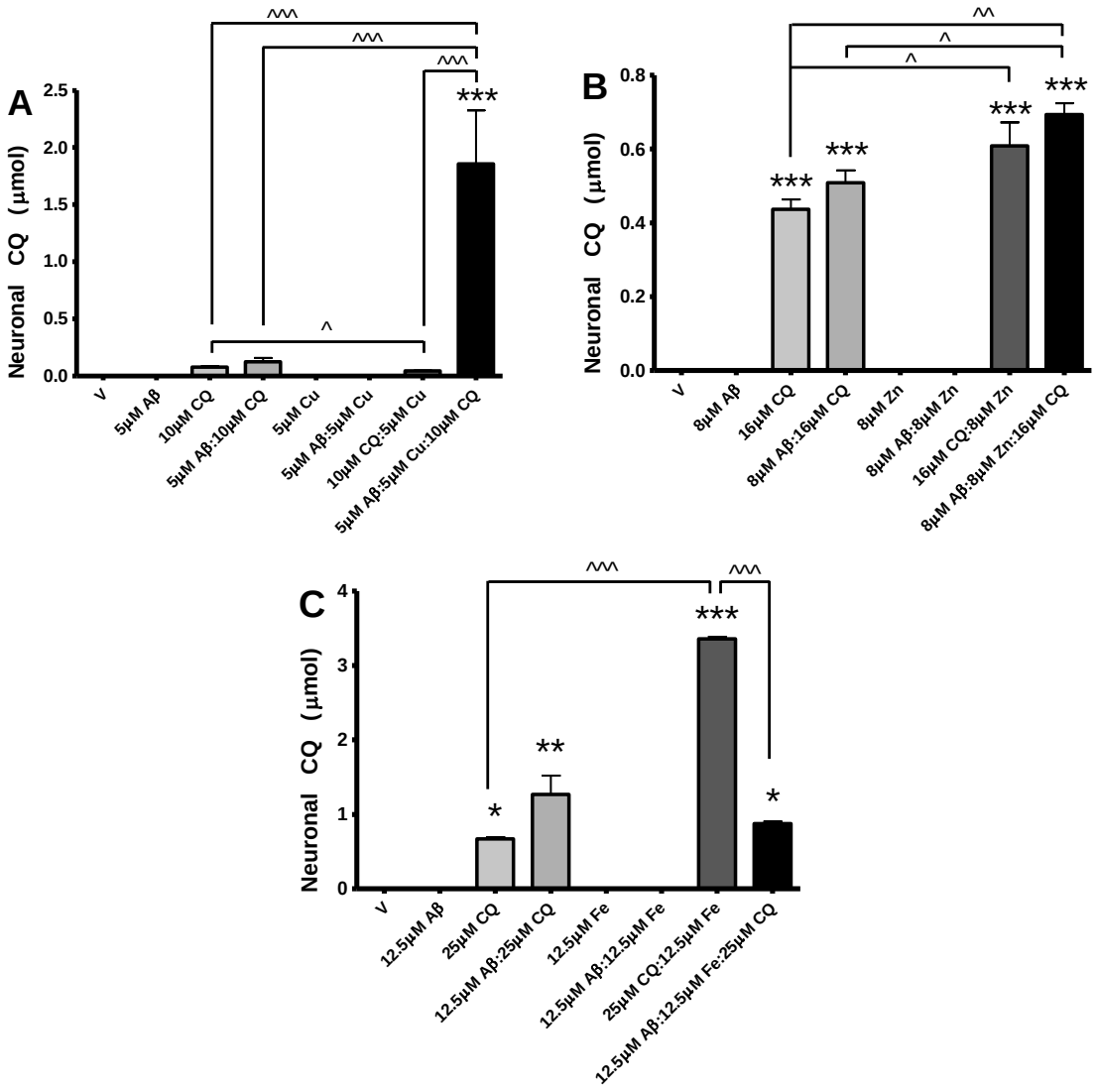

Figure 5.3.11 Effect of Aβ and/or metals on neuronal CQ uptake

*Aβ on its own did not affect CQ uptake into neuronal cells (**A**-**C**); yet, in the presence of either Cu (**A**) or Zn (**B**), it augmented neuronal CQ uptake, compared to CQ alone. ANOVA with Tukey post-hoc test; *p < 0.05, **p < 0.01, ***p < 0.001 compared to vehicle-control; ^p < 0.05; ^^p < 0.01; ^^^p < 0.001*

Bars represent mean ± S.E.M, n ≥ 2

5.3.12 Effect of metals and/or CQ on neuronal Aβ uptake

Finally, the uptake of $A\beta_{42}$ into mouse primary cortical neuronal cells was investigated, in the absence and presence of CQ and/or metals (technique detailed in **section 5.2.6**). As expected, $A\beta_{42}$ levels were undetected in neuronal cultures that were treated with either vehicle or with metals and/or CQ (**Fig. 5.3.12 A-C**); while significant levels of $A\beta_{42}$ were detected in cultured neurons treated with $A\beta_{42}$, in the absence and presence of metals and/or CQ (**Fig. 5.3.12 A-C**).

Data showed that treatment with 10 or 16 μM CQ (**Fig. 5.3.12 A** and **B**, respectively), but not 25 μM CQ (**Fig. 5.3.12 C**), together with $A\beta_{42}$ (2:1 molar ratio) promoted the uptake of $A\beta_{42}$ into mouse primary cortical neuronal cells, compared to neuronal cultures treated with $A\beta_{42}$ alone. These findings were unexpected, as it was hypothesized that any affect CQ may have on Aβ would be metal-mediated; instead, findings may be consistent with direct interaction between Aβ and CQ.

Results demonstrated that co-treatment with 5 μM $A\beta_{42}$ and $CuCl_2$ (1:1 molar ratio) did not affect the neuronal uptake of $A\beta_{42}$, relative to cultured neurons treated with $A\beta_{42}$ on its own; yet, it did diminish neuronal $A\beta_{42}$ uptake, in comparison to mouse primary cortical neuronal cells treated with 5 μM $A\beta_{42}$ and CQ (1:2 molar ratio; **Fig. 5.3.12 A**).

Concomitant treatment with $A\beta_{42}$ (8 or 12.5 μM) and either $ZnCl_2$ or $FeCl_3$ (1:1 molar ratio, respectively) stimulated the neuronal uptake of $A\beta_{42}$, as compared to treatment with $A\beta_{42}$, in the absence of these metals (**Fig. 5.3.12 B** and **C**, respectively). However, while treatment of mouse primary cortical neuronal cells with 8 μM $A\beta_{42}$ and $ZnCl_2$ (1:1 molar ratio) did not alter the uptake of $A\beta_{42}$, relative to neuronal cultures treated with 8 μM $A\beta_{42}$ and CQ (1:2 molar ratio; **Fig. 5.3.12 B**); parallel treatment with 12.5 μM $A\beta_{42}$ and $FeCl_3$ (1:1 molar ratio) increased $A\beta_{42}$ uptake, compared to cultured neurons treated with 12.5 μM $A\beta_{42}$ and CQ (1:2 molar ratio; **Fig. 5.3.12 C**).

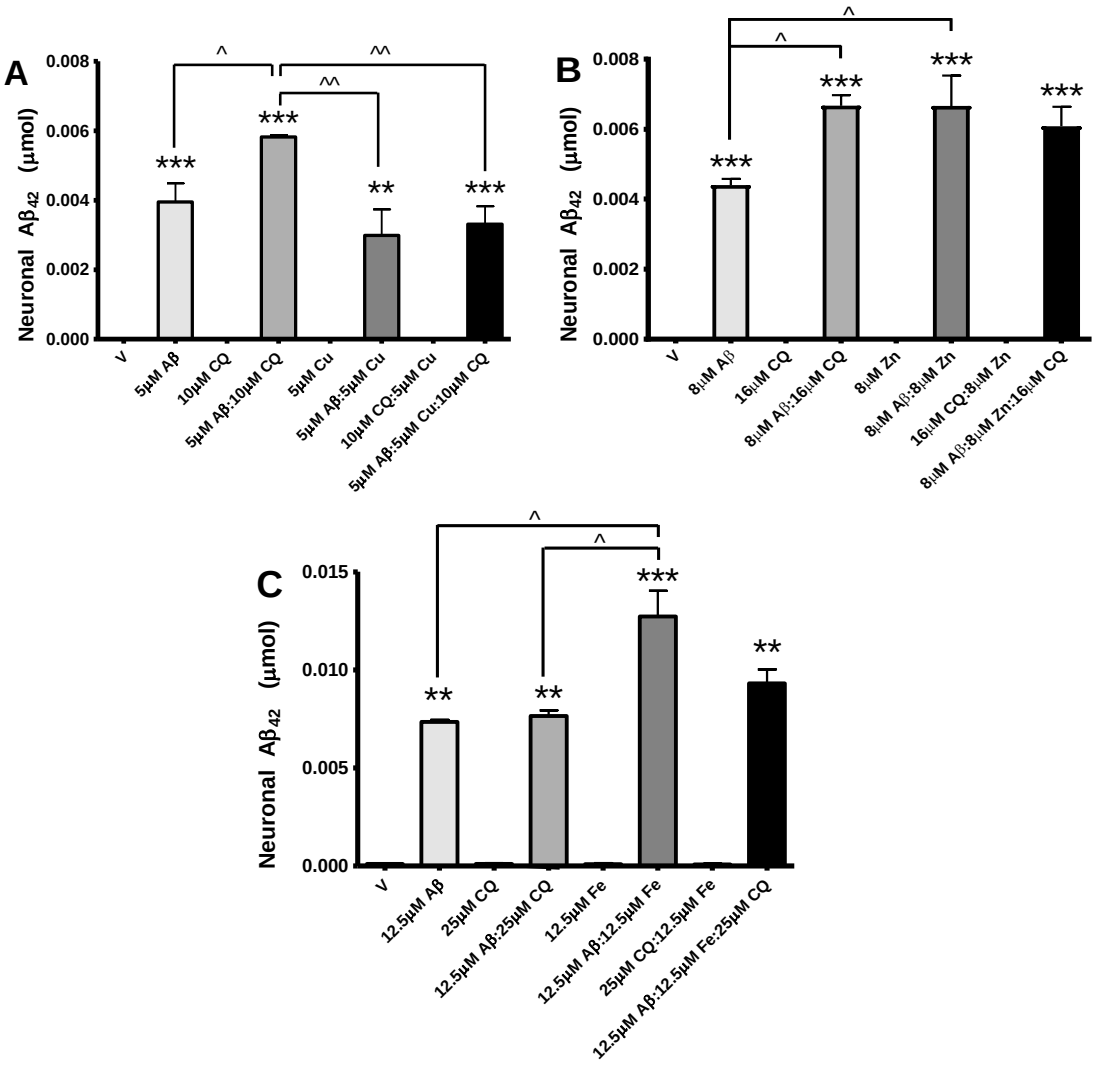

Figure 5.3.12 Effect of metals and/or CQ on neuronal Aβ uptake

*Zn (**B**) and Fe (**C**), but not Cu (**A**), enhanced neuronal Aβ uptake.*

*Moderate (**A** and **B**), but not high (**C**), doses of CQ stimulated neuronal Aβ uptake.*

*Cu suppressed the CQ-induced Aβ uptake into neuronal cells (**A**), while Zn and Fe did not affect CQ-induced Aβ uptake into neuronal cells (**B** and **C**, respectively).*

*ANOVA with Tukey post-hoc test;**$p < 0.01$, ***$p < 0.001$ compared to vehicle-control ^$p < 0.05$; ^^$p < 0.01$*

Bars represent mean ± S.E.M, $n \geq 2$

Interestingly, $A\beta_{42}$ uptake into mouse primary cortical neuronal cells treated with $A\beta_{42}$ (8 or 12.5 μM), combined with CQ (1:2 molar ratio) and $ZnCl_2$ or $FeCl_3$ (1:1 molar ratio, respectively), was no different to that of neuronal cultures treated with $A\beta_{42}$ on its own, or with either metals or CQ (**Fig. 5.3.12 B** and **C**, respectively).
Conversely, treatment with 5 μM $A\beta_{42}$, $CuCl_2$ and CQ (1:1:2 molar ratio) did not alter neuronal $A\beta_{42}$ uptake, in comparison to mouse primary cortical neuronal cells treated with 5 μM $A\beta_{42}$, in the absence and presence of 5 μM $CuCl_2$; yet, it did suppress the uptake of $A\beta_{42}$ induced by 10 μM CQ in the absence of 5 μM $CuCl_2$ (**Fig. 5.3.12 A**).

It could be concluded that the differential effects of CQ and metals on neuronal uptake of Aβ may be related to the different conformations of metallo-CQ complexes, as well as those of metallated-Aβ.

5.4 Discussion

Extensive literature exists on the interaction of metals and Aβ (see **sections 1.4.3.3-1.4.4**) and that of metals and CQ (refer to **section 1.5.5**). In contrast, the information available on the triad relationship between CQ, metal ions and Aβ protein is scarce and is drawn from *in vivo* trials in Tg animal models of AD (444, 699, 700, 709, 746, 763, 826, 829) and AD patients (710, 711, 745), as well as *in vitro* studies utilizing immortalized cells (436, 752, 811).

From experiments conducted in clonal cell lines it was inferred that the therapeutic window of metal complexes with CQ and other compounds is not dependant solely on the drug itself, but also on the dose and bioavailability of biometals (436, 607, 700). Similar conclusions can be reached for neuronal cultures, based on work presented in this chapter.

In general, there was a direct correlation between the rise of metal levels within neurons (**sections 5.3.2-5.3.4**) and neurotoxicity (**section 5.3.1**). Acute administration of physiological concentrations of CQ was shown to be non-neurotoxic (**Fig. 5.3.1 A** and **Fig. 5.3.9**); nor did it alter endogenous neuronal Cu, Zn and Fe levels (**Fig. 5.3.2**, **panel A** in **Fig. 5.3.5–5.3.7**, and **Fig. 5.3.10**). As for CQ-metal complexes, the observed toxicity at high doses (**Fig. 5.3.1 C, E** and **G**) was presumably dependant on the type of ion (Cu and Zn, but not Fe) and on its intra-neuronal level (**Fig. 5.3.3 B, D** and **F**, and **Fig. 5.3.4**).

Together, data imply that neurons possess sophisticated mechanisms to monitor changes in extracellular metal levels and to maintain their survival, in spite of metal influx. For example, no neurotoxicity was observed at any of the tested $CuCl_2$ doses (**Fig. 5.3.1 B**), despite significant neuronal ion uptake following treatment with $CuCl_2$ at doses equal to or higher than 4 μM (**Fig. 5.3.3 A**). Yet, even these refined homeostatic systems have an upper limit (different for each of the metals investigated) that, once crossed, eventuates in regulatory failure, cellular dysfunction and neuronal death.

Neurons are able to efficiently adapt and stave off increasing levels of Cu and Zn in their milieu to a certain extent. However, high doses of CQ-Cu and CQ-Zn complexes import such large amounts of metals in a short period of time that the systems in place can no longer uphold balanced metal levels. As a result, Cu and Zn continue to enter and accumulate within these cells in an unrestricted fashion (**Fig. 5.3.3 B** and **D**, **panels A-B** in **Fig. 5.3.4** and **Fig. 5.3.8**) causing neurons to die rapidly (**Fig. 5.3.1 C** and **E**).

The significance of these findings is in the insight they provide into the therapeutic window of CQ, metals and their combination. It could be deduced that, in relation to the broad therapeutic spectrum of CQ, the therapeutic range of metallo-CQ is much narrower. This could have profound implications for the design, synthesis, dosage and use not only of other 8-HQ derivatives, such as PBT2 (Prana Biotechnology; Parkville, Melbourne, VIC, Australia), but also of other metal-targeting candidate drugs for the treatment of AD (see **Fig. 1.5**) and additional neurodegenerative diseases. On a broader scope, this could also have a bearing on the development of therapeutic agents for disorders involving impaired metal metabolism - both inherited (refer to **section 1.4.1**) and acquired (like cancer, diabetes, skin conditions and coronary heart disease).

A major breakthrough was achieved by harnessing ICPMS technology for the simultaneous tracking of both metals and CQ (method detailed in **sections 5.2.7-5.2.8**). Results showed that free CQ is taken into neurons (**panel B** in **Fig. 5.3.5-5.3.7**, and **Fig. 5.3.11**). This is not surprising given the properties of the drug (listed in **Table 1.5**), but still does not provide a lead as to whether CQ enters neurons *via* a passive or active mechanism (see **section 3.3.5**). Instead of being internalized, the possibility that CQ is either inserted into the cell membrane or attached to the cell's exterior surface (despite neurons being extensively washed; full protocol in **section 5.2.6**), cannot be excluded.

Data also revealed that all metal-CQ complexes potentiated neuronal metal uptake, according to the binding affinity of the drug towards the ions (i.e., Cu > Zn > Fe), by mobilizing metals from the extracellular environment into neurons (**Fig. 5.3.4**, **panels A** and **C** in **Fig. 5.3.5-5.3.7**, and **Fig. 5.3.10**). Interestingly, metal-CQ complexes had opposing effects on neuronal CQ uptake (i.e., CQ-Cu complexes suppressed neuronal CQ uptake *versus* CQ-Zn and CQ-Fe complexes, which enhanced neuronal CQ uptake), with negligible change in the percentage of CQ between the incubating media and neurons (**panels B** and **D** in **Fig. 5.3.5-5.3.7**, and **Fig. 5.3.11**). Alternatively, these data can be interpreted as elevated CQ efflux or cellular retention, respectively.

CQ is a bi-dentate ligand that forms chelates with a broad range of cations, including Cu^{2+} and Zn^{2+} (694-696, 698, 770). Both of these ions are bound by the phenolic oxygen atom and the pyridine nitrogen atom on CQ; but, while Cu^{2+} assumes a square planar geometry, Zn^{2+} is coordinated in a trigonal bipyramidal environment (694). This suggests that the neuronal uptake of metal-bound CQ may be dependent on its spatial arrangement. Additionally, whilst the structure of CQ-Fe has not yet been resolved, these results indicate that it could resemble that of CQ-Zn, rather than CQ-Cu.

In case metal-CQ enter cells as intact complexes, rather than individual molecules, it was predicted that the levels of both CQ and metals should decrease in the treatment media and, in parallel, increase within neurons; all the time maintaining their respective 2:1 molar ratio. The concurrent, yet differential, uptake and distribution of the drug *versus* the biometals suggested otherwise.

Indeed, a pharmacodynamic study of metal-CQ uptake into neurons demonstrated that CQ entered neurons rapidly (within 10 minutes) and, following its initial rise, maintained a steady and low level (**Fig. 5.3.8**). At the same time, the rate of neuronal metal uptake increased (Cu in a linear mode; Zn and Fe gradually), at a much higher proportion than that of CQ (**Fig. 5.3.8**).

Based on findings in **sections 5.3.5 – 5.3.8**, it is proposed the MOA of metal-CQ is by crossing the plasma membrane as one unit and then separating into its constituents. Once within neurons, CQ dissociates from and releases its metal cargo that, most likely, binds to intracellular chaperone molecules. Metal ions are likely utilized immediately for essential cellular functions, stored for later use or are directed for removal. All the while, the metal-free drug might recycle back to the extracellular space, where it could potentially bind additional metal ions and transports them into neurons.

The aforementioned fits computational modelling of neuronal Zn homeostasis, which estimated that CQ passes through the plasma membrane and delivers Zn^{2+} into neurons, where the ions are sequestered to storage sites (825). In an attempt to corroborate this supposition, the study in **section 5.3.8** should be repeated in future, using CQ at a molar ratio equal to or lower than that of the metals; thereby, allowing for excess, free metal ions. If the results of such an investigation remain similar to those illustrated in **Fig. 5.3.8**, this will indicate that CQ is capable not only of chaperoning metals into neurons, but also has an ability to leave the cells in order to ferry remaining extracellular metal ions into the cells.

In addition, while several recent studies have utilized CQ as a chemical means to manipulate cerebral Zn (836-842), data in this chapter demonstrated that CQ is even more efficient in mobilizing Cu (**Fig. 5.3.4** and **Fig. 5.3.8**). Since the AD brain was found to contain a pool of labile Cu (378), it is suggested that future studies would also measure changes in this ion's levels in the brain and examine its effects. Based on the findings of such investigations, it could be determined whether CQ may be used as a pharmacological tool to modulate Cu levels in brains of animal models for research purposes.

With regards to the AD brain environment, it is important to acknowledge the predominant presence of APP, Aβ and other AD-related cerebral proteins, which affect metal ions and *vice versa* (as discussed in **sections 1.4.2-1.4.4**). These could also have significant implications on the mode CQ, PBT2 (and other metal-targeting compounds, such as the ones reviewed in **section 1.5** and depicted in **Fig. 1.5**) operate and result in the therapeutic benefits observed in animal and human AD trials.

As previously mentioned in **section 5.1**, cell-based *in vitro* studies cannot fully recapitulate the events that occur in the brain following drug administration. However, adding synthetic Aβ, metals and CQ to neuronal cultures, at approximate concentrations to those found in brains of AD patients, allows the formation of a working model as to the MOA of CQ in AD, which can later be further tested and verified by other means – both *in vitro* and *in vivo*.

Despite hypothesizing that the extracellular interaction of Aβ and metals would diminish the neuronal uptake of both the protein and the ions, experimental results demonstrated that while Aβ did not alter neuronal metal uptake (**Fig. 5.3.10**), metals differentially affected neuronal Aβ (i.e., Cu had no effect on, but both Zn and Fe induced, the neuronal uptake of Aβ; **Fig. 5.3.12**).

These findings probably reflect the different binding affinities of metal ions towards Aβ and the dissimilar resultant spatial arrangement and/or aggregation of the peptide (refer to **section 1.4.3.3**). This means that metal-mediated Aβ entry into neuronal cells may be dependent on its conformation. If so, any drug design should target the desired metallated-Aβ structure, in order to assist in its influx and potential intra-neuronal degradation. An alternate explanation is that Zn and Fe could lead to impaired intracellular degradation (for example, through the lysosomal-autophagy system), which may result in Aβ accumulation or retention within neurons.

To date, there have only been three published studies of CQ and Aβ in primary cultures; all of which highlight the role of CQ in neuroprotection and/or neurorescue against Aβ-mediated neurotoxicity. Barnham *et. al.* demonstrated that 1 μM CQ inhibits the toxicity exerted by $A\beta_{42}$ on mouse primary cortical neuronal cells following 4-day exposure (549). A similar dose of CQ was found to block the $A\beta_{25-35}$-induced Ca^{2+} influx in cortical astrocytes and to protect against $A\beta_{25-35}$-induced cell death of hippocampal neurons, with and without astrocytes (707).

Recently, co-treatment with $A\beta_{42}$ and CQ was shown not only to restore the activity of mouse primary cortical neurons cultured on multi-electrode array (MEA) chips that were compromised by treatment with $A\beta_{42}$ alone; but to augment it significantly beyond baseline levels (704).

Work presented here provides a first look into the reciprocal relationship between Aβ and CQ in terms of neuronal uptake. While neuronal CQ uptake remained unvaried by Aβ (**Fig. 5.3.11**); moderate (10 and 16 μM), but not high (25 μM), doses of CQ stimulated the uptake of Aβ (**Fig. 5.3.12**). These data point to a possible dose-dependent direct interaction between CQ and Aβ, which might be saturated at high concentrations. It is reasonable to assume that CQ interacts with the aromatic residue(s) on Aβ.

These novel results are significant as they contradict current thinking that any effect CQ may exert on Aβ is mediated by metals, but at the same time are not without precedence. Our research group has shown in the past that bathocuproine (BC), a chelator with high affinity towards Cu, forms direct intercalating interactions with Aβ in the absence of Cu (481).

Importantly, the mutual effect of Aβ and either metals or CQ was different to that of all three components together. Aβ attenuated the CQ-induced neuronal uptake of Cu (**Fig. 5.3.10 A**) and Cu suppressed the CQ-stimulated Aβ uptake (**Fig. 5.3.12 A**), but Aβ and Cu synergistically enhanced CQ uptake (**Fig. 5.3.11 A**). Aβ enhanced the CQ-induced neuronal uptake of Zn (**Fig. 5.3.10 B**), yet did not affect Zn-stimulated neuronal CQ uptake (**Fig. 5.3.11 B**). While CQ and Zn individually enhanced Aβ's neuronal uptake; combined, they did not influence Aβ's uptake into neurons (**Fig. 5.3.12 B**). Aβ attenuated both CQ-stimulated neuronal Fe uptake and Fe-induced neuronal CQ uptake (**panel C** in **Fig. 5.3.10** and **5.3.11**, respectively); however, CQ and Fe together did not impact the neuronal uptake of Aβ (**Fig. 5.3.12 C**). Once more, these data could infer dose, affinity and/or conformation-dependency and reinforce the complexity of studies of this kind.

It is important to note that studies in this chapter are limited in that neuronal uptake cannot be differentiate from degradation and/or efflux. In order to settle this point, similar studies could be performed with the addition of various endocytosis/exocytosis, lysosomal-autophagy and/or proteasome inhibitors, such as those used in **sections 3.3.5-3.3.15**.

In summary, the findings described in this chapter have significantly contributed to the understanding of the interactions between CQ, metals and Aβ in neurons, as part of an ongoing investigation into the pathogenesis of AD. Foremost, these data strengthen "the metal hypothesis of AD" (explained in **section 1.4.5**) and support the development of pharmacotherapeutics that target metal ions for the treatment of AD, as well as other neurodegenerative diseases (discussed in detail in **section 1.5**).

Experimental outcomes have also added a significant tier to our continuously evolving understanding of the drug's actions, which lead to its clinical benefits. Moreover, results encourage future studies, using various techniques, to provide additional evidence for a direct interaction between CQ and Aβ, since it will have profound implications on other 8-HQs (PBT2 for example) and, perhaps even, certain metal-complexes (such as Cu^{2+}-GTSM) that are being developed as diagnostic and/or therapeutic agents (as described in **sections 1.5.3-1.5.5**).

Chapter 6

Concluding Remarks and Future Directions

Chapter 6

6.1 Major conclusions

The current and projected AD prevalence, incidence and mortality rate statistics, as well as the accompanying societal economic cost, are alarming (6, 7, 874). These make finding a treatment, or better yet a preventative, for AD all the more imperative (875). While major advances have been made in the last few decades, the root cause(s) of AD have yet to be uncovered and, consequently, a cure for the disease is still not in sight. Reviewing the existing literature, it seems there are as many compounds being trialled as AD pharmacotherapeutics as there are theories for the origin of the disease (refer to **Chapter 1** and **Appendix A** of this thesis).

Based on a growing school of thought that considers aberrant metal metabolism to be an important contributor to the pathogenesis of neurodegenerative diseases, in general, and AD in particular (see **sections 1.4.1** and **1.4.5**), research groups worldwide are attempting to resolve this issue. Efforts are focused on therapeutics with potential to modulate cerebral location, distribution, levels and oxidative state of metal ions in a targeted fashion. One such investigational drug, which is the subject of this dissertation, is CQ (properties listed in **Table 1.5**).

Our comprehension and perspective of CQ's MOA is continuously evolving. For several decades, CQ was prescribed as a medication for conditions varying from skin disorders to intestinal infections. It was believed that CQ acts as a conventional metal chelator. Years later, it was alleged that this MOA was responsible for SMON and saw to the withdrawal of oral CQ from pharmacopeia. However, nowadays, it is thought that SMON was not directly caused by CQ (detailed in **section 1.5.5**).

Renewed interest in CQ as a potential therapeutic for AD and various other diseases, while re-igniting the scientific debate with regards to the drug's safety (876-878), has also produced data showing CQ to be an MPAC that binds extracellular metals, thereby preventing them from interacting with Aβ and forming toxic oligomers (699). Further testing rendered CQ and its homologue, PBT2, as metal chaperones/ionophores, which restore cerebral metal homeostasis and, subsequently, activate diverse neuroprotective signalling pathways that are responsible for preserving neuronal structure and function, as well as maintaining cognitive ability (436, 700, 713, 752).

According to evidence presented in this thesis, and by other researchers (436, 699, 700, 702-704, 713, 753), it is becoming clear that CQ, PBT2 and their 8-HQ homologues cannot be simply classified as having a distinct MOA; but rather that their neuro-protective, neuro-rescue and neuro-generative benefits are considered multi-functional.

8-HQs can bind directly to Aβ and stabilise its low-molecular weight, non-neurotoxic oligomeric forms; thus, operating as Aβ aggregation inhibitors. 8-HQs may also act as Aβ degradation enhancers that, directly and indirectly, promote the dissociation of high-molecular weight Aβ assemblies and/or fibrils.

Owing to their metal chaperone or ionophoric activity, 8-HQs can facilitate the transport of extracellular cations into neurons. Being MPACs, 8-HQs could form ternary complexes with Aβ and metal ions, which inhibit ROS generated by the interaction of the latter two.

Simultaneously binding metals and certain neurotransmitters, 8-HQs may also modulate various signalling pathways in the CNS involved with memory, learning and other cognitive functions.

The combination of *in vitro* biophysical techniques and cellular experiments, together with *in vivo* trials in AD animal models and patients, point to the diverse MOA of 8-HQs as pharmacotherapeutics for AD (and possibly other neurodegenerative diseases), which are not mutually exclusive. It seems CQ, PBT2 and other 8-HQs are capable of influencing Aβ, metals and neurotransmitters - individually or combined. Interestingly, an independent screen of over 100,000 compounds has identified 8-HQs (including CQ) as the most effective in rescuing Aβ toxicity in yeast models of AD (703).

Overall, this body of work adds a significant tier to existing knowledge with regards to the MOA of CQ in the treatment of AD. These data indicate that targeting metal homeostasis in the brain is a promising therapeutic strategy, and support the research and development of novel 8-HQs as therapeutics for AD and other neurodegenerative diseases. The scope of these findings also merits further exploration of 8-HQs and their metal complexes as potential diagnostics and/or therapeutics for diseases in which metals may be central to their pathogenesis (for example cancer, diabetes, skin disorders and maybe even cardiovascular diseases, malaria and/or tuberculosis (TB)).

6.2 Future Directions

Compelling evidence has been presented herein as to the effect of CQ, metals and Aβ on each other's uptake. While efforts were made to eliminate any attachment of these components to the cell surface (i.e., cell cultures were washed with cold pronase, sodium carbonate and/or PBS post treatment), this possibility could not be excluded. Internalization into neurons could be confirmed by cell fractionation studies, but these are expected to entail large volumes of primary neurons and require the ICPMS and ELISA to be sensitive enough to detect the amounts of CQ, metal ions and Aβ, respectively, in the various cellular components.

Alternatively, uptake and bioavailability of Zn could be detected, using cell-permeable fluorophores, such as 6-methoxy-(8-*p*-toluenesulfonamido)quinoline (TSQ), zinquin or FluoZin-3. Internalization of Aβ could be verified by treating primary neuronal cultures with 5-carboxyfluoroscein labelled Aβ (CF-Aβ) (862, 879) followed by cross-sectional visualization, using confocal microscopy.

Due to time constraints, the mechanism for neuronal CQ, metals and Aβ uptake (i.e., passive or active) was not fully characterized. This could be easily achieved by repeating the neuronal uptake experiments at varying temperatures (0 ^{o}c *versus* 37 ^{o}c), saturation state (saturable as oppose to non-saturable concentrations), under energy depletion conditions and/or using inhibitors (such as methyl-β-cyclodextrin (MβCD) and nocodazole against endocytosis).

If the neuronal uptake of CQ, metal ions and Aβ was found to be an active one, it will most likely involve a cell-surface receptor. Preliminary experiments were conducted in which homogenates of cells treated with CQ, metals and metallo-CQ complexes were ran on narrow immobilized pH gradient (IPG) strips, which were later subjected to laser ablation (LA)-ICPMS to separate the protein(s) that co-localize with metals and/or CQ. These experimental procedures need to be repeated and the techniques optimized.

Immobilised metal-ion affinity chromatographic (IMAC) columns of 8-HQ and CQ were also prepared, but were not used due to time shortage. In future, it is intended that neuronal cell lysates and/or brain homogenates will be applied onto these columns in order to characterize the binding and/or selectivity of metals and/or proteins toward CQ. Relevant fractions will be collected and could undergo two-dimensional gel electrophoresis (2DE) to identify a potential receptor for CQ.

As immortal cell lines originating from neuronal tumours are unsuitable for the evaluation of metallo-CQ complexes as pharmacotherapeutics for AD, and since primary neuronal cultures are resource and time-consuming, in future the use of stem cells may be recommended (880, 881).

Bibliography

1. Berchtold NC, Cotman CW. Evolution in the Conceptualization of Dementia and Alzheimer's Disease: Greco-Roman Period to the 1960s. Neurobiology of Aging. 1998;19(3):173-89.

2. Boller F, Forbes MM. History of dementia and dementia in history: An overview. Journal of the Neurological Sciences. 1998;158(2):125-33.

3. Alzheimer A. Über eine eigenartige erkrankung der hirnrinde. Allgemeine Zeitschrift für Psychiatrie und Psychisch-gerichtliche Medizin. 1907;109(64):146-8.

4. Alzheimer A. Über eigenartige Krankheitsfälle des späteren Alters. Zbl ges Neurol Psych. 1911;4:356-85.

5. Australian Bureau of Statistics. Causes of Death, Australia, 2009 2011.

6. Alzheimer's Association. 2017 Alzheimer's disease facts and figures. Alzheimer's and Dementia. 2017.

7. Alzheimer's Disease International. World Alzheimer Report 2015: The Global Impact of Dementia. London; 2015.

8. Access Economics. Caring places: planning for aged care and dementia 2010-2050. 2010.

9. Alzheimer's Association. 2013 Alzheimer's disease facts and figures. Alzheimer's & Dementia. 2013;9(2):208-45.

10. Hebert LE, Weuve J, Scherr PA, Evans DA. Alzheimer disease in the United States (2010–2050) estimated using the 2010 census. Neurology. 2013.

11. Australian Institute of Health and Welfare. Dementia in Australia. Canberra; 2012.

12. Bateman R, Aisen P, De Strooper B, Fox N, Lemere C, Ringman J, et al. Autosomal-dominant Alzheimer's disease: a review and proposal for the prevention of Alzheimer's disease. Alzheimer's Research & Therapy. 2011;3(1).

13. Tomiyama T, Nagata T, Shimada H, Teraoka R, Fukushima A, Kanemitsu H, et al. A new amyloid β variant favoring oligomerization in Alzheimer's-type dementia. Annals of Neurology. 2008;63(3):377-87.

14. Cruts M, Theuns J, Van Broeckhoven C. Locus-specific mutation databases for neurodegenerative brain diseases. Human Mutation. 2012;33(9):1340-4.

15. Alzheimer Disease & Frontotemporal Dementia Mutation Database [Internet]. [cited May 20th 2011]. Available from: http://www.molgen.ua.ac.be/ADMutations.

16. AlzGene [Internet]. Available from: http://www.alzgene.org/.

17. Lemere CA, Blusztajn JK, Yamaguchi H, Wisniewski T, Saido TC, Selkoe DJ. Sequence of deposition of heterogeneous amyloid β-peptides and APO E in Down syndrome: implications for initial events in amyloid plaque formation. Neurobiology of Disease. 1996;3(1):16-32.

18. Vetrivel KS, Thinakaran G. Amyloidogenic processing of β-amyloid precursor protein in intracellular compartments. Neurology. 2006;66(2, Supplement 1):S69-73.

19. Sherrington R, Froelich S, Sorbi S, Campion D, Chi H, Rogaeva EA, et al. Alzheimer's disease associated with mutations in presenilin 2 is rare and variably penetrant. Human Molecular Genetics. 1996;5(7):985-8.

20. Sloane PD, Zimmerman S, Suchindran C, Reed P, Wang L, Boustani M, et al. The public health impact of Alzheimer's disease, 2000-2050: potential implication of treatment advances. Annual Review of Public Health. 2002;23:213-31.

21. Brookmeyer R, Johnson E, Ziegler-Graham K, Arrighi HM. Forecasting the global burden of Alzheimer's disease. Alzheimer's & Dementia. 2007;3(3):186-91.

22. Alzheimer's Association. Changing the Trajectory of Alzheimer's Disease: A National Imperative. 2010.

23. Vickland V, Morris T, Draper B, Low L-F, Brodaty H. Modelling the impact of interventions to delay the onset of dementia in Australia. A report for Alzheimer's Australia.; 2012.

24. The AlzRisk Database. Alzheimer Research Forum [Internet]. [cited Febuary 11th 2013]. Available from: http://www.alzforum.org.

25. Zannis VI, Just PW, Breslow JL. Human apolipoprotein E isoprotein subclasses are genetically determined. American Journal of Human Genetics. 1981;33(1):11-24.

26. Rall SC, Weisgraber KH, Mahley RW. Human apolipoprotein E. The complete amino acid sequence. Journal of Biological Chemistry. 1982;257(8):4171-8.

27. Mahley RW. Apolipoprotein E: cholesterol transport protein with expanding role in cell biology. Science. 1988;240(4852):622-30.

28. Mahley RW, Rall SC, Jr. Apolipoprotein E: far more than a lipid transport protein. Annual Review of Genomics and Human Genetics. 2000;1:507-37.

29. Dumanis SB, Tesoriero JA, Babus LW, Nguyen MT, Trotter JH, Ladu MJ, et al. ApoE4 Decreases Spine Density and Dendritic Complexity in Cortical Neurons *In Vivo*. Journal of Neuroscience. 2009;29(48):15317-22.

30. Verghese PB, Castellano JM, Holtzman DM. Apolipoprotein E in Alzheimer's disease and other neurological disorders. Lancet Neurology. 2011;10(3):241-52.

31. Corder EH, Saunders AM, Risch NJ, Strittmatter WJ, Schmechel DE, Gaskell PC, Jr., et al. Protective effect of apolipoprotein E type 2 allele for late onset Alzheimer disease. Nature Genetics. 1994;7(2):180-4.

32. West HL, William Rebeck G, Hyman BT. Frequency of the apolipoprotein E ε2 allele is diminished in sporadic Alzheimer disease. Neuroscience Letters. 1994;175(1-2):46-8.

33. Corder EH, Saunders AM, Strittmatter WJ, Schmechel DE, Gaskell PC, Small GW, et al. Gene dose of apolipoprotein E type 4 allele and the risk of Alzheimer's disease in late onset families. Science. 1993;261(5123):921-3.

34. Poirier J, Bertrand P, Kogan S, Gauthier S, Davignon J, Bouthillier D. Apolipoprotein E polymorphism and Alzheimer's disease. Lancet. 1993;342(8873):697-9.

35. Schmechel DE, Saunders AM, Strittmatter WJ, Crain BJ, Hulette CM, Joo SH, et al. Increased amyloid β-peptide deposition in cerebral cortex as a consequence of apolipoprotein E genotype in late-onset Alzheimer disease. Proceedings of the National Academy of Sciences of the United States of America. 1993;90(20):9649-53.

36. Strittmatter WJ, Saunders AM, Schmechel D, Pericak-Vance M, Enghild J, Salvesen GS, et al. Apolipoprotein E: high-avidity binding to β-amyloid and increased frequency of type 4 allele in late-onset familial Alzheimer disease. Proceedings of the National Academy of Sciences of the United States of America. 1993;90(5):1977-81.

37. Strittmatter WJ, Weisgraber KH, Huang DY, Dong LM, Salvesen GS, Pericak-Vance M, et al. Binding of human apolipoprotein E to synthetic amyloid β peptide: isoform-specific effects and implications for late-onset Alzheimer disease. Proceedings of the National Academy of Sciences of the United States of America. 1993;90(17):8098-102.

38. Strittmatter WJ, Saunders AM, Goedert M, Weisgraber KH, Dong LM, Jakes R, et al. Isoform-specific interactions of apolipoprotein E with microtubule-associated protein tau: implications for Alzheimer disease. Proceedings of the National Academy of Sciences of the United States of America. 1994;91(23):11183-6.

39. Verghese PB, Castellano JM, Garai K, Wang Y, Jiang H, Shah A, et al. ApoE influences amyloid-β (Aβ) clearance despite minimal apoE/Aβ association in physiological conditions. Proceedings of the National Academy of Sciences. 2013;110(19):E1807-E16.

40. Brautigam H, Klingstedt T, Prokop S, Holtzman DM, Heppner FL, Haroutunian V, et al. New Conformation-Sensing Imaging Compounds Distinguish Protein Deposits In ApoE ε3/ε3 Alzheimer's Patients From that in ApoE ε4/ε4 Alzheimer's Patients. Alzheimer's & Dementia. 2010;6(4, Supplement):e19-20.

41. Castellano JM, Kim J, Stewart FR, Jiang H, DeMattos RB, Patterson BW, et al. Human apoE Isoforms Differentially Regulate Brain Amyloid-β Peptide Clearance. Science Translational Medicine. 2011;3(89):89ra57.

42. Meng Y, Lee JH, Cheng R, St George-Hyslop P, Mayeux R, Farrer LA. Association between SORL1 and Alzheimer’s disease in a genome-wide study. NeuroReport. 2007;18(17):1761-4.

43. Rogaeva E, Meng Y, Lee JH, Gu Y, Kawarai T, Zou F, et al. The neuronal sortilin-related receptor SORL1 is genetically associated with Alzheimer disease. Nature Genetics. 2007;39(2):168-77.

44. Harold D, Abraham R, Hollingworth P, Sims R, Gerrish A, Hamshere ML, et al. Genome-wide association study identifies variants at CLU and PICALM associated with Alzheimer's disease. Nature Genetics. 2009;41(10):1088-93.

45. Lambert JC, Heath S, Even G, Campion D, Sleegers K, Hiltunen M, et al. Genome-wide association study identifies variants at CLU and CR1 associated with Alzheimer's disease. Nature Genetics. 2009;41(10):1094-9.

46. Jun G, Naj AC, Beecham GW, Wang L-S, Buros J, Gallins PJ, et al. Meta-analysis Confirms CR1, CLU, and PICALM as Alzheimer Disease Risk Loci and Reveals Interactions With APOE Genotypes. Archives of Neurology. 2010;67(12):1473-84.

47. Hollingworth P, Harold D, Sims R, Gerrish A, Lambert J-C, Carrasquillo MM, et al. Common variants at ABCA7, MS4A6A/MS4A4E, EPHA1, CD33 and CD2AP are associated with Alzheimer's disease. Nature Genetics. 2011;43(5):429-35.

48. Naj AC, Jun G, Beecham GW, Wang L-S, Vardarajan BN, Buros J, et al. Common variants at MS4A4/MS4A6E, CD2AP, CD33 and EPHA1 are associated with late-onset Alzheimer's disease. Nature Genetics. 2011;43(5):436-41.

49. Cruchaga C, Kauwe John SK, Harari O, Jin Sheng C, Cai Y, Karch Celeste M, et al. GWAS of Cerebrospinal Fluid Tau Levels Identifies Risk Variants for Alzheimer's Disease. Neuron. 2013;78(2):256–68.

50. Reitz C, Jun G, Naj A, Rajbhandary R, Vardarajan BN, Wang L-S, et al. Variants in the ATP-binding cassette transporter (*ABCA7*), apolipoprotein e ε4,and the risk of late-onset alzheimer disease in African Americans. Journal of the American Medical Association. 2013;309(14):1483-92.

51. Zhang B, Gaiteri C, Bodea L-G, Wang Z, McElwee J, Podtelezhnikov Alexei A, et al. Integrated Systems Approach Identifies Genetic Nodes and Networks in Late-Onset Alzheimer's Disease. Cell. 2013;153(3):707-20.

52. Sherva R, Tripodis Y, Bennett DA, Chibnik LB, Crane PK, de Jager PL, et al. Genome-wide association study of the rate of cognitive decline in Alzheimer's disease. Alzheimer's & Dementia.

53. Lambert JC, Ibrahim-Verbaas CA, Harold D, Naj AC, Sims R, Bellenguez C, et al. Meta-analysis of 74,046 individuals identifies 11 new susceptibility loci for Alzheimer's disease. Nature Genetics. 2013;45(12):1452-8.

54. Jonsson T, Atwal JK, Steinberg S, Snaedal J, Jonsson PV, Bjornsson S, et al. A mutation in *APP* protects against Alzheimer's disease and age-related cognitive decline. Nature. 2012;488(7409):96-9.

55. Guerreiro R, Wojtas A, Bras J, Carrasquillo M, Rogaeva E, Majounie E, et al. TREM2 Variants in Alzheimer's Disease. New England Journal of Medicine. 2013;368(2):117-27.

56. Jonsson T, Stefansson H, Steinberg S, Jonsdottir I, Jonsson PV, Snaedal J, et al. Variant of TREM2 Associated with the Risk of Alzheimer's Disease. New England Journal of Medicine. 2013;368(2):107-16.

57. Chandra V, Bharucha NE, Schoenberg BS. Conditions associated with Alzheimer's disease at death: case-control study. Neurology. 1986;36(2):209-11.

58. Alzheimer’s Association. Changing the Trajectory of Alzheimer’s Disease: A National Imperative. 2010.

59. Zanetti O, Solerte SB, Cantoni F. Life expectancy in Alzheimer's disease (AD). Archives of Gerontology and Geriatrics. 2009;49(Supplement 1):237-43.

60. Lippa CF, Nee LE, Mori H, St George-Hyslop P. $A\beta_{-42}$ deposition precedes other changes in PS-1 Alzheimer's disease. Lancet. 1998;352(9134):1117-8.

61. Klunk WE, Price JC, Mathis CA, Tsopelas ND, Lopresti BJ, Ziolko SK, et al. Amyloid Deposition Begins in the Striatum of Presenilin-1 Mutation Carriers from Two Unrelated Pedigrees. Journal of Neuroscience. 2007;27(23):6174–84.

62. Pike KE, Savage G, Villemagne VL, Ng S, Moss SA, Maruff P, et al. β-amyloid imaging and memory in non-demented individuals: evidence for preclinical Alzheimer's disease. Brain. 2007;130(11):2837-44.

63. Jack CR, Lowe VJ, Weigand SD, Wiste HJ, Senjem ML, Knopman DS, et al. Serial PIB and MRI in normal, mild cognitive impairment and Alzheimer's disease: implications for sequence of pathological events in Alzheimer's disease. Brain. 2009;132(5):1355-65.

64. Sperling RA, LaViolette PS, O'Keefe K, O'Brien J, Rentz DM, Pihlajamaki M, et al. Amyloid Deposition Is Associated with Impaired Default Network Function in Older Persons without Dementia. Neuron. 2009;63(2):178-88.

65. Villemagne VL, Ataka S, Mizuno T, Brooks WS, Wada Y, Kondo M, et al. High Striatal Amyloid β-Peptide Deposition Across Different Autosomal Alzheimer Disease Mutation Types. Archives of Neurology. 2009;66(12):1537-44.

66. Rowe CC, Ellis KA, Rimajova M, Bourgeat P, Pike KE, Jones G, et al. Amyloid imaging results from the Australian Imaging, Biomarkers and Lifestyle (AIBL) study of aging. Neurobiology of Aging. 2010;31(8):1275-83.

67. Klunk W. FDG-PET and amyloid imaging in the dominantly inherited Alzheimer network. Alzheimer's & Dementia. 2011;7(4, Supplement):S680.

68. Bateman RJ, Xiong C, Benzinger TL, Fagan AM, Goate A, Fox NC, et al. Clinical and Biomarker Changes in Dominantly Inherited Alzheimer's Disease. New England Journal of Medicine. 2012;367(9):795-804.

69. Fleisher AS, Chen K, Quiroz YT, Jakimovich LJ, Gomez MG, Langois CM, et al. Florbetapir PET analysis of amyloid-β deposition in the presenilin 1 E280A autosomal dominant Alzheimer's disease kindred: a cross-sectional study. Lancet Neurology. 2012;11(12):1057-65.

70. Reiman EM, Quiroz YT, Fleisher AS, Chen K, Velez-Pardo C, Jimenez-Del-Rio M, et al. Brain imaging and fluid biomarker analysis in young adults at genetic risk for autosomal dominant Alzheimer's disease in the presenilin 1 E280A kindred: a case-control study. Lancet Neurology. 2012;11(12):1048-56.

71. Alzheimer's Disease International. World Alzheimer Report 2011: The benefits of early diagnosis and intervention. London; 2011.

72. Folstein MF, Folstein SE, McHugh PR. "Mini-mental state": A practical method for grading the cognitive state of patients for the clinician. Journal of Psychiatric Research. 1975;12(3):189-98.

73. Rosen WG, Mohs RC, Davis KL. A new rating scale for Alzheimer's disease. American Journal of Psychiatry. 1984;141(11):1356-64.

74. McKhann G, Drachman D, Folstein M, Katzman R, Price D, Stadlan EM. Clinical diagnosis of Alzheimer's disease: report of the NINCDS-ADRDA Work Group under the auspices of Department of Health and Human Services Task Force on Alzheimer's Disease. Neurology. 1984;34(7):939-44.

75. American Psychiatric Association. Diagnostic and Statistical Manual of Mental Disorders. 4th ed. Washington, DC: American Psychiatric Association; 2000.

76. Dubois B, Feldman HH, Jacova C, Dekosky ST, Barberger-Gateau P, Cummings J, et al. Research criteria for the diagnosis of Alzheimer's disease: revising the NINCDS-ADRDA criteria. Lancet Neurology. 2007;6(8):734-46.

77. Dubois B, Feldman HH, Jacova C, Cummings JL, DeKosky ST, Barberger-Gateau P, et al. Revising the definition of Alzheimer's disease: a new lexicon. Lancet Neurology. 2010;9(11):1118-27.

78. Sperling RA, Aisen PS, Beckett LA, Bennett DA, Craft S, Fagan AM, et al. Toward defining the preclinical stages of Alzheimer's disease: Recommendations from the National Institute on Aging and the Alzheimer's Association workgroup. Alzheimer's & Dementia. 2011;7(3):280-92.

79. Albert MS, DeKosky ST, Dickson D, Dubois B, Feldman HH, Fox NC, et al. The diagnosis of mild cognitive impairment due to Alzheimer's disease: Recommendations from the National Institute on Aging and Alzheimer's Association workgroup. Alzheimer's & Dementia. 2011;7(3):270-9.

80. McKhann GM, Knopman DS, Chertkow H, Hyman BT, Jack CR, Kawas CH, et al. The diagnosis of dementia due to Alzheimer's disease: Recommendations from the National Institute on Aging and the Alzheimer's Association workgroup. Alzheimer's & Dementia. 2011;7(3):263-9.

81. American Psychiatric Association. Diagnostic and Statistical Manual of Mental Disorders. 5th ed. Washington, DC: American Psychiatric Association; 2013.

82. Montine TJ, Phelps CH, Beach TG, Bigio EH, Cairns NJ, Dickson DW, et al. National Institute on Aging–Alzheimer's Association guidelines for the neuropathologic assessment of Alzheimer's disease: a practical approach. Acta Neuropathologica. 2012;123(1):1-11.

83. Blennow K, Hampel H, Weiner M, Zetterberg H. Cerebrospinal fluid and plasma biomarkers in Alzheimer disease. Nature Reviews Neurology. 2010;6(3):131-44.

84. Villemagne V, Fodero-Tavoletti M, Pike K, Cappai R, Masters C, Rowe C. The ART of Loss: Aβ Imaging in the Evaluation of Alzheimer's Disease and other Dementias. Molecular Neurobiology. 2008;38(1):1-15.

85. Okamura N, Yanai K. Florbetapir (18F), a PET imaging agent that binds to amyloid plaques for the potential detection of Alzheimer's disease. IDrugs. 2010;13(12):890-9.

86. Vandenberghe R, Van Laere K, Ivanoiu A, Salmon E, Bastin C, Triau E, et al. ^{18}F-flutemetamol amyloid imaging in Alzheimer disease and mild cognitive impairment: A phase 2 trial. Annals of Neurology. 2010;68(3):319-29.

87. Johnson KA, Minoshima S, Bohnen NI, Donohoe KJ, Foster NL, Herscovitch P, et al. Appropriate use criteria for amyloid PET: A report of the Amyloid Imaging Task Force, the Society of Nuclear Medicine and Molecular Imaging, and the Alzheimer's Association. Alzheimer's & Dementia. 2013;9(1):E1-E16.

88. Johnson KA, Minoshima S, Bohnen NI, Donohoe KJ, Foster NL, Herscovitch P, et al. Update on Appropriate Use Criteria for Amyloid PET Imaging: Dementia Experts, Mild Cognitive Impairment, and Education. Journal of Nuclear Medicine. 2013;54(7):1011-3.

89. aibl Australian Biomarker, Imaging & Lifestyle [Available from: http://www.aibl.csiro.au/.

90. ADNI Alzheimer's Disease Neuroimaging Initiative [Available from: http://adni.loni.ucla.edu/.

91. Koncept Analytics. Global Alzheimer Drugs Market: An Analysis. U.P., India; 2009.

92. BBC Research. Alzheimer's Disease Therapeutics and Diagnostics: Global Markets. 2010. Contract No.: PHM062A.

93. BBC Research. Alzheimer's Disease Therapeutics and Diagnostics: Global Markets. 2013. Contract No.: PHM062B.

94. Lleo A, Greenberg SM, Growdon JH. Current Pharmacotherapy for Alzheimer's Disease. Annual Review of Medicine. 2006;57(1):513-33.

95. Alzheimer's Disease Education and Referral (ADEAR) Center. Alzheimer's Disease Medications Fact Sheet. 2012.

96. Hynd MR, Scott HL, Dodd PR. Glutamate-mediated excitotoxicity and neurodegeneration in Alzheimer's disease. Neurochemistry International. 2004;45(5):583-95.

97. Sonkusare SK, Kaul CL, Ramarao P. Dementia of Alzheimer's disease and other neurodegenerative disorders--memantine, a new hope. Pharmacological Research. 2005;51(1):1-17.

98. Parsons CG, Stoffler A, Danysz W. Memantine: a NMDA receptor antagonist that improves memory by restoration of homeostasis in the glutamatergic system - too

little activation is bad, too much is even worse. Neuropharmacology. 2007;53(6):699-723.

99. Li L, Sengupta A, Haque N, Grundke-Iqbal I, Iqbal K. Memantine inhibits and reverses the Alzheimer type abnormal hyperphosphorylation of tau and associated neurodegeneration. FEBS Letters. 2004;566(1-3):261-9.

100. Tariot PN, Farlow MR, Grossberg GT, Graham SM, McDonald S, Gergel I. Memantine Treatment in Patients With Moderate to Severe Alzheimer Disease Already Receiving Donepezil: A Randomized Controlled Trial. JAMA. 2004;291(3):317-24.

101. Raina P, Santaguida P, Ismaila A, Patterson C, Cowan D, Levine M, et al. Effectiveness of Cholinesterase Inhibitors and Memantine for Treating Dementia: Evidence Review for a Clinical Practice Guideline. Annals of Internal Medicine. 2008;148(5):379-W85.

102. Alzheimer Research Forum [Available from: http://www.alzforum.org/drg/drc/default.asp.

103. ClinicalTrials.gov [Internet]. [cited November 1st 2011]. Available from: http://clinicaltrials.gov/ct2/home.

104. Sparks DL, Sabbagh MN, Connor DJ, Lopez J, Launer LJ, Browne P, et al. Atorvastatin for the Treatment of Mild to Moderate Alzheimer Disease: Preliminary Results. Archives of Neurology. 2005;62(5):753-7.

105. Sparks DL, Sabbagh MN, Connor DJ, Lopez J, Launer LJ, Petanceska S, et al. Atorvastatin Therapy Lowers Circulating Cholesterol but not Free Radical Activity in Advance of Identifiable Clinical Benefit in the Treatment of Mild-to-Moderate AD. Current Alzheimer Research. 2005;2(3):343-53.

106. Sparks DL, Petanceska S, Sabbagh M, Connor D, Soares H, Adler C, et al. Cholesterol, Copper and Aβ in Controls, MCI, AD and the AD Cholesterol-Lowering Treatment Trial (ADCLT). Current Alzheimer Research. 2005;2(5):527-39.

107. Sparks DL, Connor DJ, Sabbagh MN, Petersen RB, Lopez J, Browne P. Circulating cholesterol levels, apolipoprotein E genotype and dementia severity influence the benefit of atorvastatin treatment in Alzheimer's disease: results of the Alzheimer's Disease Cholesterol-Lowering Treatment (ADCLT) trial. Acta Neurologica Scandinavica Supplementum. 2006;114:3-7.

108. Aisen PS. The potential of anti-inflammatory drugs for the treatment of Alzheimer's disease. Lancet Neurology. 2002;1(5):279-84.

109. Szekelya CA, Thornea JE, Zandia PP, Eka M, Messiasa E, Breitnerc JCS, et al. Nonsteroidal Anti-Inflammatory Drugs for the Prevention of Alzheimer's Disease: A Systematic Review. Neuroepidemiology. 2004;23(4):159-69.

110. Reger MA. Intranasal insulin improves cognition and modulates β-amyloid in early AD. Neurology. 2008;70(6):440-8.

111. Craft S, Baker LD, Montine TJ, Minoshima S, Watson GS, Claxton A, et al. Intranasal Insulin Therapy for Alzheimer Disease and Amnestic Mild Cognitive Impairment: A Pilot Clinical Trial. Archives of Neurology. 2012;69(1):29-38.

112. Landreth G. Therapeutic use of agonists of the nuclear receptor PPARγ in Alzheimer's disease. Current Alzheimer Research. 2007;4(2):159-64.

113. Miller BW, Willett KC, Desilets AR. Rosiglitazone and pioglitazone for the treatment of Alzheimer's disease. Annals of Pharmacotherapy. 2011;45(11):1416-24.

114. Oliveira AAJ, Hodges HM. Alzheimer's Disease and Neural Transplantation as Prospective Cell Therapy. Current Alzheimer Research. 2005;2(1):79-95.

115. Tuszynski MH, Thal L, Pay M, Salmon DP, U HS, Bakay R, et al. A phase 1 clinical trial of nerve growth factor gene therapy for Alzheimer disease. Nature Medicine. 2005;11(5):551-5.

116. Sugaya K, Alvarez A, Marutle A, Kwak Y, Choumkina E. Stem cell strategies for Alzheimer's disease therapy. Panminerva Medica. 2006;48(2):87-96.

117. Bishop KM, Hofer EK, Mehta A, Ramirez A, Sun L, Tuszynski M, et al. Therapeutic potential of CERE-110 (AAV2-NGF): Targeted, stable, and sustained NGF delivery and trophic activity on rodent basal forebrain cholinergic neurons. Experimental Neurology. 2008;211(2):574-84.

118. Hardy JA, Higgins GA. Alzheimer's disease: the amyloid cascade hypothesis. Science. 1992;256(5054):184-5.

119. Hardy J, Selkoe DJ. The amyloid hypothesis of Alzheimer's disease: progress and problems on the road to therapeutics. Science. 2002;297(5580):353-6.

120. Hardy J. The amyloid hypothesis for Alzheimer's disease: a critical reappraisal. Journal of Neurochemistry. 2009;110(4):1129-34.

121. Tanzi RE, Bertram L. Twenty years of the Alzheimer's disease amyloid hypothesis: a genetic perspective. Cell. 2005;120(4):545-55.

122. Biran Y, Masters CL, Barnham KJ, Bush AI, Adlard PA. Pharmacotherapeutic targets in Alzheimer's disease. Journal of Cellular and Molecular Medicine. 2009;13(1):61-86.

123. Goedert M, Spillantini MG, Jakes R, Rutherford D, Crowther RA. Multiple isoforms of human microtubule-associated protein tau: sequences and localization in neurofibrillary tangles of Alzheimer's disease. Neuron. 1989;3(4):519-26.

124. Goedert M, Spillantini MG, Potier MC, Ulrich J, Crowther RA. Cloning and sequencing of the cDNA encoding an isoform of microtubule-associated protein tau containing four tandem repeats: differential expression of tau protein mRNAs in human brain. EMBO Journal. 1989;8(2):393-9.

125. Weingarten MD, Lockwood AH, Hwo SY, Kirschner MW. A protein factor essential for microtubule assembly. Proceedings of the National Academy of Sciences of the United States of America. 1975;72(5):1858-62.

126. Hirokawa N, Shiomura Y, Okabe S. Tau proteins: the molecular structure and mode of binding on microtubules. Journal of Cell Biology. 1988;107(4):1449-59.

127. Pooler AM, Phillips EC, Lau DH, Noble W, Hanger DP. Physiological release of endogenous tau is stimulated by neuronal activity. EMBO Reports. 2013;14(4):389-94.

128. Kuret J, Chirita CN, Congdon EE, Kannanayakal T, Li G, Necula M, et al. Pathways of tau fibrillization. Biochimica et Biophysica Acta (BBA) - Molecular Basis of Disease. 2005;1739(2-3):167-78.

129. Braak H, Braak E. Neuropathological stageing of Alzheimer-related changes. Acta Neuropathologica. 1991;82(4):239-59.

130. de Calignon A, Polydoro M, Suárez-Calvet M, William C, Adamowicz David H, Kopeikina Kathy J, et al. Propagation of Tau Pathology in a Model of Early Alzheimer's Disease. Neuron. 2012;73(4):685-97.

131. Liu L, Drouet V, Wu JW, Witter MP, Small SA, Clelland C, et al. Trans-Synaptic Spread of Tau Pathology *In Vivo*. PLoS ONE. 2012;7(2):e31302.

132. Alonso ADC, Zaidi T, Grundke-Iqbal I, Iqbal K. Role of Abnormally Phosphorylated Tau in the Breakdown of Microtubules in Alzheimer Disease. Proceedings of the National Academy of Sciences of the United States of America. 1994;91(12):5562-6.

133. Tolnay M, Probst A. REVIEW: tau protein pathology in Alzheimer's disease and related disorders. Neuropathology and Applied Neurobiology. 1999;25(3):171-87.

134. Lee VMY, Goedert M, Trojanowski JQ. Neurodegenerative Tauopathies. Annual Review of Neuroscience. 2001;24(1):1121-59.

135. Mandelkow E-M, Mandelkow E. Tau in Alzheimer's disease. Trends in Cell Biology. 1998;8(11):425-7.

136. Brandt R, Lee G. The balance between tau protein's microtubule growth and nucleation activities: implications for the formation of axonal microtubules. Journal of Neurochemistry. 1993;61(3):997-1005.

137. Trojanowski JQ, Schmidt ML, Shin RW, Bramblett GT, Rao D, Lee VM. Altered tau and neurofilament proteins in neuro-degenerative diseases: diagnostic implications for Alzheimer's disease and Lewy body dementias. Brain Pathology. 1993;3(1):45-54.

138. Maeda S, Sahara N, Saito Y, Murayama M, Yoshiike Y, Kim H, et al. Granular Tau Oligomers as Intermediates of Tau Filaments. Biochemistry. 2007;46(12):3856-61.

139. Yoshiyama Y, Higuchi M, Zhang B, Huang S-M, Iwata N, Saido Takaomi C, et al. Synapse Loss and Microglial Activation Precede Tangles in a P301S Tauopathy Mouse Model. Neuron. 2007;53(3):337-51.

140. Wittmann CW, Wszolek MF, Shulman JM, Salvaterra PM, Lewis J, Hutton M, et al. Tauopathy in Drosophila: Neurodegeneration Without Neurofibrillary Tangles. Science. 2001;293(5530):711-4.

141. SantaCruz K, Lewis J, Spires T, Paulson J, Kotilinek L, Ingelsson M, et al. Tau Suppression in a Neurodegenerative Mouse Model Improves Memory Function. Science. 2005;309(5733):476-81.

142. Kayed R, Jackson GR. Prefilament tau species as potential targets for immunotherapy for Alzheimer disease and related disorders. Current Opinion in Immunology. 2009;21(3):359-63.

143. Tharp W, Sarkar I. Origins of amyloid-beta. BMC Genomics. 2013;14(1):290.

144. Goldgaber D, Lerman MI, McBride WO, Saffiotti U, Gajdusek DC. Isolation, characterization, and chromosomal localization of human brain cDNA clones coding for the precursor of the amyloid of brain in Alzheimer's disease, Down's syndrome and aging. Journal of Neural Transmission Supplementum. 1987;24:23-8.

145. Robakis NK, Ramakrishna N, Wolfe G, Wisniewski HM. Molecular cloning and characterization of a cDNA encoding the cerebrovascular and the neuritic plaque amyloid peptides. Proceedings of the National Academy of Sciences of the United States of America. 1987;84(12):4190-4.

146. Tanzi RE, Gusella JF, Watkins PC, Bruns GA, St George-Hyslop P, Van Keuren ML, et al. Amyloid β protein gene: cDNA, mRNA distribution, and genetic linkage near the Alzheimer locus. Science. 1987;235(4791):880-4.

147. Sprecher CA, Grant FJ, Grimm G, O'Hara PJ, Norris F, Norris K, et al. Molecular cloning of the cDNA for a human amyloid precursor protein homolog: evidence for a multigene family. Biochemistry. 1993;32(17):4481-6.

148. Wasco W, Gurubhagavatula S, Paradis MD, Romano DM, Sisodia SS, Hyman BT, et al. Isolation and characterization of APLP2 encoding a homologue of the Alzheimer's associated amyloid β protein precursor. Nature Genetics. 1993;5(1):95-100.

149. Reinhard C, Hebert SS, De Strooper B. The amyloid-β precursor protein: integrating structure with biological function. EMBO Journal. 2005;24(23):3996-4006.

150. Panegyres PK, Atkins ER. The Functions of the Amyloid Precursor Protein Gene and Its Derivative Peptides: I Molecular Biology and Metabolic Processing. Neurocience & Medicine. 2011;2(2):120-31.

151. De Strooper B, Annaert W. Proteolytic processing and cell biological functions of the amyloid precursor protein. Journal of Cell Science. 2000;113(11):1857-70.

152. Turner PR, O'Connor K, Tate WP, Abraham WC. Roles of amyloid precursor protein and its fragments in regulating neural activity, plasticity and memory. Progress in Neurobiology. 2003;70(1):1-32.

153. Priller C, Bauer T, Mitteregger G, Krebs B, Kretzschmar HA, Herms J. Synapse Formation and Function Is Modulated by the Amyloid Precursor Protein. Journal of Neuroscience. 2006;26(27):7212-21.

154. Zheng H, Koo E. The amyloid precursor protein: beyond amyloid. Molecular Neurodegeneration. 2006;1(1):1-12.

155. Panegyres PK, Atkins ER. The Functions of the Amyloid Precursor Protein Gene and Its Derivative Peptides: II Experimental Evidence and Clinical Studies. Neuroscience & Medicine. 2011;2(3):239-67.

156. Tu Z, Keller MP, Zhang C, Rabaglia ME, Greenawalt DM, Yang X, et al. Integrative Analysis of a Cross-Loci Regulation Network Identifies *App* as a Gene Regulating Insulin Secretion from Pancreatic Islets. PLoS Genetics. 2012;8(12):e1003107.

157. Yamazaki T, Koo EH, Selkoe DJ. Trafficking of cell-surface amyloid β-protein precursor. II. Endocytosis, recycling and lysosomal targeting detected by immunolocalization. Journal of Cell Science. 1996;109(Pt 5):999-1008.

158. Forloni G, Terreni L, Bertani I, Fogliarino S, Invernizzi R, Assini A, et al. Protein misfolding in Alzheimer's and Parkinson's disease: genetics and molecular mechanisms. Neurobiology of Aging. 2002;23(5):957-76.

159. Nixon RA. Autophagy in neurodegenerative disease: friend, foe or turncoat? Trends in Neurosciences. 2006;29(9):528-35.

160. Nixon RA. Autophagy, amyloidogenesis and Alzheimer's disease. Journal of Cell Science. 2007;120(23):4081-91.

161. Nixon RA, Wegiel J, Kumar A, Yu WH, Peterhoff C, Cataldo A, et al. Extensive involvement of autophagy in Alzheimer disease: an immuno-electron microscopy study. Journal of Neuropathology & Experimental Neurology. 2005;64(2):113-22.

162. Yu WH, Cuervo AM, Kumar A, Peterhoff CM, Schmidt SD, Lee J-H, et al. Macroautophagy - a novel β-amyloid peptide-generating pathway activated in Alzheimer's disease. Journal of Cell Biology. 2005;171(1):87-98.

163. Nunan J, Small DH. Regulation of APP cleavage by α-, β- and γ-secretases. FEBS Letters. 2000;483(1):6-10.

164. Esch FS, Keim PS, Beattie EC, Blacher RW, Culwell AR, Oltersdorf T, et al. Cleavage of amyloid-β peptide during constitutive processing of its precursor. Science. 1990;248(4959):1122-4.

165. Haass C, Hung AY, Schlossmacher MG, Teplow DB, Selkoe DJ. β-Amyloid peptide and a 3-kDa fragment are derived by distinct cellular mechanisms. Journal of Biological Chemistry. 1993;268(5):3021-4.

166. Cao X, Sudhof TC. Dissection of amyloid-β precursor protein-dependent transcriptional transactivation. Journal of Biological Chemistry. 2004;279(23):24601-11.

167. Hussain I, Powell D, Howlett DR, Tew DG, Meek TD, Chapman C, et al. Identification of a novel aspartic protease (Asp 2) as β-secretase. Molecular and Cellular Neuroscience. 1999;14(6):419-27.

168. Vassar R, Bennett BD, Babu-Khan S, Kahn S, Mendiaz EA, Denis P, et al. β-secretase cleavage of Alzheimer's amyloid precursor protein by the transmembrane aspartic protease BACE. Science. 1999;286(5440):735-41.

169. Yan R, Bienkowski MJ, Shuck ME, Miao H, Tory MC, Pauley AM, et al. Membrane-anchored aspartyl protease with Alzheimer's disease β-secretase activity. Nature. 1999;402(6761):533-7.

170. Lin X, Koelsch G, Wu S, Downs D, Dashti A, Tang J. Human aspartic protease memapsin 2 cleaves the β-secretase site of β-amyloid precursor protein. Proceedings of the National Academy of Sciences of the United States of America. 2000;97(4):1456-60.

171. Seubert P, Oltersdorf T, Lee MG, Barbour R, Blomquist C, Davis DL, et al. Secretion of β-amyloid precursor protein cleaved at the amino terminus of the β-amyloid peptide. Nature. 1993;361(6409):260-3.

172. Haass C, Hung AY, Schlossmacher MG, Oltersdorf T, Teplow DB, Selkoe DJ. Normal cellular processing of the β-amyloid precursor protein results in the secretion of the amyloid-β peptide and related molecules. Annals of the New York Academy of Sciences. 1993;695:109-16.

173. Miravalle L, Calero M, Takao M, Roher AE, Ghetti B, Vidal R. Amino-Terminally Truncated Aβ Peptide Species Are the Main Component of Cotton Wool Plaques. Biochemistry. 2005;44(32):10810-21.

174. Morgan C, Colombres M, Nunez MT, Inestrosa NC. Structure and function of amyloid in Alzheimer's disease. Progress in Neurobiology. 2004;74(6):323-49.

175. Saito T, Suemoto T, Brouwers N, Sleegers K, Funamoto S, Mihira N, et al. Potent amyloidogenicity and pathogenicity of Aβ43. Nature Neuroscience. 2011;14(8):1023-32.

176. Saavedra L, Mohamed A, Ma V, Kar S, de Chaves EP. Internalization of β-Amyloid Peptide by Primary Neurons in the Absence of Apolipoprotein E. Journal of Biological Chemistry. 2007;282(49):35722-32.

177. Jiang Q, Lee CYD, Mandrekar S, Wilkinson B, Cramer P, Zelcer N, et al. ApoE Promotes the Proteolytic Degradation of Aβ. Neuron. 2008;58(5):681-93.

178. Savage MJ, Trusko SP, Howland DS, Pinsker LR, Mistretta S, Reaume AG, et al. Turnover of Amyloid β-Protein in Mouse Brain and Acute Reduction of Its Level by Phorbol Ester. Journal of Neuroscience. 1998;18(5):1743-52.

179. Bateman RJ, Munsell LY, Morris JC, Swarm R, Yarasheski KE, Holtzman DM. Human amyloid-β synthesis and clearance rates as measured in cerebrospinal fluid *in vivo*. Nature Medicine. 2006;12(7):856-61.

180. Seubert P, Vigo-Pelfrey C, Esch F, Lee M, Dovey H, Davis D, et al. Isolation and quantification of soluble Alzheimer's β-peptide from biological fluids. Nature. 1992;359(6393):325-7.

181. Kuhnke D, Jedlitschky G, Grube M, Krohn M, Jucker M, Mosyagin I, et al. MDR1-P-Glycoprotein (ABCB1) Mediates Transport of Alzheimer's Amyloid-β Peptides - Implications for the Mechanisms of Aβ Clearance at the Blood-Brain Barrier. Brain Pathology. 2007;17(4):347-53.

182. Deane R, Du Yan S, Submamaryan RK, LaRue B, Jovanovic S, Hogg E, et al. RAGE mediates amyloid-β peptide transport across the blood-brain barrier and accumulation in brain. Nature Medicine. 2003;9(7):907-13.

183. Basak JM, Verghese PB, Yoon H, Kim J, Holtzman DM. Low-density Lipoprotein Receptor Represents an Apolipoprotein E-independent Pathway of Aβ Uptake and Degradation by Astrocytes. Journal of Biological Chemistry. 2012;287(17):13959-71.

184. Deane R, Sagare A, Zlokovic BV. The Role of the Cell Surface LRP and Soluble LRP in Blood-Brain Barrier Aβ Clearance in Alzheimer's Disease. Current Pharmaceutical Design. 2008;14(16):1601-5.

185. Hammad SM, Ranganathan S, Loukinova E, Twal WO, Argraves WS. Interaction of Apolipoprotein J-Amyloid β-Peptide Complex with Low Density Lipoprotein Receptor-related Protein-2/Megalin. A Mechanism to Prevent Pathological Accumulation of Amyloid β Petptide. Journal of Biological Chemistry. 1997;272(30):18644-9.

186. Tanzi RE, Moir RD, Wagner SL. Clearance of Alzheimer's Aβ peptide: the many roads to perdition. Neuron. 2004;43(5):605-8.

187. Bell RD, Sagare AP, Friedman AE, Bedi GS, Holtzman DM, Deane R, et al. Transport pathways for clearance of human Alzheimer's amyloid β-peptide and apolipoproteins E and J in the mouse central nervous system. Journal of Cerebral Blood Flow and Metabolism. 2006;27(5):909-18.

188. Herz J. LRP: a bright beacon at the blood-brain barrier. Journal of Clinical Investigation. 2003;112(10):1483-5.

189. Deane R, Wu Z, Sagare A, Davis J, Du Yan S, Hamm K, et al. LRP/Amyloid β-Peptide Interaction Mediates Differential Brain Efflux of Aβ Isoforms. Neuron. 2004;43(3):333-44.

190. Tamaki C, Ohtsuki S, Iwatsubo T, Hashimoto T, Yamada K, Yabuki C, et al. Major Involvement of Low-Density Lipoprotein Receptor-Related Protein 1 in the Clearance of Plasma Free Amyloid β-Peptide by the Liver. Pharmaceutical Research. 2006;23(7):1407-16.

191. Sagare A, Deane R, Bell RD, Johnson B, Hamm K, Pendu R, et al. Clearance of amyloid-β by circulating lipoprotein receptors. Nature Medicine. 2007;13(9):1029-31.

192. Cao G, Bales KR, DeMattos RB, Paul SM. Liver X receptor-mediated gene regulation and cholesterol homeostasis in brain: relevance to Alzheimer's disease therapeutics. Current Alzheimer Research. 2007;4(2):179-84.

193. Koldamova R, Lefterov I. Role of LXR and ABCA1 in the Pathogenesis of Alzheimer's Disease - Implications for a New Therapeutic Approach Current Alzheimer Research. 2007;4(2):171-8.

194. Sparks DL. Cholesterol Metabolism and Brain Amyloidosis: Evidence for a Role of Copper in the Clearance of Aβ Through the Liver. Current Alzheimer Research. 2007;4(2):165-9.

195. Selkoe DJ. Clearing the Brain's Amyloid Cobwebs. Neuron. 2001;32(2):177-80.

196. Kurochkin IV, Goto S. Alzheimer's β-amyloid peptide specifically interacts with and is degraded by insulin degrading enzyme. FEBS Letters. 1994;345(1):33-7.

197. Qiu WQ, Walsh DM, Ye Z, Vekrellis K, Zhang J, Podlisny MB, et al. Insulin-degrading enzyme regulates extracellular levels of amyloid β-protein by degradation. Journal of Biological Chemistry. 1998;273(49):32730-8.

198. Vekrellis K, Ye Z, Qiu WQ, Walsh D, Hartley D, Chesneau V, et al. Neurons Regulate Extracellular Levels of Amyloid β-Protein via Proteolysis by Insulin-Degrading Enzyme. Journal of Neuroscience. 2000;20(5):1657-65.

199. Zhao L, Teter B, Morihara T, Lim GP, Ambegaokar SS, Ubeda OJ, et al. Insulin-Degrading Enzyme as a Downstream Target of Insulin Receptor Signaling Cascade: Implications for Alzheimer's Disease Intervention. Journal of Neuroscience. 2004;24(49):11120-6.

200. Iwata N, Tsubuki S, Takaki Y, Watanabe K, Sekiguchi M, Hosoki E, et al. Identification of the major Aβ1-42-degrading catabolic pathway in brain parenchyma: Suppression leads to biochemical and pathological deposition. Nature Medicine. 2000;6(2):143-50.

201. Iwata N, Satoshi T, Yoshie T, Keiro S, Bao L, Gerard NP, et al. Metabolic Regulation of Brain Aβ by Neprilysin. Science. 2001;292(5521):1550-2.

202. Yasojima K, Akiyama H, McGeer EG, McGeer PL. Reduced neprilysin in high plaque areas of Alzheimer brain: a possible relationship to deficient degradation of β-amyloid peptide. Neuroscience Letters. 2001;297(2):97-100.

203. Iwata N, Takaki Y, Fukami S, Tsubuki S, Saido TC. Region-specific reduction of Aβ-degrading endopeptidase, neprilysin, in mouse hippocampus upon aging. Journal of Neuroscience Research. 2002;70(3):493-500.

204. Eckman EA, Reed DK, Eckman CB. Degradation of the Alzheimer's Amyloid β Peptide by Endothelin-converting Enzyme. Journal of Biological Chemistry. 2001;276(27):24540-8.

205. Eckman EA, Watson M, Marlow L, Sambamurti K, Eckman CB. Alzheimer's Disease β-Amyloid Peptide Is Increased in Mice Deficient in Endothelin-converting Enzyme. Journal of Biological Chemistry. 2003;278(4):2081-4.

206. Roher AE, Kasunic TC, Woods AS, Cotter RJ, Ball MJ, Fridman R. Proteolysis of Aβ Peptide from Alzheimer Disease Brain by Gelatinase A. Biochemical and Biophysical Research Communications. 1994;205(3):1755-61.

207. Backstrom JR, Lim GP, Cullen MJ, Tokes ZA. Matrix Metalloproteinase-9 (MMP-9) Is Synthesized in Neurons of the Human Hippocampus and Is Capable of Degrading the Amyloid-β Peptide (1-40). Journal of Neuroscience. 1996;16(24):7910-9.

208. Yin K-J, Cirrito JR, Yan P, Hu X, Xiao Q, Pan X, et al. Matrix Metalloproteinases Expressed by Astrocytes Mediate Extracellular Amyloid-β Peptide Catabolism. Journal of Neuroscience. 2006;26(43):10939-48.

209. Abdul-Hay S, Sahara T, McBride M, Kang D, Leissring M. Identification of BACE2 as an avid β-amyloid-degrading protease. Molecular Neurodegeneration. 2012;7.

210. Esteban JA. Living with the enemy: a physiological role for the β-amyloid peptide. Trends in Neurosciences. 2004;27(1):1-3.

211. Soscia SJ, Kirby JE, Washicosky KJ, Tucker SM, Ingelsson M, Hyman B, et al. The Alzheimer's Disease-Associated Amyloid β-Protein Is an Antimicrobial Peptide. PLoS ONE. 2010;5(3):e9505.

212. Berthon G. Does human βA4 exert a protective function against oxidative stress in Alzheimer's disease? Medical Hypotheses. 2000;54(4):672-7.

213. Kontush A. Amyloid-β: an antioxidant that becomes a pro-oxidant and critically contributes to Alzheimer's disease. Free Radical Biology and Medicine. 2001;31(9):1120-31.

214. Zou K, Gong J-S, Yanagisawa K, Michikawa M. A Novel Function of Monomeric Amyloid β-Protein Serving as an Antioxidant Molecule against Metal-Induced Oxidative Damage. Journal of Neuroscience. 2002;22(12):4833-41.

215. Atwood CS, Obrenovich ME, Liu T, Chan H, Perry G, Smith MA, et al. Amyloid-β: a chameleon walking in two worlds: a review of the trophic and toxic properties of amyloid-β. Brain Research Reviews. 2003;43(1):1-16.

216. Kontush A, Atwood CS. Amyloid-β: phylogenesis of a chameleon. Brain Research Reviews. 2004;46(1):118-20.

217. Kontush A. Amyloid-β: Acute-phase apolipoprotein with metal-binding activity. Journal of Alzheimer's Disease. 2005;8(2):129-37.

218. Abramov E, Dolev I, Fogel H, Ciccotosto GD, Ruff E, Slutsky I. Amyloid-β as a positive endogenous regulator of release probability at hippocampal synapses. Nature Neuroscience. 2009;12(12):1567-76.

219. Cao L, Schrank BR, Rodriguez S, Benz EG, Moulia TW, Rickenbacher GT, et al. Aβ alters the connectivity of olfactory neurons in the absence of amyloid plaques *in vivo*. Nature Communications. 2012;3.

220. Maia LF, Kaeser SA, Reichwald J, Hruscha M, Martus P, Staufenbiel M, et al. Changes in Amyloid-β and Tau in the Cerebrospinal Fluid of Transgenic Mice Overexpressing Amyloid Precursor Protein. Science Translational Medicine. 2013;5(194):194re2.

221. Yankner BA, Dawes LR, Fisher S, Villa-Komaroff L, Oster-Granite ML, Neve RL. Neurotoxicity of a fragment of the amyloid precursor associated with Alzheimer's disease. Science. 1989;245(4916):417-20.

222. Frautschy SA, Baird A, Cole GM. Effects of injected Alzheimer β-amyloid cores in rat brain. Proceedings of the National Academy of Sciences of the United States of America. 1991;88(19):8362-6.

223. Liu ST, Howlett G, Barrow CJ. Histidine-13 Is a Crucial Residue in the Zinc Ion-Induced Aggregation of the Aβ Peptide of Alzheimer's Disease. Biochemistry. 1999;38(29):9373-8.

224. Teplow DB. Structural and kinetic features of amyloid β-protein fibrillogenesis. Amyloid. 1998;5(2):121-42.

225. Walsh DM, Hartley DM, Kusumoto Y, Fezoui Y, Condron MM, Lomakin A, et al. Amyloid β-protein fibrillogenesis. Structure and biological activity of protofibrillar intermediates. Journal of Biological Chemistry. 1999;274(36):25945-52.

226. Serpell LC. Alzheimer’s amyloid fibrils: structure and assembly. Biochimica et Biophysica Acta (BBA) - Molecular Basis of Disease. 2000;1502(1):16-30.

227. Gong Y, Chang L, Viola KL, Lacor PN, Lambert MP, Finch CE, et al. Alzheimer's disease-affected brain: Presence of oligomeric Aβ ligands (ADDLs) suggests a molecular basis for reversible memory loss. Proceedings of the National Academy of Sciences of the United States of America. 2003;100(18):10417-22.

228. Aizenstein HJ, Nebes RD, Saxton JA, Price JC, Mathis CA, Tsopelas ND, et al. Frequent Amyloid Deposition Without Significant Cognitive Impairment Among the Elderly. Archives of Neurology. 2008;65(11):1509-17.

229. O'Brien RJ, Resnick SM, Zonderman AB, Ferrucci L, Crain BJ, Pletnikova O, et al. Neuropathologic Studies of the Baltimore Longitudinal Study of Aging (BLSA). Journal of Alzheimer's Disease. 2009;18(3):665-75.

230. Price JL, McKeel Jr DW, Buckles VD, Roe CM, Xiong C, Grundman M, et al. Neuropathology of nondemented aging: Presumptive evidence for preclinical Alzheimer disease. Neurobiology of Aging. 2009;30(7):1026-36.

231. Reiman EM, Chen K, Liu X, Bandy D, Yu M, Lee W, et al. Fibrillar amyloid-β burden in cognitively normal people at 3 levels of genetic risk for Alzheimer's disease. Proceedings of the National Academy of Sciences of the United States of America. 2009;106(16):6820-5.

232. Kadir A, Marutle A, Gonzalez D, Schöll M, Almkvist O, Mousavi M, et al. Positron emission tomography imaging and clinical progression in relation to molecular

pathology in the first Pittsburgh Compound B positron emission tomography patient with Alzheimer's disease. Brain. 2011;134(1):301-17.

233. Jack CR, Wiste HJ, Lesnick TG, Weigand SD, Knopman DS, Vemuri P, et al. Brain β-amyloid load approaches a plateau. Neurology. 2013;80(10):890-6.

234. Villemagne VL, Burnham S, Bourgeat P, Brown B, Ellis KA, Salvado O, et al. Amyloid beta deposition, neurodegeneration, and cognitive decline in sporadic Alzheimer's disease: a prospective cohort study. Lancet Neurology. 2013;12(4):357-67.

235. Stine WB, Jr., Dahlgren KN, Krafft GA, LaDu MJ. *In Vitro* Characterization of Conditions for Amyloid-β Peptide Oligomerization and Fibrillogenesis. Journal of Biological Chemistry. 2003;278(13):11612-22.

236. LaFerla FM, Tinkle BT, Bieberich CJ, Haudenschild CC, Jay G. The Alzheimer's Aβ peptide induces neurodegeneration and apoptotic cell death in transgenic mice. Nature Genetics. 1995;9(1):21-30.

237. Lambert MP, Barlow AK, Chromy BA, Edwards C, Freed R, Liosatos M, et al. Diffusible, nonfibrillar ligands derived from Aβ1-42 are potent central nervous system neurotoxins. Proceedings of the National Academy of Sciences of the United States of America. 1998;95(11):6448-53.

238. Hartley DM, Walsh DM, Ye CP, Diehl T, Vasquez S, Vassilev PM, et al. Protofibrillar intermediates of amyloid β-protein induce acute electrophysiological changes and progressive neurotoxicity in cortical neurons. Journal of Neuroscience. 1999;19(20):8876-84.

239. Lue LF, Kuo YM, Roher AE, Brachova L, Shen Y, Sue L, et al. Soluble amyloid β peptide concentration as a predictor of synaptic change in Alzheimer's disease. American Journal of Pathology. 1999;155(3):853-62.

240. Kirkitadze MD, Bitan G, Teplow DB. Paradigm shifts in Alzheimer's disease and other neurodegenerative disorders: The emerging role of oligomeric assemblies. Journal of Neuroscience Research. 2002;69(5):567-77.

241. Walsh DM, Klyubin I, Fadeeva JV, Cullen WK, Anwyl R, Wolfe MS, et al. Naturally secreted oligomers of amyloid β protein potently inhibit hippocampal long-term potentiation *in vivo*. Nature. 2002;416(6880):535-9.

242. Walsh DM, Selkoe DJ. Oligomers on the brain: the emerging role of soluble protein aggregates in neurodegeneration. Protein and Peptide Letters. 2004;11(3):213-28.

243. Deshpande A, Mina E, Glabe C, Busciglio J. Different Conformations of Amyloid β Induce Neurotoxicity by Distinct Mechanisms in Human Cortical Neurons. Journal of Neuroscience. 2006;26(22):6011-8.

244. De Felice FG, Velasco PT, Lambert MP, Viola K, Fernandez SJ, Ferreira ST, et al. Aβ Oligomers Induce Neuronal Oxidative Stress through an *N*-Methyl-$_D$-aspartate Receptor-dependent Mechanism That Is Blocked by the Alzheimer Drug Memantine. Journal of Biological Chemistry. 2007;282(15):11590-601.

245. Walsh DM, Selkoe DJ. Aβ Oligomers - a decade of discovery. Journal of Neurochemistry. 2007;101(5):1172-84.

246. Decker H, Lo KY, Unger SM, Ferreira ST, Silverman MA. Amyloid-β Peptide Oligomers Disrupt Axonal Transport through an NMDA Receptor-Dependent Mechanism That Is Mediated by Glycogen Synthase Kinase 3β in Primary Cultured Hippocampal Neurons. Journal of Neuroscience. 2010;30(27):9166-71.

247. Johnson RD, Schauerte JA, Wisser KC, Gafni A, Steel DG. Direct Observation of Single Amyloid-β(1-40) Oligomers on Live Cells: Binding and Growth at Physiological Concentrations. PLoS ONE. 2011;6(8):e23970.

248. Hellstrand E, Boland B, Walsh DM, Linse S. Amyloid β-Protein Aggregation Produces Highly Reproducible Kinetic Data and Occurs by a Two-Phase Process. ACS Chemical Neuroscience. 2009;1(1):13-8.

249. Cohen SIA, Linse S, Luheshi LM, Hellstrand E, White DA, Rajah L, et al. Proliferation of amyloid-β42 aggregates occurs through a secondary nucleation mechanism. Proceedings of the National Academy of Sciences. 2013;110(24):9758-63.

250. Jeong JS, Ansaloni A, Mezzenga R, Lashuel HA, Dietler G. Novel Mechanistic Insight into the Molecular Basis of Amyloid Polymorphism and Secondary Nucleation during Amyloid Formation. Journal of Molecular Biology. 2013;425(10):1765-81.

251. Koffie RM, Meyer-Luehmann M, Hashimoto T, Adams KW, Mielke ML, Garcia-Alloza M, et al. Oligomeric amyloid β associates with postsynaptic densities and correlates with excitatory synapse loss near senile plaques. Proceedings of the National Academy of Sciences of the United States of America. 2009;106(10):4012-7.

252. Wogulis M, Wright S, Cunningham D, Chilcote T, Powell K, Rydel RE. Nucleation-Dependent Polymerization Is an Essential Component of Amyloid-Mediated Neuronal Cell Death. Journal of Neuroscience. 2005;25(5):1071-80.

253. Jan A, Gokce O, Luthi-Carter R, Lashuel HA. The Ratio of Monomeric to Aggregated Forms of Aβ40 and Aβ42 Is an Important Determinant of Amyloid-β Aggregation, Fibrillogenesis, and Toxicity. Journal of Biological Chemistry. 2008;283(42):28176-89.

254. Jan A, Adolfsson O, Allaman I, Buccarello A-L, Magistretti PJ, Pfeifer A, et al. Aβ42 Neurotoxicity Is Mediated by Ongoing Nucleated Polymerization Process Rather than by Discrete Aβ42 Species. Journal of Biological Chemistry. 2011;286(10):8585-96.

255. Crouch PJ, Harding S-ME, White AR, Camakaris J, Bush AI, Masters CL. Mechanisms of Aβ mediated neurodegeneration in Alzheimer's disease. International Journal of Biochemistry and Cell Biology. 2008;40(2):181-98.

256. Talaga P, Quere L. The plasma membrane: a target and hurdle for the development of anti-Aβ drugs? Current Drug Targets CNS and Neurological Disorders. 2002;1(6):567-74.

257. Verdier Y, Zarandi M, Penke B. Amyloid β-peptide interactions with neuronal and glial cell plasma membrane: binding sites and implications for Alzheimer's disease. Journal of Peptide Science. 2004;10(5):229-48.

258. Lauren J, Gimbel DA, Nygaard HB, Gilbert JW, Strittmatter SM. Cellular prion protein mediates impairment of synaptic plasticity by amyloid β oligomers. Nature. 2009;457(7233):1128-32.

259. Maloney B, Lahiri DK. The Alzheimer's amyloid β-peptide (Aβ) binds a specific DNA Aβ-interacting domain (AβID) in the APP, BACE1, and APOE promoters in a sequence-specific manner: Characterizing a new regulatory motif. Gene. 2011;488(1–2):1-12.

260. Penke B, Tóth AM, Földi I, Szűcs M, Janáky T. Intraneuronal β-amyloid and its interactions with proteins and subcellular organelles. Electrophoresis. 2012;33(24):3608-16.

261. Roher AE, Chaney MO, Kuo YM, Webster SD, Stine WB, Haverkamp LJ, et al. Morphology and toxicity of Aβ-(1-42) dimer derived from neuritic and vascular amyloid deposits of Alzheimer's disease. Journal of Biological Chemistry. 1996;271(34):20631-5.

262. Loo DT, Copani A, Pike CJ, Whittemore ER, Walencewicz AJ, Cotman CW. Apoptosis is induced by β-amyloid in cultured central nervous system neurons. Proceedings of the National Academy of Sciences of the United States of America. 1993;90(17):7951-5.

263. Su JH, Zhao M, Anderson AJ, Srinivasan A, Cotman CW. Activated caspase-3 expression in Alzheimer's and aged control brain: correlation with Alzheimer pathology. Brain Research. 2001;898(2):350-7.

264. Oddo S, Caccamo A, Shepherd JD, Murphy MP, Golde TE, Kayed R, et al. Triple-transgenic model of Alzheimer's disease with plaques and tangles: intracellular Aβ and synaptic dysfunction. Neuron. 2003;39(3):409-21.

265. Mattson MP, Cheng B, Davis D, Bryant K, Lieberburg I, Rydel RE. β-Amyloid peptides destabilize calcium homeostasis and render human cortical neurons vulnerable to excitotoxicity. Journal of Neuroscience. 1992;12(2):376-89.

266. Bezprozvanny I. Amyloid Goes Global. Science Signaling. 2009;2(63):pe16.

267. Schenk D, Barbour R, Dunn W, Gordon G, Grajeda H, Guido T, et al. Immunization with amyloid-β attenuates Alzheimer-disease-like pathology in the PDAPP mouse. Nature. 1999;400(6740):173-7.

268. Janus C, Pearson J, McLaurin J, Mathews PM, Jiang Y, Schmidt SD, et al. Amyloid β peptide immunization reduces behavioural impairment and plaques in a model of Alzheimer's disease. Nature. 2000;408(6815):979-82.

269. Morgan D, Diamond DM, Gottschall PE, Ugen KE, Dickey C, Hardy J, et al. Amyloid β peptide vaccination prevents memory loss in an animal model of Alzheimer's disease. Nature. 2000;408(6815):982.

270. Weiner HL, Lemere CA, Maron R, Spooner ET, Grenfell TJ, Mori C, et al. Nasal administration of amyloid-β peptide decreases cerebral amyloid burden in a mouse model of Alzheimer's disease. Annals of Neurology. 2000;48(4):567-79.

271. Das P, Murphy MP, Younkin LH, Younkin SG, Golde TE. Reduced effectiveness of Aβ1-42 immunization in APP transgenic mice with significant amyloid deposition. Neurobiology of Aging. 2001;22(5):721-7.

272. Sigurdsson EM, Scholtzova H, Mehta PD, Frangione B, Wisniewski T. Immunization with a Nontoxic/Nonfibrillar Amyloid-β Homologous Peptide Reduces Alzheimer's Disease-Associated Pathology in Transgenic Mice. American Journal of Pathology. 2001;159(2):439-47.

273. Maier M, Seabrook TJ, Lazo ND, Jiang L, Das P, Janus C, et al. Short Amyloid-β (Aβ) Immunogens Reduce Cerebral Aβ Load and Learning Deficits in an Alzheimer's Disease Mouse Model in the Absence of an Aβ-Specific Cellular Immune Response. Journal of Neuroscience. 2006;26(18):4717-28.

274. Buttini M, Masliah E, Barbour R, Grajeda H, Motter R, Johnson-Wood K, et al. β-Amyloid Immunotherapy Prevents Synaptic Degeneration in a Mouse Model of Alzheimer's Disease. Journal of Neuroscience. 2005;25(40):9096-101.

275. Solomon B, Koppel R, Hanan E, Katzav T. Monoclonal antibodies inhibit *in vitro* fibrillar aggregation of the Alzheimer β-amyloid peptide. Proceedings of the National Academy of Sciences of the United States of America. 1996;93(1):452-5.

276. Solomon B, Koppel R, Frankel D, Hanan-Aharon E. Disaggregation of Alzheimer β-amyloid by site-directed mAb. Proceedings of the National Academy of Sciences of the United States of America. 1997;94(8):4109-12.

277. Bard F, Cannon C, Barbour R, Burke R-L, Games D, Grajeda H, et al. Peripherally administered antibodies against amyloid β-peptide enter the central nervous system and reduce pathology in a mouse model of Alzheimer disease. Nature Medicine. 2000;6(8):916-9.

278. DeMattos RB, Bales KR, Cummins DJ, Dodart J-C, Paul SM, Holtzman DM. Peripheral anti-Aβ antibody alters CNS and plasma Aβ clearance and decreases brain Aβ burden in a mouse model of Alzheimer's disease. Proceedings of the National Academy of Sciences of the United States of America. 2001;98(15):8850-5.

279. Chauhan NB, Siegel GJ. Reversal of amyloid β toxicity in Alzheimer's disease model Tg2576 by intraventricular antiamyloid β antibody. Journal of Neuroscience Research. 2002;69(1):10-23.

280. Dodart J-C, Bales KR, Gannon KS, Greene SJ, DeMattos RB, Mathis C, et al. Immunization reverses memory deficits without reducing brain Aβ burden in Alzheimer's disease model. Nature Neuroscience. 2002;5(5):452-7.

281. Kotilinek LA, Bacskai B, Westerman M, Kawarabayashi T, Younkin L, Hyman BT, et al. Reversible Memory Loss in a Mouse Transgenic Model of Alzheimer's Disease. Journal of Neuroscience. 2002;22(15):6331-5.

282. Bard F, Barbour R, Cannon C, Carretto R, Fox M, Games D, et al. Epitope and isotype specificities of antibodies to β-amyloid peptide for protection against Alzheimer's disease-like neuropathology. Proceedings of the National Academy of Sciences of the United States of America. 2003;100(4):2023-8.

283. Chauhan NB, Siegel GJ. Intracerebroventricular passive immunization with anti-Aβ antibody in Tg2576. Journal of Neuroscience Research. 2003;74(1):142-7.

284. Oddo S, Billings L, Kesslak JP, Cribbs DH, LaFerla FM. Aβ Immunotherapy Leads to Clearance of Early, but Not Late, Hyperphosphorylated Tau Aggregates via the Proteasome. Neuron. 2004;43(3):321-32.

285. Wilcock DM, Rojiani A, Rosenthal A, Levkowitz G, Subbarao S, Alamed J, et al. Passive Amyloid Immunotherapy Clears Amyloid and Transiently Activates Microglia in a Transgenic Mouse Model of Amyloid Deposition. Journal of Neuroscience. 2004;24(27):6144-51.

286. Brendza RP, Bacskai BJ, Cirrito JR, Simmons KA, Skoch JM, Klunk WE, et al. Anti-Aβ antibody treatment promotes the rapid recovery of amyloid-associated neuritic dystrophy in PDAPP transgenic mice. Journal of Clinical Investigation. 2005;115(2):428-33.

287. Chauhan NB, Siegel GJ. Efficacy of anti-Aβ antibody isotypes used for intracerebroventricular immunization in TgCRND8. Neuroscience Letters. 2005;375(3):143-7.

288. Hartman RE, Izumi Y, Bales KR, Paul SM, Wozniak DF, Holtzman DM. Treatment with an Amyloid-β Antibody Ameliorates Plaque Load, Learning Deficits, and Hippocampal Long-Term Potentiation in a Mouse Model of Alzheimer's Disease. Journal of Neuroscience. 2005;25(26):6213-20.

289. Klyubin I, Walsh DM, Lemere CA, Cullen WK, Shankar GM, Betts V, et al. Amyloid β protein immunotherapy neutralizes Aβ oligomers that disrupt synaptic plasticity *in vivo*. Nature Medicine. 2005;11(5):556-61.

290. Klyubin I, Betts V, Welzel AT, Blennow K, Zetterberg H, Wallin A, et al. Amyloid β Protein Dimer-Containing Human CSF Disrupts Synaptic Plasticity: Prevention by Systemic Passive Immunization. Journal of Neuroscience. 2008;28(16):4231-7.

291. Bush AI. Metals and neuroscience. Current Opinion in Chemical Biology. 2000;4(2):184-91.

292. Koh J-Y. Zinc and disease of the brain. Molecular Neurobiology. 2001;24(1):99-106.

293. Barnham KJ, Bush AI. Metals in Alzheimer's and Parkinson's Diseases. Current Opinion in Chemical Biology. 2008;12(2):222-8.

294. Bush AI. The metallobiology of Alzheimer's disease. Trends in Neurosciences. 2003;26(4):207-14.

295. Adlard PA, Bush AI. Metals and Alzheimer's disease. Journal of Alzheimer's Disease. 2006;10(2-3):145-63.

296. Sensi SL, Paoletti P, Bush AI, Sekler I. Zinc in the physiology and pathology of the CNS. Nature Reviews Neuroscience. 2009;10(11):780-91.

297. Duce JA, Bush AI. Biological metals and Alzheimer's disease: Implications for therapeutics and diagnostics. Progress in Neurobiology. 2010;92(1):1-18.

298. Hung YH, Bush A, Cherny R. Copper in the brain and Alzheimer's disease. Journal of Biological Inorganic Chemistry. 2010;15(1):61-76.

299. Madsen E, Gitlin JD. Copper and Iron Disorders of the Brain. Annual Review of Neuroscience. 2007;30(1):317-37.

300. Parker SJ, Koistinaho J, White AR, Kanninen KM. Biometals in rare neurodegenerative disorders of childhood. Frontiers in Aging Neuroscience. 2013;5.

301. Skovronsky DM, Lee VMY, Trojanowski JQ. NEURODEGENERATIVE DISEASES: New Concepts of Pathogenesis and Their Therapeutic Implications. Annual Review of Pathology: Mechanisms of Disease. 2006;1(1):151-70.

302. McMaster D, McCrum E, Patterson C, Kerr M, O'Reilly D, Evans A, et al. Serum copper and zinc in random samples of the population of Northern Ireland. American Journal of Clinical Nutrition. 1992;56(2):440-6.

303. Iskra M, Patelski J, Majewski W. Concentrations of calcium, magnesium, zinc and copper in relation to free fatty acids and cholesterol in serum of atherosclerotic men. Journal of Trace Elementa and Electrolytes in Health and Disease. 1993;7(3):185-8.

304. Menditto A, Morisi G, Alimonti A, Caroli S, Petrucci F, Spagnolo A, et al. Association of serum copper and zinc with serum electrolytes and with selected risk factors for cardiovascular disease in men aged 55-75 years. NFR Study Group. Journal of Trace Elements and Electrolytes in Health and Disease. 1993;7(4):251-3.

305. Milne D, Johnson P. Assessment of copper status: effect of age and gender on reference ranges in healthy adults. Clinical Chemistry. 1993;39(5):883-7.

306. Ekmekcioglu C. The role of trace elements for the health of elderly individuals. Die Nahrung. 2001;45(5):309-16.

307. Bunker V, Hinks L, Lawson M, Clayton B. Assessment of zinc and copper status of healthy elderly people using metabolic balance studies and measurement of leucocyte concentrations. American Journal of Clinical Nutrition. 1984;40(5):1096-102.

308. Madarić A, Ginter E, Kadrabová J. Serum copper, zinc and copper/zinc ratio in males: influence of aging. Physiological Research. 1994;43(2):107-11.

309. Bunker V, Hinks L, Stansfield M, Lawson M, Clayton B. Metabolic balance studies for zinc and copper in housebound elderly people and the relationship between zinc balance and leukocyte zinc concentrations. American Journal of Clinical Nutrition. 1987;46(2):353-9.

310. Monget AL, Galan P, Preziosi P, Keller H, Bourgeois C, Arnaud J, et al. Micronutrient status in elderly people. Geriatrie/Min. Vit. Aux Network. International Journal for Vitamamin and Nutrition Research. 1996;66(1):71-6.

311. Del Corso L, Pastine F, Protti MA, Romanelli AM, Moruzzo D, Ruocco L, et al. Blood zinc, copper and magnesium in aging. A study in healthy home-living elderly. Panminerva Medica. 2000;42(4):273-7.

312. Ahluwalia N, Gordon MA, Handte G, Mahlon M, Li NQ, Beard JL, et al. Iron status and stores decline with age in Lewis rats. Journal of Nutrition. 2000;130(9):2378-83.

313. Martínez LE, Solé J, Arola L, Mas A. Changes in plasma copper and zinc during rat development. Biology of the Neonate. 1993;64(1):47-52.

314. Morris MC, Evans DA, Tangney CC, Bienias JL, Schneider JA, Wilson RS, et al. Dietary Copper and High Saturated and trans Fat Intakes Associated With Cognitive Decline. Archives of Neurology. 2006;63(8):1085-8.

315. Milward EA, Bruce DG, Knuiman MW, Divitini ML, Cole M, Inderjeeth CA, et al. A Cross-Sectional Community Study of Serum Iron Measures and Cognitive Status in Older Adults. Journal of Alzheimer's Disease. 2010;20(2):617-23.

316. Marcellini F, Giuli C, Papa R, Gagliardi C, Dedoussis G, Herbein G, et al. Zinc status, psychological and nutritional assessment in old people recruited in five European countries: Zincage study. Biogerontology. 2006;7(5):339-45.

317. Lam PK, Kritz-Silverstein D, Barrett-Connor E, Milne D, Nielsen F, Gamst A, et al. Plasma trace elements and cognitive function in older men and women: the Rancho Bernardo study. Jurnal of Nutritional Health Aging. 2008;12(1):22-7.

318. Baum L, Chan IH, Cheung SK, Goggins WB, Mok V, Lam L, et al. Serum zinc is decreased in Alzheimer's disease and serum arsenic correlates positively with cognitive ability. BioMetals. 2010;23(1):173-9.

319. Brewer GJ, Kanzer SH, Zimmerman EA, Molho ES, Celmins DF, Heckman SM, et al. Subclinical Zinc Deficiency in Alzheimer’s Disease and Parkinson’s Disease. American Journal of Alzheimer's Disease and Other Dementias. 2010;25(7):572-5.

320. Molina JA, Jimenez-Jimenez FJ, Aguilar MV, Meseguer I, Mateos-Vega CJ, Gonzalez-Munoz MJ, et al. Cerebrospinal fluid levels of transition metals in patients with Alzheimer's disease. Journal of Neural Transmission. 1998;105(4-5):479-88.

321. Basun H, Forssell LG, Wetterberg L, Winblad B. Metals and trace elements in plasma and cerebrospinal fluid in normal ageing and Alzheimer's disease. Journal of Neural Transmission Parkinsons Disease and Dementia Section. 1991;3(4):231-58.

322. Vural H, Demirin H, Kara Y, Eren I, Delibas N. Alterations of plasma magnesium, copper, zinc, iron and selenium concentrations and some related erythrocyte antioxidant enzyme activities in patients with Alzheimer’s disease. Journal of Trace Elements in Medicine and Biology. 2010;24(3):169-73.

323. Squitti R, Rossini PM, Cassetta E, Moffa F, Pasqualetti P, Cortesi M, et al. D-penicillamine reduces serum oxidative stress in Alzheimer's disease patients. European Journal of Clinical Investigation. 2002;32(1):51-9.

324. Faux NG, Ellis KA, Ames D, Fowler CJ, Martins RM, Pertile KK, et al. Alzheimer's disease is associated with lower hemoglobin levels and anemia: The Australian Imaging Biomarker Lifestyle (AIBL) study of aging. Alzheimer's & Dementia. 2010;6(4, Supplement):S528.

325. Hong CH, Falvey C, Harris TB, Simonsick EM, Satterfield S, Ferrucci L, et al. Anemia and risk of dementia in older adults: Findings from the Health ABC study. Neurology. 2013;81(6):528-33.

326. Rembach A, Doecke JD, Roberts BR, Watt AD, Faux NG, Volitakis I, et al. Longitudinal Analysis of Serum Copper and Ceruloplasmin in Alzheimer's Disease. Journal of Alzheimer's Disease. 2013;34(1):171-82.

327. Quinn JF, Harris C, Kaye JA, Lind B, Carter R, Anekonda T, et al. Gender Effects on Plasma and Brain Copper. International Journal of Alzheimer’s Disease. 2011;2011.

328. Snaedal J, Kristinsson J, Gunnarsdóttir S, Olafsdóttir A, Baldvinsson M, Jóhannesson T. Copper, ceruloplasmin and superoxide dismutase in patients with Alzheimer's diease: A case control study. Dementia and Geriatric Cognitive Disorders. 1998;9(5):239-42.

329. Bucossi S, Ventriglia M, Panetta V, Salustri C, Pasqualetti P, Mariani S, et al. Copper in Alzheimer's Disease: A Meta-Analysis of Serum,Plasma, and Cerebrospinal Fluid Studies. Journal of Alzheimer's Disease. 2011;24(1):175-85.

330. Ventriglia M, Bucossi S, Panetta V, Squitti R. Copper in Alzheimer's Disease: A Meta-Analysis of Serum, Plasma, and Cerebrospinal Fluid Studies. Journal of Alzheimer's Disease. 2012;30(4):981-4.

331. Squitti R, Pasqualetti P, Dal Forno G, Moffa F, Cassetta E, Lupoi D, et al. Excess of serum copper not related to ceruloplasmin in Alzheimer disease. Neurology. 2005;64(6):1040-6.

332. Squitti R, Barbati G, Rossi L, Ventriglia M, Dal Forno G, Cesaretti S, et al. Excess of nonceruloplasmin serum copper in AD correlates with MMSE, CSF β-amyloid, and h-tau. Neurology. 2006;67(1):76-82.

333. Squitti R, Bressi F, Pasqualetti P, Bonomini C, Ghidoni R, Binetti G, et al. Longitudinal prognostic value of serum “free” copper in patients with Alzheimer disease. Neurology. 2009;72(1):50-5.

334. Pajonk F-G, Kessler H, Supprian T, Hamzei P, Bach D, Schweickhardt J, et al. Cognitive decline correlates with low plasma concentrations of copper in patients with mild to moderate Alzheimer's disease. Journal Of Alzheimer's Disease. 2005;8(1):23-7.

335. Smorgon C, Mari E, Atti AR, Dalla Nora E, Zamboni PF, Calzoni F, et al. Trace elements and cognitive impairment: an elderly cohort study. Archives of Gerontology and Geriatrics. 2004;38, Supplement:393-402.

336. Agarwal R, Kushwaha S, Tripathi C, Singh N, Chhillar N. Serum copper in Alzheimer's disease and vascular dementia. Indian Journal of Clinical Biochemistry. 2008;23(4):369-74.

337. Arnal N, Cristalli DO, de Alaniz MJT, Marra CA. Clinical utility of copper, ceruloplasmin, and metallothionein plasma determinations in human neurodegenerative patients and their first-degree relatives. Brain Research. 2010;1319:118-30.

338. Brewer GJ, Kanzer SH, Zimmerman EA, Celmins DF, Heckman SM, Dick R. Copper and Ceruloplasmin Abnormalities in Alzheimer's Disease. American Journal of Alzheimer's Disease and Other Dementias. 2010;25(6):490-7.

339. Squitti R, Polimanti R, Siotto M, Bucossi S, Ventriglia M, Mariani S, et al. ATP7B Variants as Modulators of Copper Dyshomeostasis in Alzheimer's Disease. Neuromolecular Medicine. 2013;15(3):515-22.

340. Strozyk D, Launer LJ, Adlard PA, Cherny RA, Tsatsanis A, Volitakis I, et al. Zinc and copper modulate Alzheimer Aβ levels in human cerebrospinal fluid. Neurobiology of Aging. 2009;30(7):1069-77.

341. Kuiper M, Mulder C, van Kamp G, Scheltens P, Wolters E. Cerebrospinal fluid ferritin levels of patients with Parkinson's disease, Alzheimer's disease, and multiple system atrophy. Journal of Neural Transmission Parkinsons Disease and Dementia Section. 1994;7(2):109-14.

342. Loeffler DA, DeMaggio AJ, Juneau PL, Brickman CM, Mashour GA, Finkelman JH, et al. Ceruoplasmin Is Increased in Cerebrospinal Fluid in Alzheimer's Disease but Not Parkinson's Disease. Alzheimer Disease & Associated Disorders. 1994;8(3):190-7.

343. Boll M-C, Alcaraz-Zubeldia M, Montes S, Rios C. Free Copper, Ferroxidase and SOD1 Activities, Lipid Peroxidation and NO_x Content in the CSF. A Different Marker Profile in Four Neurodegenerative Diseases. Neurochemical Research. 2008;33(9):1717-23.

344. Ayton S, Faux NG, Bush AI. Ferritin levels in the cerebrospinal fluid predict Alzheimer's disease outcomes and are regulated by APOE. Nature Communications. 2015;6:6760.

345. Loeffler DA, LeWitt PA, Juneau PL, Sima AAF, Nguyen HU, DeMaggio AJ, et al. Increased regional brain concentrations of ceruloplasmin in neurodegenerative disorders. Brain Research. 1996;738(2):265-74.

346. Szymanski M, Wang R, Fallin MD, Bassett SS, Avramopoulos D. Neuroglobin and Alzheimer's dementia: Genetic association and gene expression changes. Neurobiology of Aging. 2010;31(11):1835-42.

347. Kawamata T, Tooyama I, Yamada T, Walker DG, McGeer PL. Lactotransferrin immunocytochemistry in Alzheimer and normal human brain. American Journal of Pathology. 1993;142(5):1574-85.

348. Connor JR, Snyder BS, Beard JL, Fine RE, Mufson EJ. Regional distribution of iron and iron-regulatory proteins in the brain in aging and Alzheimer's disease. Journal of Neuroscience Research. 1992;31(2):327-35.

349. Kalaria RN, Sromek SM, Grahovac I, Harik SI. Transferrin receptors of rat and human brain and cerebral microvessels and their status in Alzheimer's disease. Brain Research. 1992;585(1-2):87-93.

350. Colangelo V, Schurr J, Ball MJ, Pelaez RP, Bazan NG, Lukiw WJ. Gene expression profiling of 12633 genes in Alzheimer hippocampal CA1: Transcription and neurotrophic factor down-regulation and up-regulation of apoptotic and pro-inflammatory signaling. Journal of Neuroscience Research. 2002;70(3):462-73.

351. Jacob C, Maret W, Vallee BL. Control of zinc transfer between thionein, metallothionein, and zinc proteins. Proceedings of the National Academy of Sciences of the United States of America. 1998;95(7):3489-94.

352. Uchida Y, Takio K, Titani K, Ihara Y. The growth-inhibitory factor that is deficient in the Alzheimer's disease brain is a 68-amino acid metallothionein-like protein. Neuron. 1991;7(2):337-47.

353. Tsuji S, Kobayashi H, Uchida Y, Ihara Y, Miyatake T. Molecular cloning of human growth inhibitory factor cDNA and its down-regulation in Alzheimer's disease. EMBO Journal. 1992;11(13):4843–50.

354. Yu WH, Lukiw WJ, Bergeron C, Niznik HB, Fraser PE. Metallothionein III is reduced in Alzheimer’s disease. Brain Research. 2001;894(1):37-45.

355. Frederickson CJ, Bush AI. Synaptically released zinc: Physiological functions and pathological effects. BioMetals. 2001;14(3):353-66.

356. Linkous DH, Flinn JM, Koh JY, Lanzirotti A, Bertsch PM, Jones BF, et al. Evidence That the ZNT3 Protein Controls the Total Amount of Elemental Zinc in Synaptic Vesicles. Journal of Histochemistry and Cytochemistry. 2008;56(1):3-6.

357. Adlard PA, Parncutt JM, Finkelstein DI, Bush AI. Cognitive Loss in Zinc Transporter-3 Knock-Out Mice: A Phenocopy for the Synaptic and Memory Deficits of Alzheimer's Disease? Journal of Neuroscience. 2010;30(5):1631-6.

358. Maurer I, Zierz S, Möller H-J. A selective defect of cytochrome c oxidase is present in brain of Alzheimer disease patients. Neurobiology of Aging. 2000;21(3):455-62.

359. Lovell MA, Robertson JD, Teesdale WJ, Campbell JL, Markesbery WR. Copper, iron and zinc in Alzheimer's disease senile plaques. Journal of the Neurological Sciences. 1998;158(1):47-52.

360. Martin WR, Ye FQ, Allen PS. Increasing striatal iron content associated with normal aging. Movement Disorders. 1998;13(2):281-6.

361. Bartzokis G, Beckson M, Hance DB, Marx P, Foster JA, Marder SR. MR evaluation of age-related increase of brain iron in young adult and older normal males. Magnetic Resonance Imaging. 1997;15(1):29-35.

362. Drayer B, Burger P, Darwin R, Riederer S, Herfkens R, Johnson GA. MRI of brain iron. American Journal of Roentgenology. 1986;147(1):103-10.

363. Wender M, Szczech J, Hoffmann S, Hilczer W. Electron paramagnetic resonance analysis of heavy metals in the aging human brain. Neuropatologia Polska. 1992;30(1):65-72.

364. Zecca L, Gallorini M, Schunemann V, Trautwein AX, Gerlach M, Riederer P, et al. Iron, neuromelanin and ferritin content in the substantia nigra of normal subjects at different ages: consequences for iron storage and neurodegenerative processes. Journal of Neurochemistry. 2001;76(6):1766-73.

365. Zecca L, Zucca FA, Toscani M, Adorni F, Giaveri G, Rizzio E, et al. Iron, copper and their proteins in substantia nigra of human brain during aging. Journal of Radioanalytical & Nuclear Chemistry. 2005;263(3):733-7.

366. House E, Esiri M, Forster G, Ince PG, Exley C. Aluminium, iron and copper in human brain tissues donated to the medical research council's cognitive function and ageing study. Metallomics. 2012;4(1):56-65.

367. Vasudevaraju P, Bharathi TJ, Shamasundar NM, Subba Rao K, Balaraj BM, Ksj R, et al. New evidence on iron, copper accumulation and zinc depletion and its correlation with DNA integrity in aging human brain regions. Indian Journal of Psychiatry. 2010;52(2):140-4.

368. Morita A, Kimura M, Itokawa Y. The effect of aging on the mineral status of female mice. Biological Trace Element Research. 1994;42(2):165-77.

369. Maynard CJ, Cappai R, Volitakis I, Cherny RA, White AR, Beyreuther K, et al. Overexpression of Alzheimer's Disease Amyloid-β Opposes the Age-dependent Elevations of Brain Copper and Iron. Journal of Biological Chemistry. 2002;277(47):44670-6.

370. Maynard CJ, Cappai R, Volitakis I, Cherny RA, Masters CL, Li Q-X, et al. Gender and genetic background effects on brain metal levels in APP transgenic and normal mice: Implications for Alzheimer β-amyloid pathology. Journal of Inorganic Biochemistry. 2006;100(5-6):952-62.

371. Singh I, Sagare AP, Coma M, Perlmutter D, Gelein R, Bell RD, et al. Low levels of copper disrupt brain amyloid-β homeostasis by altering its production and clearance. Proceedings of the National Academy of Sciences. 2013;110(36):14771-6.

372. Lee J-Y, Cho E, Seo J-W, Hwang JJ, Koh J-Y. Alteration of the Cerebral Zinc Pool in a Mouse Model of Alzheimer Disease. Journal of Neuropathology & Experimental Neurology. 2012;71(3):211-22.

373. Religa D, Strozyk D, Cherny RA, Volitakis I, Haroutunian V, Winblad B, et al. Elevated cortical zinc in Alzheimer disease. Neurology. 2006;67(1):69-75.

374. Cornett CR, Markesbery WR, Ehmann WD. Imbalances of trace elements related to oxidative damage in Alzheimer's disease brain. NeuroToxicology. 1998;19(3):339-45.

375. Leite REP, Jacob-Filho W, Saiki M, Grinberg L, Ferretti REL. Determination of trace elements in human brain tissues using neutron activation analysis. Journal of Radioanalytical & Nuclear Chemistry. 2008;278(3):581-4.

376. Deibel MA, Ehmann WD, Markesbery WR. Copper, iron, and zinc imbalances in severely degenerated brain regions in Alzheimer's disease: possible relation to oxidative stress. Journal of the Neurological Sciences. 1996;143(1-2):137-42.

377. Andrási E, Farkas É, Scheibler H, Réffy A, Bezúr L. Al, Zn, Cu, Mn and Fe levels in brain in Alzheimer's disease. Archives of Gerontology and Geriatrics. 1995;21(1):89-97.

378. James SA, Volitakis I, Adlard PA, Duce JA, Masters CL, Cherny RA, et al. Elevated labile Cu is associated with oxidative pathology in Alzheimer disease. Free Radical Biology and Medicine. 2012;52(2):298-302.

379. Schrag M, Mueller C, Oyoyo U, Smith MA, Kirsch WM. Iron, zinc and copper in the Alzheimer's disease brain: A quantitative meta-analysis. Some insight on the influence of citation bias on scientific opinion. Progress in Neurobiology. 2011;94(3):296-306.

380. Bartzokis G, Sultzer D, Cummings J, Holt LE, Hance DB, Henderson VW, et al. *In Vivo* Evaluation of Brain Iron in Alzheimer Disease Using Magnetic Resonance Imaging. Archives of General Psychiatry. 2000;57(1):47-53.

381. Loeffler DA, Connor JR, Juneau PL, Snyder BS, Kanaley L, DeMaggio AJ, et al. Transferrin and Iron in Normal, Alzheimer's Disease, and Parkinson's Disease Brain Regions. Journal of Neurochemistry. 1995;65(2):710-6.

382. Ding B, Chen K-M, Ling H-W, Sun F, Li X, Wan T, et al. Correlation of iron in the hippocampus with MMSE in patients with Alzheimer's disease. Journal of Magnetic Resonance Imaging. 2009;29(4):793-8.

383. Leskovjan AC, Kretlow A, Lanzirotti A, Barrea R, Vogt S, Miller LM. Increased brain iron coincides with early plaque formation in a mouse model of Alzheimer's disease. NeuroImage. 2011;55(1):32-8.

384. Schrag M, Crofton A, Zabel M, Jiffry A, Kirsch D, Dickson A, et al. Effect of Cerebral Amyloid Angiopathy on Brain Iron, Copper, and Zinc in Alzheimer's Disease. Journal of Alzheimer's Disease. 2011;24(1):137-49.

385. Suh SW, Jensen KB, Jensen MS, Silva DS, Kesslak PJ, Danscher G, et al. Histochemically-reactive zinc in amyloid plaques, angiopathy, and degenerating neurons of Alzheimer's diseased brains. Brain Research. 2000;852(2):274-8.

386. Smith MA, Wehr K, Harris PLR, Siedlak SL, Connor JR, Perry G. Abnormal localization of iron regulatory protein in Alzheimer's disease. Brain Research. 1998;788(1-2):232-6.

387. Grundke-Iqbal I, Fleming J, Tung YC, Lassmann H, Iqbal K, Joshi JG. Ferritin is a component of the neuritic (senile) plaque in Alzheimer dementia. Acta Neuropathologica. 1990;81(2):105-10.

388. Connor JR, Menzies SL, St. Martin SM, Mufson EJ. A histochemical study of iron, transferrin, and ferritin in Alzheimer's diseased brains. Journal of Neuroscience Research. 1992;31(1):75-83.

389. Robinson SR, Noone DF, Kril J, Halliday GM. Most amyloid plaques contain ferritin-rich cells. Alzheimer's Research. 1995;1:191-6.

390. Batton CI, O'Dowd BS, Noone DF, Kril J, Robinson SR. Ferritin-rich microglia are concentrated within β-amyloid plaques. Alzheimer's Research. 1997;3:23-8.

391. Zhang L-H, Wang X, Stoltenberg M, Danscher G, Huang L, Wang Z-Y. Abundant expression of zinc transporters in the amyloid plaques of Alzheimer's disease brain. Brain Research Bulletin. 2008;77(1):55-60.

392. Zhang L-H, Wang X, Zheng Z-H, Ren H, Stoltenberg M, Danscher G, et al. Altered expression and distribution of zinc transporters in APP/PS1 transgenic mouse brain. Neurobiology of Aging. 2010;31(1):74-87.

393. Smith MA, Harris PLR, Sayre LM, Perry G. Iron accumulation in Alzheimer disease is a source of redox-generated free radicals. Proceedings of the National Academy of Sciences of the United States of America. 1997;94(18):9866-8.

394. Lee J-Y, Mook-Jung I, Koh J-Y. Histochemically Reactive Zinc in Plaques of the Swedish Mutant β-Amyloid Precursor Protein Transgenic Mice. Journal of Neuroscience. 1999;19(11):RC10:1-5.

395. Miller LM, Wang Q, Telivala TP, Smith RJ, Lanzirotti A, Miklossy J. Synchrotron-based infrared and X-ray imaging shows focalized accumulation of Cu and Zn co-localized with β-amyloid deposits in Alzheimer's disease. Journal of Structural Biology. 2006;155(1):30-7.

396. Liu G, Huang W, Moir RD, Vanderburg CR, Lai B, Peng Z, et al. Metal exposure and Alzheimer's pathogenesis. Journal of Structural Biology. 2006;155(1):45-51.

397. Rajendran R, Minqin R, Ynsa MD, Casadesus G, Smith MA, Perry G, et al. A novel approach to the identification and quantitative elemental analysis of amyloid deposits - Insights into the pathology of Alzheimer's disease. Biochemical and Biophysical Research Communications. 2009;382(1):91-5.

398. Assaf SY, Chung S-H. Release of endogenous Zn^{2+} from brain tissue during activity. Nature. 1984;308(5961):734-6.

399. Howell GA, Welch MG, Frederickson CJ. Stimulation-induced uptake and release of zinc in hippocampal slices. Nature. 1984;308(5961):736-8.

400. Hartter DE, Barnea A. Brain tissue accumulates 67copper by two ligand-dependent saturable processes. A high affinity, low capacity and a low affinity, high capacity process. Journal of Biological Chemistry. 1988;263(2):799-805.

401. Kardos J, Kovacs I, Hajos F, Kalman M, Simonyi M. Nerve endings from rat brain tissue release copper upon depolarization. A possible role in regulating neuronal excitability. Neuroscience Letters. 1989;103(2):139-44.

402. Schlief ML, Craig AM, Gitlin JD. NMDA Receptor Activation Mediates Copper Homeostasis in Hippocampal Neurons. Journal of Neuroscience. 2005;25(1):239-46.

403. Deshpande A, Kawai H, Metherate R, Glabe CG, Busciglio J. A Role for Synaptic Zinc in Activity-Dependent Aβ Oligomer Formation and Accumulation at Excitatory Synapses. Journal of Neuroscience. 2009;29(13):4004-15.

404. Yamamoto A, Shin RW, Hasegawa K, Naiki H, Sato H, Yoshimasu F, et al. Iron (III) induces aggregation of hyperphosphorylated τ and its reduction to iron (II) reverses the aggregation: implications in the formation of neurofibrillary tangles of Alzheimer's disease. Journal of Neurochemistry. 2002;82(5):1137-47.

405. Shin R-W, Kruck TPA, Murayama H, Kitamoto T. A novel trivalent cation chelator Feralex dissociates binding of aluminum and iron associated with hyperphosphorylated τ of Alzheimer's disease. Brain Research. 2003;961(1):139-46.

406. Mo Z-Y, Zhu Y-Z, Zhu H-L, Fan J-B, Chen J, Liang Y. Low micromolar zinc accelerates the fibrillization of human Tau via bridging Cys291 and Cys322. Journal of Biological Chemistry. 2009;284(50):34648-57.

407. An W-L, Bjorkdahl C, Liu R, Cowburn RF, Winblad B, Pei J-J. Mechanism of zinc-induced phosphorylation of p70 S6 kinase and glycogen synthase kinase 3β in SH-SY5Y neuroblastoma cells. Journal of Neurochemistry. 2005;92(5):1104-15.

408. Bjorkdahl C, Sjogren MJ, Winblad B, Pei J-JCA. Zinc induces neurofilament phosphorylation independent of p70 S6 kinase in N2a cells. Neuroreport. 2005;16(6):591-5.

409. Kim I, Park EJ, Seo J, Ko SJ, Lee J, Kim CH. Zinc stimulates tau S214 phosphorylation by the activation of Raf/mitogen-activated protein kinase-kinase/extracellular signal-regulated kinase pathway. Neuroreport. 2011;22(16):839-44.

410. Xiong Y, Jing X-P, Zhou X-W, Wang X-L, Yang Y, Sun X-Y, et al. Zinc induces protein phosphatase 2A inactivation and tau hyperphosphorylation through Src dependent PP2A (tyrosine 307) phosphorylation. Neurobiology of Aging. 2013;34(3):745-56.

411. Sun X-Y, Wei Y-P, Xiong Y, Wang X-C, Xie A-J, Wang X-L, et al. Synaptic released zinc promotes tau hyperphosphorylation by inhibition of PP2A. Journal of Biological Chemistry. 2012;287(14):11174-82.

412. Malm TM, Iivonen H, Goldsteins G, Keksa-Goldsteine V, Ahtoniemi T, Kanninen K, et al. Pyrrolidine Dithiocarbamate Activates Akt and Improves Spatial Learning in APP/PS1 Mice without Affecting β-Amyloid Burden. Journal of Neuroscience. 2007;27(14):3712-21.

413. Pierson KB, Evenson MA. 200 KD neurofilament protein binds Al, Cu and Zn. Biochemical and Biophysical Research Communications. 1988;152(2):598-604.

414. Rogers JT, Randall JD, Cahill CM, Eder PS, Huang X, Gunshin H, et al. An Iron-responsive Element Type II in the 5'-Untranslated Region of the Alzheimer's

Amyloid Precursor Protein Transcript. Journal of Biological Chemistry. 2002;277(47):45518-28.

415. Venti A, Giordano T, Eder P, Bush AI, Lahiri DK, Greig NH, et al. The Integrated Role of Desferrioxamine and Phenserine Targeted to an Iron-Responsive Element in the APP-mRNA 5'-Untranslated Region. Annals of the New York Academy of Sciences. 2004;1035(1):34-48.

416. Bandyopadhyay S, Huang X, Cho H, Greig N, Youdim M, Rogers J. Metal specificity of an iron-responsive element in Alzheimer's APP mRNA 5′ untranslated region, tolerance of SH-SY5Y and H4 neural cells to desferrioxamine, clioquinol, VK-28, and a piperazine chelator. Journal of Neural Transmission Supplementum. 2006;71:237-47.

417. Guo C, Wang T, Zheng W, Shan Z-Y, Teng W-P, Wang Z-Y. Intranasal deferoxamine reverses iron-induced memory deficits and inhibits amyloidogenic APP processing in a transgenic mouse model of Alzheimer's disease. Neurobiology of Aging. 2013;34(2):562-75.

418. Bellingham SA, Lahiri DK, Maloney B, La Fontaine S, Multhaup G, Camakaris J. Copper Depletion Down-regulates Expression of the Alzheimer's Disease Amyloid-β Precursor Protein Gene. Journal of Biological Chemistry. 2004;279(19):20378-86.

419. Cater MA, McInnes KT, Li Q-X, Volitakis I, La fontaine S, Mercer JFB, et al. Intracellular copper deficiency increases amyloid-β secretion by diverse mechanisms. Biochemical Journal. 2008;412(1):141-52.

420. Armendariz AD, Gonzalez M, Loguinov AV, Vulpe CD. Gene expression profiling in chronic copper overload reveals upregulation of *Prnp* and *App*. Physiological Genomics. 2004;20(1):45-54.

421. Lin R, Chen X, Li W, Han Y, Liu P, Pi R. Exposure to metal ions regulates mRNA levels of APP and BACE1 in PC12 cells: Blockage by curcumin. Neuroscience Letters. 2008;440(3):344-7.

422. Bellingham SA, Ciccotosto GD, Needham BE, Fodero LR, White AR, Masters CL, et al. Gene knockout of amyloid precursor protein and amyloid precursor-like protein-2 increases cellular copper levels in primary mouse cortical neurons and embryonic fibroblasts. Journal of Neurochemistry. 2004;91(2):423-8.

423. Lahiri DK, Chen D, Maloney B, Holloway HW, Yu Q-s, Utsuki T, et al. The Experimental Alzheimer's Disease Drug Posiphen [(+)-Phenserine] Lowers Amyloid-β Peptide Levels in Cell Culture and Mice. Journal of Pharmacology and Experimental Therapeutics. 2007;320(1):386-96.

424. Maccecchini M, Greig N, Rogers J. Mechanism of action of Posiphen®: From model to human. Alzheimer's & Dementia. 2011;7(4, Supplement):S567-8.

425. Bush AI, Multhaup G, Moir RD, Williamson TG, Small DH, Rumble B, et al. A novel zinc(II) binding site modulates the function of the βA4 amyloid protein precursor of Alzheimer's disease. Journal of Biological Chemistry. 1993;268(22):16109-12.

426. Hesse L, Beher D, Masters CL, Multhaup G. The βA4 amyloid precursor protein binding to copper. FEBS Letters. 1994;349(1):109-16.

427. Barnham KJ, McKinstry WJ, Multhaup G, Galatis D, Morton CJ, Curtain CC, et al. Structure of the Alzheimer's Disease Amyloid Precursor Protein Copper Binding Domain. A Regulator of Neuronal Copper Homeostasis. Journal of Biological Chemistry. 2003;278(19):17401-7.

428. Dahms SO, Könnig I, Roeser D, Gührs K-H, Mayer MC, Kaden D, et al. Metal Binding Dictates Conformation and Function of the Amyloid Precursor Protein (APP) E2 Domain. Journal of Molecular Biology. 2012;416(3):438-52.

429. Streltsov V. X-ray absorption and diffraction studies of the metal binding sites in amyloid β -peptide. European Biophysics Journal. 2008;37(3):257-63.

430. Streltsov VA, J. Titmuss SJ, Epa VC, Barnham KJ, Masters CL, Varghese JN. The structure of the Amyloid β-peptide high affinity Copper II binding site in Alzheimer's Disease. Biophysical Journal. 2008;95(7):3447-56.

431. Wang C-Y, Wang T, Zheng W, Zhao B-L, Danscher G, Chen Y-H, et al. Zinc Overload Enhances APP Cleavage and Aβ Deposition in the Alzheimer Mouse Brain. PLoS ONE. 2010;5(12):e15349.

432. Noda Y, Asada M, Kubota M, Maesako M, Watanabe K, Uemura M, et al. Copper enhances APP dimerization and promotes Aβ production. Neuroscience Letters. 2013;547:10-5.

433. Hung YH, Robb EL, Volitakis I, Ho M, Evin G, Li Q-X, et al. Paradoxical Condensation of Copper with Elevated β-Amyloid in Lipid Rafts under Cellular Copper Deficiency Conditions. Journal of Biological Chemistry. 2009;284(33):21899-907.

434. Acevedo KM, Hung YH, Dalziel AH, Li Q-X, Laughton K, Wikhe K, et al. Copper Promotes the Trafficking of the Amyloid Precursor Protein. Journal of Biological Chemistry. 2011;286(10):8252-62.

435. Borchardt T, Camakaris J, Cappai R, Masters CL, Beyreuther K, Multhaup G. Copper inhibits β-amyloid production and stimulates the non-amyloidogenic pathway of amyloid-precursor-protein secretion. Biochemical Journal. 1999;344(2):461-7.

436. White AR, Du T, Laughton KM, Volitakis I, Sharples RA, Xilinas ME, et al. Degradation of the Alzheimer Disease Amyloid β-Peptide by Metal-dependent Up-regulation of Metalloprotease Activity. Journal of Biological Chemistry. 2006;281(26):17670-80.

437. Park I-H, Jung MW, Mori H, Mook-Jung I. Zinc Enhances Synthesis of Presenilin 1 in Mouse Primary Cortical Culture. Biochemical and Biophysical Research Communications. 2001;285(3):680-8.

438. Cross JB, Duca JS, Kaminski JJ, Madison VS. The Active Site of a Zinc-Dependent Metalloproteinase Influences the Computed pKa of Ligands Coordinated to the Catalytic Zinc Ion. Journal of the American Chemical Society. 2002;124(37):11004-7.

439. Angeletti B, Waldron KJ, Freeman KB, Bawagan H, Hussain I, Miller CCJ, et al. BACE1 Cytoplasmic Domain Interacts with the Copper Chaperone for Superoxide Dismutase-1 and Binds Copper. Journal of Biological Chemistry. 2005;280(18):17930-7.

440. Dingwall C. A copper-binding site in the cytoplasmic domain of BACE1 identifies a possible link to metal homoeostasis and oxidative stress in Alzheimer's disease. Biochemical Society Transactions. 2007;35:571–3.

441. Greenough MA, Volitakis I, Li Q-X, Laughton K, Evin G, Ho M, et al. Presenilins Promote the Cellular Uptake of Copper and Zinc and Maintain Copper Chaperone of SOD1-dependent Copper/Zinc Superoxide Dismutase Activity. Journal of Biological Chemistry. 2011;286(11):9776-86.

442. Southon A, Greenough MA, Ganio G, Bush AI, Burke R, Camakaris J. Presenilin Promotes Dietary Copper Uptake. PLoS ONE. 2013;8(5):e62811.

443. Duce JA, Tsatsanis A, Cater MA, James SA, Robb E, Wikhe K, et al. Iron-Export Ferroxidase Activity of β-Amyloid Precursor Protein Is Inhibited by Zinc in Alzheimer's Disease. Cell. 2010;142(6):857-67.

444. Lei P, Ayton S, Finkelstein DI, Spoerri L, Ciccotosto GD, Wright DK, et al. Tau deficiency induces parkinsonism with dementia by impairing APP-mediated iron export. Nature Medicine. 2012;18(2):291-5.

445. Faller P, Hureau C, Berthoumieu O. Role of Metal Ions in the Self-assembly of the Alzheimer's Amyloid-β Peptide. Inorganic Chemistry. 2013;52(21):12193-206.

446. Mantyh PW, Ghilardi JR, Rogers S, DeMaster E, Allen CJ, Stimson ER, et al. Aluminum, Iron, and Zinc Ions Promote Aggregation of Physiological Concentrations of β-Amyloid Peptide. Journal of Neurochemistry. 1993;61(3):1171-4.

447. Bush AI, Pettingell Jr WH, Paradis MD, Tanzi RE. Modulation of Aβ adhesiveness and secretase site cleavage by zinc. Journal of Biological Chemistry. 1994;269(16):12152-8.

448. Bush AI, Pettingell WH, Multhaup G, d Paradis M, Vonsattel JP, Gusella JF, et al. Rapid induction of Alzheimer Aβ amyloid formation by zinc. Science. 1994;265(5177):1464-7.

449. Esler WP, Stimson ER, Jennings JM, Ghilardi JR, Mantyh PW, Maggio JE. Zinc-Induced Aggregation of Human and Rat β-Amyloid Peptides *In Vitro*. Journal of Neurochemistry. 1996;66(2):723-32.

450. Brown AM, Tummolo DM, Rhodes KJ, Hofmann JR, Jacobsen JS, Sonnenberg-Reines J. Selective Aggregation of Endogenous β-Amyloid Peptide and Soluble Amyloid Precursor Protein in Cerebrospinal Fluid by Zinc. Journal of Neurochemistry. 1997;69(3):1204-12.

451. Dong J, Shokes JE, Scott RA, Lynn DG. Modulating Amyloid Self-Assembly and Fibril Morphology with Zn(II). Journal of the American Chemical Society. 2006;128(11):3540-2.

452. Miller Y, Ma B, Nussinov R. Zinc ions promote Alzheimer Aβ aggregation via population shift of polymorphic states. Proceedings of the National Academy of Sciences of the United States of America. 2010;107(21):9490-5.

453. Atwood CS, Moir RD, Huang X, Scarpa RC, Bacarra NME, Romano DM, et al. Dramatic aggregation of Alzheimer Aβ by Cu(II) is induced by conditions representing physiological acidosis. Journal of Biological Chemistry. 1998;273(21):12817-26.

454. Miura T, Suzuki K, Kohata N, Takeuchi H. Metal binding modes of Alzheimer's amyloid β-peptide in insoluble aggregates and soluble complexes. Biochemistry. 2000;39(23):7024-31.

455. Atwood CS, Scarpa RC, Huang X, Moir RD, Jones WD, Fairlie DP, et al. Characterization of Copper Interactions with Alzheimer Amyloid β Peptides. Identification of an Attomolar-Affinity Copper Binding Site on Amyloid β1-42. Journal of Neurochemistry. 2000;75(3):1219-33.

456. Karr JW, Akintoye H, Kaupp LJ, Szalai VA. N-Terminal Deletions Modify the Cu^{2+} Binding Site in Amyloid-β. Biochemistry. 2005;44(14):5478-87.

457. Clements A, Allsop D, Walsh DM, Williams CH. Aggregation and Metal-Binding Properties of Mutant Forms of the Amyloid β Peptide of Alzheimer's Disease. Journal of Neurochemistry. 1996;66(2):740-7.

458. Mekmouche Y, Coppel Y, Hochgräfe K, Guilloreau L, Talmard C, Mazarguil H, et al. Characterization of the Zn(II) Binding to the Peptide Amyloid-β_{1-16} linked to Alzheimer's Disease. ChemBioChem. 2005;6(9):1663-71.

459. Jiang D, Men L, Wang J, Zhang Y, Chickenyen S, Wang Y, et al. Redox Reactions of Copper Complexes Formed with Different β-Amyloid Peptides and Their Neuropathological Relevance. Biochemistry. 2007;46(32):9270-82.

460. Syme CD, Viles JH. Solution 1H NMR investigation of Zn^{2+} and Cd^{2+} binding to amyloid-β peptide (Aβ) of Alzheimer's disease. Biochimica et Biophysica Acta (BBA) - Proteins & Proteomics. 2006;1764(2):246-56.

461. Kozin SA, Zirah S, Rebuffat S, Hui Bon Hoa G, Debey P. Zinc Binding to Alzheimer's Aβ(1-16) Peptide Results in Stable Soluble Complex. Biochemical and Biophysical Research Communications. 2001;285(4):959-64.

462. Atwood CS, Huang X, Khatri A, Scarpa RC, Kim YS, Moir RD, et al. Copper catalyzed oxidation of Alzheimer Aβ. Cellular and Molecular Biology 2000;46(4):777-83.

463. Guilloreau L, Damian L, Coppel Y, Mazarguil H, Winterhalter M, Faller P. Structural and thermodynamical properties of CuII amyloid-β16/28 complexes associated with Alzheimer's disease. Journal of Biological Inorganic Chemistry. 2006;11(8):1024-38.

464. Ha C, Ryu J, Park CB. Metal Ions Differentially Influence the Aggregation and Deposition of Alzheimer's β-Amyloid on a Solid Template. Biochemistry. 2007;46(20):6118-25.

465. Garzon-Rodriguez W, Yatsimirsky AK, Glabe CG. Binding of Zn(II), Cu(II), and Fe(II) ions to alzheimer's Aβ peptide studied by fluorescence. Bioorganic & Medicinal Chemistry Letters. 1999;9(15):2243-8.

466. Morgan DM, Dong J, Jacob J, Lu K, Apkarian RP, Thiyagarajan P, et al. Metal Switch for Amyloid Formation: Insight into the Structure of the Nucleus. Journal of the American Chemical Society. 2002;124(43):12644-5.

467. Li W, Zhang J, Su Y, Wang J, Qin M, Wang W. Effects of Zinc Binding on the Conformational Distribution of the Amyloid-β Peptide Based on Molecular Dynamics Simulations. Journal of Physical Chemistry. 2007;111(49):13814-21.

468. Han D, Wang H, Yang P. Molecular modeling of zinc and copper binding with Alzheimer's amyloid β-peptide. BioMetals. 2008;21(2):189-96.

469. Dong J, Canfield JM, Mehta AK, Shokes JE, Tian B, Childers WS, et al. Engineering metal ion coordination to regulate amyloid fibril assembly and toxicity. Proceedings of the National Academy of Sciences of the United States of America. 2007;104(33):13313-8.

470. Sangmi J, Sunil S. The Aggregated State of Amyloid-β Peptide *In Vitro* Depends on Cu^{2+} Ion Concentration. Angewandte Chemie International Edition in English. 2007;46(21):3959-61.

471. Liu B, Moloney A, Meehan S, Morris K, Thomas SE, Serpell LC, et al. Iron promotes the toxicity of amyloid β peptide by impeding its ordered aggregation. Journal of Biological Chemistry. 2011;286(6):4248-56.

472. Khmeleva SA, Mezentsev YV, Kozin SA, Tsvetkov PO, Ivanov AS, Bodoev NV, et al. Zinc-Induced Interaction of the Metal-Binding Domain of Amyloid-β Peptide with DNA. Journal of Alzheimer's Disease. 2013;36(4):633-6.

473. Baruch-Suchodolsky R, Fischer B. Soluble Amyloid β_{1-28}-Copper(I)/Copper(II)/Iron(II) Complexes Are Potent Antioxidants in Cell-Free Systems. Biochemistry. 2008;47(30):7796-806.

474. Jiang D, Li X, Williams R, Patel S, Men L, Wang Y, et al. Ternary Complexes of Iron, Amyloid-β, and Nitrilotriacetic Acid: Binding Affinities, Redox Properties, and Relevance to Iron-Induced Oxidative Stress in Alzheimer's Disease. Biochemistry. 2009;48(33):7939-47.

475. Huang X, Atwood CS, Hartshorn MA, Multhaup G, Goldstein LE, Scarpa RC, et al. The Aβ Peptide of Alzheimer's Disease Directly Produces Hydrogen Peroxide through Metal Ion Reduction. Biochemistry. 1999;38(24):7609-16.

476. Schubert D, Chevion M. The Role of Iron in β Amyloid Toxicity. Biochemical and Biophysical Research Communications. 1995;216(2):702-7.

477. Rottkamp CA, Raina AK, Zhu X, Gaier E, Bush AI, Atwood CS, et al. Redox-active iron mediates amyloid-β toxicity. Free Radical Biology and Medicine. 2001;30(4):447-50.

478. Huang X, Atwood CS, Moir RD, Hartshorn MA, Vonsattel J-P, Tanzi RE, et al. Zinc-induced Alzheimer's Aβ1-40 Aggregation Is Mediated by Conformational Factors. Journal of Biological Chemistry. 1997;272(42):26464-70.

479. Cherny RA, Legg JT, McLean CA, Fairlie DP, Huang X, Atwood CS, et al. Aqueous Dissolution of Alzheimer's Disease Aβ Amyloid Deposits by Biometal Depletion. Journal of Biological Chemistry. 1999;274(33):23223-8.

480. Huang X, Cuajungco MP, Atwood CS, Hartshorn MA, Tyndall JDA, Hanson GR, et al. Cu(II) Potentiation of Alzheimer Aβ Neurotoxicity. Correlation with Cell-Free Hydrogen Peroxide Production and Metal Reduction. Journal of Biological Chemistry. 1999;274(52):37111-6.

481. Cherny RA, Barnham KJ, Lynch T, Volitakis I, Li Q-X, McLean CA, et al. Chelation and Intercalation: Complementary Properties in a Compound for the Treatment of Alzheimer's Disease. Journal of Structural Biology. 2000;130(2-3):209-16.

482. Tõugu V, Karafin A, Palumaa P. Binding of zinc(II) and copper(II) to the full-length Alzheimer's amyloid-β peptide. Journal of Neurochemistry. 2008;104(5):1249-59.

483. Danielsson J, Pierattelli R, Banci L, Graslund A. High-resolution NMR studies of the zinc-binding site of the Alzheimer's amyloid β-peptide. FEBS Journal. 2007;274(1):46-59.

484. Gaggelli E, Janicka-Klos A, Jankowska E, Kozlowski H, Migliorini C, Molteni E, et al. NMR Studies of the Zn^{2+} Interactions with Rat and Human β-Amyloid (1-28) Peptides in Water-Micelle Environment. Journal of Physical Chemistry. 2008;112(1):100-9.

485. Yang D-S, McLaurin J, Qin K, Westaway D, Fraser PE. Examining the zinc binding site of the amyloid-β peptide. European Journal of Biochemistry. 2000;267(22):6692-8.

486. Curtain CC, Ali FE, Smith DG, Bush AI, Masters CL, Barnham KJ. Metal ions, pH, and cholesterol regulate the interactions of Alzheimer's disease amyloid-β peptide with membrane lipid. Journal of Biological Chemistry. 2003;278(5):2977-82.

487. Curtain CC, Ali F, Volitakis I, Cherny RA, Norton RS, Beyreuther K, et al. Alzheimer's Disease Amyloid-β Binds Copper and Zinc to Generate an Allosterically Ordered Membrane-penetrating Structure Containing Superoxide Dismutase-like Subunits. Journal of Biological Chemistry. 2001;276(23):20466-73.

488. Stellato F, Menestrina G, Serra M, Potrich C, Tomazzolli R, Meyer-Klaucke W, et al. Metal binding in amyloid β-peptides shows intra- and inter-peptide coordination modes. European Biophysics Journal. 2006;35(4):340-51.

489. Dong J, Atwood CS, Anderson VE, Siedlak SL, Smith MA, Perry G, et al. Metal binding and oxidation of amyloid-β within isolated senile plaque cores: Raman microscopic evidence. Biochemistry. 2003;42(10):2768-73.

490. Kowalik-Jankowska T, Ruta M, Wisniewska K, Lankiewicz L. Coordination abilities of the 1-16 and 1-28 fragments of β-amyloid peptide towards copper(II) ions: a combined potentiometric and spectroscopic study. Journal of Inorganic Biochemistry. 2003;95(4):270-82.

491. Zirah S, Rebuffat S, Kozin SA, Debey P, Fournier F, Lesage D, et al. Zinc binding properties of the amyloid fragment Aβ(1-16) studied by electrospray-ionization mass spectrometry. International Journal of Mass Spectrometry. 2003;228(2-3):999-1016.

492. Karr JW, Kaupp LJ, Szalai VA. Amyloid-β Binds Cu^{2+} in a Mononuclear Metal Ion Binding Site. Journal of the American Chemical Society. 2004;126(41):13534-8.

493. Karr JW, Szalai VA. Role of Aspartate-1 in Cu(II) Binding to the Amyloid-β Peptide of Alzheimer's Disease. Journal of the American Chemical Society. 2007;129(13):3796-7.

494. Bousejra-ElGarah F, Bijani C, Coppel Y, Faller P, Hureau C. Iron(II) Binding to Amyloid-β, the Alzheimer's Peptide. Inorganic Chemistry. 2011;50(18):9024-30.

495. Drew SC, Masters CL, Barnham KJ. Alanine-2 Carbonyl is an Oxygen Ligand in Cu^{2+} Coordination of Alzheimer's Disease Amyloid-β Peptide − Relevance to N-Terminally Truncated Forms. Journal of the American Chemical Society. 2009;131(25):8760-1.

496. Zirah S, Kozin SA, Mazur AK, Blond A, Cheminant M, Segalas-Milazzo I, et al. Structural Changes of Region 1-16 of the Alzheimer Disease Amyloid β-Peptide upon Zinc Binding and *in Vitro* Aging. Journal of Biological Chemistry. 2006;281(4):2151-61.

497. Dorlet P, Gambarelli S, Faller P, Hureau C. Pulse EPR Spectroscopy Reveals the Coordination Sphere of Copper(II) Ions in the 1-16 Amyloid-β Peptide: A Key Role of the First Two N-Terminus Residues. Angewandte Chemie International Edition. 2009;48(49):9273-6.

498. Drew SC, Noble CJ, Masters CL, Hanson GR, Barnham KJ. Pleomorphic Copper Coordination by Alzheimer's Disease Amyloid-β Peptide. Journal of the American Chemical Society. 2009;131(3):1195-207.

499. Hureau C, Coppel Y, Dorlet P, Solari PL, Sayen S, Guillon E, et al. Deprotonation of the Asp1-Ala2 Peptide Bond Induces Modification of the Dynamic Copper(II) Environment in the Amyloid-β Peptide near Physiological pH. Angewandte Chemie International Edition. 2009;48(50):9522-5.

500. Drew SC, Barnham KJ. The Heterogeneous Nature of Cu^{2+} Interactions with Alzheimer's Amyloid-β Peptide. Accounts of Chemical Research. 2011;44(11):1146-55.

501. Treiber C, Simons A, Strauss M, Hafner M, Cappai R, Bayer TA, et al. Clioquinol mediates copper uptake and counteracts Cu efflux activities of the amyloid precursor protein of Alzheimer's disease. Journal of Biological Chemistry. 2004;279:59158-1964.

502. Vaughan DW, Peters A. The structure of neuritic plaque in the cerebral cortex of aged rats. Journal of Neuropathology and Experimental Neurology. 1981;40(4):472-87.

503. Atamna H, Frey WH, Ko N. Human and rodent amyloid-β peptides differentially bind heme: Relevance to the human susceptibility to Alzheimer's disease. Archives of Biochemistry and Biophysics. 2009;487(1):59-65.

504. Moechars D, Dewachter I, Lorent K, Reverse D, Baekelandt V, Naidu A, et al. Early phenotypic changes in transgenic mice that overexpress different mutants of amyloid precursor protein in brain. Journal of Biological Chemistry. 1999;274(10):6483-92.

505. Hsiao K, Chapman P, Nilsen S, Eckman C, Harigaya Y, Younkin S, et al. Correlative memory deficits, Aβ elevation, and amyloid plaques in transgenic mice. Science. 1996;274(5284):99-102.

506. Phinney AL, Drisaldi B, Schmidt SD, Lugowski S, Coronado V, Liang Y, et al. *In vivo* reduction of amyloid-β by a mutant copper transporter. Proceedings of the National Academy of Sciences of the United States of America. 2003;100(24):14193-8.

507. Li QX, Maynard C, Cappai R, McLean CA, Cherny RA, Lynch T, et al. Intracellular accumulation of detergent-soluble amyloidogenic Aβ fragment of Alzheimer's disease precursor protein in the hippocampus of aged transgenic mice. Journal of Neurochemistry. 1999;72(6):2479-87.

508. Ciavardelli D, Consalvo A, Caldaralo V, Di Vacri ML, Nisi S, Corona C, et al. Characterisation of element profile changes induced by long-term dietary supplementation of zinc in the brain and cerebellum of 3xTg-AD mice by alternated cool and normal plasma ICP-MS. Metallomics. 2012;4(12):1321-32.

509. Zheng H, Jiang M, Trumbauer ME, Sirinathsinghji DJ, Hopkins R, Smith DW, et al. β-Amyloid precursor protein-deficient mice show reactive gliosis and decreased locomotor activity. Cell. 1995;81(4):525-31.

510. White AR, Reyes R, Mercer JFB, Camakaris J, Zheng H, Bush AI, et al. Copper levels are increased in the cerebral cortex and liver of APP and APLP2 knockout mice. Brain Research. 1999;842(2):439-44.

511. Pype S, Moechars D, Dillen L, Mercken M. Characterization of amyloid β peptides from brain extracts of transgenic mice overexpressing the London mutant of human amyloid precursor protein. Journal of Neurochemistry. 2003;84(3):602-9.

512. van Groen T, Kiliaan AJ, Kadish I. Deposition of mouse amyloid β in human APP/PS1 double and single AD model transgenic mice. Neurobiology of Disease. 2006;23(3):653-62.

513. Leskovjan AC, Lanzirotti A, Miller LM. Amyloid Plaques in PSAPP Mice Bind Less Metal than Plaques in Human Alzheimer's Disease. NeuroImage. 2009;47(4):1215-20.

514. Varela-Nallar L, Toledo EM, Larrondo LF, Cabral ALB, Martins VR, Inestrosa NC. Induction of cellular prion protein gene expression by copper in neurons. American Journal of Physiology - Cell Physiology. 2006;290(1):C271-C81.

515. Kralovicova S, Fontaine SN, Alderton A, Alderman J, Ragnarsdottir KV, Collins SJ, et al. The effects of prion protein expression on metal metabolism. Molecular and Cellular Neuroscience. 2009;41(2):135-47.

516. Pushie MJ, Pickering IJ, Martin GR, Tsutsui S, Jirik FR, George GN. Prion protein expression level alters regional copper, iron and zinc content in the mouse brain. Metallomics. 2011;3(2).

517. Chishti MA, Yang D-S, Janus C, Phinney AL, Horne P, Pearson J, et al. Early-onset Amyloid Deposition and Cognitive Deficits in Transgenic Mice Expressing a Double Mutant Form of Amyloid Precursor Protein 695. Journal of Biological Chemistry. 2001;276(24):21562-70.

518. Coronado V, Nanji M, Cox DW. The Jackson toxic milk mouse as a model for copper loading. Mammalian Genome. 2001;12(10):793-5.

519. Sturchler-Pierrat C, Abramowski D, Duke M, Wiederhold K-H, Mistl C, Rothacher S, et al. Two amyloid precursor protein transgenic mouse models with Alzheimer disease-like pathology. Proceedings of the National Academy of Sciences of the United States of America. 1997;94(24):13287-92.

520. Bayer TA, Schafer S, Simons A, Kemmling A, Kamer T, Tepest R, et al. Dietary Cu stabilizes brain superoxide dismutase 1 activity and reduces amyloid Aβ production in APP23 transgenic mice. Proceedings of the National Academy of Sciences of the United States of America. 2003;100(24):14187-92.

521. Kitazawa M, Cheng D, LaFerla FM. Chronic copper exposure exacerbates both amyloid and tau pathology and selectively dysregulates cdk5 in a mouse model of AD. Journal of Neurochemistry. 2009;108(6):1550-60.

522. Lu J, Zheng Y-l, Wu D-m, Sun D-x, Shan Q, Fan S-h. Trace amounts of copper induce neurotoxicity in the cholesterol-fed mice through apoptosis. FEBS Letters. 2006;580(28-29):6730-40.

523. Lu J, Wu DM, Zheng YL, Sun DX, Hu B, Shan Q, et al. Trace amounts of copper exacerbate β amyloid-induced neurotoxicity in the cholesterol-fed mice through TNF-mediated inflammatory pathway. Brain, Behavior, and Immunity. 2009;23(2):193-203.

524. McGowan E, Sanders S, Iwatsubo T, Takeuchi A, Saido T, Zehr C, et al. Amyloid Phenotype Characterization of Transgenic Mice Overexpressing both Mutant Amyloid Precursor Protein and Mutant Presenilin 1 Transgenes. Neurobiology of Disease. 1999;6(4):231-44.

525. Sparks DL, Friedland R, Petanceska S, Schreurs BG, Shi J, Perry G, et al. Trace copper levels in the drinking water, but not zinc or aluminum influence CNS Alzheimer-like pathology. Journal of Nutrition, Health and Aging. 2006;10(4):247-54.

526. Savonenko A, Xu GM, Melnikova T, Morton JL, Gonzales V, Wong MPF, et al. Episodic-like memory deficits in the APPswe/PS1dE9 mouse model of Alzheimer's disease: Relationships to β-amyloid deposition and neurotransmitter abnormalities. Neurobiology of Disease. 2005;18(3):602-17.

527. Manso Y, Comes G, Hidalgo J, Bush AI, Adlard PA. Copper Modulation as a Therapy for Alzheimer's Disease? International Journal of Alzheimer's Disease. 2011;2011.

528. Bolognin S, Pasqualetto F, Mucignat-Caretta C, Scancar J, Milacic R, Zambenedetti P, et al. Effects of a Copper-Deficient Diet on the Biochemistry, Neural Morphology and Behavior of Aged Mice. PLoS ONE. 2012;7(10):e47063.

529. Kessler H, Bayer T, Bach D, Schneider-Axmann T, Supprian T, Herrmann W, et al. Intake of copper has no effect on cognition in patients with mild Alzheimer's disease: a pilot phase 2 clinical trial. Journal of Neural Transmission. 2008;115(8):1181-7.

530. Kessler H, Pajonk F-G, Bach D, Schneider-Axmann T, Falkai P, Herrmann W, et al. Effect of copper intake on CSF parameters in patients with mild Alzheimer's disease: a pilot phase 2 clinical trial. Journal of Neural Transmission. 2008;115(12):1651-9.

531. Hung YH, Bush AI, La Fontaine S. Links between copper and cholesterol in Alzheimer's disease. Frontiers in Physiology. 2013;4.

532. Sparks DL, Schreurs BG. Trace amounts of copper in water induce β-amyloid plaques and learning deficits in a rabbit model of Alzheimer's disease. Proceedings of the National Academy of Sciences of the United States of America. 2003;100(19):11065-9.

533. Sparks DL, Ziolkowski C, Lawmaster T, Martin T. Influence of Water Quality on Cholesterol-Induced Tau Pathology: Preliminary Data. International Journal of Alzheimer's Disease. 2011;2011.

534. Lee JY, Cole TB, Palmiter RD, Suh SW, Koh JY. Contribution by synaptic zinc to the gender-disparate plaque formation in human Swedish mutant APP transgenic mice. Proceedings of the National Academy of Sciences of the United States of America. 2002;99(11):7705-10.

535. Friedlich AL, Lee J-Y, van Groen T, Cherny RA, Volitakis I, Cole TB, et al. Neuronal Zinc Exchange with the Blood Vessel Wall Promotes Cerebral Amyloid Angiopathy in an Animal Model of Alzheimer's Disease. Journal of Neuroscience. 2004;24(13):3453-9.

536. Stoltenberg M, Bush AI, Bach G, Smidt K, Larsen A, Rungby J, et al. Amyloid plaques arise from zinc-enriched cortical layers in APP/PS1 transgenic mice and are paradoxically enlarged with dietary zinc deficiency. Neuroscience. 2007;150(2):357-69.

537. Maynard CJ, Cappai R, Volitakis I, Laughton KM, Masters CL, Bush AI, et al. Chronic Exposure to High Levels of Zinc or Copper has Little Effect on Brain Metal Homeostasis or Aβ Accumulation in Transgenic APP-C100 Mice. Cellular and Molecular Neurobiology. 2009;29(5):757-67.

538. Corona C, Masciopinto F, Silvestri E, Viscovo AD, Lattanzio R, Sorda RL, et al. Dietary zinc supplementation of 3xTg-AD mice increases BDNF levels and prevents cognitive deficits as well as mitochondrial dysfunction. Cell Death and Disease. 2010;1(10):e91-e8.

539. Linkous DH, Adlard PA, Wanschura PB, Conko KM, Flinn JM. The effects of enhanced zinc on spatial memory and plaque formation in transgenic mice. Journal of Alzheimers Disease. 2009;18(3):565-79.

540. Railey AM, Groeber CM, Flinn JM. The Effect of Metals on Spatial Memory in a Transgenic Mouse Model of Alzheimer's Disease. Journal of Alzheimer's Disease. 2011;24(2):375-81.

541. Zhu Z, Sun Z-Y, Ye Y, Voigt J, Strickland C, Smith EM, et al. Discovery of Cyclic Acylguanidines as Highly Potent and Selective β-Site Amyloid Cleaving Enzyme (BACE) Inhibitors: Part I—Inhibitor Design and Validation. Journal of Medicinal Chemistry. 2010;53(3):951-65.

542. Zlokovic BV, Martel CL, Matsubara E, McComb JG, Zheng G, McCluskey RT, et al. Glycoprotein 330/megalin: Probable role in receptor-mediated transport of apolipoprotein J alone and in a complex with Alzheimer disease amyloid β at the blood-brain and blood-cerebrospinal fluid barriers. Proceedings of the National Academy of Sciences of the United States of America. 1996;93(9):4229-34.

543. Constantinidis J. Treatment of Alzheimer's disease by zinc compounds. Drug Development Research. 1992;27(1):1-14.

544. Brewer GJ. Zinc deficiency and zinc therapy in Alzheimer's disease. International Society for Zinc Biology (ISZB) Conference; St Kilda, Victoria, Australia 2012.

545. Bush AI, Tanzi RE. Therapeutics for Alzheimer's Disease Based on the Metal Hypothesis. Neurotherapeutics. 2008;5(3):421-32.

546. Bush AI. The Metal Theory of Alzheimer's Disease. Journal of Alzheimer's Disease. 2013;33(Supplement 1):S277-81.

547. Yoshiike Y, Tanemura K, Murayama O, Akagi T, Murayama M, Sato S, et al. New Insights on How Metals Disrupt Amyloid β -Aggregation and Their Effects on Amyloid-β Cytotoxicity. Journal of Biological Chemistry. 2001;276(34):32293-9.

548. Tew DJ, Bottomley SP, Smith DP, Ciccotosto GD, Babon J, Hinds MG, et al. Stabilization of neurotoxic soluble β-sheet-rich conformations of the Alzheimer's disease amyloid-β peptide. Biophysical Journal. 2007;94(7):2752-66.

549. Barnham KJ, Ciccotosto GD, Tickler AK, Ali FE, Smith DG, Williamson NA, et al. Neurotoxic, Redox-competent Alzheimer's β-Amyloid Is Released from Lipid Membrane by Methionine Oxidation. Journal of Biological Chemistry. 2003;278(44):42959-65.

550. Atwood CS, Perry G, Zeng H, Kato Y, Jones WD, Ling KQ, et al. Copper Mediates Dityrosine Cross-Linking of Alzheimer's Amyloid-β. Biochemistry. 2004;43(2):560-8.

551. Barnham KJ, Haeffner F, Ciccotosto GD, Curtain CC, Tew D, Mavros C, et al. Tyrosine gated electron transfer is key to the toxic mechanism of Alzheimer's disease β-amyloid. FASEB Journal. 2004;18(12):1427-9.

552. Hou L, Shao H, Zhang Y, Li H, Menon NK, Neuhaus EB, et al. Solution NMR Studies of the Aβ(1-40) and Aβ(1-42) Peptides Establish that the Met35 Oxidation State Affects the Mechanism of Amyloid Formation. Journal of the American Chemical Society. 2004;126(7):1992-2005.

553. Crouch PJ, Barnham KJ, Duce JA, Blake RE, Masters CL, Trounce IA. Copper-dependent inhibition of cytochrome c oxidase by $A\beta_{1-42}$ requires reduced methionine at residue 35 of the Aβ peptide. Journal of Neurochemistry. 2006;99(1):226-36.

554. Smith DP, Ciccotosto GD, Tew DJ, Fodero-Tavoletti MT, Johanssen T, Masters CL, et al. Concentration Dependent Cu^{2+} Induced Aggregation and Dityrosine Formation of the Alzheimer's Disease Amyloid-β Peptide. Biochemistry. 2007;46(10):2881-91.

555. Tõugu V, Karafin A, Zovo K, Chung RS, Howells C, West AK, et al. Zn(II)- and Cu(II)-induced non-fibrillar aggregates of amyloid-β (Aβ) peptide are transformed to amyloid fibrils, both spontaneously and under the influence of metal chelators. Journal of Neurochemistry. 2009;110(6):1784-95.

556. Tõugu V, Tiiman A, Palumaa P. Interactions of Zn(II) and Cu(II) ions with Alzheimer's amyloid-β peptide. Metal ion binding, contribution to fibrillization and toxicity. Metallomics. 2011;3(3):250-61.

557. Hureau C, Faller P. Aβ-mediated ROS production by Cu ions: Structural insights, mechanisms and relevance to Alzheimer's disease. Biochimie. 2009;91(10):1212-7.

558. Lau T-L, Ambroggio EE, Tew DJ, Cappai R, Masters CL, Fidelio GD, et al. Amyloid-β Peptide Disruption of Lipid Membranes and the Effect of Metal Ions. Journal of Molecular Biology. 2006;356(3):759-70.

559. Ciccotosto GD, Tew D, Curtain CC, Smith D, Carrington D, Masters CL, et al. Enhanced Toxicity and Cellular Binding of a Modified Amyloid β Peptide with a Methionine to Valine Substitution. Journal of Biological Chemistry. 2004;279(41):42528-34.

560. Barnham KJ, Masters CL, Bush AI. Neurodegenerative diseases and oxidative stress. Nature Reviews Drug Discovery. 2004;3(3):205-14.

561. Atwood CS, Huang X, Moir RD, Tanzi RE, Bush AI. Role of free radicals and metal ions in the pathogenesis of Alzheimer's disease. Metal Ions in Biological Systems. 1999;36:309-64.

562. Sayre LM, Perry G, Harris PLR, Liu Y, Schubert KA, Smith MA. *In Situ* Oxidative Catalysis by Neurofibrillary Tangles and Senile Plaques in Alzheimer's Disease. Journal of Neurochemistry. 2000;74(1):270-9.

563. Huang X, Atwood CS, Moir RD, Hartshorn MA, Tanzi RE, Bush AI. Trace metal contamination initiates the apparent auto-aggregation, amyloidosis, and oligomerization of Alzheimer's Aβ peptides. Journal of Biological Inorganic Chemistry. 2004;9(8):954-60.

564. Masayoshi Y, Masatsugu K, Shoji O. Role of zinc as an activator of mitochondrial function in rat liver. Biochemical Pharmacology. 1982;31(7):1289-93.

565. Rossi L, Lombardo M, Ciriolo M, Rotilio G. Mitochondrial Dysfunction in Neurodegenerative Diseases Associated with Copper Imbalance. Neurochemical Research. 2004;29(3):493-504.

566. Ortiz E, Pasquini JM, Thompson K, Felt B, Butkus G, Beard J, et al. Effect of manipulation of iron storage, transport, or availability on myelin composition and brain iron content in three different animal models. Journal of Neuroscience Research. 2004;77(5):681-9.

567. Smart TG, Hosie AM, Miller PS. Zn^{2+} Ions: Modulators of Excitatory and Inhibitory Synaptic Activity. Neuroscientist. 2004;10(5):432-42.

568. Bhatnagara S, Tanejaa S. Zinc and cognitive development. British Journal of Nutrition. 2001;85(Supplement 2):S139-45

569. Takeda A. Zinc homeostasis and functions of zinc in the brain. BioMetals. 2001;14(3):343-51.

570. Gaeta A, Hider RC. The crucial role of metal ions in neurodegeneration: the basis for a promising therapeutic strategy. British Journal of Pharmacology. 2005;146(8):1041-59.

571. Que EL, Domaille DW, Chang CJ. Metals in Neurobiology: Probing Their Chemistry and Biology with Molecular Imaging. Chemical Reviews. 2008;108(5):1517-49.

572. Bush AI, Curtain C. Twenty years of metallo-neurobiology: where to now? European Biophysics Journal. 2008;37(3):241-5.

573. Bush AI. Metal complexing agents as therapies for Alzheimer's disease. Neurobiology of Aging. 2002;23(6):1031-8.

574. Finefrock AE, Bush AI, Doraiswamy PM. Current Status of Metals as Therapeutic Targets in Alzheimer's Disease. Journal of the American Geriatrics Society. 2003;51(8):1143-8.

575. Crouch PJ, White AR, Bush AI. The modulation of metal bio-availability as a therapeutic strategy for the treatment of Alzheimer's disease. FEBS Journal. 2007;274(15):3775-83.

576. Brown DR. Interactions between metals and α-synuclein - function or artefact? FEBS Journal. 2007;274(15):3766-74.

577. Doraiswamy PM, Finefrock AE. Metals in our minds: therapeutic implications for neurodegenerative disorders. Lancet Neurology. 2004;3(7):431-4.

578. Behl C, Moosmann B. Antioxidant neuroprotection in Alzheimer's disease as preventive and therapeutic approach. Free Radical Biology and Medicine. 2002;33(2):182-91.

579. Zatta P, Tognon G, Carampin P. Melatonin prevents free radical formation due to the interaction between β-amyloid peptides and metal ions [Al(III), Zn(II), Cu(II), Mn(II), Fe(II)]. Journal of Pineal Research. 2003;35(2):98-103.

580. Shishodia S, Sethi G, Aggarwal BB. Curcumin: Getting Back to the Roots. Annals of the New York Academy of Sciences. 2005;1056(1):206-17.

581. Defeudis FV. Bilobalide and neuroprotection. Pharmacological Research. 2002;46(6):565-8.

582. Matsubara E, Bryant-Thomas T, Pacheco Quinto J, Henry TL, Poeggeler B, Herbert D, et al. Melatonin increases survival and inhibits oxidative and amyloid pathology in a transgenic model of Alzheimer's disease. Journal of Neurochemistry. 2003;85(5):1101-8.

583. Feng Z, Chang Y, Cheng Y, Zhang B-l, Qu Z-w, Qin C, et al. Melatonin alleviates behavioral deficits associated with apoptosis and cholinergic system dysfunction in the APP 695 transgenic mouse model of Alzheimer's disease. Journal of Pineal Research. 2004;37(2):129-36.

584. Yang F, Lim GP, Begum AN, Ubeda OJ, Simmons MR, Ambegaokar SS, et al. Curcumin Inhibits Formation of Amyloid β Oligomers and Fibrils, Binds Plaques, and Reduces Amyloid *in Vivo*. Journal of Biological Chemistry. 2005;280(7):5892-901.

585. Cheng Y, Feng Z, Zhang Q-z, Zhang J-t. Beneficial effects of melatonin in experimental models of Alzheimer disease. Acta Pharmacologica Sinica. 2006;27(2):129-39.

586. Oken BS, Storzbach DM, Kaye JA. The Efficacy of Ginkgo biloba on Cognitive Function in Alzheimer Disease. Archives of Neurology. 1998;55(11):1409-15.

587. Zandi PP, Anthony JC, Khachaturian AS, Stone SV, Gustafson D, Tschanz JT, et al. Reduced Risk of Alzheimer Disease in Users of Antioxidant Vitamin Supplements: The Cache County Study. Archives of Neurology. 2004;61(1):82-8.

588. Schneider LS, DeKosky ST, Farlow MR, Tariot PN, Hoerr R, Kieser M. A Randomized, Double-Blind, Placebo-Controlled Trial of Two Doses of Ginkgo Biloba Extract in Dementia of the Alzheimer's Type. Current Alzheimer Research. 2005;2(5):541-51.

589. Cavalli A, Bolognesi ML, Capsoni S, Andrisano V, Bartolini M, Margotti E, et al. A Small Molecule Targeting the Multifactorial Nature of Alzheimer's Disease. Angewandte Chemie International Edition. 2007;46(20):3689-92.

590. Bolognesi ML, Cavalli A, Melchiorre C. Memoquin: A Multi-Target-Directed Ligand as an Innovative Therapeutic Opportunity for Alzheimer's Disease. Neurotherapeutics. 2009;6(1):152-62.

591. Keberle H. The biochemistry of desferrioxamine and its relation to iron metabolism. Annals of the New York Academy of Sciences. 1964;119:758-68.

592. McLachlan DRC, Dalton AJ. Intramuscular desferrioxamine in patients with Alzheimer's disease. Lancet. 1991;337(8753):1304-8.

593. Cuajungco MP, Faget KY, Huang X, Tanzi RE, Bush AI. Metal chelation as a potential therapy for Alzheimer's disease. Annals of the New York Academy of Sciences. 2000;920:292-304.

594. May PM, Bulman RA. The present status of chelating agents in medicine. Progress in Medicinal Chemistry. 1983;20:225-336.

595. Fine JM, Baillargeon AM, Renner DB, Hoerster NS, Tokarev J, Colton S, et al. Intranasal deferoxamine improves performance in radial arm water maze, stabilizes HIF-1α, and phosphorylates GSK3β in P301L tau transgenic mice. Experimental Brain Research. 2012;219(3):381-90.

596. Angel I, Bar A, Horovitz T, Taler G, Krakovsky M, Resnitsky D, et al. Metal ion chelation in neurodegenerative disorders. Drug Development Research. 2002;56(3):300-9.

597. Kolusheva S, Friedman J, Angel I, Jelinek R. Membrane Interactions and Metal Ion Effects on Bilayer Permeation of the Lipophilic Ion Modulator DP-109. Biochemistry. 2005;44(36):12077-85.

598. Lee J-Y, Friedman JE, Angel I, Kozak A, Koh J-Y. The lipophilic metal chelator DP-109 reduces amyloid pathology in brains of human β-amyloid precursor protein transgenic mice. Neurobiology of Aging. 2004;25(10):1315-21.

599. Hua H, Münter L, Harmeier A, Georgiev O, Multhaup G, Schaffner W. Toxicity of Alzheimer's disease-associated Aβ peptide is ameliorated in a Drosophila model by tight control of zinc and copper availability. Biological Chemistry. 2011;392(10):919-26.

600. Petri S, Calingasan NY, Alsaied OA, Wille E, Kiaei M, Friedman JE, et al. The lipophilic metal chelators DP-109 and DP-460 are neuroprotective in a transgenic mouse model of amyotrophic lateral sclerosis. Journal of Neurochemistry. 2007;102(3):991-1000.

601. Moret V, Laras Y, Pietrancosta N, Garino C, Quelever G, Rolland A, et al. 1,1'-Xylyl bis-1,4,8,11-tetraaza cyclotetradecane: A new potential copper chelator agent for neuroprotection in Alzheimer's disease. Its comparative effects with clioquinol on rat brain copper distribution. Bioorganic & Medicinal Chemistry Letters. 2006;16(12):3298-301.

602. Liu G, Garrett MR, Men P, Zhu X, Perry G, Smith MA. Nanoparticle and other metal chelation therapeutics in Alzheimer disease. Biochimica et Biophysica Acta (BBA) - Molecular Basis of Disease. 2005;1741(3):246-52.

603. Liu G, Men P, Harris PLR, Rolston RK, Perry G, Smith MA. Nanoparticle iron chelators: A new therapeutic approach in Alzheimer disease and other neurologic disorders associated with trace metal imbalance. Neuroscience Letters. 2006;406(3):189-93.

604. Cui Z, Lockman PR, Atwood CS, Hsu C-H, Gupte A, Allen DD, et al. Novel D-penicillamine carrying nanoparticles for metal chelation therapy in Alzheimer's and other CNS diseases. European Journal of Pharmaceutics and Biopharmaceutics. 2005;59(2):263-72.

605. Mufamadi MS, Choonara YE, Kumar P, Modi G, Naidoo D, Ndesendo VK, et al. Surface-Engineered Nanoliposomes by Chelating Ligands for Modulating the Neurotoxicity Associated with β-Amyloid Aggregates of Alzheimer's disease. Pharmaceutical Research. 2012;29(11):3075-89.

606. Liu G, Men P, Kudo W, Perry G, Smith MA. Nanoparticle-chelator conjugates as inhibitors of amyloid-β aggregation and neurotoxicity: A novel therapeutic approach for Alzheimer disease. Neuroscience Letters. 2009;455(3):187-90.

607. Donnelly PS, Caragounis A, Du T, Laughton KM, Volitakis I, Cherny RA, et al. Selective Intracellular Release of Copper and Zinc Ions from Bis(thiosemicarbazonato) Complexes Reduces Levels of Alzheimer Disease Amyloid-β Peptide. Journal of Biological Chemistry. 2008;283(8):4568-77.

608. Crouch PJ, Hung LW, Adlard PA, Cortes M, Lal V, Filiz G, et al. Increasing Cu bioavailability inhibits Aβ oligomers and tau phosphorylation. Proceedings of the National Academy of Sciences of the United States of America. 2009;106(2):381-6.

609. Treiber C, Quadir MA, Voigt P, Radowski M, Xu S, Munter L-M, et al. Cellular Copper Import by Nanocarrier Systems, Intracellular Availability, and Effects on Amyloid β Peptide Secretion. Biochemistry. 2009;48(20):4273-84.

610. Schreck R, Meier B, Mannel DN, Droge W, Baeuerle PA. Dithiocarbamates as potent inhibitors of nuclear factor κ B activation in intact cells. Journal of Experimental Medicine. 1992;175(5):1181-94.

611. Liu SF, Ye X, Malik AB. Inhibition of NF-κB Activation by Pyrrolidine Dithiocarbamate Prevents *In Vivo* Expression of Proinflammatory Genes. Circulation. 1999;100(12):1330-7.

612. Hayakawa M, Miyashita H, Sakamoto I, Kitagawa M, Tanaka H, Yasuda H, et al. Evidence that reactive oxygen species do not mediate NF-κB activation. EMBO Journal. 2003;22(13):3356-66.

613. Nobel CSI, Kimland M, Lind B, Orrenius S, Slater AFG. Dithiocarbamates Induce Apoptosis in Thymocytes by Raising the Intracellular Level of Redox-active Copper. Journal of Biological Chemistry. 1995;270(44):26202-8.

614. Nobel CSI, Burgess DH, Zhivotovsky B, Burkitt MJ, Orrenius S, Slater AFG. Mechanism of Dithiocarbamate Inhibition of Apoptosis: Thiol Oxidation by Dithiocarbamate Disulfides Directly Inhibits Processing of the Caspase-3 Proenzyme. Chemical Research in Toxicology. 1997;10(6):636-43.

615. Verhaegh GW, Richard MJ, Hainaut P. Regulation of p53 by metal ions and by antioxidants: dithiocarbamate down-regulates p53 DNA-binding activity by increasing the intracellular level of copper. Molecular and Cellular Biology. 1997;17(10):5699-706.

616. Burkitt MJ, Bishop HS, Milne L, Tsang SY, Provan GJ, Nobel CSI, et al. Dithiocarbamate Toxicity toward Thymocytes Involves Their Copper-Catalyzed Conversion to Thiuram Disulfides, Which Oxidize Glutathione in a Redox Cycle without the Release of Reactive Oxygen Species. Archives of Biochemistry and Biophysics. 1998;353(1):73-84.

617. Kim CH, Kim JH, Hsu CY, Ahn YS. Zinc is required in pyrrolidine dithiocarbamate inhibition of NF-κB activation. FEBS Letters. 1999;449(1):28-32.

618. Iseki A, Kambe F, Okumura K, Niwata S, Yamamoto R, Hayakawa T, et al. Pyrrolidine Dithiocarbamate Inhibits TNF-α-Dependent Activation of NF-κB by Increasing Intracellular Copper Level in Human Aortic Smooth Muscle Cells. Biochemical and Biophysical Research Communications. 2000;276(1):88-92.

619. Furuta S, Ortiz F, Zhu Sun X, Wu H-H, Mason A, Momand J. Copper uptake is required for pyrrolidine dithiocarbamate-mediated oxidation and protein level increase of p53 in cells. Biochemical Journal. 2002;365(3):639-48.

620. Zhang X, Luhrs KJ, Ryff KA, Malik WT, Driscoll MJ, Culver B. Suppression of NF-κB ameliorates astrogliosis but not amyloid burden in APPswe/PS1dE9 Mice. Neuroscience. 2009;161(1):53-8.

621. Daniel K, Chen D, Orlu S, Cui Q, Miller F, Dou QP. Clioquinol and pyrrolidine dithiocarbamate complex with copper to form proteasome inhibitors and apoptosis inducers in human breast cancer cells. Breast Cancer Research. 2005;7(6):R897-R908.

622. Ding W-Q, Yu H-J, Lind SE. Zinc-binding compounds induce cancer cell death via distinct modes of action. Cancer Letters. 2008;271(2):251-9

623. Milacic V, Chen D, Giovagnini L, Diez A, Fregona D, Dou QP. Pyrrolidine dithiocarbamate-zinc(II) and -copper(II) complexes induce apoptosis in tumor cells by inhibiting the proteasomal activity. Toxicology and Applied Pharmacology. 2008;231(1):24-33.

624. Dearling J, Lewis J, Mullen G, Welch M, Blower P. Copper bis(thiosemicarbazone) complexes as hypoxia imaging agents: structure-activity relationships. Journal of Biological Inorganic Chemistry. 2002;7(3):249-59.

625. Fodero-Tavoletti MT, Villemagne VL, Paterson BM, White AR, Li QX, Camakaris J, et al. Bis(thiosemicarbazonato) Cu-64 complexes for positron emission tomography imaging of Alzheimer's disease. Journal of Alzheimer's Disease. 2010;20(1):49-55.

626. Petering DH. Concerning the role of zinc in the antitumor activity of 3-ethoxy-2-oxobutyraldehyde bis(thiosemicarbazonato) zinc(II) and related chelates. Biochemical Pharmacology. 1974;23(3):567-76.

627. Beraldo H, Gambino D. The wide pharmacological versatility of semicarbazones, thiosemicarba-zones and their metal complexes. Mini Reviews In Medicinal Chemistry. 2004;4(1):31-9.

628. Maurer RI, Blower PJ, Dilworth JR, Reynolds CA, Zheng Y, Mullen GED. Studies on the Mechanism of Hypoxic Selectivity in Copper Bis(Thiosemicarbazone) Radiopharmaceuticals. Journal of Medicinal Chemistry. 2002;45(7):1420-31.

629. Lewis JS, Laforest R, Buettner TL, Song S-K, Fujibayashi Y, Connett JM, et al. Copper-64-diacetyl-bis(N 4 -methylthiosemicarbazone): An agent for radiotherapy. Proceedings of the National Academy of Sciences of the United States of America. 2001;98(3):1206-11.

630. Cowley AR, Davis J, Dilworth JR, Donnelly PS, Dobson R, Nightingale A, et al. Fluorescence studies of the intra-cellular distribution of zinc bis(thiosemicarbazone) complexes in human cancer cells. Chemical Communications. 2005(7):845-7.

631. Holland JP, Aigbirhio FI, Betts HM, Bonnitcha PD, Burke P, Christlieb M, et al. Functionalized Bis(thiosemicarbazonato) Complexes of Zinc and Copper: Synthetic Platforms Toward Site-Specific Radiopharmaceuticals. Inorganic Chemistry. 2007;46(2):465-85.

632. Fujibayashi Y, Taniuchi H, Yonekura Y, Ohtani H, Konishi J, Yokoyama A. Copper-62-ATSM: A New Hypoxia Imaging Agent with High Membrane Permeability and Low Redox Potential. Journal of Nuclear Medicine. 1997;38(7):1155-60.

633. Vavere AL, Lewis JS. Cu-ATSM: A radiopharmaceutical for the PET imaging of hypoxia. Dalton Transactions. 2007(43):4893-902.

634. Kraker A, Krezoski S, Schneider J, Minkel D, Petering DH. Reaction of 3-ethoxy-2-oxobutyraldehyde bis(thiosemicarbazonato) Cu(II) with Ehrlich cells. Binding of copper to metallothionein and its relationship to zinc metabolism and cell proliferation. Journal of Biological Chemistry. 1985;260(25):13710-8.

635. Xiao Z, Donnelly PS, Zimmermann M, Wedd AG. Transfer of Copper between Bis(thiosemicarbazone) Ligands and Intracellular Copper-Binding Proteins. Insights into Mechanisms of Copper Uptake and Hypoxia Selectivity. Inorganic Chemistry. 2008;47(10):4338-47.

636. Morris RGM. Spatial localization does not require the presence of local cues. Learning and Motivation. 1981;12(2):239-60.

637. Olton DS, Samuelson RJ. Remembrance of Places Passed: Spatial Memory in Rats. Journal of Experimental Psychology Animal Behavior Processes. 1976;2(2):97-116.

638. Hung LW, Ciccotosto GD, Giannakis E, Tew DJ, Perez K, Masters CL, et al. Amyloid-β Peptide (Aβ) Neurotoxicity Is Modulated by the Rate of Peptide Aggregation: Aβ Dimers and Trimers Correlate with Neurotoxicity. Journal of Neuroscience. 2008;28(46):11950-8.

639. Barnham KJ, Kenche VB, Ciccotosto GD, Smith DP, Tew DJ, Liu X, et al. Platinum-based inhibitors of amyloid-β as therapeutic agents for Alzheimer's disease.

Proceedings of the National Academy of Sciences of the United States of America. 2008;105(19):6813-8.

640. Ma G, Huang F, Pu X, Jia L, Jiang T, Li L, et al. Identification of [PtCl2(phen)] Binding Modes in Amyloid-β Peptide and the Mechanism of Aggregation Inhibition. Chemistry – A European Journal. 2011;17(41):11657-66.

641. Kenche VB, Hung LW, Perez K, Volitakes I, Ciccotosto G, Kwok J, et al. Development of a Platinum Complex as an anti-Amyloid Agent for the Therapy of Alzheimer's Disease. Angewandte Chemie International Edition. 2013;52(12):3374-8.

642. Dedeoglu A, Cormier K, Payton S, Tseitlin KA, Kremsky JN, Lai L, et al. Preliminary studies of a novel bifunctional metal chelator targeting Alzheimer's amyloidogenesis. Experimental Gerontology. 2004;39(11-12):1641-9.

643. Choi JS, Braymer JJ, Nanga RP, Ramamoorthy A, Lim MH. Design of small molecules that target metal-Aβ species and regulate metal-induced Aβ aggregation and neurotoxicity. Proceedings of the National Academy of Sciences of the United States of America. 2010;107(51):21990-5.

644. Hindo SS, Mancino AM, Braymer JJ, Liu Y, Vivekanandan S, Ramamoorthy A, et al. Small Molecule Modulators of Copper-Induced Aβ Aggregation. Journal of the American Chemical Society. 2009;131(46):16663-5.

645. Rodríguez-Rodríguez C, Sánchez de Groot N, Rimola A, Álvarez--Larena An, Lloveras V, Vidal-Gancedo J, et al. Design, Selection, and Characterization of Thioflavin-Based Intercalation Compounds with Metal Chelating Properties for Application in Alzheimer's Disease. Journal of the American Chemical Society. 2009;131(4):1436-51.

646. Bolognesi ML, Cavalli A, Valgimigli L, Bartolini M, Rosini M, Andrisano V, et al. Multi-Target-Directed Drug Design Strategy: From a Dual Binding Site Acetylcholinesterase Inhibitor to a Trifunctional Compound against Alzheimer's Disease. Journal of Medicinal Chemistry. 2007;50(26):6446-9.

647. Fernández-Bachiller MaI, Pérez Cn, González-Muñoz GC, Conde S, López MG, Villarroya M, et al. Novel Tacrine−8-Hydroxyquinoline Hybrids as Multifunctional Agents for the Treatment of Alzheimer's Disease, with Neuroprotective, Cholinergic, Antioxidant, and Copper-Complexing Properties. Journal of Medicinal Chemistry. 2010;53(13):4927-37.

648. Rizzo S, Bisi A, Bartolini M, Mancini F, Belluti F, Gobbi S, et al. Multi-target strategy to address Alzheimer's disease: Design, synthesis and biological evaluation of new tacrine-based dimers. European Journal of Medicinal Chemistry. 2011;46(9):4336-43.

649. Weinstock M, Bejar C, Wang RH, Poltyrev T, Gross A, Finberg JP, et al. TV3326, a novel neuroprotective drug with cholinesterase and monoamine oxidase inhibitory activities for the treatment of Alzheimer's disease. Journal of Neural Transmission Supplementum. 2000(60):157-69.

650. Weinreb O, Amit T, Bar-Am O, Youdim MBH. Induction of Neurotrophic Factors GDNF and BDNF Associated with the Mechanism of Neurorescue Action of Rasagiline and Ladostigil. Annals of the New York Academy of Sciences. 2007;1122(1):155-68.

651. Zheng H, Weiner LM, Bar-Am O, Epsztejn S, Cabantchik ZI, Warshawsky A, et al. Design, synthesis, and evaluation of novel bifunctional iron-chelators as potential agents for neuroprotection in Alzheimer's, Parkinson's, and other neurodegenerative diseases. Bioorganic & Medicinal Chemistry. 2005;13(3):773-83.

652. Zheng H, Gal S, Weiner LM, Bar-Am O, Warshawsky A, Fridkin M, et al. Novel multifunctional neuroprotective iron chelator-monoamine oxidase inhibitor drugs for neurodegenerative diseases: *in vitro* studies on antioxidant activity, prevention of lipid peroxide formation and monoamine oxidase inhibition. Journal of Neurochemistry. 2005;95(1):68-78.

653. Gal S, Zheng H, Fridkin M, Youdim MBH. Novel multifunctional neuroprotective iron chelator-monoamine oxidase inhibitor drugs for neurodegenerative diseases. *In vivo* selective brain monoamine oxidase inhibition and prevention of MPTP-induced striatal dopamine depletion. Journal of Neurochemistry. 2005;95(1):79-88.

654. Kupershmidt L, Weinreb O, Amit T, Mandel S, Bar-Am O, Youdim MBH. Novel molecular targets of the multi-functional brain-permeable iron chelating drug M30 in mouse brain. Neuroscience. 2011;189:345–58.

655. Yogev-Falach M, Amit T, Bar-Am O, Weinstock M, Youdim MBH. The involvement of mitogen-activated protein (MAP) kinase in the regulation of amyloid precursor protein processing by novel cholinesterase inhibitors derived from rasagiline. FASEB Journal. 2002;16(12):1674-6.

656. Bar-Am O, Yogev-Falach M, Amit T, Sagi Y, Youdim MBH. Regulation of protein kinase C by the anti-Parkinson drug, MAO-B inhibitor, rasagiline and its derivatives, *in vivo*. Journal of Neurochemistry. 2004;89(5):1119-25.

657. Yogev-Falach M, Bar-Am O, Amit T, Weinreb O, Youdim MBH. A multifunctional, neuroprotective drug, ladostigil (TV3326), regulates holo-APP translation and processing. FASEB Journal. 2006;20(12):2177-9.

658. Avramovich-Tirosh Y, Reznichenko L, Amit T, Zheng H, Fridkin M, Weinreb O, et al. Neurorescue Activity, APP Regulation and Amyloid-β Peptide Reduction by Novel Multi-Functional Brain Permeable Iron- Chelating- Antioxidants,M-30 and Green Tea Polyphenol, EGCG. Current Alzheimer Research. 2007;4(4):403-11.

659. Avramovich-Tirosh Y, Amit T, Bar-Am O, Zheng H, Fridkin M, Youdim MBH. Therapeutic targets and potential of the novel brain-permeable multifunctional iron chelator-monoamine oxidase inhibitor drug, M-30, for the treatment of Alzheimer's disease. Journal of Neurochemistry. 2007;100(2):490-502.

660. Avraham Pharmaceuticals [Available from: http://www.avphar.com/ladostigil/clinical-data/.

661. Masters CL, Beyreuther K. Alzheimer's centennial legacy: prospects for rational therapeutic intervention targeting the Aβ amyloid pathway. Brain. 2006;129(11):2823-39.

662. Hayashi M, Fuwa T, Awazu S, Hanano M. Differences in species of iodochlorhydroxyquin absorption, metabolism, and excretion. Chemical & Pharmaceutical Bulletin. 1976;24(11):2589-96.

663. Liewendahl K, Lamberg BA. Metabolism of 125-iodochloroxyquinoline in man. I. Absorption, binding and excretion. Nuclear-Medizin. 1967;6(1):20-31.

664. Liewendahl K, Kivikangas V, Lamberg BA. Metabolism of 125-iodochloroxyquinoline in man. II. Metabolites in plasma, urine and faeces. Nuclear-Medizin. 1967;6(1):32-43.

665. Kotaki H, Yamamura Y, Tanimura Y, Saitoh Y, Nakagawa F, Tamura Z. Intestinal absorption and metabolism of clioquinol in the rat. Journal of Pharmacobio-dynamics. 1983;6(11):881-7.

666. Kotaki H, Yamamura Y, Tanimura Y, Saitoh Y, Nakagawa F, Tamura Z. Determination of chinoform and its metabolites in plasma by gas chromatography--mass spectrometry. Chemical & Pharmaceutical Bulletin. 1983;31(1):299-304.

667. Bondiolotti GP, Pollera C, Pirola R, Bareggi SR. Determination of 5-chloro-7-iodo-8-quinolinol (clioquinol) in plasma and tissues of hamsters by high-performance liquid chromatography and electrochemical detection. Journal of Chromatography B: Biomedical Sciences and Applications. 2006;837(1-2):87-91.

668. Bondiolotti G, Sala M, Pollera C, Gervasoni M, Puricelli M, Ponti W, et al. Pharmacokinetics and distribution of clioquinol in golden hamsters. Journal of Pharmacy and Pharmacology. 2007;59(3):387-93.

669. Neldner KH, Hambidge KM. Zinc therapy of acrodermatitis enteropathica. New England Journal of Medicine. 1975;292(17):879-82.

670. Flagstad T. Intestinal absorption of 65 Zinc in A46 (Adema disease) after treatment with oxychinolines. Nordisk Veterinar Medicine. 1977;29(2):96-100.

671. Geiser J, De Lisle RC, Finkelstein D, Adlard PA, Bush AI, Andrews GK. Clioquinol Synergistically Augments Rescue by Zinc Supplementation in a Mouse Model of Acrodermatitis Enteropathica. PLoS ONE. 2013;8(8):e72543.

672. David NA, Johnstone HG, Reed AC, Leake CD. The treatment of amebiasis with iodochlorhydroxyquinoline (vioform n. n. r.). Journal of the American Medical Association. 1933;100(21):1658-61.

673. Gholz LM, Arons WL. Prophylaxis and Therapy of Amebiasis and Shigellosis with Iodochlorhydroxyquin. American Journal of Tropical Medicine and Hygiene. 1964;13(3):396-401.

674. Richards DA. Prophylactic value of clioquinol against travellers' diarrhoea. Lancet. 1971;297(7688):44-5.

675. Clioquinol and neurological disease. British Medical Journal. 1971;2(5757):291-2.

676. Osterman PO. Myelopathy after clioquinol treatment. Lancet. 1971;2(7723):544.

677. Shimada Y, Tsuji T, Igata A, Steinitz H. Halogenated oxyquinoline derivatives and neurological syndromes. Lancet. 1971;298(7714):41-3.

678. Tsubaki T, Honma Y, Hoshi M. Neurological syndrome associated with clioquinol. Lancet. 1971;297(7701):696-7.

679. . Japanese Journal of Medical Science and Biology. 1975;28(Supplement 1):1-293.

680. Mumenthaler M, Kaeser HE, Meyer A, Hess T. Transient global amnesia after clioquinol: five personal observations from outside Japan. Journal of Neurology, Neurosurgery & Psychiatry. 1979;42(12):1084-90.

681. Kaeser HE. Transient global amnesia due to clioquinol. Acta Neurologica Scandinavica Supplementum. 1984(Supplement 100):175-83.

682. Ferrier TM, Schwieger AC, Eadie MJ. Delayed onset of partial epilepsy of temporal lobe origin following acute clioquinol encephalopathy. Journal of Neurology, Neurosurgery & Psychiatry. 1987;50(1):93-5.

683. Tateishi J. Subacute myelo-optico-neuropathy: Clioquinol intoxication in humans and animals. Neuropathology. 2000;20:S20-S4.

684. Konagaya M, Matsumoto A, Takase S, Mizutani T, Sobue G, Konishi T, et al. Clinical analysis of longstanding subacute myelo-optico-neuropathy: sequelae of clioquinol at 32 years after its ban. Journal of the Neurological Sciences. 2004;218(1-2):85-90.

685. Nakae K, Yamamoto S-I, Shigematsu I, Kono R. Relation between subacute myelo-optic neuropathy (S.M.O.N.) and clioquinol: nationwide survey. Lancet. 1973;301(7796):171-3.

686. Ohtsuka K, Ohishi N, Eguchi G, Yagi K. Degeneration of retinal neuroblasts by chinoform-ferric chelate. Cellular and Molecular Life Sciences. 1982;38(1):120-2.

687. Yagi K, Ohtsuka K, Ohishi N. Lipid peroxidation caused by chinoform-ferric chelate in cultured neural retinal cells. Cellular and Molecular Life Sciences. 1985;41(12):1561-3.

688. Yagi Y, Matsuda M, Yagi K. Formation of lipoperoxide in isolated sciatic nerve by chinoform-ferric chelate. Cellular and Molecular Life Sciences. 1976;32(7):905-6.

689. Arbiser JL, Kraeft SK, van Leeuwen R, Hurwitz SJ, Selig M, Dickersin GR, et al. Clioquinol-zinc chelate: a candidate causative agent of subacute myelo-optic neuropathy. Molecular Medicine 1998;4(10):665-70.

690. Kumar N, Knopman DS. SMON, clioquinol, and copper. Postgraduate Medical Journal. 2005;81(954):227.

691. Yassin MS, Ekblom J, fberg C, Oreland L. Transmethylation Reactions and Autoradiographic Distribution of Vitamin B12: Effects of Clioquinol Treatment in Mice. Japanese Journal of Pharmacology. 1998;78(1):55-61.

692. Yassin MS, Ekblom J, Xilinas M, Gottfries CG, Oreland L. Changes in uptake of vitamin B12 and trace metals in brains of mice treated with clioquinol. Journal of the Neurological Sciences. 2000;173(1):40-4.

693. Wadia NH. Some observations on SMON from Bombay. Journal of Neurology, Neurosurgery & Psychiatry. 1977;40(3):268-75.

694. DiVaira M, Bazzicalupi C, Orioli P, Messori L, Bruni B, Zatta P. Clioquinol, a Drug for Alzheimer's Disease Specifically Interfering with Brain Metal Metabolism: Structural Characterization of Its Zinc(II) and Copper(II) Complexes. Inorganic Chemistry. 2004;43(13):3795-7.

695. Ferrada E, Arancibia V, Loeb B, Norambuena E, Olea-Azar C, Huidobro-Toro JP. Stoichiometry and conditional stability constants of Cu(II) or Zn(II) clioquinol complexes; implications for Alzheimer's and Huntington's disease therapy. NeuroToxicology. 2007;28(3):445-9.

696. Wagner CC, Calvo S, Torre MH, Baran EJ. Vibrational spectra of clioquinol and its Cu(II) complex. Journal of Raman Spectroscopy. 2007;38(4):373-6.

697. Říha M, Karlíčková J, Filipský T, Macáková K, Hrdina R, Mladěnka P. Novel method for rapid copper chelation assessment confirmed low affinity of D-penicillamine for copper in comparison with trientine and 8-hydroxyquinolines. Journal of Inorganic Biochemistry. 2013;123:80-7.

698. Pushie MJ, Nienaber KH, Summers KL, Cotelesage JJH, Ponomarenko O, Nichol HK, et al. The solution structure of the copper clioquinol complex. Journal of Inorganic Biochemistry. 2014;133(Supplement C):50-6.

699. Cherny RA, Atwood CS, Xilinas ME, Gray DN, Jones WD, McLean CA, et al. Treatment with a Copper-Zinc Chelator Markedly and Rapidly Inhibits β-Amyloid Accumulation in Alzheimer's Disease Transgenic Mice. Neuron. 2001;30(3):665-76.

700. Adlard PA, Cherny RA, Finkelstein DI, Gautier E, Robb E, Cortes M, et al. Rapid Restoration of Cognition in Alzheimer's Transgenic Mice with 8-Hydroxy Quinoline Analogs Is Associated with Decreased Interstitial Aβ. Neuron. 2008;59(1):43-55.

701. Crouch PJ, Tew DJ, Du T, Nguyen DN, Caragounis A, Filiz G, et al. Restored degradation of the Alzheimer's amyloid-β peptide by targeting amyloid formation. Journal of Neurochemistry. 2009;108(5):1198-207.

702. LeVine HI, Ding Q, Walker JA, Voss RS, Augelli-Szafran CE. Clioquinol and other hydroxyquinoline derivatives inhibit Aβ(1-42) oligomer assembly. Neuroscience Letters. 2009;465(1):99-103.

703. Matlack KES, Tardiff DF, Narayan P, Hamamichi S, Caldwell KA, Caldwell GA, et al. Clioquinol promotes the degradation of metal-dependent amyloid-β (Aβ)

oligomers to restore endocytosis and ameliorate Aβ toxicity. Proceedings of the National Academy of Sciences. 2014;111(11):4013-8.

704. Ryan TM, Roberts BR, McColl G, Hare DJ, Doble PA, Li Q-X, et al. Stabilization of Nontoxic Aβ-Oligomers: Insights into the Mechanism of Action of Hydroxyquinolines in Alzheimer's Disease. The Journal of Neuroscience. 2015;35(7):2871-84.

705. Mancino AM, Hindo SS, Kochi A, Lim MH. Effects of Clioquinol on Metal-Triggered Amyloid-β Aggregation Revisited. Inorganic Chemistry. 2009;48(20):9596-8.

706. Raman B, Ban T, Yamaguchi K-i, Sakai M, Kawai T, Naiki H, et al. Metal Ion-dependent Effects of Clioquinol on the Fibril Growth of an Amyloid β Peptide. Journal of Biological Chemistry. 2005;280(16):16157-62.

707. Abramov A, Canevari L, Duchen M. Changes in intracellular calcium and glutathione in astrocytes as the primary mechanism of amyloid neurotoxicity. Journal of Neuroscience. 2003;23(12):5088-95.

708. Wang T, Wang C-Y, Shan Z-Y, Teng W-P, Wang Z-Y. Clioquinol Reduces Zinc Accumulation in Neuritic Plaques and Inhibits the Amyloidogenic Pathway in AβPP/PS1 Transgenic Mouse Brain. Journal of Alzheimer's Disease. 2012;29(3):549-59.

709. Zhang YH, Raymick J, Sarkar S, Lahiri DK, Ray B, Holtzman D, et al. Efficacy and Toxicity of Clioquinol Treatment and A-β42 Inoculation in the APP/PSI Mouse Model of Alzheimer's Disease. Current Alzheimer Research. 2013;10(5):494-506.

710. Regland B, Lehmann W, Abedini I, Blennow K, Jonsson M, Karlsson I, et al. Treatment of Alzheimer's Disease with Clioquinol. Dementia and Geriatric Cognitive Disorders 2001;12(6):408-14.

711. Ritchie CW, Bush AI, Mackinnon A, Macfarlane S, Mastwyk M, MacGregor L, et al. Metal-Protein Attenuation With Iodochlorhydroxyquin (Clioquinol) Targeting Aβ Amyloid Deposition and Toxicity in Alzheimer Disease: A Pilot Phase 2 Clinical Trial. Archives of Neurology. 2003;60(12):1685-91.

712. Barnham KJ, Gautier ECL, Kok GB, Krippner G, inventors; Prana Biotechnology Limited, assignee. 8-Hydroxyquinoline Derivatives patent USP 7,619,091 B2. 2003 16th July.

713. Adlard PA, Bica L, White AR, Nurjono M, Filiz G, Crouch PJ, et al. Metal Ionophore Treatment Restores Dendritic Spine Density and Synaptic Protein Levels in a Mouse Model of Alzheimer's Disease. PLoS ONE. 2011;6(3):e17669.

714. Crouch PJ, Savva MS, Hung LW, Donnelly PS, Mot AI, Parker SJ, et al. The Alzheimer's therapeutic PBT2 promotes amyloid-β degradation and GSK3 phosphorylation via a metal chaperone activity. Journal of Neurochemistry. 2011;119(1):220-30.

715. McColl G, Roberts BR, Pukala TL, Kenche VB, Roberts CM, Link CD, et al. Utility of an improved model of amyloid-β ($A\beta_{1-42}$) toxicity in Caenorhabditis elegans for drug screening for Alzheimer's disease. Molecular Neurodegeneration. 2012;7:57.

716. Adlard PA, Hung LW, Gunawan L, Sedjahtera A, Sherratt N, Bray L, et al. Metal Chaperones Are Novel Therapeutic Agents for Tauopathy. The 11th International Conference on Alzheimer's & Parkinson's Diseases; Florence, Italy2013.

717. Lannfelt L, Blennow K, Zetterberg H, Batsman S, Ames D, Harrison J, et al. Safety, efficacy, and biomarker findings of PBT2 in targeting Aβ as a modifying therapy for Alzheimer's disease: a phase IIa, double-blind, randomised, placebo-controlled trial. Lancet Neurology. 2008;7(9):779-86.

718. Faux NG, Ritchie CW, Gunn A, Rembach A, Tsatsanis A, Bedo J, et al. PBT2 rapidly improves cognition in Alzheimer's Disease: additional phase II analyses. Journal of Alzheimer's Disease. 2010;20(2):509-16.

719. Villemagne VL, Rowe CC, Barnham KJ, Cherny R, Woodward M, Bozinosvski S, et al. A randomized, exploratory molecular imaging study targeting amyloid β with a novel 8-OH quinoline in Alzheimer's disease: The PBT2-204 IMAGINE study. Alzheimer's & Dementia: Translational Research & Clinical Interventions. 2017;3(4):622-35.

720. Nguyen T, Hamby A, Massa SM. Clioquinol down-regulates mutant huntingtin expression *in vitro* and mitigates pathology in a Huntington's disease mouse model. Proceedings of the National Academy of Sciences of the United States of America. 2005;102(33):11840-5.

721. Park MH, Lee SJ, Byun HR, Kim Y, Oh YJ, Koh JY, et al. Clioquinol induces autophagy in cultured astrocytes and neurons by acting as a zinc ionophore. Neurobiology of Disease. 2011;42(3):242-51.

722. Cherny RA, Ayton S, Finkelstein DI, Bush AI, McColl G, Massa SM. PBT2 Reduces Toxicity in a C. elegans Model of polyQ Aggregation and Extends Lifespan, Reduces Striatal Atrophy and Improves Motor Performance in the R6/2 Mouse Model of Huntington's Disease. Journal of Huntington's Disease. 2012;1(2):211-9.

723. Huntington Study Group Reach2HD Investigators. Safety, tolerability, and efficacy of PBT2 in Huntington's disease: a phase 2, randomised, double-blind, placebo-controlled trial. The Lancet Neurology. 2015;14(1):39-47.

724. Roney CA, Arora V, Kulkarni PV, Antich PP, Bonte FJ. Nanoparticulate Radiolabelled Quinolines Detect Amyloid Plaques in Mouse Models of Alzheimer's Disease. International Journal of Alzheimer's Disease. 2009;2009.

725. Kulkarni PV, Roney CA, Antich PP, Bonte FJ, Raghu AV, Aminabhavi TM. Quinoline-*n*-butylcyanoacrylate-based nanoparticles for brain targeting for the diagnosis of Alzheimer's disease. Wiley Interdisciplinary Reviews: Nanomedicine and Nanobiotechnology. 2010;2(1):35-47.

726. Kaur D, Yantiri F, Rajagopalan S, Kumar J, Mo JQ, Boonplueang R, et al. Genetic or Pharmacological Iron Chelation Prevents MPTP-Induced Neurotoxicity *In Vivo*: A Novel Therapy for Parkinson's Disease. Neuron. 2003;37(6):899-909.

727. Pollera C, Lucchini B, Formentin E, Bareggi S, Poli G, Ponti W. Evaluation of Anti-Prionic Activity of Clioquinol in an *in vivo* Model (*Mesocricetus auratus*). Veterinary Research Communications. 2005;29:253-5.

728. Choi SM, Choi K-O, Park Y-K, Cho H, Yang EG, Park H. Clioquinol, a Cu(II)/Zn(II) Chelator, Inhibits Both Ubiquitination and Asparagine Hydroxylation of Hypoxia-inducible Factor-1α, Leading to Expression of Vascular Endothelial Growth Factor and Erythropoietin in Normoxic Cells. Journal of Biological Chemistry. 2006;281(45):34056-63.

729. Ding W-Q, Liu B, Vaught JL, Palmiter RD, Lind SE. Clioquinol and docosahexaenoic acid act synergistically to kill tumor cells. Molecular Cancer Therapeutics. 2006;5(7):1864-72.

730. Chen WH, Wang M, Yu SS, Su L, Zhu DM, She JQ, et al. Clioquinol and vitamin B12 (cobalamin) synergistically rescue the lead-induced impairments of synaptic plasticity in hippocampal dentate gyrus area of the anesthetized rats *in vivo*. Neuroscience. 2007;147(3):853-64.

731. Masuda T, Hida H, Kanda Y, Aihara N, Ohta K, Yamada K, et al. Oral administration of metal chelator ameliorates motor dysfunction after a small hemorrhage near the internal capsule in rat. Journal of Neuroscience Research. 2007;85(1):213-22.

732. Ponti W, Sala M, Pollera C, Braida D, Poli G, Bareggi S. *In vivo* Model for the Evaluation of Molecules Active Towards Transmissible Spongiform Encephalopathies. Veterinary Research Communications. 2004;28(Supplement 1):307-10.

733. Priel T, Aricha-Tamir B, Sekler I. Clioquinol attenuates zinc-dependent beta-cell death and the onset of insulitis and hyperglycemia associated with experimental type I diabetes in mice. European Journal of Pharmacology. 2007;565(1-3):232-9.

734. Olaleye O, Raghunand TR, Bhat S, Chong C, Gu P, Zhou J, et al. Characterization of clioquinol and analogues as novel inhibitors of methionine aminopeptidases from Mycobacterium tuberculosis. Tuberculosis. 2011;91(Supplement 1):S61-5.

735. Schimmer AD. Clioquinol - a novel copper-dependent and independent proteasome inhibitor. Current Cancer Drug Targets. 2011;11(3):325-31.

736. Suh S, Choi B, Jang B, Kim J, Kwon L, Sohn M, et al. Clioquinol reduces spinal cord white matter damage and behavioral deficits in MOG-induced multiple sclerosis model mice. International Society for Zinc Biology (ISZB) Conference; St Kilda, Victoria, Australia 2012.

737. Papazian V, Jackson T, Pham T, Liu X, Greguric I, Loc'h C, et al. The preparation of $^{123/125}$I-clioquinol for the study of Aβ protein in Alzheimer's disease. Journal of Labelled Compounds and Radiopharmaceuticals. 2005;48(7):473-84.

738. George AJ, Holsinger RMD, McLean CA, Laughton KM, Beyreuther K, Evin G, et al. APP intracellular domain is increased and soluble Aβ is reduced with diet-induced hypercholesterolemia in a transgenic mouse model of Alzheimer disease. Neurobiology of Disease. 2004;16(1):124-32.

739. Li QX, Mok SS, Laughton KM, McLean CA, Volitakis I, Cherny RA, et al. Overexpression of Aβ is associated with acceleration of onset of motor impairment and superoxide dismutase 1 aggregation in an amyotrophic lateral sclerosis mouse model. Aging Cell. 2006;5(2):153-65.

740. Tominaga H, Ishiyama M, Ohseto F, Sasamoto K, Hamamoto T, Suzuki K, et al. A water-soluble tetrazolium salt useful for colorimetric cell viability assay. Analytical Communications. 1999;36(2):47-50.

741. Mosmann T. Rapid colorimetric assay for cellular growth and survival: Application to proliferation and cytotoxicity assays. Journal of Immunological Methods. 1983;65(1–2):55-63.

742. Denizot F, Lang R. Rapid colorimetric assay for cell growth and survival: Modifications to the tetrazolium dye procedure giving improved sensitivity and reliability. Journal of Immunological Methods. 1986;89(2):271-7.

743. Cory AH, Owen TC, Barltrop JA, Cory JG. Use of an aqueous soluble tetrazolium/formazan assay for cell growth assays in culture. Cancer Communications. 1991;3(7):207-12.

744. Korzeniewski C, Callewaert DM. An enzyme-release assay for natural cytotoxicity. Journal of Immunological Methods. 1983;64(3):313-20.

745. Ibach B, Haen E, Marienhagen J, Hajak G. Clioquinol treatment in familiar early onset of Alzheimer's disease: a case report. Pharmacopsychiatry. 2005;38(4):178-9.

746. Wang Y, Branicky R, Stepanyan Z, Carroll M, Guimond MP, Hihi A, et al. The Anti-neurodegeneration Drug Clioquinol Inhibits the Aging-associated Protein CLK-1. Journal of Biological Chemistry. 2009;284(1):314-23.

747. Li C, Wang J, Zhou B. The Metal Chelating and Chaperoning Effects of Clioquinol: Insights from Yeast Studies. Journal of Alzheimer's Disease. 2010;21(4):1249–62.

748. Cater MA, Haupt Y. Clioquinol induces cytoplasmic clearance of the X-linked inhibitor of apoptosis protein (XIAP): therapeutic indication for prostate cancer. Biochemical Journal. 2011;436(2):481-91.

749. Cameron AR, Wallace K, Logie L, Prescott AR, Unterman TG, Harthill J, et al. The antineurodegenerative agent clioquinol regulates the transcription factor FOXO1a. Biochemical Journal. 2012;443(1):57-64.

750. Katsuyama M, Iwata K, Ibi M, Matsuno K, Matsumoto M, Yabe-Nishimura C. Clioquinol induces DNA double-strand breaks, activation of ATM, and subsequent activation of p53 signaling. Toxicology. 2012;299(1):55-9.

751. Tardiff DF, Tucci ML, Caldwell KA, Caldwell GA, Lindquist S. Different 8-hydroxyquinolines protect models of TDP-43, α-synuclein, and polyglutamine proteotoxicity through distinct mechanisms. Journal of Biological Chemistry. 2012;287(6):4107-20.

752. Caragounis A, Du T, Filiz G, Laughton KM, Volitakis I, Sharples RA, et al. Differential modulation of Alzheimer's disease amyloid β-peptide accumulation by diverse classes of metal ligands. Biochemical Journal. 2007;407(3):435-50.

753. Kenche VB, Zawisza I, Masters CL, Bal W, Barnham KJ, Drew SC. Mixed Ligand Cu^{2+} Complexes of a Model Therapeutic with Alzheimer's Amyloid-β Peptide and Monoamine Neurotransmitters. Inorganic Chemistry. 2013;52(8):4303-18.

754. Jack DB, Riess W. Pharmacokinetics of iodochlorhydroxyquin in man. Journal of Pharmaceutical Sciences. 1973;62(12):1929-32.

755. Chen C, Samejima K, Tamura Z. A gas chromatographic determination method of 5-chloro-7-iodo-8-quinolinol and its conjugates in biological fluids. Chemical & Pharmaceutical Bulletin. 1976;24(1):97-101.

756. Ohshima N, Kotaki H, Saitoh Y, Nakagawa F, Tamura Z. Sex difference of the metabolic disposition of clioquinol in rats. Journal of Pharmacobio-dynamics. 1989;12(7):371-7.

757. Hayakawa K, Kitada K, Hamaki M, Miyazaki M. High-performance liquid chromatographic determination of clioquinol and its conjugates in biological materials. Journal of Chromatography B: Biomedical Sciences and Applications. 1982;229(1):159-65.

758. Ezzedeen FW, Stohs SJ, Stublar M. Analysis of iodochlorhydroxyquin in biological materials by high-performance liquid chromatography. Journal of Chromatography B: Biomedical Sciences and Applications. 1983;276:121-8.

759. Ogata M, Watanabe S, Tateishi J, Kuroda S, Tomokuni K. Metabolism of ^{14}C-iodochlorohydroxyquinoline (chinoform) in mice. Acta Medicinae Okayama. 1971;25(3):199-204.

760. Watanabe S, Tateishi J, Kuroda S, Otsuki S, Ogata M. Incorporation of radioactive chinoform into the nervous tissues. Igaku To Seibutsugaku. 1971;83(1):15-9.

761. Ogata M, Watanabe S, Tateishi J, Kuroda S, Otsuki S. Accumulation of clioquinol in mice. Lancet. 1973;301(7815):1325.

762. Ogata M, Watanabe S, Tateishi J, Kuroda S, Otsuki S. Distribution of radioactive clioquinol in animals. Lancet. 1973;301(7814):1248-9.

763. Opazo C, Luza S, Villemagne VL, Volitakis I, Rowe C, Barnham KJ, et al. Radioiodinated clioquinol as a biomarker for β-amyloid: Zn^{2+} complexes in Alzheimer's disease. Aging Cell. 2006;5(1):69-79.

764. Klebe R, Ruddle F. Neuroblastoma: Cell culture analysis of a differentiating stem cell system. Journal of Cell Biology. 1969;43:69A.

765. Gunn AP, Roberts BR, Bush AI. Rapid Generation of Dityrosine Cross-linked Aβ Oligomers *via* Cu-Redox Cycling. In: Sigurdsson EM, Calero M, Gasset M, editors. Amyloid Proteins - Methods and Protocols. Methods in Molecular Biology. 849. 2nd ed: Humana Press; 2012. p. 3-10.

766. Smith PK, Krohn RI, Hermanson GT, Mallia AK, Gartner FH, Provenzano MD, et al. Measurement of protein using bicinchoninic acid. Analytical Biochemistry. 1985;150(1):76-85.

767. Ida N, Hartmann T, Pantel J, Schroder J, Zerfass R, Forstl H, et al. Analysis of heterogeneous β-A4 peptides in human cerebrospinal fluid and blood by a newly developed sensitive western blot assay. Journal of Biological Chemistry. 1996;271(37):22908-14.

768. Smith DP, Smith DG, Curtain CC, Boas JF, Pilbrow JR, Ciccotosto GD, et al. Copper-mediated Amyloid-β Toxicity Is Associated with an Intermolecular Histidine Bridge. Journal of Biological Chemistry. 2006;281(22):15145-54.

769. Jin L, Wu W-H, Li Q-Y, Zhao Y-F, Li Y-M. Copper inducing Aβ42 rather than Aβ40 nanoscale oligomer formation is the key process for Aβ neurotoxicity. Nanoscale. 2011;3(11):4746-51.

770. Padmanabhan G, Becue I, Smith JB. Clioquinol. In: Florey K, Al-Badr AA, Forcier GA, Brittain HG, Grady LT, editors. Analytical Profiles of Drug Substances. 18: Academic Press; 1989. p. 57-90.

771. Ben-Ze'ev A, Farmer SR, Penman S. Mechanisms of regulating tubulin synthesis in cultured mammalian cells. Cell. 1979;17(2):319-25.

772. Lee JC, Field DJ, Lee LLY. Effects of nocodazole on structures of calf brain tubulin. Biochemistry. 1980;19(26):6209-15.

773. Jung SM, Yamazaki H, Tetsuka T, Moroi M. Effect of nocodazole, a new microtubule inhibitor, on platelet aggregation and release. Thrombosis Research. 1981;23(4-5):401-10.

774. Rennison ME, Handel SE, Wilde CJ, Burgoyne RD. Investigation of the role of microtubules in protein secretion from lactating mouse mammary epithelial cells. Journal of Cell Science. 1992;102(2):239-47.

775. Lee J-H, Yu WH, Kumar A, Lee S, Mohan PS, Peterhoff CM, et al. Lysosomal Proteolysis and Autophagy Require Presenilin 1 and Are Disrupted by Alzheimer-Related PS1 Mutations. Cell. 2010;141(7):1146-U91.

776. Nixon RA, Cataldo AM, Mathews PM. The Endosomal-Lysosomal System of Neurons in Alzheimer's Disease Pathogenesis: A Review. Neurochemical Research. 2000;25(9):1161-72.

777. Ohkuma S, Poole B. Fluorescence Probe Measurement of the Intralysosomal pH in Living Cells and the Perturbation of pH by Various Agents. Proceedings of the National Academy of Sciences of the United States of America. 1978;75(7):3327-31.

778. Seglen PO, Gordon PB. 3-Methyladenine: Specific inhibitor of autophagic/lysosomal protein degradation in isolated rat hepatocytes. Proceedings of the National Academy of Sciences of the United States of America. 1982;79(6):1889-92.

779. Blommaart EFC, Krause U, Schellens JPM, Vreeling-Sindelárová H, Meijer AJ. The Phosphatidylinositol 3-Kinase Inhibitors Wortmannin and LY294002 Inhibit Autophagy in Isolated Rat Hepatocytes. European Journal of Biochemistry. 1997;243(1-2):240-6.

780. Nixon RA. Endosome function and dysfunction in Alzheimer's disease and other neurodegenerative diseases. Neurobiology of Aging. 2005;26(3):373-82.

781. Barnham KJ, Cherny RA, Cappai R, Melov S, Masters CL, Bush AI. Metal-Protein Attenuating Compounds (MPACs) for the Treatment of Alzheimers Disease. Drug Design Reviews-Online. 2004;1:75-82.

782. Frederickson CJ. Neurobiology of Zinc and Zinc-Containing Neurons. In: John RS, Ronald JB, editors. International Review of Neurobiology. 31: Academic Press; 1989. p. 145-238.

783. Lee J, Prohaska JR, Dagenais SL, Glover TW, Thiele DJ. Isolation of a murine copper transporter gene, tissue specific expression and functional complementation of a yeast copper transport mutant. Gene. 2000;254(1–2):87-96.

784. Gruenheid S, Cellier M, Vidal S, Gros P. Identification and characterization of a second mouse Nramp gene. Genomics. 1995;25(2):514-25.

785. Zheng W, Xin N, Chi Z-H, Zhao B-L, Zhang J, Li J-Y, et al. Divalent metal transporter 1 is involved in amyloid precursor protein processing and Aβ generation. FASEB Journal. 2009;23(12):4207-17.

786. Weinreb O, Mandel S, Bar-Am O, Amit T. Iron-chelating backbone coupled with monoamine oxidase inhibitory moiety as novel pluripotential therapeutic agents for Alzheimer's disease: a tribute to Moussa Youdim. Journal of Neural Transmission. 2011;118(3):479-92.

787. Ding W-Q, Liu B, Vaught JL, Yamauchi H, Lind SE. Anticancer Activity of the Antibiotic Clioquinol. Cancer Research. 2005;65(8):3389-95.

788. Du T, Filiz G, Caragounis A, Crouch PJ, White AR. Clioquinol Promotes Cancer Cell Toxicity through Tumor Necrosis Factor α Release from Macrophages. Journal of Pharmacology and Experimental Therapeutics. 2008;324(1):360-7.

789. Tuller ER, Brock AL, Yu H, Lou JR, Benbrook DM, Ding W-Q. PPARα signaling mediates the synergistic cytotoxicity of clioquinol and docosahexaenoic acid in human cancer cells. Biochemical Pharmacology. 2009;77(9):1480-6.

790. Tardito S, Bassanetti I, Bignardi C, Elviri L, Tegoni M, Mucchino C, et al. Copper Binding Agents Acting as Copper Ionophores Lead to Caspase Inhibition and Paraptotic Cell Death in Human Cancer Cells. Journal of the American Chemical Society. 2011;133(16):6235-42.

791. Tardito S, Barilli A, Bassanetti I, Tegoni M, Bussolati O, Franchi-Gazzola R, et al. Copper-dependent cytotoxicity of 8-Hydroxyquinoline derivatives correlates with their hydrophobicity and does not require caspase activation. Journal of Medicinal Chemistry. 2012;55(23):10448-59.

792. Chen H-L, Chang C-Y, Lee H-T, Lin H-H, Lu P-J, Yang C-N, et al. Synthesis and pharmacological exploitation of clioquinol-derived copper-binding apoptosis inducers triggering reactive oxygen species generation and MAPK pathway activation. Bioorganic & Medicinal Chemistry. 2009;17(20):7239-47.

793. Barrea RA, Chen D, Irving TC, Dou QP. Synchrotron X-ray imaging reveals a correlation of tumor copper speciation with Clioquinol's anticancer activity. Journal of Cellular Biochemistry. 2009;108:96-105.

794. Yu H, Zhou Y, Lind SE, Ding WQ. Clioquinol targets zinc to lysosomes in human cancer cells. Biochemical Journal. 2009;417(1):133-9.

795. Moret V, Laras Y, Cresteil T, Aubert G, Ping DQ, Di C, et al. Discovery of a new family of bis-8-hydroxyquinoline substituted benzylamines with pro-apoptotic activity in cancer cells: Synthesis, structure-activity relationship, and action mechanism studies. European Journal of Medicinal Chemistry. 2009;44(2):558-67.

796. Cater MA, Pearson HB, Wolyneic K, Klaver P, Bilandzic M, Paterson BM, et al. Increasing intracellular bioavailable copper selectively targets prostate cancer cells. ACS Chemical Biology.

797. Ding W-Q, Lind SE. Metal ionophores - An emerging class of anticancer drugs. IUBMB Life. 2009;61(11):1013-8.

798. Xue J, Wang S, Wu J, Hannafon BN, Ding WQ. Zinc at Sub-Cytotoxic Concentrations Induces Heme Oxygenase-1 Expression in Human Cancer Cells. Cellular Physiology and Biochemistry. 2013;32(1):100-10.

799. Cao B, Li J, Zhu J, Shen M, Han K, Zhang Z, et al. The anti-parasitic clioquinol induces apoptosis in leukemia and myeloma cells by inhibiting histone deacetylase activity. Journal of Biological Chemistry. 2013;288(47):34181-9.

800. Chen D, Cui QC, Yang H, Barrea RA, Sarkar FH, Sheng S, et al. Clioquinol, a Therapeutic Agent for Alzheimer's Disease, Has Proteasome-Inhibitory, Androgen Receptor-Suppressing, Apoptosis-Inducing, and Antitumor Activities in Human Prostate Cancer Cells and Xenografts. Cancer Research. 2007;67(4):1636-44.

801. Mao X, Li X, Sprangers R, Wang X, Venugopal A, Wood T, et al. Clioquinol inhibits the proteasome and displays preclinical activity in leukemia and myeloma. Leukemia. 2009;23(3):585-90.

802. Zhai S, Yang L, Cui Q, Sun Y, Dou Q, Yan B. Tumor cellular proteasome inhibition and growth suppression by 8-hydroxyquinoline and clioquinol requires their capabilities to bind copper and transport copper into cells. Journal of Biological Inorganic Chemistry. 2010;15(2):259-69.

803. Biedler JL, Roffler-Tarlov S, Schachner M, Freedman LS. Multiple Neurotransmitter Synthesis by Human Neuroblastoma Cell Lines and Clones. Cancer Research. 1978;38(11 Part 1):3751-7.

804. Biedler JL, Helson L, Spengler BA. Morphology and Growth, Tumorigenicity, and Cytogenetics of Human Neuroblastoma Cells in Continuous Culture. Cancer Research. 1973;33(11):2643-52.

805. Ross RA, Spengler BA, Biedler JL. Coordinate morphological and biochemical interconversion of human neuroblastoma cells. Journal of the National Cancer Institute. 1983;71:741-7.

806. Biedler JL, Spengler BA. A novel chromosome abnormality in human neuroblastoma and antifolate-resistant Chinese hamster cell lives in culture. Journal of the National Cancer Institute. 1976;57(3):683-95.

807. Barnes EN, Biedler JL, Spengler BA, Lyser KM. The Fine Structure of Continuous Human Neuroblastoma Lines SK-N-SH, SK-N-BE(2), and SK-N-MC. In Vitro. 1981;17(7):619-31.

808. Day SRr, Ziolkowski HJC. Human brain tumour cell strains with deficient host-cell reactivation of *N*-methyl-*N'*-nitro-*N*-nitrosoguanidine-damaged adenovirus 5. Nature. 1979;279(5716):797-9.

809. Puck TT, Cieciura SJ, Robinson A. Genetics of somatic mammalian cells: III. Long-term cultivation of euploid cells from human and animal subjects. Journal of Experimental Medicine. 1958;108(6):945-56.

810. Filiz G, Caragounis A, Bica L, Du T, Masters CL, Crouch PJ, et al. Clioquinol inhibits peroxide-mediated toxicity through up-regulation of phosphoinositol-3-kinase and inhibition of p53 activity. International Journal of Biochemistry and Cell Biology. 2008;40(5):1030-42.

811. Price KA, Filiz G, Caragounis A, Du T, Laughton KM, Masters CL, et al. Activation of epidermal growth factor receptor by metal-ligand complexes decreases levels of extracellular amyloid β peptide. International Journal of Biochemistry and Cell Biology. 2008;40(9):1901-17.

812. Russell WMS, Burch RL. The Principle of Humane Experimental Technique. London: Methuen & Co. Ltd.; 1959.

813. Liddell JR, Obando D, Liu J, Ganio G, Volitakis I, San Mok S, et al. Lipophilic adamantyl- or deferasirox-based conjugates of desferrioxamine B have enhanced neuroprotective capacity: Implications for Parkinson's disease. Free Radical Biology and Medicine. 2013;60:147-56.

814. Chen D, Milacic V, Frezza M, Dou QP. Metal complexes, their cellular targets and potential for cancer therapy. Current Pharmaceutical Design. 2009;15(7):777-91.

815. Schimmer AD, Jitkova Y, Gronda M, Wang Z, Brandwein J, Chen C, et al. A Phase I Study of the Metal Ionophore Clioquinol in Patients With Advanced Hematologic Malignancies. Clinical Lymphoma Myeloma and Leukemia. 2012;12(5):330-6.

816. Chen D, Dou QP. New uses for old copper-binding drugs: converting the pro-angiogenic copper to a specific cancer cell death inducer. Expert Opinion on Therapeutic Targets. 2008;12(6):739-48.

817. Neldner KH. The halogenated 8-hydroxyquinolines. International Journal of Dermatology. 1977;16(4):267-73.

818. Schaumburg HH, Spencer PS. Clioquinol. In: Spencer PS, Schaumburg HH, editors. Experimental and Clinical Neurotoxicology Baltimore, MD: Williams and Wilkins; 1980. p. 395-406.

819. Mao X, Schimmer AD. The toxicology of Clioquinol. Toxicology Letters. 2008;182(1-3):1-6.

820. Atamna H, Frey WH. A role for heme in Alzheimer's disease: heme binds amyloid β and has altered metabolism. Proceedings of the National Academy of Sciences of the United States of America. 2004;101(30):11153-8.

821. Asakura K, Ueda A, Kawamura N, Ueda M, Mihara T, Mutoh T. Clioquinol inhibits NGF-induced Trk autophosphorylation and neurite outgrowth in PC12 cells. Brain Research. 2009;1301:110-5.

822. Yu H, Lou JR, Ding WQ. Clioquinol independently targets NF-κB and lysosome pathways in human cancer cells. Anticancer Research. 2010;30(6):2087-92.

823. Barcia E, Salama A, Fernández-Carballido A, Negro S. Protective effects of clioquinol on human neuronal-like cells: a new formulation of clioquinol-loaded PLGA microspheres for Alzheimer's disease. Journal of Drug Targeting. 2011;19(8):637-46.

824. Benvenisti-Zarom L, Chen J, Regan RF. The oxidative neurotoxicity of clioquinol. Neuropharmacology. 2005;49(5):687-94.

825. Colvin RA, Bush AI, Volitakis I, Fontaine CP, Thomas D, Kikuchi K, et al. Insights into Zn^{2+} homeostasis in neurons from experimental and modeling studies. American Journal of Physiology - Cell Physiology. 2008;294(3):C726-42.

826. Rival T, Page RM, Chandraratna DS, Sendall TJ, Ryder E, Liu B, et al. Fenton chemistry and oxidative stress mediate the toxicity of the β amyloid peptide in a *Drosophila* model of Alzheimer's disease. European Journal of Neuroscience. 2009;29(7):1335-47.

827. Tjälve H, Ståhl K. Effect of 5-chloro-7-iodo-8-hydroxy-quinoline (clioquinol) on the uptake and distribution of nickel, zinc and mercury in mice. Acta Pharmacologica et Toxicologica. 1984;55(1):65-72.

828. Nitzan YB, Sekler I, Frederickson CJ, Coulter DA, Balaji RV, Liang SL, et al. Clioquinol effects on tissue chelatable zinc in mice. Journal of Molecular Medicine. 2003;81(10):637-44.

829. Schäfer S, Pajonk F-G, Multhaup G, Bayer T. Copper and clioquinol treatment in young APP transgenic and wild-type mice: effects on life expectancy, body weight, and metal-ion levels. Journal of Molecular Medicine. 2007;85(4):405-13.

830. Ismail T, Mauerhofer E, Slomianka L. The hippocampal region of rats and mice after a single i.p. dose of clioquinol: Loss of synaptic zinc, cell death and c-Fos induction. Neuroscience. 2008;157(3):697-707.

831. Kaur D, Rajagopalan S, Andersen JK. Chronic expression of H-ferritin in dopaminergic midbrain neurons results in an age-related expansion of the labile iron pool and subsequent neurodegeneration: implications for Parkinson's disease. Brain Research. 2009;1297:17-22.

832. Grossi C, Francese S, Casini A, Rosi MC, Luccarini I, Fiorentini A, et al. Clioquinol decreases amyloid-β burden and reduces working memory impairment in a transgenic mouse model of Alzheimer's disease. Journal of Alzheimer's Disease. 2009;17(2):423-40.

833. Weismann K, Knudsen L. Effects of penicillamine and hydroxyquinoline on absorption of orally ingested 65zinc in the rat. Journal of Investigative Dermatology. 1978;71(4):242-4.

834. Tamura Z, Kotaki H, Nakajima K, Tanimura Y, Saitoh Y, Nakagawa F. Clioquinol causes ataxia in rats. Lancet. 1982;320(8301):776.

835. Ozawa K, Saida K, Saida T. Experimental clioquinol intoxication in rats: Abnormalities in optic nerves and small nerve cells of dorsal root ganglia. Acta Neuropathologica. 1986;69(3):272-7.

836. Suh SW, Won SJ, Hamby AM, Yoo BH, Fan Y, Sheline CT, et al. Decreased brain zinc availability reduces hippocampal neurogenesis in mice and rats. Journal of Cerebral Blood Flow and Metabolism. 2009;29(9):1579-88.

837. Takeda A, Takada S, Ando M, Itagaki K, Tamano H, Suzuki M, et al. Impairment of recognition memory and hippocampal long-term potentiation after acute exposure to clioquinol. Neuroscience. 2010;171(2):443-50.

838. Takeda A, Takada S, Nakamura M, Suzuki M, Tamano H, Ando M, et al. Transient Increase in Zn^{2+} in Hippocampal CA1 Pyramidal Neurons Causes Reversible Memory Deficit. PLoS ONE. 2011;6(12):e28615.

839. Kim JH, Jang BG, Choi BY, Kwon LM, Sohn M, Song HK, et al. Zinc Chelation Reduces Hippocampal Neurogenesis after Pilocarpine-Induced Seizure. PLoS ONE. 2012;7(10):e48543.

840. Takeda A, Tamano H, Ogawa T, Takada S, Ando M, Oku N, et al. Significance of serum glucocorticoid and chelatable zinc in depression and cognition in zinc deficiency. Behavioural Brain Research. 2012;226(1):259-64.

841. Takeda A, Suzuki M, Tamano H, Takada S, Ide K, Oku N. Involvement of glucocorticoid-mediated Zn^{2+} signaling in attenuation of hippocampal CA1 LTP by acute stress. Neurochemistry International. 2012;60(4):394-9.

842. Takeda A, Iida M, Ando M, Nakamura M, Tamano H, Oku N. Enhanced Susceptibility to Spontaneous Seizures of Noda Epileptic Rats by Loss of Synaptic Zn^{2+}. PLoS ONE. 2013;8(8):e71372.

843. Wang T, Zheng W, Xu H, Zhou J-M, Wang Z-Y. Clioquinol Inhibits Zinc-Triggered Caspase Activation in the Hippocampal CA1 Region of a Global Ischemic Gerbil Model. PLoS ONE. 2010;5(7):e11888.

844. Bareggi SR, Braida D, Pollera C, Bondiolotti G, Formentin E, Puricelli M, et al. Effects of clioquinol on memory impairment and the neurochemical modifications induced by scrapie infection in golden hamsters. Brain Research. 2009;1280 195-200.

845. Tateishi J, Kuroda S, Saito A, Otsuki S. Myelo-optic neuropathy induced by clioquinol in animals. Lancet. 1971;298(7736):1263-4.

846. Hess R, Keberle H, Koella W, Schmid K, Gelzer J. Clioquinol: absence of neurotoxicity in laboratory animals. Lancet. 1972;300(7774):424-5.

847. Tateishi J, Kuroda S, Saito A, Otsuki S. Neurotoxicity of clioquinol in laboratory animals. Lancet. 1972;300(7786):1095.

848. Heywood R, Chesterman H, Worden AN. The oral toxicity of clioquinol (5-chloro-7-iodo-8-hydroxyquinoline) in beagle dogs. Toxicology. 1976;6(1):41-6.

849. Worden A, Heywood R. Clioquinol toxicity. Lancet. 1978;311(8057):212.

850. Krinke G, Schaumburg HH, Spencer PS, Thomann P, Hess R. Clioquinol and 2,5-hexanedione induce different types of distal axonopathy in the dog. Acta Neuropathologica. 1979;47(3):213-21.

851. Hoover DM, Carlton WW. The Subacute Neurotoxicity of Excess Pyridoxine HCl and Clioquinol (5-Chloro-7-Iodo-8-Hydroxyquinoline) in Beagle Dogs. I. Clinical Disease. Veterinary Pathology Online. 1981;18(6):745-56.

852. Hoover DM, Carlton WW. The Subacute Neurotoxicity of Excess Pyridoxine HCl and Clioquinol (5-Chloro-7-Iodo-8-Hydroxyquinoline) in Beagle Dogs. II. Pathology. Veterinary Pathology Online. 1981;18(6):757-68.

853. Goto M, Akahane K, Ono H, Kaneko T, Fukuda H, Tamura Z. Deterioration of spinal reflex in beagles orally ingesting clioquinol. Journal of Toxicological Sciences. 1982;7(1):1-12.

854. Goto M, Akahane K, Kato K, Fukuda H. Impairment of visual system of beagles orally ingesting clioquinol. Journal of Toxicological Sciences. 1982;7(1):19-25.

855. Koyama N, Terada M, Yokota T. Electrophysiological changes in the fasciculus gracilis of the cat following chronic clioquinol administration. Journal of the Neurological Sciences. 1989;94(1-3):271-82.

856. Moir RD, Atwood CS, Romano DM, Laurans MH, Huang X, Bush AI, et al. Differential Effects of Apolipoprotein E Isoforms on Metal-Induced Aggregation of Aβ Using Physiological Concentrations. Biochemistry. 1999;38(14):4595-603.

857. Thomas PK, Bradley DJ, Bradley WA, Degen PH, Krinke G, Muddle J, et al. Correlated nerve conduction, somatosensory evoked potential and neuropathological studies in clioquinol and 2,5-hexanedione neurotoxicity in the baboon. Journal of the Neurological Sciences. 1984;64(3):277-95.

858. Prana Biotechnology [Available from: http://www.pranabio.com/.

859. Brewer GJ, Torricelli JR, Evege EK, Price PJ. Optimized survival of hippocampal neurons in B27-supplemented neurobasal™, a new serum-free medium combination. Journal of Neuroscience Research. 1993;35(5):567-76.

860. Cuajungco MP, Goldstein LE, Nunomura A, Smith MA, Lim JT, Atwood CS, et al. Evidence that the β-amyloid plaques of Alzheimer's disease represent the redox-silencing and entombment of Aβ by zinc. Journal of Biological Chemistry. 2000;275(26):19439-42.

861. Opazo C, Huang X, Cherny RA, Moir RD, Roher AE, White AR, et al. Metalloenzyme-like Activity of Alzheimer's Disease β-Amyloid. Cu-Dependent Catalytic conversion of Dopamine, Cholesterol and Biological Reducing Agents to Neurotoxic H_2O_2. Journal of Biological Chemistry. 2002;277(43):40302-8.

862. Ciccotosto GD, Tew DJ, Drew SC, Smith DG, Johanssen T, Lal V, et al. Stereospecific interactions are necessary for Alzheimer disease amyloid-β toxicity. Neurobiology of Aging. 2011;32(2): 235-48.

863. White AR, Bush AI, Beyreuther K, Masters CL, Cappai R. Exacerbation of Copper Toxicity in Primary Neuronal Cultures Depleted of Cellular Glutathione. Journal of Neurochemistry. 1999;72(5):2092-8.

864. White AR, Zheng H, Galatis D, Maher F, Hesse L, Multhaup G, et al. Survival of Cultured Neurons from Amyloid Precursor Protein Knock-Out Mice against Alzheimer's Amyloid-β Toxicity and Oxidative Stress. Journal of Neuroscience. 1998;18(16):6207-17.

865. Fezoui Y, Hartley DM, Harper JD, Khurana R, Walsh DM, Condron MM, et al. An improved method of preparing the amyloid β-protein for fibrillogenesis and neurotoxicity experiments. Amyloid. 2000;7(3):166-78.

866. Teplow DB. Preparation of Amyloid β-Protein for Structural and Functional Studies. In: Indu K, Ronald W, editors. Methods in Enzymology. 413: Academic Press; 2006. p. 20-33.

867. Allain P, Mauras Y, Douge C, Jaunault L, Delaporte T, Beaugrand C. Determination of iodine and bromine in plasma and urine by inductively coupled plasma mass spectrometry. Analyst. 1990;115(6):813-5.

868. Baumann H. Rapid and sensitive determination of iodine in fresh milk and milk powder by inductively coupled plasma — mass spectrometry (ICP-MS). Fresenius' Journal of Analytical Chemistry. 1990;338(7):809-12.

869. Vanhoe H, Van Allemeersch F, Versieck J, Dams R. Effect of solvent type on the determination of total iodine in milk powder and human serum by inductively coupled plasma mass spectrometry. Analyst. 1993;118(8):1015-9.

870. Schramel P, Hasse S. Iodine determination in biological materials by ICP-MS. Microchimica Acta. 1994;116(4):205-9.

871. Dyke JV, Dasgupta PK, Kirk AB. Trace iodine quantitation in biological samples by mass spectrometric methods: The optimum internal standard. Talanta. 2009;79(2):235-42.

872. Cutler P, Brown F, Camilleri P, Carpenter D, George A, Gray C, et al. The recognition of haemoglobin by antibodies raised for the immunoassay of β-amyloid. FEBS Letters. 1997;412(2):341-5.

873. White AR, Multhaup G, Maher F, Bellingham S, Camakaris J, Zheng H, et al. The Alzheimer's Disease Amyloid Precursor Protein Modulates Copper-Induced Toxicity and Oxidative Stress in Primary Neuronal Cultures. Journal of Neuroscience. 1999;19(21):9170-9.

874. Taylor CAG, Sujay F., McGuire LC, Lu H, Croft JB. Deaths from Alzheimer's Disease - United States, 1999–2014. Atlanta, GA: Center for Surveillance, Epidemiology, and Laboratory Services, Centers for Disease Control and Prevention (CDC), U.S. Department of Health and Human Services; 2017.

875. Alzheimer's Association. Changing the Trajectory of Alzheimer's Disease: How a Treatment by 2025 Saves Lives and Dollars. 2015.

876. Tabira T. Clioquinol's return: cautions from Japan. Science. 2001;292(5525):2251-2.

877. Bush AI, Masters CL. Clioquinol's return: cautions from Japan [response]. Science. 2001;292(5525):2251-2.

878. Cahoon L. The curious case of clioquinol. Nature Medicine. 2009;15(4):356-9.

879. Smith DG, Ciccotosto GD, Tew DJ, Perez K, Curtain CC, Boas JF, et al. Histidine 14 modulates membrane binding and neurotoxicity of the Alzheimer's disease amyloid-β peptide. Journal of Alzheimer's Disease. 2010;19(4):1387-400.

880. Israel MA, Yuan SH, Bardy C, Reyna SM, Mu Y, Herrera C, et al. Probing sporadic and familial Alzheimer's disease using induced pluripotent stem cells. Nature. 2012;482(7384):216-20.

881. Qiang L, Fujita R, Yamashita T, Angulo S, Rhinn H, Rhee D, et al. Directed Conversion of Alzheimer's Disease Patient Skin Fibroblasts into Functional Neurons. Cell. 2011;146(3):359-71.

Appendix A

Alzheimer Review Series *J. Cell. Mol. Med. Vol 13, No 1, 2009 pp. 61-86*

Guest Editor: B. O. Popescu

Pharmacotherapeutic targets in Alzheimer's disease

Yif'at Biran [a, b], Colin L. Masters [a, b], Kevin J. Barnham [a, c, d], Ashley I. Bush [a, c], Paul A. Adlard [a, c, *]

[a] *The Oxidation Biology Laboratory, The Mental Health Research Institute, Parkville, Victoria, Australia*
[b] *Centre for Neuroscience, University of Melbourne, Parkville, Victoria, Australia*
[c] *Department of Pathology, University of Melbourne, Parkville, Victoria, Australia*
[d] *Bio21 Molecular Science & Biotechnology Institute, University of Melbourne, Parkville, Victoria, Australia*

Received: September 1, 2008; Accepted: November 7, 2008

Abstract

Alzheimer's disease (AD) is a progressive neurodegenerative disorder which is characterized by an increasing impairment in normal memory and cognitive processes that significantly diminishes a person's daily functioning. Despite decades of research and advances in our understanding of disease aetiology and pathogenesis, there are still no effective disease-modifying drugs available for the treatment of AD. However, numerous compounds are currently undergoing pre-clinical and clinical evaluations. These candidate pharmacotherapeutics are aimed at various aspects of the disease, such as the microtubule-associated τ-protein, the amyloid-β (Aβ) peptide and metal ion dyshomeostasis – all of which are involved in the development and progression of AD. We will review the way these pharmacological strategies target the biochemical and clinical features of the disease and the investigational drugs for each category.

Keywords: Alzheimer's disease • τ • amyloid-β • metals • therapeutics

Current pharmacotherapies for the treatment of AD

Alzheimer's disease (AD) is the most prevalent cause of dementia in the elderly population, affecting approximately 35–40 million patients worldwide [1], and is the third leading cause of death in developed countries [2]. As such, AD represents a major socio-economic problem, which requires better diagnostic tools, management and effective therapies in order to ease the burden of this disease. While there are advances being made in all these areas, particularly with the identification of new biomarkers and the development of novel brain imaging compounds for the early detection of disease, it is clear that an effective treatment for AD is as elusive as ever. To date, the only Food and Drugs Administration (FDA)-approved drugs for the treatment of AD patients are the acetylcholinesterase inhibitors (AChEIs) tacrine, donepezil, galantamine and rivastigmine, and the non-competitive N-methyl-D-aspartate (NMDA)-receptor antagonist memantine. The AChEIs exert their affect by preventing the enzymatic degradation of the neurotransmitter acetylcholine (AChE), resulting in increased AChE concentrations in the synaptic cleft and enhanced cholinergic transmission [3]. Memantine, however, protects neurons against NMDA receptor activation-mediated glutamate excitotoxicity [4–6] and also inhibits τ-hyperphosphorylation and aggregation [7]. A new approach, using combination therapy of donepezil and memantine, has been reported to have significant beneficial effects on cognitive function, activities of daily living and behaviour [8]. Meanwhile, potent and more selective AChEIs (Huperzine A, Neuro-Hitech Inc., New York, NY, USA) and NMDA-receptor antagonists (Dimebon, Medivation Inc., San Francisco, CA, USA) are being assessed.

*Correspondence to: Paul A. ADLARD,
The Mental Health Research Institute, 155 Oak Street,
Parkville, Victoria 3052, Australia.
Tel.: +61 3 93892955
Fax: +61 3 93806182
E-mail: padlard@mhri.edu.au

doi:10.1111/j.1582-4934.2008.00595.x

However, irrespective of the form of therapy utilized, the current approaches for the treatment of AD provide only temporary symptomatic relief and do not inhibit and/or reverse the underlying disease mechanisms. This stresses the urgent need for disease-modifying drugs for AD – small, easily administrated, well-tolerated, bioavailable compounds that cross the blood-brain barrier (BBB) and have little or no adverse effects and/or contraindications. There are currently more than 50 compounds in various stages of clinical investigation for the treatment of AD (www.alzforum.org) including: statins [9–12], peroxisome proliferator-activated receptor-γ agonists [13–16], non-steroidal anti-inflammatory drugs [17–19], neurotrophic molecules and even metabolic or nutritional drinks (Ketasyn™, Accera, Broomfield, CO, USA; Souvenaid™, Danone Research-Centre for Specialized Nutrition, respectively, Palaiseau, France). In addition, there are many more candidate molecules that are at the pre-clinical stage of development and are likely to proceed into clinical trials. Most of these pharmacological agents have been designed and/or developed based upon a notion that has been dominating the AD field for the past two decades – the 'amyloid cascade hypothesis'. This theory claims that the metabolism of the amyloid-β (Aβ) peptide (both generation and clearance) is the main initiator of AD, which together with the downstream formation of the τ-protein aggregates, leads to neuronal and synaptic dysfunction and loss, microglial activation and neuronal death [20, 21]. Thus, most of the pharma-cological agents being developed target one or both of the principal cerebral proteins implicated in the pathogenesis of AD: τ and Aβ. In this review, we will provide a broad overview of the therapeutic approaches currently being developed for the treatment of AD.

AD pharmacotherapies targeting τ

Neurofibrillary tangles (NFTs), which are found in AD and other forms of dementia, consist of insoluble, intra-neuronal inclusions [22, 23] comprised paired helical filaments that are formed from hyperphosphorylated τ [24, 25]. Hyperphosphorylation of the microtubule-associated τ-protein is likely to result from an imbalance in kinase and phosphatases activities, and leads to destabilization of microtubules [26], loss of neuronal cytoskeletal architecture and/or plasticity [27], impaired neuronal transport, dystrophy and ultimately neuronal cell death [28, 29]. Based on these findings, small molecules that interfere with the formation of τ-aggregates, selectively inhibit τ-kinases and/or activate τ-phosphatases are being pursued as therapeutic targets (see Fig. 1).

Modulators of τ kinases or phosphatases

The biological function of the microtubule-associated τ-protein [30] is regulated by several kinases and phosphatases [31–33]. An imbalance in activity between kinases and phosphatases results in the abnormal phosphorylation of 38 or more serine and/or threonine amino acids on τ in the AD brain [34–37]. Phosphorylation of a tyrosine residue at position 18 (Tyr^{18}) on τ by the tyrosine kinase fyn has also been reported [38]. Decreased mRNA levels [39] and activity of the main τ-protein phosphatases (PP)1 and PP2A, as well as other τ-phosphatases such as PP2B and PP5, have been observed in AD [40–42]. This can lead to a direct reduction in τ-dephosphorylation or indirect hyperphosphorylation by the inability of these phosphatases to inhibit τ-hyperphosphorylation by different kinases [43], therefore τ-phosphatases have been proposed as therapeutic targets [44]. Major kinases, whose protein levels and activities are reported to be up-regulated in AD and other tauopathies [45–48], involved in the phosphorylation of τ include glycogen synthase kinase (GSK)-3, cyclin-dependent protein kinase-5, casein kinase-1, protein kinase A (cyclic adenosine monophosphate (cAMP)-dependent protein kinase), protein kinase C, calcium and calmodulin-dependent protein kinase-II, microtubule-affinity regulation kinase and mitogen-activated protein kinase family members [49–53]. These proteins have also been suggested as therapeutic targets for AD. Recent reports have highlighted the importance of GSK-3β in the developments of both τ and Aβ pathologies in AD and concluded that this kinase is a vital drug target for the treatment of AD and other neurodegenerative diseases [54–57]. Several animal studies, for example, have demonstrated that the inhibition of GSK-3β activity by lithium [58] results in decreased levels of both Aβ (in PDAPP mice) and τ-phospho-rylation, τ-aggregation and NFT formation (in JNPL3 mutant τ-mice) [59–61]. Other GSK-3β inhibitors are being developed, such as AR-A014418 [61], as well as other kinase inhibitors [62–67]; however, this approach is hindered due to the ubiquitous expression of these kinases, their pleiotropic activities in countless cellular functions and the low selectivity of inhibitors for specific kinases, isoforms of a particular kinase, cellular compartment and/or pathological, rather than physiological, activity of the kinase [68–70].

τ aggregation inhibitors (TAIs)

Screening for TAIs started in the early 1990s with reports on the ability of phenothiazines [71], anthraquinones [72] and low molecular weight N-phenylamine derivatives [73] to prevent τ-aggregation and associated toxicity in cell lines [74]. The most clinically advanced TAI is AL-108 or NAP (Allon Therapeutics Inc., Vancouver, BC, Canada), which is an intra-nasal formulation of an 8 amino-acid peptide (NAPVSIPQ) derived from the biological activity-dependent neuroprotective protein secreted by the brain in response to various insults [75]. Studies in transgenic mice suggest that AL-108 interacts with microtubules, reduces τ-hyperphosphorylation and increases soluble τ levels leading to an improvement in cognition [76, 77]. Data from a recently completed phase IIa trial evaluating AL-108 in 144 patients with amnestic mild cognitive impairment demonstrated that it is safe and well tolerated, and the high dose (15 mg twice a day) resulted in a significant and lasting improvement in short term and working

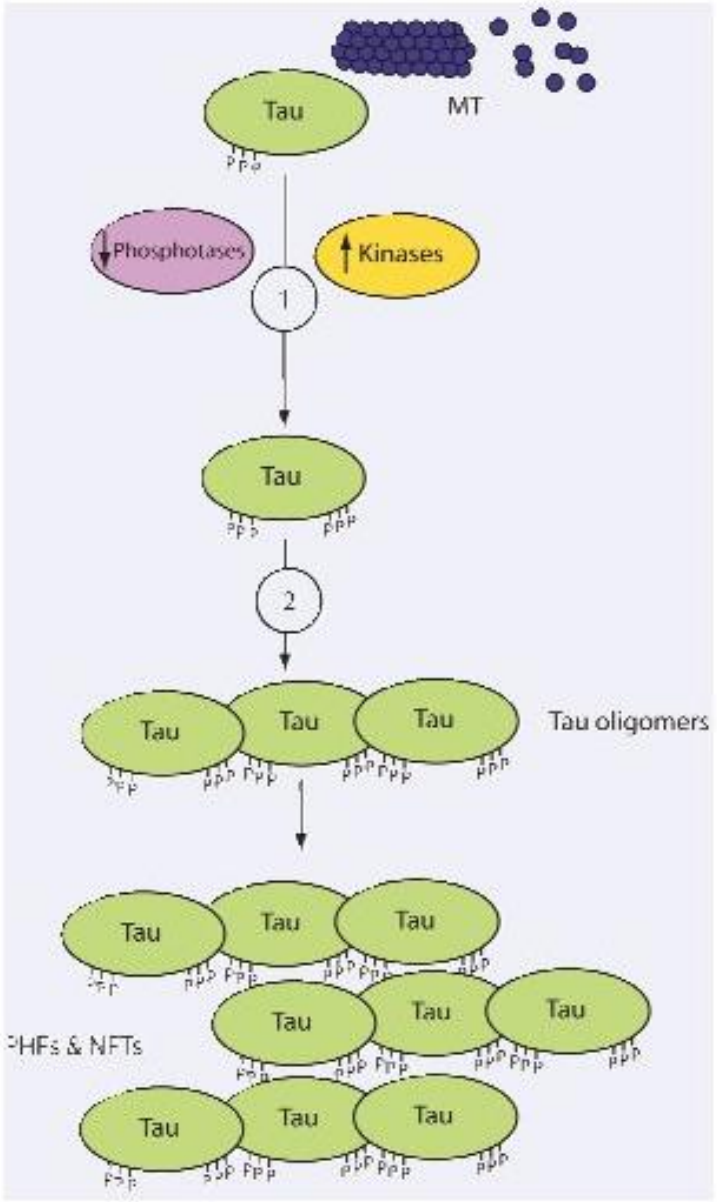

Fig. 1 Pharmacotherapeutic strategies for the treatment of Alzheimer's disease targeting τ. Schematic representation of the anti-τ targets for potential pharmacotherapies: (*i*) Modulators of τ-kinases or phosphatases, (ii) τ-aggregation inhibitors (TAIs). Abbreviations: MT (microtubule); NFTs (neurofibrillary tangles); PHFs (paired helical filaments).

memory (but not in tests that involved executive functions). AL-108 is now being tested as a treatment for other neurodegenerative diseases, mental disorders and ocular disease. An intravenous (IV) formulation of NAP, known as AL-208, is also under clinical investigation for mild cognitive impairment associated with coronary artery bypass graft surgery as well as other indications [78].

A recently announced TAI is Rember™ (TauRx Therapeutics Ltd., Singapore), which has methylthioninium chloride (MTC; also known as the histochemical dye methylene blue) as its active constituent. It is proposed that this compound is not only able to prevent the oligomerization and self-aggregation of τ, but also dissolve pre-formed τ-oligomers and paired helical filaments into truncated

τ-fragments, which can then be naturally degraded and eliminated (http://www.taurx.com/). At the 11th International Conference on Alzheimer's Disease (ICAD, Chicago, 2008), pre-clinical data (01–06-04, P2–383, P2–428) and results of a recently completed 24-week, multi-centred, randomized, double-blind, dose-ranging (30, 60 or 100 mg, three times per day), placebo-controlled phase IIb trial followed by a 60-week, blinded, active treatment extension study were presented (03–04-07, P4–347, P4–384). Patients with moderate AD who received MTC at 60 mg three times/day showed a significant improvement in the Alzheimer's Disease Assessment Scale-Cognitive Subscale (ADAS-Cog) scores, compared to placebo control, at the end of the 24-week-long trial. This result was further verified after 50 weeks of treatment and again at the conclusion of the trial (84 weeks in total). Another measure of the drug's efficacy that was utilized was single photon emission computed tomography (SPECT) analysis at week 24 compared to baseline, which revealed that the regional cerebral blood flow decline seen in the hippocampus and entorhinal cortex of individuals treated with placebo, was not observed in individuals treated with MTC (60 mg three times/day). Despite these seemingly encouraging results, great reservations have been expressed, mainly due to unusual trial design and an unconventional method of analysis. However, TauRx Therapeutics Ltd. has announced that it intends to take Rember™ into a phase III clinical trial, and that it is already testing a second generation TAI molecule, LMT-X, in τ-transgenic animal models.

AD pharmacotherapies targeting Aβ

Although the exact mechanism is still unclear, it is widely believed that dysfunctional Aβ metabolism is the underlying cause for the neurodegeneration and dementia observed in AD. Therefore, a leading strategy for the development of AD pharmacotherapies is modulation of Aβ production, aggregation and/or clearance. It is assumed that altering these processes will stop and/or reverse the pathological neuronal loss and the clinical cognitive decline. We will briefly summarize key findings of the major AD pharmacological strategies being development to target various aspects of Aβ metabolism (see Fig. 2).

Inhibitors and/or modulators of the secretases

The amyloid precursor protein (APP) is an evolutionary conserved type I transmembrane glycoprotein [79] that belongs to a family of proteins, including amyloid protein precursor-like protein1 (APLP1) and APLP2 [80, 81]. Both the amino and carboxyl terminals of APP can be divided into several regions, each with its own characteristics and functions [82]. The overall function of APP is unclear; however, it is believed to be important during the development of the CNS and in response to stress or injury [83]. APP has been suggested to act as a cell-surface receptor and may also be involved in cell adhesion and/or neurite outgrowth [84, 85]. APP is synthesized in the endoplasmic reticulum, undergoes N- and O-glycosylation in the Golgi, and is translocated from the trans-Golgi network to the cell surface *via* the secretory pathway [86]. During and/or after trafficking, APP undergoes degradation *via* the ubiquitin–proteasome system [87] and/or various forms of autophagy [88, 89]. Neuronal macroautophagy induction and impaired clearance of several autophagy intermediates is evident in the AD brain, leading to an overproduction and accumulation of intracellular Aβ in autophagic vacuoles [90, 91].

APP also undergoes proteolytic processing through either the non-amyloidogenic or the amyloidogenic pathways [92]. During the non-amyloidogenic pathway, the membrane-bound enzyme α-secretase cleaves APP within its Aβ domain, resulting in the extracellular secretion of soluble APP-α (sAPP-α) and the production of a short membrane-bound COOH-terminal fragment (CTF), α-CTF or C83 [93]. Subsequent γ-secretase cleavage of C83 results in the secretion of a 3-kD peptide termed p3 out of the cell [94], and release of the APP intracellular domain (AICD) into the cytoplasm [95]. Enzymes that have been suggested to have α-secretase activity include members of a disintegrin and metalloprotease family of proteins, ADAM 10 and ADAM 17 or TACE (tumour necrosis factor-α converting enzyme) [96–98]. The amyloidogenic pathway is initiated when β-secretase, identified as the aspartyl protease β-site APP cleaving enzyme (BACE1, Asp-2 or memapsin-2) [99, 100], cleaves APP at the N-terminal part of the Aβ domain. This cleavage leads to the extracellular release of sAPPβ, while the β-CTF or C99 fragment remains membrane bound. Sequential γ-secretase cleavage of C99, at the C-terminal of Aβ, allows the shedding of the AICD and the secretion of Aβ species of variable length, into the lumen or extracellular space [101]. γ-Secretase is thought to be an intramembranous-cleaving polytopic aspartyl protease [102], comprised a complex of presenilin1 (PS1), presenilin2 (PS2), nicastrin, aph-1 and pen-2 [103–105]. The presenilins (PSs) are transmembrane homologue proteins [106], which have been shown to be essential for the γ-secretase cleavage of APP [107, 108] as well as other type I proteins [109]. Mutations in PSs have been shown to alter APP processing and Aβ levels in mice [110] and are associated with the inheritance of early onset familial AD in human beings [111].

Following their discovery and characterization, the APP secretases became attractive targets in the quest for an AD treatment. The logic behind modulating the APP secretases is two fold: stimulating α-secretase cleavage in order to direct APP processing towards the non-amyloidogenic pathway or suppressing β- and/or γ-secretase cleavage in order to reduce the amount of Aβ produced. It has been shown that muscarinic AChE-receptor agonists can foster α-secretase processing of APP to subsequently result in a reduction in Aβ levels [112, 113]. This has been further demonstrated in animal models of AD, where the treatment of triple transgenic mice [114] with the M1 AChR agonist NGX267 (Torrey Pines Therapeutics, La Jolla, CA, USA) resulted in reduced $A\beta_{1-42}$, reduced amyloid load and decreased τ-phosphorylation as well as improved behaviour [115]. Numerous β- and γ-secretase inhibitors and/or modulators have also been designed; however,

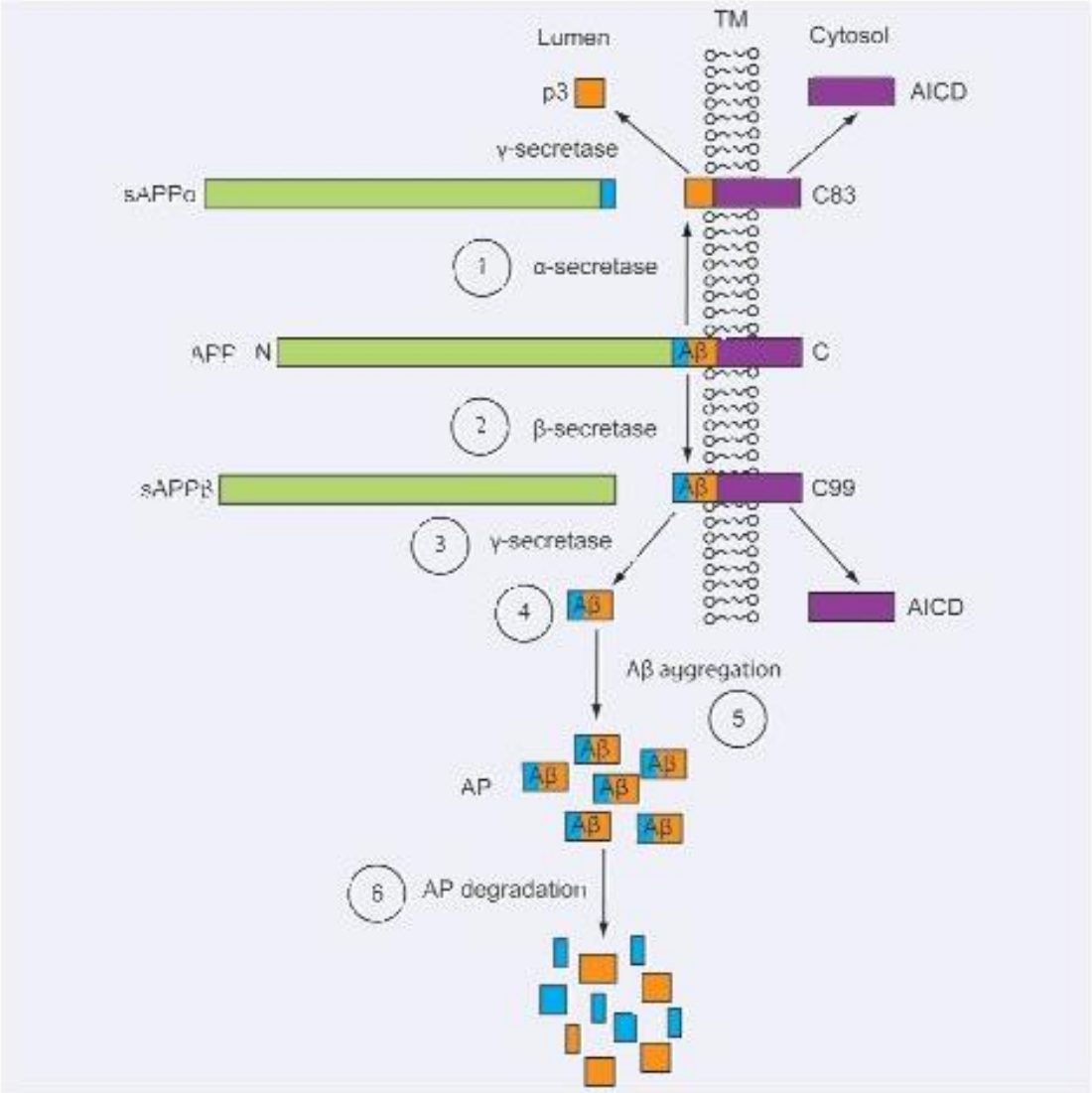

Fig. 2 Pharmacotherapeutic strategies for the treatment of Alzheimer's disease targeting Aβ. Schematic representation of the anti-amyloidogenic targets for potential pharmacotherapies: (*i*) α-secretase activators, (*ii*) β-secretase modulators/inhibitors, (*iii*) γ-secretase modulators/inhibitors, (*iv*) Aβ immunotherapy, (*v*) Aβ aggregation inhibitors, (*vi*) Amyloid-plaque degredation enhancers. Abbreviations: Aβ (amyloid-β), AICD (APP intracellular domain); AP (amyloid plaque); APP (amyloid precursor protein); sAPPα (soluble APP-α); sAPPβ (soluble APP-β); TM (trans-membrane).

the majority of these agents are not specific for the secretase cleavage of APP and thus may prevent the cleavage and processing of additional substrates, which could result in various adverse effects [116, 117]. At the moment, the β-secretase inhibitor TAK-070 (Takeda Pharmaceutical Co. Ltd., Osaka, Japan) is undergoing a phase I clinical trial. A number of γ-secretase-targeting compounds are in early clinical development, including a selective γ-secretase inhibitor (BMS-708163; Bristol-Myers Squibb, New York, NY, USA) and a γ-secretase modulator (E2012; Eisai Inc., Wooddiff Lake, NJ, USA). The most advanced compound, however, is the γ-secretase inhibitor hydroxyl-valeryl monobenzocaprolactam/LY450139 dihydrate (Eli Lilly, Indianapolis, IN, USA). A 40-week, multi-centre, randomized, double-blinded, dose escalation, placebo-controlled, parallel assignment phase II study (safety, tolerability

and biomarker assessment) with LY450139 dihydrate in individuals with mild-to-moderate AD showed that individuals who received either the low (100 mg/day) or high (140 mg/day) dose of the drug had a significant (~60%) decrease in plasma $A\beta_{1-40}$ compared to placebo; however, $A\beta_{1-40}$ changes in cerebrospinal fluid (CSF) were not statistically significant [118]. Recruitment of approximately 1,500 individuals for a phase III trial to study the effects of LY450139 dihydrate (100 or 140 mg per day) on the rate of cognitive and functional decline *versus* placebo over a 2-year period has begun, with the clinical trial estimated to be complete in the first quarter of 2012.

A focal point at ICAD 2008 was the announcement by Myriad Genetics (Salt Lake City, UT, USA) that the most extensive (1,649 patients treated over 18 months in a phase III) AD clinical trial ever to be completed (tarenflurbil/Flurizan™ 800 mg/twice daily or placebo) had failed to demonstrate significant differences in any of its outcome measures, including ADAS-Cog and Alzheimer's Disease Cooperative Study Activities of Daily Living (ADCS-ADL) scores. Thus, the γ-secretase modulator Flurizan™ was ineffective in slowing disease progression. The failure of this trial has raised many issues within the AD research community with the main question being whether or not β- and/or γ-secretase modulators should still be considered as a therapeutic target. Many scientists believe that a wiser strategy to targeting Aβ production is to target Aβ after it has been synthesized.

Aβ aggregation inhibitors

As described above, Aβ is constitutively synthesized at the membrane surface by proteolytic cleavage and is then secreted [119]. Aβ typically ranges between 38 and 43 amino acid residues in length with $A\beta_{1-40}$ and $A\beta_{1-42}$ being the most prominent types in AD [120]. Following its secretion, extracellular Aβ can later be internalized back into the cell by poorly understood molecular mechanisms. Recently, it was reported that in the absence of apolipoprotein E (ApoE), $A\beta_{1-42}$ is internalized in axons of primary neurons *via* a clathrin-independent endocytic pathway involving lipid rafts [121]. The rapid turnover of Aβ in the brain [122, 123] suggests efficient clearance and/or degradation mechanism(s) of the peptide are in place. Detection of Aβ in plasma and CSF [124], implies that Aβ can be transported from the CNS across the BBB into the periphery. In this regard, a few receptors (involved in cholesterol and/or lipid metabolism) have been suggested to mediate Aβ efflux from the brain, including MDR1-P-glycoprotein (P-gp/ABCB1) [125], receptor for advanced glycation end products (RAGE) [126] and the extensively studied low-density lipoprotein receptor-related protein (LRP). Aβ has been shown to bind directly to LRP-1 and LRP-2/megalin or indirectly, by binding to their ligands: apolipoprotein J and E (ApoJ and ApoE, respectively) and α2-macroglobulin (α2 M) [127–129]. Aβ-LRP1/2 complexes can be internalized and delivered to the endosomal/lysosomal compartments, where they either undergo autophagy in a similar manner to APP, or they may undergo transcytosis into the CSF or plasma [130, 131]. Aβ is finally eliminated through the kidney and liver *via* LRP [132, 133] or by liver X receptor [134–136]. Alternatively, Aβ can be catabolized *via* enzymatic degradation [137]. To this end, several classes of enzymes have been identified, including the serine proteases plasmin and tissue plasminogen activator [138–140], and the metalloproteases neprilysin [141–144], insulin degrading enzyme [145–148], as well as the zinc-dependent endothelin-converting enzyme 1 [149, 150] and matrix metalloproteinases 2 and 9 (MMP2 and MMP9, respectively) [151–153].

The fact that Aβ is normally produced in the body throughout life, is present in various organs and bodily fluids, and that the body has evolved sophisticated mechanisms for its metabolism (as detailed above) suggest that Aβ has a physiological role [154]. Although the function of Aβ is yet to be elucidated, Aβ has been proposed as an acute-phase apolipoprotein with metal-binding and antioxidant activities [155–160]. The idea that Aβ has a functional role leads us to the conclusion that with old age, and more specifically with the late onset of AD, Aβ either losses its physiological function or gains a pathological function [155, 156]. There are several theories as to factor(s) that may turn Aβ from being a physiological to a pathological agent; however, none of these hypotheses are definite and all of them still have many caveats. However, it has been consistently demonstrated that Aβ exerts neurotoxic and synaptotoxic affects both *in vitro* [161] and *in vivo* [162]. Researchers have turned to the study of Aβ structure in search of clues as to its toxic effects. It was found that soluble Aβ monomers assume a random coil or α-helix conformation; however, in AD they undergo a structural change into a pleated β-sheet [163]. This induces the peptide to form low molecular weight oligomers, higher molecular weight complexes (protofibrils and amyloid-β derived diffusible ligands or ADDLs), mature fibrils and amyloid plaques (APs) in the neuropil and the vasculature [164–166]. *In vitro* studies have shown that amyloidogenesis and fibrillogenesis can be affected not only by the type of Aβ produced and its conformation, but also by factors such as time, concentration, temperature, pH and metal ion concentration [167]. For many years it was believed that the toxic effects of Aβ were a result of the mature Aβ fibrils; however, recent studies suggest that low molecular weight, soluble, oligomeric forms of $A\beta_{1-42}$ rather than $A\beta_{1-40}$ [168] are more neurotoxic than the mature Aβ fibrils [169–173]. Indeed, the severity of AD correlates more closely with cerebral concentrations of soluble Aβ rather than insoluble Aβ load (reviewed by Lesne and Kotilinek [174]). As our understanding of Aβ structure improves and with the advent of more advanced techniques, the development of inhibitors of Aβ oligomers will improve [175]. Candidate drugs in this category are synthetic peptides based on the $A\beta_{17-21}$ sequence, with the five-amino-acid β-sheet breaker peptide Ac-LPFFD-NH2 (iAβ5p) as its lead compound [176, 177], the discontinued tramiprosate/Alzhemed™ (Neurochem Inc.) and ELND-005/AZD-103 (developed as a joint venture by Elan Pharma International Ltd., Dublin, Ireland and Transition Therapeutics, Toronto, ON, Canada). Tramiprosate/Alzhemed™ is in fact a variant of the amino acid taurine (3-amino-1-propanylsulfonic acid [3-APS]) [178], which prevents sulphated glycosaminoglycans from promoting the

oligomerization of soluble Aβ [179], but at the same time also enhances non-toxic τ-aggregation *in vitro* [180, 181]. Unfortunately, pre-clinical studies of tramiprosate/ Alzhemed™ in TgCRND8 mice did not include an investigation of τ-pathology or any behavioural testing. Phase II trial results showed the only significant effect of tramiprosate/Alzhemed™ treatment was a dose-dependent reduction in CSF $A\beta_{1-42}$, but had no significant impact on CSF $A\beta_{1-40}$ and τ, or on psychometric scores [182, 183]. Despite these disappointing results, the investigational drug progressed into a phase III trial in Northern America, which was recently declared by the FDA to have failed. As a result, the European Phase III study of tramiprosate/Alzhemed™ has been abandoned and the compound is being marketed as a nutraceutical, although a phase II trial for its use as a preventative of hemorrhagic stroke in patients with cerebral amyloid angiopathy (CAA) is ongoing. Another investigational drug, ELND-005/AZD-103 (Transition Therapeutics, Toronto, ON, Canada and Elan, Dublin, Ireland), is an orally administrated compound that crosses the BBB and is believed to break-down Aβ aggregates and prevent further Aβ oligomerization from taking place. In transgenic mouse models of AD, ELND-005/AZD-103 treatment improved their spatial memory performance in the Morris Water Maze. In several phase I studies, single and multiple ascending doses of ELND-005/AZD-103 were shown to have good safety, tolerability and pharmacokinetic profiles. At present, ELND-005/AZD-103 is undergoing an 18-month phase II trial in 340 patients with mild-to-moderate AD in order to confirm its safety and to evaluate its efficacy on cognition and functionality.

Another approach has been to try and characterize the mechanism(s) involved in the neurotoxicity of Aβ as a basis for developing pharmacotherapeutics that modulate these processes. Aβ-associated neurotoxicity may be attributed to various factors [184], including: Aβ interactions with intracellular target(s) and/or extracellular Aβ interaction with membrane surface receptor(s), cholesterol, lipids and lipoproteins [185, 186]. Activation of microglia and inflammatory factors [187] and induction of apoptosis by Aβ-mediated activation of cysteine aspartyl proteases termed caspases [114, 188, 189] have also been proposed to have neurotoxic effects. Berman and colleagues recently demonstrated that Aβ oligomer-induced neurotoxicity is due to the destabilization of phosphatidylinositol-4,5-bisphosphate ($PtdIns(4,5)P_2$) metabolism [190]. Another proposed mechanism of Aβ toxicity is the promotion of ion-channel formation and calcium ion (Ca^{2+}) influx [191]. This theory gained support from pre-clinical and early clinical trials with different neuronal L-type calcium channel blockers, such as S-312-d, nimodipine and MEM 1003 (Memory Pharmaceuticals, Montvale, NJ, USA) [192–195]. However, meta-analysis of clinical studies revealed that nimodipine only slows down the disease progression and may be effective only in certain types of dementia [196]. As for MEM 1003, late last year Memory Pharmaceuticals announced that the drug failed to show changes in ADAS-Cog scores between treated and control mild-to-moderate AD patients in a phase IIa trial, yet the company is still testing the efficacy of MEM 1003 in individuals with bipolar disorder (www.memorypharma.com).

Passive or active immunization

A novel and controversial approach to treating AD is based on vaccine therapy. Transgenic mouse models of AD actively immunized with Aβ [197–200] or passively immunized with humanized anti-Aβ antibodies [201–208] showed reduced Aβ and τ-pathology, neutralized soluble Aβ oligomers, attenuated synaptic degeneration and improved synaptic plasticity, all of which were accompanied by improved learning. Immunization against Aβ thus appeared to be the much-anticipated breakthrough in the development of AD therapeutics, in addition to being the primary test of the amyloid cascade hypothesis. An active immunization strategy was rapidly advanced into clinical trials by Elan, and following successful completion of the phase I trial, a phase IIa trial with AN-1792/Betabloc was initiated by Elan/Wyeth. This study was terminated after four patients presented with symptoms consistent with autoimmune meningoencephalitis [209, 210] and by the end of 2002 there were 18 known cases [211]. A subsequent autopsy analysis of a phase I study patient, who died 20 months after the first inoculation, indicated evidence of encephalitis [212]. This, together with three later autopsy cases of AN-1792-immunized AD patients, highlighted the persistence of CAA despite the removal of Aβ from plaques [213], consistent with observations from studies in PDAPP mice [214, 215] and monkeys [216]. A follow-up study of a further 36 patients demonstrated that many developed anti-Aβ antibodies, which was consistent with a slowing in the rate of cognitive decline 12 months after completion of the trial [217]. Patients with the highest titres also displayed the greatest slowing in cognitive decline [218]. While encouraging, MRI scans of the antibody responders revealed a reduction in total brain volume and the rates of cognitive decline in the non-responders appeared more rapid than typical [219]. However, a composite neuropsychological performance study has shown that the patients developing Aβ antibodies showed improvements in memory, attention and concentration, along with decreases in the level of τ-protein in CSF [220]. The most recent data to emerge from the original immunization trial, however, appear to confound some of these earlier reports. The long-term clinical follow-up of 80 patients demonstrated that, despite a varied degree of Aβ plaque removal, there was no prevention of progressive neurodegeneration and no evidence for improved survival [221]. Of note, seven of the eight immunized patients that underwent autopsy, including two patients with near complete removal of plaques, had severe end-stage dementia prior to death [221]. Despite its tragic outcome, valuable lessons learnt from this failed trial have lead researchers to develop more selective, advanced immunotherapies [222–225], including another active Aβ vaccine developed by Elan and Wyeth (Madison, NJ, USA) (ACC-001). Affiris GmbH (Vienna, Austria) is also developing an active immunization program with AFFITOPE AD01 (phase I study due to be completed in November 2008) and AFFITOPE AD02 (recruitment stage for a phase I trial due to be completed in early 2009).

The development of intravenous recombinant humanized anti-Aβ monoclonal immunoglobulins (IVIg), which avoid the induction

of an immune response, continues in parallel. Two small, independent phase I investigations of AD patients with IVIg over six months proved to be safe, stopped the cognitive deterioration and in most cases even resulted in a slight improvement of ADAS-Cog scores [226]. Examples of passive vaccines against Aβ in various stages of research and development are: phase I (V950, Merck, Whitehouse Station, NJ, USA; PF-04360365, Pfizer, New York, NY, USA), completed phase II (LY2062430, Eli Lilly, Indianapolis, IN, USA), and ongoing parallel phase II and III (AAB-001/Bapineuzumab, Elan with Wyeth, Madison, NJ, USA). Data from a phase II study with LY2062430 indicate that the monoclonal antibodies lead to elevated levels of $A\beta_{1-40}$ and $A\beta_{1-42}$, both in serum and CSF; however, SPECT analysis did not reveal any reduction in APs and no improvement in cognition was detected. Despite this, the company has announced its intention to commence a phase III study with LY2062430 in the coming year. With regards to AAB-001/bapineuzumab, modified intent-to-treat (MITT) interim analysis of phase II studies showed no significant changes in ADAS-Cog and Disability Assessment Scale for Dementia in the total study population and no statistically significant changes in any of the cognitive or functional efficacy endpoints in the ApoE4 carrier sub-group. In fact, a significant elevation in ventricular volume was observed in ApoE4 carriers treated with the drug. However, *post hoc* MITT analysis of the results did show statistically significant differences from baseline in ADAS-Cog, the Neuropsychological Test Battery and the Clinical Dementia Rating Sum of Boxes, as well as the Brain Boundary Shift Integral in the non-ApoE4 carrier sub-group treated with AAB-001/bapineuzumab compared to placebo. It should be noted that individuals treated with the drug experienced significantly more cases of cataracts, deep vein thrombosis, syncope, seizures and pulmonary embolism, as compared to placebo control patients. Importantly, vasogenic edema was observed only in drug-treated patients and mostly in ApoE4 carriers treated with the highest dose of the drug (2.0 mg/kg). The significance of the results, however, will only be made clear once a final analysis is done after the completion of all phase II and III trials.

The metal hypothesis of AD

It is evident that both Aβ and τ are involved in the development and progression of AD; however, pharmacological strategies directed at these targets have not yet proven to be disease modifying in human studies. In particular, several investigational drugs that target Aβ have failed to show any correlation between a reduction in amyloid burden and improvement in cognitive functions in large-scale clinical trials (as mentioned above). While such data might indicate that the 'amyloid hypothesis' of AD is not necessarily the correct one, there remains considerable debate as to whether it has yet to be truly tested in the clinic. Numerous factors have been proposed to account for the poor performance of several frontline drugs, including: patient confounds (*e.g.* ApoE genotype, overall rates of cognitive decline in placebo groups), trial design (*e.g.* is a 'treatment' protocol, as opposed to a 'prevention' protocol, the best way to test the hypothesis) and drug penetration (*e.g.* it is suggested that Flurizan may have failed because of a poor pharmacodynamic profile). While the debate over the validity of the amyloid cascade hypothesis will no doubt continue, it remains likely that there are other critical factors playing a role in AD pathogenesis.

Metal ions are one such possibility, as cerebral concentrations of zinc (Zn), copper (Cu) and iron (Fe) ions are significantly elevated in AD, compared to age-matched controls [227–230], and metals have been implicated in several other neurodegenerative diseases [231–234]. Here, we will review the various events in AD pathogenesis in which metal ions are involved, and then discuss the pharmacotherapeutics being developed to modulate metal ions in AD.

There is an increasing amount of evidence suggesting that τ and NFTs may in some way be involved in, or regulated by, metal metabolism. Zinc ions (Zn^{2+}) [235] and the iron regulatory protein-2 [236], for example, have been found to co-localize with NFT-containing neurons. Addition of Zn^{2+} to mouse and human neuroblastoma cells (N2a and SH-SY5Y, respectively) induces τ-hyperphosphorylation [237], whereas the opposite result is seen in hippocampal neurons with the addition of pyrolidium dithiocarbamate (PDTC) [238] or iron citrate ($FeC_6H_5O_7$) [239]. Ferric ions (Fe^{3+}) and cupric ions (Cu^{2+}) can bind to various 'repeat' motifs on τ, thus altering the protein's conformation, promoting its phosphorylation [238] and inducing its aggregation [240–242]. In the case of iron, this effect can be reversed by reducing Fe^{3+} to Fe^{2+} (ferrous ions) [243]. As for APs, they have been shown to be enriched with Cu (400 μM), Zn (1 mM) and Fe (1 mM) [114, 176, 192–194], suggesting that there may be an interaction between metals, APP and Aβ that may influence Aβ aggregation and Aβ-associated toxicity.

It has been demonstrated that APP contains putative zinc and copper-binding domains (CuBD) both in its ectodomain and in its Aβ sequence (see Fig. 3). Little is known about the APP Zn-binding domain; however, it has been established that its CuBD consists of a tyrosine (Tyr^{168}), a methionine (Met^{170}) and two histidine ($His^{147,151}$) residues that are able to coordinate Cu^{2+} and reduce it to Cu^{+} [244]. The similarities between the CuBD on APP and Cu chaperone proteins suggest that APP may play a role in metal homeostasis [245]. This notion has recently gained support from findings that the translation of APP mRNA is governed by the binding of an iron-regulatory element to its 5'-untranslated region such that in an Fe-enriched environment APP translation is up-regulated, whereas it is down-regulated in response to an Fe-deficient milieu [246, 247]. Moreover, increasing Cu levels *in vitro* can shift APP processing towards the non-amyloidogenic pathway and result in decreased Aβ production [222–225]. This may result from an increase in GSK-3β phosphorylation, which activates phosphatidylinositol-3-kinase (PI3K) to result in the secretion of MMPs that can degrade Aβ [225]. In addition, genetically modified animal models of AD provide vital clues as to the affects of APP and Aβ on metal-ions and *vice versa*. Tg2576 mice that overexpress the Swedish double mutant APP_{695} (K-670-N and M-671-L)

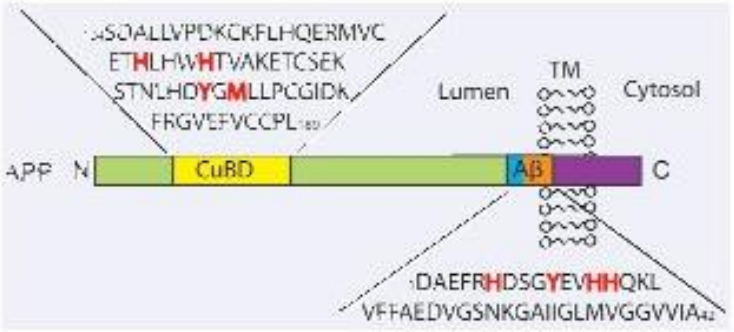

Fig. 3 Copper binding domains on APP. APP contains two high-affinity copper binding domains: one on its N-terminus and the other on the Aβ sequence. Highlighted in red are the copper binding ligands in the CuBD and in the $Aβ_{1-42}$ sequence. Abbreviations: Aβ (amyloid-β); APP (amyloid precursor protein); CuBD (copper binding domains); TM (trans-membrane).

exhibit AD-related behavioural and cognitive changes (memory and spatial learning impairments) [248] and AD-related pathology (substantially elevated levels of full-length APP, CTFs and cerebral extracellular Aβ) [249]. However, their cerebral Cu (but not Fe) levels are significantly reduced [224, 250]. C100 mice over-express Aβ and the C-terminal of APP, yet have significantly lower levels of both Cu and Fe in the brain [250]. Conversely, APP (and APLP2) knockout mice have raised brain and liver Cu levels [251] and develop reactive cerebral gliosis and locomotor-behavioural changes with age [252]. These studies all suggest a role for APP in metal homeostasis. As a further demonstration that metal homeostasis is important in the pathogenesis of AD, when APP_{SWE}/$PS1_{P-264-L}$-expressing mice, which also have ~15% lower brain Cu levels compared to non-transgenic controls, are crossed with TxJ 'toxic milk' mice (that have a mutated ATPase7b transporter and a consequent elevation in Cu levels), the resulting progeny have markedly reduced AP load and Aβ levels [224]. Similarly, increasing dietary copper intake in APP23 mice (carrying the Swedish mutation of human APP_{751}, regulated by the murine Thy-1.2 promoter [253]) resulted in reduced Aβ levels and a prolonged lifespan [222]. Conversely, increasing dietary Cu intake in normal rabbits resulted in elevated Aβ levels and impaired learning [134, 254]. Thus, metal homeostasis appears to be intimately involved in Aβ metabolism.

These *in vivo* studies are supported by a wealth of *in vitro* data demonstrating that low concentrations of Zn^{2+} promote the rapid aggregation of Aβ at physiological pH [255–259]. At mildly acidic pH, Cu^{2+} (and Fe^{3+}) have also been shown to induce Aβ precipitation [227, 230, 260–262]. These data suggest that the synaptic cleft is an ideal location for Aβ metallation and aggregation, as neurotransmission results in peak concentrations of ~300 μM Zn^{2+} [263, 264] and up to 100 μM Cu^{2+} [265–267]. This is supported by observations of a significant reduction in plaque formation in a transgenic mouse model of AD (Tg2576) lacking the zinc transporter 3 (ZnT3) protein ($Tg2576/ZnT3^{-/-}$) [268, 269], which is responsible for zinc enrichment and transport into pre-synaptic vesicles [270, 271]. The complicated process of Aβ aggregation makes it is difficult to characterize the binding of metals to Aβ, and while there have been numerous reports on the affinity and stoichiometry of Aβ-metal binding, results have varied depending on: the Aβ source (mouse, rat or human), Aβ sequence or length ($Aβ_{X-16/28/40/42}$), Aβ species (monomers, oligomers, etc.), as well as the reaction conditions (sample preparation, type and concentration of buffer, pH, incubation time and/or technique used). Most researchers are in agreement that Aβ binds Cu^{2+} and Zn^{2+} in a 1:1 ratio [272–276]; however, there have also been reports of Zn^{2+} binding to Aβ in a 2:1 [277] and 3:1 stoichiometry [278], and of Cu^{2+} binding to Aβ in a 2:1 ratio when copper is in excess [279, 280]. Mounting evidence indicates that the Aβ:metal ions ratio modulates not only Aβ conformation (random coil, α-helix or β-sheet) and aggregation [281–283], but also the morphology of the Aβ aggregates (amorphous, non-fibrillar or fibrillar) [280, 284, 285]. There is also an ongoing debate as to the binding affinity and kinetics of Aβ to Cu^{2+} and Zn^{2+}, with dissociation constants (K_D) ranging from nM to μM for Cu^{2+}-Aβ [272, 286, 287] and for Zn^{2+}-Aβ [255, 276, 287–291]. A novel study has even suggested an initial, weak Zn^{2+}-$Aβ_{40}$ complex, which quickly turns into a high-affinity complex, possibly due to a conformational change of the peptide [287]. In order to resolve the issues above, it is imperative that the metal-binding site(s) of Aβ and APP are defined and that the relationship between the structural features of the protein and its function in health and disease can be elucidated. Recent studies [287, 292] utilizing the electrospray-ionization mass spectrometry, Raman spectroscopy, electron paramagnetic resonance, circular dichroism, nuclear magnetic resonance, X-ray diffraction and extended X-ray absorption fine structure spectroscopies have determined the coordination of Cu and Zn by His^6, His^{13}, His^{14} [163, 255, 262, 272, 284, 286, 293–301] and a fourth ligand. The fourth donor could be Tyr^{10} [293, 301] and/or Glu^{11} [288, 302] for Zn^{2+}, or Tyr^{10} [293, 296] and/or Asp^1 [272, 298, 299] for Cu^{2+}. Interestingly, mouse and rat Aβ contains three amino acid substitutions (R-5-G, Y-10-F and H-13-R), which prevent the formation of intermolecular histidine bridges [293, 303, 304] and therefore do not allow metal-induced Aβ aggregation *in vitro* [256, 260] and cerebral Aβ deposits *in vivo* [305].

In summary, the above findings demonstrate APP and/or Aβ play a major physiological role in regulating metal-ion levels. This cumulative data has lead Bush, Tanzi and colleagues to propose 'the metal theory of AD' [306], which stipulates that age-related endogenous metal dyshomeostasis in the brain allows binding of

redox-active metal ions (Cu^{2+} and Fe^{3+}) to Aβ. This can lead to neurotoxicity as Cu^{2+} stabilizes the neurotoxic, oligomeric Aβ species [307–309], induces the covalent di-tyrosine crosslink of Aβ [274, 286, 287, 310–317] and promotes the generation of SDS-resistant copper-derived diffusible ligands [278, 286, 316]. Metallated-Aβ also has an increased affinity for the phospholipid heads of the membrane bilayer [318, 319], which acts as a reductant in the production of reactive oxygen species (ROS) *via* Fenton and Haber–Weiss chemistry [320, 321]. The resulting radicals, such as hydrogen peroxide (H_2O_2) and superoxide (OH^-), induce oxidative stress damage of lipids, proteins and DNA, ultimately leading to synaptic and neuronal loss [230, 231, 320–326]. Based on this hypothesis, pharmacotherapeutics that aim to restore metal homeostasis, inhibit Aβ-metal interactions and/or inhibit metallated Aβ-catalysed oxidation are being developed.

AD pharmacotherapies targeting metal ions

The equilibrium (concentrations, distribution, stability and bioavailability) of metal ions is critical for many physiological functions. This is particularly true for the CNS, where metals are essential for development and maintenance of enzymatic activities, mitochondrial function [327, 328], myelination [329], neurotransmission [330], learning and memory [331, 332]. Due to their importance, cells have evolved complex machinery for controlling metal-ion homeostasis. However, when these mechanisms fail, the altered homeostasis of metal ions can result in a disease state, including several neurodegenerative disorders [333, 334]. Understanding the complex structural and functional interactions of metal ions with the various intracellular and extracellular components of the CNS, under normal conditions and during neurodegeneration, is essential for the development of effective therapies [335]. Accordingly, modulation of metal ions has been proposed as a disease-modifying therapeutic strategy for AD [336–338] and other neurodegenerative diseases [339, 340]. Antioxidants and metal-modulators represent two such therapeutic strategies.

Antioxidants

Antioxidant molecules are capable of neutralizing free or incorrectly bound metals, thereby interfering with the 'down-stream' generation of ROS and other radicals. Therefore, antioxidants may be used mainly as a preventative approach [341]. Numerous molecules with antioxidant properties, such as oestrogen, melatonin, vitamin C and E (L-ascorbate and α- topopherol, respectively), ginkgo biloba extract, curcumin and flavonoids, have been shown to have neuroprotective effects against Aβ-induced toxicity in cell-based experiments [342, 343] and animal models [344–348], but have had conflicting results in a clinical setting [349–351].

Metal chelators

By definition, metal chelators bind strongly to two or more metal ions and form a cyclic ring, which converts the metal ions into an inert form and depletes the total pool of bioavailable metals. Desferrioxamine (DFO), an Fe chelator with high binding affinities for Zn, Cu and aluminium (Al) [352], was the first such agent to enter clinical investigations for the treatment of AD. Results of a 2-year-long, blinded phase II trial with a cohort of 48 AD patients demonstrated that 125 mg intramuscular injections twice daily for 5 days a week significantly slowed down the decline of some cognitive functions, compared to the two control arms (an oral placebo or no treatment) [353]. DFO, however, is a large hydrophilic molecule, which is not orally bio-available and does not normally penetrate the BBB. Hence, it is unknown whether the beneficial effect seen with the DFO treatment was due to the drug's interaction and/or chelation of metals, or due to a different mechanism all together [354]. Another hexadentate chelator, DP-109 (DPharm, Rehovot, Israel), is a large synthetic pro-drug that becomes activated following the cleavage of its two long-chain esters. Daily administration of DP-109 by oral gavage to female Tg2576 mice over a 3-month period reduced the formation and deposition of CAA and APs, as well as re-solubilized Aβ [355]. Like DFO, DP-109 is not expected to cross the BBB, therefore the way it exerts its anti-amyloidogenic effect is still not clear. Recently, DP-109 and DP-460 (another Ca, Cu and Zn lipophilic chelator) were reported to have neuroprotective effects in a G93A transgenic mouse model of amyotrophic lateral sclerosis [356], another neurodegenerative disease associated with metal imbalance [357, 358]. Other chelating agents have been reported to have different effects *in vitro*, including reduced $Aβ_{42}$-induced oxidative stress [359], and the solubilization of hypophosphorylated τ [360] and Aβ from AD brain [361]. Further *in vivo* studies with these chelators is required to further advance this therapeutic route and to rule out any systemic effects.

An alternative approach to chelation is to modulate metals with metallo-complexes. Such an approach serves to remove metals from biologically deleterious sites and potentially deliver them to areas of deficiency, thereby maintaining overall metal homeostasis.

Metal complexes

Metallo-complexes are emerging as a new potential therapeutic for AD. The rational guiding this strategy is the delivery of Cu, for example, to cellular compartment which are Cu-deficient, using metallo-complexes of pyrrolidine dithiocarbamate (M^{2+}-PDTC) or *bis*(thiosemicarbazone) (M^{2+}-BTSC), or preventing the harmful binding of Cu to Aβ, using platinum (Pt) complexed to 1,10 phenanthroline derivatives (L-$PtCl_2$).

PDTC is traditionally considered an inhibitor of the transcription-factor regulator nuclear factor-κB (NF-κB) with anti-inflammatory, antioxidant and anti-apoptotic properties [362–364] – all of which have been attributed to the synergistic interaction

between PDTC, Cu and/or Zn [365–371]. As well as preventing the nuclear translocation of NF-κB in a neonatal hypoxia-ischaemia model, PDTC also activates Akt and inhibits GSK-3β [372]. *In vivo*, oral PDTC treatment of APP/PS1 double transgenic mice resulted in increased cerebral Cu levels, as compared to non-treated APP/PS1 mice, as well as down-regulation of the GSK-3β signalling cascade, which lead to a decrease in τ-phosphorylation and an improvement in spatial memory, but had no effect on amyloid burden, glial activation or oxidative stress [238]. The latest data to emerge indicate that PDTC complexed to either Cu^{2+} or Zn^{2+} can act as proteasome inhibitors to induce apoptosis in numerous human cancer cells [373–375]. It would be of interest to examine if the same effects occur in cellular and/or animal models of AD.

The metallo-complexes of diacetyl*bis*(N^4-methylthiosemicarbazone) (M^{2+}-ATSM) and glyoxal*bis*(N^4-methylthiosemicarbazone) (M^{2+}-GTSM) have both been shown to have anti-bacterial, anti-fungal and anti-neoplastic/cytotoxic activities, by selectively delivering exogenous metal ions into metal-deficient cells [376, 377]. Cu^{2+}-ATSM is membrane permeable, selective for oxygen-deprived (hypoxic) cells, and is redox inactive therefore the ligand retains its Cu molecule [378, 379]. These properties are being exploited for its development as a radiotherapeutic agent [380–382] and as a radiopharmaceutical for positron emission tomography imaging [383, 384]. Cu^{2+}-GTSM can also cross the BBB; however, once inside the cell it is reduced by various cellular reductants and releases its Cu molecule, which is made available for the cell [378, 385, 386]. Treatment of hAPP$_{695}$-overexpressing CHO cells with Cu^{2+}/Zn^{2+}-BTSC ligands resulted in increased intracellular metal levels that, in turn, activated Akt/PI3K, c-Jun N-terminal kinase and GSK-3 [387]. Phosphorylation of the above kinases lead to the up-regulation of MMPs, which reduced extracellular levels of Aβ [387]. Examination of the effects of Cu^{2+}/Zn^{2+}-BTSC ligands on τ and translation of these studies to animal models of AD is currently underway.

Other radiopharmaceutical-based compounds being evaluated for treatment of AD are 1,10 phenanthroline derivatives complexed to platinum (Pt^{2+}). These ligand-$PtCl_2$ complexes have been designed to bind and alkylate the imidazole side chains on histidine residues 6, 13 and 14 on Aβ, thereby preventing the detrimental binding of Cu^{2+} to this Aβ metal binding site and subsequent Aβ-Cu^{2+} binding to the cell membrane [388]. This study identified the Pt(4,7-diphenyl-[1,10] phenanthroline)Cl_2 as a compound that binds to Aβ, changes the conformation of Aβ and inhibits Aβ aggregation [388]. In addition, this complex is able to inhibit Aβ-related neurotoxicity (restore the cell viability of primary mouse cortical neurons and suppresses the Cu^{2+}-Aβ-dependent H_2O_2 generation), and reverse Aβ-inhibited long-term potentiation (LTP) of mouse hippocampal slices as a measure of synaptotoxicity [388]. Future evaluation of the compound's ability to cross the BBB and exert beneficial effects in animal models for AD need to be performed prior to its advanced development as an AD pharmacotherapeutic.

The Aβ-metal interaction can be targeted not only to the Aβ sequence that binds metals, but also to the metals themselves.

Metal-protein attenuating compounds (MPACs)

MPACs have weak, reversible affinity towards metals, which enables them to compete with endogenous ligands for metal ions, target the harmful 'up stream' metal-protein reactions and restore normal metal levels in specific cellular compartments [389]. The first-generation series of MPACs were based on clioquinol (CQ; 5-chloro-7-iodo-8-hydroxyquinoline). CQ is highly lipophilic, absorbed quickly, can convert to glucuronated and sulphate metabolites, is able to cross the BBB and is excreted in urine and faeces [390–395]. CQ had been used as a therapeutic in cattle and human beings with Zn-deficiency diseases and for many decades was prescribed as an oral anti-amebic in addition to being used for the treatment of dysentery and diarrhoea [396, 397]. However, its oral preparation was withdrawn from the market during the 1960s to 1970s, as it was suspected to be involved in the development of subacute myelo-optico-neuropathy (SMON) [398–401]. SMON is characterized by sensory and motor disorders in the lower limbs, peripheral neuropathy and visual impairment due to demyelation of the spinal cord, optic nerve and peripheral nerves [402]. SMON affected people worldwide; however, it reached near-epidemic proportions in Japan, where a few related deaths were reported [403]. At the time, a mechanistic link between CQ and SMON was not established [404]. Later, it was suggested that CQ may transport metals into the CNS, which leads to neurotoxicity. Early studies demonstrated that CQ-Fe^{3+}, but not CQ or Fe^{3+} alone, induced degeneration of cultured retinal neuroblasts [405] by increasing cellular Fe concentrations and promoting lipid peroxidation [406]. However, it is now believed that intake of CQ at doses far exceeding the recommended ones and for prolonged periods, together with a post-World War II iron-deficient diet, are the reasons for a vitamin B12 deficiency that presented as SMON in Japan [407, 408].

CQ binds Cu^{2+} and Zn^{2+} (2:1 ratio) in a square, planar arrangement [409, 410] and exerts different effects on Cu and Zn, depending on its route of administration and the system in which it is tested [411–413]. The known interaction of CQ with Cu^{2+} and Zn^{2+} thus prompted an investigation into the effects of CQ on AD-related pathology. CQ was initially shown to dissolve synthetic Aβ-Cu^{2+}/Zn^{2+} aggregates and amyloid deposits from post-mortem AD brain [414]. This then prompted a study of the oral administration of CQ to Tg2576 mice over 9 weeks, which resulted in the normalization of cerebral Cu and Zn levels, a reduction in H_2O_2 synthesis, and a significant decrease in cortical amyloid deposition by ~49%, compared to control littermates [415]. Subsequently, CQ was shown to reverse Cu-suppressed, but not Zn-suppressed $A\beta_{1-40}$ fibril formation [416], and to rescue Ca^{2+}-mediated Aβ toxicity in neuronal cell culture [417]. Other studies, however, have suggested that CQ increases oxidative neurotoxicity [418]. As previously mentioned, CQ treatment caused a reduction in Aβ levels in CHO-APP cells, accompanied by increased phosphorylation of GSK-3 and MMP2/3 activity [225]. The cumulative data led to CQ being entered into clinical trials for the treatment of AD (PBT-1, Prana Biotechnology, Melbourne, Victoria, Australia), in which CQ slowed the cognitive decline of moderate to severe AD patients, with no signs of

severe adverse effects. It also influenced CSF-τ, lowered plasma $A\beta_{1-42}$ with no change to CSF-$A\beta_{1-42}$ levels [419]. Subsequent phase II/III studies, however, were stalled by the difficulties encountered in preventing di-iodo-8-hydroxy quinoline contamination during the required larger scale chemical synthesis for such trials [420]. The subsequent drug discovery program identified PBT2 (Prana Biotechnology) as an 8-hydroxy quinoline that lacks iodine, thereby enabling easier chemical synthesis, and which also has higher solubility and increased BBB permeability than CQ. This compound was then extensively screened in a variety of pre-clinical assays. In APP/PS1 Tg mice, PBT2 was shown to decrease soluble interstitial Aβ within hours, and to improve cognitive performance to levels equivalent to or greater than wild-type controls within days of treatment [421]. In addition, there was a significant decrease in insoluble Aβ load and the phosphorylation of τ, as well as a significant increase in synaptophysin levels – suggesting that a number of primary indices that characterize the AD brain had been successfully modulated by this orally bioavailable MPAC [421]. PBT2 then progressed into human clinical trial, and following a successful phase I study, it entered into a randomized, double blind, placebo-controlled, multi-centred, 12-week-long phase IIa trial with 78 mild AD patients (Prana Biotechnology). This study demonstrated safety and tolerability, reduced CSF levels of $A\beta_{1-42}$ and improved cognition in patients taking PBT2 as compared to placebo [422]. Taken together, these data support the notion that the modulation of metals may be sufficient to significantly alter the onset and progression of AD, and that targeting metals may represent a more potent disease intervention than systemically targeting the production or degradation of the Aβ protein; however, these concepts need to be further explored in a larger phase III trial.

While CQ is continuing to be examined as a therapeutic for other diseases, such as Parkinson's disease, Prion diseases, Huntington's disease, diabetes and cancer [373, 411, 423–431], a finer dissection of the mechanism of action of drugs such as CQ and PBT2 will enable researchers to better design additional pharmacotherapies for the treatment of AD and other diseases.

Conclusion

It is evident that AD pathogenesis is a complex process involving both genetic and environmental factors; therefore development of effective disease-modifying drugs is proving to be a difficult task. Aβ, τ and metals are some of the therapeutic targets identified and compounds that modulate them represent promising drug candidates. With ongoing basic science and clinical research, we look forward to a greater understanding of the pathogenesis of AD, the completion of several comprehensive clinical trials and the development of new potential pharmacotherapeutic agents for the treatment and/or prevention of AD.

Disclosers and Acknowledgements

The authors would like to acknowledge Dr. Robert Cherny for discussing the ideas presented. Y.B. is supported by the Commonwealth Scientific and Industrial Research Organization (CSIRO) Preventative-Health Flagship. P.A.A., C.L.M., K.J.B. and A.I.B. are consultants to Prana Biotechnology. We gratefully acknowledge the support of the National Health and Medical Research Council of Australia, Australian Research Council and the Alzheimer's Association (USA).

References

1. **Mount C, Downton C.** Alzheimer disease: progress or profit? *Nat Med.* 2006; 12: 780–4.
2. **Nagy Z.** The last neuronal division: a unifying hypothesis for the pathogenesis of Alzheimer's disease. *J Cell Mol Med.* 2005; 9: 531–41.
3. **Lleo A, Greenberg SM, Growdon JH.** Current pharmacotherapy for Alzheimer's disease. *Annu Rev Med.* 2006; 57: 513–33.
4. **Hynd MR, Scott HL, Dodd PR.** Glutamate-mediated excitotoxicity and neurodegeneration in Alzheimer's disease. *Neurochem Int.* 2004; 45: 583–95.
5. **Sonkusare SK, Kaul CL, Ramarao P.** Dementia of Alzheimer's disease and other neurodegenerative disorders–memantine, a new hope. *Pharmacol Res.* 2005; 51: 1–17.
6. **Parsons CG, Stoffler A, Danysz W.** Memantine: a NMDA receptor antagonist that improves memory by restoration of homeostasis in the glutamatergic system–too little activation is bad, too much is even worse. *Neuropharmacology.* 2007; 53: 699–723.
7. **Li L, Sengupta A, Haque N, Grundke-Iqbal I, Iqbal K.** Memantine inhibits and reverses the Alzheimer type abnormal hyperphosphorylation of tau and associated neurodegeneration. *FEBS Lett.* 2004; 566: 261–9.
8. **Tariot PN, Farlow MR, Grossberg GT, Graham SM, McDonald S, Gergel I.** Memantine treatment in patients with moderate to severe Alzheimer disease already receiving donepezil: a randomized controlled trial. *JAMA.* 2004; 291: 317–24.
9. **Sparks DL, Connor DJ, Sabbagh MN, Petersen RB, Lopez J, Browne P.** Circulating cholesterol levels, apolipoprotein E genotype and dementia severity influence the benefit of atorvastatin treatment in Alzheimer's disease: results of the Alzheimer's Disease Cholesterol-Lowering Treatment (ADCLT) trial. *Acta Neurol Scand Suppl.* 2006; 114: 3–7.
10. **Sparks DL, Petanceska S, Sabbagh M, Connor D, Soares H, Adler C, Lopez J, Ziolkowski C, Lochhead J, Browne P.** Cholesterol, copper and Aβ in controls, MCI, AD and the AD Cholesterol-Lowering Treatment Trial (ADCLT). *Curr Alzheimer Res.* 2005; 2: 527–39.
11. **Sparks DL, Sabbagh MN, Connor DJ, Lopez J, Launer LJ, Browne P, Wasser D, Johnson-Traver S, Lochhead J, Ziolwolski**

C. Atorvastatin for the treatment of mild to moderate Alzheimer disease: preliminary results. *Arch Neurol.* 2005; 62: 753–7.

12. **Sparks DL, Sabbagh MN, Connor DJ, Lopez J, Launer LJ, Petanceska S, Browne P, Wasser D, Johnson-Traver S, Lochhead J, Zielkowski C.** Atorvastatin therapy lowers circulating cholesterol but not free radical activity in advance of identifiable clinical benefit in the treatment of mild-to-moderate AD. *Curr Alzheimer Res.* 2005; 2: 343–53.
13. **Landreth G.** Therapeutic use of agonists of the nuclear receptor PPARγ in Alzheimer's disease. *Curr Alzheimer Res.* 2007; 4: 159–64.
14. **Pedersen WA, McMillan PJ, Kulstad JJ, Leverenz JB, Craft S, Haynatzki GR.** Rosiglitazone attenuates learning and memory deficits in Tg2576 Alzheimer mice. *Exp Neurol.* 2006; 199: 265–73.
15. **Risner ME, Saunders AM, Altman JFB, Ormandy GC, Craft S, Foley IM, Zvartau-Hind ME, Hosford DA, Roses AD.** Efficacy of rosiglitazone in a genetically defined population with mild-to-moderate Alzheimer's disease. *Pharmacogenomics J.* 2006; 6: 246–54.
16. **Watson GS, Cholerton BA, Reger MA, Baker LD, Plymate SR, Asthana S, Fishel MA, Kulstad JJ, Green PS, Cook DG, Kahn SE, Keeling ML, Craft S.** Preserved cognition in patients with early Alzheimer disease and amnestic mild cognitive impairment during treatment with rosiglitazone: a preliminary study. *Am J Geriatr Psychiatry.* 2005; 13: 950–8.
17. **Doraiswamy PM, Xiong GL.** Pharmacological strategies for the prevention of Alzheimer's disease. *Expert Opin Pharmacother.* 2006; 7: 1–10.
18. **Szekely a CA, Thorne a JE, Zandi PP, Ek a M, Messias a E, Breitner JCS, Goodman a SN.** Nonsteroidal anti-inflammatory drugs for the prevention of Alzheimer's disease: a systematic review. *Neuroepidemiology.* 2004; 23: 159–69.
19. **Aisen PS.** The potential of anti-inflammatory drugs for the treatment of Alzheimer's disease. *Lancet Neurol.* 2002; 1: 279–84.
20. **Hardy J, Selkoe DJ.** The amyloid hypothesis of Alzheimer's disease: progress and problems on the road to therapeutics. *Science.* 2002; 297: 353–6.
21. **Tanzi RE, Bertram L.** Twenty years of the Alzheimer's disease amyloid hypothesis: a genetic perspective. *Cell.* 2005; 120: 545–55.
22. **Tolnay M, Probst A.** Review: tau protein pathology in Alzheimer's disease and related disorders. *Neuropathol Appl Neurobiol.* 1999; 25: 171–87.
23. **Lee VMY, Goedert M, Trojanowski JQ.** Neurodegenerative tauopathies. *Annu Rev Neurosci.* 2001; 24: 1121–59.
24. **Grundke-Iqbal I, Iqbal K, Tung YC, Quinlan M, Wisniewski HM, Binder LI.** Abnormal phosphorylation of the microtubule-associated protein tau (tau) in Alzheimer cytoskeletal pathology. *Proc Natl Acad Sci USA.* 1986; 83: 4913–7.
25. **Kosik KS, Joachim CL, Selkoe DJ.** Microtubule-associated protein tau (tau) is a major antigenic component of paired helical filaments in Alzheimer disease. *Proc Natl Acad Sci USA.* 1986; 83: 4044–8.
26. **Alonso ADC, Zaidi T, Grundke-Iqbal I, Iqbal K.** Role of abnormally phosphorylated tau in the breakdown of microtubules in Alzheimer disease. *Proc Natl Acad Sci USA.* 1994; 91: 5562–6.
27. **Mandelkow E-M, Mandelkow E.** Tau in Alzheimer's disease. *Trends Cell Biol.* 1998; 8: 425–7.
28. **Brandt R, Lee G.** The balance between tau protein's microtubule growth and nucleation activities: implications for the formation of axonal microtubules. *J Neurochem.* 1993; 61: 997–1005.
29. **Trojanowski JQ, Schmidt ML, Shin RW, Bramblett GT, Rao D, Lee VM.** Altered tau and neurofilament proteins in neurodegenerative diseases: diagnostic implications for Alzheimer's disease and Lewy body dementias. *Brain Pathol.* 1993; 3: 45–54.
30. **Weingarten MD, Lockwood AH, Hwo SY, Kirschner MW.** A protein factor essential for microtubule assembly. *Proc Natl Acad Sci USA.* 1975; 72: 1858–62.
31. **Gail VWJ, Judith AH.** Tau protein in normal and Alzheimer's disease brain: an update. *J Alzheimers Dis.* 1999; 1: 329–51.
32. **Watanabe A, Hasegawa M, Suzuki M, Takio K, Morishima-Kawashima M, Titani K, Arai T, Kosik KS, Ihara Y.** In vivo phosphorylation sites in fetal and adult rat tau. *J Biol Chem.* 1993; 268: 25712–7.
33. **Mandelkow EM, Biernat J, Drewes G, Gustke N, Trinczek B, Mandelkow E.** Tau domains, phosphorylation, and interactions with microtubules. *Neurobiol Aging.* 1995; 16: 355–62.
34. **Morishima-Kawashima M, Hasegawa M, Takio K, Suzuki M, Yoshida H, Titani K, Ihara Y.** Proline-directed and Non-proline-directed Phosphorylation of PHF-tau. *J Biol Chem.* 1995; 270: 823–9.
35. **Betts JC, Loviny TLF, Blackstock WP, Anderton BH.** New phosphorylation sites identified in hyperphosphorylated tau (paired helical filament-tau) from Alzheimer's disease brain using nanoelectrospray mass spectrometry. *J Neurochem.* 1998; 71: 2465–76.
36. **Iqbal K, Grundke-Iqbal I.** Metabolic/signal transduction hypothesis of Alzheimer's disease and other tauopathies. *Acta Neuropathol.* 2005; 109: 25–31.
37. **Iqbal K, del C. Alonso A, Chen S, Chohan MO, El-Akkad E, Gong C-X, Khatoon S, Li B, Liu F, Rahman A, Tanimukai H, Grundke-Iqbal I.** Tau pathology in Alzheimer disease and other tauopathies. *Biochim Biophys Acta.* 2005; 1739: 198–210.
38. **Lee G, Thangavel R, Sharma VM, Litersky JM, Bhaskar K, Fang SM, Do LH, Andreadis A, Van Hoesen G, Ksiezak-Reding H.** Phosphorylation of tau by fyn: implications for Alzheimer's disease. *J Neurosci.* 2004; 24: 2304–12.
39. **Vogelsberg-Ragaglia V, Schuck T, Trojanowski JQ, Lee VMY.** PP2A mRNA expression is quantitatively decreased in Alzheimer's disease hippocampus. *Exp Neurol.* 2001; 168: 402–12.
40. **Cheng-Xin Gong TJSIG-IKI.** Phosphoprotein phosphatase activities in Alzheimer disease brain. *J Neurochem.* 1993; 61: 921–7.
41. **Fei Liu IG-IKIC-XG.** Contributions of protein phosphatases PP1, PP2A, PP2B and PP5 to the regulation of tau phosphorylation. *Eur J Neurosci.* 2005; 22: 1942–50.
42. **Gong CX, Grundke-Iqbal I, Iqbal K.** Dephosphorylation of Alzheimer's disease abnormally phosphorylated tau by protein phosphatase-2A. *Neuroscience.* 1994; 61: 765–72.
43. **Pei J-J, Gong C-X, An W-L, Winblad B, Cowburn RF, Grundke-Iqbal I, Iqbal K.** Okadaic-acid-induced inhibition of protein phosphatase 2A produces activation of mitogen-activated protein kinases ERK1/2, MEK1/2, and p70 S6, similar to that in Alzheimer's disease. *Am J Pathol.* 2003; 163: 845–58.
44. **Iqbal K, Grundke-Iqbal I.** Tau phosphatase activity as a therapeutic target for AD. *Drug News Perspect.* 1998; 11: 10–4.
45. **Ferrer I, Gomez-Isla T, Puig B, Freixes M, RibÉ E, Dalfó E, Avila J.** Current advances on different kinases involved in tau phosphorylation, and implications in Alzheimer's disease and tauopathies. *Curr Alzheimer Res.* 2005; 2: 3–18.
46. **Savage MJ, Lin Y-G, Ciallella JR, Flood DG, Scott RW.** Activation of c-Jun N-terminal kinase and p38 in an Alzheimer's

disease model is associated with amyloid deposition. *J Neurosci.* 2002; 22: 3376–85.

47. **Harris FM, Brecht WJ, Xu Q, Mahley RW, Huang Y.** Increased tau phosphorylation in apolipoprotein E4 transgenic mice is associated with activation of extracellular signal-regulated kinase: modulation by zinc. *J Biol Chem.* 2004; 279: 44795–801.
48. **Lee K-Y, Clark AW, Rosales JL, Chapman K, Fung T, Johnston RN.** Elevated neuronal Cdc2-like kinase activity in the Alzheimer disease brain. *Neurosci Res.* 1999; 34: 21–9.
49. **Biernat J, Gustke N, Drewes G, Mandelkow EM, Mandelkow E.** Phosphorylation of Ser262 strongly reduces binding of tau to microtubules: distinction between PHF-like immunoreactivity and microtubule binding. *Neuron.* 1993; 11: 153–63.
50. **Drewes G, Trinczek B, Illenberger S, Biernat J, Schmitt-Ulms G, Meyer HE, Mandelkow E-M, Mandelkow E.** Microtubule-associated protein/microtubule affinity-regulating kinase. *J Biol Chem.* 1995; 270: 7679–88.
51. **Ishiguro K, Ihara Y, Uchida T, Imahori K.** A novel tubulin-dependent protein kinase forming a paired helical filament epitope on tau. *J Biochem.* 1988; 104: 319–21.
52. **Ishiguro K, Omori A, Sato K, Tomizawa K, Imahori K, Uchida T.** A serine/threonine proline kinase activity is included in the tau protein kinase fraction forming a paired helical filament epitope. *Neurosci Lett.* 1991; 128: 195–8.
53. **Ishiguro K, Shiratsuchi A, Sato S, Omori A, Arioka M, Kobayashi S, Uchida T, Imahori K.** Glycogen synthase kinase 3β is identical to tau protein kinase I generating several epitopes of paired helical filaments. *FEBS Lett.* 1993; 325: 167–72.
54. **Bhat RV, Haeberlein SLB, Avila J.** Glycogen synthase kinase 3: a drug target for CNS therapies. *J Neurochem.* 2004; 89: 1313–7.
55. **Cohen P, Goedert M.** GSK3 inhibitors: development and therapeutic potential. *Nat Rev Drug Discov.* 2004; 3: 479–87.
56. **Martinez A, Castro A, Dorronsoro I, Alonso M.** Glycogen synthase kinase 3 (GSK-3) inhibitors as new promising drugs for diabetes, neurodegeneration, cancer, and inflammation. *Med Res Rev.* 2002; 22: 373–84.
57. **Meijer L, Flajolet M, Greengard P.** Pharmacological inhibitors of glycogen synthase kinase 3. *Trends Pharmacol Sci.* 2004; 25: 471–80.
58. **Phiel CJ, Klein PS.** Molecular targets of lithium action. *Annu Rev Pharmacol Toxicol.* 2001; 41: 789–813.
59. **Ryder J, Su Y, Liu F, Li B, Zhou Y, Ni B.** Divergent roles of GSK3 and CDK5 in APP processing. *Biochem Biophys Res Commun* 2003; 312: 922–9.
60. **Su Y, Ryder J, Li B, Wu X, Fox N, Solenberg P, Brune K, Paul S, Zhou Y, Liu F, Ni B.** Lithium, a common drug for bipolar disorder treatment, regulates amyloid-β precursor protein processing. *Biochemistry.* 2004; 43: 6899–908.
61. **Noble W, Planel E, Zehr C, Olm V, Meyerson J, Suleman F, Gaynor K, Wang L, LaFrancois J, Feinstein B, Burns M, Krishnamurthy P, Wen Y, Bhat R, Lewis J, Dickson D, Duff K.** Inhibition of glycogen synthase kinase-3 by lithium correlates with reduced tauopathy and degeneration *in vivo*. *Proc Natl Acad Sci USA.* 2005; 102: 6990–5.
62. **Rapoport M, Ferreira A.** PD98059 prevents neurite degeneration induced by fibrillar β-amyloid in mature hippocampal neurons. *J Neurochem.* 2000; 74: 125–33.
63. **Samo S, Ruzzene M, Frascella P, Pagano MA, Meggio F, Zambon A, Mazzorana M, Maira GD, Lucchini V, Pinna LA.** Development and exploitation of CK2 inhibitors. *Mol Cell Biochem.* 2005; 274: 69–76.
64. **Pedersen LM, Lien GF, Bollerud I, Gjerstad J.** Induction of long-term potentiation in single nociceptive dorsal horn neurons is blocked by the CaMKII inhibitor AIP. *Brain Res.* 2005; 1041: 66–71.
65. **Knockaert M, Greengard P, Meijer L.** Pharmacological inhibitors of cyclin-dependent kinases. *Trends Pharmacol Sci* 2002; 23: 417–25.
66. **Pallas M, Canudas AM, Ventaguer E, Allgaier C, De Arriba SG, Alvira D, Sureda FX, Camins A.** Inhibitors of cyclin-dependent kinases: potential drugs for the treatment of neurodegenerative disorders? *Curr Med Chem Cent Nerv Syst Agents.* 2005; 5: 101–9.
67. **Le Corre S, Klafki HW, Plesnila N, Hubinger G, Obermeier A, Sahagun H, Monse B, Seneci P, Lewis J, Eriksen J, Zehr C, Yue M, McGowan E, Dickson DW, Hutton M, Roder HM.** An inhibitor of tau hyperphosphorylation prevents severe motor impairments in tau transgenic mice. *Proc Natl Acad Sci USA.* 2006; 103: 9673–8.
68. **Churcher I.** Tau therapeutic strategies for the treatment of Alzheimer's disease. *Curr Top Med Chem.* 2006; 6: 579–95.
69. **Iqbal K, Grundke-Iqbal I.** Alzheimer neurofibrillary degeneration: significance, etiopathogenesis, therapeutics and prevention. *J Cell Mol Med.* 2008; 12: 38–55.
70. **Stoothoff WH, Johnson GVW.** Tau phosphorylation: physiological and pathological consequences. *Biochim Biophys Acta.* 2005; 1739: 280–97.
71. **Mischik CM, Edwards PC, Lai RY, Roth M, Harrington CR.** Selective inhibition of Alzheimer disease-like tau aggregation by phenothiazines. *Proc Natl Acad Sci USA.* 1996; 93: 11213–8.
72. **Pickhardt M, Gazova Z, von Bergen M, Khlistunova I, Wang Y, Hascher A, Mandelkow E-M, Biernat J, Mandelkow E.** Anthraquinones inhibit tau aggregation and dissolve Alzheimer's paired helical filaments *in vitro* and in cells. *J Biol Chem.* 2005; 280: 3628–35.
73. **Pickhardt M, Biernat J, Khlistunova I, Wang YP, Gazova Z, Mandelkow EM, Mandelkow E.** N-Phenylamine derivatives as aggregation inhibitors in cell models of tauopathy. *Curr Alzheimer Res.* 2007; 4: 397–402.
74. **Khlistunova I, Pickhardt M, Biernat J, Yipeng W, Mandelkow E-M, Mandelkow E.** Inhibition of tau aggregation in cell models of tauopathy. *Curr Alzheimer Res.* 2007; 4: 544–6.
75. **Gozes I, Zaltzman R, Hauser J, Brenneman DE, Shohami E, Hill JM.** The expression of activity-dependent neuroprotective protein (ADNP) is regulated by brain damage and treatment of mice with the ADNP derived peptide, NAP, reduces the severity of traumatic head injury. *Curr Alzheimer Res.* 2005; 2: 149–53.
76. **Vulih-Shultzman I, Pinhasov A, Mandel S, Grigoriadis N, Touloumi O, Pittel Z, Gozes I.** Activity-dependent neuroprotective protein snippet NAP reduces tau hyperphosphorylation and enhances learning in a novel transgenic mouse model. *J Pharmacol Exp Ther.* 2007; 323: 438–49.
77. **Gozes I, Spivak-Pohis I.** Neurotrophic effects of the peptide NAP: a novel neuroprotective drug candidate. *Curr Alzheimer Res.* 2006; 3: 197–9.
78. **Geerts H.** AL-108 and AL-208, formulations of the neuroprotective NAP fragment of activity-dependent neuroprotective protein, for cognitive disorders. *Curr Opin Investig Drugs.* 2008 2008; 9: 800–11.
79. **Rosen DR, Martin-Morris L, Luo LQ, White K.** A *Drosophila* gene encoding a protein resembling the human β-amyloid protein precursor. *Proc Natl Acad Sci USA.* 1989; 86: 2478–82.

80. **Sprecher CA, Grant FJ, Grimm G, O'Hara PJ, Norris F, Norris K, Foster DC.** Molecular cloning of the cDNA for a human amyloid precursor protein homolog: evidence for a multigene family. *Biochemistry*. 1993; 32: 4481–6.
81. **Wasco W, Gurubhagavatula S, Paradis MD, Romano DM, Sisodia SS, Hyman BT, Neve RL, Tanzi RE.** Isolation and characterization of APLP2 encoding a homologue of the Alzheimer's associated amyloid β protein precursor. *Nat Genet*. 1993; 5: 95–100.
82. **Reinhard C, Hebert SS, De Strooper B.** The amyloid-β precursor protein: integrating structure with biological function. *EMBO J*. 2005; 24: 3996–4006.
83. **Panegyres PK.** The functions of the amyloid precursor protein gene. *Rev Neurosci*. 2001; 12: 1–39.
84. **De Strooper B, Annaert W.** Proteolytic processing and cell biological functions of the amyloid precursor protein. *J Cell Sci*. 2000; 113: 1857–70.
85. **Zheng H, Koo E.** The amyloid precursor protein: beyond amyloid. *Mol Neurodegener*. 2006; 1: 1–12.
86. **Yamazaki T, Koo EH, Selkoe DJ.** Trafficking of cell-surface amyloid β-protein precursor. II. Endocytosis, recycling and lysosomal targeting detected by immunolocalization. *J Cell Sci*. 1996; 109: 999–1008.
87. **Forloni G, Terreni L, Bertani I, Fogliarino S, Invernizzi R, Assini A, Ribizzi G, Negro A, Calabrese E, Volonte MA, Mariani C, Franceschi M, Tabaton M, Bertoli A.** Protein misfolding in Alzheimer's and Parkinson's disease: genetics and molecular mechanisms. *Neurobiol Aging*. 2002; 23: 957–76.
88. **Nixon RA.** Autophagy in neurodegenerative disease: friend, foe or turncoat? *Trends Neurosci*. 2006; 29: 528–35.
89. **Nixon RA.** Autophagy, amyloidogenesis and Alzheimer's disease. *J Cell Sci*. 2007; 120: 4081–91.
90. **Nixon RA, Wegiel J, Kumar A, Yu WH, Peterhoff C, Cataldo A, Cuervo AM.** Extensive involvement of autophagy in Alzheimer disease: an immuno-electron microscopy study. *J Neuropathol Exp Neurol*. 2005; 64: 113–22.
91. **Yu WH, Cuervo AM, Kumar A, Peterhoff CM, Schmidt SD, Lee J-H, Mohan PS, Mercken M, Farmery MR, Tjernberg LO, Jiang Y, Duff K, Uchiyama Y, Naslund J, Mathews PM, Cataldo AM, Nixon RA.** Macroautophagy – a novel β-amyloid peptide-generating pathway activated in Alzheimer's disease. *J Cell Biol*. 2005; 171: 87–98.
92. **Nunan J, Small DH.** Regulation of APP cleavage by α-, β- and γ-secretases. *FEBS Lett*. 2000; 483: 6–10.
93. **Esch FS, Keim PS, Beattie EC, Blacher RW, Culwell AR, Oltersdorf T, McClure D, Ward PJ.** Cleavage of amyloid-β peptide during constitutive processing of its precursor. *Science*. 1990; 248: 1122–4.
94. **Haass C, Hung AY, Schlossmacher MG, Teplow DB, Selkoe DJ.** β-Amyloid peptide and a 3-kDa fragment are derived by distinct cellular mechanisms. *J Biol Chem*. 1993; 268: 3021–4.
95. **Cao X, Sudhof TC.** Dissection of amyloid-β precursor protein-dependent transcriptional transactivation. *J Biol Chem*. 2004; 279: 24601–11.
96. **Black RA, Rauch CT, Kozlosky CJ, Peschon JJ, Slack JL, Wolfson MF, Castner BJ, Stocking KL, Reddy P, Srinivasan S, Nelson N, Boiani N, Schooley KA, Gerhart M, Davis R, Fitzner JN, Johnson RS, Paxton RJ, March CJ, Cerretti DP.** A metalloproteinase disintegrin that releases tumour-necrosis factor-α from cells. *Nature*. 1997; 385: 729–33.
97. **Buxbaum JD, Liu KN, Luo Y, Slack JL, Stocking KL, Peschon JJ, Johnson RS, Castner BJ, Cerretti DP, Black RA.** Evidence that tumor necrosis factor alpha converting enzyme is involved in regulated α-secretase cleavage of the Alzheimer amyloid protein precursor. *J Biol Chem*. 1998; 273: 27765–7.
98. **Lammich S, Kojro E, Postina R, Gilbert S, Pfeiffer R, Jasionowski M, Haass C, Fahrenholz F.** Constitutive and regulated α-secretase cleavage of Alzheimer's amyloid precursor protein by a disintegrin metalloprotease. *Proc Natl Acad Sci USA*. 1999; 96: 3922–7.
99. **Hussain I, Powell D, Howlett DR, Tew DG, Meek TD, Chapman C, Gloger IS, Murphy KE, Southan CD, Ryan DM, Smith TS, Simmons DL, Walsh FS, Dingwall C, Christie G.** Identification of a novel aspartic protease (Asp 2) as β-secretase. *Mol Cell Neurosci*. 1999; 14: 419–27.
100. **Yan R, Bienkowski MJ, Shuck ME, Miao H, Tory MC, Pauley AM, Brashler JR, Stratman NC, Mathews WR, Buhl AE, Carter DB, Tomasselli AG, Parodi LA, Heinrikson RL, Gurney ME.** Membrane-anchored aspartyl protease with Alzheimer's disease β-secretase activity. *Nature*. 1999; 402: 533–7.
101. **Seubert P, Oltersdorf T, Lee MG, Barbour R, Blomquist C, Davis DL, Bryant K, Fritz LC, Galasko D, Thal LJ.** Secretion of β-amyloid precursor protein cleaved at the amino terminus of the β-amyloid peptide. *Nature*. 1993; 361: 260–3.
102. **Wolfe MS, Xia W, Moore CL, Leatherwood DD, Ostaszewski B, Rahmati T, Donkor IO, Selkoe DJ.** Peptidomimetic probes and molecular modeling suggest that Alzheimer's γ-secretase is an intramembrane-cleaving aspartyl protease. *Biochemistry*. 1999; 38: 4720–7.
103. **Edbauer D, Winkler E, Regula JT, Pesold B, Steiner H, Haass C.** Reconstitution of γ-secretase activity. *Nat Cell Biol*. 2003; 5: 486–8.
104. **Francis R, McGrath G, Zhang J, Ruddy DA, Sym M, Apfeld J, Nicoll M, Maxwell M, Hai B, Ellis MC, Parks AL, Xu W, Li J, Gurney M, Myers RL, Himes CS, Hiebsch R, Ruble C, Nye JS, Curtis D.** aph-1 and pen-2 are required for Notch pathway signaling, γ-secretase cleavage of βAPP, and presenilin protein accumulation. *Dev Cell*. 2002; 3: 85–97.
105. **Periz G, Fortini ME.** Functional reconstitution of γ-secretase through coordinated expression of presenilin, nicastrin, Aph-1, and Pen-2. *J Neurosci Res*. 2004; 77: 309–22.
106. **Li X, Greenwald I.** Additional evidence for an eight-transmembrane-domain topology for Caenorhabditis elegans and human presenilins. *Proc Natl Acad Sci USA*. 1998; 95: 7109–14.
107. **Wolfe MS, Xia W, Ostaszewski BL, Diehl TS, Kimberly WT, Selkoe DJ.** Two transmembrane aspartates in presenilin-1 required for presenilin endoproteolysis and γ-secretase activity. *Nature*. 1999; 398: 513–7.
108. **Zhang Z, Nadeau P, Song W, Donoviel D, Yuan M, Bernstein A, Yankner BA.** Presenilins are required for γ-secretase cleavage of β-APP and transmembrane cleavage of Notch-1. *Nat Cell Biol*. 2000; 2: 463–5.
109. **Kopan R, Ilagan MXG.** γ-secretase: proteasome of the membrane? *Nat Rev Mol Cell Biol*. 2004; 5: 499–504.
110. **Selkoe DJ.** The cell biology of β-amyloid precursor protein and presenilin in Alzheimer's disease. *Trends Cell Biol*. 1998; 8: 447–53.
111. **St George-Hyslop PH, Petit A.** Molecular biology and genetics of Alzheimer's disease. *C R Biol*. 2005; 328: 119–30.
112. **Fisher A, Michaelson DM, Brandeis R, Haring R, Chapman S, Pittel Z.** M1 muscarinic agonists as potential

disease-modifying agents in Alzheimer's disease: rationale and perspectives. *Ann N Y Acad Sci.* 2000; 920: 315–20.

113. **Wolf BA, Wertkin AM, Jolly YC, Yasuda RP, Wolfe BB, Konrad RJ, Manning D, Ravi S, Williamson JR, Lee VMY.** Muscarinic regulation of Alzheimer's disease amyloid precursor protein secretion and amyloid β-protein production in human neuronal NT2N cells. *J Biol Chem.* 1995; 270: 4916–22.
114. **Oddo S, Caccamo A, Shepherd JD, Murphy MP, Golde TE, Kayed R, Metherate R, Mattson MP, Akbari Y, LaFerla FM.** Triple-transgenic model of Alzheimer's disease with plaques and tangles: intracellular Aβ and synaptic dysfunction. *Neuron.* 2003; 39: 409–21.
115. **Caccamo A, Oddo S, Billings LM, Green KN, Martinez-Coria H, Fisher A, LaFerla FM.** M1 receptors play a central role in modulating AD-like pathology in transgenic mice. *Neuron.* 2006; 49: 671–82.
116. **Evin G, Sernee MF, Masters CL.** Inhibition of γ-secretase as a therapeutic intervention for Alzheimer's disease: prospects, limitations and strategies. *CNS Drugs.* 2006; 20: 351.
117. **Tschape J-A, Hartmann T.** Therapeutic perspectives in Alzheimers disease. *Recent Patents CNS Drug Discov.* 2006; 1: 119–27.
118. **Fleisher AS, Raman R, Siemers ER, Becerra L, Clark CM, Dean RA, Farlow MR, Galvin JE, Peskind ER, Quinn JF, Sherzai A, Sowell BB, Aisen PS, Thal LJ.** Phase 2 safety trial targeting amyloid-β production with a γ-secretase inhibitor in Alzheimer disease. *Arch Neurol.* 2008; 65: 1031–8.
119. **Haass C, Hung AY, Schlossmacher MG, Oltersdorf T, Teplow DB, Selkoe DJ.** Normal cellular processing of the β-amyloid precursor protein results in the secretion of the amyloid-β peptide and related molecules. *Ann N Y Acad Sci.* 1993; 695: 109–16.
120. **Morgan C, Colombres M, Nunez MT, Inestrosa NC.** Structure and function of amyloid in Alzheimer's disease. *Prog Neurobiol.* 2004; 74: 323–49.
121. **Saavedra L, Mohamed A, Ma V, Kar S, de Chaves EP.** Internalization of β-amyloid peptide by primary neurons in the absence of apolipoprotein E. *J Biol Chem.* 2007; 282: 35722–32.
122. **Bateman RJ, Munsell LY, Morris JC, Swarm R, Yarasheski KE, Holtzman DM.** Human amyloid-β synthesis and clearance rates as measured in cerebrospinal fluid *in vivo*. *Nat Med.* 2006; 12: 856–61.
123. **Savage MJ, Trusko SP, Howland DS, Pinsker LR, Mistretta S, Reaume AG, Greenberg BD, Siman R, Scott RW.** Turnover of amyloid β-protein in mouse brain and acute reduction of its level by phorbol ester. *J Neurosci.* 1998; 18: 1743–52.
124. **Seubert P, Vigo-Pelfrey C, Esch F, Lee M, Dovey H, Davis D, Sinha S, Schlossmacher M, Whaley J, Swindlehurst C.** Isolation and quantification of soluble Alzheimer's β-peptide from biological fluids. *Nature.* 1992; 359: 325–7.
125. **Kuhnke D, Jedlitschky G, Grube M, Krohn M, Jucker M, Mosyagin I, Cascorbi I, Walker LC, Kroemer HK, Warzok RW, Vogelgesang S.** MDR1-P-glycoprotein (*ABCB1*) mediates transport of Alzheimer's amyloid-β peptides – implications for the mechanisms of Aβ clearance at the blood-brain barrier. *Brain Pathol.* 2007; 17: 347–53.
126. **Deane R, Du Yan S, Submamaryan RK, LaRue B, Jovanovic S, Hogg E, Welch D, Manness L, Lin C, Yu J, Zhu H, Ghiso J, Frangione B, Stern A, Schmidt AM, Armstrong DL, Arnold B, Liliensiek B, Nawroth P, Hofman F, Kindy M, Stern D, Zlokovic B.** RAGE mediates amyloid-β peptide transport across the blood-brain barrier and accumulation in brain. *Nat Med.* 2003; 9: 907–13.
127. **Tanzi RE, Moir RD, Wagner SL.** Clearance of Alzheimer's Aβ peptide: the many roads to perdition. *Neuron.* 2004; 43: 605–8.
128. **Bell RD, Sagare AP, Friedman AE, Bedi GS, Holtzman DM, Deane R, Zlokovic BV.** Transport pathways for clearance of human Alzheimer's amyloid β-peptide and apolipoproteins E and J in the mouse central nervous system. *J Cereb Blood Flow Metab.* 2006; 27: 909–18.
129. **Hammad SM, Ranganathan S, Loukinova E, Twal WO, Argraves WS.** Interaction of apolipoprotein j-amyloid β-peptide complex with low density lipoprotein receptor-related protein-2/megalin. A mechanism to prevent pathological accumulation of amyloid β peptide. *J Biol Chem.* 1997; 272: 18644–9.
130. **Deane R, Wu Z, Sagare A, Davis J, Du Yan S, Hamm K, Xu F, Parisi M, LaRue B, Hu HW, Spijkers P, Guo H, Song X, Lenting PJ, Van Nostrand WE, Zlokovic BV.** LRP/amyloid β-peptide interaction mediates differential brain efflux of Aβ isoforms. *Neuron.* 2004; 43: 333–44.
131. **Herz J.** LRP: a bright beacon at the blood-brain barrier. *J Clin Invest.* 2003; 112: 1483–5.
132. **Tamaki C, Ohtsuki S, Iwatsubo T, Hashimoto T, Yamada K, Yabuki C, Terasaki T.** Major involvement of low-density lipoprotein receptor-related protein 1 in the clearance of plasma free amyloid β-peptide by the liver. *Pharm Res.* 2006; 23: 1407–16.
133. **Sagare A, Deane R, Bell RD, Johnson B, Hamm K, Pendu R, Marky A, Lenting PJ, Zhenhua W, Zarcone T, Goate A, Mayo K, Perlmutter D, Coma M, Zhihui Z, Zlokovic BV.** Clearance of amyloid-β by circulating lipoprotein receptors. *Nat Med.* 2007; 13: 1029–31.
134. **Sparks DL.** Chdesterol metabdism and brain amyloidosis: evidence for a role of copper in the clearance of Aβ through the liver. *Curr Alzheimer Res.* 2007; 4: 165–9.
135. **Koldamova R, Lefterov I.** Role of LXR and *ABCA1* in the pathogenesis of Alzheimer's disease – implications for a new therapeutic approach. *Curr Alzheimer Res.* 2007; 4: 171–8.
136. **Cao G, Bales KR, DeMattos RB, Paul SM.** Liver X receptor-mediated gene regulation and cholesterol homeostasis in brain: relevance to Alzheimer's disease therapeutics. *Curr Alzheimer Res.* 2007; 4: 179–84.
137. **Selkoe DJ.** Clearing the brain's amyloid cobwebs. *Neuron.* 2001; 32: 177–80.
138. **Kinston IB, Castro MJM, Anderson S.** *In vitro* stimulation of tissue-type plasminogen activator by Alzheimer amyloid β-peptide analogues. *Nat Med.* 1995; 1: 138–42.
139. **Tucker HM, Kihiko-Ehmann M, Wright S, Rydel RE, Estus S.** Tissue plasminogen activator requires plasminogen to modulate amyloid-β neurotoxicity and deposition. *J Neurochem.* 2000; 75: 2172–7.
140. **Tucker HM, Kihiko M, Caldwell JN, Wright S, Kawarabayashi T, Price D, Walker D, Scheff S, McGillis JP, Rydel RE, Estus S.** The plasmin system is induced by and degrades amyloid-β aggregates. *J Neurosci.* 2000; 20: 3937–46.
141. **Yasojima K, Akiyama H, McGeer EG, McGeer PL.** Reduced neprilysin in high plaque areas of Alzheimer brain: a possible relationship to deficient degradation of β-amyloid peptide. *Neurosci Lett.* 2001; 297: 97–100.
142. **Iwata N, Tsubuki S, Takaki Y, Watanabe K, Sekiguchi M, Hosoki E, Kawashima-Morishima M, Lee H-J, Hama E, Sekine-Aizawa Y, Saido TC.** Identification of the major Aβ1–42-degrading catabolic pathway

in brain parenchyma: Suppression leads to biochemical and pathological deposition. *Nat Med.* 2000; 6: 143–50.

143. **Iwata N, Satoshi T, Yoshie T, Keiro S, Bao L, Gerard NP, Gerard C, Emi H, Lee H-J, Saido TC.** Metabolic regulation of brain Aβ by neprilysin. *Science.* 2001; 292: 1550–2.
144. **Iwata N, Takaki Y, Fukami S, Tsubuki S, Saido TC.** Region-specific reduction of Aβ-degrading endopeptidase, neprilysin, in mouse hippocampus upon aging. *J Neurosci Res.* 2002; 70: 493–500.
145. **Qiu WQ, Walsh DM, Ye Z, Vekrellis K, Zhang J, Podlisny MB, Rosner MR, Safavi A, Hersh LB, Selkoe DJ.** Insulin-degrading enzyme regulates extracellular levels of amyloid β-protein by degradation. *J Biol Chem.* 1998; 273: 32730–8.
146. **Kurochkin IV, Goto S.** Alzheimer's β-amyloid peptide specifically interacts with and is degraded by insulin degrading enzyme. *FEBS Lett.* 1994; 345: 33–7.
147. **Zhao L, Teter B, Morihara T, Lim GP, Ambegaokar SS, Ubeda OJ, Frautschy SA, Cole GM.** Insulin-degrading enzyme as a downstream target of insulin receptor signaling cascade: implications for Alzheimer's disease intervention. *J Neurosci.* 2004; 24: 11120–6.
148. **Vekrellis K, Ye Z, Qiu WQ, Walsh D, Hartley D, Chesneau V, Rosner MR, Selkoe DJ.** Neurons regulate extracellular levels of amyloid β-protein via proteolysis by insulin-degrading enzyme. *J Neurosci.* 2000; 20: 1657–65.
149. **Eckman EA, Reed DK, Eckman CB.** Degradation of the Alzheimer's amyloid β peptide by endothelin-converting enzyme. *J Biol Chem.* 2001; 276: 24540–8.
150. **Eckman EA, Watson M, Marlow L, Sambamurti K, Eckman CB.** Alzheimer's disease β-amyloid peptide is increased in mice deficient in endothelin-converting enzyme. *J Biol Chem.* 2003; 278: 2081–4.
151. **Roher AE, Kasunic TC, Woods AS, Cotter RJ, Ball MJ, Fridman R.** Proteolysis of Aβ peptide from Alzheimer disease brain by gelatinase A. *Biochem Biophys Res Commun.* 1994; 205: 1755–61.
152. **Backstrom JR, Lim GP, Cullen MJ, Tokes ZA.** Matrix metalloproteinase-9 (MMP-9) is synthesized in neurons of the human hippocampus and is capable of degrading the amyloid-β peptide (1–40). *J Neurosci.* 1996; 16: 7910–9.
153. **Yin K-J, Cirrito JR, Yan P, Hu X, Xiao Q, Pan X, Bateman R, Song H, Hsu F-F, Turk J, Xu J, Hsu CY, Mills JC, Holtzman DM, Lee J-M.** Matrix metalloproteinases expressed by astrocytes mediate extracellular amyloid-β peptide catabolism. *J Neurosci.* 2006; 26: 10939–48.
154. **Esteban JA.** Living with the enemy: a physiological role for the β-amyloid peptide. *Trends Neurosci.* 2004; 27: 1–3.
155. **Atwood CS, Obrenovich ME, Liu T, Chan H, Perry G, Smith MA, Martins RN.** Amyloid-β: a chameleon walking in two worlds: a review of the trophic and toxic properties of amyloid-β. *Brain Res Rev.* 2003; 43: 1–16.
156. **Kontush A.** Amyloid-β: an antioxidant that becomes a pro-oxidant and critically contributes to Alzheimer's disease. *Free Radic Biol Med.* 2001; 31: 1120–31.
157. **Kontush A.** Amyloid-β: Acute-phase apolipoprotein with metal-binding activity. *J Alzheimers Dis.* 2005; 8: 129–37.
158. **Kontush A, Atwood CS.** Amyloid-β: phylogenesis of a chameleon. *Brain Res Rev.* 2004; 46: 118–20.
159. **Berthon G.** Does human βA4 exert a protective function against oxidative stress in Alzheimer's disease? *Med Hypotheses.* 2000; 54: 672–7.
160. **Zou K, Gong J-S, Yanagisawa K, Michikawa M.** A novel function of monomeric amyloid β-protein serving as an antioxidant molecule against metal-induced oxidative damage. *J Neurosci.* 2002; 22: 4833–41.
161. **Yankner BA, Dawes LR, Fisher S, Villa-Komaroff L, Oster-Granite ML, Neve RL.** Neurotoxicity of a fragment of the amyloid precursor associated with Alzheimer's disease. *Science.* 1989; 245: 417–20.
162. **Frautschy SA, Baird A, Cole GM.** Effects of injected Alzheimer β-amyloid cores in rat brain. *Proc Natl Acad Sci USA.* 1991; 88: 8362–6.
163. **Liu ST, Howlett G, Barrow CJ.** Histidine-13 is a crucial residue in the zinc ion-induced aggregation of the Aβ peptide of Alzheimer's disease. *Biochemistry.* 1999; 38: 9373–8.
164. **Serpell LC.** Alzheimer's amyloid fibrils: structure and assembly. *Biochim Biophys Acta.* 2000; 1502: 16–30.
165. **Teplow DB.** Structural and kinetic features of amyloid beta-protein fibrillogenesis. *Amyloid.* 1998; 5: 121–42.
166. **Walsh DM, Hartley DM, Kusumoto Y, Fezoui Y, Condron MM, Lomakin A, Benedek GB, Selkoe DJ, Teplow DB.** Amyloid beta-protein fibrillogenesis. Structure and biological activity of protofibrillar intermediates. *J Biol Chem.* 1999; 274: 25945–52.
167. **Stine WB Jr, Dahlgren KN, Krafft GA, LaDu MJ.** *In vitro* characterization of conditions for amyloid-β peptide oligomerization and fibrillogenesis. *J Biol Chem.* 2003; 278: 11612–22.
168. **Lambert MP, Barlow AK, Chromy BA, Edwards C, Freed R, Liosatos M, Morgan TE, Rozovsky I, Trommer B, Viola KL, Wals P, Zhang C, Finch CE, Krafft GA, Klein WL.** Diffusible, nonfibrillar ligands derived from Aβ1–42 are potent central nervous system neurotoxins. *Proc Natl Acad Sci USA.* 1998; 95: 6448–53.
169. **Hartley DM, Walsh DM, Ye CP, Diehl T, Vasquez S, Vassilev PM, Teplow DB, Selkoe DJ.** Protofibrillar intermediates of amyloid β-protein induce acute electrophysiological changes and progressive neurotoxicity in cortical neurons. *J Neurosci.* 1999; 19: 8876–84.
170. **Lue LF, Kuo YM, Roher AE, Brachova L, Shen Y, Sue L, Beach T, Kurth JH, Rydel RE, Rogers J.** Soluble amyloid β peptide concentration as a predictor of synaptic change in Alzheimer's disease. *Am J Pathol.* 1999; 155: 853–62.
171. **Walsh DM, Selkoe DJ.** Oligomers on the brain: the emerging role of soluble protein aggregates in neurodegeneration. *Protein Pept Lett.* 2004; 11: 213–28.
172. **Deshpande A, Mina E, Glabe C, Busciglio J.** Different conformations of amyloid β induce neurotoxicity by distinct mechanisms in human cortical neurons. *J Neurosci.* 2006; 26: 6011–8.
173. **LaFerla FM, Green KN, Oddo S.** Intracellular amyloid-β in Alzheimer's disease. *Nat Rev Neurosci.* 2007; 8: 499–509.
174. **Lesne S, Kotilinek L.** Amyloid plaques and amyloid-β oligomers: an ongoing debate. *J Neurosci.* 2005; 25: 9319–20.
175. **Look GC, Jerecic J, Cherbavaz DB, Pray TR, Breach J-CR, Crosier WJ, Igoudin L, Hiromoka CM, Lowe RM, McEntee M, Ruslim-Litrus L, Hsiu-Mei W, Sue Z, Catalano SM, Goure WF, Summa D, Krafft GA.** Discovery of ADDL-targeting small molecule drugs for Alzheimer's disease. *Curr Alzheimer Res.* 2007; 4: 562–7.
176. **Chacon MA, Barria MI, Soto C, Inestrosa NC.** β-sheet breaker peptide prevents Aβ-induced spatial memory impairments with partial reduction of amyloid deposits. *Mol Psychiatry.* 2004; 9: 953–61.
177. **Giordano C, Masi A, Pizzini A, Sansone A, Consalvi V, Chiaraluce R, Lucente G.** Synthesis and activity of fibrillogenesis peptide inhibitors related to the 17–21 β-amyloid sequence. *Eur J Med Chem.* In Press.
178. **Goedert M, Jakes R, Spillantini MG, Hasegawa M, Smith MJ, Crowther RA.**

Assembly of microtubule-associated protein tau into Alzheimer-like filaments induced by sulphated glycosaminoglycans. *Nature*. 1996; 383: 550–3.

179. **Gervais F, Paquette J, Morissette C, Krzywkowski P, Yu M, Azzi M, Lacombe D, Kong X, Aman A, Laurin J, Szarek WA, Tremblay P.** Targeting soluble Aβ peptide with tramiprosate for the treatment of brain amyloidosis. *Neurobiol Aging*. 2007; 28: 537–47.
180. **Santa-Maria I, Hernandez F, Del Rio J, Moreno F, Avila J.** Tramiprosate, a drug of potential interest for the treatment of Alzheimer's disease, promotes an abnormal aggregation of tau. *Mol Neurodegener*. 2007; 2: 1–12.
181. **Santa-Maria I, Hernández F, Moreno FJ, Avila J.** Taurine, an inducer for tau polymerization and a weak inhibitor for amyloid-β-peptide aggregation. *Neurosci Lett*. 2007; 429: 91–4.
182. **Aisen PS, Saumier D, Briand R, Laurin J, Gervais F, Tremblay P, Garceau D.** A phase II study targeting amyloid-β with 3APS in mild-to-moderate Alzheimer disease. *Neurology*. 2006; 67: 1757–63.
183. **Geents H.** NC-531 (Neurochem). *Curr Opin Investig Drugs*. 2004; 5: 95–100.
184. **Crouch PJ, Harding S-ME, White AR, Camakaris J, Bush AI, Masters CL.** Mechanisms of Aβ mediated neurodegeneration in Alzheimer's disease. *Int J Biochem Cell Biol*. 2008; 40: 181–98.
185. **Talaga P, Quere L.** The plasma membrane: a target and hurdle for the development of anti-Aβ drugs? *Curr Drug Targets CNS Neurol Disord*. 2002; 1: 567–74.
186. **Verdier Y, Zarandi M, Penke B.** Amyloid β-peptide interactions with neuronal and glial cell plasma membrane: binding sites and implications for Alzheimer's disease. *J Pept Sci*. 2004; 10: 229–48.
187. **Roher AE, Chaney MO, Kuo YM, Webster SD, Stine WB, Haverkamp LJ, Woods AS, Cotter RJ, Tuohy JM, Krafft GA, Bonnell BS, Emmerling MR.** Morphology and toxicity of Aβ-(1–42) dimer derived from neuritic and vascular amyloid deposits of Alzheimer's disease. *J Biol Chem*. 1996; 271: 20631–5.
188. **Loo DT, Copani A, Pike CJ, Whittemore ER, Walencewicz AJ, Cotman CW.** Apoptosis is induced by β-amyloid in cultured central nervous system neurons. *Proc Natl Acad Sci USA*. 1993; 90: 7951–5.
189. **Su JH, Zhao M, Anderson AJ, Srinivasan A, Cotman CW.** Activated caspase-3 expression in Alzheimer's and aged control brain: correlation with Alzheimer pathology. *Brain Res*. 2001; 898: 350–7.
190. **Berman DE, Dall'armi C, Voronov SV, McIntire LB, Zhang H, Moore AZ, Staniszewski A, Arancio O, Kim TW, Di Paolo G.** Oligomeric amyloid-β peptide disrupts phosphatidylinositol-4,5-bisphosphate metabolism. *Nat Neurosci*. 2008; 11: 547–54.
191. **Mattson MP, Cheng B, Davis D, Bryant K, Lieberburg I, Rydel RE.** β-Amyloid peptides destabilize calcium homeostasis and render human cortical neurons vulnerable to excitotoxicity. *J Neurosci*. 1992; 12: 376–89.
192. **Fritze J, Walden J.** Clinical findings with nimodipine in dementia: test of the calcium hypothesis. *J Neural Transm Suppl*. 1995; 46: 439–53.
193. **Pierrot N, Ghisdal P, Caumont A-S, Octave J-N.** Intraneuronal amyloid-β1–42 production triggered by sustained increase of cytosolic calcium concentration induces neuronal death. *J Neurochem*. 2004; 88: 1140–50.
194. **Rose GM, Ong VS, Woodruff-Pak DS.** Efficacy of MEM 1003, a novel calcium channel blocker, in delay and trace eyeblink conditioning in older rabbits. *Neurobiol Aging*. 2007; 28: 766–73.
195. **Yagami T, Ueda K, Sakaeda T, Itoh N, Sakaguchi G, Okamura N, Hori Y, Fujimoto M.** Protective effects of a selective L-type voltage-sensitive calcium channel blocker, S-312-d, on neuronal cell death. *Biochem Pharmacol*. 2004; 67: 1153–65.
196. **López-Arrieta J, Birks J.** Nimodipine for primary degenerative, mixed and vascular dementia. *Cochrane Database Syst Rev*. 2002; 3: 1–56.
197. **Buttini M, Masliah E, Barbour R, Grajeda H, Motter R, Johnson-Wood K, Khan K, Seubert P, Freedman S, Schenk D, Games D.** β-Amyloid immunotherapy prevents synaptic degeneration in a mouse model of Alzheimer's disease. *J Neurosci*. 2005; 25: 9096–101.
198. **Janus C, Pearson J, McLaurin J, Mathews PM, Jiang Y, Schmidt SD, Chishti MA, Horne P, Heslin D, French J, Mount HTJ, Nixon RA, Mercken M, Bergeron C, Fraser PE, St. George-Hyslop P, Westaway D.** Aβ peptide immunization reduces behavioural impairment and plaques in a model of Alzheimer's disease. *Nature*. 2000; 408: 979–82.
199. **Town T, Tan J, Sansone N, Obregon D, Klein T, Mullan M.** Characterization of murine immunoglobulin G antibodies against human amyloid-β1–42. *Neurosci Lett*. 2001; 307: 101–4.
200. **Morgan D, Diamond DM, Gottschall PE, Ugen KE, Dickey C, Hardy J, Duff K, Jantzen P, DiCarlo G, Wilcock D, Connor K, Hatcher J, Hope C, Gordon M, Arendash GW.** Aβ peptide vaccination prevents memory loss in an animal model of Alzheimer's disease. *Nature*. 2000; 408: 982.
201. **Bard F, Cannon C, Barbour R, Burke R-L, Games D, Grajeda H, Guido T, Hu K, Huang J, Johnson-Wood K, Khan K, Kholodenko D, Lee M, Lieberburg I, Motter R, Nguyen M, Soriano F, Vasquez N, Weiss K, Welch B, Seubert P, Schenk D, Yednock T.** Peripherally administered antibodies against amyloid β-peptide enter the central nervous system and reduce pathology in a mouse model of Alzheimer disease. *Nat Med*. 2000; 6: 916–9.
202. **Brendza R, Bacskai B, Cirrito J, Simmons K, Skoch J, Klunk W, Mathis C, Bales K, Paul S, Hyman B, Holtzman D.** Anti-abeta antibody treatment promotes the rapid recovery of amyloid-associated neuritic dystrophy in PDAPP transgenic mice. *J Clin Invest*. 2005; 115: 428–33.
203. **DeMattos RB, Bales KR, Cummins DJ, Dodart J-C, Paul SM, Holtzman DM.** Peripheral anti-Aβ antibody alters CNS and plasma Aβ clearance and decreases brain Aβ burden in a mouse model of Alzheimer's disease. *Proc Natl Acad Sci USA*. 2001; 98: 8850–5.
204. **Dodart J-C, Bales KR, Gannon KS, Greene SJ, DeMattos RB, Mathis C, DeLong CA, Wu S, Wu X, Holtzman DM, Paul SM.** Immunization reverses memory deficits without reducing brain Aβ burden in Alzheimer's disease model. *Nat Neurosci*. 2002; 5: 452–7.
205. **Du Y, Wei X, Dodel R, Sommer N, Hampel H, Gao F, Ma Z, Zhao L, Oertel WH, Farlow M.** Human anti-β-amyloid antibodies block β-amyloid fibril formation and prevent β-amyloid-induced neurotoxicity. *Brain*. 2003; 126: 1935–9.
206. **Hartman RE, Izumi Y, Bales KR, Paul SM, Wozniak DF, Holtzman DM.** Treatment with an amyloid-β antibody ameliorates plaque load, learning deficits, and hippocampal long-term potentiation in a mouse model of Alzheimer's disease. *J Neurosci*. 2005; 25: 6213–20.
207. **Klyubin I, Betts V, Welzel AT, Blennow K, Zetterberg H, Wallin A, Lemere CA, Cullen WK, Peng Y, Wisniewski T, Selkoe DJ, Anwyl R, Walsh DM, Rowan MJ.**

Amyloid β protein dimer-containing human CSF disrupts synaptic plasticity: prevention by systemic passive immunization. *J Neurosci.* 2008; 28: 4231–7.

208. **Lombardo JA, Stern EA, McLellan ME, Kajdasz ST, Hickey GA, Bacskai BJ, Hyman BT.** *Amyloid-β antibody treatment leads to rapid normalization of plaque-induced neuritic alterations. J Neurosci.* 2003; 23: 10879–83.
209. **Check E.** Nerve inflammation halts trial for *Alzheimer's drug. Nature.* 2002; 415: 462.
210. **Senior K.** Dosing in phase II trial of Alzheimer's vaccine suspended. *Lancet Neurol.* 2002; 1: 3.
211. **Orgogozo JMM, Gilman SMF, Dartigues JFMDP, Laurent BM, Puel MM, Kirby LCM, Jouanny PMDP, Dubois BM, Eisner LM, Flitman SM, Michel BFM, Boada MM, Frank AMDP, Hock CM.** Subacute meningoencephalitis in a subset of patients with AD after Aβ42 immunization. *Neurology.* 2003; 61: 46–54.
212. **Nicoll JAR, Wilkinson D, Holmes C, Steart P, Markham H, Weller RO.** Neuropathology of human Alzheimer disease after immunization with amyloid-b peptide: a case report. *Nat Med.* 2003 04; 9: 448.
213. **Nicoll JA, Barton E, Boche D, Neal JW, Ferrer I, Thompson P, Vlachouli C, Wilkinson D, Bayer A, Games D, Seubert P, Schenk D, Holmes C.** *Aβ species removal after Aβ42 immunization. J Neuropathol Exp Neurol.* 2006; 65: 1040–8.
214. **Schenk D, Barbour R, Dunn W, Gordon G, Grajeda H, Guido T, Hu K, Huang J, Johnson-Wood K, Khan K, Kholodenko D, Lee M, Liao Z, Lieberburg I, Motter R, Mutter L, Soriano F, Shopp G, Vasquez N, Vandevert C, Walker S, Wogulis M, Yednock T, Games D, Seubert P.** Immunization with amyloid-β attenuates Alzheimer-disease-like pathology in the PDAPP mouse. *Nature.* 1999; 400: 173–7.
215. **Bacskai BJ, Kajdasz ST, Christie RH, Carter C, Games D, Seubert P, Schenk D, Hyman BT.** Imaging of amyloid-β deposits in brains of living mice permits direct observation of clearance of plaques with immunotherapy. *Nat Med.* 2001; 7: 369–72.
216. **Lemere CA, Beierschmitt A, Iglesias M, Spooner ET, Bloom JK, Leverone JF, Zheng JB, Seabrook TJ, Louard D, Li D, Selkoe DJ, Palmour RM, Ervin FR.** Alzheimer's disease Aβ vaccine reduces central nervous system Aβ levels in a non-human primate, the Caribbean vervet. *Am J Pathol.* 2004; 165: 283–97.
217. **Hock C, Konietzko U, Papassotiropoulos A, Wollmer A, Streffer J, von Rotz RC, Davey G, Moritz E, Nitsch RM.** Generation of antibodies specific for β-amyloid by vaccination of patients with Alzheimer disease. *Nat Med.* 2002; 8: 1270–6.
218. **Hock C, Konietzko U, Streffer JR, Tracy J, Signorell A, Müller-Tillmanns B, Lemke U, Henke K, Moritz E, Garcia E, Wollmer MA, Umbricht D, de Quervain DJF, Hofmann M, Maddalena A, Papassotiropoulos A, Nitsch RM.** Antibodies against β-amyloid slow cognitive decline in Alzheimer's disease. *Neuron.* 2003; 38: 547–54.
219. **Fox NCMF, Black RSM, Gilman SMF, Rossor MNMF, Griffith SGMDPM, Jenkins LP, Koller MMM, for the ANST.** Effects of Aβ immunization (*AN*1792) on MRI measures of cerebral volume in Alzheimer disease. *Neurology.* 2005; 64: 1563–72.
220. **Gilman S, Koller M, Black RS, Jenkins L, Griffith SGMD, Fox NC, Eisner L, Kirby L, Rovira M, D. BM, Forette F, Orgogozo JM, Team ANS.** Clinical effects of *Aβ* immunization (*AN*1792) in patients with *AD* in an interrupted trial. *Neurology.* 2005; 64: 1553–62.
221. **Holmes C, Boche D, Wilkinson D, Yadegarfar G, Hopkins V, Bayer A, Jones RW, Bullock R, Love S, Neal JW, Zotova E, Nicoll JAR.** Long-term effects of Aβ42 immunisation in *Alzheimer's disease: follow-up of a randomised, placebo-controlled phase I trial. Lancet.* 2008; 372: 216–23.
222. **Bayer TA, Schafer S, Simons A, Kemmling A, Kamer T, Tepest R, Eckert A, Schussel K, Eikenberg O, Sturchler-Pierrat C, Abramowski D, Staufenbiel M, Multhaup G.** Dietary Cu stabilizes brain superoxide dismutase 1 activity and reduces amyloid Aβ production in APP23 transgenic mice. *Proc Natl Acad Sci USA.* 2003; 100: 14187–92.
223. **Borchardt T, Camakaris J, Cappai R, Masters CL, Beyreuther K, Multhaup G.** Copper inhibits β-amyloid production and stimulates the non-amyloidogenic pathway of amyloid-precursor-protein secretion. *Biochem J.* 1999; 344: 461–7.
224. **Phinney AL, Drisaldi B, Schmidt SD, Lugowski S, Coronado V, Liang Y, Horne P, Yang J, Sekoulidis J, Coomaraswamy J, Chishti MA, Cox DW, Mathews PM, Nixon RA, Carlson GA, George-Hyslop PS, Westaway D.** *In vivo reduction of amyloid-β by a mutant copper transporter. Proc Natl Acad Sci USA.* 2003; 100: 14193–8.
225. **White AR, Du T, Laughton KM, Volitakis I, Sharples RA, Xilinas ME, Hoke DE, Holsinger RMD, Evin G, Cherny RA, Hill AF, Barnham KJ, Li Q-X, Bush AI, Masters CL.** Degradation of the *Alzheimer disease amyloid β-peptide by metal-dependent up-regulation of metalloprotease activity. J Biol Chem.* 2006; 281: 17670–80.
226. **Dodel RC, Du Y, Depboylu C, Hampel H, Frolich L, Haag A, Hemmeter U, Paulsen S, Teipel SJ, Brettschneider S, Spottke A, Nolker C, Moller HJ, Wei X, Farlow M, Sommer N, Oertel WH.** Intravenous immunoglobulins containing antibodies against β-amyloid for the treatment of *Alzheimer's disease. J Neurol Neurosurg Psychiatry.* 2004; 75: 1472–4.
227. **Adlard PA, Bush AI.** Metals and Alzheimer's disease. *J Alzheimers Dis.* 2006; 10: 145–63.
228. **Lovell MA, Robertson JD, Teesdale WJ, Campbell JL, Markesbery WR.** Copper, iron and zinc in Alzheimer's disease senile plaques. *J Neurol Sci.* 1998; 158: 47–52.
229. **Basun H, Forssell LG, Wetterberg L, Winblad B.** Metals and trace elements in plasma and cerebrospinal fluid in normal ageing and Alzheimer's disease. *J Neural Transm Park Dis Dement Sect.* 1991; 3: 231–58.
230. **Bush AI.** The metallobiology of Alzheimer's disease. *Trends Neurosci.* 2003; 26: 207–14.
231. **Bush AI.** Metals and neuroscience. *Curr Opin Chem Biol.* 2000; 4: 184–91.
232. **Koh J-Y.** Zinc and disease of the brain. *Mol Neurobiol.* 2001; 24: 99–106.
233. **Madsen E, Gitlin JD.** Copper and iron disorders of the brain. *Annu Rev Neurosci.* 2007; 30: 317–37.
234. **Barnham KJ, Bush AI.** Metals in Alzheimer's and Parkinson's diseases. *Curr Opin Chem Biol.* 2008; 12: 222–8.
235. **Suh SW, Jensen KB, Jensen MS, Silva DS, Kesslak PJ, Danscher G, Frederickson CJ.** Histochemically-reactive zinc in amyloid plaques, angiopathy, and degenerating neurons of Alzheimer's diseased brains. *Brain Res.* 2000; 852: 274–8.
236. **Smith MA, Wehr K, Harris PLR, Siedlak SL, Connor JR, Perry G.** Abnormal localization of iron regulatory protein in Alzheimer's disease. *Brain Res.* 1998; 788: 232–6.
237. **Bjorkdahl C, Sjogren MJ, Winblad B, Pei J-JCA.** Zinc induces neurofilament

phosphorylation independent of p70 S6 kinase in N2a cells. *Neuroreport*. 2005; 16: 591–5.

238. **Malm TM, Iivonen H, Goldsteins G, Keksa-Goldsteine V, Ahtoniemi T, Kanninen K, Salminen A, Auriola S, Van Groen T, Tanila H, Koistinaho J.** Pyrrolidine dithiocarbamate activates Akt and improves spatial learning in APP/PS1 mice without affecting β-amyloid burden. *J Neurosci*. 2007; 27: 3712–21.
239. **Egaña JT, Zambrano C, Nuñez MT, Gonzalez-Billault C, Maccioni RB.** Iron-induced oxidative stress modify tau phosphorylation patterns in hippocampal cell cultures. *Biometals*. 2003; 16: 215–23.
240. **Ma Q, Li Y, Du J, Kanazawa K, Nemoto T, Nakanishi H, Zhao Y.** Binding of copper (II) ion to an Alzheimer's tau peptide as revealed by MALDI-TOF MS, CD, and NMR. *Biopolymers*. 2005; 79: 74–85.
241. **Ma Q, Li Y, Du J, Liu H, Kanazawa K, Nemoto T, Nakanishi H, Zhao Y.** Copper binding properties of a tau peptide associated with Alzheimer's disease studied by CD, NMR, and MALDI-TOF MS. *Peptides*. 2006; 27: 841–9.
242. **Zhou L-X, Du J-T, Zeng Z-Y, Wu W-H, Zhao Y-F, Kanazawa K, Ishizuka Y, Nemoto T, Nakanishi H, Li Y-M.** Copper (II) modulates in vitro aggregation of a tau peptide. *Peptides*. 2007; 28: 2229–34.
243. **Yamamoto A, Shin RW, Hasegawa K, Naiki H, Sato H, Yoshimasu F, Kitamoto T.** Iron (III) induces aggregation of hyperphosphorylated τ and its reduction to iron (II) reverses the aggregation: implications in the formation of neurofibrillary tangles of Alzheimer's disease. *J Neurochem*. 2002; 82: 1137–47.
244. **Barnham KJ, McKinstry WJ, Multhaup G, Galatis D, Morton CJ, Curtain CC, Williamson NA, White AR, Hinds MG, Norton RS, Beyreuther K, Masters CL, Parker MW, Cappai R.** Structure of the Alzheimer's disease amyloid precursor protein copper binding domain. A regulator of neuronal copper homeostasis. *J Biol Chem*. 2003; 278: 17401–7.
245. **Bayer TA, Multhaup G.** Involvement of amyloid β precursor protein (AβPP) modulated copper homeostasis in Alzheimer's disease. *J Alzheimers Dis*. 2005; 8: 201–6.
246. **Rogers JT, Randall JD, Cahill CM, Eder PS, Huang X, Gunshin H, Leiter L, McPhee J, Sarang SS, Utsuki T, Greig NH, Lahiri DK, Tanzi RE, Bush AI, Giordano T, Gullans SR.** An iron-responsive element type II in the 5'-untranslated region of the Alzheimer's amyloid precursor protein transcript. *J Biol Chem*. 2002; 277: 45518–28.
247. **Venti A, Giordano T, Eder P, Bush AI, Lahiri DK, Greig NH, Rogers JT.** The integrated role of desferrioxamine and phenserine targeted to an iron-responsive element in the APP-mRNA 5'-untranslated region. *Ann N Y Acad Sci*. 2004; 1035: 34–48.
248. **Moechars D, Dewachter I, Lorent K, Reverse D, Baekelandt V, Naidu A, Tesseur I, Spittaels K, Haute CV, Checler F, Godaux E, Cordell B, Van Leuven F.** Early phenotypic changes in transgenic mice that overexpress different mutants of amyloid precursor protein in brain. *J Biol Chem*. 1999; 274: 6483–92.
249. **Hsiao K, Chapman P, Nilsen S, Eckman C, Harigaya Y, Younkin S, Yang F, Cole G.** Correlative memory deficits, Aβ elevation, and amyloid plaques in transgenic mice. *Science*. 1996; 274: 99–102.
250. **Maynard CJ, Cappai R, Volitakis I, Cherny RA, White AR, Beyreuther K, Masters CL, Bush AI, Li Q-X.** Overexpression of Alzheimer's disease amyloid-β opposes the age-dependent elevations of brain copper and iron. *J Biol Chem*. 2002; 277: 44670–6.
251. **White AR, Reyes R, Mercer JFB, Camakaris J, Zheng H, Bush AI, Multhaup G, Beyreuther K, Masters CL, Cappai R.** Copper levels are increased in the cerebral cortex and liver of APP and APLP2 knockout mice. *Brain Res*. 1999; 842: 439–44.
252. **Zheng H, Jiang M, Trumbauer ME, Sirinathsinghji DJ, Hopkins R, Smith DW, Heavens RP, Dawson GR, Boyce S, Conner MW, Stevens KA, Slunt HH, Sisoda SS, Chen HY, Van der Ploeg LH.** β-Amyloid precursor protein-deficient mice show reactive gliosis and decreased locomotor activity. *Cell*. 1995; 81: 525–31.
253. **Stuchlik-Pierrat C, Abramowski D, Duke M, Wiederhold K-H, Misti C, Rothacher S, Ledermann B, Burki K, Frey P, Paganetti PA, Waridel C, Calhoun ME, Jucker M, Probst A, Staufenbiel M, Sommer B.** Two amyloid precursor protein transgenic mouse models with Alzheimer disease-like pathology. *Proc Natl Acad Sci USA*. 1997; 94: 13287–92.
254. **Sparks DL, Schreurs BG.** Trace amounts of copper in water induce β-amyloid plaques and learning deficits in a rabbit model of Alzheimer's disease. *Proc Natl Acad Sci USA*. 2003; 100: 11065–9.
255. **Bush AI, Pettingell Jr WH, Paradis MD, Tanzi RE.** Modulation of Aβ adhesiveness and secretase site cleavage by zinc. *J Biol Chem*. 1994; 269: 12152–8.
256. **Bush AI, Pettingell WH, Multhaup G, d Paradis M, Vonsattel JP, Gusella JF, Beyreuther K, Masters CL, Tanzi RE.** Rapid induction of Alzheimer Aβ amyloid formation by zinc. *Science*. 1994; 265: 1464–7.
257. **Esler WP, Stimson ER, Jennings JM, Ghilardi JR, Mantyh PW, Maggio JE.** Zinc-induced aggregation of human and rat β-amyloid peptides *in vitro*. *J Neurochem*. 1996; 66: 723–32.
258. **Brown AM, Tummolo DM, Rhodes KJ, Hofmann JR, Jacobsen JS, Sonnenberg-Reines J.** Selective aggregation of endogenous β-amyloid peptide and soluble amyloid precursor protein in cerebrospinal fluid by zinc. *J Neurochem*. 1997; 69: 1204–12.
259. **Mantyh PW, Ghilardi JR, Rogers S, DeMaster E, Allen CJ, Stimson ER, Maggio JE.** Aluminum, iron, and zinc ions promote aggregation of physiological concentrations of β-amyloid peptide. *J Neurochem*. 1993; 61: 1171–4.
260. **Atwood CS, Moir RD, Huang X, Scarpa RC, Bacarra NME, Romano DM, Hartshorn MA, Tanzi RE, Bush AI.** Dramatic aggregation of Alzheimer Aβ by Cu(II) is induced by conditions representing physiological acidosis. *J Biol Chem*. 1998; 273: 12817–26.
261. **Gaggelli E, Kozlowski H, Valensin D, Valensin G.** Copper homeostasis and neurodegenerative disorders (Alzheimer's, Prion, and Parkinson's diseases and amyotrophic lateral sclerosis). *Chem Rev*. 2006; 106: 1995–2044.
262. **Miura T, Suzuki K, Kohata N, Takeuchi H.** Metal binding modes of Alzheimer's amyloid β-peptide in insoluble aggregates and soluble complexes. *Biochemistry*. 2000; 39: 7024–31.
263. **Assaf SY, Chung S-H.** Release of endogenous Zn^{2+} from brain tissue during activity. *Nature*. 1984; 308: 734–6.
264. **Howell GA, Welch MG, Frederickson CJ.** Stimulation-induced uptake and release of zinc in hippocampal slices. *Nature*. 1984; 308: 736–8.
265. **Hartter DE, Barnea A.** Brain tissue accumulates 67copper by two ligand-dependent saturable processes. A high affinity, low capacity and a low affinity, high capacity process. *J Biol Chem*. 1988; 263: 799–805.
266. **Kardos J, Kovacs I, Hajos F, Kalman M, Simonyi M.** Nerveendings from rat brain tissue release copper upon depolarization. A

possible role in regulating neuronal excitability. *Neurosci Lett.* 1989; 103: 139–44.

267. **Schlief ML, Craig AM, Gitlin JD.** NMDA receptor activation mediates copper homeostasis in hippocampal neurons. *J Neurosci.* 2005; 25: 239–46.
268. **Friedlich AL, Lee J-Y, van Groen T, Cherny RA, Volitakis I, Cole TB, Palmiter RD, Koh J-Y, Bush AI.** Neuronal zinc exchange with the blood vessel wall promotes cerebral amyloid angiopathy in an animal model of Alzheimer's disease. *J Neurosci.* 2004; 24: 3453–9.
269. **Lee JY, Cole TB, Palmiter RD, Suh SW, Koh JY.** Contribution by synaptic zinc to the gender-disparate plaque formation in human Swedish mutant APP transgenic mice. *Proc Natl Acad Sci USA.* 2002; 99: 7705–10.
270. **Linkous DH, Flinn JM, Koh JY, Lanzirotti A, Bertsch PM, Jones BF, Giblin LJ, Frederickson CJ.** Evidence that the ZNT3 protein controls the total amount of elemental zinc in synaptic vesides. *J Histochem Cytochem.* 2008; 56: 3–6.
271. **Frederickson CJ, Bush AI.** Synaptically released zinc: physiological functions and pathological effects. *Biometals.* 2001; 14: 353–66.
272. **Karr JW, Akintoye H, Kaupp LJ, Szalai VA.** N-Terminal deletions modify the Cu^{2+} binding site in amyloid-β. *Biochemistry.* 2005; 44: 5478–87.
273. **Syme CD, Viles JH.** Solution 1H NMR investigation of Zn^{2+} and Cd^{2+} binding to amyloid-β peptide (Aβ) of Alzheimer's disease. *Biochim Biophys Acta.* 2006; 1764: 246–56.
274. **Jiang D, Men L, Wang J, Zhang Y, Chickenyen S, Wang Y, Zhou F.** Redox reactions of copper complexes formed with different β-amyloid peptides and their neuropathological relevance. *Biochemistry.* 2007; 46: 9270–82.
275. **Clements A, Allsop D, Walsh DM, Williams CH.** Aggregation and metal-binding properties of mutant forms of the amyloid β peptide of Alzheimer's disease. *J Neurochem.* 1996; 66: 740–7.
276. **Mekmouche Y, Coppel Y, Hochgräfe K, Guilloreau L, Talmard C, Mazarguil H, Faller P.** Characterization of the Zn(II) binding to the peptide amyloid-β_{1-16} linked to Alzheimer's disease. *Chembiochem.* 2005; 6: 1663–71.
277. **Kozin SA, Zirah S, Rebuffat S, Hui Bon Hoa G, Debey P.** Zinc binding to Alzheimer's Aβ(1–16) peptide results in stable soluble complex. *Biochem Biophys Res Commun.* 2001; 285: 959–64.
278. **Atwood CS, Huang X, Khatri A, Scarpa RC, Kim YS, Moir RD, Tanzi RE, Roher AE, Bush AI.** Copper catalyzed oxidation of Alzheimer Aβ. *Cell Mol Biol.* 2000; 46: 777–83.
279. **Guilloreau L, Damian L, Coppel Y, Mazarguil H, Winterhalter M, Faller P.** Structural and thermodynamical properties of Cull amyloid-β16/28 complexes associated with Alzheimer's disease. *J Biol Inorg Chem.* 2006; 11: 1024–38.
280. **Ha C, Ryu J, Park CB.** Metal ions differentially influence the aggregation and deposition of Alzheimer's β-amyloid on a solid template. *Biochemistry.* 2007; 46: 6118–25.
281. **Han D, Wang H, Yang P.** Molecular modeling of zinc and copper binding with Alzheimer's amyloid β-peptide. *Biometals.* 2008; 21: 189–96.
282. **Li W, Zhang J, Su Y, Wang J, Qin M, Wang W.** Effects of zinc binding on the conformational distribution of the amyloid-β peptide based on molecular dynamics simulations. *J Phys Chem.* 2007; 111: 13814–21.
283. **Morgan DM, Dong J, Jacob J, Lu K, Apkarian RP, Thiyagarajan P, Lynn DG.** Metal switch for amyloid formation: insight into the structure of the nucleus. *J Am Chem Soc.* 2002; 124: 12644–5.
284. **Dong J, Canfield JM, Mehta AK, Shokes JE, Tian B, Childers WS, Simmons JA, Mao Z, Scott RA, Wamcke K, Lynn DG.** Engineering metal ion coordination to regulate amyloid fibril assembly and toxicity. *Proc Natl Acad Sci USA.* 2007; 104: 13313–8.
285. **Sangmi J, Sunil S.** The aggregated state of amyloid-β peptide *in vitro* depends on Cu^{2+} ion concentration. *Angew Chem Int Ed Engl.* 2007; 46: 3959–61.
286. **Atwood CS, Scarpa RC, Huang X, Moir RD, Jones WD, Fairlie DP, Tanzi RE, Bush AI.** Characterization of copper interactions with Alzheimer amyloid β peptides. Identification of an attomolar-affinity copper binding site on amyloid β1–42. *J Neurochem.* 2000; 75: 1219–33.
287. **Tougu V, Karafin A, Palumaa P.** Binding of zinc(II) and copper(II) to the full-length Alzheimer's amyloid-β peptide. *J Neurochem.* 2008; 104: 1249–59.
288. **Gaggelli E, Janicka-Klos A, Jankowska E, Kozlowski H, Migliorini C, Molteni E, Valensin D, Valensin G, Wieczerzak E.** NMR studies of the Zn^{2+} interactions with rat and human β-amyloid (1–28) peptides in water-micelle environment. *J Phys Chem.* 2008; 112: 100–9.
289. **Danielsson J, Pierattelli R, Banci L, Graslund A.** High-resolution NMR studies of the zinc-binding site of the Alzheimer's amyloid β-peptide. *FEBS J.* 2007; 274: 46–59.
290. **Garzon-Rodriguez W, Yatsimirsky AK, Glabe CG.** Binding of Zn(II), Cu(II), and Fe(II) ions to Alzheimer's Aβ peptide studied by fluorescence. *Bioorg Med Chem Lett.* 1999; 9: 2243–8.
291. **Clements A, Allsop D, Walsh DM, Williams CH.** Aggregation and metal-binding properties of mutant forms of the amyloid Aβ peptide of Alzheimer's disease. *J Neurochem.* 1996; 66: 740–7.
292. **Streltsov V.** X-ray absorption and diffraction studies of the metal binding sites in amyloid β-peptide. *Eur Biophys J.* 2008; 37: 257–63.
293. **Curtain CC, Ali F, Volitakis I, Cherny RA, Norton RS, Beyreuther K, Barrow CJ, Masters CL, Bush AI, Barnham KJ.** Alzheimer's disease amyloid-β binds copper and zinc to generate an allosterically ordered membrane-penetrating structure containing superoxide dismutase-like subunits. *J Biol Chem.* 2001; 276: 20466–73.
294. **Yang D-S, McLaurin J, Qin K, Westaway D, Fraser PE.** Examining the zinc binding site of the amyloid-β peptide. *Eur J Biochem.* 2000; 267: 6692–8.
295. **Zirah S, Rebuffat S, Kozin SA, Debey P, Foumier F, Lesage D, Tabet J-C.** Zinc binding properties of the amyloid fragment Aβ(1–16) studied by electrospray-ionization mass spectrometry. *Int J Mass Spectrom.* 2003; 228: 999–1016.
296. **Curtain CC, Ali FE, Smith DG, Bush AI, Masters CL, Barnham KJ.** Metal ions, pH, and cholesterol regulate the interactions of Alzheimer's disease amyloid-β peptide with membrane lipid. *J Biol Chem.* 2003; 278: 2977–82.
297. **Dong J, Atwood CS, Anderson VE, Siedlak SL, Smith MA, Perry G, Carey PR.** Metal binding and oxidation of amyloid-β within isolated senile plaque cores: Raman microscopic evidence. *Biochemistry.* 2003; 42: 2768–73.
298. **Karr JW, Kaupp LJ, Szalai VA.** Amyloid-β binds Cu^{2+} in a mononuclear metal ion binding site. *J Am Chem Soc.* 2004; 126: 13534–8.
299. **Karr JW, Szalai VA.** Role of aspartate-1 in Cu(II) binding to the amyloid-β peptide of Alzheimer's disease. *J Am Chem Soc.* 2007; 129: 3796–7.
300. **Kowalik-Jankowska T, Ruta M, Wisniewska K, Lankiewicz L.** Coordination abilities of the 1–16 and 1–28 fragments of

β-amyloid peptide towards copper(II) ions: a combined potentiometric and spectroscopic study. *J Inorg Biochem.* 2003; 95: 270–82.

301. **Stellato F, Menestrina G, Serra M, Potrich C, Tomazzolli R, Meyer-Klaucke W, Morante S.** Metal binding in amyloid β-peptides shows intra- and inter-peptide coordination modes. *Eur Biophys J.* 2006; 35: 340–51.
302. **Zirah S, Kozin SA, Mazur AK, Blond A, Cheminant M, Segalas-Milazzo I, Debey P, Rebuffat S.** Structural changes of region 1–16 of the *Alzheimer* disease amyloid β-peptide upon zinc binding and *in vitro* aging. *J Biol Chem.* 2006; 281: 2151–61.
303. **Liu ST, Howlett G, Barrow CJ.** Histidine-13 is a crucial residue in the zinc ion-induced aggregation of the abeta peptide of Alzheimer's disease. *Biochemistry.* 1999; 38: 9373–8.
304. **Morgan DM, Dong J, Jacob J, Lu K, Apkarian RP, Thiyagarajan P, Lynn DG.** Metal switch for amyloid formation: insight into the structure of the nucleus. *J Am Chem Soc.* 2002; 124: 12644–5.
305. **Vaughan D, Peters A.** The structure of neuritic plaque in the cerebral cortex of aged rats. *J Neuropathol Exp Neurol.* 1981; 40: 472–87.
306. **Bush AI, Tanzi RE.** Therapeutics for *Alzheimer's* disease based on the metal hypothesis. *Neurotherapeutics.* 2008; 5: 421–32.
307. **Ganai K, Sahoo B, Kaushalya SK, Desai R, Maiti S.** Zinc lowers amyloid-β toxicity by selectively precipitating aggregation intermediates. *Biochemistry.* 2007; 46: 10655–63.
308. **Tew DJ, Bottomley SP, Smith DP, Ciccotosto GD, Babon J, Hinds MG, Masters CL, Cappai R, Barnham KJ.** Stabilization of neurotoxic soluble β-sheet-rich conformations of the *Alzheimer's* disease amyloid-β peptide. *Biophys J.* 2008; 94: 2752–66.
309. **Yoshiike Y, Tanemura K, Murayama O, Akagi T, Murayama M, Sato S, Sun X, Tanaka N, Takashima A.** New insights on how metals disrupt amyloid β -aggregation and their effects on amyloid-β cytotoxicity. *J Biol Chem.* 2001; 276: 32293–9.
310. **Barnham KJ, Haeffner F, Ciccotosto GD, Curtain CC, Tew D, Mavros C, Beyreuther K, Carrington D, Masters CL, Cherny RA, Cappai R, Bush AI.** Tyrosine gated electron transfer is key to the toxic mechanism of *Alzheimer's* disease β-amyloid. *FASEB J.* 2004; 18: 1427–9.
311. **Atwood CS, Perry G, Zeng H, Kato Y, Jones WD, Ling KQ, Huang X, Moir RD, Wang D, Sayre LM, Smith MA, Chen SG, Bush AI.** Copper mediates dityrosine cross-linking of Alzheimer's amyloid-beta. *Biochemistry.* 2004; 43: 560–8.
312. **Smith DP, Ciccotosto GD, Tew DJ, Fodero-Tavoletti MT, Johanssen T, Masters CL, Barnham KJ, Cappai R.** Concentration dependent Cu^{2+} induced aggregation and dityrosine formation of the *Alzheimer's* disease amyloid-β peptide. *Biochemistry.* 2007; 46: 2881–91.
313. **Barnham KJ, Ciccotosto GD, Tickler AK, Ali FE, Smith DG, Williamson NA, Lam Y-H, Carrington D, Tew D, Kocak G, Volitakis I, Separovic F, Barrow CJ, Wade JD, Masters CL, Cherny RA, Curtain CC, Bush AI, Cappai R.** Neurotoxic, redox-competent Alzheimer's β-amyloid is released from lipid membrane by methionine oxidation. *J Biol Chem.* 2003; 278: 42959–65.
314. **Crouch PJ, Barnham KJ, Duce JA, Blake RE, Masters CL, Trounce IA.** Copper-dependent inhibition of cytochrome c oxidase by Aβ1 42 requires reduced methionine at residue 35 of the Aβ peptide. *J Neurochem.* 2006; 99: 226–36.
315. **Hou L, Shao H, Zhang Y, Li H, Menon NK, Neuhaus EB, Brewer JM, Byeon IJL, Ray DG, Vitek MP, Iwashita T, Makula RA, Przybyla AB, Zagorski MG.** Solution NMR studies of the Aβ(1–40) and Aβ(1–42) peptides establish that the Met35 oxidation state affects the mechanism of amyloid formation. *J Am Chem Soc.* 2004; 126: 1992–2005.
316. **Atwood CS, Perry G, Zeng H, Kato Y, Jones WD, Ling KQ, Huang X, Moir RD, Wang D, Sayre LM, Smith MA, Chen SG, Bush AI.** Copper mediates dityrosine cross-linking of Alzheimer's amyloid-β. *Biochemistry.* 2004; 43: 560–8.
317. **Naylor R, Hill A, Barnham K.** Neurotoxicity in *Alzheimer's* disease: is covalently crosslinked Aβ responsible? *Eur Biophys J.* 2008; 37: 265–8.
318. **Lau T-L, Ambroggio EE, Tew DJ, Cappai R, Masters CL, Fidelio GD, Barnham KJ, Separovic F.** Amyloid-β peptide disruption of lipid membranes and the effect of metal ions. *J Mol Biol.* 2006; 356: 759–70.
319. **Ciccotosto GD, Tew D, Curtain CC, Smith D, Carrington D, Masters CL, Bush AI, Cherny RA, Cappai R, Barnham KJ.** Enhanced toxicity and cellular binding of a modified amyloid β peptide with a methionine to valine substitution. *J Biol Chem.* 2004; 279: 42528–34.
320. **Barnham KJ, Masters CL, Bush AI.** Neurodegenerative diseases and oxidative stress. *Nat Rev Drug Discov.* 2004; 3: 205–14.
321. **Smith DG, Cappai R, Barnham KJ.** The redox chemistry of the *Alzheimer's* disease amyloid β peptide. *Biochim Biophys Acta.* 2007; 1768: 1976–90.
322. **Atwood CS, Huang X, Moir RD, Tanzi RE, Bush AI.** Role of free radicals and metal ions in the pathogenesis of *Alzheimer's* disease. *Met Ions Biol Syst.* 1999; 36: 309–64.
323. **Huang X, Atwood CS, Hartshorn MA, Multhaup G, Goldstein LE, Scarpa RC, Cuajungco MP, Gray DN, Lim J, Moir RD, Tanzi RE, Bush AI.** The Aβ peptide of *Alzheimer's* disease directly produces hydrogen peroxide through metal ion reduction. *Biochemistry.* 1999; 38: 7609–16.
324. **Huang X, Atwood CS, Moir RD, Hartshorn MA, Tanzi RE, Bush AI.** Trace metal contamination initiates the apparent auto-aggregation, amyloidosis, and oligomerization of *Alzheimer's* Aβ peptides. *J Biol Inorg Chem.* 2004; 9: 954–60.
325. **Huang X, Cuajungco MP, Atwood CS, Hartshorn MA, Tyndall JDA, Hanson GR, Stokes KC, Leopold M, Multhaup G, Goldstein LE, Scarpa RC, Saunders AJ, Lim J, Moir RD, Glabe C, Bowden EF, Masters CL, Fairlie DP, Tanzi RE, Bush AI.** Cu(II) potentiation of *Alzheimer* Aβ neurotoxicity. correlation with cell-free hydrogen peroxide production and metal reduction. *J Biol Chem.* 1999; 274: 37111–6.
326. **Sayre LM, Perry G, Harris PLR, Liu Y, Schubert KA, Smith MA.** In situ oxidative catalysis by neurofibrillary tangles and senile plaques in *Alzheimer's* disease. *J Neurochem.* 2000; 74: 270–9.
327. **Rossi L, Lombardo M, Ciriolo M, Rotilio G.** Mitochondrial dysfunction in neurodegenerative diseases associated with copper imbalance. *Neurochem Res.* 2004; 29: 493–504.
328. **Masayoshi Y, Masatsugu K, Shoji O.** Role of zinc as an activator of mitochondrial function in rat liver. *Biochem Pharmacol.* 1982; 31: 1289–93.
329. **Ortiz E, Pasquini JM, Thompson K, Felt B, Butkus G, Beard J, Connor JR.** Effect of manipulation of iron storage, transport, or availability on myelin composition and brain iron content in three different animal models. *J Neurosci Res.* 2004; 77: 681–9.
330. **Smart TG, Hosie AM, Miller PS.** Zn^{2+} Ions: Modulators of Excitatory and

Inhibitory Synaptic Activity. *Neuroscientist*. 2004; 10: 432–42.
331. **Takeda A.** Zinc homeostasis and functions of zinc in the brain. *Biometals*. 2001; 14: 343–51.
332. **Bhatnagara S, Tanejaa S.** Zinc and cognitive development. *Br J Nutr*. 2001; 85: S139–S45.
333. **Gaeta A, Hider RC.** The crucial role of metal ions in neurodegeneration: the basis for a promising therapeutic strategy. *Br J Pharmacol*. 2005; 146: 1041–59.
334. **Que EL, Domaille DW, Chang CJ.** Metals in neurobiology: probing their chemistry and biology with molecular imaging. *Chem Rev*. 2008; 108: 1517–49.
335. **Bush AI, Curtain C.** Twenty years of metallo-neurobiology: where to now? *Eur Biophys J*. 2008; 37: 241–5.
336. **Crouch PJ, White AR, Bush AI.** The modulation of metal bio-availability as a therapeutic strategy for the treatment of Alzheimer's disease. *FEBS J*. 2007; 274: 3775–83.
337. **Finefrock AE, Bush AI, Doraiswamy PM.** Current Status of Metals as Therapeutic Targets in Alzheimer's Disease. *J Am Geriatr Soc*. 2003; 51: 1143–8.
338. **Bush AI.** Metal complexing agents as therapies for Alzheimer's disease. *Neurobiol Aging*. 2002; 23: 1031–8.
339. **Brown DR.** Interactions between metals and α-synuclein – function or artefact? *FEBS J*. 2007; 274: 3766–74.
340. **Doraiswamy PM, Finefrock AE.** Metals in our minds: therapeutic implications for neurodegenerative disorders. *Lancet Neurol*. 2004; 3: 431–4.
341. **Behl C, Moosmann B.** Antioxidant neuroprotection in Alzheimer's disease as preventive and therapeutic approach. *Free Radic Biol Med*. 2002; 33: 182–91.
342. **Zatta P, Tognon G, Carampin P.** Melatonin prevents free radical formation due to the interaction between β-amyloid peptides and metal ions [Al(III), Zn(II), Cu(II), Mn(II), Fe(II)]. *J Pineal Res*. 2003; 35: 98–103.
343. **Shishodia S, Sethi G, Aggarwal BB.** Curcumin: Getting Back to the Roots. *Ann N Y Acad Sci*. 2005; 1056: 206–17.
344. **Yang F, Lim GP, Begum AN, Ubeda OJ, Simmons MR, Ambegaokar SS, Chen PP, Kayed R, Glabe CG, Frautschy SA, Cole GM.** Curcumin inhibits formation of amyloid β oligomers and fibrils, binds plaques, and reduces amyloid *in vivo*. *J Biol Chem*. 2005; 280: 5892–901.
345. **Feng Z, Chang Y, Cheng Y, Zhang B-l, Qu Z-w, Qin C, Zhang J-t.** Melatonin alleviates behavioral deficits associated with apoptosis and cholinergic system dysfunction in the APP 695 transgenic mouse model of Alzheimer's disease. *J Pineal Res*. 2004; 37: 129–36.
346. **Matsubara E, Bryant-Thomas T, Pacheco Quinto J, Henry TL, Poeggeler B, Herbert D, Cruz-Sanchez F, Chyan Y-J, Smith MA, Perry G, Shoji M, Abe K, Leone A, Grundke-Ikbal I, Wilson GL, Ghiso J, Williams C, Refolo LM, Pappolla MA.** Melatonin increases survival and inhibits oxidative and amyloid pathology in a transgenic model of Alzheimer's disease. *J Neurochem*. 2003; 85: 1101–8.
347. **Cheng Y, Feng Z, Zhang Q-z, Zhang J-t.** Beneficial effects of melatonin in experimental models of Alzheimer disease1. *Acta Pharmacol Sin*. 2006; 27: 129–39.
348. **Defeudis FV.** Bilobalide and neuroprotection. *Pharmacol Res*. 2002; 46: 565–8.
349. **Zandi PP, Anthony JC, Khachaturian AS, Stone SV, Gustafson D, Tschanz JT, Norton MC, Welsh-Bohmer KA, Breitner JCS.** Reduced risk of Alzheimer disease in users of antioxidant vitamin supplements: The Cache County Study. *Arch Neurol*. 2004; 61: 82–8.
350. **Oken BS, Storzbach DM, Kaye JA.** The Efficacy of Ginkgo biloba on cognitive function in Alzheimer disease. *Arch Neurol*. 1998; 55: 1409–15.
351. **Schneider LS, DeKosky ST, Farlow MR, Tariot PN, Hoerr R, Kieser M.** A randomized, double-blind, placebo-controlled trial of two doses of ginkgo biloba extract in dementia of the Alzheimer's type. *Curr Alzheimer Res*. 2005; 2: 541–51.
352. **Kebede H.** The biochemistry of desferrioxamine and its relation to iron metabolism. *Ann N Y Acad Sci*. 1964; 119: 758–68.
353. **McLachlan DRC, Dalton AJ.** Intramuscular desferrioxamine in patients with Alzheimer's disease. *Lancet*. 1991; 337: 1304–8.
354. **Cuajungco MP, Faget KY, Huang X, Tanzi RE, Bush AI.** Metal chelation as a potential therapy for Alzheimer's disease. *Ann N Y Acad Sci*. 2000; 920: 292–304.
355. **Lee J-Y, Friedman JE, Angel I, Kozak A, Koh J-Y.** The lipophilic metal chelator DP-109 reduces amyloid pathology in brains of human β-amyloid precursor protein transgenic mice. *Neurobiol Aging*. 2004; 25: 1315–21.
356. **Petri S, Calingasan NY, Alsaied OA, Wille E, Kiaei M, Friedman JE, Baranova O, Chavez JC, Beal MF.** The lipophilic metal chelators DP-109 and DP-460 are neuroprotective in a transgenic mouse model of amyotrophic lateral sclerosis. *J Neurochem*. 2007; 102: 991–1000.
357. **Carrì MT, Ferri A, Cozzolino M, Calabrese L, Rotilio G.** Neurodegeneration in amyotrophic lateral sclerosis: the role of oxidative stress and altered homeostasis of metals. *Brain Res Bull*. 2003; 61: 365–74.
358. **Roos PM, Vesterberg O, Nordberg M.** Metals in motor neuron diseases. *Exp Biol Med*. 2006; 231: 1481–7.
359. **Penluigi M, Joshi G, Sultana R, Calabrese V, De Marco C, Coccia R, Butterfield DA.** *In vivo* protection by the xanthate tricyclodecan-9-yl-xanthogenate against amyloid β-peptide (1–42)-induced oxidative stress. *Neuroscience*. 2006; 138: 1161–70.
360. **Shin R-W, Kruck TPA, Murayama H, Kitamoto T.** A novel trivalent cation chelator Feralex dissociates binding of aluminum and iron associated with hyperphosphorylated τ of Alzheimer's disease. *Brain Res*. 2003; 961: 139–46.
361. **Cherny RA, Barnham KJ, Lynch T, Volitakis I, Li Q-X, McLean CA, Multhaup G, Beyreuther K, Tanzi RE, Masters CL, Bush AI.** Chelation and intercalation: complementary properties in a compound for the treatment of Alzheimer's disease. *J Struct Biol*. 2000; 130: 209–16.
362. **Schreck R, Meier B, Mannel DN, Droge W, Baeuerle PA.** Dithiocarbamates as potent inhibitors of nuclear factor κ B activation in intact cells. *J Exp Med*. 1992; 175: 1181–94.
363. **Liu SF, Ye X, Malik AB.** Inhibition of NF-κB activation by pyrrolidine dithiocarbamate prevents *in vivo* expression of proinflammatory genes. *Circulation*. 1999; 100: 1330–7.
364. **Hayakawa M, Miyashita H, Sakamoto I, Kitagawa M, Tanaka H, Yasuda H, Karin M, Kikugawa K.** Evidence that reactive oxygen species do not mediate NF-κB activation. *EMBO J*. 2003; 22: 3356–66.
365. **Burkitt MJ, Bishop HS, Milne L, Tsang SY, Provan GJ, Nobel CSI, Orrenius S, Slater AFG.** Dithiocarbamate toxicity toward thymocytes involves their copper-catalyzed conversion to thiuram disulfides, which oxidize glutathione in a redox cycle without the release of reactive oxygen species. *Arch Biochem Biophys*. 1998; 353: 73–84.
366. **Nobel CSI, Burgess DH, Zhivotovsky B, Burkitt MJ, Orrenius S, Slater AFG.** Mechanism of dithiocarbamate inhibition of apoptosis: thiol oxidation by dithiocarbamate disulfides directly inhibits processing

of the caspase-3 proenzyme. *Chem Res Toxicol.* 1997; 10: 636–43.

367. **Nobel CSI, Kimland M, Lind B, Orrenius S, Slater AFG.** Dithiocarbamates induce apoptosis in thymocytes by raising the intracellular level of redox-active copper. *J Biol Chem.* 1995; 270: 26202–8.
368. **Verhaegh GW, Richard MJ, Hainaut P.** Regulation of p53 by metal ions and by antioxidants: dithiocarbamate down-regulates p53 DNA-binding activity by increasing the intracellular level of copper. *Mol Cell Biol.* 1997; 17: 5699–706.
369. **Kim CH, Kim JH, Hsu CY, Ahn YS.** Zinc is required in pyrrolidine dithiocarbamate inhibition of NF-κB activation. *FEBS Lett.* 1999; 449: 28–32.
370. **Iseki A, Kambe F, Okumura K, Niwata S, Yamamoto R, Hayakawa T, Seo H.** Pyrrolidine dithiocarbamate inhibits TNF-α-dependent activation of NF-κB by increasing intracellular copper level in human aortic smooth muscle cells. *Biochem Biophys Res Commun.* 2000; 276: 88–92.
371. **Furuta S, Ortiz F, Zhu Sun X, Wu H-H, Mason A, Momand J.** Copper uptake is required for pyrrolidine dithiocarbamate-mediated oxidation and protein level increase of p53 in cells. *Biochem J.* 2002; 365: 639–48.
372. **Nurmi A, Goldsteins G, Närväinen J, Pihlaja R, Ahtoniemi T, Gröhn O, Koistinaho J.** Antioxidant pyrrolidine dithiocarbamate activates Akt-GSK signaling and is neuroprotective in neonatal hypoxia-ischemia. *Free Radic Biol Med.* 2006; 40: 1776–84.
373. **Daniel K, Chen D, Orlu S, Cui Q, Miller F, Dou QP.** Clioquinol and pyrrolidine dithiocarbamate complex with copper to form proteasome inhibitors and apoptosis inducers in human breast cancer cells. *Breast Cancer Res.* 2005; 7: R897–908.
374. **Milacic V, Chen D, Giovagnini L, Diez A, Fregona D, Dou QP.** Pyrrolidine dithiocarbamate-zinc(II) and -copper(II) complexes induce apoptosis in tumor cells by inhibiting the proteasomal activity. *Toxicol Appl Pharmacol.* 2008; 231: 24–33.
375. **Ding W-Q, Yu H-J, Lind SE.** Zinc-binding compounds induce cancer cell death *via* distinct modes of action. *Cancer Lett.* 2008; 271: 251–9.
376. **Beraldo H, Gambino D.** The wide pharmacological versatility of semicarbazones, thiosemicarbazones and their metal complexes. *Mini Rev Med Chem.* 2004; 4: 31–9.
377. **Petering DH.** Concerning the role of zinc in the antitumor activity of 3-ethoxy-2-oxobutyraldehyde bis(thiosemicarbazonato) zinc(II) and related chelates. *Biochem Pharmacol.* 1974; 23: 567–76.
378. **Deanling J, Lewis J, Mullen G, Welch M, Blower P.** Copper bis(thiosemicarbazone) complexes as hypoxia imaging agents: structure-activity relationships. *J Biol Inorg Chem.* 2002; 7: 249–59.
379. **Maurer RI, Blower PJ, Dilworth JR, Reynolds CA, Zheng Y, Mullen GED.** Studies on the mechanism of hypoxic selectivity in copper bis(thiosemicarbazone) radiopharmaceuticals. *J Med Chem.* 2002; 45: 1420–31.
380. **Lewis JS, Laforest R, Buettner TL, Song S-K, Fujibayashi Y, Connett JM, Welch MJ.** Copper-64-diacetyl-bis(N4-methylthiosemicarbazone): An agent for radiotherapy. *Proc Natl Acad Sci USA.* 2001; 98: 1206–11.
381. **Cowley AR, Davis J, Dilworth JR, Donnelly PS, Dobson R, Nightingale A, Peach JM, Shore B, Kerr D, Seymour L.** Fluorescence studies of the intra-cellular distribution of zinc bis(thiosemicarbazone) complexes in human cancer cells. *Chem Commun.* 2005; 7: 845–7.
382. **Holland JP, Aighthio FI, Betts HM, Bonnitcha PD, Burke P, Christlieb M, Churchill GC, Cowley AR, Dilworth JR, Donnelly PS, Green JC, Peach JM, Vasudevan SR, Warren JE.** Functionalized bis(thiosemicarbazonato) complexes of zinc and copper: synthetic platforms toward site-specific radiopharmaceuticals. *Inorg Chem.* 2007; 46: 465–85.
383. **Fujibayashi Y, Taniuchi H, Yonekura Y, Ohtani H, Konishi J, Yokoyama A.** Copper-62-ATSM: a new hypoxia imaging agent with high membrane permeability and low redox potential. *J Nucl Med.* 1997; 38: 1155–60.
384. **Vavere AL, Lewis JS.** Cu-ATSM: A radiopharmaceutical for the PET imaging of hypoxia. *Dalton Trans.* 2007; 43: 4893–902.
385. **Xiao Z, Donnelly PS, Zimmermann M, Wedd AG.** Transfer of copper between bis(thiosemicarbazone) ligands and intracellular copper-binding proteins. insights into mechanisms of copper uptake and hypoxia selectivity. *Inorg Chem.* 2008; 47: 4338–47.
386. **Kraker A, Krezoski S, Schneider J, Minkel D, Petering DH.** Reaction of 3-ethoxy-2-oxobutyraldehyde bis(thiosemicarbazonato) Cu(II) with Ehrlich cells. Binding of copper to metallothionein and its relationship to zinc metabolism and cell proliferation. *J Biol Chem.* 1985; 260: 13710–8.
387. **Donnelly PS, Caragounis A, Du T, Laughton KM, Volitakis I, Cherny RA, Sharples RA, Hill AF, Li Q-X, Masters CL, Barnham KJ, White AR.** Selective intracellular release of copper and zinc ions from bis(thiosemicarbazonato) complexes reduces levels of Alzheimer disease amyloid-β peptide. *J Biol Chem.* 2008; 283: 4568–77.
388. **Barnham KJ, Kenche VB, Ciccotosto GD, Smith DP, Tew DJ, Liu X, Perez K, Cranston GA, Johanssen TJ, Volitakis I, Bush AI, Masters CL, White AR, Smith JP, Cherny RA, Cappai R.** Platinum-based inhibitors of amyloid-β as therapeutic agents for Alzheimer's disease. *Proc Natl Acad Sci USA.* 2008; 105: 6813–8.
389. **Masters CL, Beyreuther K.** Alzheimer's centennial legacy: prospects for rational therapeutic intervention targeting the Aβ amyloid pathway. *Brain.* 2006; 129: 2823–39.
390. **Bondiolotti G, Sala M, Pollera C, Gervasoni M, Puricelli M, Ponti W, Baneggi SR.** Pharmacokinetics and distribution of clioquinol in golden hamsters. *J Pharm Pharmacol.* 2007; 59: 387–93.
391. **Bondiolotti GP, Pollera C, Pirola R, Baneggi SR.** Determination of 5-chloro-7-iodo-8-quinolinol (clioquinol) in plasma and tissues of hamsters by high-performance liquid chromatography and electrochemical detection. *J Chromatogr B Analyt Technol Biomed Life Sci.* 2006; 837: 87–91.
392. **Hayashi M, Fuwa T, Awazu S, Hanano M.** Differences in species of iodochlorhydroxyquin absorption, metabolism, and excretion. *Chem Pharm Bull.* 1976; 24: 2589–96.
393. **Kotaki H, Yamamura Y, Tanimura Y, Saitoh Y, Nakagawa F, Tamura Z.** Intestinal absorption and metabolism of clioquinol in the rat. *J Pharmacobiodyn.* 1983; 6: 881–7.
394. **Kotaki H, Yamamura Y, Tanimura Y, Saitoh Y, Nakagawa F, Tamura Z.** Determination of chinoform and its metabolites in plasma by gas chromatography–mass spectrometry. *Chem Pharm Bull.* 1983; 31: 299–304.
395. **Liewendahl K, Kivikangas V, Lamberg BA.** Metabolism of ^{125}-iodochloroxyquinoline in man. II. Metabolites in plasma, urine and faeces. *Nuclear-Medizin.* 1967; 6: 32–43.
396. **Neldner KH, Hambidge KM.** Zinc therapy of acrodermatitis enteropathica. *N Engl J Med.* 1975; 292: 879–82.
397. **Flagstad T.** Intestinal absorption of 65 Zinc in A46 (Adema disease) after treatment with oxychinolines. *Nordisk Veterinar Medicine.* 1977; 29: 96–100.

398. **Tsubaki T, Honma Y, Hoshi M.** Neurological syndrome associated with clioquindl. *Lancet*. 1971; 297: 696–7.
399. Clioquinol and neurological disease. *Br Med J*. 1971; 2: 291–2.
400. **Osterman PO.** Myelopathy after clioquinol treatment. *Lancet*. 1971; 2: 544.
401. **Shimada Y, Tsuji T, Igata A, Steinitz H.** Halogenated oxyquindine derivatives and neurological syndromes. *Lancet*. 1971; 2: 41–3.
402. **Tateishi J.** Subacute myelo-optico-neuropathy: Clioquinol intoxication in humans and animals. *Neuropathology*. 2000; 20: S20–S24.
403. **Konagaya M, Matsumoto A, Takase S, Mizutani T, Sobue G, Konishi T, Hayabara T, Iwashita H, Ujihira T, Miyata K, Matsuoka Y.** Clinical analysis of longstanding subacute myelo-optico-neuropathy: sequelae of clioquinol at 32 years after its ban. *J Neurol Sci*. 2004; 218: 85–90.
404. **Nakae K, Yamamoto S-I, Shigematsu I, Kono R.** RElation between subacute myelo-optic neuropathy (S.M.O.N.) and clioquinol: nationwide survey. *Lancet*. 1973; 301: 171–3.
405. **Ohtsuka K, Ohishi N, Eguchi G, Yagi K.** Degeneration of retinal neuroblasts by chinoform-ferric chelate. *Cell Mol Life Sci*. 1982; 38: 120–2.
406. **Yagi K, Ohtsuka K, Ohishi N.** Lipid peroxidation caused by chinoform-ferric chelate in cultured neural retinal cells. *Cell Mol Life Sci*. 1985; 41: 1561–3.
407. **Yassin MS, Ekblom J, Iberg C, Oreland L.** Transmethylation Reactions and Autoradiographic Distribution of Vitamin B12: Effects of Clioquinol Treatment in Mice. *Jpn J Pharmacol*. 1998; 78: 55–61.
408. **Yassin MS, Ekblom J, Xilinas M, Gottfries CG, Oreland L.** Changes in uptake of vitamin B12 and trace metals in brains of mice treated with clioquinol. *J Neurol Sci*. 2000; 173: 40–4.
409. **DiVaira M, Bazzicalupi C, Orioli P, Messori L, Bruni B, Zatta P.** Clioquinol, a drug for Alzheimer's disease specifically interfering with brain metal metabolism: structural characterization of its zinc(II) and copper(II) complexes. *Inorg Chem*. 2004; 43: 3795–7.
410. **Wagner CC, Calvo S, Torre MH, Baran EJ.** Vibrational spectra of clioquinol and its Cu(II) complex. *J Raman Spec*. 2007; 38: 373–6.
411. **Ding W-Q, Liu B, Vaught JL, Palmiter RD, Lind SE.** Clioquinol and docosahexaenoic acid act synergistically to kill tumor cells. *Mol Cancer Ther*. 2006; 5: 1864–72.
412. **Treiber C, Simons A, Strauss M, Hafner M, Cappai R, Bayer TA, Multhaup G.** Clioquinol mediates copper uptake and counteracts copper efflux activities of the amyloid precursor protein of Alzheimer's disease. *J Biol Chem*. 2004; 279: 51958–64.
413. **Nitzan Y, Sekler I, Frederickson C, Coulter D, Balaji R, Liang S-L, Margulis A, Hershfinkel M, Silverman W.** Clioquinol effects on tissue chelatable zinc in mice. *J Mol Med*. 2003; 81: 637–44.
414. **Cherny RA, Legg JT, McLean CA, Fairlie DP, Huang X, Atwood CS, Beyreuther K, Tanzi RE, Masters CL, Bush AI.** Aqueous dissolution of Alzheimer's disease Aβ amyloid deposits by biometal depletion. *J Biol Chem*. 1999; 274: 23223–8.
415. **Cherny RA, Atwood CS, Xilinas ME, Gray DN, Jones WD, McLean CA, Barnham KJ, Volitakis I, Fraser FW, Kim Y-S, Huang X, Goldstein LE, Moir RD, Lim JT, Beyreuther K, Zheng H, Tanzi RE, Masters CL, Bush AI.** Treatment with a copper-zinc chelator markedly and rapidly inhibits β-amyloid accumulation in Alzheimer's disease transgenic mice. *Neuron*. 2001; 30: 665–76.
416. **Raman B, Ban T, Yamaguchi K-i, Sakai M, Kawai T, Naiki H, Goto Y.** Metal ion-dependent effects of clioquindl on the fibril growth of an amyloid β peptide. *J Biol Chem*. 2005; 280: 16157–62.
417. **Abramov AY, Canevari L, Duchen MR.** Changes in intracellular calcium and glutathione in astrocytes as the primary mechanism of amyloid neurotoxicity. *J Neurosci*. 2003; 23: 5088–95.
418. **Benvenisti-Zarom L, Chen J, Regan RF.** The oxidative neurotoxicity of clioquinol. *Neuropharmacology*. 2005; 49: 687–94.
419. **Regland B, Lehmann W, Abedini I, Blennow K, Jonsson M, Karlsson I, S¨qren M, Wallin A, Xilinas M, Gottfries CG.** Treatment of Alzheimer's disease with clioquinol. *Dement Geriatr Cogn Disord*. 2001; 12: 408–14.
420. **Ritchie CW, Bush AI, Mackinnon A, Macfarlane S, Mastwyk M, MacGregor L, Kiers L, Cherny R, Li Q-X, Tammer A, Carrington D, Mavros C, Volitakis I, Xilinas M, Ames D, Davis S, Beyreuther K, Tanzi RE, Masters CL.** Metal-protein attenuation with iodochlorhydroxyquin (clioquindl) targeting aβ amyloid deposition and toxicity in Alzheimer disease: a pilot phase 2 clinical trial. *Arch Neurol*. 2003; 60: 1685–91.
421. **Adlard PA, Cherny RA, Finkelstein DI, Gautier E, Robb E, Cortes M, Volitakis I, Liu X, Smith JP, Perez K, Laughton K, Li Q-X, Charman SA, Nicolazzo JA, Wilkins S, Deleva K, Lynch T, Kok G, Ritchie CW, Tanzi RE, Cappai R, Masters CL, Barnham KJ, Bush AI.** Rapid restoration of cognition in Alzheimer's transgenic mice with 8-hydroxy quinoline analogs is associated with decreased interstitial Aβ. *Neuron*. 2008; 59: 43–55.
422. **Lannfelt L, Blennow K, Zetterberg H, Batsman S, Ames D, Harrison J, Masters CL, Targum S, Bush AI, Murdoch R, Wilson J, Ritchie CW.** Safety, efficacy, and biomarker findings of PBT2 in targeting Aβ as a modifying therapy for Alzheimer's disease: a phase IIa, double-blind, randomised, placebo-controlled trial. *Lancet Neurol*. 2008; 7: 779–86.
423. **Arbiser JL, Kraeft SK, van Leeuwen R, Hurwitz SJ, Selig M, Dickersin GR, Flint A, Byers HR, Chen LB.** Clioquinol-zinc chelate: a candidate causative agent of subacute myelo-optic neuropathy. *Mol Med*. 1998; 4: 665–70.
424. **Chen WH, Wang M, Yu SS, Su L, Zhu DM, She JQ, Cao XJ, Ruan DY.** Clioquinol and vitamin B12 (cobalamin) synergistically rescue the lead-induced impairments of synaptic plasticity in hippocampal dentate gyrus area of the anesthetized rats *in vivo*. *Neuroscience*. 2007; 147: 853–64.
425. **Choi SM, Choi K-O, Park Y-K, Cho H, Yang EG, Park H.** Clioquinol, a Cu(II)/Zn(II) chelator, inhibits both ubiquitination and asparagine hydroxylation of hypoxia-inducible factor-1α, leading to expression of vascular endothelial growth factor and erythropoietin in normoxic cells. *J Biol Chem*. 2006; 281: 34056–63.
426. **Kaur D, Yantiri F, Rajagopalan S, Kumar J, Mo JQ, Boonplueang R, Viswanath V, Jacobs R, Yang L, Beal MF, DiMonte D, Volitaskis I, Ellerby L, Cherny RA, Bush AI, Andersen JK.** Genetic or pharmacological iron chelation prevents mptp-induced neurotoxicity *in vivo*: a novel therapy for Parkinson's disease. *Neuron*. 2003; 37: 899–909.
427. **Masuda T, Hida H, Kanda Y, Aihara N, Ohta K, Yamada K, Nishino H.** Oral administration of metal chelator ameliorates motor dysfunction after a small hemorrhage near the internal capsule in rat. *J Neurosci Res*. 2007; 85: 213–22.
428. **Nguyen T, Hamby A, Massa SM.** Clioquinol down-regulates mutant huntingtin

expression in vitro and mitigates pathology in a Huntington's disease mouse model. *Proc Natl Acad Sci USA.* 2005; 102: 11840–5.

429. **Pollera C, Lucchini B, Formentin E, Bareggi S, Poli G, Ponti W.** Evaluation of anti-prionic activity of clioquinol in an *in vivo* model (Mesocricetus auratus). *Vet Res Commun.* 2005; 29: 253–5.

430. **Ponti W, Sala M, Pollera C, Braida D, Poli G, Bareggi S.** *In vivo* model for the evaluation of molecules active towards transmissible spongiform encephalopathies. *Vet Res Commun.* 2004; 28: 307–10.

431. **Priel T, Aricha-Tamir B, Sekler I.** Clioquinol attenuates zinc-dependent beta-cell death and the onset of insulitis and hyperglycemia associated with experimental type I diabetes in mice. *Eur J Pharmacol.* 2007; 565: 232–9.